

This is a digital document from the collections of the *Wyoming Water Resources Data System (WRDS) Library.*

For additional information about this document and the document conversion process, please contact WRDS at wrds@uwyo.edu and include the phrase **“Digital Documents”** in your subject heading.

To view other documents please visit the WRDS Library online at:
<http://library.wrds.uwyo.edu>

Mailing Address:

Water Resources Data System
University of Wyoming, Dept 3943
1000 E University Avenue
Laramie, WY 82071

Physical Address:

Wyoming Hall, Room 249
University of Wyoming
Laramie, WY 82071

Phone: (307) 766-6651

Fax: (307) 766-3785

Funding for WRDS and the creation of this electronic document was provided by the Wyoming Water Development Commission
(<http://wwdc.state.wy.us>)

This PDF is intended to represent the document delivered to the Wyoming Water Development Office in hard copy; however variations may exist from the printed version.

Weather Modification— Medicine Bow/Sierra Madre Ranges Final Design and Permitting Study

**Final Report prepared for
Wyoming Water Development Commission
State of Wyoming**

by

National Center for Atmospheric Research
Research Applications Laboratory
P.O. Box 3000
Boulder, CO 80307



NCAR

Investigators:

Sarah Tessendorf¹, Roy Rasmussen¹, Lulin Xue¹, Courtney Weeks¹, Kyoko Ikeda¹, Jamie Wolff¹, Michelle Harrold¹, Bruce Boe², Patrick Golden³, Logan Karsten¹, David Gochis¹,
Duncan Axisa¹

¹Research Applications Laboratory, National Center for Atmospheric Research (NCAR)

²Weather Modification International (WMI)

³Heritage Environmental Consultants (HEC)

8 December 2017

Weather Modification—Medicine Bow/Sierra Madre Final Design and Permitting Study

Table of Contents

Executive Summary	i
1. Introduction	1
1.1. Task Overview	1
1.2. Personnel and Organizations	3
2. Task 1: Scoping Meeting/Project Meetings	4
2.1. Scoping Meetings in Saratoga and Savery, WY	4
2.2. 27 January 2016, Cheyenne, WY	4
3. Task 2: Review and Summarization of Previous Data	6
3.1. Background	6
3.1.1. Conceptual Model	7
3.2. History of Wintertime Orographic Cloud Seeding	9
3.2.1. Randomized Studies - Historical	9
3.2.2. Randomized Studies - Recent	10
3.2.3. Physical Experiments	12
3.2.4. Numerical Modeling	13
3.3. Meteorological and Climatological Observations	14
3.4. History of Cloud Seeding In and Near the Targeted Areas	14
4. Task 3: Climatology of the Project Area	16
4.1. Data and Methodology	17
4.1.1. Observations	17
4.1.2. Model (WRF-CONUS)	17
4.1.3. Seeding Potential Analysis Methods	18
4.2. Climatology of precipitation	22
4.2.1. SNOTEL Precipitation Observations	23
4.2.2. Comparison of model vs SNOTEL	28
4.2.3. Comparison of the 8-year Headwaters and CONUS WRF model simulations	33
4.3. Model-based Climatology	45
4.3.1. Single Site Analysis	45
4.3.2. Area-based Analysis	49
4.3.3. Spatial Mapping Analysis	60
4.4. Climatology of Cloud Seeding Opportunities	64
4.4.1. Model-based Analysis Results	64
4.5. Seedable Precipitation	80
4.6. Climatological Analysis Summary	81
5. Task 4: Development of a Preliminary Project Design	82
5.1. Project Scope and Targeting	82
5.2. Delivery Methods and Seeding Agent Selection	83
5.3. Selection of Test Cases	85
5.4. Initial Ground-based Tests	85
5.5. Additional Ground Generator Tests	87

5.6.	Airborne Tests	88
5.7.	Ground-based Generator Locations	89
5.8.	Summary Remarks	89
6.	Task 5: Model Evaluation of the Preliminary Project Design	91
6.1.	Overview of the model	91
6.1.1.	Updates to ASPEN and the Microphysical Scheme	92
6.2.	Model setup.....	94
6.3.	Case overviews	95
6.4.	Case study simulations	95
6.4.1.	Case 1: 23 January 2010 results.....	96
6.4.2.	Case 2: 10 January 2014 results.....	105
6.4.3.	Case 3: 13 January 2014 results.....	112
6.4.4.	Case 4: 21 February 2012 results.....	122
6.5.	Model Simulation Comparison with Observations	133
6.5.1.	Comparison between model and observed soundings	133
6.5.2.	Comparison between model and observed precipitation	138
6.6.	Summary of Case Study Simulation Results	140
7.	Task 6: Field Surveys: Proposed Ground-Based Generator Locations	142
7.1.	Proposed Ground-Based Generator Locations: Siting Areas.....	142
7.1.1.	Proposed Ground-Based Generator Locations: Field Surveys.....	143
7.2.	Proposed Viable Ground-based Generator Locations	149
7.2.1.	Medicine Bow Range.....	149
7.2.2.	Sierra Madre Range	149
8.	Task 7: Access/Easements & Environmental Permitting/Reporting	156
8.1.	Private Lands.....	156
8.2.	Public Lands.....	157
8.2.1.	Medicine Bow National Forest Service Application	157
8.3.	Weather Modification Program Permitting.....	158
8.3.1.	State of Wyoming Permit Requirements.....	158
8.3.2.	Wyoming Game and Fish Department	158
8.3.3.	National Oceanic and Atmospheric Administration Reporting.....	158
9.	Task 8: Establishment of Operational Criteria.....	160
9.1.	Information Sources.....	160
9.1.1.	Soundings.....	160
9.1.2.	Radiometer.....	160
9.1.3.	Other Sources	161
9.2.	Ground-Based Seeding with Ice Nuclei.....	161
9.3.	Airborne Seeding with Ice Nuclei.....	163
9.4.	Seeding Season	164
9.5.	Suspension Criteria	164
10.	Task 9: Environmental and Legal Considerations	167
10.1.	Downwind (Extra-area) Effects	167
10.2.	Environmental Impacts of Seeding Agents	169
10.3.	General Statements on Potential Environmental Impacts of Cloud Seeding....	172
10.4.	Legal Implications.....	174
11.	Task 10: Evaluation Methodology	175

11.1.	Statistical Evaluation	175
11.1.1.	Target/Control Method	175
11.1.2.	Evaluation by Historical Regression	176
11.1.3.	Evaluation by Ratio Statistics.....	177
11.2.	Numerical Model Evaluation	177
11.3.	Physical Evaluation	178
11.4.	Evaluation Methodology Summary	180
12.	Task 11: Potential Benefits/Hydrologic Assessment	181
12.1.	WRF-CONUS Model Estimates of Seeding Effects on Streamflow.....	181
12.1.1.	WRF-CONUS Simulation of Runoff.....	181
12.1.2.	Assumptions for Estimating Seeding Effects on Streamflow	186
12.1.3.	Regression-based Estimates of Streamflow Changes due to Seeding	187
12.2.	WRF-Hydro Simulation of Seeding Impacts on Streamflow	189
12.2.1.	Description of WRF-Hydro and Methods for this Study.....	190
12.2.2.	WRF-Hydro Results.....	193
12.2.3.	WRF-Hydro Analysis Summary.....	205
12.3.	Synthesis of Results from Multiple Methods	206
13.	Task 12: Cost Estimates	208
13.1.	Project Scope.....	208
13.2.	Length of Program Season.....	209
13.3.	Deployment of Ground-Based Ice Nucleus Generators	210
13.4.	Airborne Seeding.....	211
13.5.	Possible Cost Savings.....	213
13.5.1.	Sharing Operational Resources.....	213
13.5.2.	The Number of Operational Seasons	214
13.5.3.	Project Implementation Mode.....	214
14.	Task 13: Preliminary Cost/Benefit Analyses	217
14.1.	The Value of Water near the Medicine Bow and Sierra Madre Ranges	217
14.2.	Value of Augmented April-July Streamflow	218
14.3.	Cost per Acre Foot Estimates	219
14.4.	Cost/Benefit Summary Remarks.....	220
15.	Task 14: Finalization of Project Design	222
16.	Task 15: Environmental Analysis and Permitting.....	224
17.	Task 16: Discretionary Task.....	225
18.	Task 17: Reports and Executive Summaries	226
19.	Task 18: Report Presentations.....	227
20.	Task 19: Climatological Monitoring of the Study Area	228
21.	Task 20: Model Evaluation of the WWMPP RSE using an Ensemble Approach	229
21.1.	Description of Ensemble Modeling Approach	229
21.2.	Ensemble formulation.....	230
21.3.	Verification of the Ensemble Modeling Approach	233
21.4.	Evaluation of the WWMPP using the Ensemble Modeling Approach.....	238
21.5.	Summary of RSE Ensemble Modeling Study.....	239
21.6.	Next Steps for Modeling the Effects of Cloud Seeding.....	239
21.7.	Application of the Ensemble Approach to other Mountain Ranges	239
22.	Summary and Recommendations	241

22.1.	Summary	241
22.2.	Conclusions and Recommendations	246
22.2.1.	Recommendations	247
Appendix A: Photos from Field Surveys		249
Appendix B: Letters from the USFS.....		276
Appendix C: Public Hearing Documents		279
References		290
List of Acronyms		298

LIST OF FIGURES

Figure 1. Topography map of the Medicine Bow and Sierra Madre Ranges (m) illustrating the locations of nine ground-based generator design groups.....	iii
Figure 2. Change in precipitation (mm) due to simulated cloud seeding for model simulations using only Sierra Madre Groups A–F (RUN14 and RUN15) compared with two hours of simulated airborne seeding (RUN16) case in the 13 January 2014 case. RUN14 does not include the newly-added AgI-removal processes, while RUN15 does. The small area of negative changes in precipitation in the Medicine Bow is the result of precipitation changing phase from rain to snow (and snow falling out farther downwind) in the seeding simulation. The assessment area total change in precipitation in these cases is positive.....	iv
Figure 3. Map of the final recommended design for 23 ground-based generator sites in the Medicine Bow and Sierra Madre Ranges.	vi
Figure 4. WRF-Hydro simulation results from water year 2010: difference between seeded and unseeded snow water equivalent (SWE) for 1 May 2010 (colored), along with accumulated precipitation difference (mm; contour) on the left, and total accumulated streamflow differences (AF) for the 2010 water year from the non-seeded to seeded simulation by basin on the right. The basins shown in the right panel are outlined in thick black lines on the left for reference.	viii
Figure 5. Cost of water for usage and for two estimates of annual seeding program costs (using 70% impact area) for the three levels of estimated streamflow increases resulting from WWMPP annual seeding effects for seedable storms. Gray shading indicates estimated water costs. The solid green and red lines indicate the cost for the 23 remote generator ground-seeding option versus the single aircraft airborne seeding option, respectively, expressed as program costs per acre-foot of streamflow increase (essentially a 1:1 ratio). The dashed green and red lines show the corresponding 5:1 ratios of water costs to program costs.	ix
Figure 4.1. WRF-CONUS model domain and elevation. Red box indicates the Sierra Madre (SM) and Medicine Bow (MB) mountain ranges where the analysis is focused. For a close-up of the study region see Figure 12.1.	18
Figure 4.2. Map of the model terrain height highlighting the grid points used for each region in the seeding potential analysis (crosses or plus symbols of different colors). Precipitation gauge sites are marked by yellow circles. Sites used for analysis of 700-hPa conditions are marked by white circles.	21
Figure 4.3. Locations of SNOTEL sites (magenta dots) in Sierra Madre and Medicine Bow Ranges. Filled magenta circles indicate the SNOTEL sites used for the evaluation of the WRF-CONUS model simulation results. Open magenta circles are the SNOTEL sites not used for the evaluation.	23
Figure 4.4. (a) – (h) Monthly precipitation averaged over 13 SNOTEL sites for each of the eight water years. (i) Eight-year climatology of monthly precipitation at 13 SNOTEL sites. Vertical bars indicate one standard deviation from the area average, representing spatial variability.	24
Figure 4.5. The November–April precipitation at SNOTEL sites in each water year. Contours indicate elevation.....	25

Figure 4.6. (a) Temporal correlation coefficients of daily precipitation over eight years at each pair of SNOTEL sites. (b) Same as panel (a) but excludes seasonal data from seasons 2000–2001 to 2003–2004 during which time some sites did not have measurements. SNOTEL site names in black (blue) are the sites in the Sierra Madre (Medicine Bow) Range.....	27
Figure 4.7. Same as Figure 4.6 but for each water year.	28
Figure 4.8. The November–April precipitation in each water year from the WRF-CONUS model simulation. Magenta circles indicate the SNOTEL site locations.....	29
Figure 4.9. Climatology of annual precipitation accumulation at each SNOTEL site. Vertical bars are one standard deviation about the climatological mean. Average seasonal (1 November–30 April, shaded region) and annual precipitation differences are annotated in the upper left corner (model minus observation in mm). Values in parentheses indicate percent bias over the seasonal and annual time periods with respect to the observations. Refer to the map in the middle column for the location of the SNOTEL sites. Note that the values were averaged over eight years at all sites except at Sage Creek (7 years), Little Snake (4 years), and Cinnabar Park (5 years). ...	30
Figure 4.10. Time history of observed and simulated precipitation accumulation averaged over 13 SNOTEL sites for each water year. The difference (mm) between the model and SNOTEL precipitation observations for November–April (winter) and the full year is indicated in the upper left corners. Values in parentheses are the percent bias from the observations. The biases are taken as model minus observation.....	32
Figure 4.11. An 8-year climatology of precipitation accumulation averaged over 13 SNOTEL sites. Vertical bars are one standard deviation from the 8-year mean, representing the year-to-year variability. The difference (in mm) between the WRF-CONUS model and SNOTEL precipitation observations for November–April (winter) and the full year is indicated in the upper left corners. Values in parentheses are the percent bias from the observations. The biases are taken as model minus observation.	33
Figure 4.12. Model domain from the two high-resolution (4 km) WRF simulations. The red polygon indicates the WRF-Headwaters domain.	34
Figure 4.13. 8-year climatology of November–April precipitation from the (a) WRF-Headwaters, (b) WRF-CONUS, and (c) SNOTEL observations. Magenta circles in panels (a) and (b) show locations of the SNOTEL sites.	35
Figure 4.14. Precipitation accumulation from the WRF-Headwaters (WRF-HW) and WRF-CONUS simulations (blue and red, respectively) compared with the SNOTEL observations. Precipitation values are averaged over 13 SNOTEL sites in the study domain. Vertical bars represent one standard deviation from the spatial average.	36
Figure 4.15. December 2007 observed (red) and WRF-CONUS modeled (blue) LWP at the Cedar Creek radiometer site for the 9-degree elevation, 80-degree-azimuth scan angle. The difference (model minus twenty-minute observed mean) is shown in green (right axis).....	38
Figure 4.16. As in Figure 4.15, but for February 2008.	38
Figure 4.17. As in Figure 4.15, but for March 2008.	38
Figure 4.18. December 2007 observed (red) and WRF-Headwaters modeled (blue) LWP at the Cedar Creek radiometer site for the 9-degree elevation, 80-degree-azimuth scan angle. The difference (model minus twenty-minute observed mean) is shown in green (right axis).....	39

Figure 4.19. As in Figure 4.18, but for February 2008.	39
Figure 4.20. As in Figure 4.18, but for March 2008.	39
Figure 4.21. Monthly boxplots of non-zero (>0.05 mm) observed and modeled liquid-water path at the Cedar Creek radiometer for the 9-degree elevation, 80-degree-azimuth angle scan. The red line denotes the median value; the box extents are the 25 th and 75 th percentiles; whiskers extend to the last non-outlying point; outliers are denote by gray plusses.	40
Figure 4.22. November 2008–April 2009 observed (red) and WRF-CONUS modeled (blue) LWP at the Cedar Creek radiometer site for the 9 degree elevation, 80 degree azimuth scan angle. The difference (model minus twenty-minute observed mean) is shown in green (right axis).	41
Figure 4.23. As in Figure 4.22, but for the 2009-2010 season.	41
Figure 4.24 As in Figure 4.22, but for the 2010-2011 season.	42
Figure 4.25. As in Figure 4.22, but for the 2011-2012 season.	42
Figure 4.26. As in Figure 4.22, but for the Savery radiometer and the 2009-2010 season...	42
Figure 4.27. As in Figure 4.22, but for the Savery radiometer and the 2010-2011 season...	43
Figure 4.28. As in Figure 4.22, but for the Savery radiometer and the 2011-2012 season...	43
Figure 4.29. Seasonal boxplots of non-zero (>0.05 mm) observed and modeled LWP at the Cedar Creek radiometer for the 9 degree elevation, 80 degree azimuth angle scan. The red line denotes the median value; the box extents are the 25 th and 75 th percentiles; whiskers extend to the last non-outlying point; outliers are denote by gray plusses...	44
Figure 4.30. As in Figure 4.29, but for the Savery radiometer.	45
Figure 4.31. Wind rose plots showing the frequency of modeled 700 hPa wind direction at (clockwise from top left) Savery, Saratoga, Cedar Creek, and Centennial when precipitation occurred at the HY47 precipitation gauge site for a and b and the GLEES precipitation gauge site for c and d from November–April over the 8-year period. The amount of precipitation per 3-hourly model output time for each wind direction is indicated by the color shading within each wind direction bin.	46
Figure 4.32. Month-by-month wind roses of modeled 700-hPa wind direction during 3-hourly model output times for Savery with precipitation over HY47 gauge site from November–April over the 8-year period.	47
Figure 4.33. Month-by-month wind roses of modeled 700 hPa wind direction for 3-hourly output times at Saratoga with precipitation over HY47 gauge site from November–April over the 8-year period.	48
Figure 4.34. Histogram counts (left ordinate) of the 700 hPa modeled temperature at (clockwise from top left) Savery, Saratoga, Cedar Creek, and Centennial for all 3-hourly output between November and April from the 8-year period (red) and for all 3-hourly output that had precipitation (blue) at the precipitation gauge site of HY47 (Sierra Madre sites) or GLEES (Medicine Bow sites). Cumulative distributions for all (red) and output hours with precipitation (blue dotted) are also overlaid using the right ordinate (%).	49
Figure 4.35. Histogram counts (left ordinate) of the area-averaged 0–1 km AGL modeled temperature for ground seeding (GS) over (clockwise from top left) SMWest, SMEast, MBWest, and MBEast for all 3-hourly output between November – April from the 8-year period (red) and for all 3-hourly output that had precipitation (blue) at the precipitation gauge site of HY47 (Sierra Madre sites) or GLEES (Medicine Bow sites).	

Cumulative distributions for all (red) and output hours with precipitation (blue dotted) are also overlaid using the right ordinate (%).	50
Figure 4.36. Histogram counts (left ordinate) of the area-averaged 0–1 km AGL modeled LWC for ground seeding (GS) over (clockwise from top left) SMWest, SMEast, MBWest, and MBEast for all 3-hourly output between November and April from the 8-year period (red) and for all 3-hourly output that had precipitation (blue) at the precipitation gauge site of HY47 (Sierra Madre sites) or GLEES (Medicine Bow sites). Cumulative distributions for all (red) and output hours with precipitation (blue dotted) are also overlaid using the right ordinate (%).	51
Figure 4.37. Histogram counts (left ordinate) of the area-averaged modeled LWP over (clockwise from top left) SMWest, SMEast, MBWest, and MBEast for all 3-hourly output between November and April from the 8-year period (red) and for all 3-hourly output that had precipitation (blue) at the precipitation gauge site of HY47 (Sierra Madre sites) or GLEES (Medicine Bow sites). Cumulative distributions for all (red) and output hours with precipitation (blue dotted) are also overlaid using the right ordinate (%).	52
Figure 4.38. Histogram counts (left ordinate) of the area-averaged Froude number derived from the model over (clockwise from top left) SMWest, SMEast, MBWest, and MBEast for all 3-hourly output between November and April from the 8-year period (red) and for all 3-hourly output that had precipitation (blue) at the precipitation gauge site of HY47 (Sierra Madre sites) or GLEES (Medicine Bow sites). Cumulative distributions for all (red) and output hours with precipitation (blue dotted) are also overlaid using the right ordinate (%).	53
Figure 4.39. Histogram counts (left ordinate) of the area-averaged model cloud-base height over (clockwise from top left) SMWest, SMEast, MBWest, and MBEast for all 3-hourly output between November and April from the 8-year period (red) and for all 3-hourly output that had precipitation (blue) at the precipitation gauge site of HY47 (Sierra Madre sites) or GLEES (Medicine Bow sites). Cumulative distributions for all (red) and output hours with precipitation (blue dotted) are also overlaid using the right ordinate (%).	54
Figure 4.40. Histogram counts (left ordinate) of the area-averaged model cloud depth over (Clockwise from top left) SMWest, SMEast, MBWest, and MBEast for all 3-hourly output between November and April from the 8-year period (red) and for all 3-hourly output that had precipitation (blue) at the precipitation gauge site of HY47 (Sierra Madre sites) or GLEES (Medicine Bow sites). Cumulative distributions for all (red) and output hours with precipitation (blue dotted) are also overlaid using the right ordinate (%).	55
Figure 4.41. Histogram counts (left ordinate) of the area-average model cloud top temperature over (clockwise from top left) SMWest, SMEast, MBWest, and MBEast for all 3-hourly output between November and April from the 8-year period (red) and for all 3-hourly output that had precipitation (blue) at the precipitation gauge site of HY47 (Sierra Madre sites) or GLEES (Medicine Bow sites). Cumulative distributions for all (red) and output hours with precipitation (blue dotted) are also overlaid using the right ordinate (%).	56
Figure 4.42. Histogram counts (left ordinate) of the area-averaged modeled temperature for the (left) 3–4 km MSL [AS] and (right) 4–5 km MSL [ASH] layer over (top) SMWest	

and (bottom) MBWest for all 3-hourly output between November and April from the 8-year period (red) and for all 3-hourly output that had precipitation (blue) at the precipitation gauge site of HY47 (Sierra Madre sites) or GLEES (Medicine Bow sites). Cumulative distributions for all (red) and output hours with precipitation (blue dotted) are also overlaid using the right ordinate (%).	59
Figure 4.43. Histogram counts (left ordinate) of the area-averaged model LWC for the (left) 3–4 km MSL [AS] and (right) 4–5 km MSL [ASH] layer over (top) SMWest and (bottom) MBWest for all 3-hourly output between November – April from the 8-year period (red) and for all 3-hourly output that had precipitation (blue) at the precipitation gauge site of HY47 (Sierra Madre sites) or GLEES (Medicine Bow sites). Cumulative distributions for all (red) and output hours with precipitation (blue dotted) are also overlaid using the right ordinate (%).	60
Figure 4.44. Frequency (fraction of time) that (a) temperature and (b) LWC criteria are met for seeding conditions within the 0 – 1 km AGL (GS) layer for all 3-hourly output for November–April over the 8-year period. Thin black contours indicate the topography (every 500 m MSL). The original WWMPP generator sites (8 in each Range) are overlaid as red triangles for reference.	61
Figure 4.45. Month-by-month frequency (fraction of time) that temperature criteria is met for seeding conditions within the 0–1 km AGL (GS) layer for all 3-hourly output from November–April over the 8-year period. Thin black contours indicate the topography (every 500 m MSL). The original WWMPP generator sites (8 in each Range) are overlaid as red triangles.	62
Figure 4.46. Month-by-month frequency (fraction of time) that LWC criteria is met for seeding conditions within the 0–1 km AGL (GS) layer for all 3-hourly output from November–April over the 8-year period. Thin black contours indicate the topography (every 500 m MSL). The original WWMPP generator sites (8 in each Range) are overlaid as red triangles.	63
Figure 4.47. Frequency (fraction of time) that (a) temperature and (b) LWC criteria are met for seeding conditions within the 3–4 km MSL (AS) layer for all 3-hourly output for November–April over the 8-year period. Thin black contours indicate the topography (every 500 m MSL). The original WWMPP generator sites (8 in each Range) are overlaid as red triangles.	64
Figure 4.48. Frequency (percent of time) that both the temperature ($-18^{\circ}\text{C} < T < -6^{\circ}\text{C}$) and LWC ($> 0.01 \text{ g kg}^{-1}$) criteria are met for seeding conditions within the 0 – 1 km AGL (GS) layer for all 3-hourly output for November – April over the 8-year period. Thin black contours indicate the topography (every 500 m MSL). The original WWMPP generator sites (8 in each Range) are overlaid as red triangles.	65
Figure 4.49. Month-by-month frequency (percent of time) that both the temperature ($-18^{\circ}\text{C} < T < -6^{\circ}\text{C}$) and LWC ($> 0.01 \text{ g kg}^{-1}$) criteria are met for seeding conditions within the 0–1 km AGL (GS) layer for all 3-hourly output from November–April over the 8-year period. Thin black contours indicate the topography (every 500 m MSL). The original WWMPP generator sites (8 in each Range) are overlaid as red triangles.	66
Figure 4.50. Frequency (percent of time) that both the temperature ($-18^{\circ}\text{C} < T < -6^{\circ}\text{C}$) and LWC ($> 0.01 \text{ g kg}^{-1}$) criteria are met for seeding conditions within the 3–4 km MSL (left) and 4–5 km MSL layer (right) for all 3-hourly output for November–April over	

the 8-year period. Thin black contours indicate the topography (every 500 m MSL). The original WWMPP generator sites (8 in each Range) are overlaid as red triangles.	67
Figure 4.51. Bar chart showing the average fraction of hours in a month that met the temperature and LWC criteria averaged over (a) SMWest and (b) MBWest for ground-based seeding (0–1 km AGL; blue) and the same for hours that also had precipitation in the model near the (a) HY47 or (b) GLEES precipitation site (green).	68
Figure 4.52. Bar chart showing the number of hours in a month that met the temperature and LWC criteria averaged over (a) SMWest and (b) MBWest for ground-based seeding (0–1 km AGL). Each color represents one of the 8 years simulated by the model.	69
Figure 4.53. Bar chart showing the average fraction of hours in a winter season (November–April) that met the temperature and LWC criteria averaged over (a) SMWest and (b) MBWest for ground-based seeding (0–1 km AGL; blue) and the same for hours that also had precipitation in the model near the (a) HY47 or (b) GLEES precipitation site (green).	70
Figure 4.54. Bar chart showing the average fraction of hours in a winter season (November–April) that met the temperature, LWC, and wind direction (210 to 315 degrees) criteria averaged over (a) SMWest and (b) MBWest for ground-based seeding (0–1 km AGL; blue) and the same for hours that also had precipitation in the model near the (a) HY47 or (b) GLEES precipitation site (green).	71
Figure 4.55. Bar chart showing the average fraction of hours in a winter season (November–April) that met the temperature, LWC, wind direction, and Froude number (>0.5) criteria averaged over (a) SMWest and (b) MBWest for ground-based seeding (0–1 km AGL; blue) and the same for hours that also had precipitation in the model near the (a) HY47 or (b) GLEES precipitation site (green).	72
Figure 4.56. Bar chart showing the average fraction of hours in a winter season (November–April) that met the temperature and LWC criteria averaged over SMSouth for ground-based seeding (0–1 km AGL; blue) and the same for hours that also had precipitation in the model near the SM South precipitation site (green).	73
Figure 4.57. Bar chart showing the average fraction of hours in a winter season (November–April) that met the temperature, LWC, and wind direction (320 to 50 degrees) criteria averaged over SMSouth for ground-based seeding (0–1 km AGL; blue) and the same for hours that also had precipitation in the model near the SM South precipitation site (green).	73
Figure 4.58. Bar chart showing the average fraction of hours in a month that met the temperature and LWC criteria averaged over SMWest for the (a) AS layer and (b) ASH layer (blue) and the same for hours that also had precipitation in the model near the HY47 precipitation site (green).	74
Figure 4.59. Bar chart showing the average fraction of hours in a month that met the temperature and LWC criteria averaged over MBWest for the (a) AS layer and (b) ASH layer (blue) and the same for hours that also had precipitation in the model near the GLEES precipitation site (green).	75
Figure 4.60. Bar chart showing the average fraction of hours in a winter season (November–April) that met the temperature and LWC criteria averaged over (a) SMWest and (b) MBWest for the AS layer (3–4 km MSL; blue) and the same for hours that also had precipitation in the model near the (a) HY47 or (b) GLEES precipitation site (green).	76

Figure 4.61. Ground (0–1 km AGL; blue) versus airborne (3–4 km MSL; green) seeding opportunities (fraction of hours in the season that meet the designated criteria, listed atop the figure) by month for (a) SMWest and (b) MBWest. The frequency of occurrence of cases from the union of both ground and AS layer seeding potential is shown in the yellow bar for each time period.....	77
Figure 4.62. Ground (0–1 km AGL; blue) versus airborne (3–4 km MSL; green) seeding opportunities (fraction of hours in the season that meet the designated criteria, listed atop the figure) by November–April season, and the 8-year average, for (a) SMWest and (b) MBWest. The frequency of occurrence of cases from the union of both ground and AS layer seeding potential is shown in the yellow bar for each time period.	78
Figure 4.63. Ground (0–1 km AGL; blue) versus airborne (4–5 km MSL; green) seeding opportunities (fraction of hours in the season that meet the designated criteria, listed atop the figure) by month for (a) SMWest and (b) MBWest. The frequency of occurrence of cases from the union of both ground and AS layer seeding potential is shown in the yellow bar for each time period.....	79
Figure 4.64. Ground (0–1 km AGL; blue) versus airborne (4–5 km MSL; green) seeding opportunities (fraction of hours in the season that meet the designated criteria, listed atop the figure) by November–April season, and the 8-year average, for (a) SMWest and (b) MBWest. The frequency of occurrence of cases from the union of both ground and AS layer seeding potential is shown in the yellow bar for each time period.	80
Figure 5.1. Maps of the terrain across the study region, highlighting the assessment area for the Medicine Bow (left) and Sierra Madre (right) Ranges, defined as area greater than 8,000 ft MSL elevation.	83
Figure 5.2. Example of a remotely controlled AgI generator.....	84
Figure 5.3. Example of cloud seeding aircraft.	84
Figure 5.4. Topography map of the Medicine Bow and Sierra Madre Ranges (m) illustrating the locations of the generator sites used in the WWMPP (green), those permitted but not used in the WWMPP (blue), and the new sites surveyed in 2015 to “fill in the gaps” (red). These sites formed the basis for the site groupings illustrated in Figure 5.5.....	86
Figure 5.5. Topography map of the Medicine Bow and Sierra Madre Ranges (m) illustrating the locations of initial ground-based generator design groups.....	87
Figure 5.6. Topography map of the Medicine Bow and Sierra Madre Ranges (m) illustrating the locations of additional ground-based generator design groups.....	88
Figure 5.7. Flight track positions (red line) designed for testing in the model	89
Figure 6.1. Interactions between AgI and hydrometeors simulated in the ASPEN cloud seeding parameterization (Xue et al. 2013a).....	92
Figure 6.2. Interactions between AgI and hydrometeors simulated in the updated ASPEN cloud seeding parameterization (updated from Xue et al. 2013a).....	93
Figure 6.3. Model domain for seeding project design evaluation simulations.	94
Figure 6.4. The accumulated precipitation (mm) of the control simulation in 23 January 2010 case.....	97
Figure 6.5. The LWP (mm) from the control simulation (color scale of 0 to 0.5 mm) at 2345 23 January 2010, and 0345 and 0600 UTC 24 January 2010.	97
Figure 6.6. Simulated seeding effects for all seeding experiments except Run19. Open blue circles denote the locations of ground-based generators utilized in the given experiment. The colorscale is from -2.5 to 2.5 mm.....	99

Figure 6.7. Accumulated LWP path difference (-0.8 to 0.8 mm) during the seeding period between seeded (SEED) and control simulations for the same cases as in Figure 6.6.	101
Figure 6.8. Average AgI concentration below 1 km AGL at the end of the seeding period for the same cases as in Figure 6.6.	102
Figure 6.9. Locations of various vertical cross sections denoted as thick blue lines. Note: there are two cross section locations for Sierra Madre (SM1 and SM2), intersecting different points along those mountains.	103
Figure 6.10. South-north (top row) and west-east (bottom row) cross sections of liquid and ice-phase mixing ratio differences between SEED and CTRL of Run1 at 0145 UTC in 23 January 2010 case. Black contours indicate liquid water mixing ratio difference from -0.1 to -0.02 g kg ⁻¹ in an interval of 0.02 g kg ⁻¹ . Color shaded is the mixed-phase mixing ratio difference from -0.5 to 0.5 g kg ⁻¹ .	103
Figure 6.11. Same as Figure 6.4, but for the 10 January 2014 case.	106
Figure 6.12. Same as Figure 6.5, but for the 10 January 2014 case.	106
Figure 6.13. Same as Figure 6.6, but for the 10 January 2014 case without Run16.	107
Figure 6.14. Accumulated LWP path difference (-0.8 to 0.8 mm) during the simulated seeding period between SEED and CTRL simulations for the same cases as in Figure 6.13.	109
Figure 6.15. Average AgI concentration below 1 km AGL at the end of the simulated seeding period for the same cases as in Figure 6.13.	110
Figure 6.16. Same as Figure 6.10, but for the 10 January 2014 case at 1800 UTC. Top row is south-north cross section and bottom row is west-east cross section.	111
Figure 6.17. Same as Figure 6.4, but for the 13 January 2014 case.	114
Figure 6.18. Same as Figure 6.5, but for the 13 January 2014 case.	114
Figure 6.19. Same as Figure 6.6, but for the 13 January 2014 case without run6.	115
Figure 6.20. Accumulated LWP path difference (-0.8 to 0.8 mm) during the seeding period between SEED and CTRL simulations for the same cases as in Figure 6.19.	116
Figure 6.21. Average AgI concentration below 1 km AGL at the end of the seeding period for the same cases as in Figure 6.19.	117
Figure 6.22. Same as Figure 6.10, but for run1 of the 13 January 2014 case at 1400 UTC.	118
Figure 6.23. Control precipitation at the end of the simulation for the 13 January 2014 case.	118
Figure 6.24. Liquid-water path below 1 km AGL at 0900, 1500 and 2100 UTC from the control simulation for the 13 January 2014 case.	119
Figure 6.25. Seeding effect of precipitation of runs 14 to 16 for the 13 January 2014 case.	119
Figure 6.26. Accumulated LWP difference (-0.8 to 0.8 mm) during the seeding period between SEED and CTRL simulations of runs 14 to 16 for the 13 January 2014 case.	120
Figure 6.27. Average AgI concentration below 1 km AGL at the end of the seeding period of runs 14 and 15 and between 3 and 4 km MSL of run 16 for the 13 January 2014 case.	120
Figure 6.28. Vertical cross sections (south-north on the top and west-east at the bottom) of Run 16 at 1630 UTC for the 13 January 2014 case.	121
Figure 6.29. Same as Figure 6.4, but for the 21 February 2012 case.	124

Figure 6.30. Same as Figure 6.5, but for the 21 February 2012 case.	124
Figure 6.31. Same as Figure 6.6, but for the 21 February 2012 case with all runs.	125
Figure 6.32. Accumulated LWP path difference (-0.8 to 0.8 mm) during the seeding period between SEED and CTRL simulations for the same cases as in Figure 6.31.	126
Figure 6.33. Average AgI concentration below 1 km AGL at the end of the seeding period for the same cases as in Figure 6.31.	127
Figure 6.34. Same as Figure 6.10, but for the 21 February 2012 case at 1745 UTC.	128
Figure 6.35. Control precipitation at the end of the simulation for the 21 February 2012 case.	128
Figure 6.36. Liquid-water path below 1 km AGL at 1500, 1900 and 2300 UTC from the control simulation for the 21 February 2012 case.	129
Figure 6.37. Simulated seeding effect on precipitation (mm) of Runs 10 to 14 for the 21 February 2012 case.	129
Figure 6.38. Accumulated LWP difference (-0.8 to 0.8 mm) during the seeding period between SEED and CTRL simulations of Runs 10 to 14 for the 21 February 2012 case.	130
Figure 6.39. Average AgI concentration below 1 km AGL at the end of the seeding period of Runs 10 and 11, between 3 and 4 km MSL of Runs 12 and 14, and between 4 and 5 km MSL of Run 13 for the 21 February 2012 case.	131
Figure 6.40. Vertical cross sections (south-north on the top and west-east at the bottom) of Run 12 at 2030 UTC for the 21 February 2012 case.	131
Figure 6.41. Vertical cross sections (south-north on the top and west-east at the bottom) of Run 13 at 2030 UTC for the 21 February 2012 case.	132
Figure 6.42. Scatter plots of observed and model-simulated (a) 700-hPa geopotential height (m MSL), (b) 700-hPa temperature ($^{\circ}\text{C}$), (c) 700-hPa dew point temperature ($^{\circ}\text{C}$), (d) 700-hPa vapor mixing ratio (g kg^{-1}), (e) precipitable water (cm), (f) 700-hPa wind speed (m s^{-1}), (g) 700-hPa wind direction (deg), (h) Richardson number, (i) Froude number, and (j) the squared of Brunt-Vaisala frequency (N^2 , s^{-2}). Filled dots are color- coded by RSE cases. The sounding data are from 23 January 2010 23 UTC (case 1), 10 January 2014 16 UTC (case 2), 13 and 21 UTC 13 January 2014 (case 3), 13 and 21 UTC 21 February 2012 (case 4).	135
Figure 6.43. Skew-T comparison between the sounding launched from Saragoga and the RSE model-based sounding for 23 UTC on 23 January 2010 (Case 1).	136
Figure 6.44. Skew-T comparison for 16 UTC on 10 January 2014 (Case 2).	137
Figure 6.45. Skew-T comparison for (a) 13 UTC and (b) 21 UTC on 13 January 2014 (Case 3).	138
Figure 6.46. Skew-T comparison for (a) 13 UTC and (b) 21 UTC on 21 February 2012 (Case 4).	138
Figure 6.47. Maps of observed precipitation accumulation (mm) over the simulation period for the 23 January 2010 case (Case 1) from SNOTEL sites, with minimum accumulation in (a) and maximum accumulation in (b), compared with model-simulated precipitation accumulation at the SNOTEL sites (c) and the complete simulation of precipitation across the domain (d).	139
Figure 6.48. Same as Figure 6.47, but for 10 January 2014 (Case 2).	139
Figure 6.49. Same as Figure 6.47, but for 13 January 2014 (Case 3).	140
Figure 6.50. Same as Figure 6.47, but for 21 February 2012 (Case 4).	140

Figure 7.1. Siting areas for placement of additional proposed ground-based generators.	142
Figure 7.2. Proposed ground-based generator sites selected and visited in the field.	144
Figure 7.3. The final 35 proposed viable ground-based generator locations for the Preliminary Project Design. Consists of Sierra Madre Groups A–D and Medicine Bow Groups A–C, also illustrated in Figure 5.6.	150
Figure 7.4. Land ownership map with proposed ground-based generator sites.	155
Figure 9.1. Yield as a function of supercooling for a condensation-freezing nucleus produced by the seeding solution used in the WWMPP (blues), and another condensation-freezing nucleus produced by pyrotechnics manufactured by Ice Crystal Engineering (red, yellow). (Data from DeMott 1997, 1999.)	162
Figure 9.2. The locations of NRCS SNOTEL sites in the Sierra Madre and Medicine Bow Ranges are shown. All but Little Snake River were also used in the WWMPP for snowpack evaluation.	166
Figure 10.1. The accumulated precipitation (mm) from CTRL (left), and the simulated seeding effect (difference in precipitation from the seeding simulation minus CTRL; mm) for the WR seeding cases (right).	168
Figure 12.1. WRF-CONUS simulation of (a) precipitation, (b) total runoff (surface and sub-surface runoff), and (c) evapotranspiration averaged over 2000–2008. Top panels show annual precipitation, runoff, and evapotranspiration. Middle and bottom panels are for November – April, and May – October, respectively. The thick black solid line indicates the hydrological basins: west of the divide is the Green River basin and east of the divide is the North Platte River basin. The thin straight black line is the Colorado-Wyoming state border.	182
Figure 12.2. Ratio of annual total runoff to annual precipitation from the 8-year averaged WRF-CONUS model data. The thick black line is the divide between the North Platte River Basin to the east and the Green River Basin to the west.	183
Figure 12.3. Scatter plot of total runoff (acre feet) from the WRF-CONUS model simulation in the North Platte River Basin above 8,000 ft MSL during April through July compared with SWE (mm) on May 1 st . Red line shows the least-squared fit. r^2 is the coefficient of determination and r is the linear correlation coefficient.	185
Figure 12.4. Scatter plot of total runoff (acre feet) from the WRF-CONUS model simulation in the Green River Basin above 8,000 ft MSL during April through July compared with SWE (mm) on May 1 st . Red line shows the least-squared fit. r^2 is the coefficient of determination and r is the linear correlation coefficient.	185
Figure 12.5. Estimates of streamflow increases into the (a) North Platte River Basin and (b) Green River Basin using the 5, 10, 15% levels of seasonal seeding effects for seedable storms from the draft WWMPP report. The streamflow calculations include adjustments to relate the seeding effects to total assessment area precipitation, which requires an estimate of assessment area seeding coverage. The range of streamflow estimates for the various levels of area coverage (50–80%) are denoted by the different color-shaded areas. Different colors represent the estimates based on a ground-based (red) or airborne-based (blue) seeding program. The 70% area coverage (solid lines within the color-shaded areas) are used for streamflow estimates assumed in the benefit/cost calculations. Note: there is overlap between the shaded regions, which is indicated by the light purple shaded areas.	188

Figure 12.6. Overview of the WRF-Hydro modeling domain, along with seeding ground-based stations and targeted regions for increased precipitation.	190
Figure 12.7. WRF-Hydro sequence of operations used in this study and in the NOAA National Water Model (NWM).	191
Figure 12.8. Overview of NHDPlus V2 reaches across modeling domain.	192
Figure 12.9. Difference between seeded and unseeded SWE for 1 May 2010 (colored), along with accumulated precipitation difference (mm) (contour).	194
Figure 12.10. Difference between seeded and unseeded SWE for 1 April 2012 (colored), along with accumulated precipitation difference (mm) (contour).	195
Figure 12.11. Total accumulated streamflow differences for the 2010 water year from the non-seeded to seeded simulation by basin.	197
Figure 12.12. Total accumulated streamflow differences for the 2012 water year from the non-seeded to seeded simulation by basin.	197
Figure 12.13. Total percent streamflow differences for the 2010 water year from the non-seeded to seeded simulation by basin.	198
Figure 12.14. Total percent streamflow differences for the 2012 water year from the non-seeded to seeded simulation by basin.	198
Figure 12.15. Difference in streamflow (ft ³ /s or cfs) between the non-seeded and seeded simulation during the 2010 water year at site #6630000.	199
Figure 12.16. Streamflow differences (ft ³ /s, or cfs) for 15 June 2010 for each channel reach in the modeling domain.	200
Figure 12.17. Streamflow differences for 15 May 2012 for each channel reach in the modeling domain.	200
Figure 12.18. Accumulated streamflow for all three simulations and against observations for the 2010 water year at site #6630000.	202
Figure 12.19. Accumulated streamflow for all three simulations and against observations for the 2012 water year at site #6630000.	203
Figure 12.20. Overview of USGS GAGES-II basins located near the cloud seeding regions.	204
Figure 12.21. Simulated streamflow for the 2010 and 2012 water years for USGS site #6622700.	204
Figure 12.22. Simulated streamflow for the 2010 and 2012 water years for USGS site #6632400.	205
Figure 12.23. Simulated streamflow for the 2010 and 2012 water years for USGS site #6623800.	205
Figure 13.1. The subsets of all potential ice nucleus generator sites recommended for ground-based seeding operations in the Sierra Madre Range (left, green, 16 sites), and Medicine Bow Range (right, yellow, 7 sites). The locations of the U.S. Geological Survey (USGS) stream gaging sites are also shown (red triangles).	209
Figure 13.2. Potential aircraft flight tracks for airborne-seeding operations are shown. Location relative to the target range is determined by wind direction, distance from the range by wind speed.	212
Figure 14.1. Cost of water for usage categories and for two estimates of annual seeding program costs (using 70% impact area) for the three levels of estimated streamflow increases resulting from WWMPP annual seeding effects for seedable storms (5, 10, 15%; Section 12). Gray shading indicates estimated water costs (\$30-\$65/AF). The solid green and red lines indicate the cost for the 23 remote ground-based generator	

seeding option versus the single aircraft airborne-seeding option, respectively, expressed as program costs per acre-feet of streamflow increase (essentially a 1:1 ratio). The dashed green and red lines show the corresponding 5:1 ratios of water costs to program costs.....	220
Figure 15.1. Map of the Final Recommended Project Design for 23 ground-based generator sites in the Medicine Bow and Sierra Madre Ranges.....	223
Figure 21.1. Outer and inner domains used for model simulation of each EU. (a) The outer domain has 27 km grid spacing and is run for 24 hours per EU, (b) the inner domain has 0.9 km grid spacing and is run for 12 hours per EU.....	232
Figure 21.2. Paired errors for the gauge location declared as the control of all 1118 RSE cases. Error is the model 4-hr precipitation minus the 4-hr gauge-measured precipitation. a) All 24 ensemble members per RSE case initialized with CFSR, b) All 24 ensemble members per RSE case initialized with ERA-Interim, and c) All 24 ensemble members per RSE case initialized with the NARR reanalysis.....	234
Figure 21.3. Paired errors for the gauge location declared as the target for all 118 RSE cases. Error is the model 4-hr precipitation minus the 4-hr gauge-measured precipitation. a) All 24 ensemble members per RSE case initialized with CFSR, b) All 24 ensemble members per RSE case initialized with ERA-Interim, and c) All 24 ensemble members per RSE case initialized with the NARR reanalysis.....	235
Figure 21.4. Distribution of EU paired errors by subtracting the ensemble mean of the 24 ensemble members run using each re-analysis from the 4-hr observed precipitation accumulation at each gauge. Each box and whisker plot represents the paired differences of the 118 EU cases. Each plot provides the results for a particular EU snow-gauge location (see Figure 1 for details). HY is Highway 47 (target in the Sierra Madre range), GL is Glee (target in the Medicine Bow range), SS is Sandstone (upwind co-variate site in the Sierra Madre range), BR is Barrett Ridge (upwind co-variate in the Medicine Bow range), ER is Elk River (southern co-variate for the Sierra Madre range), and CP is Chimney Park (southern co-variate for the Medicine Bow range). The box represents 25 to 75% of the differences, while the whiskers 5 to 95% of the data. Outliers are shown as plus signs. The mean difference is represented by the horizontal red line. Results are shown in each plot for the three different analyses (CFSR, ERA and NARR) and for seeding onset lag times of 30 and 60 minutes (CFSR30, CFSR60, etc.). The statistical design specified that the lag to estimate seeding effect at a gauge site would be 30 minutes from the start of seeding.	236
Figure 21.5. ERA-Interim model-estimated seeding effect (seeding simulation 4-hr precipitation accumulation minus control simulation precipitation) for the targeted gauge site (mm), either GL or HY, in each EU from the model ensemble mean.	237
Figure 21.6. Frequency of ERA-Interim model-estimated seeding effect for the target gauge sites, either GL or HY, combined from the model ensemble mean.....	237
Figure 21.7. Distributions of the fractional increase in precipitation at the Medicine Bow range target (GL), the Sierra Madre target (HY) and both (average of the two) based on the difference between seed and no-seed model ensemble simulations (8,946 EU cases simulated). The horizontal bar is the median and the red X the mean value. The top and bottom of the boxes represent the quartile ranges.....	238

LIST OF TABLES

Table 1.1. List of key personnel from each institution that was involved in conducting this study.	3
Table 2.1. List of attendees (other than presenters) at the scoping meeting in Saratoga.	4
Table 2.2. List of attendees (other than presenters) at the scoping meeting in Savery.....	4
Table 2.3. List of attendees at the January 2016 TAT meeting in Cheyenne.	5
Table 3.1. Advantages and disadvantages of various seeding types and modes.	8
Table 4.1. WRF-CONUS model physics options.	18
Table 4.2. Average annual precipitation from SNOTEL sites and the fraction of the annual precipitation that fell between 1 November and 30 April in each water year.....	24
Table 4.3. Model setup used for the CONUS and 8-year Headwaters WRF model simulations. More details on each can be found in Rasmussen et al. (2011) and Liu et al. (2016).	35
Table 4.4. Percent bias of the November–April precipitation amount from the WRF-HW and WRF-CONUS model simulations with respect to SNOTEL observations. The percent biases were computed from observed and simulated precipitation amount averaged over the 13 SNOTEL sites.	37
Table 4.5. Seasonal (November–April) model precipitation totals from HY47 and the amount of precipitation that fell when the SMWest average 700-hPa temperature was < –6°C.	57
Table 4.6. As in Table 4.5, but 700-hPa temperatures averaged over the SMEast area.....	57
Table 4.7. As in Table 4.5, but precipitation from GLEES and 700-hPa temperatures averaged over the MBWest area.	57
Table 4.8. As in Table 4.5, but precipitation from GLEES and 700-hPa temperatures averaged over the MBEast area.	58
Table 4.9. Wintertime (November–April) 8-year average simulated total precipitation (mm) compared with the seasonal precipitation that fell during ground-seedable (“GS”, 0–1 km AGL) time periods versus lower airborne-seedable (“AS”, 3–4 km MSL), and upper airborne-seedable (“ASH”, 4–5 km MSL) times. The percent of the total seasonal precipitation that was seedable is provided in parentheses next to the absolute seedable precipitation. For ground-seeding potential, both the primary criteria (temperature and LWC only) are compared with the scenario with additional criteria included (wind direction and Froude number). The model precipitation was extracted from one of three precipitation sites (Figure 4.2) depending on the region.	81
Table 6.1. The extra AgI removal processes that are simulated in the new ASPEN	94
Table 6.2. Model configurations for cloud seeding project design evaluation simulations. .	95
Table 6.3. Seeding simulation experiments of 23 January 2010 case. The SM “oriC” group consists of the one original Group C generator shown in Figure 5.5.	96
Table 6.4. Control precipitation (CTRL; acre-feet) followed by the simulated seeding effect (SE; acre-feet and % relative to CTRL precipitation) over the entire domain, Sierra Madre assessment area (> 8,000 ft, SM), and Medicine Bow assessment area (> 8,000 ft, MB) from all experiments for the 23 January 2010 case. In addition, the area affected by positive simulated seeding effects (PSE_A) is noted (km ² and %) for each experiment and over the full domain, Sierra Madre assessment area, and Medicine	

Bow assessment area. The % impact area is relative to the total area of the domain, Sierra Madre assessment area, or Medicine Bow assessment area, which is listed in the CTRL row, respectively. Run1 is shaded in light gray to highlight it as the “baseline” experiment. The experiments that resulted in the largest Sierra Madre and Medicine Bow assessment area relative simulated seeding effects are shaded in light blue (are not always the same experiment).....	104
Table 6.5. Seeding simulations for the 10 January 2014 case. The SM “oriC” group consists of the one original Group C generator shown in Figure 5.5.	105
Table 6.6. Same as Table 6.4, but for the 10 January 2014 case.....	112
Table 6.7. Seeding simulations of the 13 January 2014 case. The SM “oriC” group consists of the one original Group C generator shown in Figure 5.5. Runs listed in light green shading were run with WRF V3.7.1 using the updated ASPEN.....	113
Table 6.8. Same as Table 6.4, but for the 13 January 2014 case. Results listed in light green shading were run with WRF V3.7.1 using the updated ASPEN.....	122
Table 6.9. Seeding simulations of the 21 February 2012 case. The SM “oriC” group consists of the one original Group C generator shown in Figure 5.5. Runs listed in light green shading were run with WRF V3.7.1 using the updated ASPEN.....	123
Table 6.10. Same as Table 6.4, but for the 21 February 2012 case.....	133
Table 7.1. Description of Proposed Ground-Based Generator Locations.....	145
Table 7.2. Description of Proposed Generator Locations – Preliminary Project Design	151
Table 12.1: 8-year average annual precipitation, runoff, runoff ratio, snowfall and rainfall averaged over the study area (Figure 12.1), North Platte River basin, and Green River basin. Values in parentheses for the snowfall and rainfall indicate the ratio of snowfall and rainfall to total precipitation. Note that the basin-averaged values are only for the area that appears in Figure 12.1, not including the entire basin.	183
Table 12.2. 8-yr (2000–2008) average annual and April–July total runoff per river basin in acre feet for areas > 8,000 ft in elevation calculated from the WRF-CONUS model simulations.	186
Table 12.3. Streamflow increase estimates using various seeding impact parameters for a ground-based seeding program (5, 10, 15% seeding effect and 50-80% seeding impact area). Estimated April–July streamflow increases (AF) are provided using the 70% impact area (shaded row) estimated increases.....	189
Table 12.4. Same as Table 12.3, except for an airborne-seeding program.....	189
Table 12.5. Summary streamflow results for the 2010 water year by basin.	196
Table 12.6. Summary streamflow results for the 2012 water year by basin.	196
Table 13.1. Estimated operational costs of a five-month, ground-based seeding program in the Medicine Bow and Sierra Madre Ranges. Cost are based upon direct and personnel costs as of the fourth quarter of calendar year 2016.	211
Table 13.2. Estimated operational costs of a possible five-month airborne-seeding program in the Medicine Bow and/or Sierra Madre Ranges.	213
Table 13.3. Contracted versus self-run projects, or project components.	215
Table 14.1. Cost of a Ground-based Program to Generate Different Benefit/Cost Ratios, assuming a water cost of \$30 and impact area of 70%. The estimated annual increase in streamflow from seeding based upon the WRF-Hydro simulation is included in the far right column (shaded in gray) for comparison.....	218

Table 14.2. Cost of an Airborne Program to Generate Different Benefit/Cost Ratios (assuming \$30 water cost and 70% impact area).....	219
Table 14.3. Annual Costs Breakdown of Seeding Options for the Proposed Winter Cloud- seeding program and Estimated Cost/AF of augmented streamflow (using 70% impact area assumption for ground and airborne).....	219
Table 19.1. Attendee list (other than presenters) from the public hearing held in Saratoga, WY on 11 July 2017.....	227
Table 21.1. Aspects of the model configuration utilized in all simulations.....	232
Table 21.2. Summary of ensemble model configurations.....	233

Weather Modification—Medicine Bow/Sierra Madre Ranges Final Design and Permitting Study

Executive Summary

A Final Design and Permitting Study was performed to establish an operational weather modification program targeting the Medicine Bow and Sierra Madre Ranges in southern Wyoming. This study was led by the National Center for Atmospheric Research (NCAR) in collaboration with Weather Modification International, and Heritage Environmental Consultants. Twenty tasks were identified by the Wyoming Water Development Commission for the study, including:

1. scoping and project meetings;
2. reviewing previous studies and data;
3. climatological analysis of the project area;
4. development of a preliminary project design;
5. model evaluation for the preliminary project design;
6. field surveys of potential ground-generator locations;
7. assessing the access/easements and permitting/reporting for potential generator sites;
8. operational criteria development;
9. reviewing environmental and legal considerations;
10. providing program evaluation methodologies;
11. potential benefits analysis;
12. cost estimates;
13. development of a cost/benefit analysis of the potential program;
14. finalization of the project design;
15. environmental analysis and permitting;
16. discretionary tasks;
17. preparation of the final report deliverable;
18. giving presentations on the final results;
19. climatological monitoring of the study area; and
20. a model evaluation of the Wyoming Weather Modification Pilot Program (WWMPP) Randomized Statistical Experiment (RSE).

Two public scoping meetings were held at the beginning of the project in locations near the Medicine Bow and Sierra Madre Ranges. The first was in Saratoga, Wyoming on 21 September 2015, and the second in Savery, Wyoming on 24 September 2015. The meetings provided the public with an overview of the scientific concept of cloud seeding, a summary of the previous studies in Wyoming, and a description of the plans for the current study.

A review of previous data found that numerous research investigations have improved the understanding of how to use silver iodide (AgI) seeding to enhance snowfall in winter orographic clouds. These include the recently concluded Wyoming Range Phase II Feasibility Study, and the draft WWMPP, which encompasses the same mountain ranges as those investigated in this study. The results from these studies were reviewed in the preparation of this report to ensure consistency with the most recent recommendations for cloud-seeding program design.

Noteworthy results from the draft WWMPP report asserted that while the RSE was statistically inconclusive, an “accumulation of evidence” analysis approach suggested seasonal precipitation increases of 5–15% in seedable storms over a winter season. It also demonstrated the capability of numerical models to realistically simulate snowfall distributions, as well as simulate seeding effects via a seeding parameterization.

The review of previous data summarized the various options for cloud seeding (e.g., seeding agents, method of delivery, etc.). Liquid-propane seeding was determined to be an ineffective seeding option for the study area because seeding impacts are spatially limited due to the requirement that the liquid propane must be released within supercooled clouds. In addition, manual ground-based AgI generators were experienced as challenging to deploy and operate in the project area, given the limited options for accessible and effective generator placement. For manual generators to be activated and deactivated during the winter months, locations would need to be sited at lower elevations around the Medicine Bow and Sierra Madre Ranges, potentially creating a situation where the AgI plume could be blocked and unable to disperse over the mountains.

A climatological analysis of the Medicine Bow and Sierra Madre Ranges was performed as part of the WWMPP by Ritzman et al. (2015). However, the criteria for seeding used during the WWMPP were established for a *research*-based cloud-seeding program. For the purpose of this study, a climatology analysis was conducted based upon seeding criteria more appropriate for an *operational* cloud-seeding program. Due to a lack of available observations (e.g., soundings and supercooled liquid-water measurements) this study utilized snow-gauge observations and an 8-year, high-resolution (4 km) Weather Research and Forecasting (WRF) model simulation run over the continental United States (CONUS) (WRF-CONUS; Liu et al. 2016) to assess the climatology of seedable conditions in the region. The results of the climatology analysis indicated that the predominant 700-hPa wind direction is westerly. Similarly, the most frequent occurrence of seedable conditions for both ground and airborne-seeding modes were located over the western regions of both mountain ranges. The analysis also indicated that seeding opportunities occurred frequently enough to warrant the placement of a few ground-based generators in southern portions of the Sierra Madre Range. The eastern regions of both ranges were found to be ineffective for ground-based seeding. Airborne seeding was shown to be feasible in all regions, and seeding opportunities were frequent enough to warrant implementation of an airborne program. The fraction of November–April precipitation that fell under seedable conditions was approximately 38% for ground-based seeding, and approximately 56% for airborne seeding. These estimates are based upon the climatological analysis results for the western regions and were used to calculate the estimated streamflow benefits.

Preliminary Project Design, Model Evaluation, and Field Surveys

To test a wide variety of program design options based upon results of the climatological analysis, several groups of potential ground-based generator sites were established. Initially, seven groups of generators were tested (Groups A–D; see Figure 1). Following initial cloud-seeding model simulations, additional generators were added to Group C along the crestline of the Sierra Madre (already pictured in Figure 1), and two additional groups of generator sites were created (Groups E–F; Figure 1) to investigate potential seeding impacts from generators located farther upwind. The preliminary project design focused on ground-based seeding and/or airborne

seeding with an operational season of mid-November through mid-April (e.g., 15 November–15 April), utilizing AgI, or more specifically, a silver iodide-salt compound as the seeding agent.

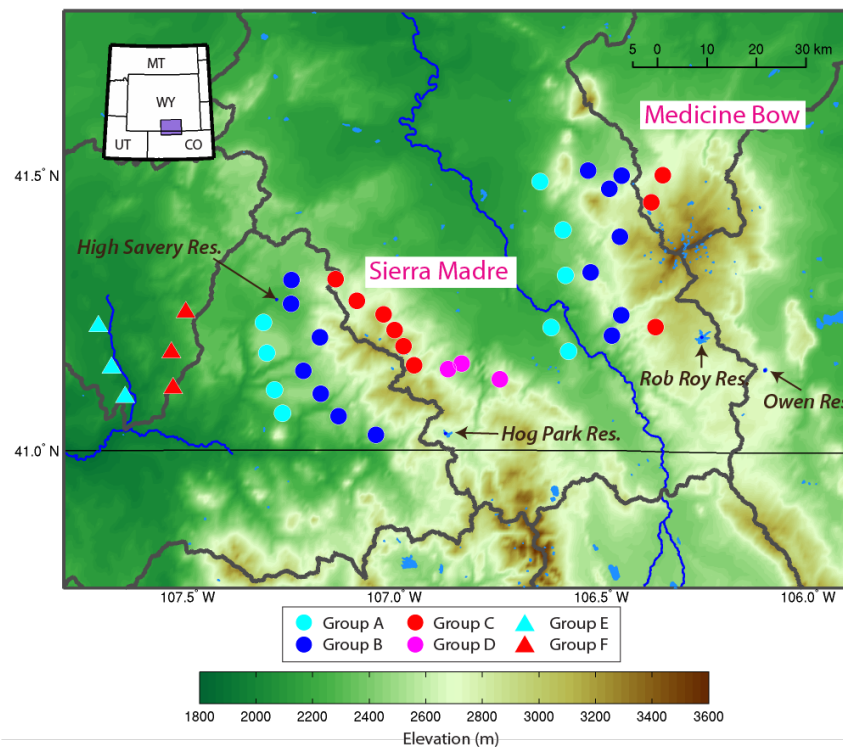


Figure 1. Topography map of the Medicine Bow and Sierra Madre Ranges (m) illustrating the locations of nine ground-based generator design groups.

Four cases were selected from the WWMPP RSE research program to represent a variety of typical seeding conditions in the Sierra Madre and Medicine Bow Ranges. To investigate the potential designs of a ground-based seeding program, these cases were assessed using the NCAR cloud-seeding model parameterization implemented in the Thompson microphysics scheme within the WRF model.

WRF “control” simulations of these four cases showed that supercooled liquid water was present in both ranges throughout the simulations in all cases, which is a necessary condition for seeding operations to commence. The WRF ground-based seeding simulations in these cases showed that: (1) seeding depleted supercooled liquid water in a shallow layer close to the terrain and increased precipitation over the mountain; (2) flow over the Medicine Bow was usually blocked, or forced around the range due to the steeper slope of the topography, although flow from some of the lower elevation generators placed upwind of the Sierra Madre were also occasionally blocked; (3) the simulated seeding effect was not as great if the natural cloud efficiently produced precipitation (as occurred in two of the four cases); (4) seeding simulations using all six of the Sierra Madre generator groups, including the two upwind groups (E–F), produced the greatest combined simulated precipitation increases in *both* ranges for most of the cases tested.

One caveat of note is that the original version of the model seeding parameterization used in this study for the ground-seeding simulations did not include precipitation scavenging of AgI

particles, AgI self-coagulation, or AgI dry deposition processes. Therefore, the particles transported from the Sierra Madre to the Medicine Bow and the subsequent simulated seeding impacts in the Medicine Bow were likely overestimated. To address this potential overestimation, two of the initial ground-based seeding cases were re-run using only the Sierra Madre generator groups and the updated seeding parameterization to better understand how additional AgI-removal processes affected the cloud and precipitation, especially downwind in the Medicine Bow Range.

The results of the ground-seeding simulations (Sierra Madre generators only) with the additional AgI-removal processes reduced the AgI concentration and the simulated seeding effect in the Medicine Bow region by about 50% for both of the re-run cases (Figure 2). However, similar or greater simulated seeding effects still resulted in the Medicine Bow when AgI was released from sites only in the Sierra Madre compared with the seeding scenario using only the Medicine Bow generators to target the Medicine Bow. In light of these results, it can be hypothesized that ground-based generators strategically placed only in the Sierra Madre Range could effectively target both the Sierra Madre and Medicine Bow Ranges.

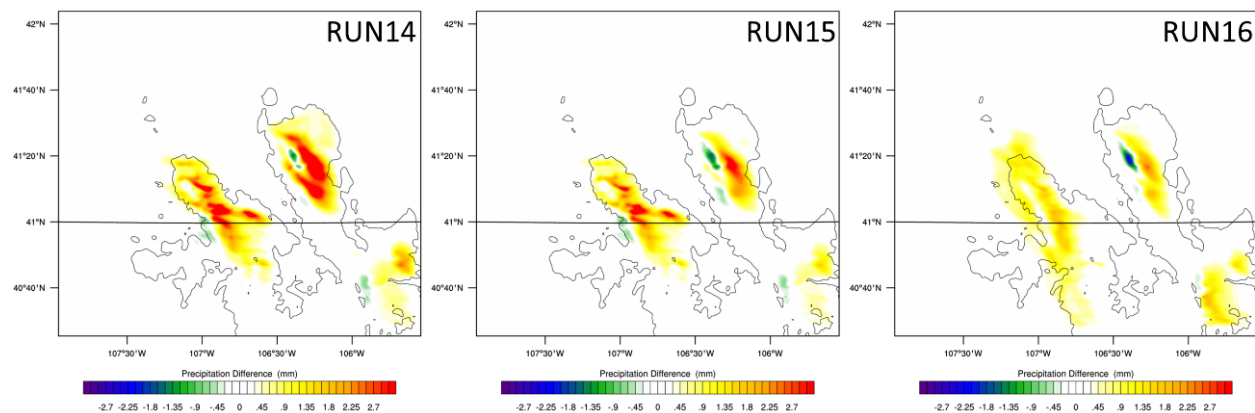


Figure 2. Change in precipitation (mm) due to simulated cloud seeding for model simulations using only Sierra Madre Groups A–F (RUN14 and RUN15) compared with two hours of simulated airborne seeding (RUN16) case in the 13 January 2014 case. RUN14 does not include the newly-added AgI-removal processes, while RUN15 does. The small area of negative changes in precipitation in the Medicine Bow is the result of precipitation changing phase from rain to snow (and snow falling out farther downwind) in the seeding simulation. The assessment area total change in precipitation in these cases is positive.

Two of the four test cases exhibited suitable airborne-seeding conditions, and therefore airborne seeding was simulated for a period of approximately 2 hours in those two cases. Airborne seeding simulations produced increases in total precipitation across the assessment areas similar to that from ground seeding (compare RUN15 and RUN16 in Figure 2 for an example). Airborne seeding simulations, in general, showed impacts over a deeper and broader portion of the atmosphere, and converted the supercooled liquid water to precipitation more efficiently than the ground-seeding scenarios.

During the field surveys, 27 potential ground-based generator sites were visited, and considered for inclusion in the operational project design. Of these 27 sites, 18 were located on federal lands, and 9 on private lands within the Medicine Bow and Sierra Madre Ranges. For each location, land ownership, access descriptions and ratings, and brief descriptions of the sites were

presented. As a result of the modeling exercise and field surveys, a total of 35 viable generator sites located on federal, state, and private lands were recommended for possible use, with 23 located on United States Forest Service (USFS) lands.

A Special Use Permit application was submitted to the USFS on 22 February 2016 for an operational cloud-seeding program designed to target the Medicine Bow and Sierra Madre Ranges. The approach for the permit application portion of this study was to provide a maximum number of potential ground-based generators that could be used in the Medicine Bow and Sierra Madre Ranges operational cloud-seeding program, and would be assessed through the federal NEPA process. The application requested USFS approval to place up to 23 ground-based generators on National Forest administered lands. The Medicine Bow National Forest sent a letter to the Wyoming Water Development Office (WWDO) on 9 August 2016 explaining that the proposed project failed to meet the minimum requirements of the initial screening criteria. The WWDO resubmitted the application on 22 December 2016. The Medicine Bow National Forest responded with a letter to the WWDO on 28 February 2017 initially accepting the amended SUP application and notifying the WWDO that USFS personnel would be in contact to discuss the application approval procedures. The WWDO is currently waiting to be contacted on this matter.

Based on additional model simulations, the total number of viable generator sites was narrowed down from 35 to 23 ground-based generators[†]. Since the model simulations indicated that seeding from sites in the Sierra Madre can produce positive simulated effects on the Medicine Bow under westerly and southwesterly wind flow, one approach to developing a cost-effective operational program would be to place generators only in the Sierra Madre to target both mountain ranges. However, to target the Medicine Bow under northwesterly winds, some sites are still needed in the Medicine Bow on the western and northwestern slopes. The final project design of 23 ground-based generators includes 16 in the Sierra Madre, and 7 in the Medicine Bow (Figure 3). Of the 16 sites in the Sierra Madre, 6 were sited specifically to target the Medicine Bow.

[†] Note that not all of these are on USFS land, and therefore this set of 23 slightly differs from the 23 included in the USFS permit application.

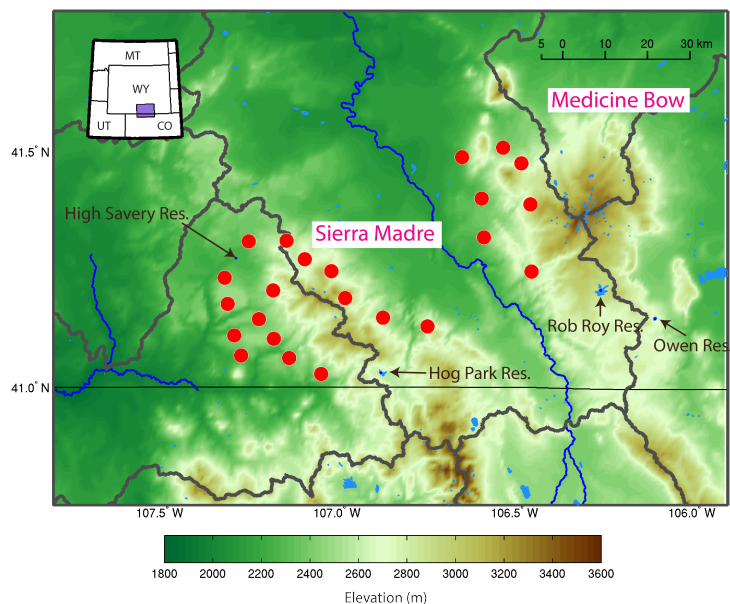


Figure 3. Map of the final recommended design for 23 ground-based generator sites in the Medicine Bow and Sierra Madre Ranges.

Operational Criteria and Other Program Considerations

Operational seeding criteria were developed for possible ground-based seeding operations as well as for potential seeding with an aircraft. The most critical data required for establishing operational seeding criteria are upper-air temperatures, wind direction and speed, and the existence of supercooled liquid water upwind and over the project target area. Weather observations to determine when most of the operational criteria are met are available in real time via a variety of products available on the internet. However, to obtain all pertinent project specific weather information, the deployment of project soundings and a radiometer is recommended, although not required. A well-designed cloud-seeding program will incorporate seeding suspension criteria to stop or suspend seeding activities that could generate unsafe conditions due to increases in precipitation. Suspension criteria recommended for an operational program implemented in the Medicine Bow and Sierra Madre Mountains can be found in Section 9.5.

Other program considerations take into account environmental concerns such as downwind (extra-area) effects, or potential impacts on water and soil quality that surface in relation to the practice of cloud seeding. A large number of studies have been conducted in the western United States related to the potential environmental impacts of winter cloud seeding. In general, these studies found that significant environmental effects due to the possible conduct of cloud-seeding programs in these areas were not expected to occur.

Potential Benefits, Cost Estimates, and Benefit/Cost Analysis Summary

Estimates of streamflow changes due to seeding impacts on precipitation were calculated two ways. One method estimated the change in streamflow relative to a change in precipitation using regressions of historical precipitation and streamflow records, either from gauge measurements and/or long-term model simulation. This method was similar to that used in other weather modification feasibility studies (i.e., Wyoming Range, Bighorn Mountains). In this design study,

the 8-year, WRF-CONUS high-resolution model simulation (Liu et al. 2016) was utilized to establish the relationship between changes in streamflow relative to a change in actual precipitation. However, there are several assumptions required for this approach, such as the magnitude of precipitation change due to seeding (i.e., the seeding effect) and the fraction of the assessment area that is impacted by seeding (i.e., the impact area). These assumptions contribute to a substantial range of uncertainty in the final results.

Secondly, streamflow changes from seeding were estimated using a new method that utilizes the WRF-Hydro model, coupled with results of cloud-seeding simulations from the WWMPP. While there are still inherent uncertainties associated with this method, many of the assumptions associated with the previous regression method are removed.

The results of the two methods compared rather well. The regression method found a range of total streamflow increase between ~11,170 and ~49,390 acre-feet (AF), depending on the assumed method of seeding (ground-based versus airborne), the assumed magnitude of the seeding effect (5, 10, or 15% based upon the WWMPP results) and assumed impact area (all assuming a 70% impact area). In contrast, the WRF-Hydro method found a range of 5,000–7,750 AF of streamflow increase (Figure 4). The WRF-Hydro simulation method helped reduce some of the uncertainties in the traditional regression analysis, because it did not need to assume anything about the spatial distribution or magnitude of the seeding effect. Rather, the spatial distribution and magnitude of the seeding effect from the seeding simulations were directly ingested as forcing into the WRF-Hydro simulation. However, at the present time, this simulation represented only two years of simulated seeding cases from the WWMPP; whereas, the regression analysis represented a multi-year average scenario from the climatology analysis. Therefore, averaging the results from the two years of WRF-Hydro simulations yields 6,375 AF of average additional streamflow.

Moreover, the regression analysis results were based upon less stringent conditions for seeding than imposed during the WWMPP (i.e., the climatology analysis used a warmer temperature criterion, no time limit on seeding periods, etc.). The 4-hour time-limit criterion and, in particular, because only one target was seeded at a time, the WWMPP will likely yield reduced seeding effects on streamflow in the WRF-Hydro method than what is estimated using the climatology analysis regression method. The reduction will depend on how long seeding criteria were actually met beyond the 4-hour limit imposed by the WWMPP, but it will likely be reduced by at least half given only one target was seeded at a time in the WWMPP. If the average WRF-Hydro results were doubled, to account for the limited seeding time periods simulated based upon the WWMPP criteria, the results indicate approximately 12,500 AF of additional streamflow could be produced from cloud seeding. This estimate is consistent with the regression analysis result (~11,170 AF) for a ground scenario with just over a 5% seeding effect in seedable storms over a winter season using an assumed 70% impact area.

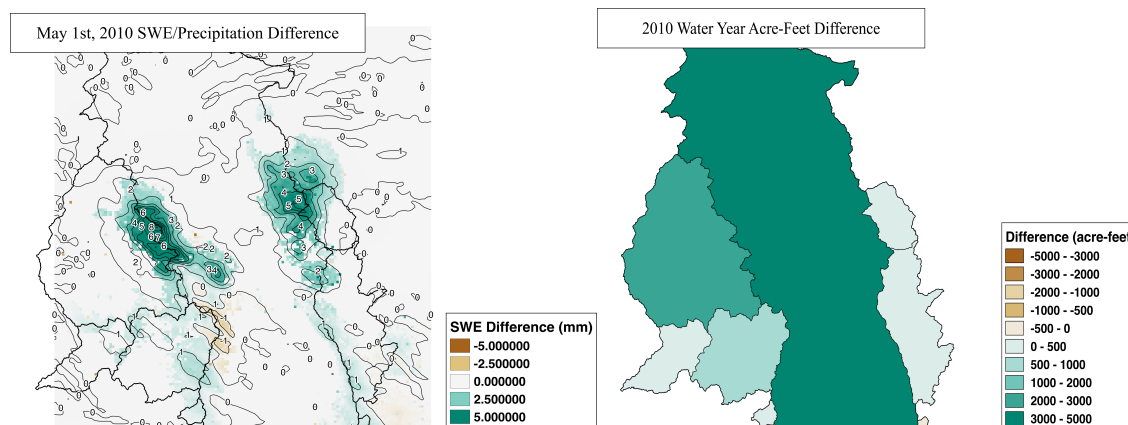


Figure 4. WRF-Hydro simulation results from water year 2010: difference between seeded and unseeded snow water equivalent (SWE) for 1 May 2010 (colored), along with accumulated precipitation difference (mm; contour) on the left, and total accumulated streamflow differences (AF) for the 2010 water year from the non-seeded to seeded simulation by basin on the right. The basins shown in the right panel are outlined in thick black lines on the left for reference.

Cost estimates were prepared for two different operational cloud-seeding program options:

- 1.) a program with 23 remote-controlled ground-based generators (estimated annual cost: \$656,685), and
- 2.) a single stand-alone aircraft seeding program (estimated annual cost: \$361,780).

A preliminary benefit/cost analysis was performed using the estimated range of enhanced average April – July runoff values. American Society of Civil Engineers (ASCE) Guidelines were considered in determining whether the program would be considered feasible. The Guidelines suggest that two questions be answered: is the proposed program technically feasible, and is the proposed program economically feasible? An affirmative answer to both questions is required for the program to be considered feasible. *The evidence presented in this study demonstrates that the program is technically feasible.*

For a program to be considered economically feasible, the ASCE Guidelines recommend that a proposed program have an estimated benefit/cost ratio of 5/1. To determine the benefit/cost ratio, several assumptions need to be considered (e.g., allocation of the water, value of the water, etc.), and were included in the ratio calculations for this study. Of the possible seeding options and levels of seeding effects, airborne seeding met the 5/1 ratio assuming 10% or greater seeding effect and depending on the actual value of water (**Error! Reference source not found.**). round seeding does not meet the 5/1 ratio, primarily due to the higher program cost when compared with airborne seeding (Figure 5). If the ground-seeding program costs could be reduced (by reducing the number of total generators) while still achieving the desired seeding effect, ground seeding could be more cost effective.

Water and program costs vs. streamflow increases from seeding

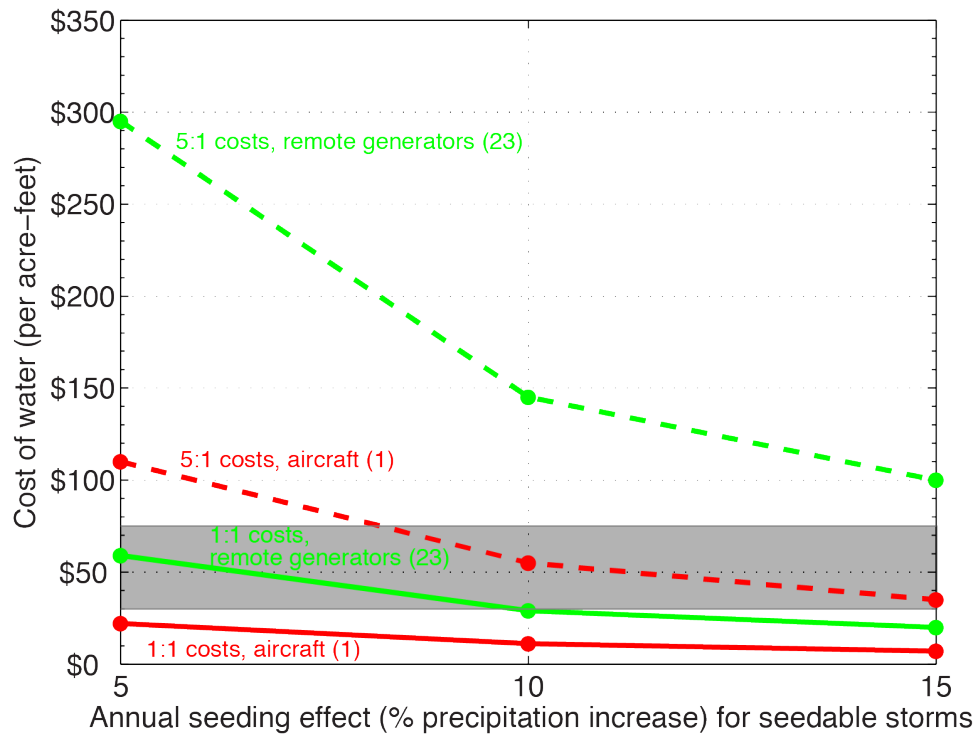


Figure 5. Cost of water for usage and for two estimates of annual seeding program costs (using 70% impact area) for the three levels of estimated streamflow increases resulting from WWMPP annual seeding effects for seedable storms. Gray shading indicates estimated water costs. The solid green and red lines indicate the cost for the 23 remote generator ground-seeding option versus the single aircraft airborne seeding option, respectively, expressed as program costs per acre-foot of streamflow increase (essentially a 1:1 ratio). The dashed green and red lines show the corresponding 5:1 ratios of water costs to program costs.

Model Evaluation of the WWMPP RSE

Instead of collecting additional randomized cases at great expense, an ensemble modeling approach to estimate the impact of ground-based seeding was conducted. This approach is advantageous because conditions with and without seeding can be simulated, allowing the difference of the model simulations to estimate the seeding effect. An ensemble modeling approach also better accounts for initial condition uncertainty, model biases, and random errors in the model simulations. A prerequisite to using a model, however, is that the simulations reasonably represent reality. The WWMPP RSE snow-gauge data and sounding data were compared with the model ensemble and showed reasonable agreement.

This snow-gauge comparison was made with twenty-four model ensemble members for each of three re-analysis forcing datasets with no seeding simulated, with a total of 8,946 simulations to simulate each of the 118 Experimental Units (EUs). The results of the model ensemble approach with and without seeding estimated a mean enhancement of precipitation of 5%, with an inner quartile range of 3 to 7%. These results provide a robust estimate of the impact of ground-based cloud seeding in the Sierra Madre and Medicine Bow Ranges in Wyoming that accounts for key uncertainties in both initial conditions and model physics.

Conclusions and Recommendations

Based on the results of this study, it can be concluded that an operational cloud-seeding program targeting the Medicine Bow and Sierra Madre Ranges is technically feasible. This assertion is supported by the climatological analysis and cloud-seeding model evaluation presented herein, as well as the results previously determined in the same project area during the WWMPP.

Based on the results of this study, an operational cloud-seeding program targeting the Medicine Bow and Sierra Madre Ranges would be economically feasible depending on which type of operational program is implemented (ground or air). The cost effectiveness of a cloud-seeding program is dependent on several factors, including the cost of water and the amount of seeding effect expected. Based on the results of this analysis, airborne seeding is a cost-effective program design option given its lower overall program cost, fewer seeding restrictions due to wind direction or atmospheric stability, and no required permitting fees. However, airborne seeding is limited by aircraft on-station time, which is not reflected in the climatology analysis. For example, a single aircraft may not be able to seed for the entirety of a seedable period if that period is longer than the aircraft can be on station (due to fuel consumption, crew duty limits, etc.). The climatology analysis did not exclude long seedable periods given the aircraft on-station time is currently unknown (dependent on the actual aircraft type selected for the seeding program, the extent of icing conditions encountered in a given flight, etc.). However, accounting for this could lead to a reduction in the amount of precipitation that falls when conditions are seedable by a single aircraft. None of the ground-based seeding scenarios met the 5/1 ratio, and therefore, cannot be considered economically feasible. However conceptually, a ground-based seeding program might be more cost effective if the number of generators in the design were reduced to lower overall program costs, while maintaining seeding effects similar to those presented in this study.

Based on the results of this study, several recommendations specific to the design and conduct of an operational cloud-seeding program in the Medicine Bow and Sierra Madre Ranges are presented:

- Seeding should be conducted using AgI as the seeding agent.
- The seeding season for ground-based and/or airborne operations should be 15 November– 15 April.
- Aircraft seeding is considered technically and economically feasible, whereas ground-based seeding is considered technically feasible only, therefore it is recommended that aircraft seeding be conducted.
- To address whether or not ground-based seeding could be considered economically feasible, an investigation focused on optimizing the operational design in relation to cost and seeding effectiveness should be considered.
- To validate the impacts from seeding with either proposed program design, it is recommended that modeled simulations of additional test cases (ideally an entire season of seeding cases), be considered.
- Basic seeding criteria should be based on readily available (and quickly accessible) meteorological data.
- To accurately assess seeding criteria in the study area specifically, a program would benefit from deploying project-specific instrumentation (i.e., radiometer and soundings),

but these would add additional costs to operate the program that were not considered in the benefit/cost analysis for this study.

- To assess the feasibility of reducing overall program cost, it is recommended that a study to investigate sharing operational resources (i.e., aircraft, staff, weather data, etc.) between seeding programs targeting multiple mountain ranges in the region should be considered.
- To determine the most cost effective approach to sharing operational resources, a cohesive evaluation of all the Wyoming (proposed and operational) weather modification projects, is recommended and should consider multiple project designs (ground-based and airborne).
- The implementation of a statewide, real-time modeling system would provide guidance to determine storm seedability, especially if multiple cloud-seeding programs are implemented within the state. A forecast modeling system will generate a cost savings by identifying when storms have high seeding potential, therefore maximizing cloud-seeding impacts. The model can also serve as a basis for seasonal program evaluation.

Disclaimer

All rights to the underlying data collected and/or generated with funding from the Wyoming Water Development Office (WWDO) from which this report was created remain with the WWDO. This report does not constitute the opinions of the State of Wyoming, the Wyoming Water Development Commission, or the Wyoming Water Development Office.

1. Introduction

A Final Design and Permitting Study was performed for the Wyoming Water Development Commission (WWDC) to establish an operational weather modification program targeting the Medicine Bow and Sierra Madre Ranges in southern Wyoming. As part of the study, 20 tasks were identified and are briefly described below. The organization of this report follows this tasking, as requested by the WWDC.

1.1. Task Overview

Task 1: Scoping and Project Meetings

A scoping meeting should be held early in the project to familiarize the WWDC, technical advisory team (TAT), governmental agencies, and local stakeholders with the scope of the project, as well as obtain input from affected parties.

Task 2: Review and Summarization of Previous Data

This review will include all available background information regarding previous weather modification research and/or activities within the State of Wyoming and within the target area (wherever possible), and projects in close proximity with the potential to affect the Medicine Bow and Sierra Madre Ranges program operations or evaluation.

Task 3: Climatology of the Project Area

The purpose of this analysis is to determine the characteristics of the storms producing precipitation over the Medicine Bow and Sierra Madre Ranges and determine the seeding potential of the project area using criteria based on an operational cloud-seeding program.

Task 4: Development of a Preliminary Project Design

A customized weather-modification project design for the Medicine Bow and Sierra Madre Ranges will be developed based on the information gathered in Tasks 1–3. The design shall include the methodology, materials, equipment, siting considerations, available meteorological observation systems, and other components necessary to operate and maintain a weather modification program in the targeted areas.

Task 5: Model Evaluation of the Preliminary Project Design

The goal of this task is to evaluate the suggested locations of ground-seeding generators and optimize seeding strategies for the project design, including the possibility for airborne seeding using sophisticated numerical models.

Task 6: Field Surveys of Proposed Ground Generator Locations

Field surveys will be conducted to inspect proposed ground-generator locations as determined from Tasks 4–5.

Task 7: Access/Easements and Environmental Permitting/Reporting

A review of all local area plans, county ordinances, and other regulations that may affect the proposed weather modification operations in the project area will be conducted. This will include identifying all easements and/or access agreements that will be necessary to implement siting of the equipment as directed by the preliminary project design, as well as summarize all permitting and/or reporting requirements necessary to implement the project design.

Task 8: Establishment of Operational Criteria

Operational seeding criteria will be developed for the project area, containing protocols and procedures necessary to operation of the programs within established Guidelines as set forth by the American Society of Civil Engineers (ASCE).

Task 9: Environmental and Legal Considerations

A summary of any potential environmental considerations associated with implementation of the project design will be provided.

Task 10: Evaluation Methodology

Methodologies for evaluating the efficacy of the cloud-seeding program in the targeted areas will be summarized, including both physical and statistical methods.

Task 11: Potential Benefits/Hydrologic Assessment

The goal of this task is to assess the potential streamflow benefits from cloud seeding utilizing the long-term high-resolution model simulation used in Task 3 (WRF-CONUS) to conduct a water balance approach. In addition, these results will be compared with those from a method that utilizes a coupled atmospheric-hydrological model (WRF-Hydro).

Task 12: Cost Estimates

Costs for establishing, operating, and maintaining the proposed weather modification program will be estimated and summarized.

Task 13: Cost/Benefit Analyses

Based on the information from Tasks 1–12 of the project, cost/benefit estimates for conducting weather modification operations in the targeted areas will be calculated on a per-acre-foot (AF) basis.

Task 14: Finalization of Project Design

A final project design for the operational weather modification program will be developed based on the information compiled and analyzed during Tasks 1 – 13 of the project.

Task 15: Environmental Analysis and Permitting

This task covers all of the preparatory work required to get any necessary permits to operate ground-based generators on federal, state and private lands, as determined by the final project design. For sites on Federal land, this would include any required environmental analysis.

Task 16: Program Discretionary Task

This task reserves funds for the Wyoming Water Development Office (WWDO) program manager to authorize spending on any unforeseen items that arise during the course of the project.

Task 17: Reports and Executive Summaries

Digital and paper copies of the final report and executive summary will be provided to the WWDC.

Task 18: Report Presentations

A public meeting/hearing will be held in the local project area to present the final results of the study.

Task 19: Climatological Monitoring of the Study Area

Pertinent climatological information and data will be collected and archived during the November 2015–April 2016 winter season for the study area.

Task 20: Model-based Evaluation of the Wyoming Weather Modification Pilot Program (WWMPP) Randomized Statistical Experiment (RSE)

The goal of this task is to simulate all of the WWMPP RSE cases with the Weather Research and Forecasting (WRF) cloud-seeding model to evaluate and determine whether the WRF cloud-seeding model can replicate a statistical result similar to that found with the WWMPP RSE snow-gauge observations.

1.2. Personnel and Organizations

The Research Applications Laboratory (RAL) of the National Center for Atmospheric Research (NCAR) collaborated with Weather Modification International (WMI) and Heritage Environmental Consultants (HEC) to conduct this study. Key personnel from each institution are listed in Table 1.1.

Table 1.1. List of key personnel from each institution that was involved in conducting this study.

Organization	Key Personnel
NCAR	Sarah Tessendorf Roy Rasmussen Lulin Xue Kyoko Ikeda Courtney Weeks Jamie Wolff Michelle Harrold Logan Karsten David Gochis Duncan Axisa Scott Landolt Al Jachcik Dan Breed
WMI	Bruce Boe
HEC	Patrick Golden

2. Task 1: Scoping Meeting/Project Meetings

The purpose of the scoping meeting is to familiarize the WWDC, TAT, governmental agencies, and local stakeholders with the scope of the project, as well as obtain input from affected parties.

2.1. Scoping Meetings in Saratoga and Savery, WY

Two public scoping meetings were held at the beginning of the project. The first was held on 21 September 2015 in Saratoga, Wyoming at the Platte Valley Community Center (PVCC). The second meeting was held on 24 September 2015 in Savery, Wyoming at the Savery Little Snake Museum.

The meetings were opened by Mr. Barry Lawrence, the WWDO Project Manager, who facilitated introductions and provided a brief history and purpose of the study. Presentations at the meeting then included an overview of the scientific concept of cloud seeding (Mr. Bruce Boe, WMI), a summary of the previous studies in Wyoming (Dr. Roy Rasmussen, NCAR), an overview of the current study (Dr. Sarah Tessendorf, Mr. Bruce Boe, and Mr. Patrick Golden). The complete attendee list is included in Table 2.1.

Table 2.1. List of attendees (other than presenters) at the scoping meeting in Saratoga.

Name	Agency		Name	Agency
Jeni Cederle	WWDO		Scott Kerbs	AG-OP
Joan McGraw	Medicine Bow Conservation District		Joe Parsons	Saratoga Encampment Rawlins Conservation Dist.
Maggie Kelly			Robert Kelly	
Dave Gloss	USFS		Joe Elder	PVCC
Kendall Cook			Kat Farris	
Justin Stern	WSEO		Jeb Steward	

Table 2.2. List of attendees (other than presenters) at the scoping meeting in Savery.

Name	Agency		Name	Agency
Jeni Cederle	WWDO		Amanda Drake	WSEO
Ray Weber			Linda Fleming	Snake River Press

2.2. 27 January 2016, Cheyenne, WY

A TAT meeting was held on 27 January 2016 in Cheyenne, Wyoming at the WWDO. Ms. Jeni Cederle, the new WWDO Project Manager, facilitated the meeting. At the meeting, NCAR gave a presentation updating the TAT on the preliminary results and progress on the Medicine Bow and Sierra Madre Ranges Study, as well as the next steps in the study. NCAR representatives included Dr. Roy Rasmussen and Dr. Sarah Tessendorf. The complete list of attendees is included in Table 2.3.

Table 2.3. List of attendees at the January 2016 TAT meeting in Cheyenne.

Name	Agency		Name	Agency
Lee Hacklemen	National Resources Conservation Service		John Mejia	Desert Research Institute (DRI)
Ty Wattenberg	--		Frank McDonough	DRI
Steve Wolff	WSEO		Brian Lovett	WY Dept Environmental Quality (DEQ)
Jeff Frazier	WY Dept Transportation		Jeff French	Univ. Wyoming (UW)
Sean Collier	Southern Nevada Water Authority		Kate Dwire	USFS Rocky Mtn Research Station (RMRS)
Nathan Haynes	USFS Medicine Bow-Routt NF and Thunder Basin NF (MBRTB)		Scot Rogers	USFS MBRTB
Terry Deshler	UW		Mitchel Cottenoir	Tribal Water Engineer
Robert Musselman	USFS RMRS		Binod Pokharel	UW
Sandy Henny	USFS		Mohammed Mahmoud	Central Arizona Project
Lee Arrington	WSEO		Jeri Trebelcock	Popo Agie Conservation Dist.
Bruce Boe	WMI		Pat Golden	HEC
Bart Geerts	UW		Barry Lawrence	WWDO
Ray DeLuna	TREC Inc.		Roy Rasmussen	NCAR
Sarah Tessendorf	NCAR		Joe Busto	Colorado Water Conservation Board
Joan McGraw	Medicine Bow Conservation Dist.		Jeni Cederle	WWDO

3. Task 2: Review and Summarization of Previous Data

3.1. Background

The potential for modifying supercooled clouds with artificial *ice nuclei* (IN) was initially championed in the literature by Findeisen (1938). After artificial ice nucleation by both dry ice and silver iodide (AgI) became known, many researchers became interested in modifying precipitation from supercooled clouds (e.g., Schaefer 1946, Vonnegut 1947, Kraus and Squires 1947, Langmuir 1948, Coons et al. 1948, and Bergeron 1949). Such modification is termed glaciogenic seeding, as it results in the formation of cloud ice.

These early scientists recognized that winter orographic clouds might be particularly well suited to seeding due to the frequency and persistence of supercooled water. Ludlum (1955) was among the first to present a conceptual model for seeding orographic clouds to enhance snowfall, a model that has remained unchanged in the essential details. However, the microphysical precipitation processes in winter clouds have proven to be far more complex than originally envisioned. Many refinements and clarifications of the conceptual model details have since been made.

Precipitation in winter orographic storms develops when ice crystals form on natural IN (typically certain dust particles) and grow through *deposition* (water vapor forming ice directly, the process that builds the smallest snow crystals), *riming* (the collection of unfrozen cloud droplets by ice crystals), and/or *aggregation* (the entanglement of ice crystals with each other to form snowflakes). Measurements indicate that most orographic clouds do not contain much ice until temperatures colder than $-12\text{ }^{\circ}\text{C}$ are reached (e.g., Geresdi et al. 2005). Natural IN are scarce at these relatively warm temperatures (Hoose and Möhler 2012). During many storms, the precipitation process is inefficient due to the lack of natural IN active at warmer cloud temperatures.

Furthermore, the weak updrafts in orographic clouds (mostly composed of very small droplets of similar sizes), limit the activity of ice multiplication processes (e.g., Hallett and Mossop 1974) that create cloud ice without additional IN. As a result, many shallow clouds, especially winter orographic clouds, may largely lack ice crystals and thereby, be inefficient in producing precipitation. The absence of ice crystals allows supercooled cloud droplets to persist for long periods in such orographic clouds, instead of being depleted by vapor diffusion, riming, and/or aggregation. This fact is well documented by the measurement of sustained supercooled liquid water (SLW) in orographic clouds taken by aircraft and ground-based instruments, such as radiometers (e.g., Rauber et al. 1986; Huggins 1995). In contrast to natural IN, artificial IN, such as AgI, will nucleate ice crystals at temperatures as warm as $-5\text{ }^{\circ}\text{C}$, enabling the creation of ice crystals in clouds warmer than $-12\text{ }^{\circ}\text{C}$ by “seeding” them with an AgI aerosol (DeMott et al. 1995).

One alternative to glaciogenic seeding with AgI is to seed with liquid propane (LP). Rather than producing ice via heterogeneous nucleation, LP is released directly into the cloud to be seeded, where the rapid evaporation of the propane droplets results in extreme supercooling and homogeneous nucleation. At temperatures colder than $-2\text{ }^{\circ}\text{C}$, approximately 10^{12} ice crystals are

produced per gram of propane (Hicks and Vali 1973). Seeding with LP is straightforward and efficient. However, there are disadvantages. First, the release must occur within a supercooled cloud. If LP is released in clear air, there are no cloud droplets to be frozen. If released in cloud but the cloud is not supercooled, the ice formation will be very transient. Further, if ice that forms should warm and melt or sublimate, it will not reform (Reynolds 1996). Therefore, to be effective, the ice produced by LP seeding must continue to grow to precipitation. If the ice thus formed melts or sublimates, there are no nuclei left behind to re-initiate ice development (as there would be when seeding with AgI), even if, or when the environment again becomes saturated and supercooled.

3.1.1. Conceptual Model

The following chain of events is hypothesized for seeding of the Medicine Bow and Sierra Madre Ranges.

When performing ground-based seeding, AgI is released from IN generators near and/or on the target mountain range, and carried upward by the wind. The plume of AgI rises and disperses within a relatively large volume of air. The AgI particles nucleate cloud ice at temperatures colder than -5°C . However, the nucleation efficiency increases by orders of magnitude (a factor of 100 to 1,000) at temperatures of -8° to -10°C ¹. The ice crystals then grow rapidly in conditions of water saturation (within the cloud), where supercooled water droplets exist. The ice crystals first grow by vapor deposition and then by riming and/or aggregation, forming precipitation-sized ice particles that fall to the surface as snow. These crystals are enhanced in number, size, and/or density from what would have fallen naturally, but otherwise are indistinguishable from natural snowfall.

The chain of events for airborne seeding is essentially the same, except transport of the AgI into the cloud is ensured, because it is released in cloud, or just above cloud. By this method, the AgI creates ice within 1 min (at -6° to -8°C) of release via flare² (DeMott 1999), which rapidly grows as ice crystals in regions of SLW. The chain is otherwise identical to ground-based seeding, although the precipitation particles often originate at greater heights.

Airborne seeding eliminates some of the uncertainties inherent in ground-based releases of AgI because the seeding agent is delivered immediately and directly to the target clouds. Using pyrotechnics, an aircraft can deliver more seeding agent to the cloud faster than ground-based generators can. A typical ground-based generator release rate is 25 grams per hour (per generator), while airborne release rates begin at ~ 37 grams per minute. Aircraft can also effectively treat clouds in some circumstances when ground-based seeding cannot.

¹ These numbers apply to the seeding solution used in the WWMPP, which functions rapidly through the condensation-freezing mechanism. More “traditional” formulas producing $\text{AgI}\cdot\text{NH}_4\text{I}$ nuclei function through the contact-freezing mechanism, and thus may require many minutes more to nucleate in clouds of lesser LWC.

² The activity of the silver iodide-based pyrotechnic quoted here is for the glaciogenic flare presently manufactured by Ice Crystal Engineering, LLC, of Kindred, North Dakota. The IN output and activity of pyrotechnics manufactured by others may vary considerably, and should be determined before any program is undertaken.

However, seeding with aircraft is often more expensive than ground-based generators, in large part because deployment costs are greater. When a large number of ground-based generators are required to ensure adequate targeting, this may not be the case. Aircraft also have limited on-station (seeding) times, as crew endurance, fuel consumption, and sometimes aircraft icing limit the length of operations. Ground-based generators can be operated continuously for a day or more, but many more are required, and only the portions of the cloud within 1 km (~3,000 ft) can be effectively targeted.

The model for LP seeding is essentially the same, but the targeting is different. While AgI nuclei can be released from any location where the flow will carry it into supercooled clouds, the LP can only be used within supercooled clouds, and must be sited where the clouds develop. The advantage of LP is that it can be used to produce ice crystals if any SLW is present, and does not require clouds to be -6°C or colder. The advantages and disadvantages of various seeding methods are listed in Table 3.1.

Table 3.1. Advantages and disadvantages of various seeding types and modes.

<i>Type/Mode</i>	<i>Siting/Positioning</i>	<i>Target Temperature Threshold</i>		<i>Seeding Rate</i> ⁴	<i>Advantages</i>	<i>Limitations</i>
		$^{\circ}\text{C}$	$^{\circ}\text{F}$			
<i>Manual, Ground-based AgI</i>	Fixed location, upwind of target. Distance from target and elevation depend upon typical flows during seeding conditions.	$\sim -6^{\circ}\text{C}^1$	$\sim (+21^{\circ}\text{F})$	$1.25 \cdot 10^{11}$ nuclei per minute.	Does not require remote communications electronics to actuate generators.	Requires an on-site operator (generators must be accessible during harsh winter weather). Their fixed locations limit (operations based to a limited range of wind direction/speeds).
<i>Remote-Controlled Ground-based AgI</i>	Fixed location, upwind of target. Distance from target and elevation depend upon typical flows during seeding conditions.	$\sim -6^{\circ}\text{C}^1$	$\sim (+21^{\circ}\text{F})$	$1.25 \cdot 10^{11}$ nuclei per minute.	Does not require an on-site operator. Allows for high-elevation deployment,	Their fixed locations limit operations to a limited range of wind direction/speeds. AgI seeding solution is expensive compared with LP. Must have remote communication link.
<i>Airborne AgI</i>	Upwind of target clouds, at an appropriate altitude and distance from target.	~ -4 to $-6^{\circ}\text{C}^{1,2}$	$\sim +25$ to $+21^{\circ}\text{F}$	At -6°C , $2.3 \cdot 10^{14}$ nuclei per minute with pyro, $6 \cdot 10^{11}$ nuclei per minute with seeding solution used by ground IN generators.	Upwind distance and altitude can be adjusted according to the cloud depth, temperature, and ambient wind speed. Deployment of surface-based equipment not required.	Minimum safe altitude must be maintained. Seeding at low altitudes close to the barrier in light winds is not possible.
<i>Ground-based Liquid Propane</i>	Fixed location, Generators must be high enough to be routinely within supercooled clouds.	$< 0^{\circ}\text{C}^3$	$< 32^{\circ}\text{F}$	$7 \cdot 10^{12}$ ice crystals per minute from 0 to -2°C , $\sim 7 \cdot 10^{14}$ ice crystals per minute at	Propane is less expensive compared with AgI based seeding solutions. Any supercooled cloud can be	Only effective if LP is released within supercooled cloud. Utilizes homogeneous nucleation (i.e., no nuclei are left behind

Type/Mode	Siting/Positioning	Target Temperature Threshold		Seeding Rate ⁴	Advantages	Limitations
		°C	°F			
				temperatures colder than -2°C. ³	treated, regardless of temperature. Does not require an on-site operator.	to re-nucleate if the ice formed initially melts or sublimates). Their fixed locations limit operations to a limited range of wind direction/speeds., Must have remote communication link.
¹ This temperature is based upon the nucleation efficiency of the seeding solution used in the WWMPP, which functions by the condensation-freezing mode. This solution contains an oxidizer, so the generator must be constructed with corrosion-resistant (e.g. stainless steel) components. ² Glaciogenic pyrotechnics manufactured by Ice Crystal Engineering produce 10 ¹¹ IN per gram active at -4°C, and 10 ¹³ IN active at -6°C (1.5 orders of magnitude more than the seeding solution cited), which can further broaden the seeding opportunity window. See Figure 12.1. ³ Per Hicks and Vali (1973). ⁴ Seeding rates for AgI nuclei calculated from efficiencies measured by DeMott (1997, 1999).						

3.2. History of Wintertime Orographic Cloud Seeding

The fundamental hypothesis for increasing precipitation through winter orographic cloud seeding is that natural precipitation efficiency can be improved by seeding. If conducted upstream (upwind) of the target mountain range, it will convert more of the supercooled cloud water to ice crystals. The newly created ice crystals then grow by diffusion, riming, and/or aggregation, and precipitate as additional snow to the surface, increasing the total snowfall.

Scientific evaluation of this hypothesis has been attempted over the last half a century using statistical comparison of surface precipitation in treated versus untreated events (randomized studies), observational studies to understand natural cloud structure and effects of seeding (physical studies), and numerical modeling of both natural and seeded clouds. Since 1948, numerous research programs have been performed to determine whether or not AgI seeding produces additional precipitation in winter orographic clouds (Huggins 2009 for a summary).

3.2.1. Randomized Studies - Historical

Two randomized programs conducted in the Rocky Mountains are of immediate relevance to winter orographic cloud seeding in Wyoming. These are the Climax experiments in the central Colorado Mountains (Mielke et al. 1981; Grant 1986), and the Bridger Range Experiment (BRE) in southwestern Montana (Super and Heimbach 1983).

The Climax Experiments (Climax I, 1960–1965, and Climax II, 1965–1970) were exploratory and confirmatory randomized seeding experiments that used instruments and observations as covariates and for ancillary (*ex post facto*) studies. The Climax I and II research used experimental units of one-day (24-h) duration, which were declared in accordance with design criteria established prior to the start of the respective experiments (Grant and Mielke 1967, Mielke et al. 1971). Both Climax I and the replication, Climax II, reported precipitation increases

with high statistical confidence (Mielke et al. 1981). A reanalysis of the complete Climax data set (I and II) showed that for warm 500-hPa temperatures, precipitation increases of 25% were realized. However, the validity of the experiments was questioned on the basis of the experimental execution and evaluation methodology (Rangno and Hobbs 1987, 1993). Much was learned from the Climax experiments, but ultimately the validity of these experiments left the conclusions in doubt.

The BRE was conducted in the Bridger Mountains of southwest Montana from 1969 to 1972 (Super 1974; Super and Heimbach 1983). To avoid trapping the seeding agent below stable atmospheric layers above, the BRE utilized ground-based IN generators that burned an AgI solution, and were sited more than midway up the upwind (western) side of the barrier. The Bangtail Ridge, a secondary barrier located 5 to 20 km to the east of the main Bridger ridgeline, was the expected target. Randomized experiments were conducted during the winters of 1970–1971 and 1971–1972, and follow-on physical measurements were later made (Super and Heimbach 1988). This project produced strong statistical evidence of seeding effects, and considerable documentation of the physical chain-of-events that began with seeding and led to the observed precipitation changes. A *post hoc* statistical analysis strongly suggests that increased target-area snowfall resulted from seeding when the AgI plume temperature was colder than approximately -9°C . An estimate of $\sim 15\%$ more seasonal target area precipitation than predicted on non-seeded days resulted, while a target-control analysis of independent snow course data strongly suggested seeding enhanced the seasonal snowpack more than 15%. Additional exploratory analysis of the BRE was later carried out by sub-partitioning the original 24-h experimental units into 6-h data blocks (Super 1986). That analysis was limited to those 6-h periods with rawinsonde observations, main ridge temperatures $\leq -9^{\circ}\text{C}$ and westerly flow. The results showed that AgI seeding was particularly effective in increasing precipitation in a small fraction of the 6-h blocks, but had little or no effect most of the time. Seeding appeared to be especially effective when cloud-top temperatures were warmer than about -25°C and the wind had a strong cross-barrier component. Super (1986) notes that, “...this analysis has not suggested any significant decreases in target precipitation due to seeding. This implies that the treatment used could be applied whenever potential storm conditions existed without concern of decreasing snowfall.” These results have been accepted, but because of the limited scale, different geography and climate, the direct transferability to Wyoming was in doubt.

3.2.2. Randomized Studies - Recent

Randomized experiments with many similar design elements were recently conducted. The Snowy Precipitation Enhancement Research Program (SPERP) in the Snowy Mountains of Australia (Manton et al. 2011, Manton et al. 2015) was conducted from 2005 through 2009.

Even more recently, the WWMPP in southern Wyoming (Breed et al. 2014, WWDC Draft Executive Summary 2014) was conducted from 2005 through 2014.

The Australian experiment, SPERP (Phase I), provided newer evidence of an increase in precipitation due to AgI seeding of winter orographic clouds based on a 5-year statistical program (Manton and Warren 2011). Analysis of the confirmatory experiment showed a 7–9% increase in snow water equivalent (SWE), depending on whether the analysis used the primary control area or an extended “total” control area. However, these experimental results did not

meet the accepted level of significance and therefore cannot be considered to be statistically different than no seeding effect.

The operational procedures and measurements taken during SPERP were designed to address and verify the issue of targeting – that is, ensuring that seeding material was affecting the seedable portion of the clouds. Therefore, exploratory analyses were performed with the targeting issue, and others, in mind. Using extensive measurements of silver-in-snow, tracers, integrated liquid water within the targeted clouds, and trajectory modeling, supported partitioning the precipitation data by the total time generators were operating during a case. Seasonal precipitation increases of 14% were established (relative to seedable storms), at a 3% significance level (p-value of 0.03) after thresholding the cases according to generator hours, which was indicative of probable AgI coverage of the target area (e.g., more generator hours being equivalent to more AgI seeding material reaching the target area). Physical studies included silver-in-snow measurements that verified effective targeting of the AgI seeding agent.

The findings from the SPERP analysis prompted a second seeding experiment in the same area, but with expanded target and control areas and different seeding criteria. Although the study is not yet published, drafts of the project description and results have been circulated within the scientific community (Manton et al. 2015 Reynolds 2015). Although the changes in the target and control areas led to a range of seeding effects, the overall result is very similar to that found in the SPERP study: a 13% increase in precipitation (in the target area for seedable storms) at a 6% significance level (p-value of 0.06). The replication of the results in response to experimental changes from the SPERP analysis is very encouraging as far as substantiating the efficacy of winter orographic cloud seeding.

The results of the Wyoming project, WWMPP, were recently summarized in a draft executive summary (WWDC 2014) and included statistical, physical, and modeling analyses. The accumulation of evidence from these analyses suggests that “cloud seeding is a viable technology to augment existing water supplies, for the Medicine Bow and Sierra Madre Ranges.” The primary statistical analysis implied a 3% increase in precipitation with a 28% probability that the result occurred by chance, which did not meet the acceptable level of significance. While this primary statistical analysis did not show a significant impact of seeding, statistical analysis stratified by generator hours, similar to the SPERP analyses, showed seasonal increases of 3–17% for seeded storm periods. Furthermore, high-resolution modeling studies that simulated three of the experimental seasons, or about half of the total number of seeding cases, showed positive seasonal seeding effects between 10–15% (relative to seedable storms).

Though no seeding effect was discerned in the primary randomized statistical experiment, ancillary studies using physical considerations (e.g., hours of generator operation, surface-based IN measurements, and numerical modeling) to stratify the WWMPP precipitation data and modeling studies over three full winter seasons yielded more positive evidence from the statistical, modeling, and physical analysis. This evidence suggested, “a positive seeding effect on the order of 5 to 15%” relative to seedable storms in a given season.” These increases apply to a single control site in the target area, so a seeding effect applicable to the whole target area needs to be calculated based on an estimate of effective seeding coverage of the target area. For

example, if the areal coverage of effective seeding were 60%, then the seeding effect for the target would be 3–9%.

Important design and operational aspects of the WWMPP included confirming the presence of SLW over the target mountain ranges. This was accomplished using a dispersion model to guide initial generator placement, radiometers, soundings, and high-resolution real-time forecast models to inform operational decisions, and utilizing additional observations from ancillary instruments and “piggy-back” experiments, such as the AgI Seeding Cloud Impact Investigation (ASCII; e.g., Pokharel et al. 2014a). Based on the preliminary results of the WWMPP, the recommendation was made to consider implementing cloud-seeding technology in Wyoming by carefully addressing each of five components: 1) barrier identification; 2) program design; 3) operational criteria; 4) program evaluation; and 5) program management. These were further detailed in the executive summary.

The consensus of a post-SPERP, post-WWMPP panel discussion was that technological advances, particularly in remote sensing and numerical modeling, bode well for the advancement of cloud-seeding operations (Tessendorf et al. 2015).

3.2.3. Physical Experiments

Several randomized seeding experiments have included some physical studies aimed at verifying the seeding conceptual model. However, a number of other non-randomized research programs have also contributed to refinement of the seeding conceptual model. Much of this work has been summarized by Golden (1995) and Super (1999), and more recently, Huggins (2009), who compiled a summary of past research studies related to winter orographic cloud seeding. The overall results of the various studies provided support for the National Research Council (NRC 2003) conclusions that “strongly suggested positive seeding effects” in these types of storms.

Observational studies in concert with the WWMPP and SPERP randomized seeding experiments have evaluated or verified steps in the seeding conceptual model. The technique of snow sampling for trace chemistry analysis (silver-in-snow) has advanced to the point of being a preferred method of evaluating the effectiveness of targeting (Warburton et al. 1995). Results have been presented the analysis of SPERP (Manton et al. 2011), and in the draft conclusions of the WWMPP (WWDC 2014). Additionally, AgI IN measurements using the NCAR acoustic IN counter (AINC) have demonstrated the variability of the seeding plume in targeting small areas, using both airborne and ground-based instruments (Heimbach et al. 2008; Boe et al. 2014).

Geerts et al. (2010) applied a high-resolution vertically-pointing millimeter-wavelength airborne Doppler radar to investigate wintertime seeding effects in orographic clouds for seven cases in conjunction with the WWMPP. Those results showed that the increase in near-surface reflectivity could be attributed to AgI seeding with statistical significance. However, the large natural variability of meteorological conditions and the small number of cases rendered the results cautionary. Consequently, the AgI Seeding Cloud Impact Investigation (ASCII) field program was carried out to better quantify the seeding signals by reducing the impact of natural variability of the orographic storms. Results showed that in some cases, increased reflectivity at low levels observed by the airborne Doppler radar was very likely to be induced by ground-released AgI particles (Pokharel et al. 2014a). The ASCII program also contributed surface radar,

precipitation, and cloud physics observations, and airborne radar, lidar, and cloud physics measurements that have aided validation of numerical modeling of winter orographic cloud seeding.

These studies, along with evidence from randomized seeding experiments provide a detailed physical picture of AgI plume transport, ice nucleation, and snow development. More sophisticated measurements and improved numerical models developed over the last decade continue to refine and validate the seeding conceptual model.

3.2.4. Numerical Modeling

Modeling natural and seeded orographic clouds has been conducted in concert with physical studies. The WRF model (Skamarock et al. 2008) was used in a number of winter snowpack studies and cloud-seeding evaluations that have verified the model's ability to reasonably simulate AgI plume transport and snowfall over a variety of time and space scales. For example, the WRF model was used to simulate eight seasons of snowfall in the Rocky Mountains, covering all of Colorado and parts of adjacent states (Ikeda et al. 2010). The model runs at various resolutions were compared with Snow Telemetry (SNOTEL) data, and grid resolutions of 6 km at a minimum were needed for reasonable agreement. Although 6-km resolution was adequate, the model run at 2-km grid resolution captured the local topographic forcing of regional snowfall even better.

Recently, Xue et al. (2013a, b) incorporated an AgI cloud-seeding parameterization into the Thompson bulk microphysics scheme (Thompson et al. 2008) within the WRF model to systematically investigate how orographic seeding outcomes are influenced by atmospheric and cloud properties under idealized and realistic conditions. Almost all idealized and realistic case simulations showed that ground-based glaciogenic seeding enhances precipitation in stable stratified orographic clouds, but were ineffective in convective clouds deep enough to produce abundant ice nucleation near the top. By examining seeding effects under various meteorological and microphysical conditions, the model simulations presented in Xue et al. (2013a, b) demonstrated that the seeding effects increase with decreasing natural precipitation efficiency and vice versa.

For smaller domains, the WRF model can be configured at very high resolution, called a large eddy simulation (LES). The LES model was run on a case in the Medicine Bow Range of southern Wyoming at 100-m resolution and proved to be successful in simulating details of the airflow and plume dispersion for that case, validated by results of airborne mapping of the seeding plumes (Xue et al. 2014; Boe et al. 2014).

These recent modeling studies incorporating AgI seeding into the processes that lead to precipitation have shown promise in simulating seeding effects. Likewise, the emergence of this state-of-the-art cloud-seeding microphysics scheme together with sufficient computing power to resolve large eddies now allows examination of the chain of events associated with glaciogenic seeding.

3.3. Meteorological and Climatological Observations

Public data sources include SNOTEL precipitation and snowpack measurements and United States Geological Survey (USGS) streamflow records. Meteorological data are also available through the National Oceanic and Atmospheric Administration (NOAA). Limited historical data are also provided in the Green River Basin Plan (WWC 2010) and the Platte River Basin Final Report (Trihydro 2006). The North American Regional Reanalysis (NARR) provides temperatures, winds, moisture, soil data, and numerous other meteorological parameters in a very useful format. Produced by the National Centers for Environmental Prediction (NCEP), the NARR takes in, or assimilates, a great amount of observational data to produce a long-term picture of weather over North America.

3.4. History of Cloud Seeding In and Near the Targeted Areas

Cloud-seeding operations are regulated and permitted by the Wyoming State Engineer's Office (WSEO).

In the 1960s, the University of Wyoming Atmospheric Water Resources Research (AWRR, later the Department of Atmospheric Science) established a research facility atop Elk Mountain, an isolated peak on the northwest flank of the Medicine Bow Range. The Elk Mountain Observatory (EMO) was utilized for cloud seeding and cloud physics research for several decades (e.g., Auer et al. 1969; Auer 1972; Cooper and Vali 1981; Politovich and Vali 1983; Deshler and Vali 1985; Rogers and Vali 1987). Much of this research was directed toward improving understanding of cloud and precipitation processes, which are directly linked to the efficacy of cloud seeding.

The earliest record of cloud seeding in the area is found in WSEO Weather Modification Permit #2, granted to Water Resources Development Corporation of Denver, Colorado, which hired Wyoming Weather, Inc., to seed clouds between 1 May 1951 and 31 December 1951. Ground-based AgI generators were chosen as the method, but the permit does not differentiate between warm-season and cold-season activities.

Cloud seeding was again attempted in 1954, to increase snowpack not only in Carbon and Albany Counties, but in the central and eastern parts of the state as well. Counties listed in that permit included Campbell, Converse, Crook, Goshen, Laramie, Johnson, Niobrara, Platte, Sheridan, and Weston. Cloud seeding operations were authorized on behalf of the Wheatland Irrigation District for February through May of that year, and for the other areas May through September only. Those permits specified that augmentation of snowpack was the purpose, though snowpack does not generally accumulate during the latter period (May through September). In November of 1954, another permit was issued to Water Resources Development Corp. for the use of 40 ground-based AgI generators in Sweetwater, Platte, Carbon, Albany, and Laramie Counties. According to records, twenty generators were also authorized for use in the areas for calendar year 1955.

The Natural Resources Research Institute (NRRI, the predecessor to the University of Wyoming Department of Atmospheric Science) was granted its first seeding permit in 1963 to seed in Carbon and Albany Counties in the vicinity of Elk Mountain, and in Sublette and Fremont

Counties along the Wind River Range. Additional permits for NRRI to operate in the same areas were subsequently approved in 1964 and 1965.

The NRRI was again permitted for seeding operations in 1969. This permit is especially noteworthy because the application specifically states that it involves cloud physics studies of cap cloud formation in the vicinity of Elk Mountain, and also “a limited number of experiments on the Medicine Bow Mountains.” The permit alluded to the use of instrumented aircraft and an NRRI radar.

A similar permit was issued to the NRRI for the period beginning in 15 November 1970 through 1 April 1971, for additional experimentation on Elk Mountain. The permit states that, “The objective of the activities within the Elk Mountain Water Resources Observatory is to develop a sound snow pack augmentation system.” The NRRI permit was renewed for the same project area and purpose for the 1972-73, and 1973-74 seasons; however, during the first renewal in 1972, the permittee was not NRRI, but its successor, the Atmospheric Science Department of the University of Wyoming.

The last cloud-seeding permit in the area, prior to those for the WWMPP, was issued to Colorado International Corporation, of Boulder, CO, on behalf of Platte Valley Weather Modification, Inc. This permit authorized the use of a twin-engine aircraft outfitted with ejectable (droppable) AgI pyrotechnics to seed the Medicine Bow Range for snowpack augmentation from 14 February through 21 May 1977.

Most recently, the WWMPP was conducted from 2005 through 2014 (WWDC 2014). That research program utilized ground-based IN generators sited on the western flanks of the Medicine Bow and Sierra Madre Ranges to target precipitation gauge clusters in each range. Seeding for this project was conducted between 15 November and 30 April in most seasons.

4. Task 3: Climatology of the Project Area

The purpose of this task was to characterize winter storms and their seeding potential over the Sierra Madre and Medicine Bow Ranges in southern Wyoming. In order to accomplish this, the following questions were addressed:

- What are the climatological averages and variability of winds, temperatures, cloud depths, stabilities, and liquid-water content (LWC) over the Sierra Madre and Medicine Bow Ranges?
- What are the prevailing winds, temperatures, cloud depths, stabilities, and liquid water content during precipitating storms over the Sierra Madre and Medicine Bow Ranges?
- What fraction of the precipitation occurs when 700-hPa temperatures are warmer than $-6\text{ }^{\circ}\text{C}$?
- What fraction of precipitation occurs during seedable conditions?

Operational cloud-seeding programs utilize a temperature threshold warmer than those used in research studies (i.e., the $-8\text{ }^{\circ}\text{C}$ threshold used in the WWMPP research program [Ritzman 2013; Ritzman et al. 2015]) because AgI has been shown to activate in temperatures as warm as $-5\text{ }^{\circ}\text{C}$ or $-6\text{ }^{\circ}\text{C}$ (DeMott 1997). To ensure moderate to strong AgI activation efficiency in this analysis, the operational cloud-seeding temperature threshold was set at $-6\text{ }^{\circ}\text{C}$.

In addition to a proper activation temperature for AgI, liquid water needs to be present for there to be the potential for cloud seeding. The presence of SLW is a sign that natural precipitation processes are inefficient, and if additional ice crystals are nucleated (via AgI activation) they could grow at the expense of the SLW and fall out as additional snow. The criteria utilized in this study define seedable LWC as greater than 0.01 g/kg and within the appropriate temperature range to be considered SLW. Therefore, at a minimum, both proper temperature and LWC criteria need to be met to determine seeding potential.

Additional variables, such as atmospheric stability and winds, play a role in determining seeding potential, especially with regard to how effectively the AgI will be transported into the seedable cloud. Therefore, assessing atmospheric stability and wind direction is important for determining locations to release AgI and the method of delivery (i.e., ground-based generators or aircraft). The observations needed to evaluate these meteorological criteria include atmospheric soundings (to assess temperature, atmospheric stability, and winds at heights where clouds form), radiometer data (to assess the presence of SLW in the atmosphere), and precipitation gauge data (to determine when and how much precipitation fell). With the exception of Natural Resource Conservation Service (NRCS) SNOTEL gauge measurements; these types of observations are quite rare, especially in the western U.S. mountains. Therefore, an alternative way to get this important information is to utilize high-resolution model simulation output. While not all publicly available model simulations include LWC as an output variable (as explained in Ritzman et al. 2015), this study uses an NCAR-generated high-resolution model simulation over an 8-year period that includes all key variables for the climatology analysis.

4.1. Data and Methodology

The climatology of the project area was investigated using SNOTEL observational data and a high-resolution WRF model simulation performed over the Continental United States (CONUS) domain spanning an 8-year period between 1 October 2000 and 30 September 2008 (hereafter, WRF-CONUS model).

4.1.1. Observations

SNOTEL observations provide a long-term record of precipitation data from gauges that weigh precipitation and snow water content via pressure-sensing snow pillows located at numerous sites throughout the Western U.S. These sites are owned and operated by the Department of Agriculture NRCS, and are typically located at elevations between 2,400 and 3,600 meters (m) above mean sea level (MSL). Historical and real-time data are available from the NRCS web site (<http://www.wcc.nrcs.usda.gov/snow/>) and have been widely used for climatological studies. These studies also describe known measurement deficiencies (Serreze et al. 1999; Serreze et al. 2001; and Johnson and Marks 2004; for example) such as an undercatch of snowfall due to wind (Serreze et al. 2001; Yang et al. 1998; Rasmussen et al. 2012). The SNOTEL gauges are often located in a forest clearing where the wind speed is typically less than 2 m s^{-1} , and an undercatch of approximately 10–15% is expected (Yang et al. 1998). The SNOTEL data resolution is 0.1 inch (2.5 mm), making it difficult to study precipitation characteristics or verify model data on a sub-daily basis. However, these data are suitable for use over monthly or longer periods.

Additional snow-gauge observations are available for this study because data were also collected during the WWMPP. The WWMPP dataset includes high-resolution snow-gauge data from eight sites (four in each Range), radiometer data (one radiometer per Range), and local sounding data released from Saratoga, WY. The soundings were released for each seeding case called during the WWMPP. In other words, they were not released on a regular schedule making them useful for the climatology analysis, but at least provide sounding data that can be used in model evaluation (Section 6.5.1).

4.1.2. Model (WRF-CONUS)

Model data used to examine the climatology of the Sierra Madre and Medicine Bow Ranges came from a high-resolution (4-km) regional climate (RCM) simulation (Liu et al. 2016) using the WRF model (Skamarock et al. 2005). This WRF-CONUS model simulation was carried out as a follow-up study to a preceding high-resolution RCM study discussed in Rasmussen et al. (2014) and the WRF-CONUS outputs are currently used in a number of climate studies. The entire simulation period was expected to run from 1 October 2000 to 30 September 2013; however, because the full 13-year dataset was not yet available at the time this analysis was conducted, the focus was concentrated on the first 8 water years (2000 to 2008). Figure 4.1 shows the WRF-CONUS model domain, which had a horizontal grid spacing of 4 km and an output frequency of 3 hours for 3-dimensional (3D) data fields (e.g., atmospheric temperature, winds, various mixing ratios) and 1 hour for 2-dimensional fields (e.g., precipitation reaching the ground, near-surface air temperature). Table 4.1 lists the physical parameterizations used in the WRF-CONUS model simulation. The model was forced with 6-hourly European Centre for Medium-Range Weather Forecasts (ECMWF) Re-Analysis (ERA)-Interim reanalysis data. See Liu et al. (2016) for a full description of the simulation setup.

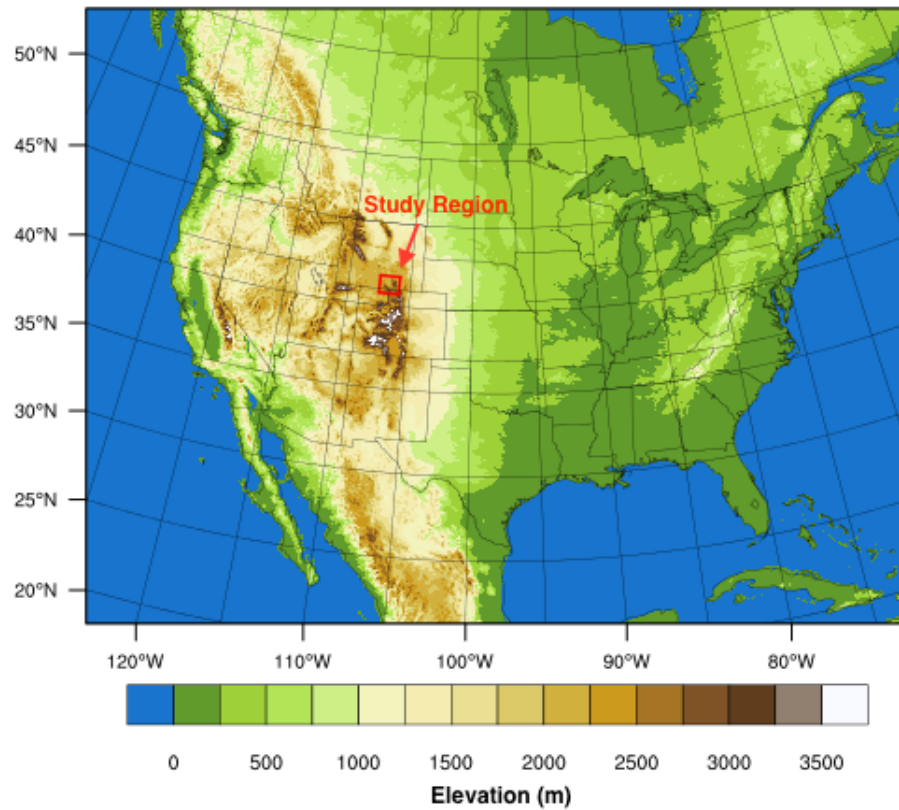


Figure 4.1. WRF-CONUS model domain and elevation. Red box indicates the Sierra Madre (SM) and Medicine Bow (MB) mountain ranges where the analysis is focused. For a close-up of the study region see Figure 12.1.

Table 4.1. WRF-CONUS model physics options.

WRF physics	Parameterization schemes	References
Land surface	Noah-MP (multi-physics) Land Surface Model	Niu et al. (2011)
Microphysics	Thompson aerosol-aware mixed-phase scheme	Thompson and Eidhammer (2014)
Planetary boundary layer	Yonsei University (YSU) PBL	Hong et al. (2006)
Longwave and shortwave radiation	RRTMG	Iacono et al. (2008)

4.1.3. Seeding Potential Analysis Methods

The frequency of instances when seeding conditions occurred over the target areas were determined by analyzing the key criteria needed for clouds to be seedable. The key criteria produced by the WRF-CONUS model output and utilized in this analysis were temperature, liquid-water path (LWP, defined as column integrated cloud water over unit area), LWC mixing ratio, horizontal components of wind velocity (U and V), and derived turbulence parameters (e.g., squared of Brunt-*Väisälä* frequency, Froude number, and Bulk Richardson number).

Of these, the primary criterion used to indicate the presence of a cloud seeding opportunity was the presence of liquid water at temperatures appropriate for AgI activation. This leads to the following criteria for assessing whether cloud seeding is viable in a region:

- Temperature between -18°C and -6°C and
- $\text{LWP} > 0.01 \text{ mm}$ and/or
- $\text{LWC} > 0.01 \text{ g kg}^{-1}$

The LWP criterion resembles information that would be available to an operational forecaster using radiometer observations; however, LWP does not specify which vertical layer in the atmosphere the liquid water exists. Therefore, the LWC criterion, provided by the model, helps identify and discriminate ground from airborne-seeding opportunities based on the vertical location of liquid water.

Meeting the above criteria indicates the potential for cloud seeding, whether ground-based or airborne. However, this potential can only be realized if the seeding material reaches the regions where those criteria exist. Because ground-based seeding requires the AgI plume to be carried over the barrier and into the suitable clouds, the inclusion of wind direction and atmospheric stability criteria are necessary. The requisite wind direction criteria vary due to the orientation and topography of each range:

- Wind direction:
 - Between 210 and 315 degrees for west slope areas of both Ranges
 - Between 20 and 100 degrees for the Medicine Bow east slope
 - Between 0 and 50 degrees for the Sierra Madre east slope
 - Between 320 and 50 degrees for the Sierra Madre southern region (see Figure 4.2)
- Froude number > 0.5

The wind direction criterion was based on the dominant wind regimes affecting the target region. These additional criteria were not assessed for airborne-seeding potential, given that aircraft can introduce AgI directly into the atmosphere wherever seeding conditions occur, and the flight track can be oriented to account for wind direction.

Stability indices were derived from the WRF-CONUS model output and analyzed to assess impacts on ground-based seeding potential. The primary index analyzed was the Froude number (Fr). The Froude number expresses the ability of upslope airflow to go over a mountain barrier. The flow will be blocked by the barrier when $Fr < 0.5$. The airflow will freely move over the barrier (unblocked) when $Fr > 1$. Froude number is computed from

$$Fr = \frac{U/h}{N}$$

where U is the average wind speed (m s^{-1}) perpendicular to the mountain barrier orientation over a depth of h (in m), and N is an average of the Brunt-*Väisälä* frequency between the same depth. N (s^{-1}) is expressed as

$$N = \left(\frac{g}{T_v} \frac{\partial \theta_v}{\partial z} \right)^{1/2}$$

where g is the gravitational acceleration (9.8 m s^{-2}), T_v is the layer average virtual temperature (K), and $\partial \theta_v / \partial z$ is the vertical gradient of virtual potential temperature (K m^{-1}). For this analysis, the wind speed of the component perpendicular to each range (Sierra Madre or Medicine Bow) at each grid point lower than the peak of the range was used. The height (h) was calculated as the difference between the range peak height and the local height at each grid point. The local Brunt-*Väisälä* frequency (N) was then used to calculate the local Fr. Using this method, a 3D field of local Fr was generated.

To determine the seeding potential of the project area, three methods were employed: a single-site analysis of 700-hPa conditions, an area-based analysis, and a spatial mapping of seeding potential. Each method provided different pieces of information to address the objectives of the climatological analysis, and are described in more detail below.

The single-site analysis was performed by looking at 700-hPa conditions at individually selected grid points around the west, north, and eastern slopes of the Sierra Madre and Medicine Bow Ranges. The single-site analysis was performed because the 700-hPa pressure level intersects the crest of the mountain range, making an area-based analysis along the 700-hPa level not possible. Several sites surrounding the Ranges were selected to assess 700-hPa temperature and wind conditions on all sides of the barriers (Figure 4.2). Four sites considered to be the most representative of the region were targeted for this report: Savery and Saratoga on the western and northeastern slopes of the Sierra Madre Range, and Cedar Creek and Centennial on the western and eastern slopes of the Medicine Bow Range (Figure 4.2). The modeled 700-hPa temperature and wind conditions at those single grid points were then assessed during periods when precipitation was simulated by the model. For the Savery and Saratoga single-site analyses, periods with precipitation were determined using the model output at the grid point closest to the HY47 snow-gauge site; and for the Cedar Creek and Centennial sites, the grid point nearest to the GLEES snow-gauge site was used (Figure 4.2).

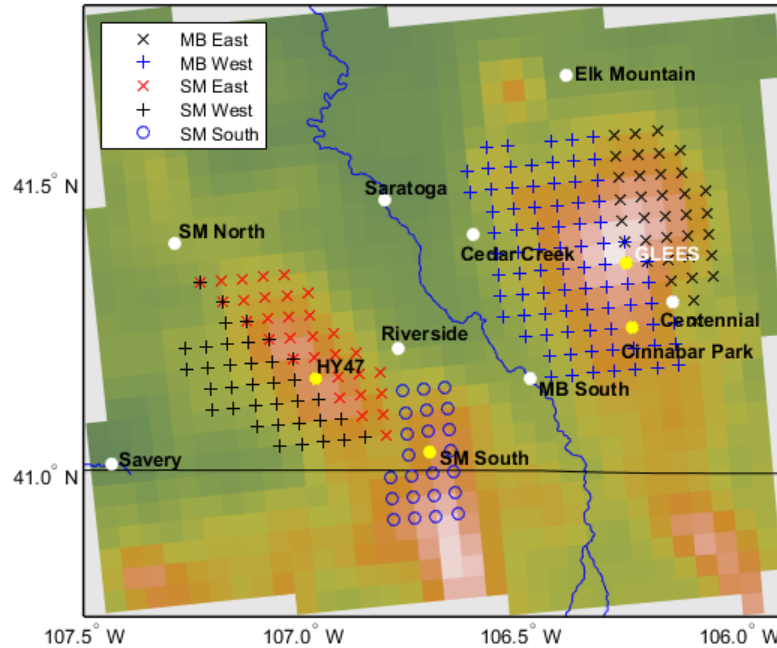


Figure 4.2. Map of the model terrain height highlighting the grid points used for each region in the seeding potential analysis (crosses or plus symbols of different colors). Precipitation gauge sites are marked by yellow circles. Sites used for analysis of 700-hPa conditions are marked by white circles.

For the area-based analysis, target regions were defined for investigation (Figure 4.2). Then areal-averaged values for each seeding criterion (for either ground-based or airborne-seeding layers) were produced at every model output time (3-hourly). Several target regions were selected to cover upslope conditions on each side of the target range where seeding conditions were possible (which was determined based on the single-site analysis). For the Sierra Madre and Medicine Bow Ranges, while upslope flow is predominantly from a westerly direction, upslope flow also occurs with easterly and northerly winds depending on seasonal storm tracks; thus, target regions are located on both the east and west slopes of the Sierra Madre and Medicine Bow Ranges, as well as the southern region of the Sierra Madre Range (SMEast, SMWest, MBEast, MBWest, and SMSouth, respectively). In particular, the temperature and LWC were assessed over these areas by producing histograms of the area-averaged values. Additionally, the frequency of time (over a given month or winter season) that the areal-averaged conditions met the thresholds defined above was determined. In order to normalize the results by when precipitation occurred, a representative SNOTEL site for the given target region was chosen for each region. Part of this selection required the site to have a good comparison between the SNOTEL data and the model (based upon the SNOTEL model evaluation in Section 4.2.2). Then the model grid point nearest that SNOTEL site was used to determine whether precipitation occurred or not.

The spatial maps were produced by utilizing the 3-hourly model output and mapping the frequency of hours in a given time period, such as monthly or seasonally, that the primary criteria were met at each grid point. This produced maps of seedability frequency for each grid point. These statistics were produced for each month and water year (November–April) starting November 2000 and ending April 2008.

For the spatial mapping and area-based analyses, ground-based seeding potential was analyzed separately from airborne-seeding potential based on the vertical layer of the atmosphere being investigated. For ground-based seeding, the 0–1 km Above Ground Level (AGL) layer was investigated and each criterion assessed was averaged over that layer at every model grid point (4-km spacing) and output time (3-hourly). For airborne-seeding potential, the 3–4-km MSL and the 4–5-km MSL layers were assessed by averaging each criterion over that vertical layer as was done for the ground-seeding layer.

4.2. Climatology of precipitation

Precipitation climatology for the project area was investigated using SNOTEL observation data from 13 sites located in the project area, and a high-resolution WRF-CONUS model simulation³ over an 8-year period between 1 October 2000–30 September 2008 (Figure 4.3).

³ Refer to Section 4.1.2 for the description of the WRF-CONUS simulation.

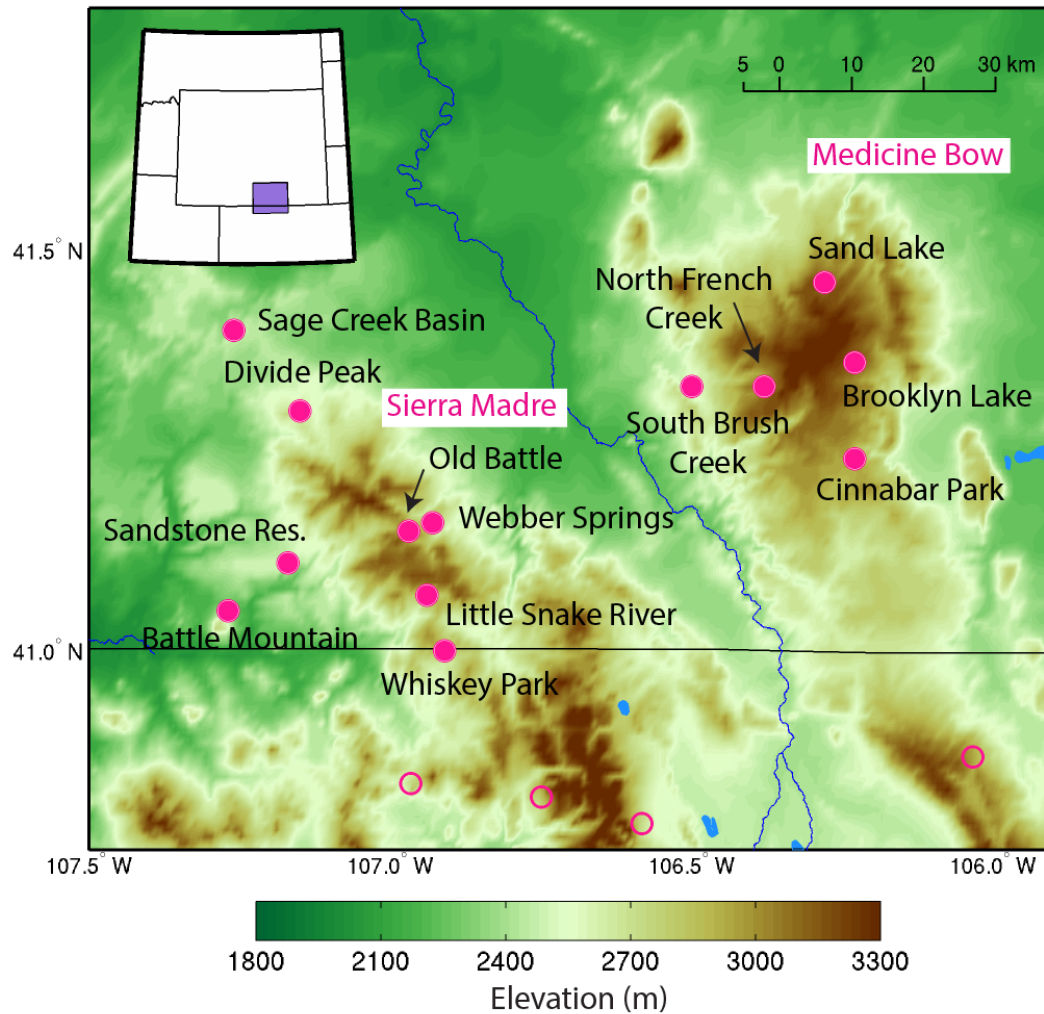


Figure 4.3. Locations of SNOTEL sites (magenta dots) in Sierra Madre and Medicine Bow Ranges. Filled magenta circles indicate the SNOTEL sites used for the evaluation of the WRF-CONUS model simulation results. Open magenta circles are the SNOTEL sites not used for the evaluation.

4.2.1. SNOTEL Precipitation Observations

In this Section, annual precipitation characteristics of the study area are presented using the SNOTEL precipitation data.

The monthly precipitation averaged over the 13 SNOTEL sites for each water year (panels a–h) and 8-year average (panel i) are shown in Figure 4.4. In Wyoming, a single snowstorm can bring heavy snowfall to the area, and the month of maximum wintertime precipitation is heavily dependent upon when big snow storms occur. As shown in Figure 4.4, the annual cycle of precipitation varies over the 8-year period. Precipitation from November through April makes up 55–75% of the annual total amount and clearly exceeds warm-season precipitation for all years examined (Table 4.2).

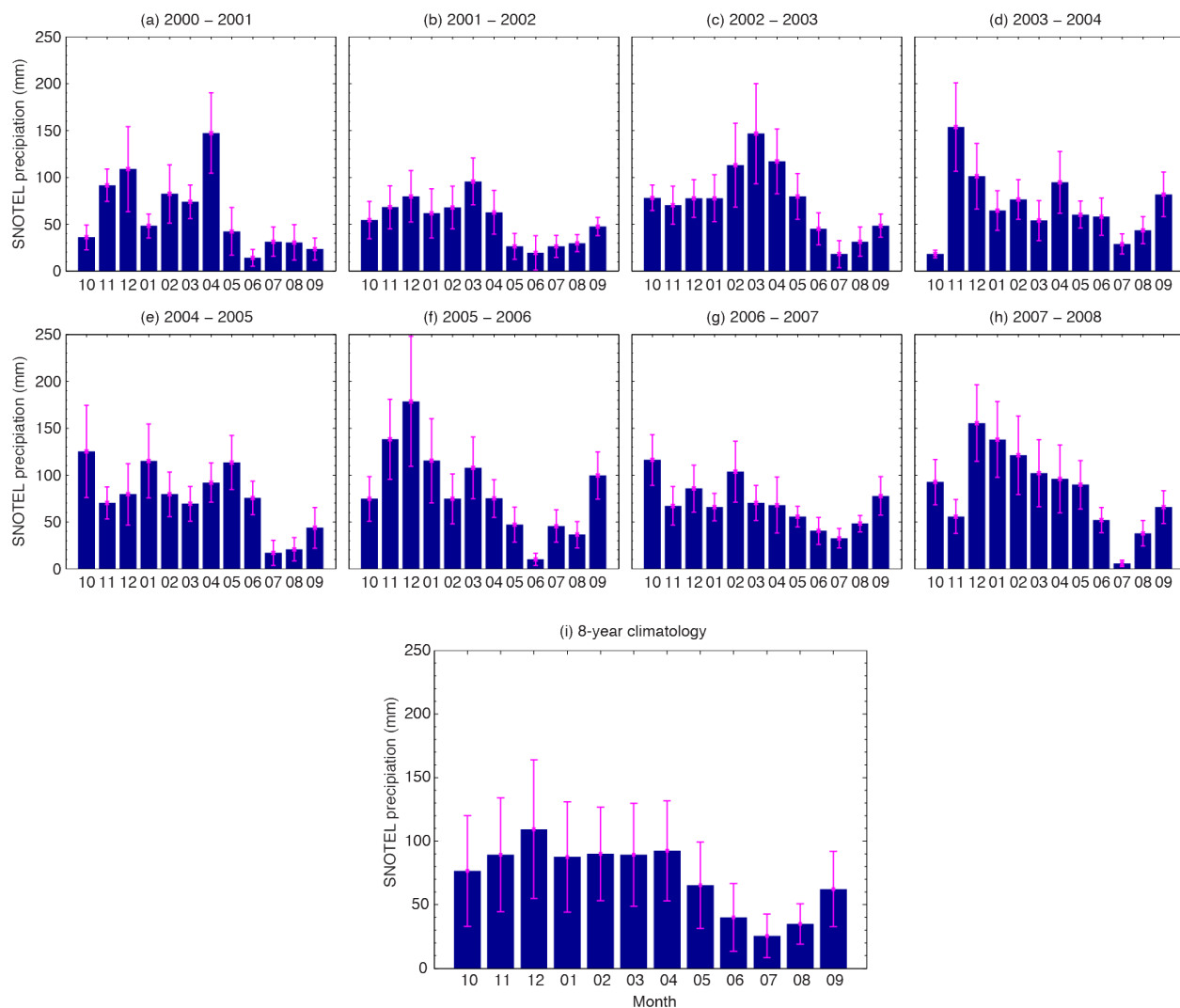


Figure 4.4. (a) – (h) Monthly precipitation averaged over 13 SNOTEL sites for each of the eight water years. (i) Eight-year climatology of monthly precipitation at 13 SNOTEL sites. Vertical bars indicate one standard deviation from the area average, representing spatial variability.

Table 4.2. Average annual precipitation from SNOTEL sites and the fraction of the annual precipitation that fell between 1 November and 30 April in each water year.

Water year	Annual precipitation (mm)	Fraction of November – April precipitation (%)
2000 – 2001	728.2	76
2001 – 2002	632.5	69
2002 – 2003	900.8	67
2003 – 2004	833.8	65
2004 – 2005	899.4	56
2005 – 2006	1001.2	69
2006 – 2007	829.2	55
2007 – 2008	1009.7	66
8-year average	854.4	65

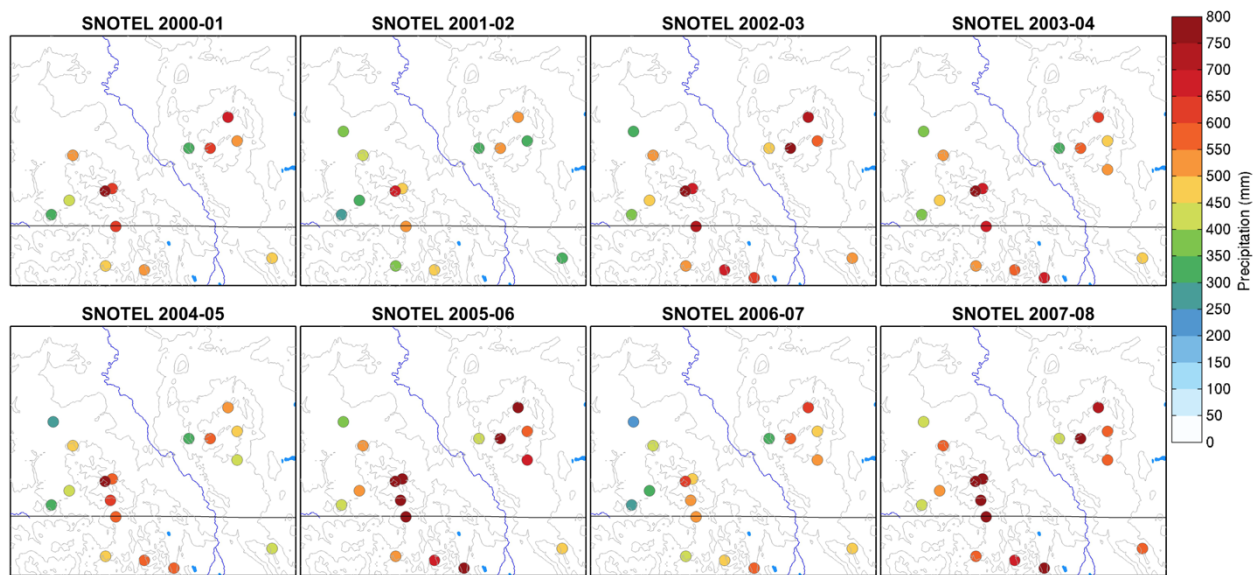


Figure 4.5. The November–April precipitation at SNOTEL sites in each water year. Contours indicate elevation.

Figure 4.5 shows the November–April precipitation at SNOTEL sites in each of the eight winter seasons. In general, high precipitation is located at high elevations.

To investigate more about precipitation characteristics over the two mountain ranges, daily SNOTEL precipitation from 1 November to 30 April was examined. Figure 4.6 shows correlation coefficients of daily precipitation between pairs of SNOTEL sites over eight, and then four winter seasons starting in the 2000–2001 and 2004–2005 seasons, respectively. The 4-year correlation coefficients are presented here because all 13 SNOTEL sites had measurements over that period while some SNOTEL sites were not active in the first 4-year period. Bright colors indicate high correlation in daily precipitation between a given pair of sites.

Overall, the correlations are high among the sites in the same range, i.e., the sites in Sierra Madre are more correlated among themselves compared with the sites in Medicine Bow and vice versa. In the Medicine Bow Range, North French Creek and Sand Lake are highly correlated in all winter seasons. This suggests that strong westerly to southwesterly storms with sufficient Froude number allow precipitation enhancement and snow to be carried over the range onto the eastern slopes. In addition, South Brush Creek is more highly correlated with North French Creek and Sand Lake than other sites in the Medicine Bow Range. Both South Brush Creek and North French Creek are on the western slope and upstream from Sand Lake (on the eastern slope) under westerly flow. The correlation among the three sites also indicates the dominance of westerly upslope storms as a mechanism of bringing snowfall over the range. Cinnabar Park precipitation seems slightly more correlated with Sand Lake and Brooklyn Lake for the years shown, all of which are located on the eastern slopes of the Medicine Bow Range. Westerly storms bring snowfall to these east slope sites as for Sand Lake, but it is difficult to make any conclusion about the westerly flow contribution to the snowfall in this area without gauge sites directly upstream (west) of Cinnabar Park.

In the Sierra Madre Range, precipitation rates at Sage Creek Basin, Divide Peak, and Sandstone Reservoir are highly correlated with each other. The three sites are located on the north and west slopes of the mountain range. The high correlations between these sites suggest that precipitation associated from northwesterly/westerly flows is dominant over this area. The correlation coefficient at Battle Mountain is the highest with Sandstone Reservoir, which also indicates the dominance of westerly storms in this area. Old Battle and Webber Springs are geographically close to each other (although Webber Springs is located downwind from Old Battle with respect to westerly flows) and have a high correlation as expected. Webber Springs, Little Snake River, and Whiskey Park, which are at high elevations in Sierra Madre, show generally high correlations with each other, suggesting orographically enhanced precipitation is the key to producing precipitation in this mountain range as it is in Medicine Bow.

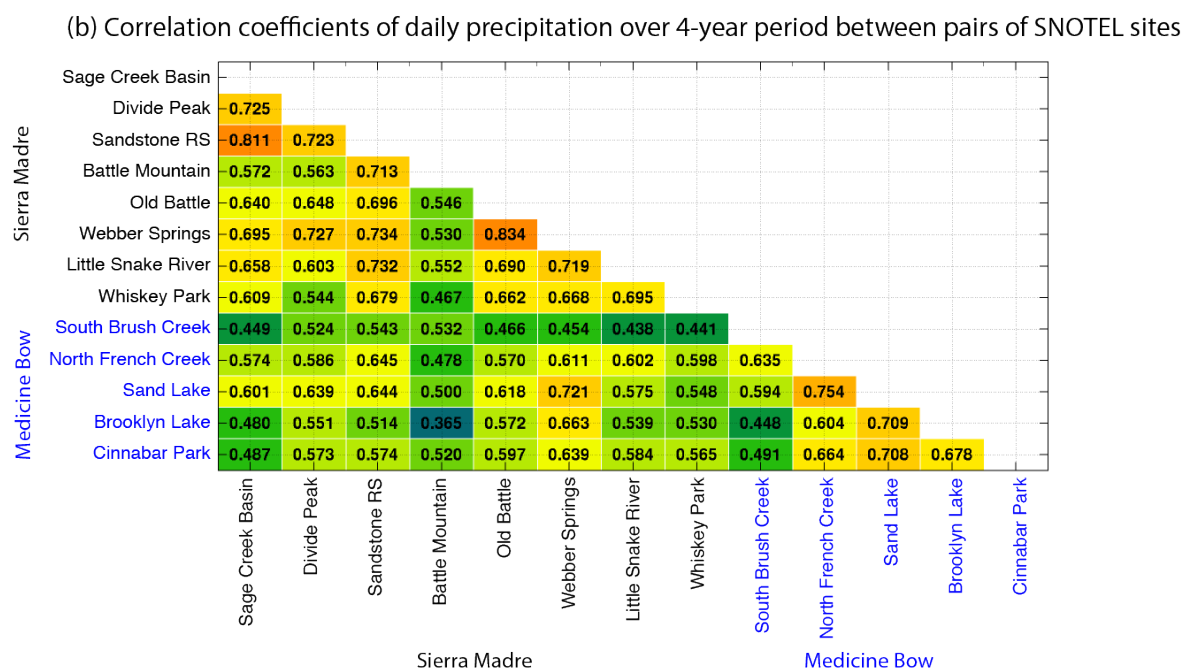
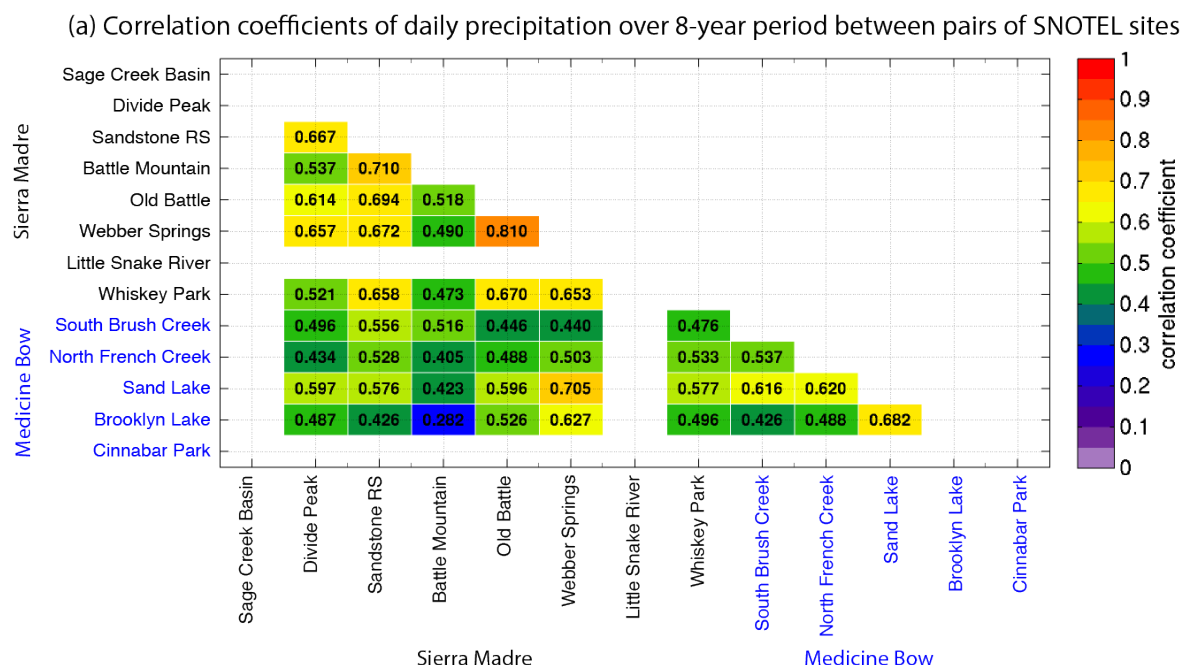


Figure 4.6. (a) Temporal correlation coefficients of daily precipitation over eight years at each pair of SNOTEL sites. (b) Same as panel (a) but excludes seasonal data from seasons 2000–2001 to 2003–2004 during which time some sites did not have measurements. SNOTEL site names in black (blue) are the sites in the Sierra Madre (Medicine Bow) Range.

Correlation coefficients for each winter season (Figure 4.7) show year-to-year variability, although similar patterns as those described based on the 8- and 4-year correlations can be seen. The year-to-year variability is related to a number of factors, such as dominant wind regimes associated with snow-producing events. For example, higher coefficients in the 2004–2005 and 2007–2008 seasons for pairs of sites in the same mountain range compared with other seasons are associated with strong southwesterly events and perhaps westerly events dominated, when

compared with other years. The low correlation coefficients from the 2001–2002 season stem from the fact that it was a dry year (and, thus, small dynamic range causing the correlation to be low).

With regard to pairs of sites between the two mountain ranges, no clear pattern is apparent from the correlation coefficient plots.

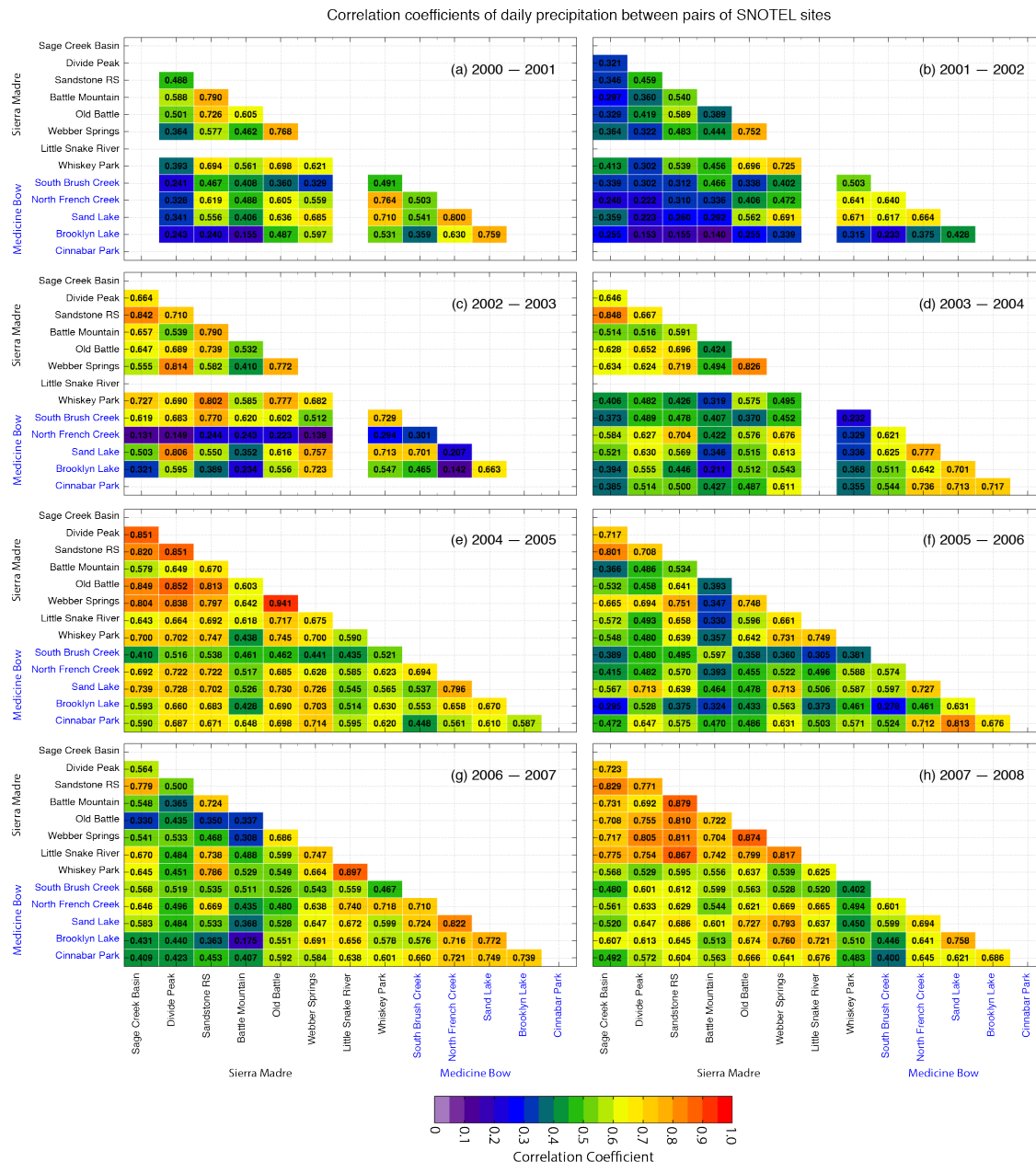


Figure 4.7. Same as Figure 4.6 but for each water year.

4.2.2. Comparison of model vs SNOTEL

Figure 4.8 shows the spatial distribution of the November–April precipitation from the WRF-CONUS simulation results for each of the winter seasons (Section 4.1.2). The spatial pattern well represents the elevation-dependent precipitation amounts as presented by the observational data

(Figure 4.5). The spatial correlation among the total seasonal precipitation from the WRF-CONUS model at each of the corresponding SNOTEL locations over the eight winter seasons ranged from 0.86 to 0.94 (although the sample size is only 5 months x 13 sites for each winter season). Averaged over the eight seasons, the spatial correlation coefficient was 0.81.

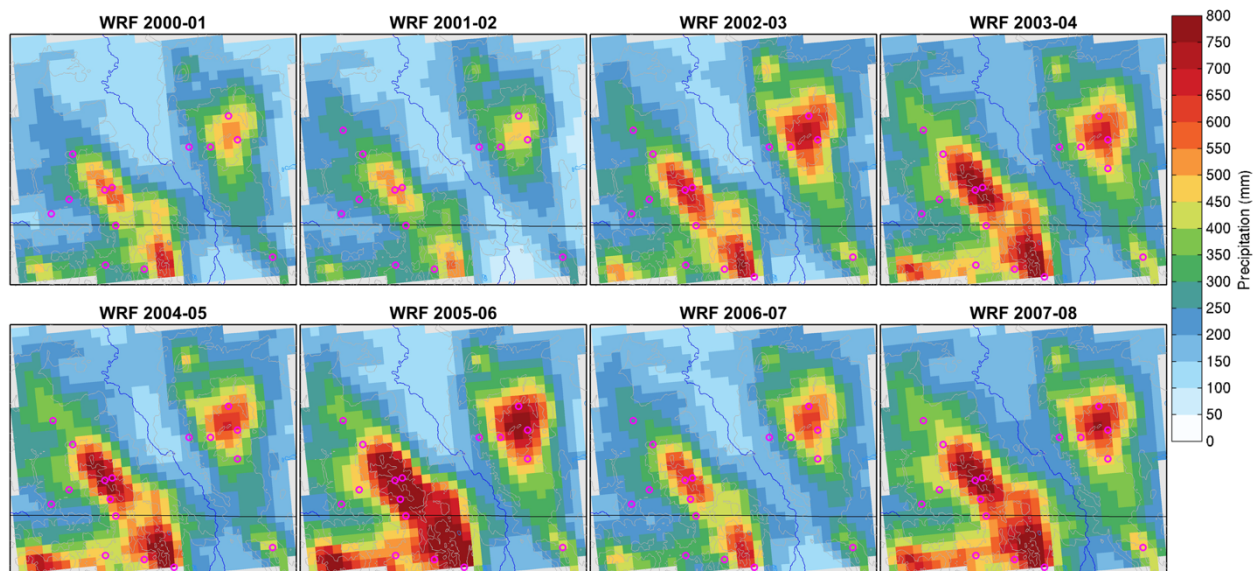


Figure 4.8. The November–April precipitation in each water year from the WRF-CONUS model simulation. Magenta circles indicate the SNOTEL site locations.

The ability for the model to reproduce observed precipitation at each site is demonstrated in Figure 4.9. The figure shows the 8-year climatology of precipitation accumulation from the model and observations at each SNOTEL site. Overall, the model is able to simulate observed precipitation well. In particular, the model performed very well at Sage Creek, Webber Springs, Little Snake (Sierra Madre sites), and Cinnabar Park (Medicine Bow site). The places at which the model had the largest systematic negative bias were Divide Peak, Old Battle, and Whiskey Park (Sierra Madre sites), and North French Creek and Sand Lake (Medicine Bow sites). With the exception of Brooklyn Lake (Medicine Bow) where a high bias in the model was noted, the remaining sites generally indicated a smaller, but still negative, bias. It is important to note that due to the availability of observations at each station, Sage Creek is a 7-year mean, Little Snake is a 4-year mean, and Cinnabar Park is a 5-year mean.

Comparisons of time-series plots of precipitation at each site for individual years (not shown) revealed that the general model tendency to simulate less precipitation than observed results from two factors: (1) relatively large snowstorms that the model missed or produced much weaker precipitation, and (2) systematic underestimation at particular SNOTEL sites. For example, the model produced significantly less snowfall than the observations for a large-scale northwesterly event in the beginning of November 2000 at nearly all of the Sierra Madre sites (not shown). A significant underestimate also occurred for a heavy westerly snowstorm in mid-December 2000. The model underestimated over both mountain ranges for this particular event (not shown).

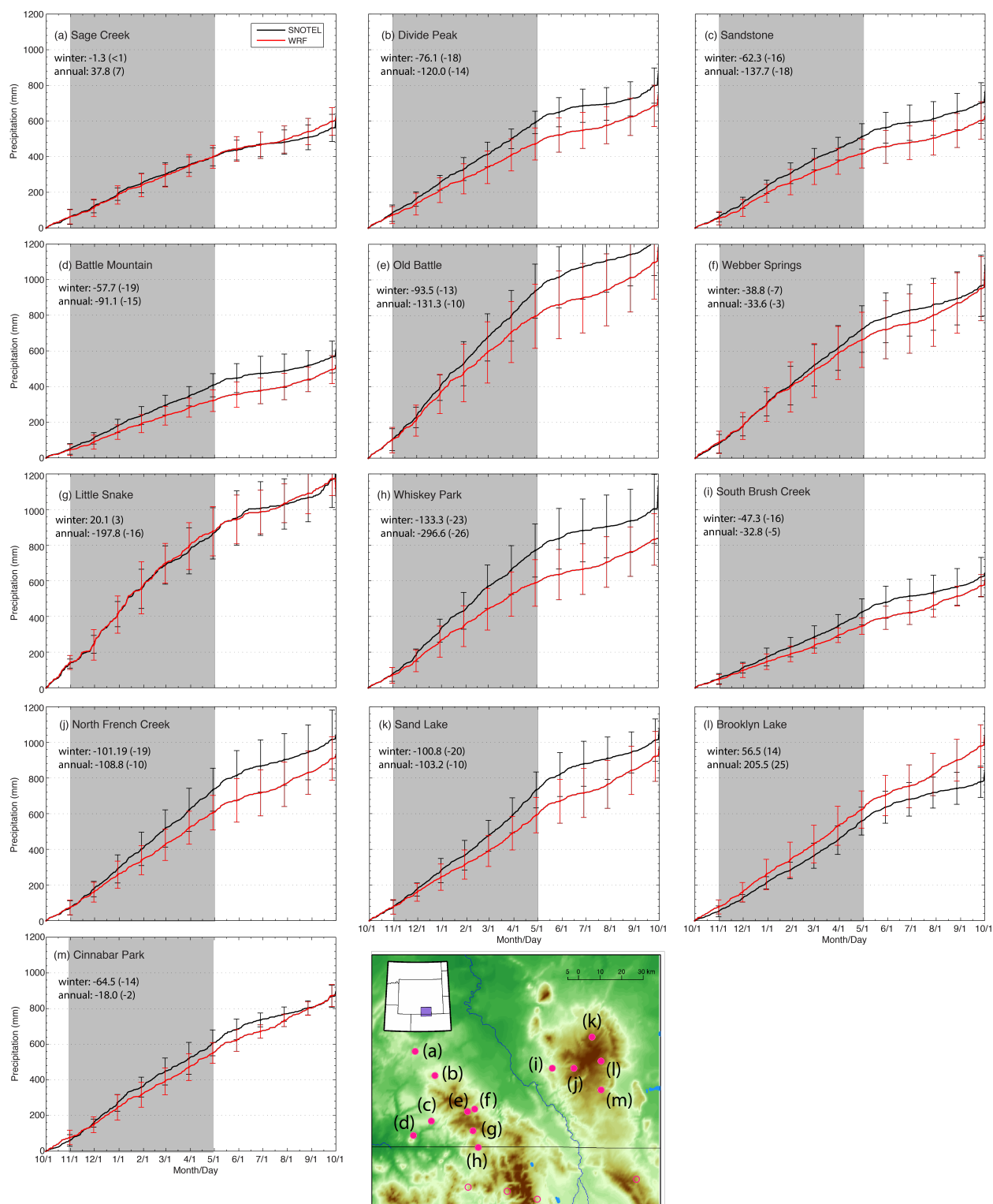


Figure 4.9. Climatology of annual precipitation accumulation at each SNOTEL site. Vertical bars are one standard deviation about the climatological mean. Average seasonal (1 November–30 April, shaded region) and annual precipitation differences are annotated in the upper left corner (model minus observation in mm). Values in parentheses indicate percent bias over the seasonal and annual time periods with respect to the observations. Refer to the map in the middle column for the location of the SNOTEL sites. Note that the values were averaged over eight years at all sites except at Sage Creek (7 years), Little Snake (4 years), and Cinnabar Park (5 years).

When precipitation is averaged over all SNOTEL sites and presented as a mean time history plot for each year (Figure 4.10), large precipitation events missed or significantly underestimated by the model are apparent. However, it is also important to emphasize that the model's ability to capture each major event is very good in some years (e.g., seasons 2004–2005 through 2006–2007).

The 8-year climatology averaged across 13 SNOTEL sites (Figure 4.11) is impacted by the large negative bias from the 2000–2001, 2002–2003, and 2007–2008 seasons. Nevertheless, the accumulation up to the end of the seeding season (30 April) is within one standard deviation from the climatological mean.

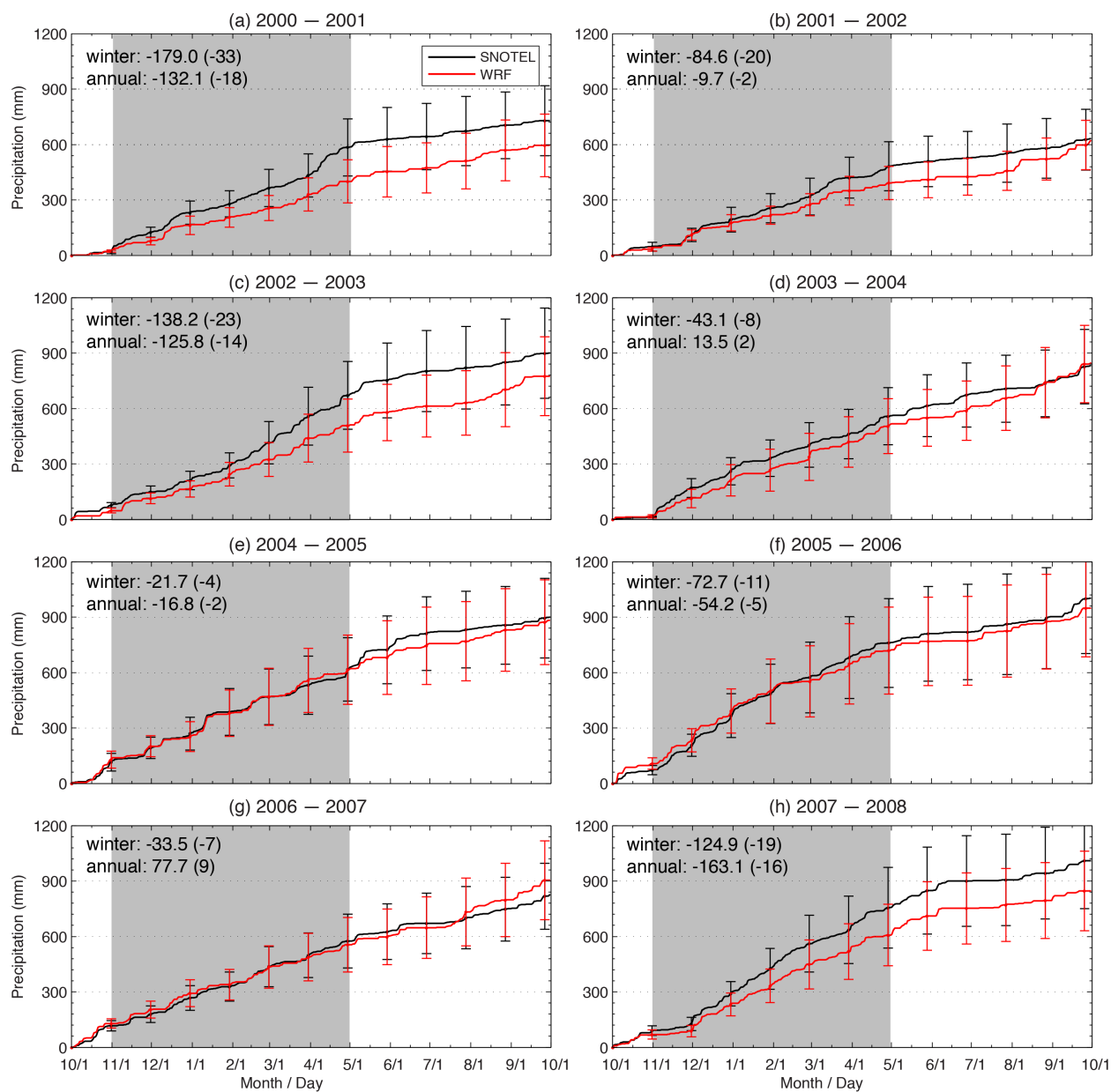


Figure 4.10. Time history of observed and simulated precipitation accumulation averaged over 13 SNOTEL sites for each water year. The difference (mm) between the model and SNOTEL precipitation observations for November–April (winter) and the full year is indicated in the upper left corners. Values in parentheses are the percent bias from the observations. The biases are taken as model minus observation.

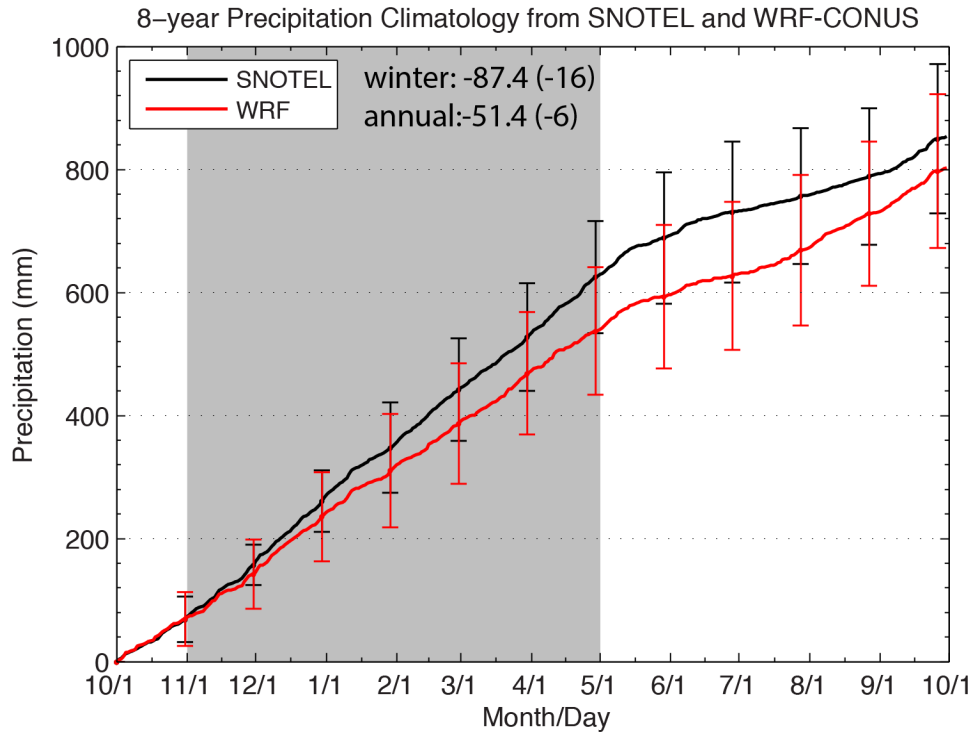


Figure 4.11. An 8-year climatology of precipitation accumulation averaged over 13 SNOTEL sites. Vertical bars are one standard deviation from the 8-year mean, representing the year-to-year variability. The difference (in mm) between the WRF-CONUS model and SNOTEL precipitation observations for November–April (winter) and the full year is indicated in the upper left corners. Values in parentheses are the percent bias from the observations. The biases are taken as model minus observation.

4.2.3. Comparison of the 8-year Headwaters and CONUS WRF model simulations

Previous subsections examined the WRF model simulation results based on a 4-km WRF run performed over CONUS (WRF-CONUS). Preceding the WRF-CONUS simulation, a WRF simulation was performed over a smaller domain covering the headwater regions of Colorado and southern Wyoming (Rasmussen et al. 2014; WRF-Headwaters, hereafter). The climatology analysis conducted by Ritzman et al. (2015) for the WWMPP utilized the WRF-Headwaters model simulation output. The WRF-CONUS simulation was performed as an extension study to the high-resolution WRF-Headwaters project to study hydrological cycle over the CONUS. Figure 4.12 displays the model domain used for the two WRF simulations. Various changes were made to the simulation setup and physical parameterization options to ensure stable and reliable model performance over a large domain for the WRF-CONUS simulation, as well as to utilize a newer version of the WRF model and updated parameterizations. Model setup and key parameterizations from the two simulations are listed in Table 4.3.

Ikeda et al. (2010) and Rasmussen et al. (2014) found that the WRF-Headwaters simulation reproduced SNOTEL measurements well over the headwater regions of Colorado. Cloud-seeding feasibility studies for other mountain ranges in Wyoming (e.g., Wind River Range, Wyoming Range) using the same dataset have also revealed that the simulation captured precipitation events over the mountain ranges well. One of the challenges inherent in a large model domain, such as in the WRF-CONUS simulation, is the deviation of weather patterns from the “truth” with increasing distance from the model boundaries (due to increasing degree of freedom in flow

fields). Consequently, moisture fields reaching the Sierra Madre and Medicine Bow Ranges may potentially differ in the WRF-CONUS run when compared with the WRF-Headwaters simulation, due to variation in time/distance for the upstream conditions to change significantly from the model boundary. While this study aimed to employ the most up-to-date high-resolution model simulation for the climatology analysis (i.e. WRF-CONUS), it is prudent to investigate the performance of the WRF-CONUS simulation compared with the WRF-Headwaters run to gauge the differences between the two model simulations. Any differences noted between the two simulations would be valuable for interpreting the results of the previous WWMPP climatology when compared with the present cloud-seeding feasibility study performed over the same region. In this subsection, the model data from the two WRF simulations are compared with explore this question.

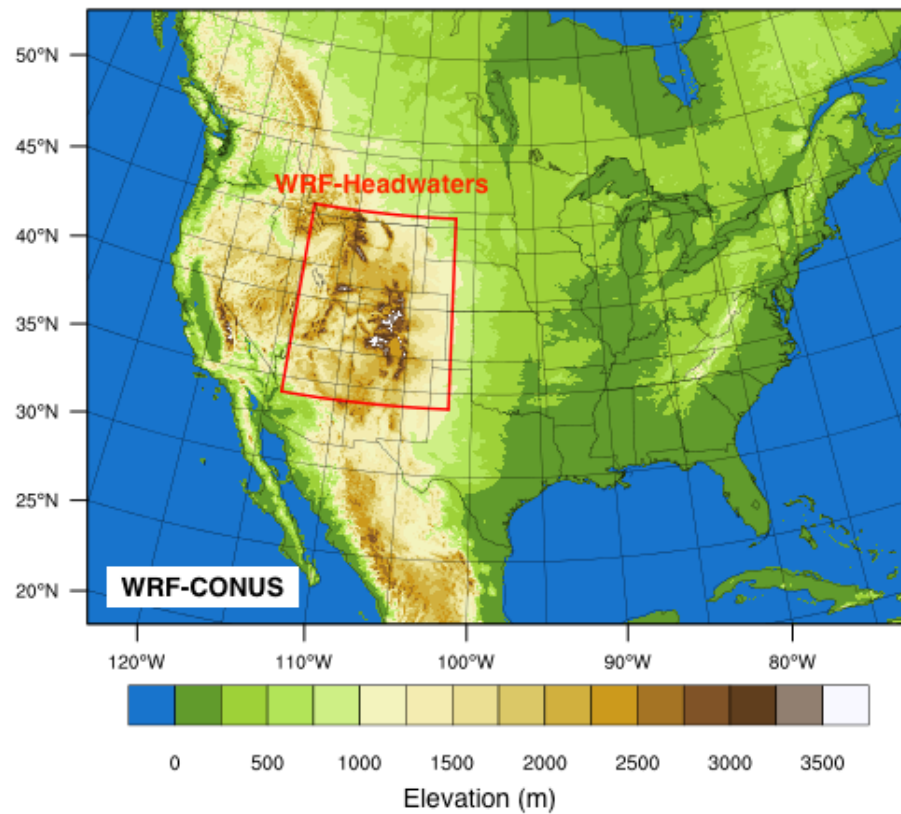


Figure 4.12. Model domain from the two high-resolution (4 km) WRF simulations. The red polygon indicates the WRF-Headwaters domain.

Table 4.3. Model setup used for the CONUS and 8-year Headwaters WRF model simulations. More details on each can be found in Rasmussen et al. (2011) and Liu et al. (2016).

	CONUS	Headwaters
WRF version	WRF v 3.4.1	WRF v 3.1.1
Horizontal Grid Resolution	4 km	4 km
Number of Vertical Levels	51	45
Microphysics	Thompson aerosol-aware scheme	Thompson scheme
Radiation	RRTMG	CAM
Land Surface	Noah-MP	Noah with improvements from Barlage et al. (2010)
Planetary Boundary Layer	Yonsei University PBL	Yonsei University PBL
Spectral Nudging	Yes	No
Number of Nest	1	1
Forcing Data	6-hourly ERA-Interim reanalysis	3-hourly North American Regional Reanalysis
Simulation Period	1 October 2000 – 30 September 2013	1 October 2000 – 30 September 2008

Figure 4.13 shows the spatial distribution of the 8-year (2000–2008) climatology of the November–April precipitation from the two models and SNOTEL observations. The spatial patterns of the two models are essentially the same, demonstrating that the overall weather systems/features are similarly reproduced. The figure also shows that the precipitation amount is slightly greater in the WRF-Headwaters run over the Sierra Madre Range than in the WRF-CONUS. The range of spatial correlation for the November–April total precipitation over the eight winter seasons was 0.73–0.91 and 0.86–0.94 from the WRF-Headwaters and WRF-CONUS simulations, respectively.

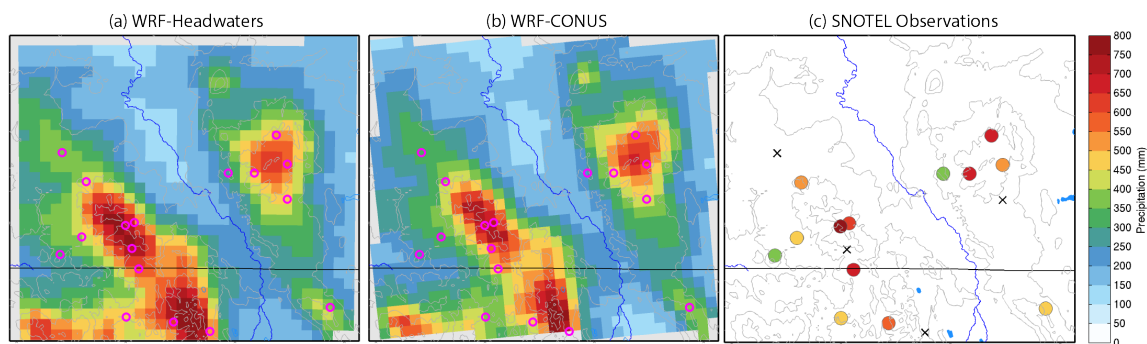


Figure 4.13. 8-year climatology of November–April precipitation from the (a) WRF-Headwaters, (b) WRF-CONUS, and (c) SNOTEL observations. Magenta circles in panels (a) and (b) show locations of the SNOTEL sites.

Comparison of precipitation accumulation between the two models shows that the WRF-Headwater has less bias for the years examined (Figure 4.14, Table 4.4), although the differences

are not statistically significant (i.e., error bars overlap in Figure 4.14) except for 2000–2001 and 2002–2003. The slightly better agreement of the WRF-Headwaters dataset for these years results from the better simulation over the Sierra Madre Range. The WRF-CONUS simulation’s relatively high negative bias at Old Battle and Whiskey Park and lesser negative bias at several other sites across the Sierra Madre Range such as Divide Peak, Webber Springs, and Sandstone was not present in the WRF-Headwaters dataset and agreed very well with the observations (not shown). This is consistent with the greater precipitation amount from the WRF-Headwaters dataset shown in Figure 4.13. Over the Medicine Bow Range, the two simulations produced nearly the same results with respect to the observations.

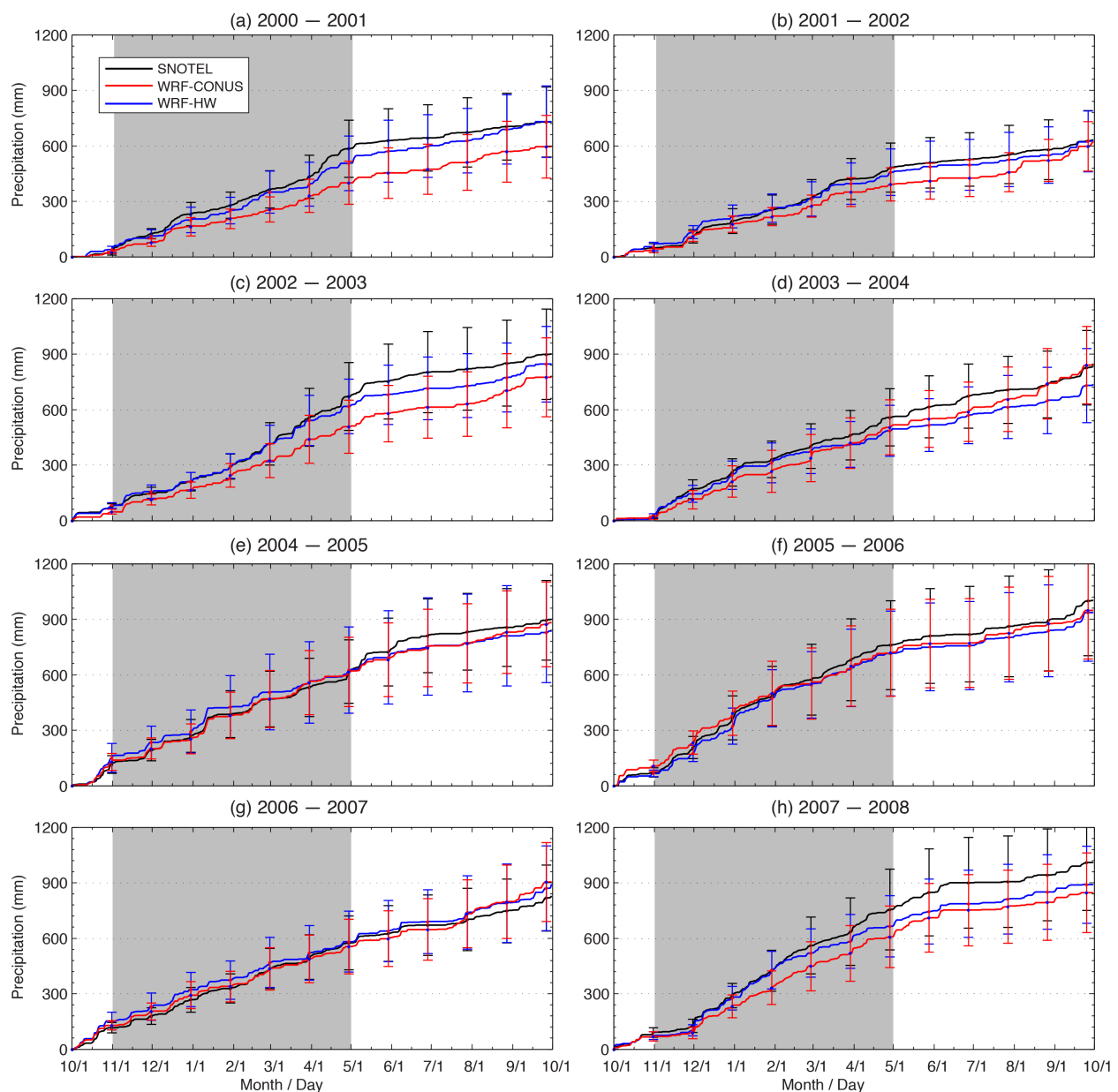


Figure 4.14. Precipitation accumulation from the WRF-Headwaters (WRF-HW) and WRF-CONUS simulations (blue and red, respectively) compared with the SNOTEL observations. Precipitation values are averaged over 13 SNOTEL sites in the study domain. Vertical bars represent one standard deviation from the spatial average.

Table 4.4. Percent bias of the November–April precipitation amount from the WRF-HW and WRF-CONUS model simulations with respect to SNOTEL observations. The percent biases were computed from observed and simulated precipitation amount averaged over the 13 SNOTEL sites.

	November–April		Annual	
	Headwaters	CONUS	Headwaters	CONUS
2000–2001	–17	–33	<1	–18
2001–2002	–11	–20	<1	–2
2002–2003	–10	–23	–6	–14
2003–2004	–16	–8	–12	2
2004–2005	–8	–4	–7	–2
2005–2006	–6	–11	–6	–5
2006–2007	–7	–7	8	9
2007–2008	–11	–19	–12	–16
8-year mean	–10	–16	–5	–6

Comparison of Model LWP with WWMPP Radiometer Observations

Data from the Cedar Creek radiometer in the Medicine Bow/Sierra Madre region are available from late 2007 through early 2012⁴, and data from the Savery radiometer are available from late 2009 through early 2012. As noted in Table 4.3, the WRF-Headwaters simulation only transpired through 2008, while the WRF-CONUS model simulation continued through 2013⁵. The short period of overlap between the model simulations and radiometer periods of record allow for a comparison of both the WRF-Headwaters and WRF-CONUS model simulations at Cedar Creek for a 1-year period (2007–2008 winter season), and a longer comparison of the WRF-CONUS model output at both radiometer sites.

2007–2008 WRF-CONUS, Headwaters, & Cedar Creek Radiometer

During the 2007–2008 winter season, the Cedar Creek radiometer operated three different scan angles. As results are very similar from each angle, but only the angle with the least outages will be considered herein. Figure 4.15 through Figure 4.17 show monthly time-series plots of observed LWP and the WRF-CONUS model LWP extracted at the Cedar Creek site along the selected scan angle. The differences between the modeled and observed values are overlaid in green. Given that the model and observations use different temporal resolutions, the mean of the observations in a 20-minute window surrounding the model time are used to calculate the differences. Note that a period of missing differences can be used to differentiate between periods of missing observations and periods of observations with a value of zero. The model shows minimal phase error and low magnitude error; errors in magnitude tend to be positive (over-predicting values during periods with liquid water or incorrectly predicting a period of liquid water).

⁴ With the exception of January 2008, during which time the Cedar Creek radiometer data is unavailable.

⁵ At the time the climatology analysis was performed for this study the entire WRF-CONUS simulation was not complete and so the climatology only focuses on the 2000–2008 period, which is coincident with the WRF-Headwater simulation period.

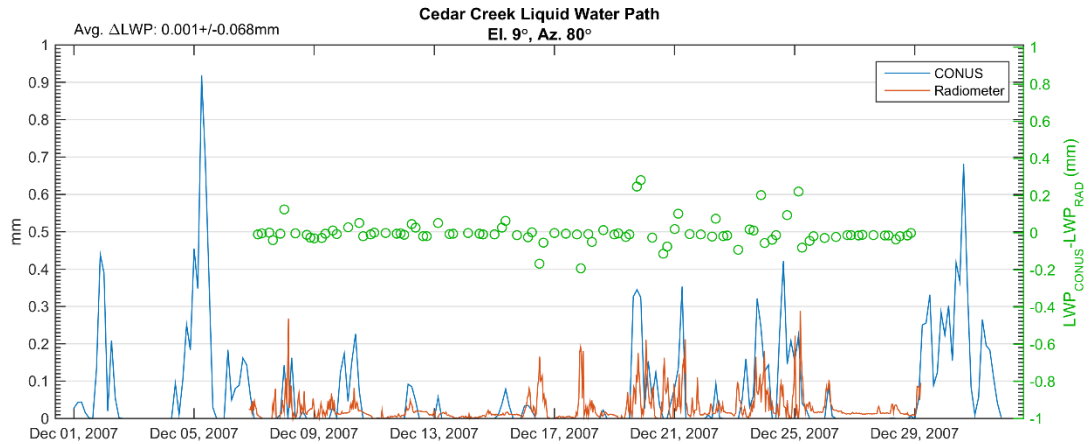


Figure 4.15. December 2007 observed (red) and WRF-CONUS modeled (blue) LWP at the Cedar Creek radiometer site for the 9-degree elevation, 80-degree-azimuth scan angle. The difference (model minus twenty-minute observed mean) is shown in green (right axis).

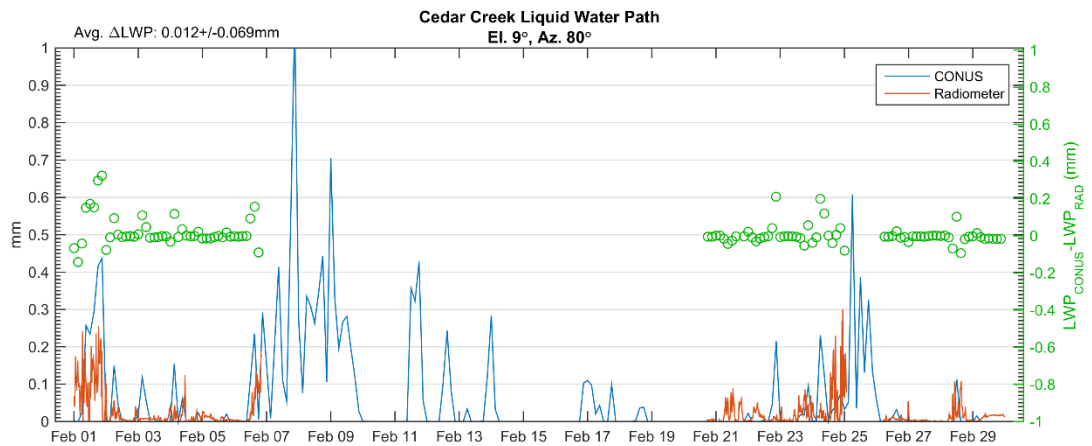


Figure 4.16. As in Figure 4.15, but for February 2008.

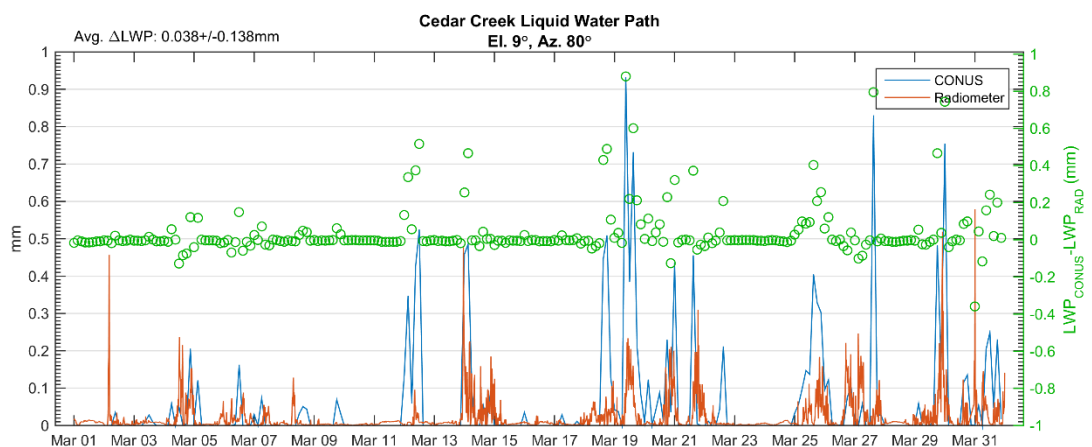


Figure 4.17. As in Figure 4.15, but for March 2008.

Monthly time series of LWP extracted from the WRF-Headwaters model compared with observations are shown in Figure 4.18–Figure 4.20. Similar to the WRF-CONUS model, the

WRF-Headwaters shows very good timing for correctly predicted events, but frequently predicted false alarms (which occurred only rarely in the WRF-CONUS comparison) and generally higher values during observed events.

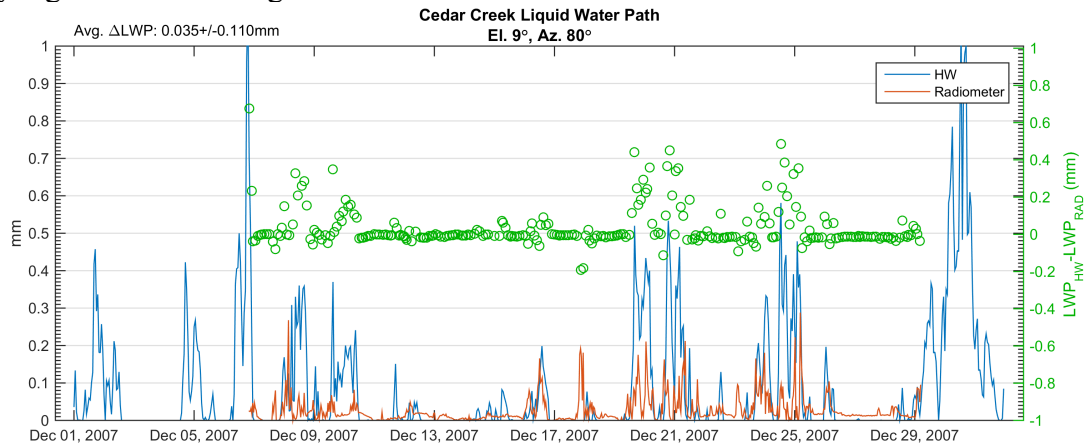


Figure 4.18. December 2007 observed (red) and WRF-Headwaters modeled (blue) LWP at the Cedar Creek radiometer site for the 9-degree elevation, 80-degree-azimuth scan angle. The difference (model minus twenty-minute observed mean) is shown in green (right axis).

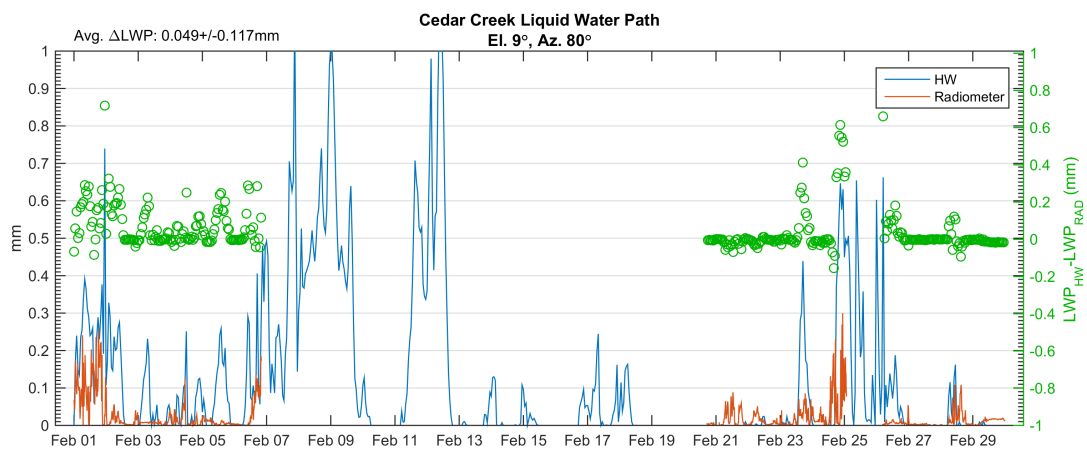


Figure 4.19. As in Figure 4.18, but for February 2008.

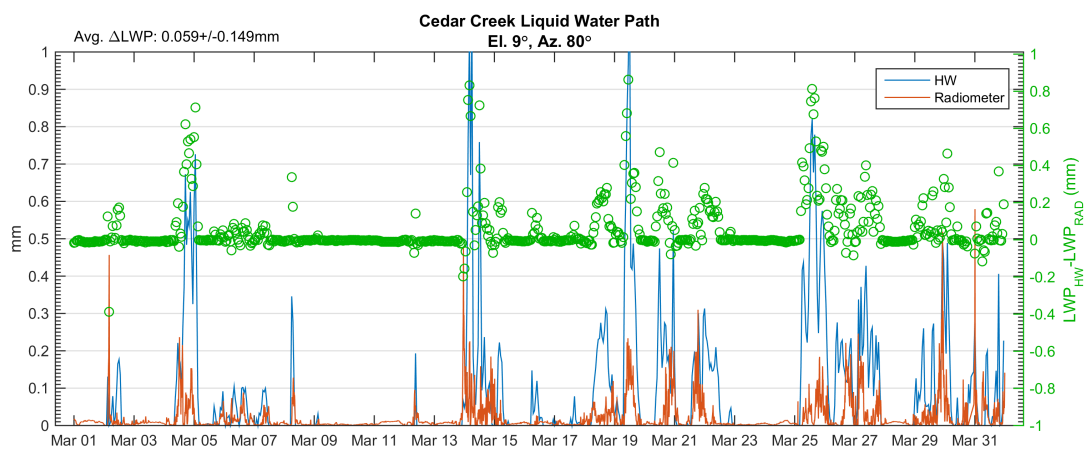


Figure 4.20. As in Figure 4.18, but for March 2008.

Figure 4.21 contains boxplots of modeled and observed nonzero LWP (defined as greater than 0.05 mm to account for high-frequency noise remaining in the observations) for each month in the 2007–2008 season that had observed data. Given the quantity and duration of data outages, only model points that have an observed value within thirty minutes are included. The boxplots confirm the belief that both models tend to over-predict values. The distribution of LWP from the WRF-Headwaters model includes even greater values than the WRF-CONUS during December, is very similar in February, and is narrower than the WRF-CONUS distribution in March. Thus, while the bias is positive for both models across the 2007–2008 season, the degree and distribution of error varies month-to-month.

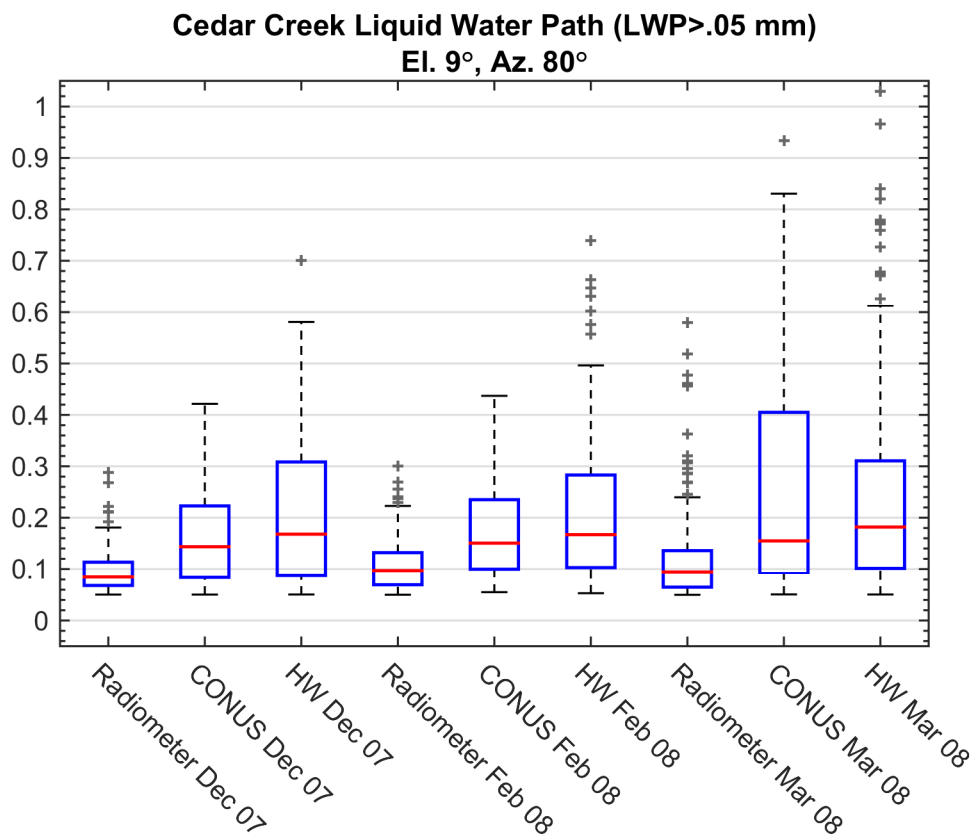


Figure 4.21. Monthly boxplots of non-zero (>0.05 mm) observed and modeled liquid-water path at the Cedar Creek radiometer for the 9-degree elevation, 80-degree-azimuth angle scan. The red line denotes the median value; the box extents are the 25th and 75th percentiles; whiskers extend to the last non-outlying point; outliers are denoted by gray plusses.

2008–2012 WRF-CONUS, Cedar Creek Radiometer, and Savery Radiometer

Because the WRF-CONUS model has a lengthier simulation period than WRF-Headwaters—extending farther into the years during the WWMPP—a comparison with the WWMPP radiometer data can be performed over a longer time period. This offers the additional benefit of then being able to include a second radiometer (Savery) for comparison. As with the 2007–2008 data, the comparisons between the model and Cedar Creek radiometer are very similar across all angle scans, and thus discussion is limited to the angle with the least data outages (again, 9-degree elevation, 80-degree azimuth); only one angle was available from the Savery radiometer.

Seasonal (November–April) time series of observed and WRF-CONUS modeled LWP are shown in Figure 4.22–Figure 4.28. As with the 2007–2008 season, the timing of events at the Cedar Creek site is very good, the frequency of false alarms is relatively low, and magnitudes compare well but are slightly high. In contrast, the timing is not as accurate at the Savery site, but the magnitudes compare exceptionally well. The boxplots shown in Figure 4.29 and Figure 4.30 corroborate this, illustrating that the modeled distributions contain higher values, but comparable medians at Cedar Creek and very similar distributions at Savery.

These results indicate that the WRF-CONUS model is capable of simulating realistic LWP and precipitation events. Given the WRF-CONUS simulated LWP events closer to those observed than WRF-Headwaters, it is the selected model simulation used for the purpose of the climatology analysis.

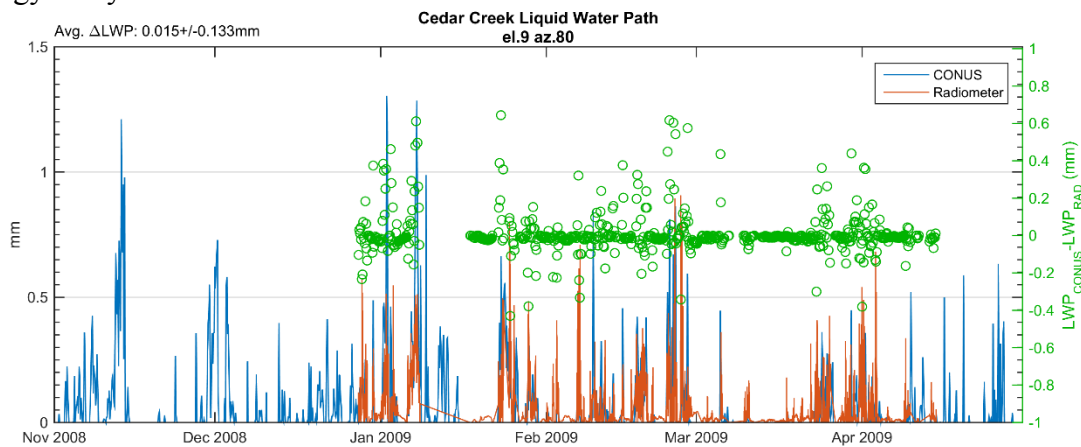


Figure 4.22. November 2008–April 2009 observed (red) and WRF-CONUS modeled (blue) LWP at the Cedar Creek radiometer site for the 9 degree elevation, 80 degree azimuth scan angle. The difference (model minus twenty-minute observed mean) is shown in green (right axis).

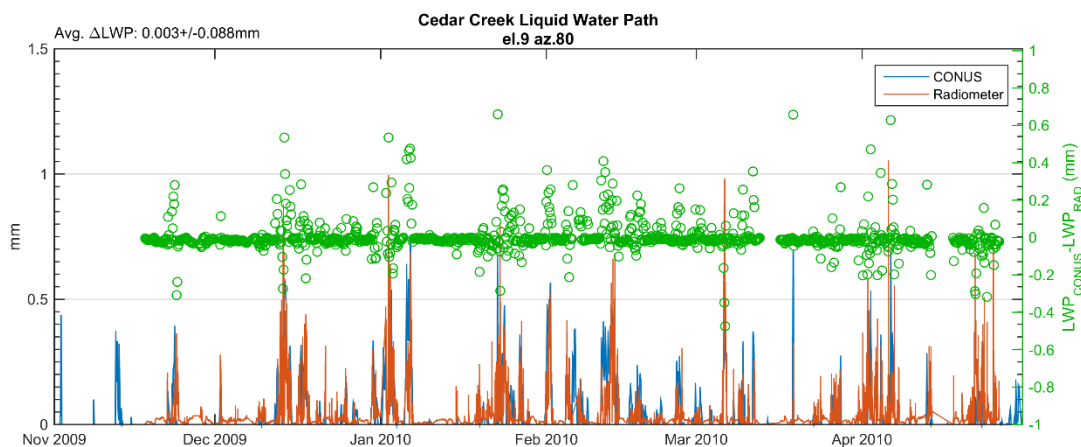


Figure 4.23. As in Figure 4.22, but for the 2009-2010 season.

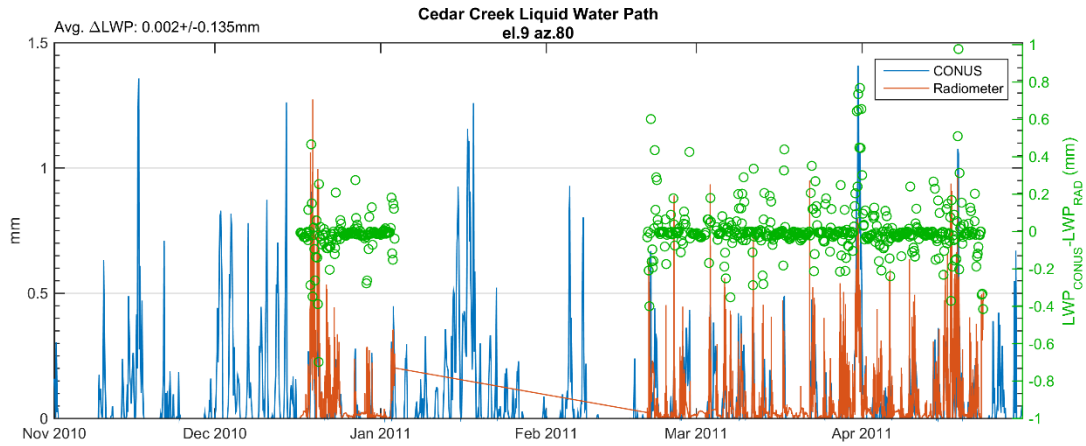


Figure 4.24 As in Figure 4.22, but for the 2010-2011 season.

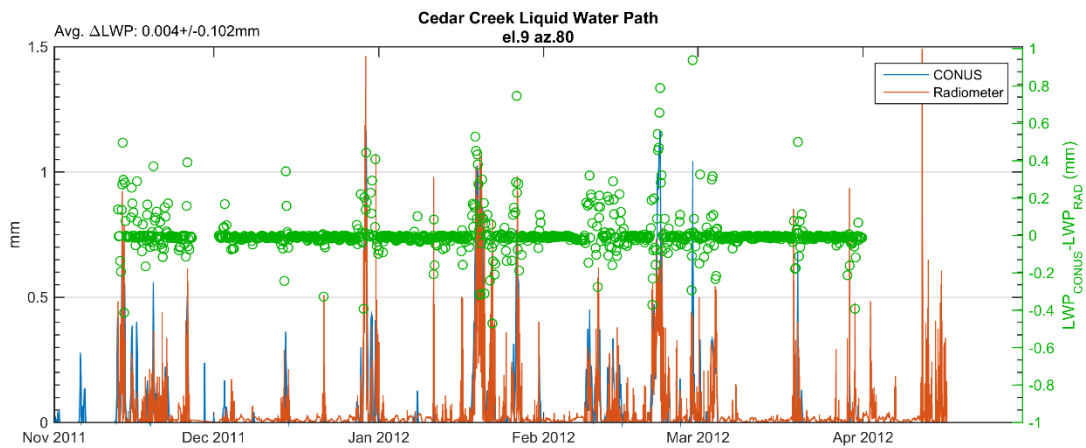


Figure 4.25. As in Figure 4.22, but for the 2011-2012 season.

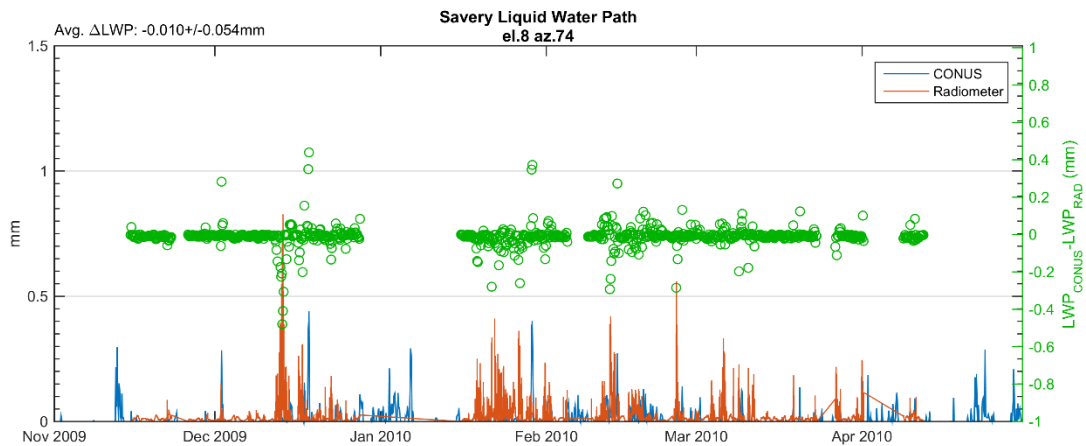


Figure 4.26. As in Figure 4.22, but for the Savery radiometer and the 2009-2010 season.

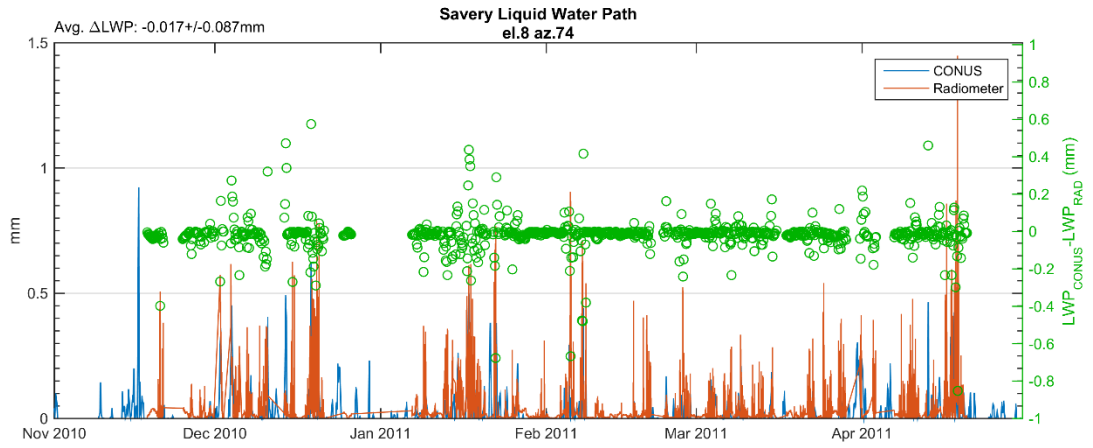


Figure 4.27. As in Figure 4.22, but for the Savery radiometer and the 2010-2011 season.

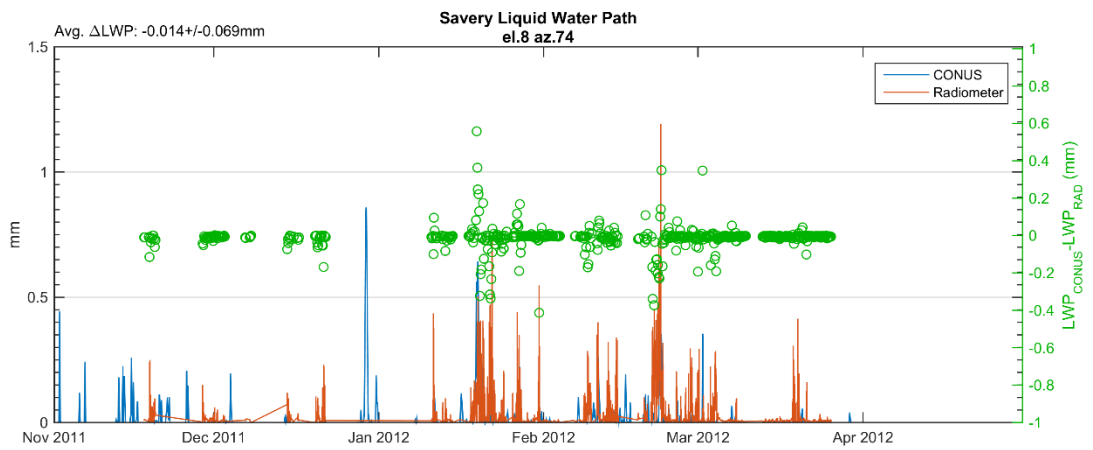


Figure 4.28. As in Figure 4.22, but for the Savery radiometer and the 2011-2012 season.

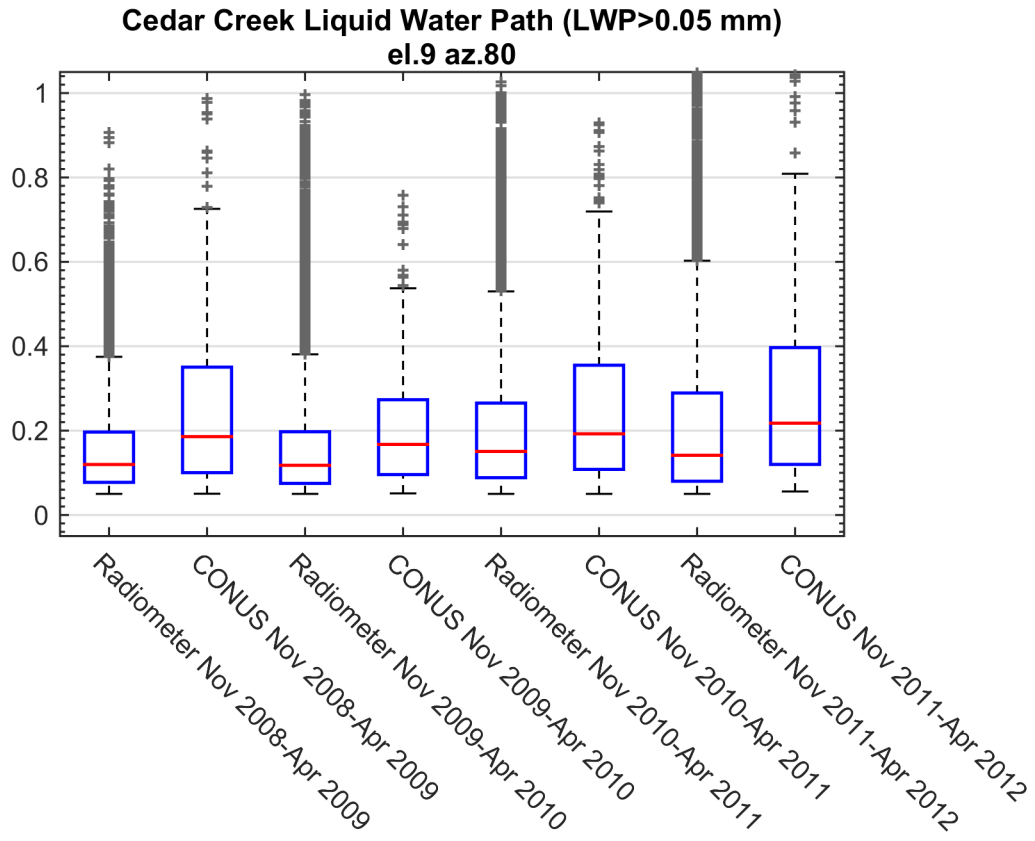


Figure 4.29. Seasonal boxplots of non-zero (>0.05 mm) observed and modeled LWP at the Cedar Creek radiometer for the 9 degree elevation, 80 degree azimuth angle scan. The red line denotes the median value; the box extents are the 25th and 75th percentiles; whiskers extend to the last non-outlying point; outliers are denote by gray plusses.

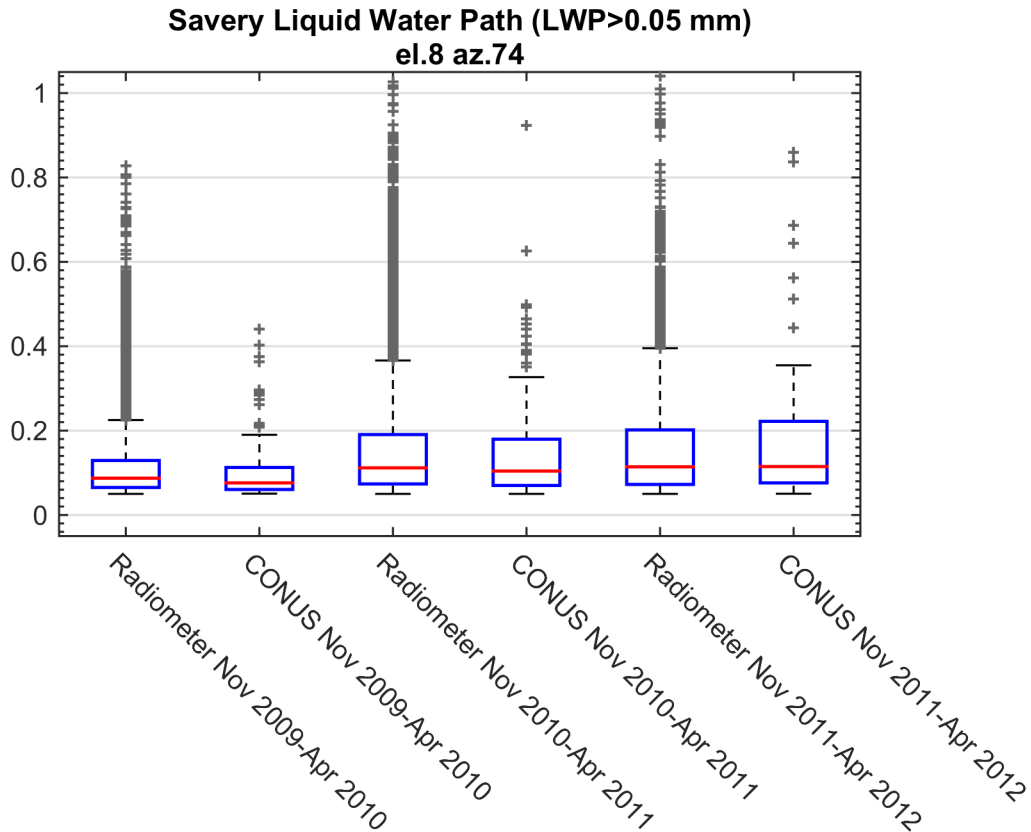


Figure 4.30. As in Figure 4.29, but for the Savery radiometer.

4.3. Model-based Climatology

4.3.1. Single Site Analysis

Single-site analysis using the WRF-CONUS model output of the 700-hPa winds during seedable conditions ($LWP > 0.01$ mm, $-18^{\circ}\text{C} < T < -6^{\circ}\text{C}$) are shown for Savery, Saratoga, Cedar Creek, and Centennial in Figure 4.31. When looking at the complete 8-year period during modeled precipitation events between November and April, the 700-hPa winds over Savery are usually just north of westerly, then due westerly, followed by fewer cases with southwesterly and north-northwesterly winds. A similar distribution to Savery is also noted at Saratoga; however, for this site the winds are less often southwesterly and more often north-northwesterly with occasional north-northeasterly cases. In general, the 700-hPa winds at Cedar Creek during precipitation events are similar to Savery with a focused distribution for west and west-northwesterly cases. For the Centennial site, precipitation occurs during a variety of wind directions, with all quadrants having at least a few events associated with those wind directions. Overall, the 700-hPa winds are most frequently from either the westerly or northeasterly directions during precipitation events at this site.

An important factor to note in this analysis is the number of total samples from each site, which represents a general frequency of seedable conditions because the sample size included in these plots depends not only on precipitation occurring at the selected gauge site, but also requires the

LWP and temperature criteria be met for seeding. While Savery and Cedar Creek experienced around 1,100 and 1,400 events, respectively, Saratoga experienced just under 700 and Centennial with much fewer at 267 total events.

For the sites that have a large sample size of precipitation events (i.e., Savery and Cedar Creek), year-to-year variability of the November–April distribution is minimal and the dominant direction is between the west-southwest to northwest quadrant. For Saratoga and Centennial, there is greater variability in the 700-hPa winds from year-to-year for the substantially fewer precipitation events (not shown).

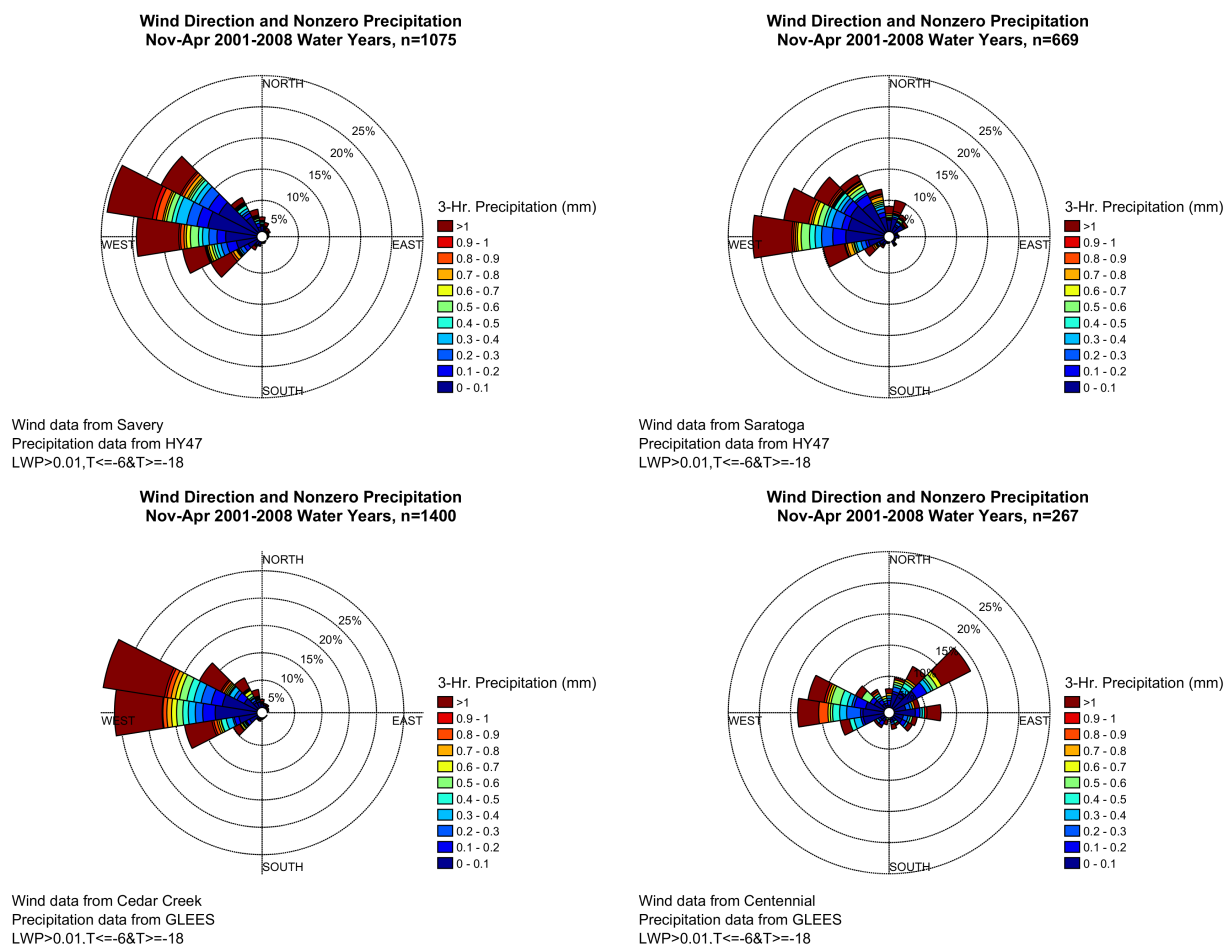
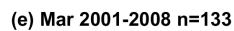
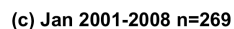


Figure 4.31. Wind rose plots showing the frequency of modeled 700 hPa wind direction at (clockwise from top left) Savery, Saratoga, Cedar Creek, and Centennial when precipitation occurred at the HY47 precipitation gauge site for a and b and the GLEES precipitation gauge site for c and d from November–April over the 8-year period. The amount of precipitation per 3-hourly model output time for each wind direction is indicated by the color shading within each wind direction bin.

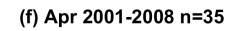
The 700-hPa wind directions during precipitation events do vary somewhat by month with a general shift towards more events occurring with northerly to northeasterly wind components into March and April, especially for the Saratoga and Centennial sites (Figure 4.32, Savery; Figure 4.33, Saratoga).

(a) Nov 2000-2007 n=104



Wind data from Savery
Precipitation data from HY47
LWP>0.01,T<=-6&T>=-18

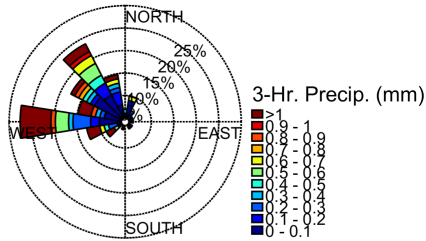
(b) Dec 2000-2007 n=320



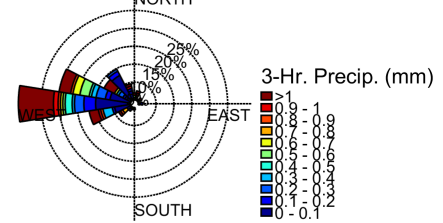
47

Wind Direction and Nonzero Precipitation

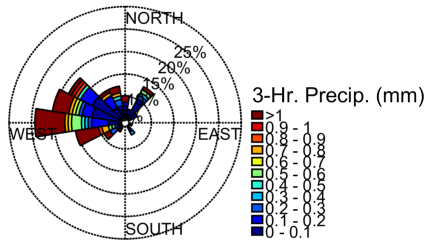
(a) Nov 2000-2007 n=102



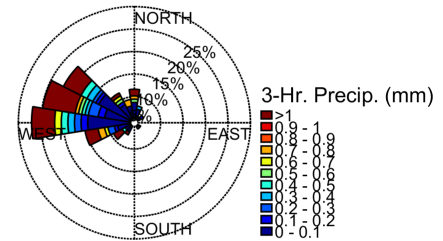
(b) Dec 2000-2007 n=153



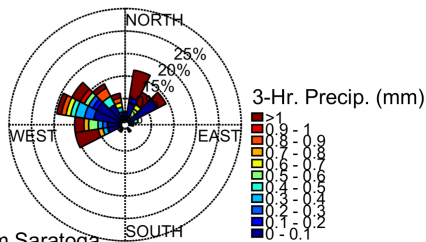
(c) Jan 2001-2008 n=135



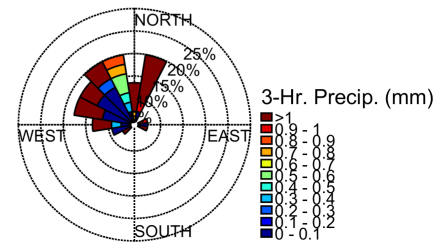
(d) Feb 2001-2008 n=136



(e) Mar 2001-2008 n=96



(f) Apr 2001-2008 n=47



Wind data from Saratoga
Precipitation data from HY47
LWP>0.01,T<=-6&T>=-18

Figure 4.33. Month-by-month wind roses of modeled 700 hPa wind direction for 3-hourly output times at Saratoga with precipitation over HY47 gauge site from November–April over the 8-year period.

The modeled 700-hPa temperatures over an average winter season at the four sites ranged consistently from 10 °C to –22 °C; however, when precipitation did occur, the range was narrowed between 2 °C to –20 °C (Figure 4.34). For Savery, Saratoga, and Cedar Creek, roughly 50% of the wintertime hours over the 8-year period were warmer than –6 °C, whereas approximately 30% of the hours with precipitation were warmer than –6 °C. The percentages were higher at Centennial with approximately 58% and 38%, respectively.

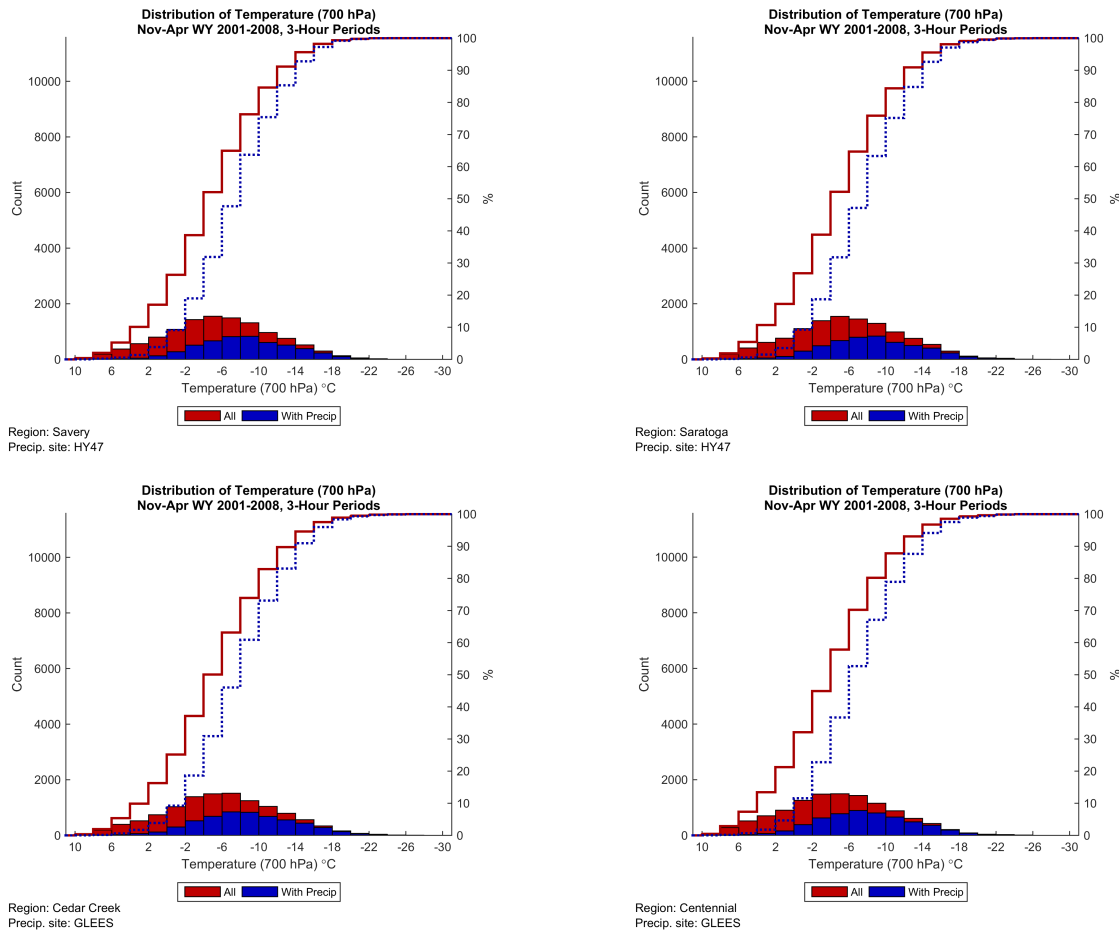


Figure 4.34. Histogram counts (left ordinate) of the 700 hPa modeled temperature at (clockwise from top left) Savery, Saratoga, Cedar Creek, and Centennial for all 3-hourly output between November and April from the 8-year period (red) and for all 3-hourly output that had precipitation (blue) at the precipitation gauge site of HY47 (Sierra Madre sites) or GLEES (Medicine Bow sites). Cumulative distributions for all (red) and output hours with precipitation (blue dotted) are also overlaid using the right ordinate (%).

4.3.2. Area-based Analysis

The Sierra Madre and Medicine Bow Ranges were separated into three and two regions, respectively, to further analyze the frequency of seedable conditions. The regions include SMWest, SMEast, SMSouth, MBWest, and MBEast (see Figure 4.2). Regardless of region examined, wintertime temperature in the ground-seeding layer (0–1 km AGL; GS) ranged from as warm as 8 °C to as cool as –22 °C; however when precipitation did occur, the temperatures were narrowed between 0 °C and –22 °C (Figure 4.35). This result is also consistent with the modeled 700-hPa temperature distribution at four selected sites in the Sierra Madre and Medicine Bow Ranges (Figure 4.34). While the minimum and maximum of the temperature range during precipitation events are similar between the regions, there is a shift in the distribution to colder temperatures for the west and south regions, when compared with the east regions for both Sierra Madre and Medicine Bow Ranges. Specifically, the temperature is colder than –6 °C when precipitation is falling 87 (88)% of the time for SMWest (MBWest), but drops to 82 (84)% of the time for SMEast (MBEast).

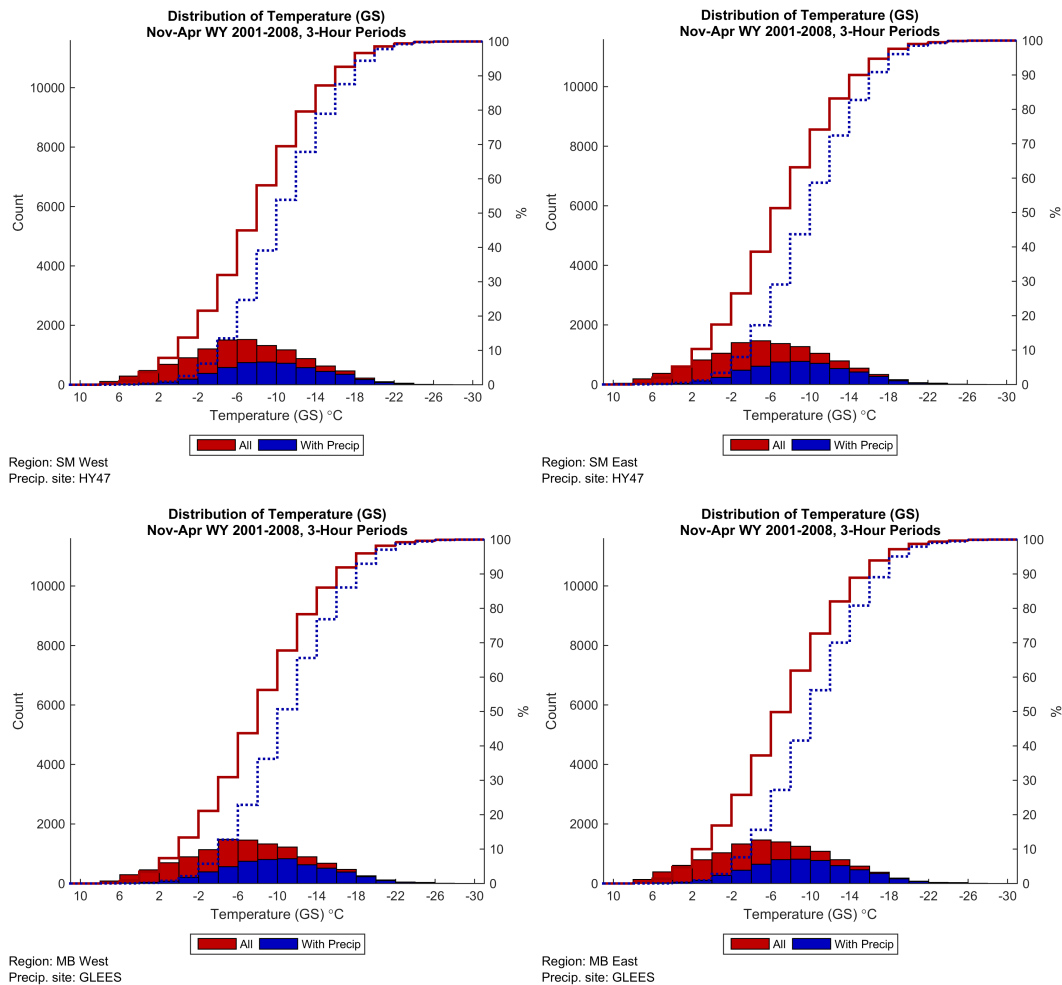


Figure 4.35. Histogram counts (left ordinate) of the area-averaged 0–1 km AGL modeled temperature for ground seeding (GS) over (clockwise from top left) SMWest, SMEast, MBWest, and MBEast for all 3-hourly output between November – April from the 8-year period (red) and for all 3-hourly output that had precipitation (blue) at the precipitation gauge site of HY47 (Sierra Madre sites) or GLEES (Medicine Bow sites). Cumulative distributions for all (red) and output hours with precipitation (blue dotted) are also overlaid using the right ordinate (%).

The distribution of LWC over each of the regions shows that approximately 50–60% of all wintertime hours exhibited no LWC and nearly 12–27% of the hours with precipitation had no LWC (Figure 4.36). The MBWest region has the highest percentage of LWC present (49% of all hours and 87% with precipitation), followed by SMWest (44%, 84%), and SMSouth (42%, 80%), with the MBEast (40%, 72%) and SMEast (39%, 78%) regions having the lowest frequency. Given this, when precipitation occurs, there is seeding potential (when considering only LWC) around 85% of the time on the western slopes of the Sierra Madre and Medicine Bow Ranges, dropping to an average of 75% of the time on the eastern slopes of each range. Of course, suitable temperatures are also necessary and the union of the requirements are explored in more detail below. In general, the SM/MBWest regions have a higher values of LWC (illustrated as a longer tail in the LWC distribution) than the East regions and the East regions have a slightly higher fraction of hours with precipitation that have zero LWC. This suggests that the East regions have less overall LWC as compared with the West regions. Figure 4.36 also suggests that some situations occur where LWC is present but there is no precipitation occurring

(red bar extending above the blue bar for $LWC > 0$). These are also potentially seedable situations if the temperature is suitable.

The histogram of LWP is similar to the LWC histogram for the ground-seeding layer (Figure 4.37) for the SMWest and MBWest regions. This implies the majority of the liquid water in the vertically integrated LWP value is concentrated in the lowest layer of the atmosphere. In contrast, for SMEast and MBEast there are relatively fewer occurrences of zero LWP (regardless of precipitation) suggesting there is more liquid water at higher levels for these regions. The implication for the feasibility of airborne seeding for each region will be described more below.

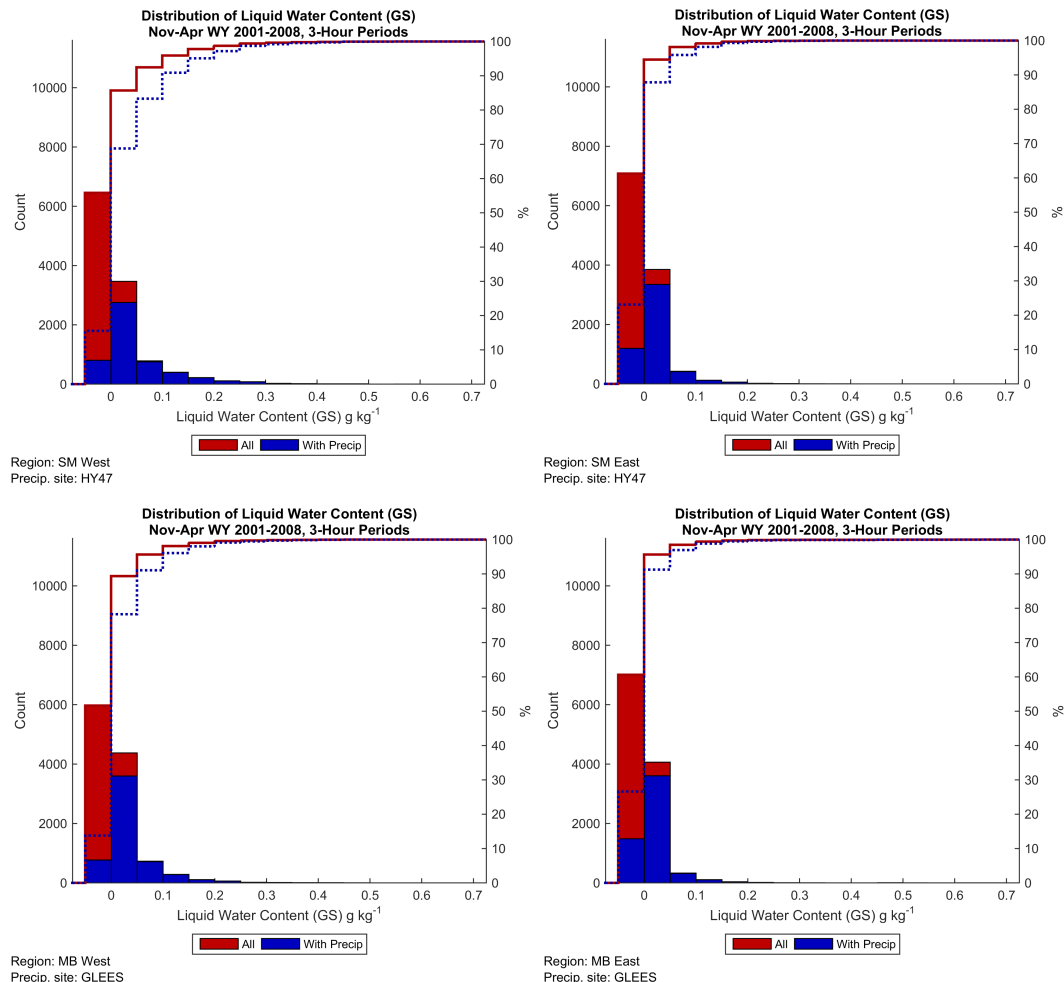


Figure 4.36. Histogram counts (left ordinate) of the area-averaged 0–1 km AGL modeled LWC for ground seeding (GS) over (clockwise from top left) SMWest, SMEast, MBWest, and MBEast for all 3-hourly output between November and April from the 8-year period (red) and for all 3-hourly output that had precipitation (blue) at the precipitation gauge site of HY47 (Sierra Madre sites) or GLEES (Medicine Bow sites). Cumulative distributions for all (red) and output hours with precipitation (blue dotted) are also overlaid using the right ordinate (%).

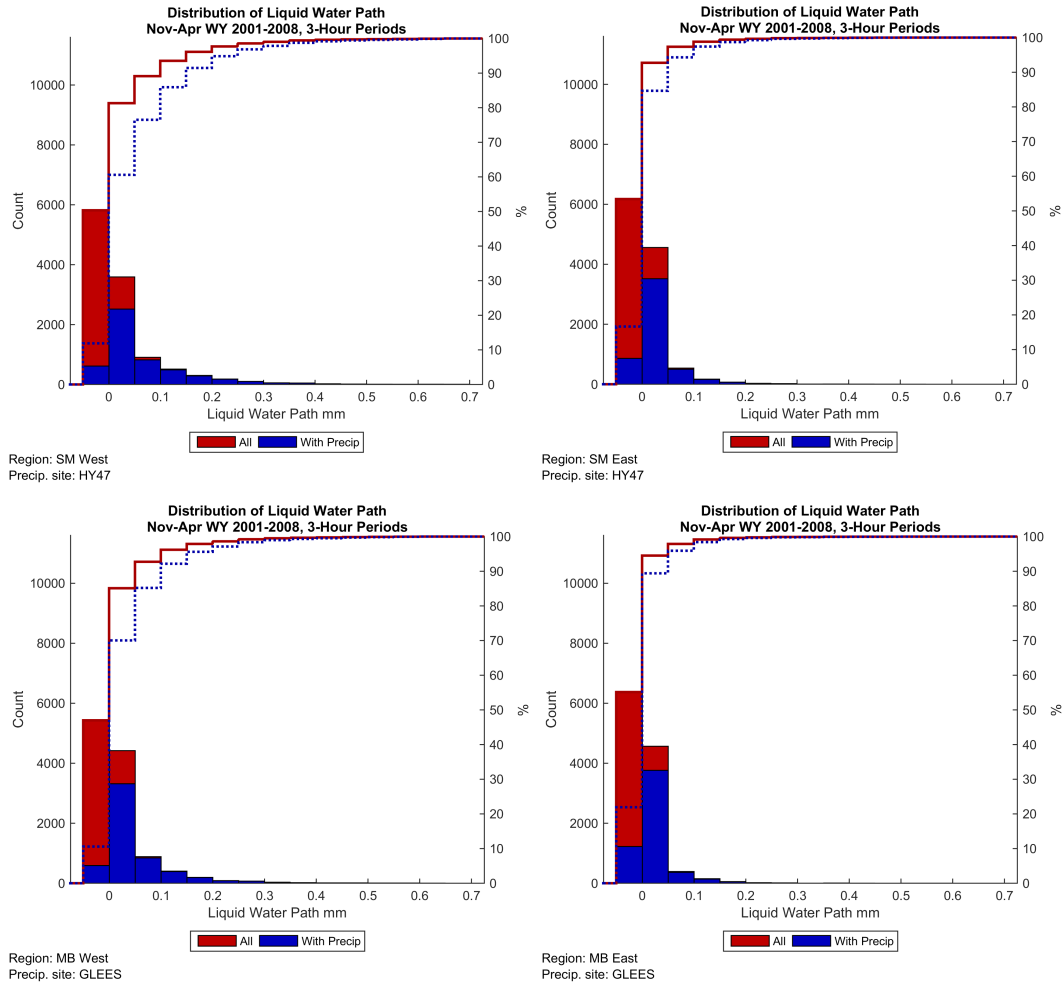


Figure 4.37. Histogram counts (left ordinate) of the area-averaged modeled LWP over (clockwise from top left) SMWest, SMEast, MBWest, and MBEast for all 3-hourly output between November and April from the 8-year period (red) and for all 3-hourly output that had precipitation (blue) at the precipitation gauge site of HY47 (Sierra Madre sites) or GLEES (Medicine Bow sites). Cumulative distributions for all (red) and output hours with precipitation (blue dotted) are also overlaid using the right ordinate (%).

The Froude number distribution illustrates that during the winter there are some situations where flow may be blocked by the mountain barrier ($Fr < 0.5$; Figure 4.38). This occurred less than 30% of the time for SMWest and closer to 20% of the time for the MBWest, MBEast, and SMEast areas. This condition was present only ~15% of the time when precipitation occurred for each region.

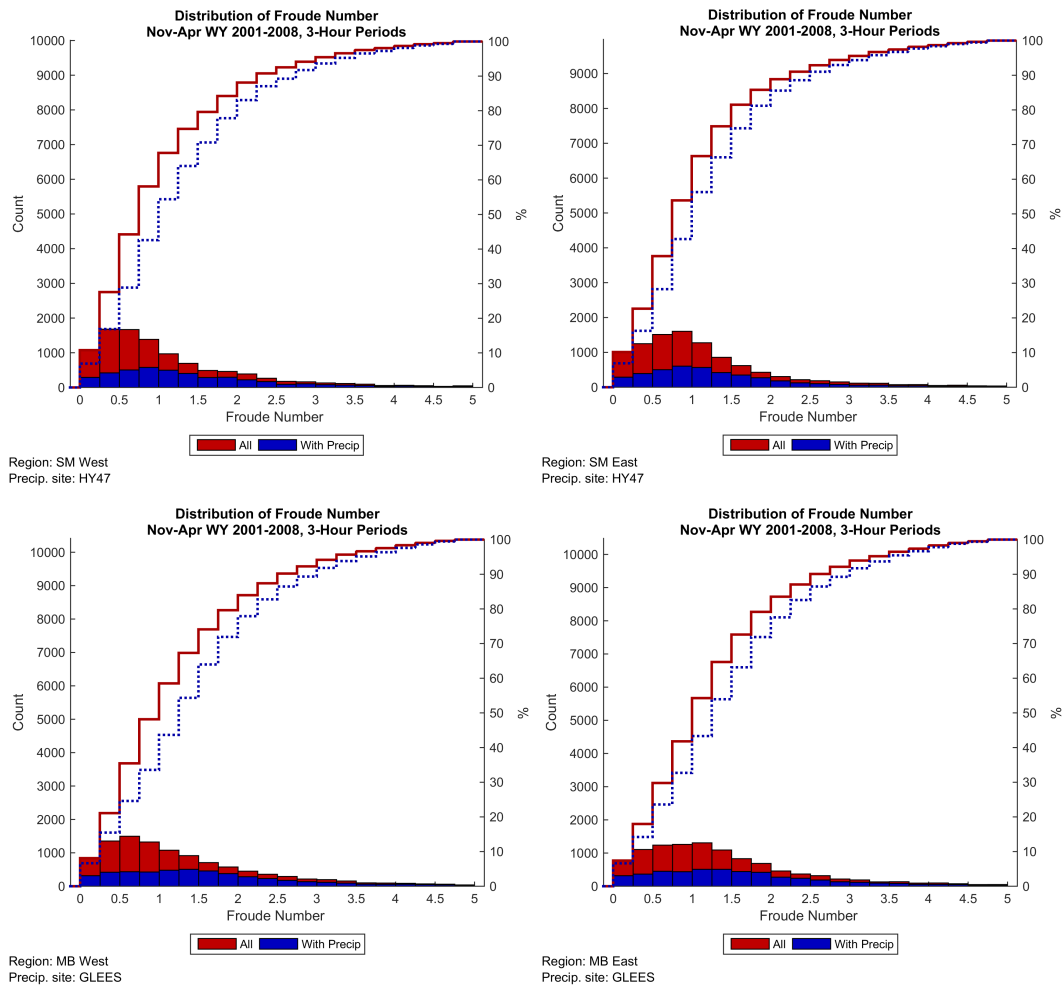


Figure 4.38. Histogram counts (left ordinate) of the area-averaged Froude number derived from the model over (clockwise from top left) SMWest, SMEast, MBWest, and MBEast for all 3-hourly output between November and April from the 8-year period (red) and for all 3-hourly output that had precipitation (blue) at the precipitation gauge site of HY47 (Sierra Madre sites) or GLEES (Medicine Bow sites). Cumulative distributions for all (red) and output hours with precipitation (blue dotted) are also overlaid using the right ordinate (%).

Characteristics of clouds, such as base height, depth, and top temperature, influence the cloud's natural precipitation efficiency. Clouds with colder cloud tops, and that are greater depth, most likely have some natural ice formation processes leading to precipitation growth. Moreover, if cloud bases are too high, then ground-based AgI generators may have difficulty targeting the clouds. The cloud-base heights (Figure 4.39) during winter are typically between 2,500 and 3,000 m MSL for all regions in the Sierra Madre Range (i.e., the distribution does not vary between the western and eastern regions). Just under 60% of all hours in the wintertime have cloud-base heights in this range and over 80% of the cloud-base heights during wintertime hours with precipitation are in this range. The second most frequent bin for cloud-base heights during winter is between 6,000 and 6,500 m MSL, which accounts for nearly 15–20% of all hours, when precipitation does not occur. For the Medicine Bow Range (Figure 4.39), the predominant category is still between 2,500 and 3,000 m MSL; however, the percentage decreases to less than 50% for all wintertime hours (70% with precipitation) as compared with the Sierra Madre Range. Both the 3,000 to 3,500 m MSL and 6,000 to 6,500 m MSL categories occur about 15% of the time for all wintertime hours. For both the Sierra Madre and Medicine Bow Ranges, cloud-base

heights are lower than 4,500 m nearly 100% of the time during wintertime hours with precipitation.

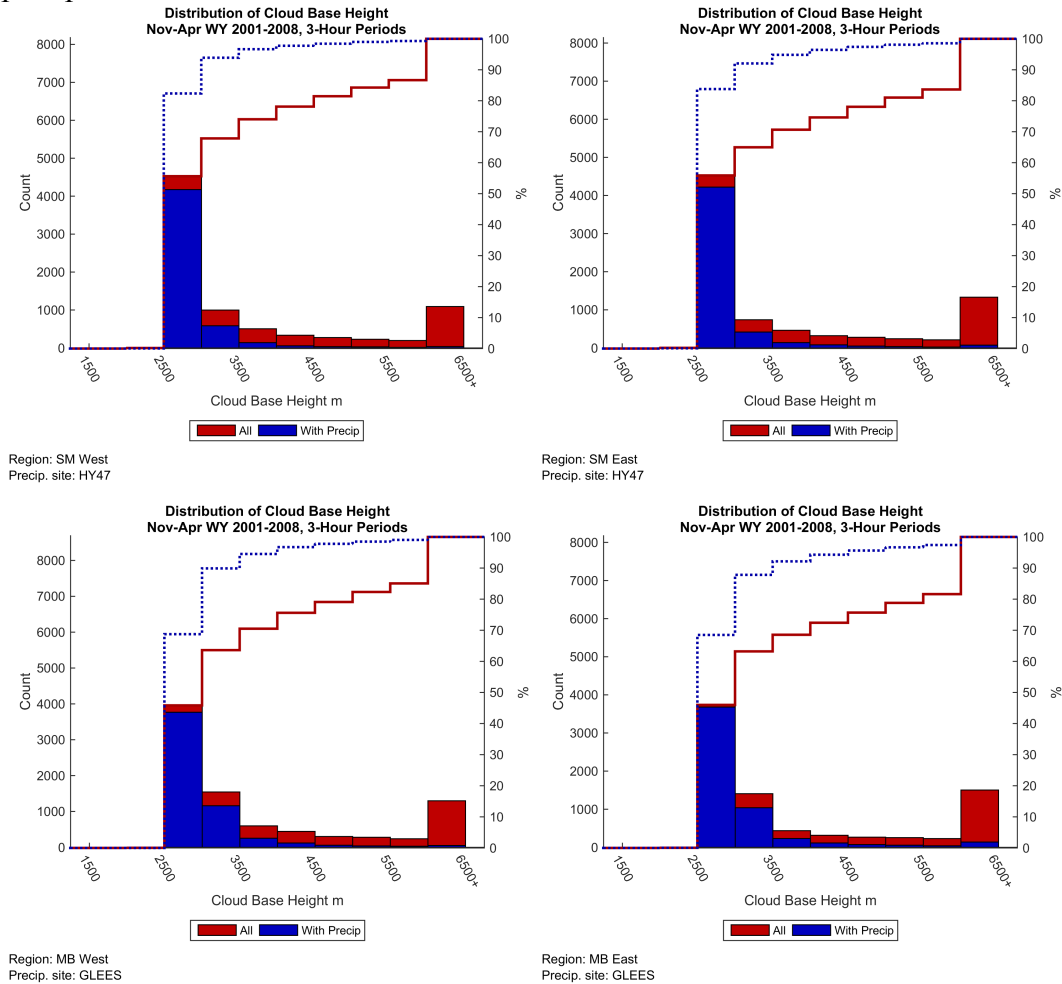


Figure 4.39. Histogram counts (left ordinate) of the area-averaged model cloud-base height over (clockwise from top left) SMWest, SMEast, MBWest, and MBEast for all 3-hourly output between November and April from the 8-year period (red) and for all 3-hourly output that had precipitation (blue) at the precipitation gauge site of HY47 (Sierra Madre sites) or GLEES (Medicine Bow sites). Cumulative distributions for all (red) and output hours with precipitation (blue dotted) are also overlaid using the right ordinate (%).

Cloud depths are as deep as 8,500 m, with just over 50% of all winter clouds being relatively shallow (<2,000 m; Figure 4.40). Slightly deeper clouds are the general trend for the eastern regions in both the Sierra Madre and Medicine Bow Ranges as compared with the western regions. Similar results are noted for all wintertime hours and those with precipitation. Cloud-top temperatures colder than -20°C for all wintertime hours over both regions in the Sierra Madre Range are noted about 60% of the time, which decreases to 50% of the time when precipitation is observed in each region (Figure 4.41). Roughly 30% of the time modeled cloud-top temperatures are in the suitable cloud seeding range of -5 to -20°C . While the overall percentage of colder cloud-top temperatures increases over the Medicine Bow study regions, the frequency of time that temperatures are suitable for seeding remains around 30% (Figure 4.41).

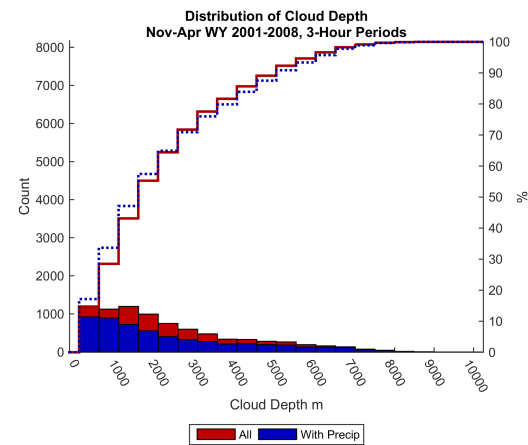
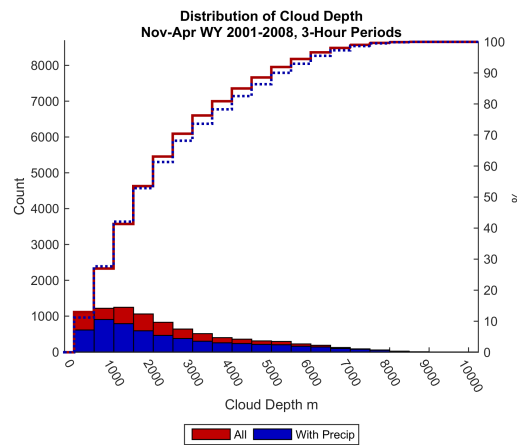
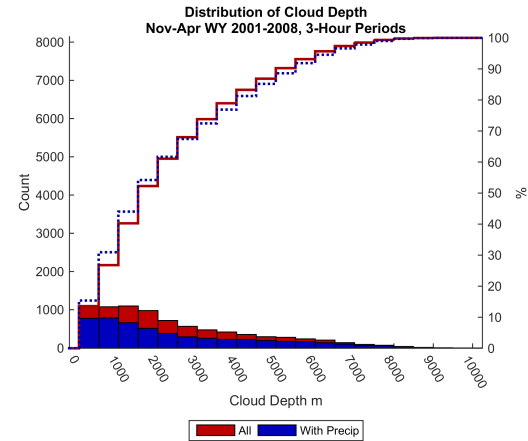
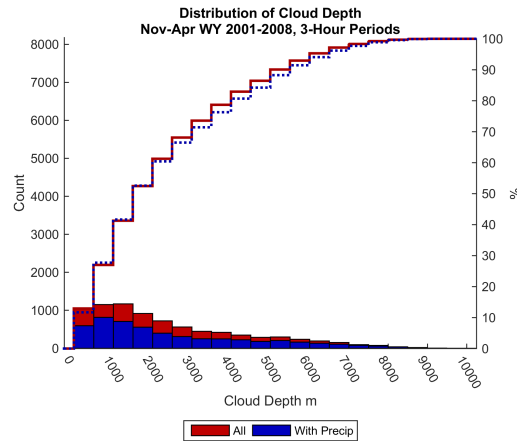


Figure 4.40. Histogram counts (left ordinate) of the area-averaged model cloud depth over (Clockwise from top left) SMWest, SMEast, MBWest, and MBEast for all 3-hourly output between November and April from the 8-year period (red) and for all 3-hourly output that had precipitation (blue) at the precipitation gauge site of HY47 (Sierra Madre sites) or GLEES (Medicine Bow sites). Cumulative distributions for all (red) and output hours with precipitation (blue dotted) are also overlaid using the right ordinate (%).

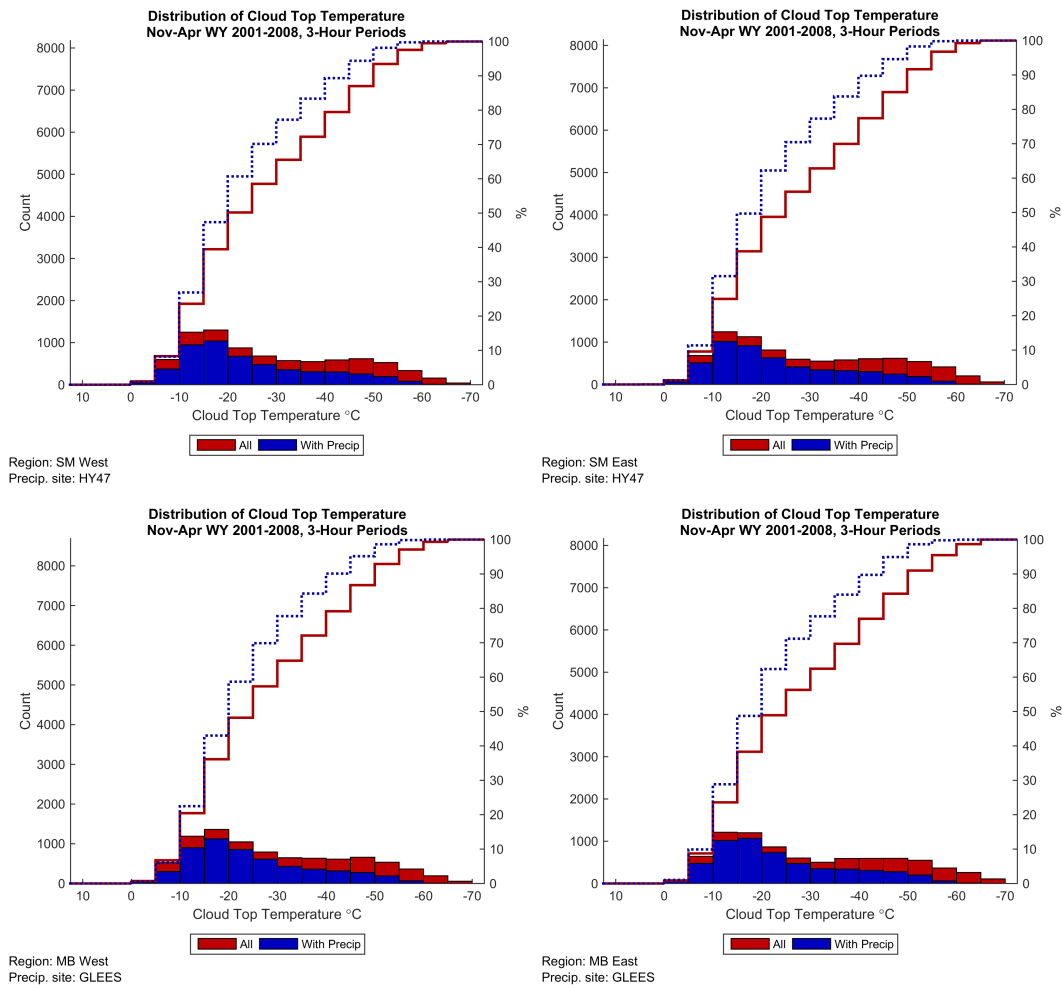


Figure 4.41. Histogram counts (left ordinate) of the area-average model cloud top temperature over (clockwise from top left) SMWest, SMEast, MBWest, and MBEast for all 3-hourly output between November and April from the 8-year period (red) and for all 3-hourly output that had precipitation (blue) at the precipitation gauge site of HY47 (Sierra Madre sites) or GLEES (Medicine Bow sites). Cumulative distributions for all (red) and output hours with precipitation (blue dotted) are also overlaid using the right ordinate (%).

The amount (and percent) of seasonal precipitation that falls when the area-averaged modeled 700-hPa temperatures are cooler than -6°C is shown by water year in Table 4.5 through Table 4.8. The 8-year seasonal average over all four areas was very similar, with just over half of the precipitation falling when 700-hPa temperatures were cooler than -6°C . All four areas varied significantly from year to year, ranging from $\sim 25\text{--}75\%$. The year-to-year fluctuations are very similar across the three regions. In all areas, water year 2008 was the coolest year, with the most precipitation falling when temperatures were cooler than -6°C .

Table 4.5. Seasonal (November–April) model precipitation totals from HY47 and the amount of precipitation that fell when the SMWest average 700-hPa temperature was < –6°C.

Season (Water Year)	Seasonal Precipitation (mm)	Seasonal Precipitation (mm) when 700-hPa T < –6°C
2001	540	395 (73%)
2002	389	210 (54%)
2003	464	123 (27%)
2004	817	433 (53%)
2005	897	560 (62%)
2006	940	543 (58%)
2007	750	395 (53%)
2008	848	628 (74%)
8-yr Average	706	411 (58%)
Standard Deviation	211	174

Table 4.6. As in Table 4.5, but 700-hPa temperatures averaged over the SMEast area.

Season (Water Year)	Seasonal Precipitation (mm)	Seasonal Precipitation (mm) when 700-hPa T < –6°C
2001	540	329 (61%)
2002	389	177 (45%)
2003	464	114 (25%)
2004	817	431 (53%)
2005	897	541 (60%)
2006	940	484 (51%)
2007	750	345 (46%)
2008	848	615 (73%)
8-yr Average	706	379 (54%)
Standard Deviation	211	174

Table 4.7. As in Table 4.5, but precipitation from GLEES and 700-hPa temperatures averaged over the MBWest area.

Season (Water Year)	Seasonal Precipitation (mm)	Seasonal Precipitation (mm) when 700-hPa T < –6°C
2001	527	340 (65%)
2002	363	163 (45%)
2003	588	139 (24%)
2004	751	487 (65%)
2005	880	524 (60%)
2006	892	448 (50%)
2007	812	462 (57%)
2008	816	572 (70%)
8-yr Average	704	392 (56%)
Standard Deviation	191	163

Table 4.8. As in Table 4.5, but precipitation from GLEES and 700-hPa temperatures averaged over the MBEast area.

Season (Water Year)	Seasonal Precipitation (mm)	Seasonal Precipitation (mm) when 700-hPa T < -6°C
2001	527	315 (60%)
2002	363	148 (41%)
2003	588	133 (23%)
2004	751	485 (64%)
2005	880	497 (56%)
2006	892	400 (45%)
2007	812	424 (52%)
2008	816	562 (69%)
8-yr Average	704	370 (53%)
Standard Deviation	191	159

In the airborne-seeding layer (3–4 km MSL; AS), the modeled temperature range in wintertime shifted slightly cooler than in the ground-seeding layer, as would be expected. In the AS layer it ranged from 2 °C to -26 °C, with the cooler range of -4 °C to -26 °C when precipitation occurred (Figure 4.42 a,c). Again, the east regions in both the Sierra Madre and Medicine Bow Ranges shifted toward warmer temperatures when compared with the west regions; it is also noted that the Medicine Bow study regions were slightly warmer than the Sierra Madre study regions. Specifically, 20% of all wintertime hours for both western regions were warmer than -6 °C, increasing slightly to near 25% for the eastern study regions. When precipitation occurred, temperatures were rarely warmer than -6 °C, regardless of the region. At the lower limit of the suitable seeding temperature range (< -18 °C), approximately 5% of all wintertime hours were too cold, increasing to 15% of the time during precipitation, regardless of range. In the higher airborne-seeding layer (4–5 km MSL; ASH), the temperatures were always colder than -6 °C, even when precipitation was not occurring (Figure 4.42 b,d). In fact, temperatures in this layer became too cold for cloud seeding with AgI in the western study regions 40% of the time in winter, increasing to 65% of the time when precipitation occurs. Thus, temperature becomes a limiting factor in the AS layer and is a significant limiting factor in the ASH layer.

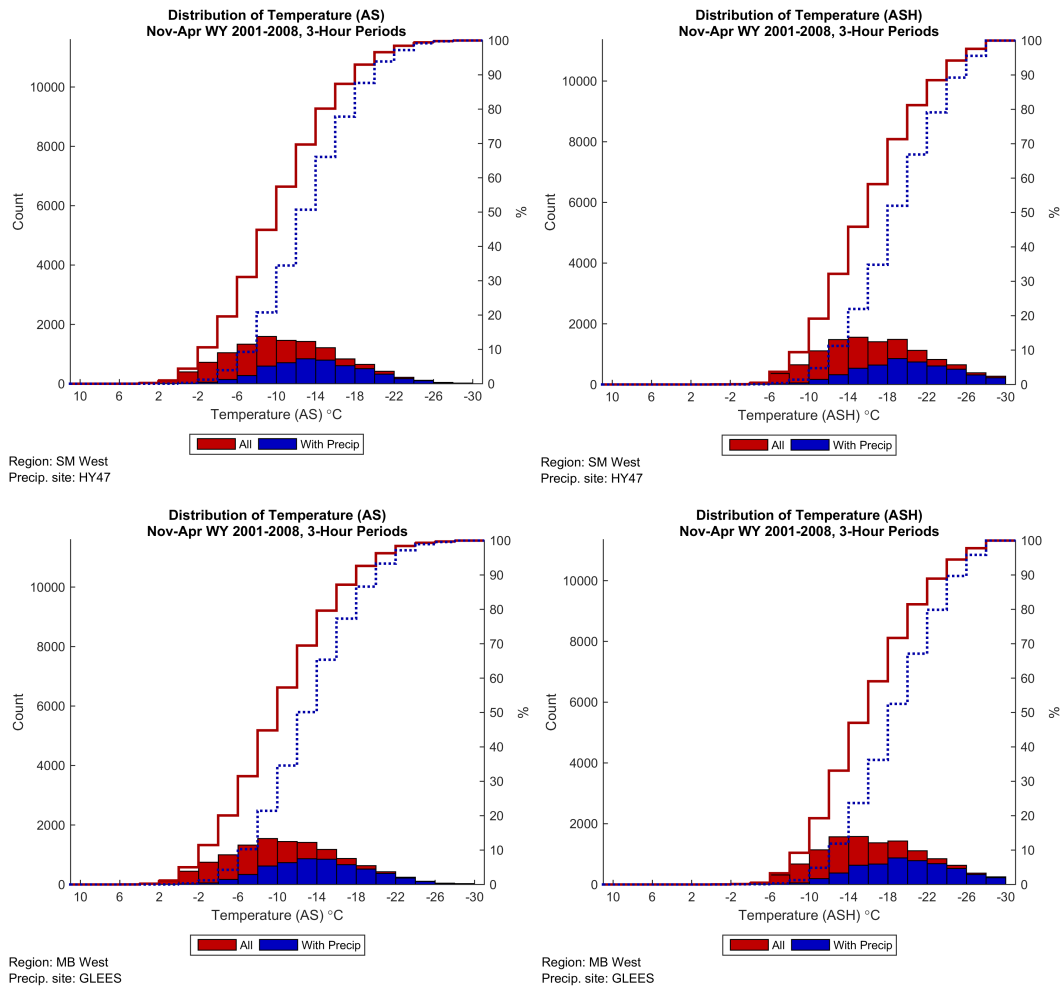


Figure 4.42. Histogram counts (left ordinate) of the area-averaged modeled temperature for the (left) 3–4 km MSL [AS] and (right) 4–5 km MSL [ASH] layer over (top) SMWest and (bottom) MBWest for all 3-hourly output between November and April from the 8-year period (red) and for all 3-hourly output that had precipitation (blue) at the precipitation gauge site of HY47 (Sierra Madre sites) or GLEES (Medicine Bow sites). Cumulative distributions for all (red) and output hours with precipitation (blue dotted) are also overlaid using the right ordinate (%).

The range of LWC in the airborne-seeding layers is narrower when compared with the ground-seeding layer (Figure 4.43). For the AS layer, 60% or more of the wintertime hours had no LWC (increases to near 70% for the east regions), with 25–30% of the wintertime hours with precipitation having zero LWC. As in the GS layer analysis, there is a discrepancy between the frequency during winter when LWC exists and when precipitation occurs, suggesting there may be occasional opportunities for seeding even when no precipitation occurred. When looking at the ASH layer, the percent of time there is no LWC increases to 80–90% for all wintertime hours and 60–80% of the time during wintertime hours with precipitation. Given these results, the ASH layer will not be a focus for the majority of the remaining discussion.

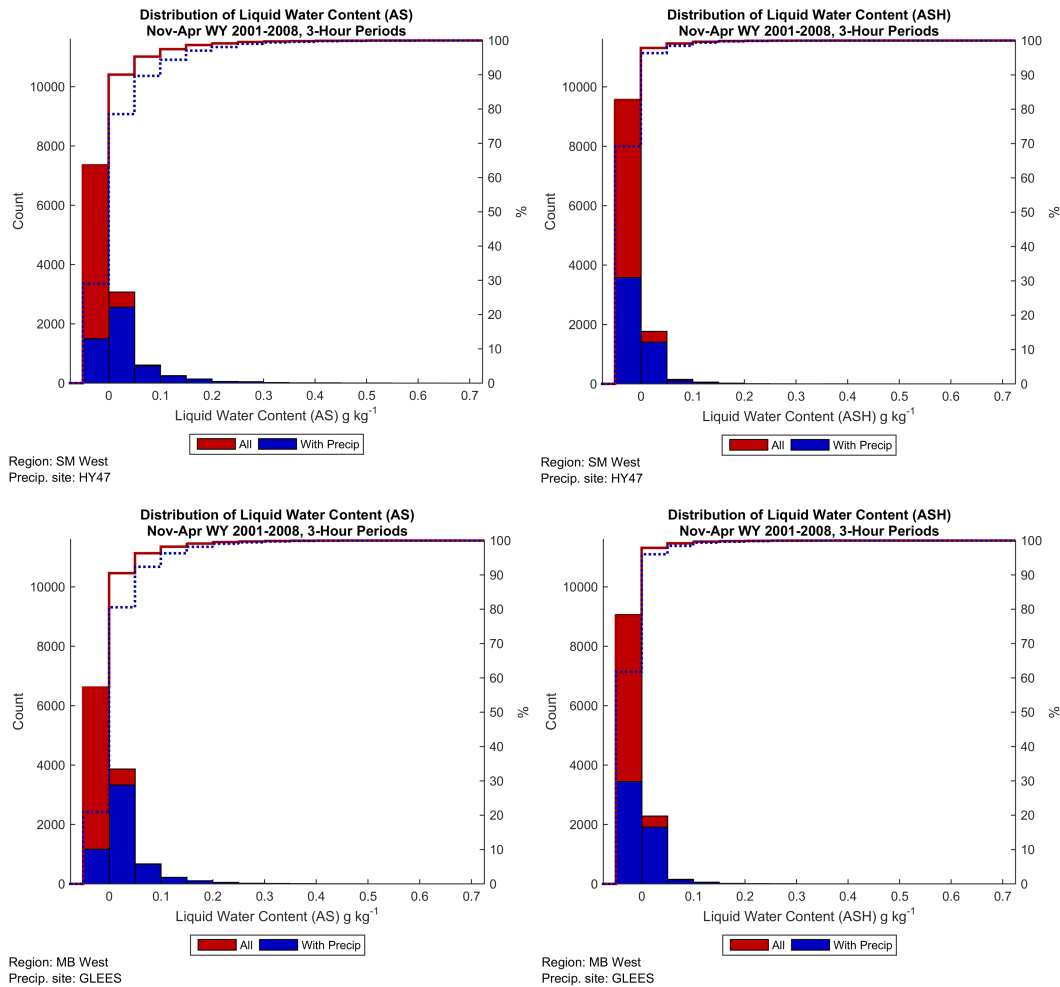


Figure 4.43. Histogram counts (left ordinate) of the area-averaged model LWC for the (left) 3–4 km MSL [AS] and (right) 4–5 km MSL [ASH] layer over (top) SMWest and (bottom) MBWest for all 3-hourly output between November – April from the 8-year period (red) and for all 3-hourly output that had precipitation (blue) at the precipitation gauge site of HY47 (Sierra Madre sites) or GLEES (Medicine Bow sites). Cumulative distributions for all (red) and output hours with precipitation (blue dotted) are also overlaid using the right ordinate (%).

4.3.3. Spatial Mapping Analysis

Spatial maps were produced indicating the frequency of time the layer average temperature ($-18^{\circ}\text{C} < T < -6^{\circ}\text{C}$) and LWC ($> 0.01 \text{ g kg}^{-1}$) in the ground-seeding layer (0–1 km AGL) met the seeding criteria across the Sierra Madre and Medicine Bow Ranges from November–April (Figure 4.44) and for each individual month (Figure 4.45 and Figure 4.46) for the full 8-year period. Naturally, the greatest frequency of suitable temperatures in the GS layer between November and April occurs over the highest terrain greater than 70% of the time (Figure 4.44). Along the lower elevations of the west and east slopes of both the Sierra Madre and Medicine Bow Ranges, the frequencies tend to be in the 35–50% range. The spatial distribution of LWC indicates the presence of liquid water will be an important factor in controlling the frequency of seeding opportunities, due to a lower frequency of LWC across the domain in the GS layer. The greatest frequencies of LWC were again noted over the higher terrain areas, with a sharp decrease to very lower frequencies of LWC on the eastern slopes of both the SM and MB ranges.

When looking at the spatial distributions by month, the cooler and frequently more suitable temperatures for seeding are evident in December–February with the typically warmer, seasonal transition months of November, March, and April having lower frequency, as expected (Figure 4.45). In addition, while relatively high values of LWC were found at the highest elevations for all months examined, the highest frequency of suitable LWC values are generally found in December–February at the lower elevations (Figure 4.46).

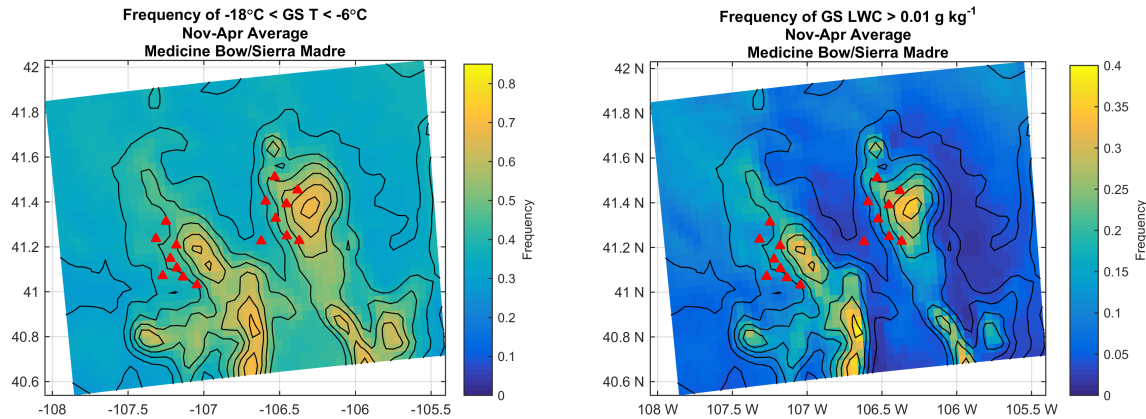


Figure 4.44. Frequency (fraction of time) that (a) temperature and (b) LWC criteria are met for seeding conditions within the 0 – 1 km AGL (GS) layer for all 3-hourly output for November–April over the 8-year period. Thin black contours indicate the topography (every 500 m MSL). The original WWMPP generator sites (8 in each Range) are overlaid as red triangles for reference.

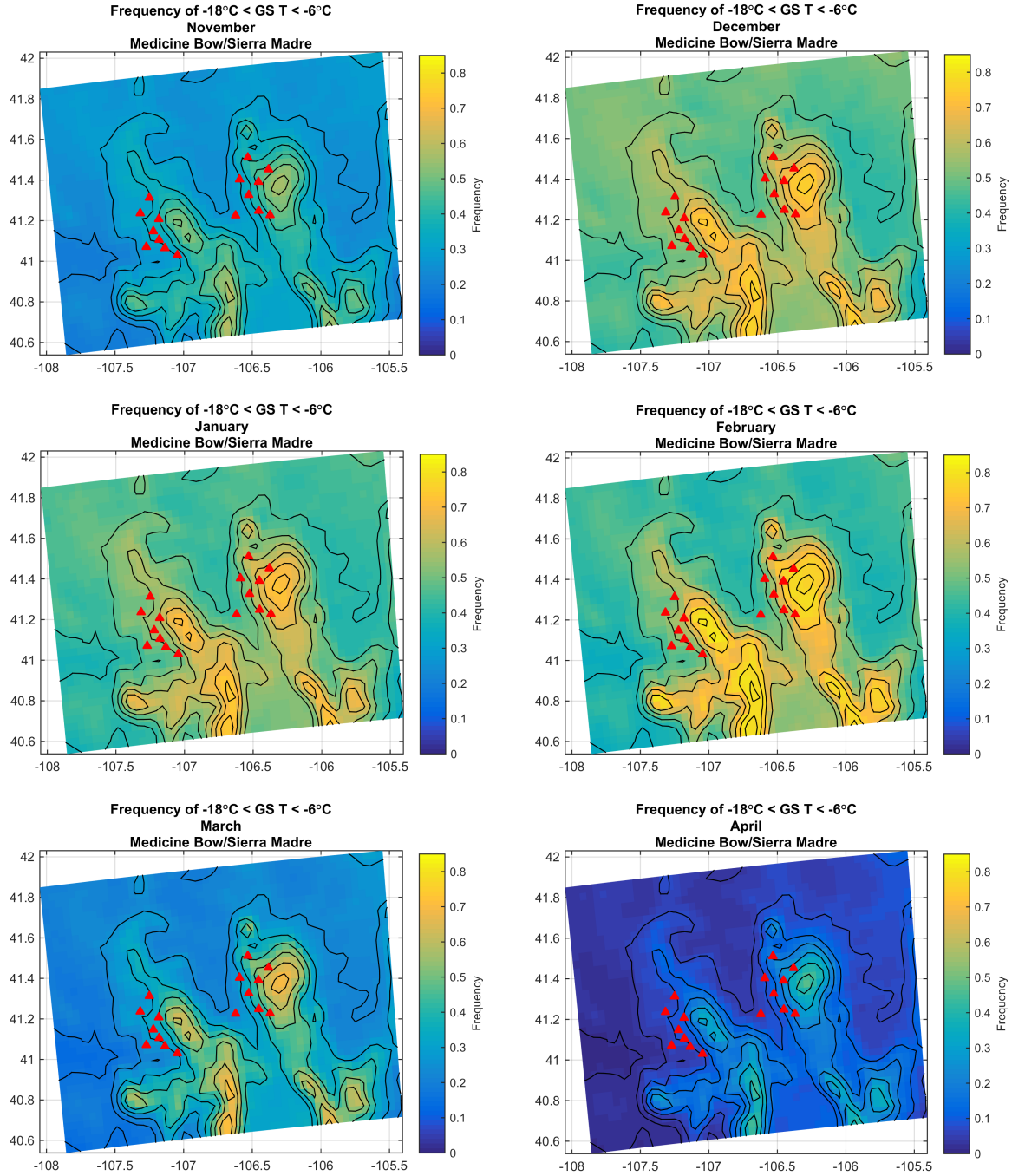


Figure 4.45. Month-by-month frequency (fraction of time) that temperature criteria is met for seeding conditions within the 0–1 km AGL (GS) layer for all 3-hourly output from November–April over the 8-year period. Thin black contours indicate the topography (every 500 m MSL). The original WWMPP generator sites (8 in each Range) are overlaid as red triangles.

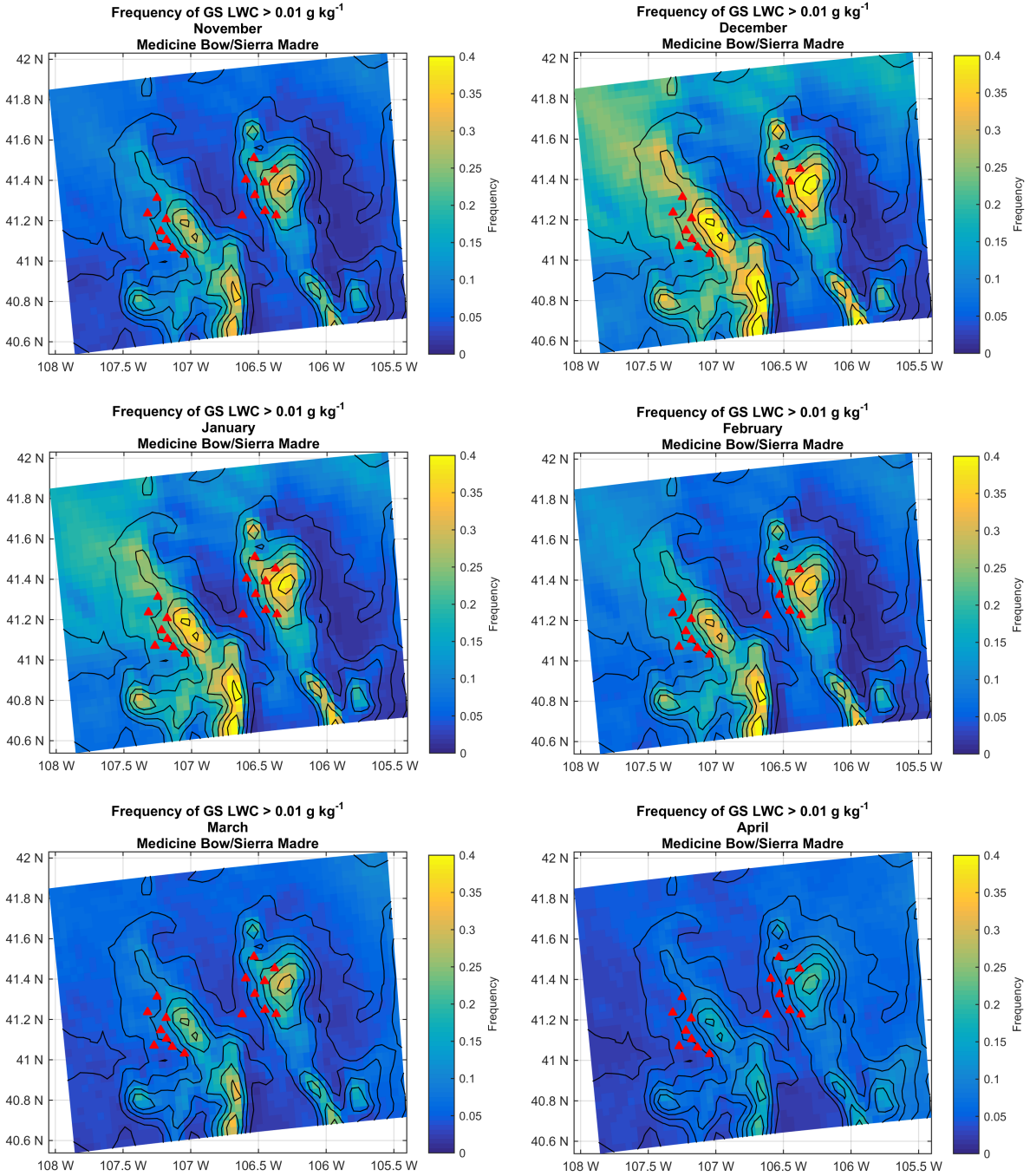


Figure 4.46. Month-by-month frequency (fraction of time) that LWC criteria is met for seeding conditions within the 0–1 km AGL (GS) layer for all 3-hourly output from November–April over the 8-year period. Thin black contours indicate the topography (every 500 m MSL). The original WWMPP generator sites (8 in each Range) are overlaid as red triangles.

For the AS layer (3–4 km MSL), the frequency of suitable temperatures between November and April was greater than 60% across the entire domain (i.e., not as highly correlated to terrain for this layer; Figure 4.47). On the other hand, the spatial distribution of LWC in the AS layer has a very similar pattern as the GS layer, but with reduced overall frequencies generally between 20

and 30% across the higher elevations and near zero along the eastern slopes of both the Sierra Madre and Medicine Bow Ranges.

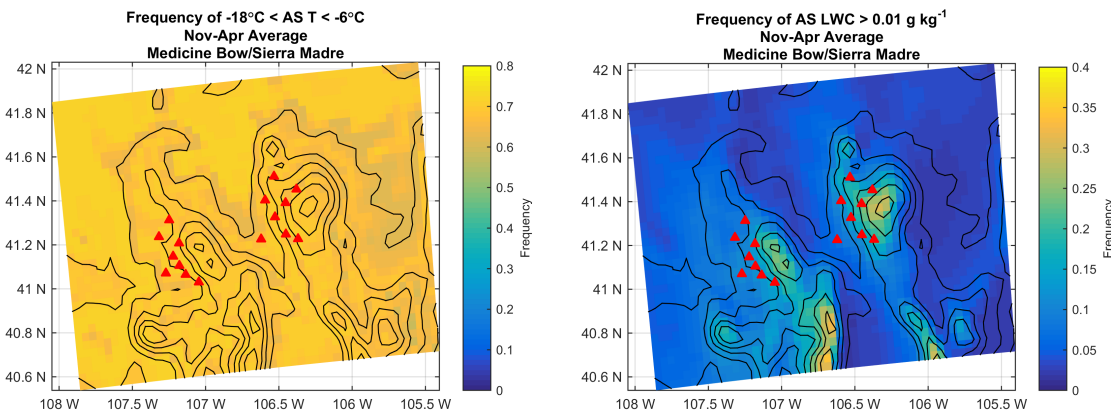


Figure 4.47. Frequency (fraction of time) that (a) temperature and (b) LWC criteria are met for seeding conditions within the 3–4 km MSL (AS) layer for all 3-hourly output for November–April over the 8-year period. Thin black contours indicate the topography (every 500 m MSL). The original WWMP generator sites (8 in each Range) are overlaid as red triangles.

4.4. Climatology of Cloud Seeding Opportunities

When considering the two most essential criteria for cloud-seeding potential, proper temperature and the presence of liquid water, the frequency that these criteria are met can be established using either observations (if available) or model output. These two criteria provide a general sense of the frequency of cloud-seeding opportunities.

Using observations, such as regular soundings to determine the 700-hPa temperature and radiometer data to determine the presence of LWC, the frequency in which these basic conditions are met can be assessed. While the WWMP data set includes radiometer data for both the Medicine Bow and Sierra Madre target ranges, regular soundings are not available. Soundings were launched only for the WWMP during periods when seeding cases were being called, so this biases the sounding data set toward seedable cases. Therefore, this analysis will be conducted using WRF-CONUS model output.

Using the WRF-CONUS model output, the fraction of hours in a given month or the entire winter season (between November and April) in which the temperature and liquid-water criteria were both met can be calculated. Additional criteria that may affect the potential for seeding are wind direction and atmospheric stability indices. These variables will be analyzed using the spatial mapping and area-based methods for both ground and airborne-seeding potential.

4.4.1. Model-based Analysis Results

Ground Seeding Spatial Mapping Analysis

Figure 4.48 shows the spatial frequency (% of time analyzed for all eight seasons) that seeding criteria are met within the 0–1 km AGL layer. Recall from Figure 4.44 that the frequency of LWC was the limiting factor in controlling the frequency of seeding opportunities and the overall

pattern when considering the criteria for both temperature and LWC is very similar to that when considering LWC alone (Figure 4.48). A gradual increase in the frequency of suitable seeding conditions across the western slopes (15–20%) of the Sierra Madre and Medicine Bow Ranges comes to a peak along the highest terrain (25–30%), which is then followed by a sharp decrease (to near zero) over the eastern slopes. When looking at the spatial distributions by month, the overall pattern remains the same but the frequencies of suitable seeding conditions are highest between December and February (Figure 4.49). During these months, a peak of 30–35% is noted over the highest terrain, while the western slopes see suitable seeding conditions closer to 20–25% of the time.

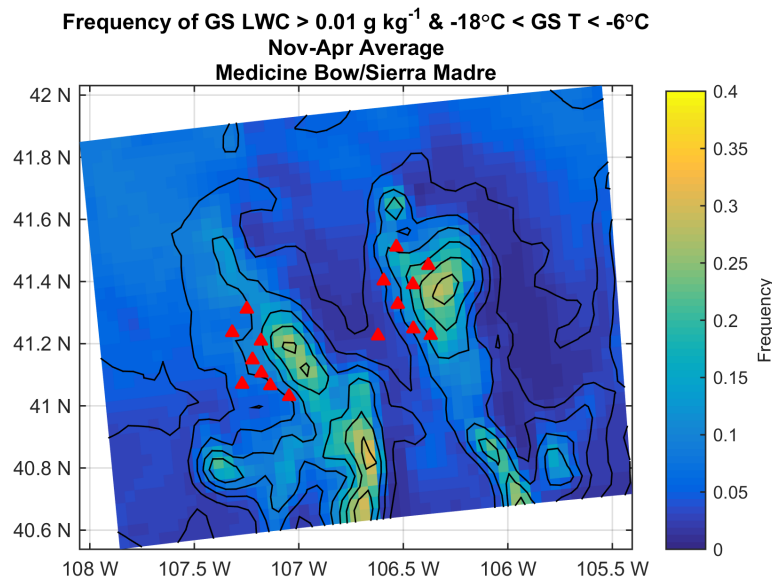


Figure 4.48. Frequency (percent of time) that both the temperature ($-18^{\circ}\text{C} < T < -6^{\circ}\text{C}$) and LWC ($> 0.01 \text{ g kg}^{-1}$) criteria are met for seeding conditions within the 0 – 1 km AGL (GS) layer for all 3-hourly output for November – April over the 8-year period. Thin black contours indicate the topography (every 500 m MSL). The original WWMPP generator sites (8 in each Range) are overlaid as red triangles.

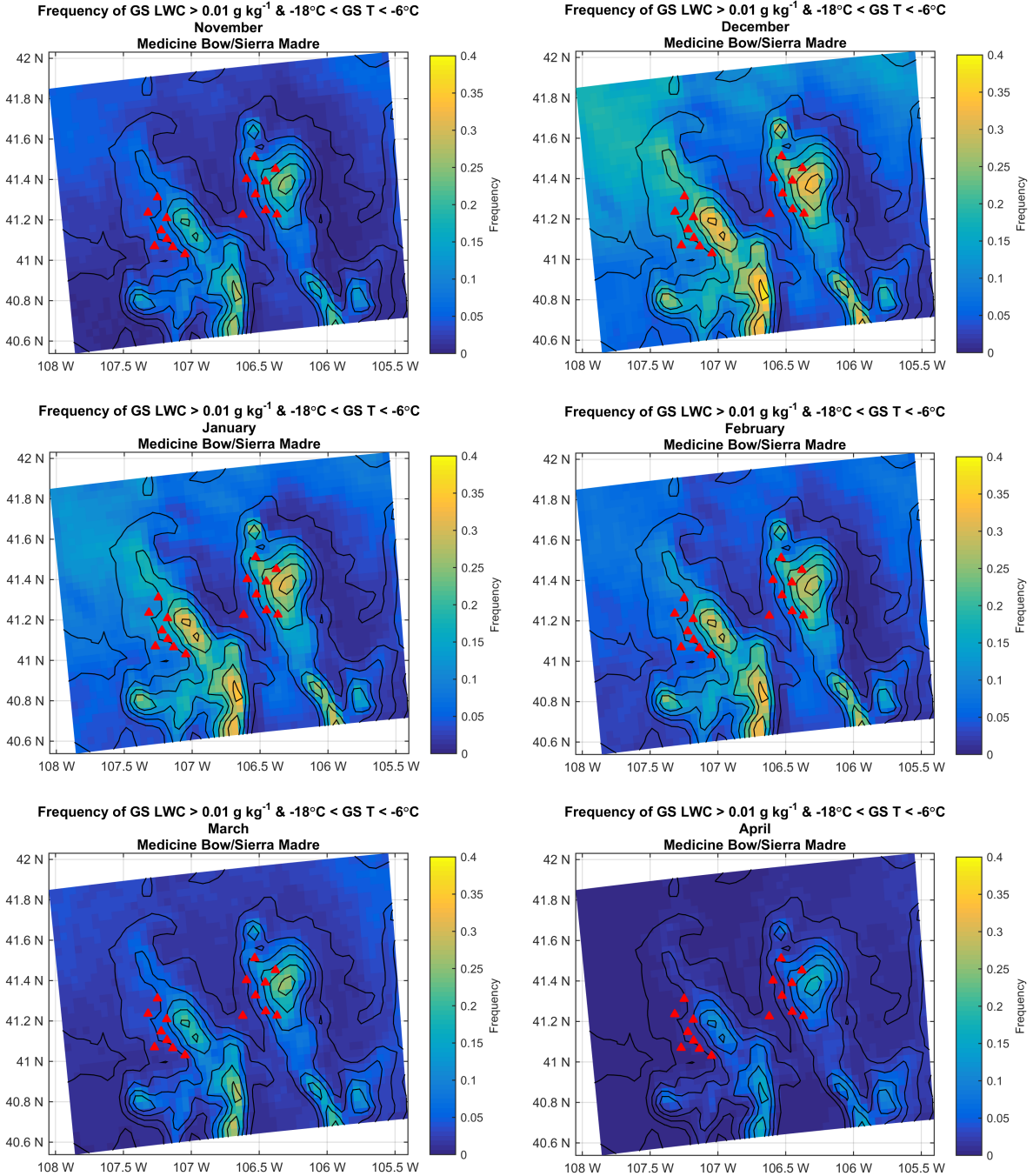


Figure 4.49. Month-by-month frequency (percent of time) that both the temperature ($-18^{\circ}\text{C} < T < -6^{\circ}\text{C}$) and LWC ($> 0.01 \text{ g kg}^{-1}$) criteria are met for seeding conditions within the 0–1 km AGL (GS) layer for all 3-hourly output from November–April over the 8-year period. Thin black contours indicate the topography (every 500 m MSL). The original WWMPP generator sites (8 in each Range) are overlaid as red triangles.

Airborne Seeding Spatial Mapping Analysis

The spatial distribution pattern of the seedable condition frequency for the AS layer across the domain is similar to that of the GS layer, suggesting a strong correlation of the seedable conditions to terrain features. However, an overall reduction of about 5% is noted in the frequency across the western slopes and the highest terrain regions (Figure 4.50a). The

frequencies in the ASH layer are significantly reduced to a maximum of about 5% over the western slopes of the highest terrain (Figure 4.50b). The reduction in frequency between November–April for the ASH layer is driven by temperatures becoming too cold and LWC being greatly reduced in the higher layers of the atmosphere on average.

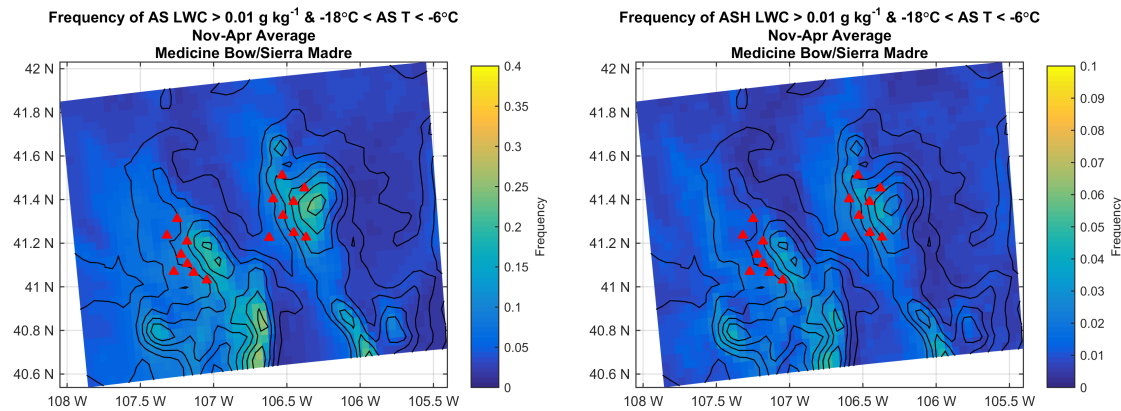


Figure 4.50. Frequency (percent of time) that both the temperature ($-18^{\circ}\text{C} < T < -6^{\circ}\text{C}$) and LWC ($> 0.01 \text{ g kg}^{-1}$) criteria are met for seeding conditions within the 3–4 km MSL (left) and 4–5 km MSL layer (right) for all 3-hourly output for November–April over the 8-year period. Thin black contours indicate the topography (every 500 m MSL). The original WWMPP generator sites (8 in each Range) are overlaid as red triangles.

Ground-Seeding Area-based Analysis

On a monthly basis, the seasonality of ground-based cloud-seeding opportunities (defined as meeting the temperature and LWC criteria) is primarily between November and April, with the highest frequency of opportunities in December–February for both SMWest and MBWest (Figure 4.51). In fact, the 8-year average fraction of hours that meet these two criteria for each of these months over SMWest is between 25 and 30% with a slight decrease over MBWest where seeding criteria was met around 25% of the time for each of the months December–February. In addition, when normalized by the presence of precipitation over the target area for each region, only a small reduction in the fraction of hours was noted. This indicates there were relatively few non-precipitating opportunities for cloud seeding.

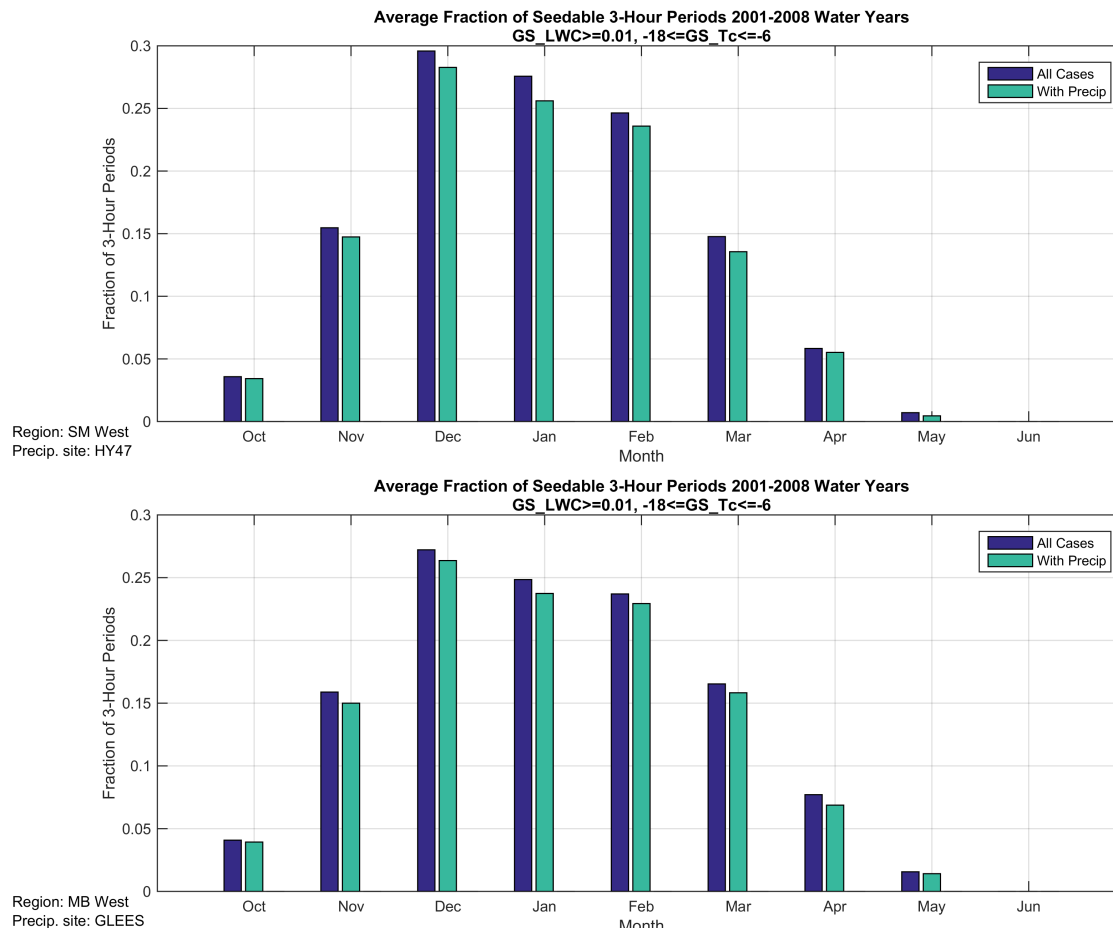


Figure 4.51. Bar chart showing the average fraction of hours in a month that met the temperature and LWC criteria averaged over (a) SMWest and (b) MBWest for ground-based seeding (0–1 km AGL; blue) and the same for hours that also had precipitation in the model near the (a) HY47 or (b) GLEES precipitation site (green).

When the monthly distribution of wintertime hours that met temperature and LWC criteria are grouped by season, the interannual variability in seeding opportunities becomes apparent (Figure 4.52). For example, the 2006–2007 (bright red) and 2001–2002 (to a smaller extent; medium blue) water years showed fewer opportunities for ground-based seeding than most of the other water years in nearly all months, which is because these years were relatively dry (Table 4.2). This is also supported by the reduction in the total fraction of hours over the season meeting the seeding criteria (temperature and LWC) for those two water years (Figure 4.53). Some years, such as water years 2005–2006 and 2007–2008, have a similar seasonal fraction of seedable hours, yet one dominant month occasionally drives the seasonal opportunities. For example, January was the dominant month in 2005–2006 (orange), while the frequency for seeding by month was more evenly split among the months of December through February in 2007–2008 (deep red). This illustrates that the seasonality of seeding opportunities varies from year-to-year, depending on storm characteristics and seasonality, but over the 8-year period of study, five of the seasons showed 20% or greater wintertime hours meeting the temperature and LWC criteria for both SMWest and MBWest (Figure 4.53). Hence, the seasonal variability often levels out over the course of the winter. In general, the seedable fraction of hours is slightly lower for MBWest when compared with SMWest, except for water years 2003–2004 and 2006–2007. The fraction of seedable hours in the lowest year (water year 2006–2007) was 13% (14%) for

SMWest (MBWest) and for a high year (multiple years) was approximately 23% (22%) for SMWest (MBWest). The 8-year average for both regions showed 19% of the wintertime hours as being seedable, based on meeting the primary criteria (temperature and LWC) in the ground-seeding layer. When precipitation was considered, the fraction of hours with seedable conditions was reduced by only a single percent or two at most (Figure 4.53), with an 8-year average at 18% of all wintertime hours characterized as seedable with precipitation. When normalized by the presence of clouds, the 8-year average frequency of ground-based seeding opportunities relative to the presence of clouds was approximately 32% for both SMWest and MBWest (not shown). This indicates that one-third of the clouds in the region met the temperature and LWC criteria for ground-based seeding.

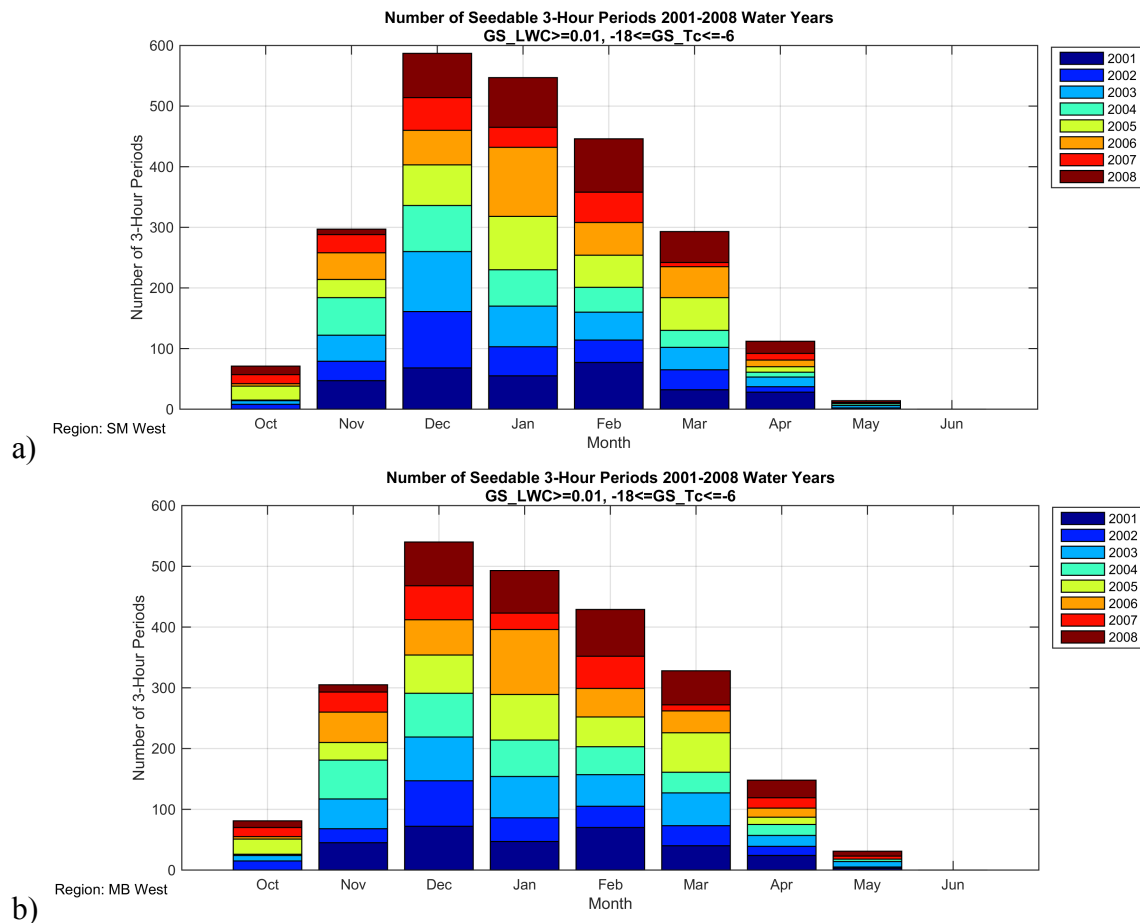


Figure 4.52. Bar chart showing the number of hours in a month that met the temperature and LWC criteria averaged over (a) SMWest and (b) MBWest for ground-based seeding (0–1 km AGL). Each color represents one of the 8 years simulated by the model.

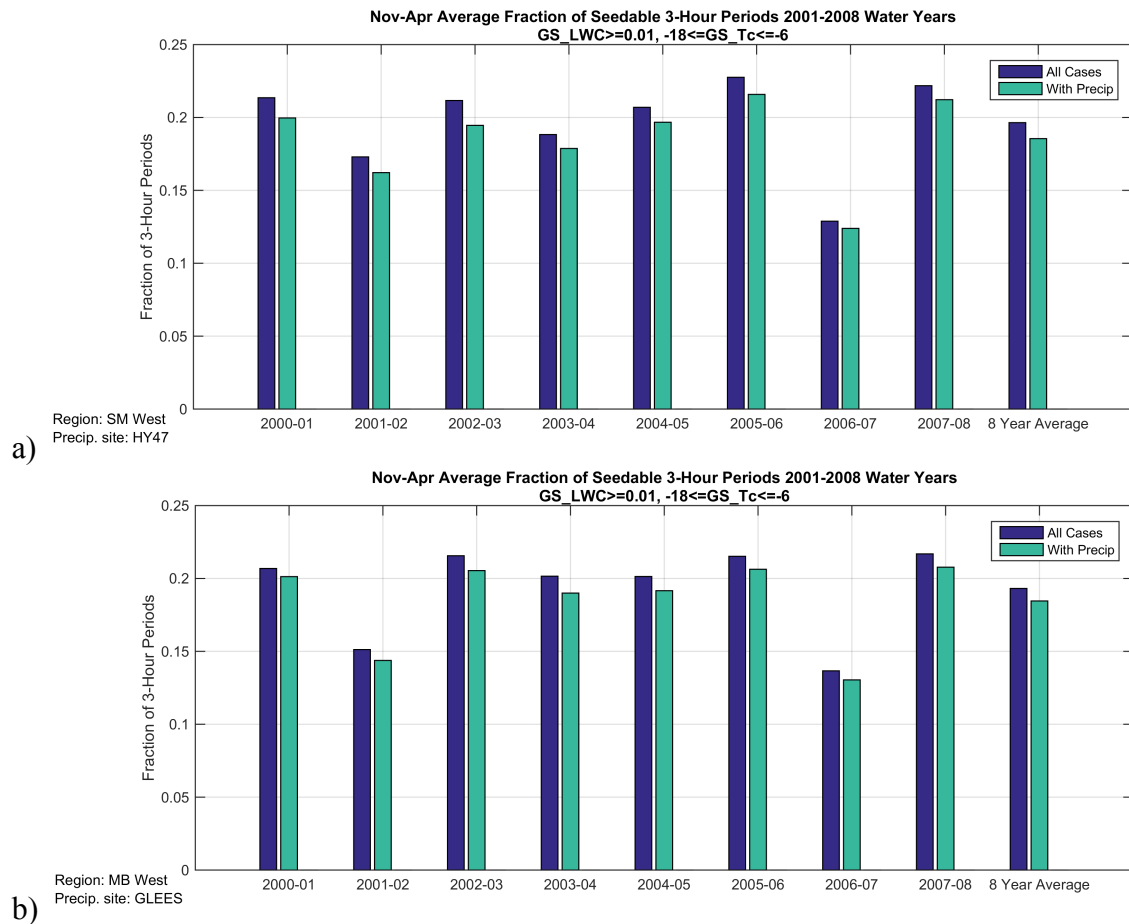


Figure 4.53. Bar chart showing the average fraction of hours in a winter season (November–April) that met the temperature and LWC criteria averaged over (a) SMWest and (b) MBWest for ground-based seeding (0–1 km AGL; blue) and the same for hours that also had precipitation in the model near the (a) HY47 or (b) GLEES precipitation site (green).

When siting ground-based seeding generators, wind direction climatology is considered in positioning the generators at optimal locations for favorable transport of ground-based seeding material over the barrier. For SMWest and MBWest, wind directions between 210 and 315 degrees were added to the seedable-condition criteria. When including this wind direction criterion on the ground-based seeding potential, the frequencies were reduced by a few percent, from an 8-year average of 19% to just under 17% of all wintertime hours, and from 18% to around 16% of wintertime hours that also experienced precipitation (Figure 4.54).

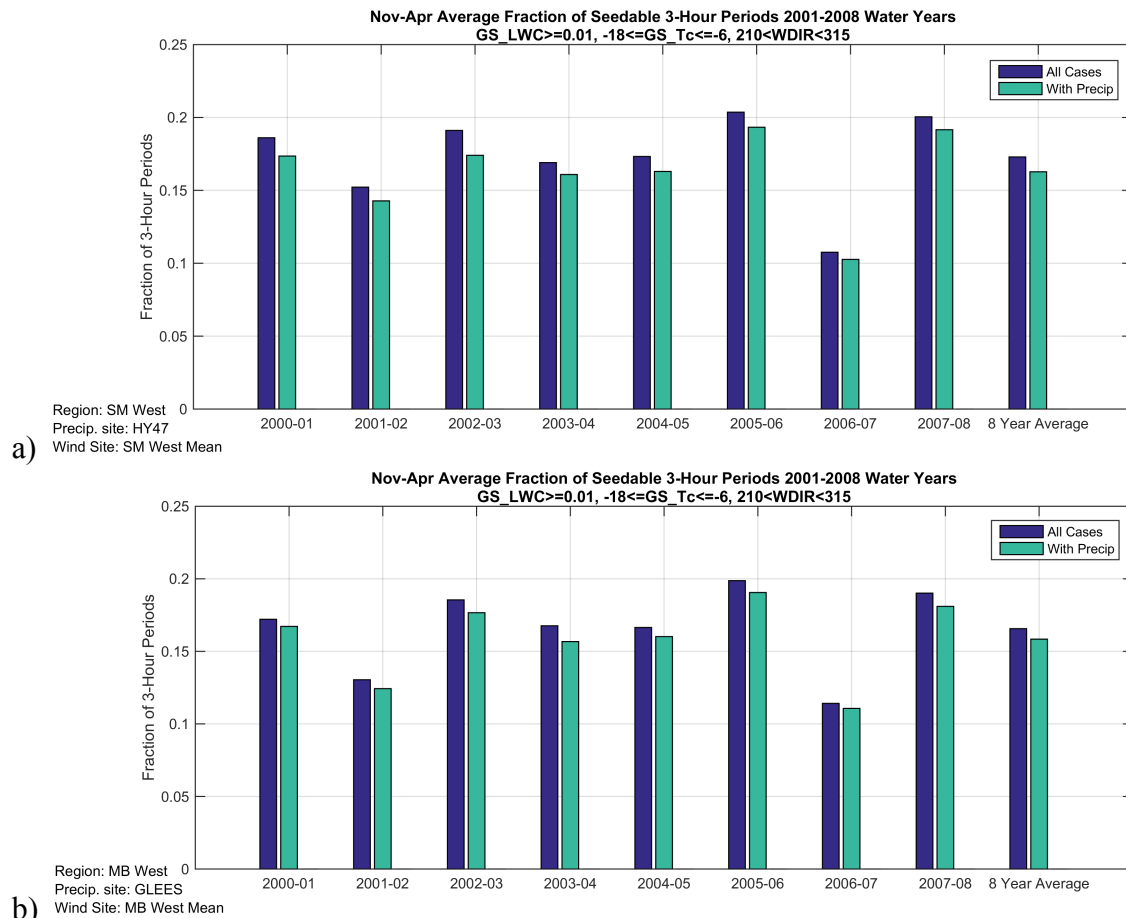


Figure 4.54. Bar chart showing the average fraction of hours in a winter season (November–April) that met the temperature, LWC, and wind direction (210 to 315 degrees) criteria averaged over (a) SMWest and (b) MBWest for ground-based seeding (0–1 km AGL; blue) and the same for hours that also had precipitation in the model near the (a) HY47 or (b) GLEES precipitation site (green).

Moreover, because AgI released from ground-based generators needs to disperse vertically up and over the mountain barrier, it is also important to assess the stability of the atmosphere. When including the additional criterion of $Fr > 0.5$ in the analysis of frequency of ground-seeding conditions indicating flow would be less likely to be blocked by the mountain barrier), the frequency of opportunities for ground-based seeding was reduced a bit more (Figure 4.55) to roughly 15–16% of the season, based on the 8-year average for both ranges.

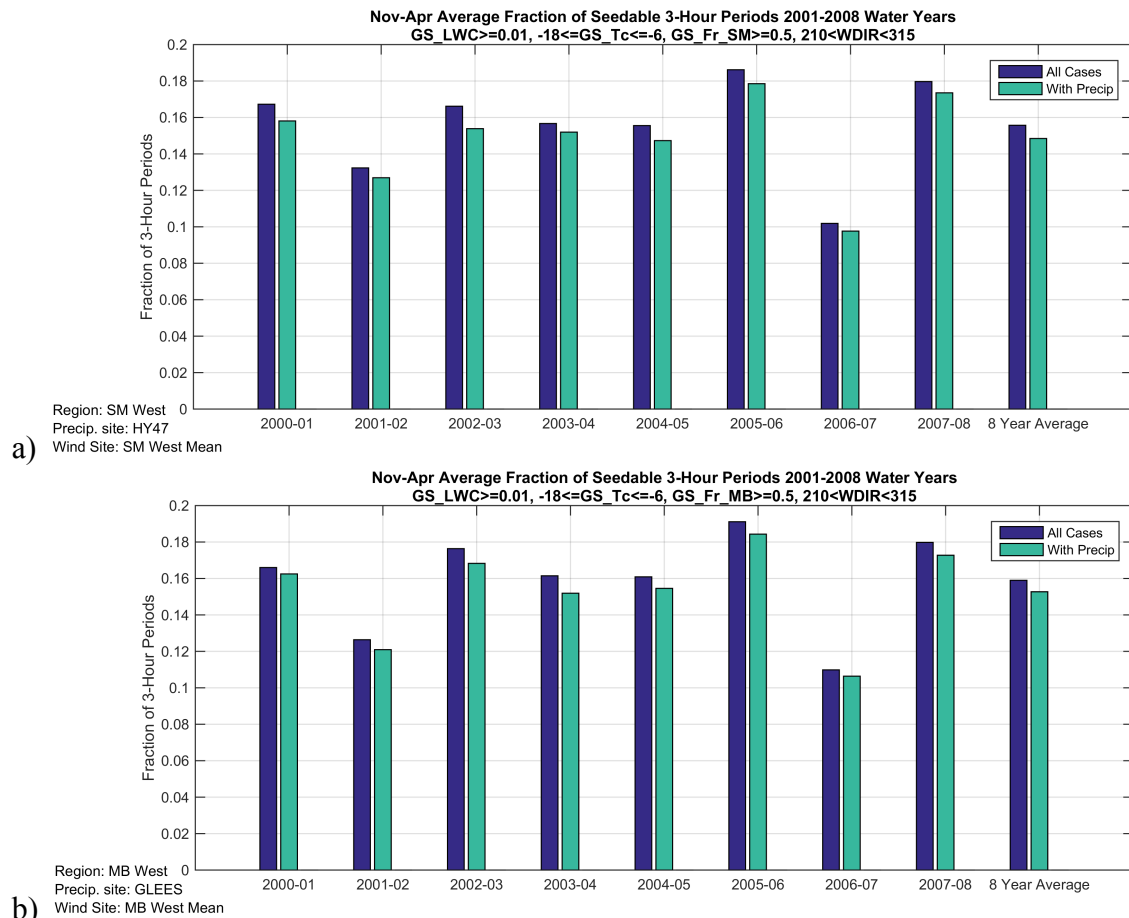


Figure 4.55. Bar chart showing the average fraction of hours in a winter season (November–April) that met the temperature, LWC, wind direction, and Froude number (>0.5) criteria averaged over (a) SMWest and (b) MBWest for ground-based seeding (0–1 km AGL; blue) and the same for hours that also had precipitation in the model near the (a) HY47 or (b) GLEES precipitation site (green).

As previously noted, seeding opportunities are limited by the lack of frequent liquid water over the eastern slopes of the Sierra Madre and Medicine Bow Ranges, and when coupled with wind direction and atmospheric stability criteria, the frequency of ground seeding in these regions is nearly zero (not shown), so these regions will not be discussed going forward. However, there are opportunities over the SMSouth region. When strictly considering the temperature and LWC criteria, SMSouth shows lower frequencies of ground-based seeding opportunities than SMWest, averaging about 13% of the time over the 8-year period (Figure 4.56). SMSouth was targeted with northerly upslope winds ranging from 320 to 50 degrees; when including the wind criterion, the frequency of seedable periods of conditions were present decreased dramatically to an average of only 2% over the 8-year period (Figure 4.57). As a result, locating generators in this area to target the SMSouth region under northerly winds is inadvisable. However, as will be illustrated in Section 6, generators located in this area could help target the southern extent of the Medicine Bow under westerly or southwesterly winds.

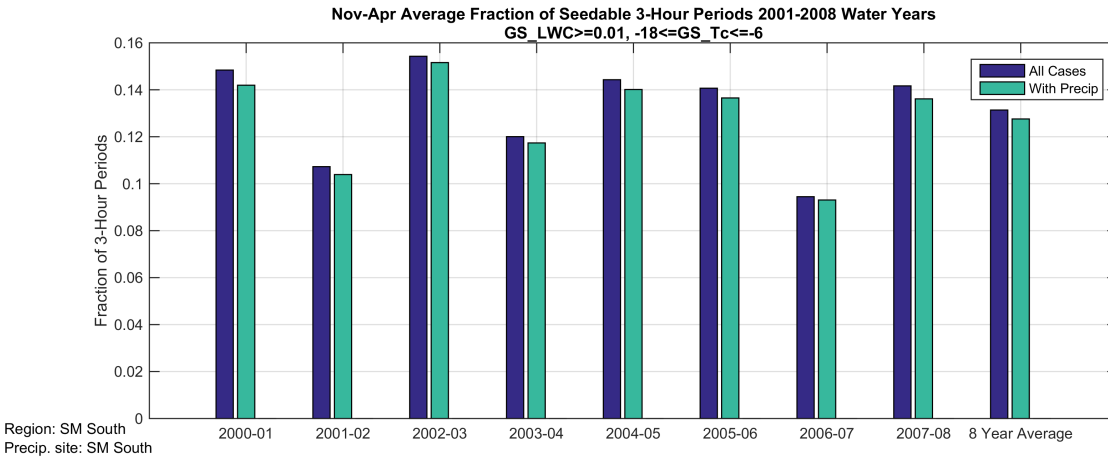


Figure 4.56. Bar chart showing the average fraction of hours in a winter season (November–April) that met the temperature and LWC criteria averaged over SMSouth for ground-based seeding (0–1 km AGL; blue) and the same for hours that also had precipitation in the model near the SM South precipitation site (green).

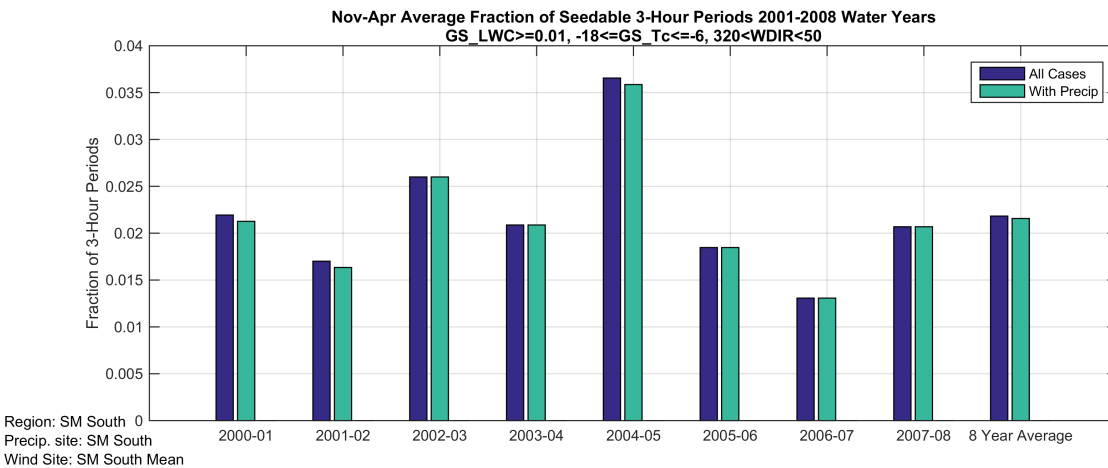


Figure 4.57. Bar chart showing the average fraction of hours in a winter season (November–April) that met the temperature, LWC, and wind direction (320 to 50 degrees) criteria averaged over SMSouth for ground-based seeding (0–1 km AGL; blue) and the same for hours that also had precipitation in the model near the SM South precipitation site (green).

Airborne Seeding Area-based Analysis

Airborne-seeding opportunities were focused on two layers: AS (3–4 km MSL) and ASH (4–5 km MSL). When the results from the SMWest (Figure 4.58) and MBWest (Figure 4.59) regions are analyzed, the November–March months encompassed the highest frequencies when the AS layer met the temperature and LWC criteria (top panel in both figures). On the other hand, the ASH layer met the temperature and LWC criteria more frequently in the transition months of October and March–May when the temperatures were not as cold in that layer (bottom panel in both figures). When the frequencies are normalized by precipitation in the target area, the fractions are reduced more for the ASH layer in those transition months, indicating that when seeding conditions are met in the ASH layer, there is a reduced likelihood of precipitation at the surface. However, the November–February period in the ASH layer shows almost no change in seedable-condition frequency when normalized by precipitation in the target area. The fraction of seedable periods by month over the 8-year period of study is higher for the AS layer in the fall

and spring than the GS layer, while the ASH layer had the lowest fraction except for the months of May and June.

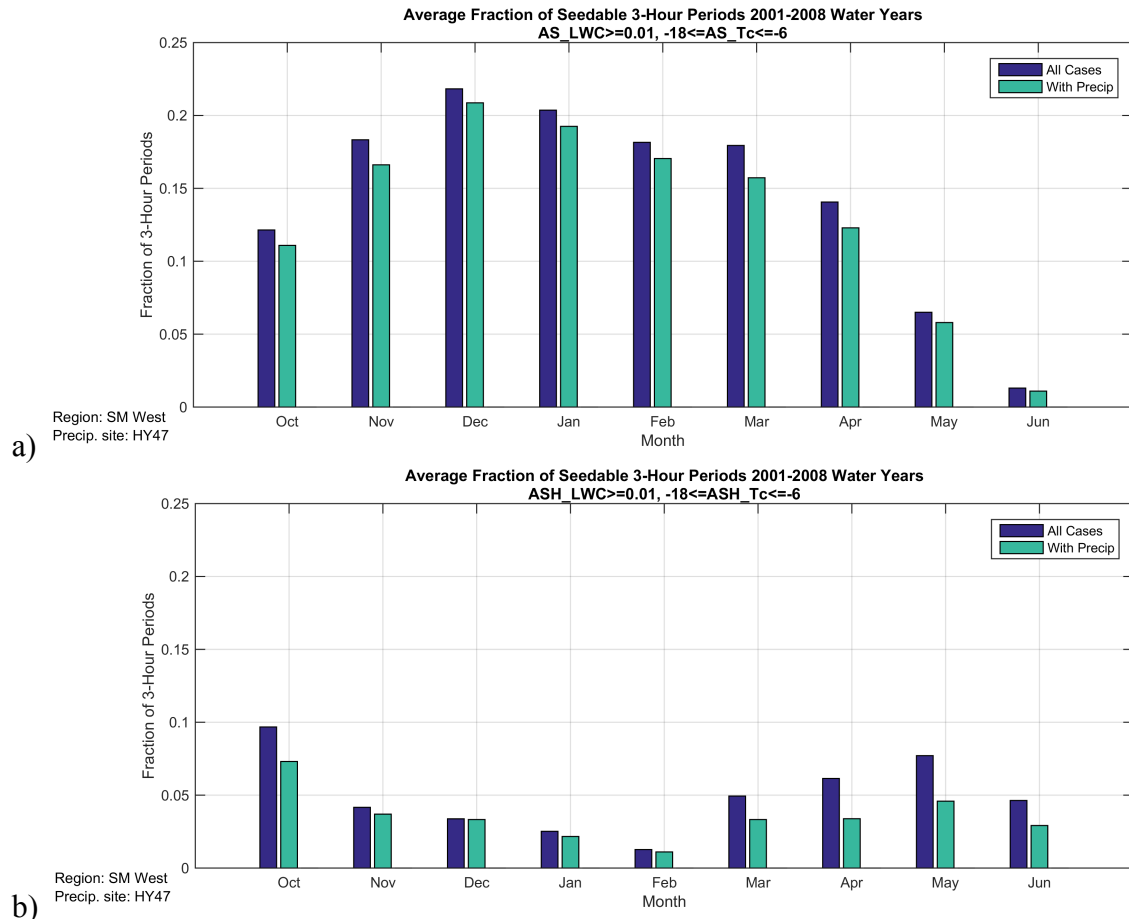


Figure 4.58. Bar chart showing the average fraction of hours in a month that met the temperature and LWC criteria averaged over SMWest for the (a) AS layer and (b) ASH layer (blue) and the same for hours that also had precipitation in the model near the HY47 precipitation site (green).

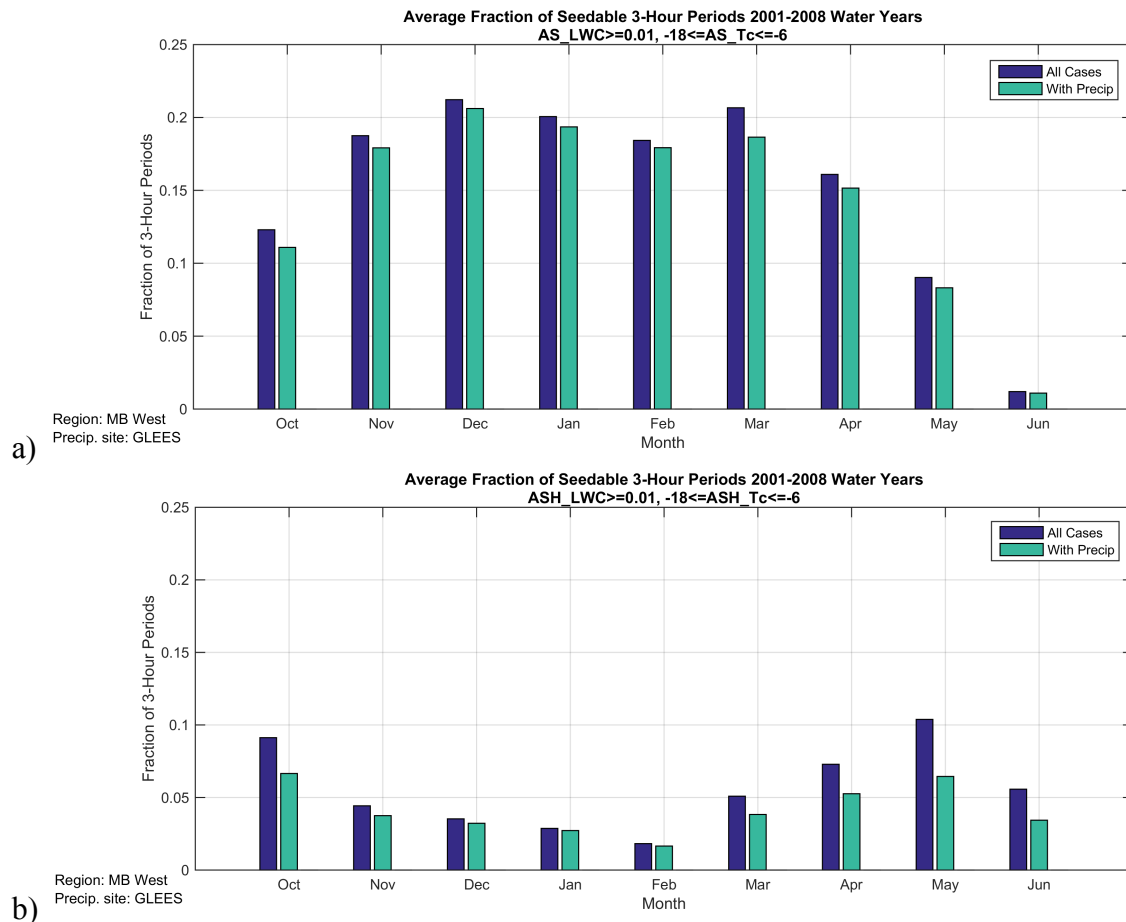


Figure 4.59. Bar chart showing the average fraction of hours in a month that met the temperature and LWC criteria averaged over MBWest for the (a) AS layer and (b) ASH layer (blue) and the same for hours that also had precipitation in the model near the GLEES precipitation site (green).

Like the ground-seeding layer, there is year-to-year variability in the fraction of seedable hours (Figure 4.60). The 2001–2002 season had the lowest frequency, while the other 7 years were similar in the total fraction of seedable 3-hour periods. The 8-year average seeding-potential frequency for the AS layer across both the SMWest and MBWest regions was about 19% of wintertime hours, and just over 17% when considering whether precipitation also occurred. When considering the AS layer over SMSouth (not shown), the 8-year average fraction of seedable conditions during wintertime hours with or without precipitation decreases to 14%. For the ASH layer (not shown), the frequency of seedable conditions decreases to about 4% (4%, 3%) for SMWest (MBWest, SMSouth) for all wintertime hours and 3% (3%, 2%) during precipitation. Note, the lack precipitation does not exclude it from being a potential cloud seeding opportunity; however it does prevent us from calculating the seedable precipitation for those events with zero precipitation.

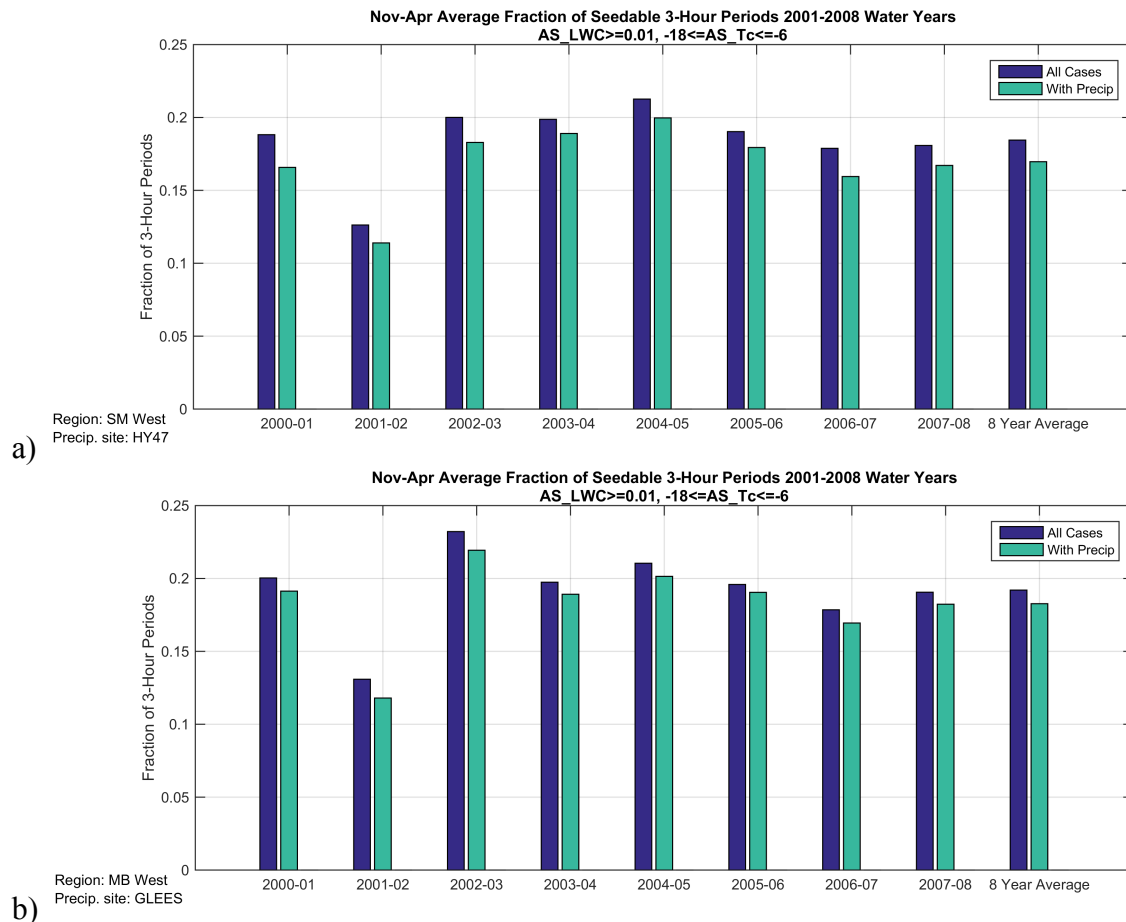
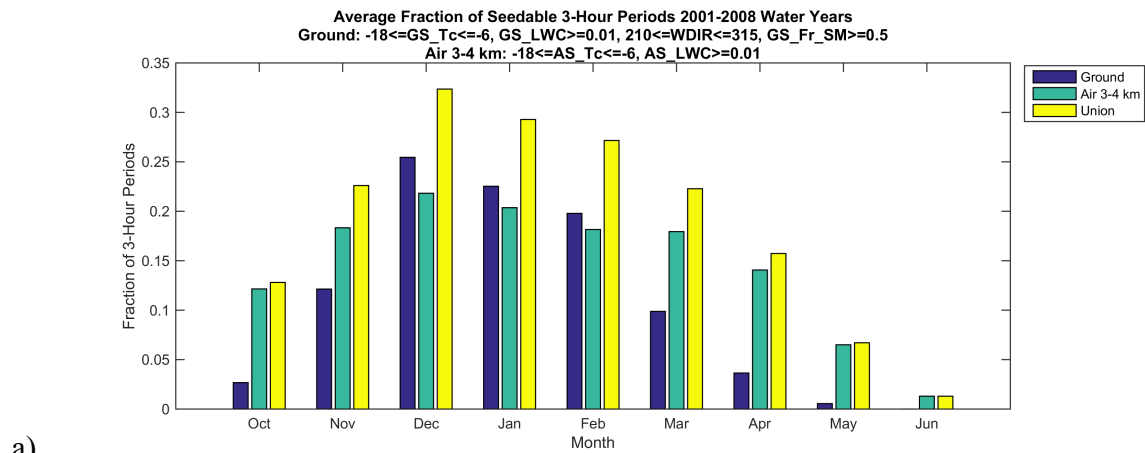


Figure 4.60. Bar chart showing the average fraction of hours in a winter season (November–April) that met the temperature and LWC criteria averaged over (a) SMWest and (b) MBWest for the AS layer (3–4 km MSL; blue) and the same for hours that also had precipitation in the model near the (a) HY47 or (b) GLEES precipitation site (green).

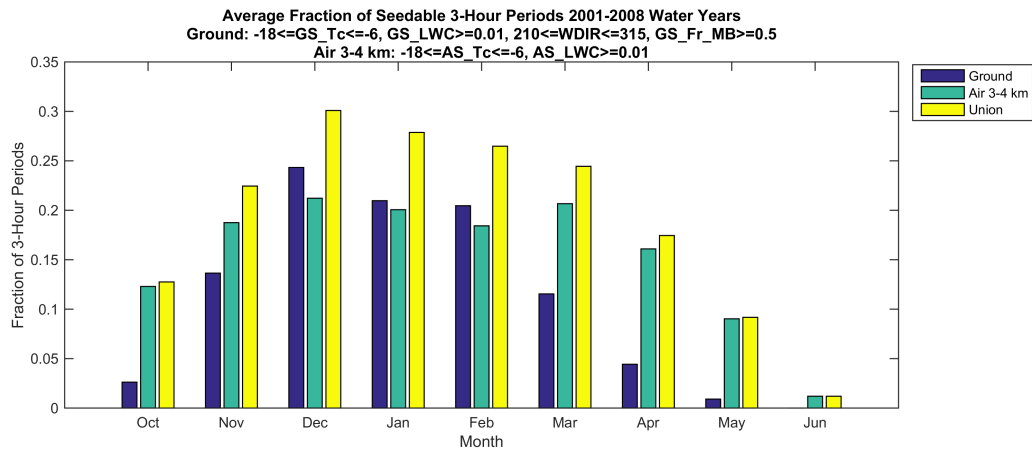
When normalized by the presence of clouds, the 8-year average frequency of AS opportunities (i.e., those that met the temperature and LWC criteria) relative to when clouds were present was 31% (not shown), nearly the same as that for ground-based seeding opportunities. For ASH, the opportunities decrease to only 6% (not shown).

Ground versus Airborne-seeding Opportunities

Using the area-based model analysis and considering all of the additional criteria that impact ground-seeding opportunities, the airborne-seeding opportunities at the 3–4 km MSL layer are a few percent lower than the ground-seeding opportunities during the December–February months, but up to 5–10% higher during November and March–April (Figure 4.61). While seedable conditions frequently exist in both layers simultaneously, a program that includes both ground and airborne options for seeding can employ either seeding method (or both simultaneously) at any given time. Therefore, the frequency of the union of the ground and airborne-seeding cases was calculated to determine how often a program could use using both options. Such a program would see an increase in frequency of seeding opportunities to about 30% during December–January and roughly 25% for the season, based on the 8-year average (Figure 4.62).

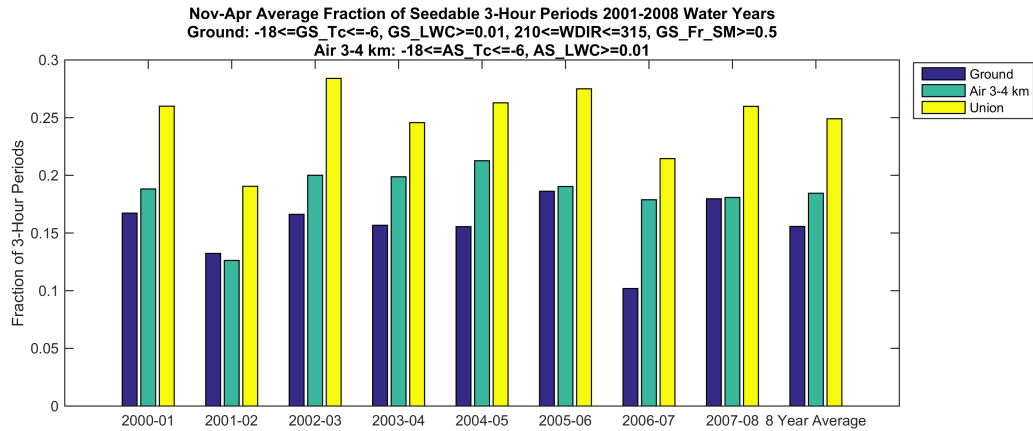


a)

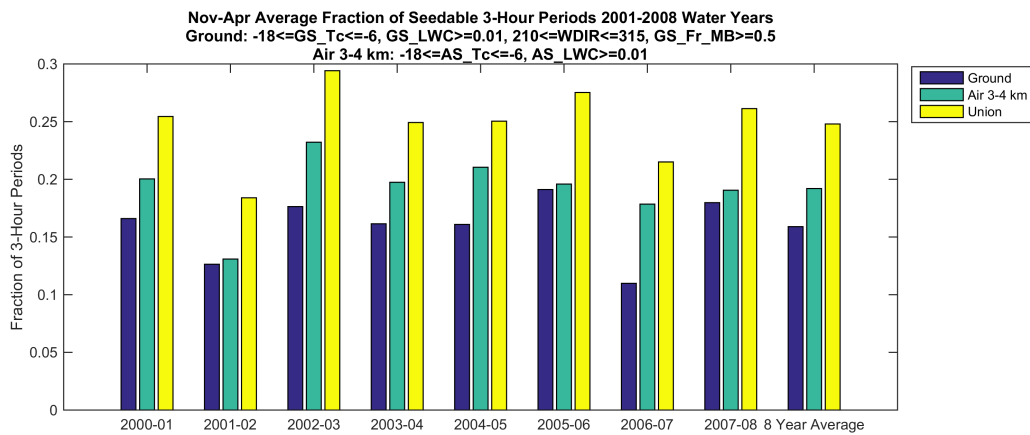


b)

Figure 4.61. Ground (0–1 km AGL; blue) versus airborne (3–4 km MSL; green) seeding opportunities (fraction of hours in the season that meet the designated criteria, listed atop the figure) by month for (a) SMWest and (b) MBWest. The frequency of occurrence of cases from the union of both ground and AS layer seeding potential is shown in the yellow bar for each time period.



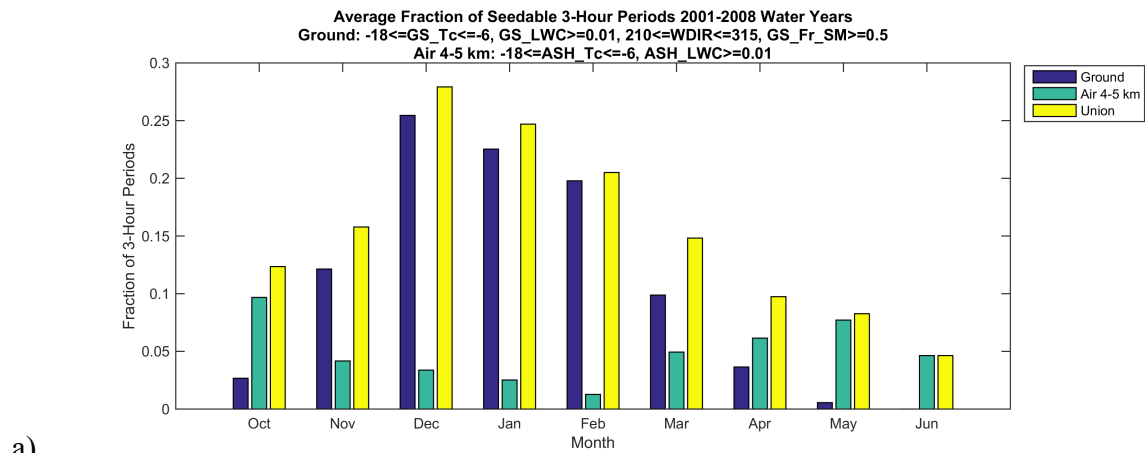
a)



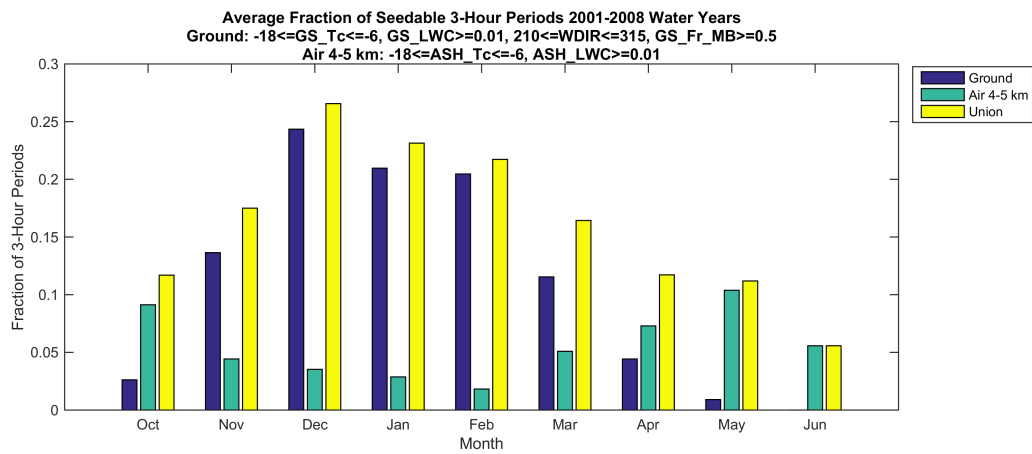
b)

Figure 4.62. Ground (0–1 km AGL; blue) versus airborne (3–4 km MSL; green) seeding opportunities (fraction of hours in the season that meet the designated criteria, listed atop the figure) by November–April season, and the 8-year average, for (a) SMWest and (b) MBWest. The frequency of occurrence of cases from the union of both ground and AS layer seeding potential is shown in the yellow bar for each time period.

As mentioned in the spatial mapping analysis above, the airborne layer at 4–5 km MSL was also assessed, but has much less potential for airborne seeding given less LWC and/or temperatures that are frequently too cold. This result is summarized again herein, showing the comparison relative to ground-based seeding potential from the area-based analysis (Figure 4.63). For the 4–5 km MSL airborne-seeding layer, the highest fraction of hours meeting the temperature and LWC criteria (still under 10%) typically occurs during the transition months of October–November and March–May. Evidently, airborne-seeding opportunities at this higher altitude occur less than 5% of the time during the November–April months, on average (Figure 4.64). However, the coincidence of the ground and 4–5 km MSL airborne cases is nearly a sum of the fractions of ground and 4–5 km MSL airborne cases. This indicates that there are only few instances of conditions simultaneously met in both layers; in other words, the 4–5 km MSL airborne layer and ground-seeding cases mostly occur at different times.

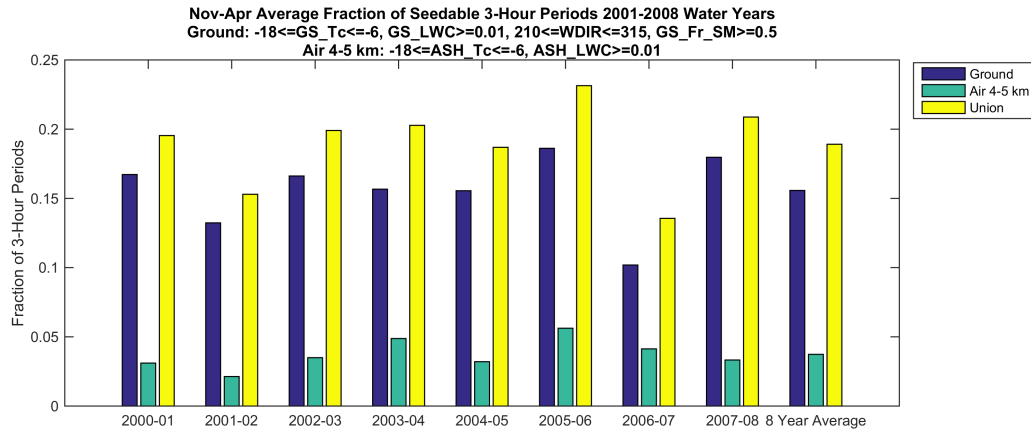


a)

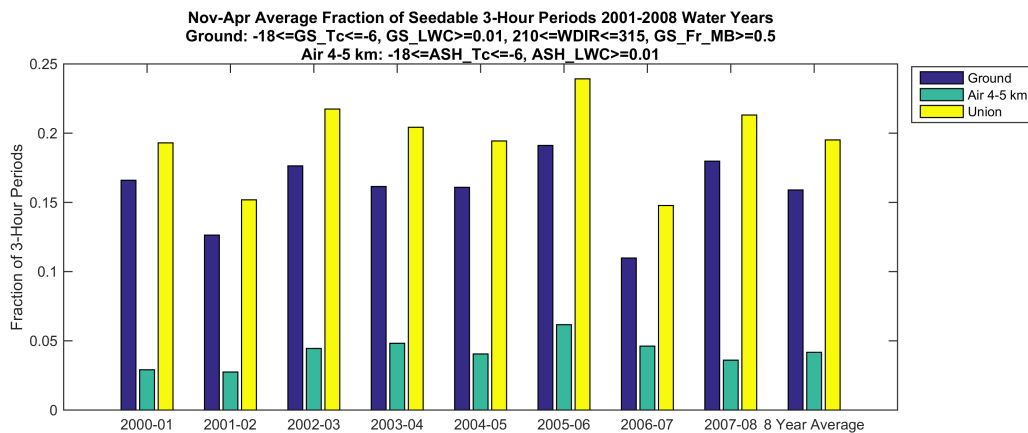


b)

Figure 4.63. Ground (0–1 km AGL; blue) versus airborne (4–5 km MSL; green) seeding opportunities (fraction of hours in the season that meet the designated criteria, listed atop the figure) by month for (a) SMWest and (b) MBWest. The frequency of occurrence of cases from the union of both ground and AS layer seeding potential is shown in the yellow bar for each time period.



a)



b)

Figure 4.64. Ground (0–1 km AGL; blue) versus airborne (4–5 km MSL; green) seeding opportunities (fraction of hours in the season that meet the designated criteria, listed atop the figure) by November–April season, and the 8-year average, for (a) SMWest and (b) MBWest. The frequency of occurrence of cases from the union of both ground and AS layer seeding potential is shown in the yellow bar for each time period.

4.5. Seedable Precipitation

Modeled precipitation falling during hours with seedable conditions was totaled throughout the wintertime months (November–April) to determine the total seasonal “seedable precipitation.” Then, the total seasonal seedable precipitation can be compared with the total wintertime precipitation to determine what fraction of the total precipitation could have been seeded. However, there may be seedable storms that did not produce precipitation (i.e., instances when temperature and LWC were suitable, but no precipitation occurred). When precipitation does not occur during seedable periods, it is impossible to quantify the potential impact relative to natural precipitation for those situations. As shown in Table 4.9, 44% of the wintertime precipitation for the western regions was seedable by ground-based seeding, 56–58% by lower-layer airborne seeding, and 15% by upper-layer airborne seeding. For ground-based seeding in the western regions when including the additional criteria (wind direction and atmospheric stability) needed to effectively transport AgI over the target areas, only 38–39% of wintertime precipitation was seedable. The additional ground-based criteria reduce the eastern regions’ seedability to 0%. Despite similar total precipitation, the precipitation that fell during seedable periods in the eastern regions was lower for all types of seeding, both absolutely and relatively. Seedable precipitation amounts in the Sierra Madre southern region for airborne seeding were similar to

the eastern regions, both in total and percentage. For ground-based seeding, the seedable precipitation in the Sierra Madre southern region was less than the western region and more than the eastern region, and the additional ground-based seeding criteria only resulted in a one-quarter reduction in the seedable precipitation. Therefore, the western regions show the most potential for seeding by aircraft or ground-based generators. The Sierra Madre southern region has some potential, and while the eastern regions have some potential for airborne seeding, the eastern regions have negligible potential for ground-based seeding.

Table 4.9. Wintertime (November–April) 8-year average simulated total precipitation (mm) compared with the seasonal precipitation that fell during ground-seedable (“GS”, 0–1 km AGL) time periods versus lower airborne-seedable (“AS”, 3–4 km MSL), and upper airborne-seedable (“ASH”, 4–5 km MSL) times. The percent of the total seasonal precipitation that was seedable is provided in parentheses next to the absolute seedable precipitation. For ground-seeding potential, both the primary criteria (temperature and LWC only) are compared with the scenario with additional criteria included (wind direction and Froude number). The model precipitation was extracted from one of three precipitation sites (Figure 4.2) depending on the region.

Region & Precip. site	Seedable Wintertime Precipitation (mm)				
	Season Total Precipitation	GS: T+LWC	GS: T+LWC+WDIR+Fr	AS: T+LWC	ASH: T+LWC
SM West & HY47	683	301 (44%)	264 (39%)	396 (58%)	104 (15%)
SM East & HY47	683	176 (26%)	0 (0%)	209 (31%)	30 (4%)
SM South & SM South	537	169 (32%)	126 (24%)	196 (37%)	38 (7%)
MB West & GLEES	623	274 (44%)	239 (38%)	347 (56%)	93 (15%)
MB East & GLEES	623	150 (24%)	0 (0%)	187 (30%)	26 (4%)

4.6. Climatological Analysis Summary

In summary, the climatological analysis indicates that the western slopes of both ranges are the most seedable in terms of storm frequency and suitability, whether seeded from the ground or by aircraft. The analysis indicates that seeding opportunities occurred frequently enough to warrant placing a few ground-based generators in the Sierra Madre south region to target the southern extents of the range; however, these sites may be better (or more frequently) used to target the southern extents of the Medicine Bow Range, as discussed in Section 6. The lower frequency of suitable seeding conditions coupled with limiting wind directions and atmospheric stability suggests that the eastern regions of both ranges should not be considered for ground-based seeding. Results show that seeding by aircraft is feasible over both ranges, and the opportunities to do so are frequent enough to warrant the implementation of an airborne program. Ground-based seeding conditions occurred when approximately 38% of the wintertime precipitation fell, whereas airborne-seeding conditions occurred during approximately 56% of the wintertime precipitation. These percentages of “seedable precipitation” are based on the results of the western regions, which form the basis for the program design and will be used to calculate the estimated streamflow benefits described in Section 12.

5. Task 4: Development of a Preliminary Project Design

The overall goal of this task was to examine and develop the components of a cloud seeding project design for the Medicine Bow and Sierra Madre Ranges. The process followed the steps outlined in ASCE Standard#42-04 (ASCE 2004):

1. Definition of project scope
2. Targeting and delivery methods
3. Seeding agent selection
4. Meteorological data collection and instrumentation
5. Selection and siting of seeding equipment
6. Legal issues
7. Environmental concerns

Some of the steps in developing a project design are reported in separate sections of this report, such as meteorological data and instrumentation (Section 9), and legal issues and environmental concerns (Section 10). The remaining steps are described in more detail below.

The design process of selecting and siting seeding equipment relies on the WRF model configured with a seeding parameterization to assess potential seeding effects resulting from various seeding scenarios and seeding delivery methods (e.g., siting of ground-based seeding generators). The WRF modeling system was used to iteratively assess and improve the preliminary project design by simulating selected case studies. Available meteorological observations in the region were used to evaluate the model performance for each case. This design process is described in Section 6. The design process was iterative based upon the results of the cloud-seeding model evaluation, therefore there are several additional aspects of the design described below that emerged as a result of initial cloud-seeding model simulations.

5.1. Project Scope and Targeting

The proposed target area is the Medicine Bow and Sierra Madre Ranges, with drainage into the North Platte and Green River Basins. The Medicine Bow Range is a nearly round-shaped mountain barrier in south central Wyoming. The Sierra Madre Range is located to the southwest of the Medicine Bow Range and is oriented from northwest to southeast. The highest peak in this region is Medicine Bow Peak at 3,662 m (12,013 ft) MSL located in the central portion of the Medicine Bow Range. The highest peak in the Sierra Madre Range is Bridger Peak at 3,354 m (11,004 ft) MSL. The total area assessed in this study was defined as elevations above 8,000 ft MSL, is 2,468 km² in the Medicine Bow and 2,459 km² in the Sierra Madre, for a combined total of 4,927 km² (Figure 5.1). The climatology analysis (Section 4) illustrated that the dominant wind direction is westerly, therefore preliminary project designs focused on targeting the western slopes of the Ranges. The climatology analysis also indicated that the best season for seeding in this region is between November and April.

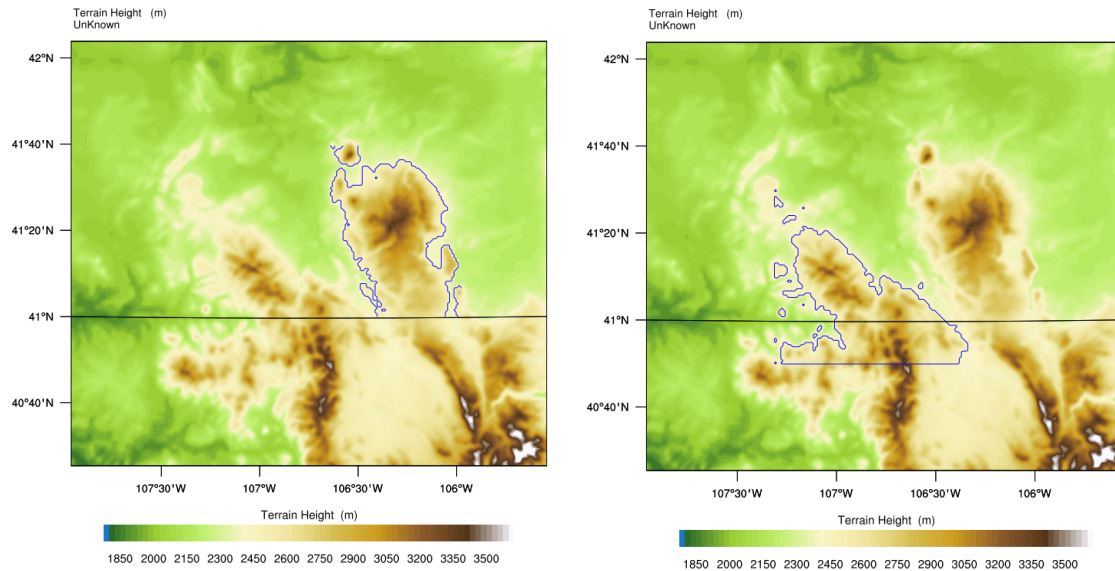


Figure 5.1. Maps of the terrain across the study region, highlighting the assessment area for the Medicine Bow (left) and Sierra Madre (right) Ranges, defined as area greater than 8,000 ft MSL elevation.

5.2. Delivery Methods and Seeding Agent Selection

A review of seeding agents for glaciogenic seeding was provided in Section 3. AgI is the recommended seeding agent because it has a longer effective lifetime than liquid propane and does not need to be released directly into supercooled clouds. Effective targeting of supercooled cloud regions depends on several factors related to the mode of seeding-agent delivery: adequate dispersion and concentration of the seeding material, costs, and logistical constraints (i.e., permissible flight altitudes, access to ground-based sites, permits and leases, reliable operation of the delivery mode). Two modes of ground-based AgI seeding (manually-operated generators and remotely-controlled generators) and the airborne release of AgI were reviewed, identifying pros and cons for each approach (Section 3). Figure 5.2–Figure 5.3 demonstrate the equipment used for the different seeding dispersion modes (i.e., ground and airborne).



Figure 5.2. Example of a remotely controlled AgI generator.



Figure 5.3. Example of cloud seeding aircraft.

5.3. Selection of Test Cases

Section 6.3 describes the selection process for the test cases (seeded storms) used to assess the seeding impacts using numerical modeling of various generator and aircraft track locations. Four storms, all from the randomized seeding cases of the WWMPP, were selected to represent a variety of regimes identified in the climatology analysis. The cases represented different wind directions at 700 hPa, neutral to weakly stable low-level atmospheric conditions, with similar (upstream) LWPs. A comparison of the WRF cloud seeding model results for these test cases against several different seeding scenarios guided the iterative design process. The various seeding modes and ground-based generator design groups were simulated for each of the cases in which conditions for the generator groups were suitable for seeding.

5.4. Initial Ground-based Tests

The preliminary project designs initially tested in the model were based upon the locations of ground-based generator sites from the WWMPP, as well as additional sites identified as part of the 2015 field survey to help complete areas not previously covered by the WWMPP sites (Figure 5.4). From the sites shown in Figure 5.4, seven groups (Figure 5.5), three in the Medicine Bow (A–C) and four in the Sierra Madre (A–D), were formed for testing with the WRF cloud-seeding model. Sites that were surveyed on the eastern slopes of both Ranges were not selected for model testing, because the results of the climatology analysis showed infrequent easterly upslope events favorable for seeding.

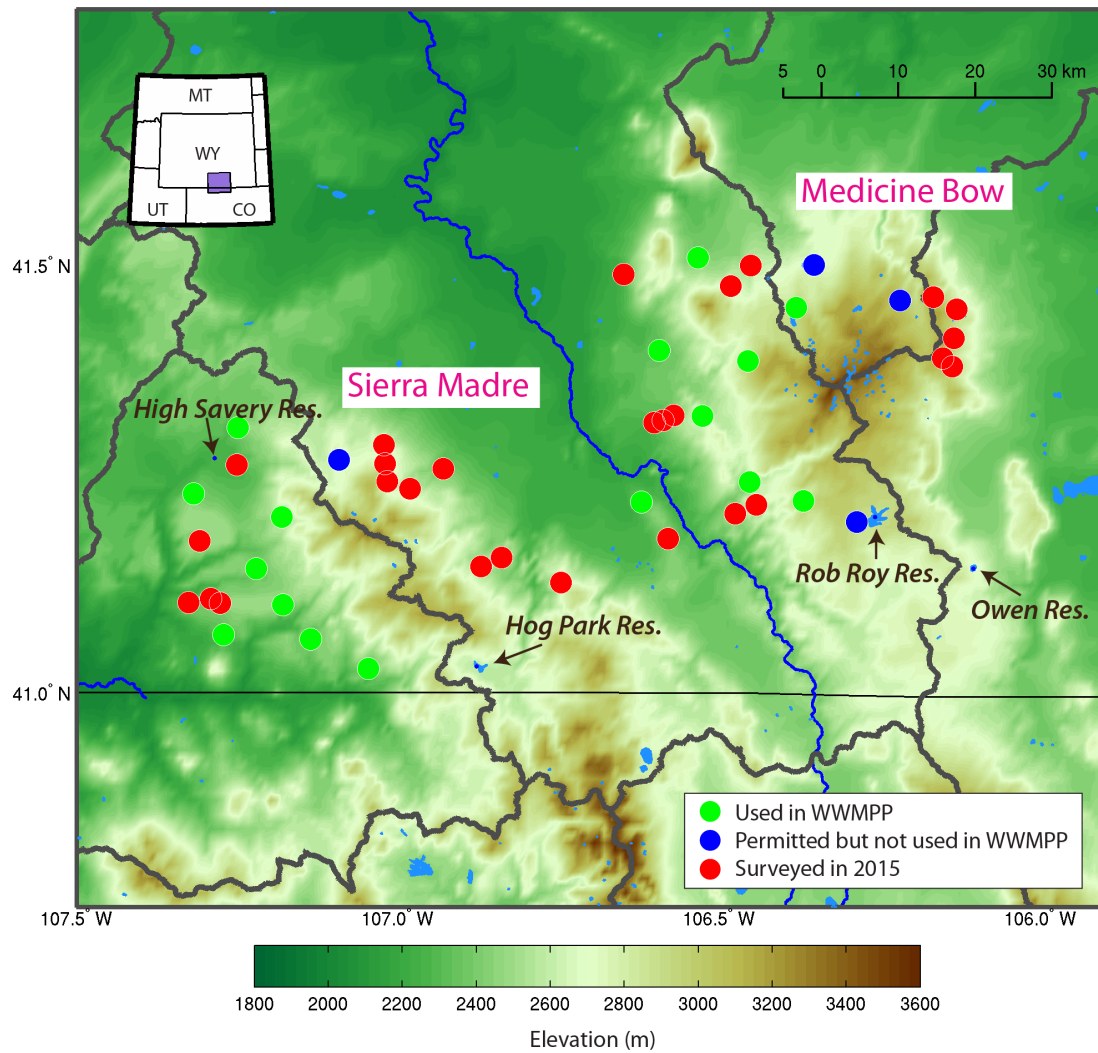


Figure 5.4. Topography map of the Medicine Bow and Sierra Madre Ranges (m) illustrating the locations of the generator sites used in the WWMPP (green), those permitted but not used in the WWMPP (blue), and the new sites surveyed in 2015 to “fill in the gaps” (red). These sites formed the basis for the site groupings illustrated in Figure 5.5.

Figure 5.5 shows the locations of the preliminary ground-based generator design groups. Group A was the most upwind group for each range, with Group C being located closest to the crest of each barrier. Group D generators were located in the Sierra Madre to test for situations when northerly-northeasterly winds created upslope flow into the southern end of the Sierra Madre, as well as to investigate potential impacts to the southern end of the Medicine Bow under westerly winds.

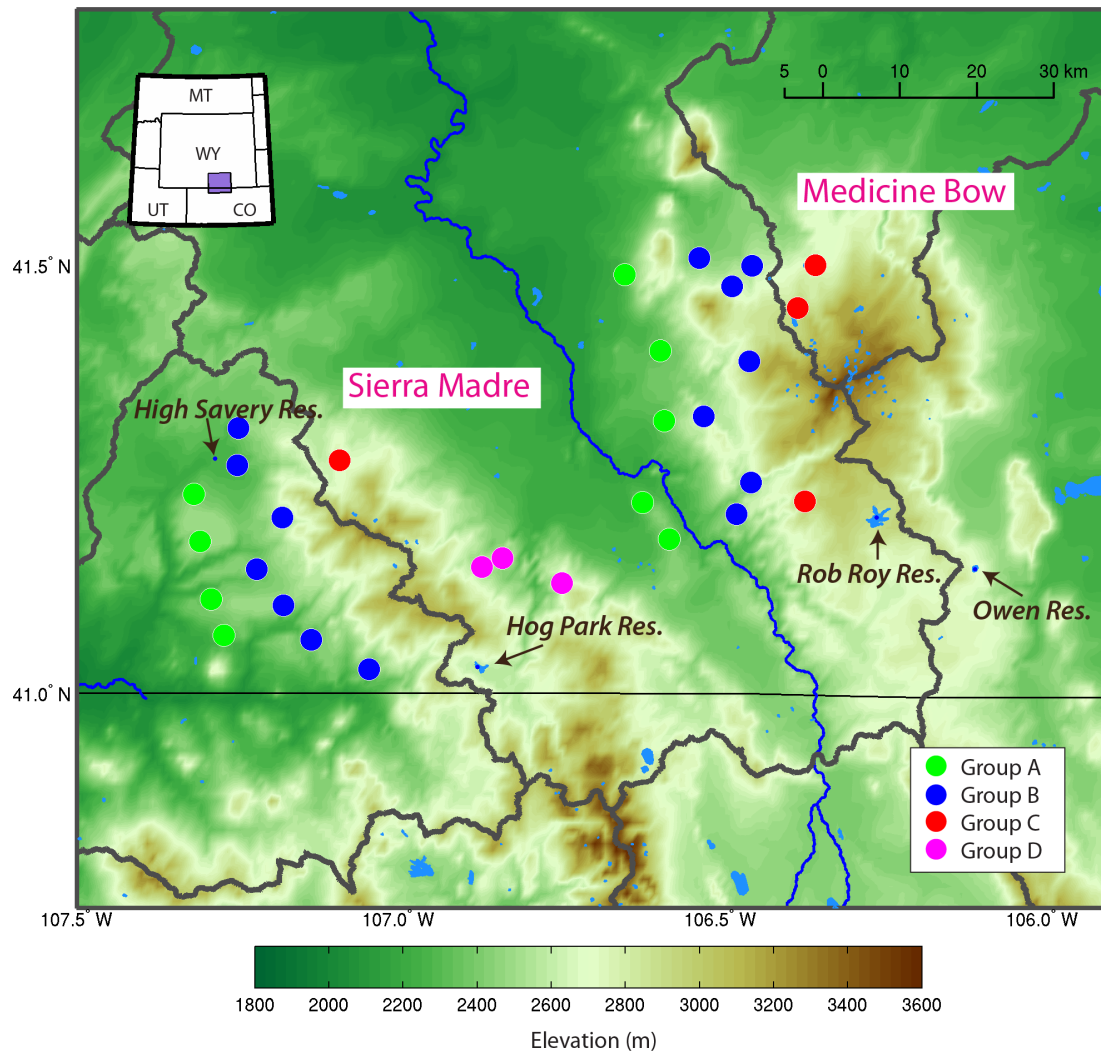


Figure 5.5. Topography map of the Medicine Bow and Sierra Madre Ranges (m) illustrating the locations of initial ground-based generator design groups.

5.5. Additional Ground Generator Tests

The early results of the ground-based seeding simulations using Groups A–D (Figure 5.5) suggested simulated impacts of seeding could occur on the Medicine Bow by seeding from the Sierra Madre. As a result, five additional generators were added into Group C along the crest line of the Sierra Madre. Furthermore, two additional groups were added west of the Sierra Madre (Groups E and F) to investigate if the Sierra Madre Range could be better targeted by generators located farther upwind (Figure 5.6).

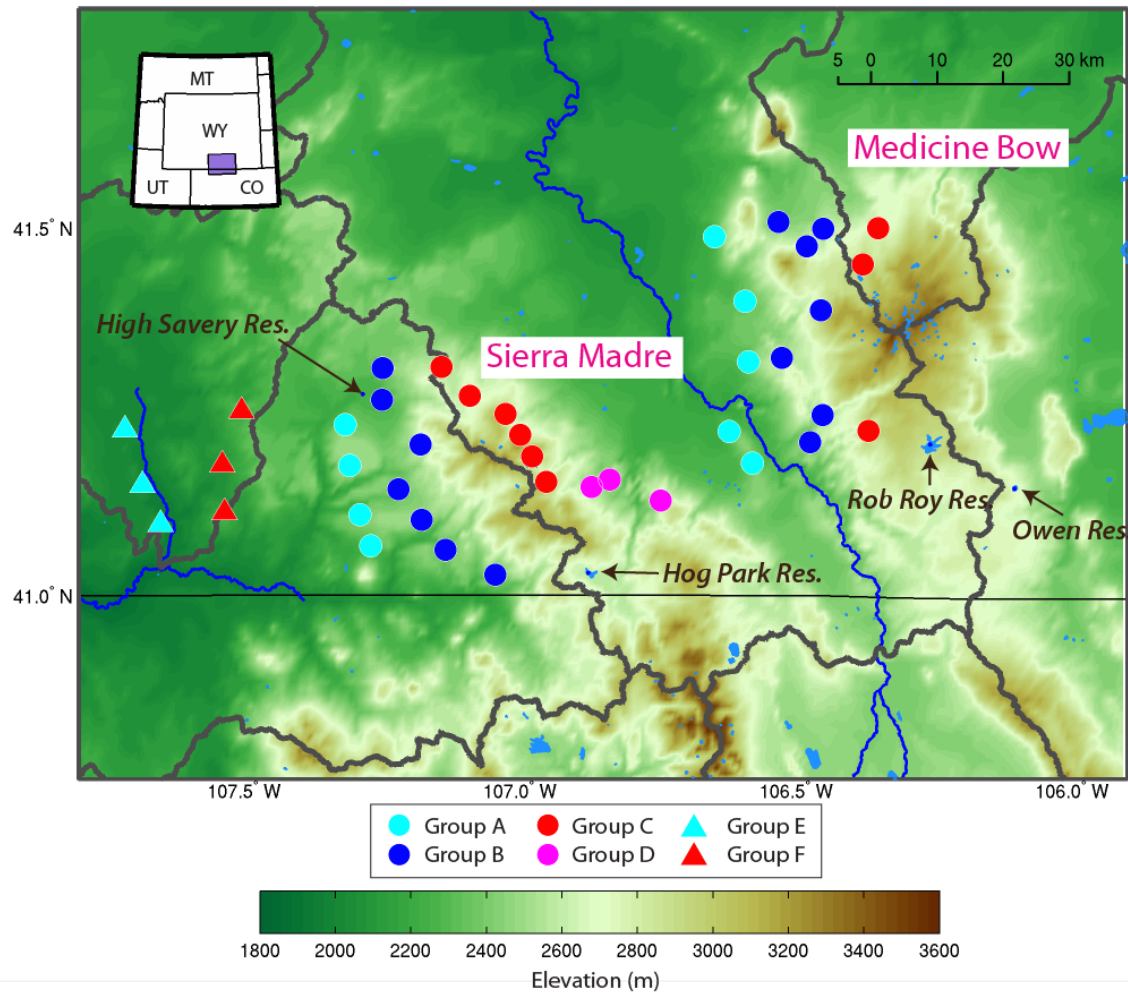


Figure 5.6. Topography map of the Medicine Bow and Sierra Madre Ranges (m) illustrating the locations of additional ground-based generator design groups.

5.6. Airborne Tests

Two airborne tracks were designed and tested in the seeding experiments for cases when seeding conditions were suitable for airborne seeding. Model simulations were performed to compare the difference of the track altitude on the simulated seeding effects in the assessment area.

A northeast-southwest oriented track (~50 km long) to the northwest of the Sierra Madre Range was designed for northwesterly winds, while a north-south track (~65 km long) to the west of the Sierra Madre Range was designed for use in westerly wind scenarios (Figure 5.7). Details of the results from these test simulations are provided in Section 6.

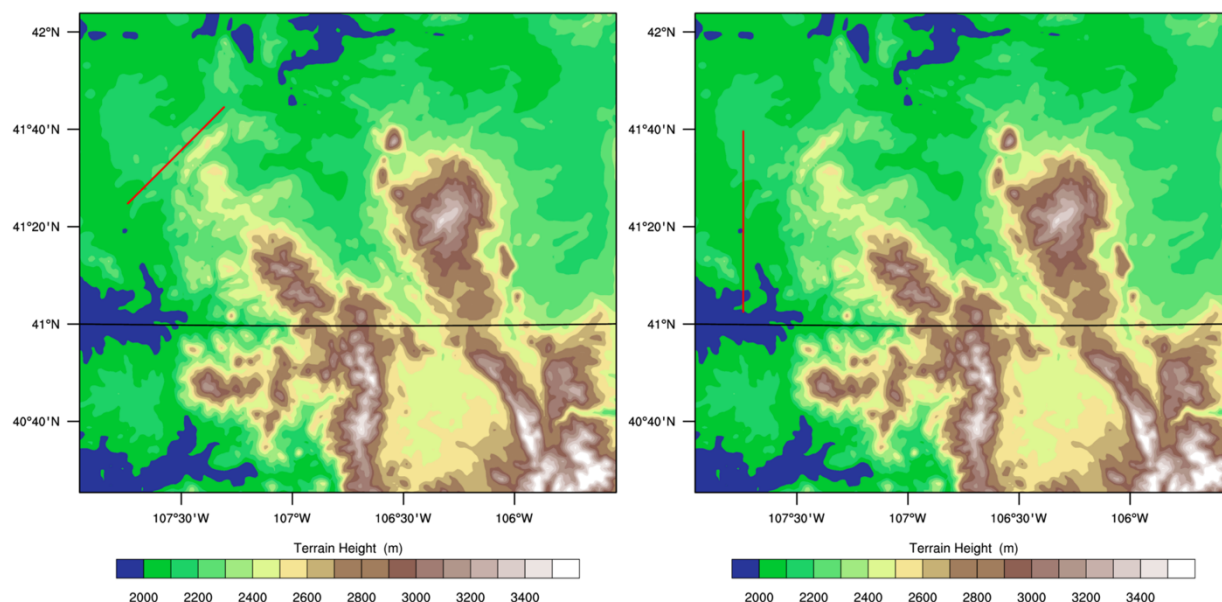


Figure 5.7. Flight track positions (red line) designed for testing in the model.

5.7. Ground-based Generator Locations

After further evaluation, Groups E and F were ruled out being less effective in targeting the Sierra Madre Range due to their location lower elevation upwind of the barrier. In some cases, the AgI plumes from these generators were blocked (or partially blocked) by the range itself, and the simulated results showed the plumes being transported around the northern tip of the Sierra Madre Range. Once Groups E and F were deemed ineffective and removed from the project design, 35 sites remained. These remaining 35 sites from Sierra Madre Groups A, B, C, and D and Medicine Bow Groups A, B, C were included in the field survey summarized below in Section 7.

5.8. Summary Remarks

A summary of the preliminary project design for seeding the Medicine Bow and Sierra Madre Ranges to enhance precipitation and streamflow into the North Platte and Green River Basins includes the following:

- the total area assessed in the Medicine Bow and Sierra Madre Ranges encompassed the North Platte and Green River Basins above 8,000 ft MSL (2,438 m). This area is approximately 4,927 km²;
- an operational season of November through mid-April (e.g., 15 November–15 April);
- silver iodide, or more specifically, a silver iodide-salt compound as the seeding agent. A ground-based cloud seeding generator network consisting of 35 remotely-controlled generators, located primarily on the western slopes of the ranges; and/or
- an airborne-seeding operation that can be positioned to target the regions of the barrier that are most suitable for seeding including those that cannot be targeted using ground-based techniques;

- the use of a prognostic numerical model with frequent updates to aid in identifying suitable seeding opportunities, possibly with an automated seeding criteria assessment; and
- in addition to, or in place of the numerical model, it is recommended that direct observations of seeding criteria parameters, such as liquid water and temperature and wind profiles are included in the project design.

Sharing operational resources (i.e., aircraft, staff, weather data, etc.) between adjacent cloud-seeding programs may be the most cost-effective way to target the Medicine Bow and Sierra Madre Mountains, and is highly recommended for consideration. Consolidating operational resources between projects would likely reduce project costs, and therefore increase the cost effectiveness for the project.

Various aspects of the design are covered in other sections of this report, such as the recommended criteria for seeding, criteria for suspending operations, environmental concerns, and the advantages and disadvantages of the different seeding dispersion modes (manual, remote, and airborne).

6. Task 5: Model Evaluation of the Preliminary Project Design

This task used a numerical model to evaluate, through an iterative process, the suggested locations of ground-based seeding generators and aircraft seeding flight tracks to optimize seeding strategies for the operational project design.

6.1. Overview of the model

The WRF numerical modeling system (Klemp et al. 2003; Skamarock et al. 2005, 2008; Mikalakes et al. 2004; Barker et al. 2004; Chen and Dudhia 2000) is a community model developed through a collaborative effort led by NCAR. Modifications to the physics parameterization in the model code simulate the dispersion and activation of AgI seeding material within the cloud (i.e., AgI cloud seeding parameterization, Xue et al. 2013a, b), and the subsequent microphysical responses leading to precipitation.

The NCAR AgI Seeding Parameterization (ASPEN; previously referred to as the Wintertime AgI Seeding Parameterization, WASP, in earlier studies) was embedded in the Thompson microphysics scheme (Thompson et al. 2008). The Thompson scheme originated in a study that tested several different microphysics schemes in an attempt to determine which one best-simulated mixed-phase clouds, including those with large amounts of SLW (Thompson et al. 2004). Several modifications to the Reisner et al. (1998) scheme resulted from this study, which produced the Thompson bulk microphysical scheme that appears to handle the sensitive balance of cloud water, snow, and graupel suitably for this study.

Using ASPEN, AgI particles can be released in the computing domain as a function of location, time, and source strength. In other words, it can represent the release of AgI from ground-based generators and/or airborne platforms (Xue et al. 2013a, b). With a prescribed source strength or release rate (g h^{-1}) and a known mean mass diameter (m), the number of AgI particles is derived. These AgI particles, acting as passive scalars, are advected and dispersed horizontally and vertically by model dynamics. The vertical diffusion, or mixing, of these particles is calculated by the PBL schemes. By default, the PBL schemes only mix water vapor, cloud water, and cloud ice vertically. To make vertical mixing of AgI particles more realistic, the PBL schemes were modified to mix all AgI related scalars vertically.

The AgI particles are assumed to be monodispersed in the AgI cloud seeding parameterization. Modifications were made to the parameterization so that a lognormal distribution of AgI particles could be simulated.

AgI particles can be collected by drops and ice-phase particles through Brownian, phoretic, and turbulent diffusion. When the conditions are favorable, these AgI particles can nucleate ice crystals through deposition, condensation freezing, contact freezing, and immersion freezing. Both mixing ratios and number concentrations of dry AgI, AgI in drops, ice, snow, and graupel are predicted. Both ground-based and airborne glaciogenic seeding effects can be simulated by this parameterization. The detailed interactions between AgI and hydrometeors are illustrated in Figure 6.1.

The WRF model with ASPEN was used before to simulate the seeding effect for the WWMPP, the Wyoming Range Phase II feasibility study, and for program design and evaluation for Idaho

Power Company (IPC). While efforts have been made to evaluate the model against available observations (i.e., soundings, radiometer, precipitation gauges), the required measurements to evaluate the physics of the cloud seeding parameterization itself have not been available. Therefore, the parameterization has not been fully evaluated and all simulated seeding results should be considered approximate. Nonetheless, the model’s ability to simulate the meteorological conditions needed for a seeding effect (i.e., temperature, winds, liquid water) can be validated with sounding and radiometer data. If these conditions are well represented by the model, it is a good indication that the resulting simulated seeding effects are reasonable. Furthermore, an assessment of the cloud seeding parameterization, simulating all of the WWMPP randomized seeding cases, has been included as part of this study (Section 21), to determine whether the model can represent the observed results of that statistical program.

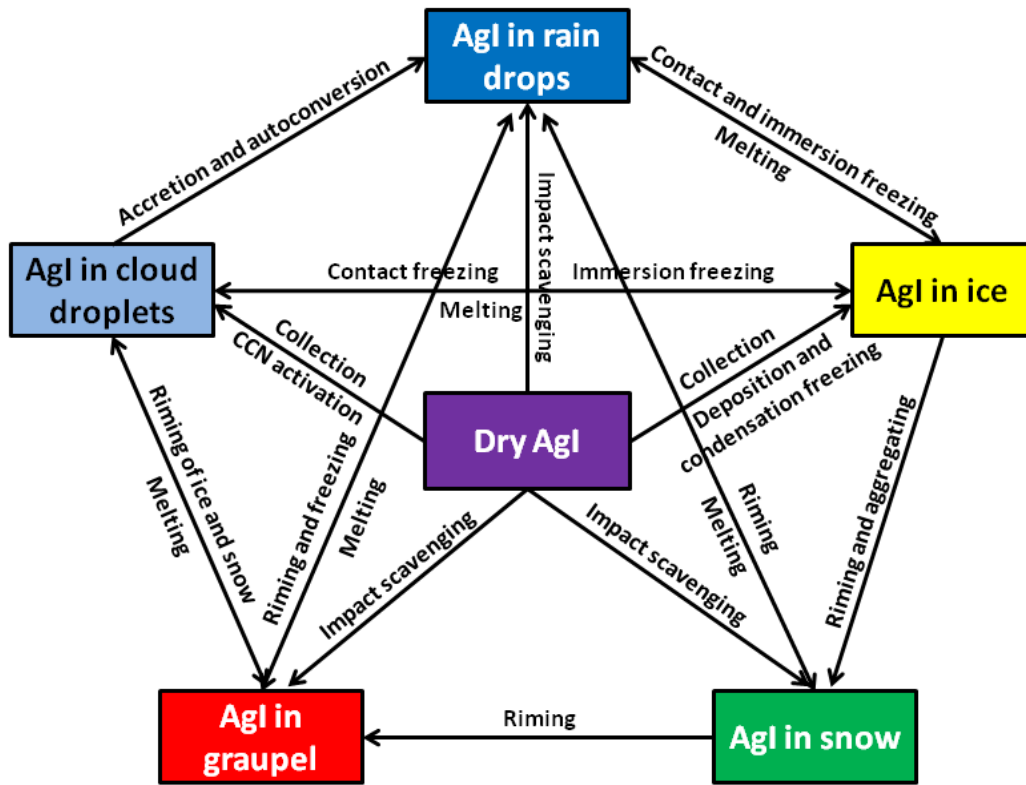


Figure 6.1. Interactions between AgI and hydrometeors simulated in the ASPEN cloud seeding parameterization (Xue et al. 2013a).

6.1.1. Updates to ASPEN and the Microphysical Scheme

Between the time that the ground-seeding test simulations were completed for this study and when the airborne test simulations were initiated, some important changes to the ASPEN seeding parameterization were made, including updating some of the physical processes, migrating ASPEN into the newest version of the Thompson microphysics scheme (Thompson and Eidhammer 2014), and migrating into a newer version of the WRF model (WRFV3.7.1).

The newest version of the Thompson microphysics scheme (Thompson and Eidhammer 2014) incorporates the explicit cloud droplet activation and ice nucleation as a function of the background CCN and IN concentration. Such an “aerosol-aware” version of the microphysical

scheme (Thompson-Eidhammer scheme) simulates more realistic clouds. The updated ASPEN was incorporated into the new Thompson-Eidhammer scheme and it was modified to simulate more AgI removal processes that were absent in the original version. In the WRFV3.7.1, the vertical mixing of all scalars was realized by all PBL schemes. The new version of ASPEN also simulates the AgI scavenging by precipitation particles (rain, snow, and graupel), AgI self-coagulation mainly through Brownian diffusion, and AgI dry deposition was added as a function of surface roughness and PBL height. The new AgI removal processes are listed in Table 6.1 for comparison with the original ASPEN processes. The detailed interactions between AgI and hydrometeors in the updated ASPEN are illustrated in Figure 6.2.

It would not have been feasible to re-run all of the previously completed ground-seeding simulations, therefore, only a few simulations were re-run to document any differences that may have resulted from using the updated ASPEN. However, it should be noted that all of the airborne-seeding test simulations were run with the newly updated ASPEN. The reason that this study migrated to the updated version of ASPEN was because it included more realistic physical processes with the potential to better represent the effects of seeding than the original version. For example, the AgI scavenging processes added into the new ASPEN could impact the simulated seeding effect in the Medicine Bow from seeding material released in the Sierra Madre, which was a key aspect of the results that needed to be explored using the newer version of ASPEN.

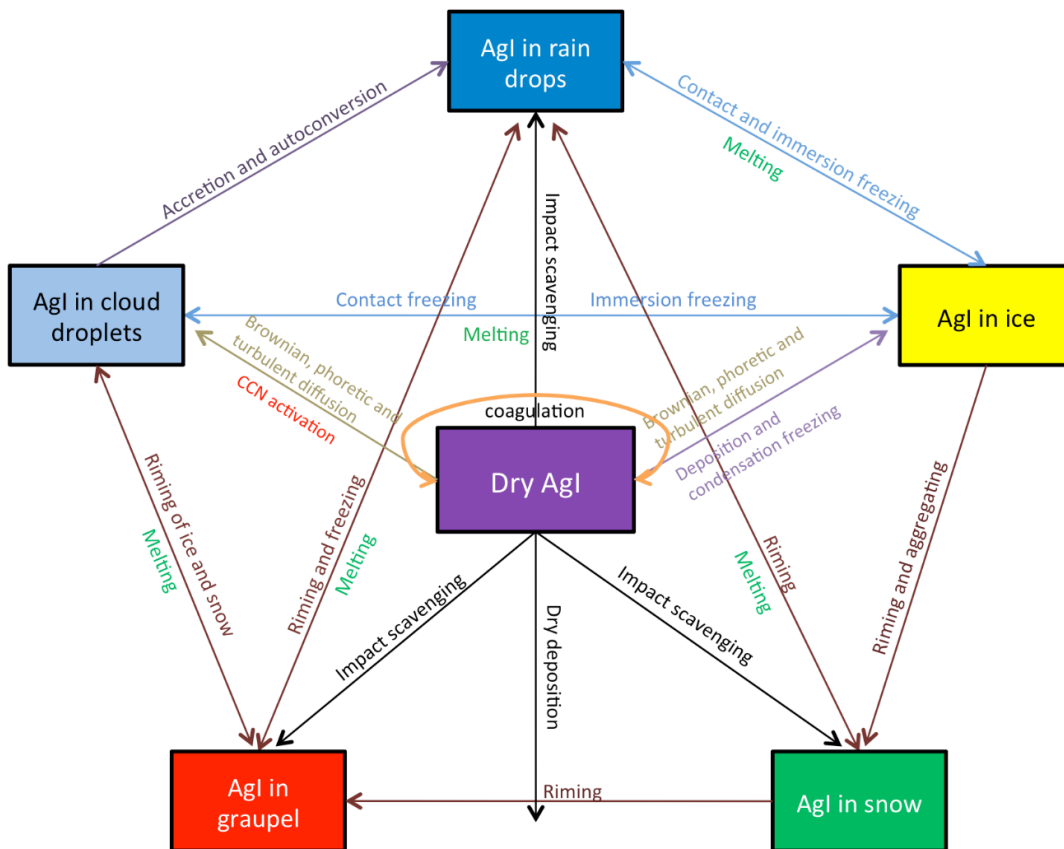


Figure 6.2. Interactions between AgI and hydrometeors simulated in the updated ASPEN cloud seeding parameterization (updated from Xue et al. 2013a).

Table 6.1. The extra AgI removal processes that are simulated in the new ASPEN

Process	Description
AgI self-coagulation	AgI number reduction due to the Brownian and phoretic process
Scavenging by rain	AgI collected by rain drops
Scavenging by snow	AgI collected by snow flakes
Scavenging by graupel	AgI collected by graupel particles
Dry deposition	AgI dry deposition due to surface roughness and PBL turbulence
Enhanced deposition	AgI dry deposition due to down draft close to the ground

6.2. Model setup

The WRFV3.4.1 model with the original ASPEN was used to simulate ground seeding in four test cases. For the airborne-seeding simulations (and a few re-runs of the ground-seeding simulations), WRFV3.7.1 was used with the updated ASPEN. A single domain was set up for the simulations (Figure 6.3). The domain covering both the Medicine Bow and Sierra Madre Ranges has a horizontal grid spacing of 900 m. The vertical coordinate consisted of 61 terrain-following vertically-stretched levels as were used in many previous studies (Xue et al. 2010, 2012, 2013a, 2013b, 2014).

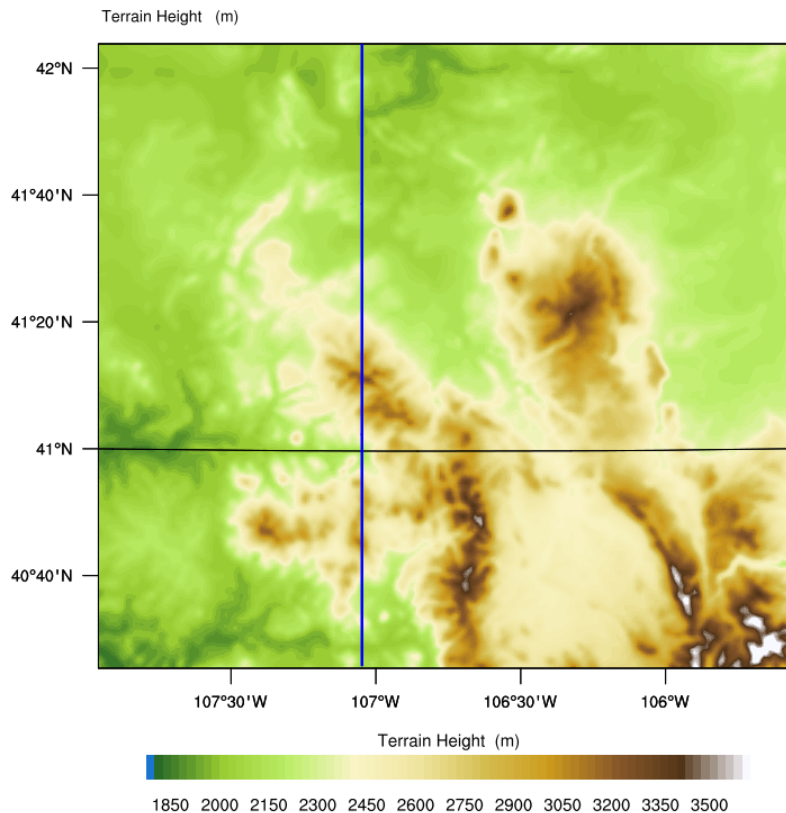


Figure 6.3. Model domain for seeding project design evaluation simulations.

The simulations were driven by analysis data of the innermost domain (2-km grid spacing) from the Real Time-Four Dimensional Data Assimilation (RT-FDDA) WRF forecast model designed

for the WWMPP. For each case, the domain was integrated for 9 to 14 hours with the first 2 to 3 hours as the spin-up period. The detailed configurations are listed in Table 6.2.

Table 6.2. Model configurations for cloud seeding project design evaluation simulations.

Configuration	Ground-seeding simulations	Airborne seeding simulations
WRF version	3.4.1	3.7.1
Horizontal grids	224 x 200	224 x 200
Grid spacing	900 m	900 m
Vertical levels	61 terrain-following Eta levels	81 terrain-following Eta levels
Driving data	RT-FDDA analysis data of the inner most domain with grid spacing of 2 km	RT-FDDA analysis data of the inner most domain with grid spacing of 2 km
Time step	5 s	5 s
PBL scheme	Mellor-Yamada-Janic (MYJ)	Mellor-Yamada-Nakanishi-Niino (MYNN)
Land surface model	Noah	Noah-MP
Cumulus scheme	N/A	N/A
Nudging	N/A	N/A
Microphysics	Thompson with the Wintertime AgI Seeding Parameterization (WASP)	Thompson-Eidhammer scheme with the updated WASP
AgI scavenging	Cloud, ice and AgI nucleation	Cloud, ice, rain, snow, graupel and AgI nucleation
AgI coagulation	N/A	Brownian and phoretic coagulation
AgI dry deposition	N/A	Due to PBL turbulence and surface roughness
Enhanced deposition	N/A	Due to downdraft close to the ground

6.3. Case overviews

Four cases were chosen to test simulated seeding impacts of different generator groups under different wind regimes. The cases were selected from three seasons of WWMPP seeding simulations. Each case represents an experimental unit (EU) from the WWMPP RSE and were chosen to represent different wind regimes. The wind regimes were determined using the measured wind direction from proximity soundings released at Saratoga, Wyoming during the WWMPP for each EU. The first two cases have generally westerly 700-hPa winds: 23 January 2010 (EU70) and 10 January 2014 (EU152). The third case has northwesterly 700-hPa winds: 13 January 2014 (EU157). The fourth case has southwesterly 700-hPa winds: 21 February 2012 (EU120). Of these four cases, only the third (13 January 2014) and fourth (21 February 2012) were identified to have airborne-seeding potential (airborne flight levels were too cold for seeding in the first two cases). Ground-seeding cases re-run with the updated ASPEN were only performed for these latter two cases (EU157 & EU120).

6.4. Case study simulations

Nine groups of generators in different locations have been tested (Figure 5.6, Section 5). For each case, one control simulation (no seeding was simulated) and then several seeding simulations with various combinations of Medicine Bow (MB) and/or Sierra Madre (SM) generator groups were performed. Based on the wind direction in the airborne-seeding layer, two

flight tracks were tested (Figure 5.7). For case 3 (13 January 2014), only one airborne-seeding case was simulated while three airborne-seeding cases with different track altitudes and duration were conducted for case 4 (21 February 2012). The airborne-seeding rate was set to 1.8 kg h^{-1} . For the ground-seeding cases that were re-run to test the impact of AgI scavenging processes using the newly updated ASPEN, seeding was simulated using all Sierra Madre generators (groups A to F) for each case.

6.4.1. Case 1: 23 January 2010 results

For this case, the control run was integrated from 23 January 2010 2100 UTC to 24 January 2010 0600 UTC. Seeding simulations were integrated between 23 January 2010 2345 UTC to 24 January 2010 0345 UTC. Various combinations of ground-generator groups were simulated in different experiments. The seeding simulation experiments are listed in Table 6.3.

Table 6.3. Seeding simulation experiments of 23 January 2010 case. The SM “oriC” group consists of the one original Group C generator shown in Figure 5.5.

Run 1	SM A+B+oriC & MB A+B+C
Run 2	SM A+B+oriC
Run 3	MB A+B+C
Run 4	SM A
Run 5	MB A
Run 6	SM B
Run 7	MB B
Run 8	MB C
Run 9	SM A+B+oriC+D
Run 10	MB A (north generator only)
Run 11	SM D
Run 12	SM oriC
Run 13	SM A+B+C
Run 14	SM A+B+C & MB A+B+C
Run 15	SM E+F
Run 16	SM E
Run 17	SM F
Run 18	SM A+B+C+D+E+F
Run 19	SM A+B+C+D

The simulated natural precipitation (accumulation over the simulation period) in case 1 is stronger in the Medicine Bow Range than in the northern (target) region of Sierra Madre Range (Figure 6.4). The LWP during and after the seeding period, however, indicated that more SLW was available in the Sierra Madre Range than in the Medicine Bow Range (Figure 6.5).

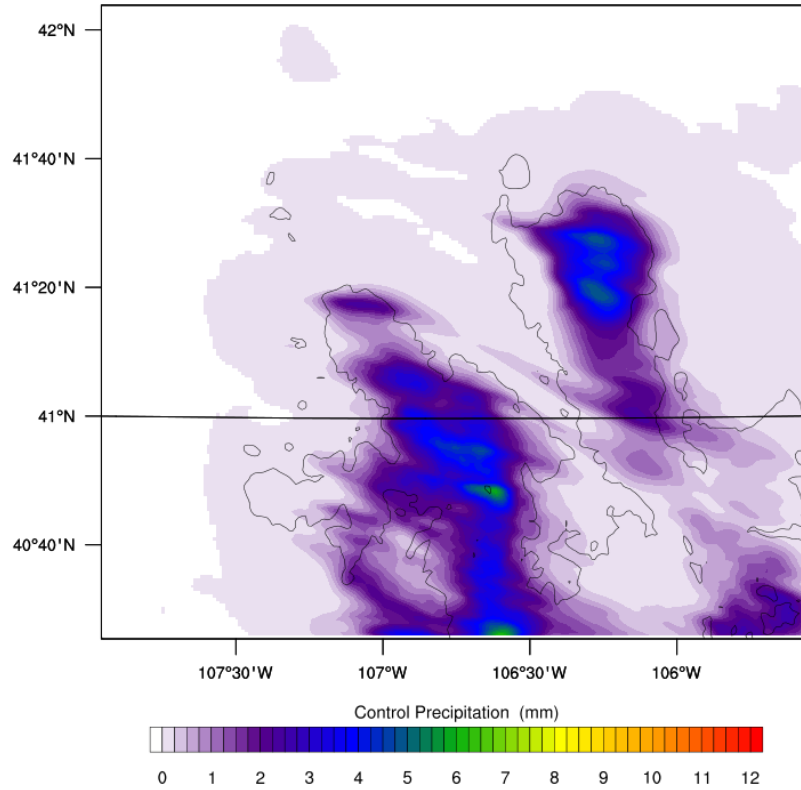


Figure 6.4. The accumulated precipitation (mm) of the control simulation in 23 January 2010 case.

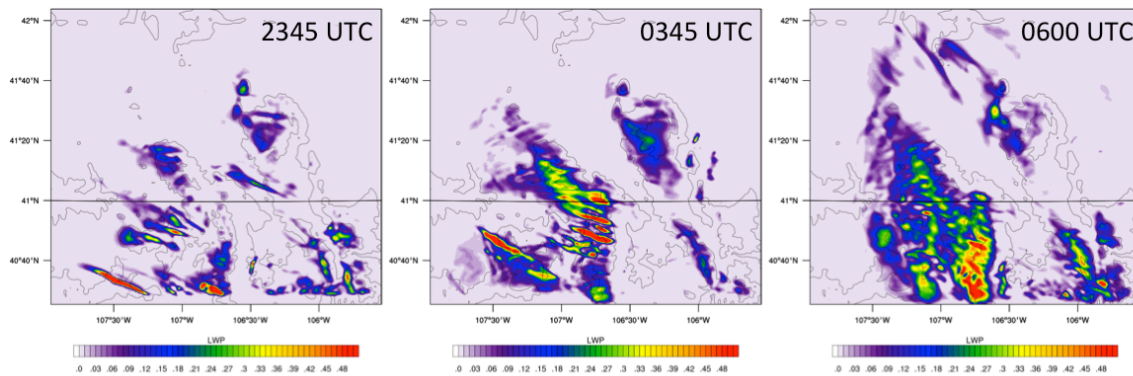
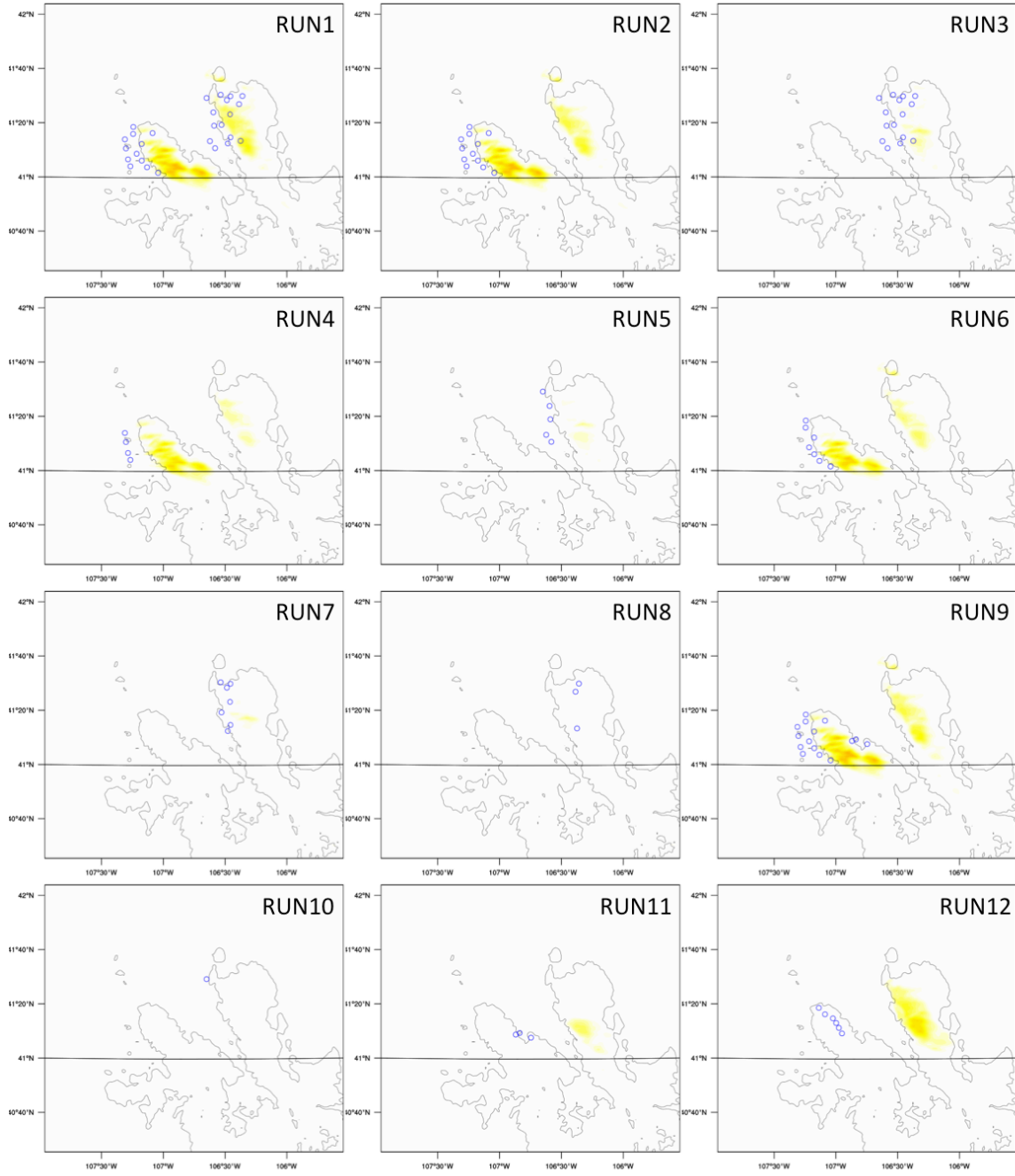


Figure 6.5. The LWP (mm) from the control simulation (color scale of 0 to 0.5 mm) at 2345 23 January 2010, and 0345 and 0600 UTC 24 January 2010.

The simulated seeding effects are defined as the difference in precipitation accumulated in the seeded simulation (SEED) minus that from the control (CTRL) simulation without seeding. These simulated seeding effects, from all case 1 seeding experiments except for Run19, are plotted in Figure 6.6. The corresponding generators used in that experiment are plotted on each map. The results of this modeling exercise show that 1) seeding from the Sierra Madre upwind region has impact on both Ranges, 2) seeding from Medicine Bow generators has little impact on the Medicine Bow Range, and 3) seeding from the top and the lee side of the Sierra Madre Range impacts the Medicine Bow Range.



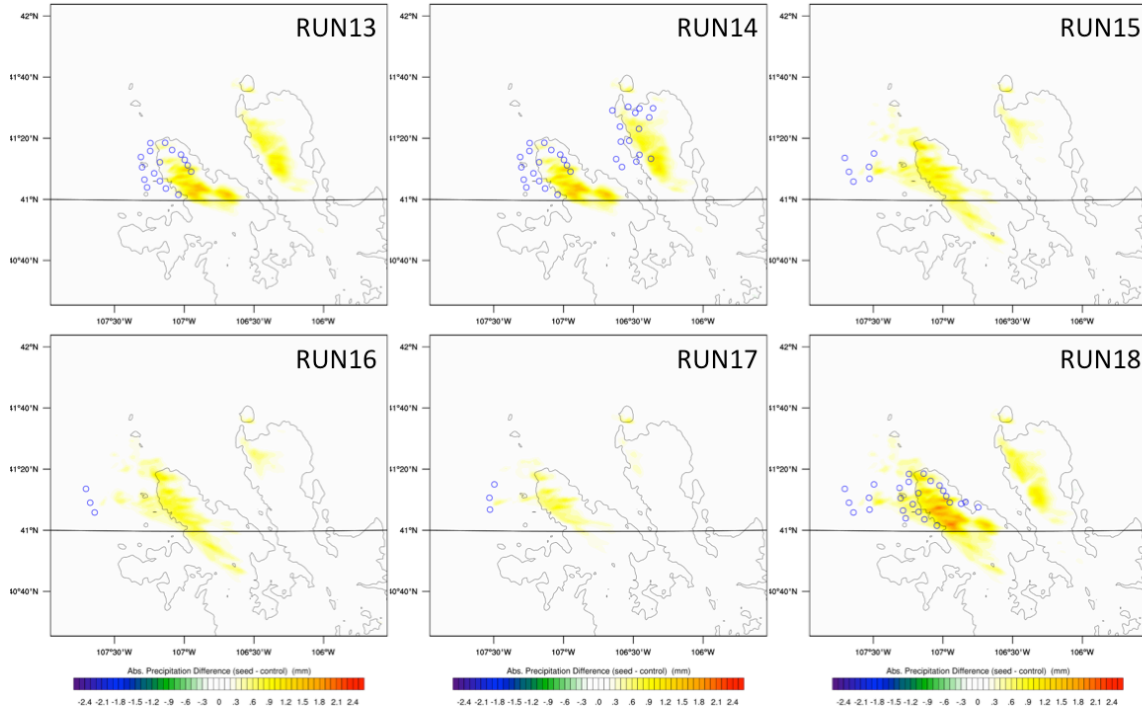
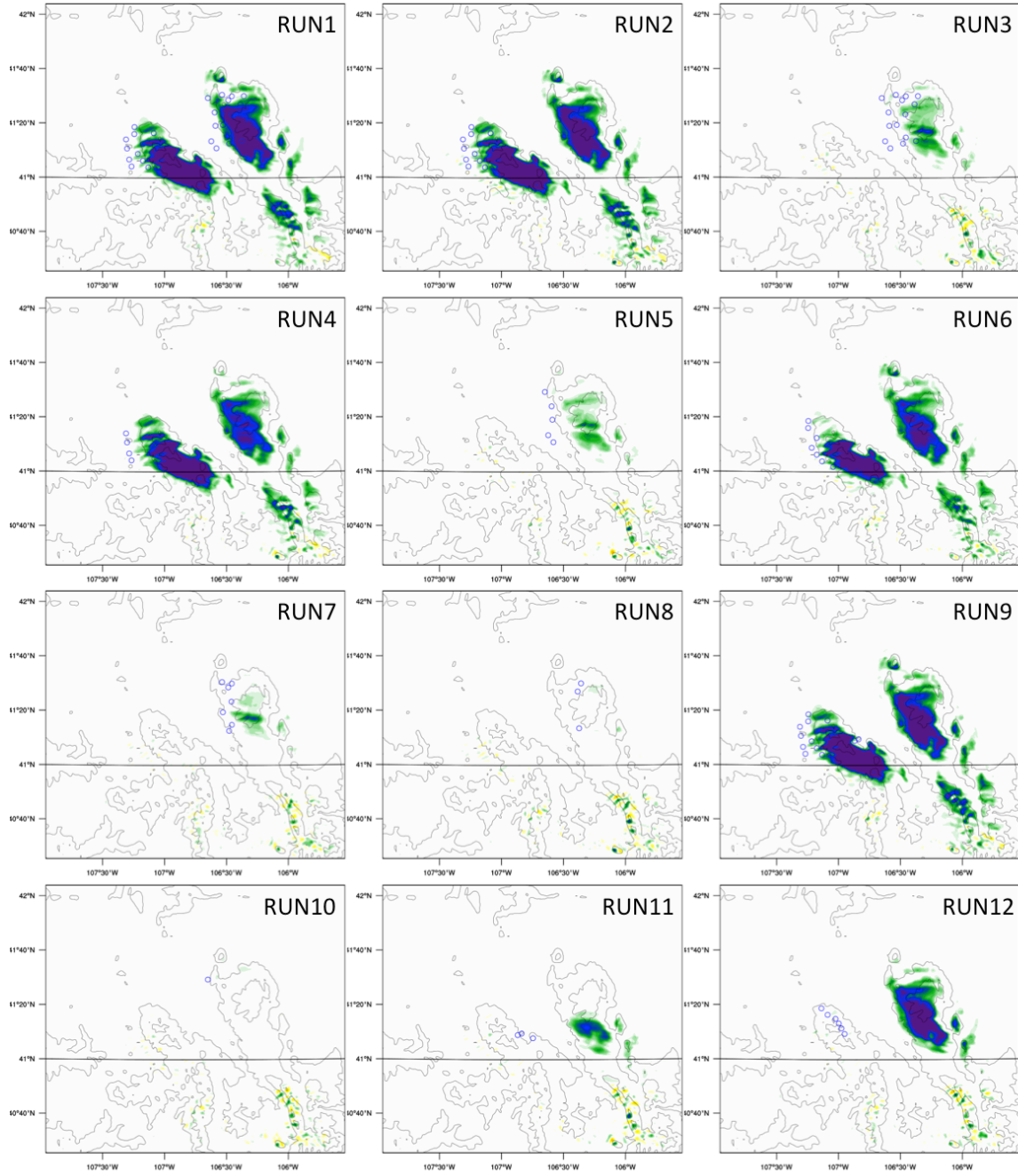


Figure 6.6. Simulated seeding effects for all seeding experiments except Run19. Open blue circles denote the locations of ground-based generators utilized in the given experiment. The colorscale is from -2.5 to 2.5 mm.

The LWP depletion patterns, shown in Figure 6.7, correspond to the simulated seeding effect in Figure 6.6 very well. The depletion of LWP is associated with the LWP distribution (Figure 6.5) and areas covered by AgI plumes (Figure 6.8). The flow over the Medicine Bow Range was slightly blocked due to stable atmospheric conditions. As a result, AgI plumes in most experiments only reached the upwind side of the Medicine Bow Range.



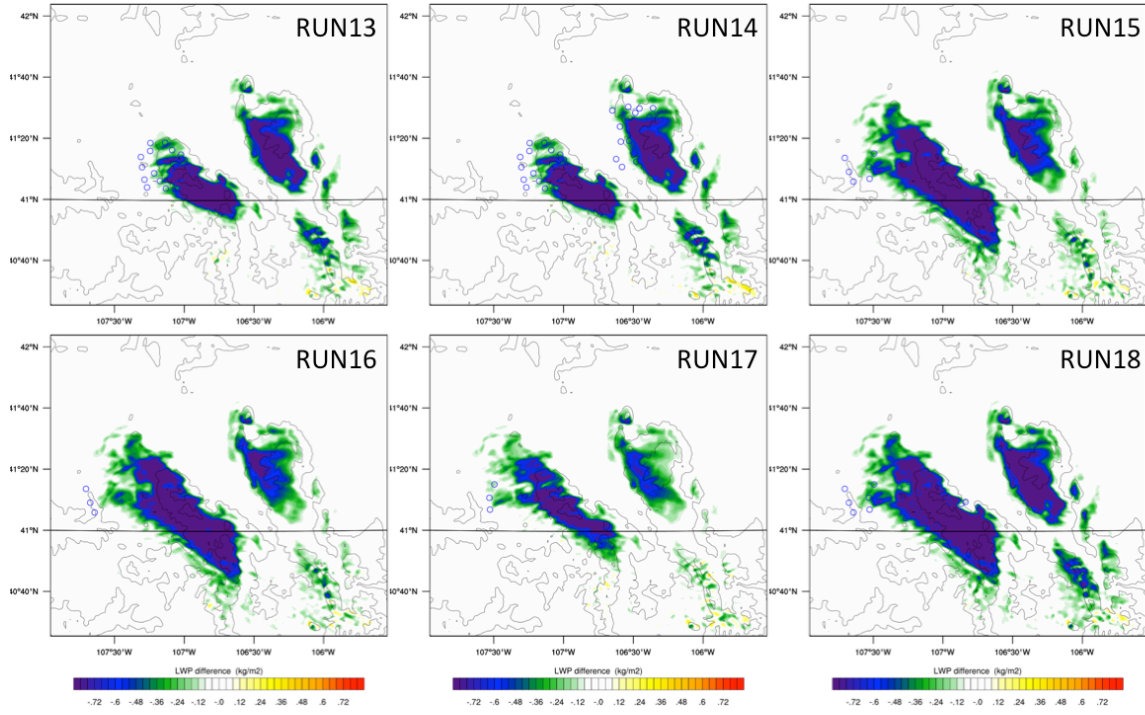
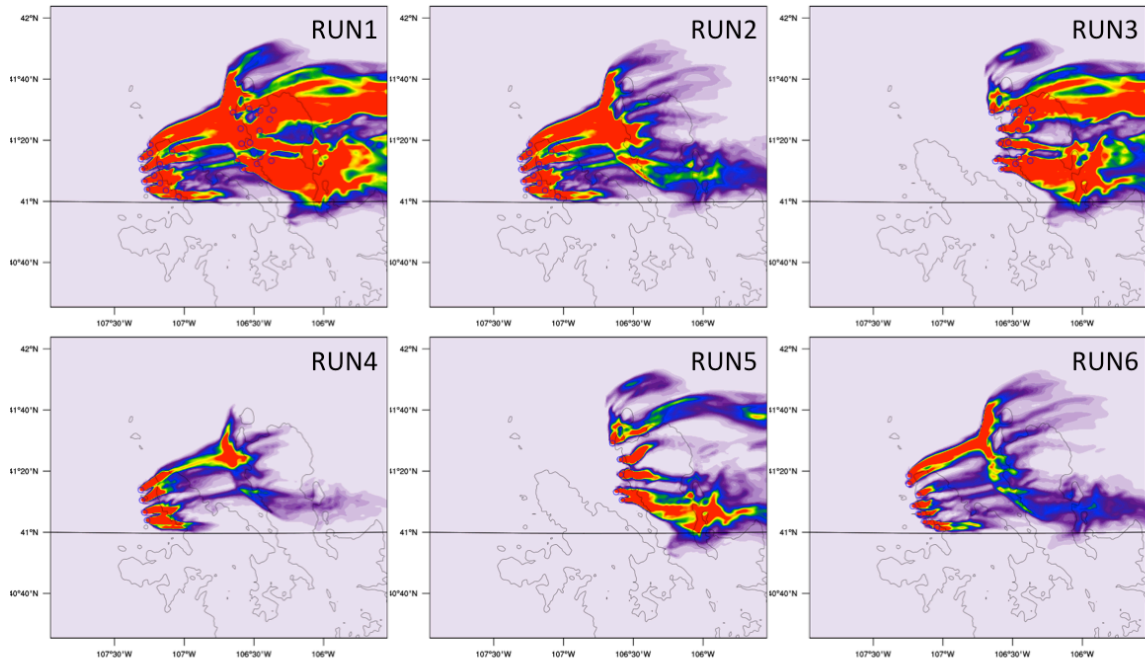


Figure 6.7. Accumulated LWP path difference (-0.8 to 0.8 mm) during the seeding period between seeded (SEED) and control simulations for the same cases as in Figure 6.6.



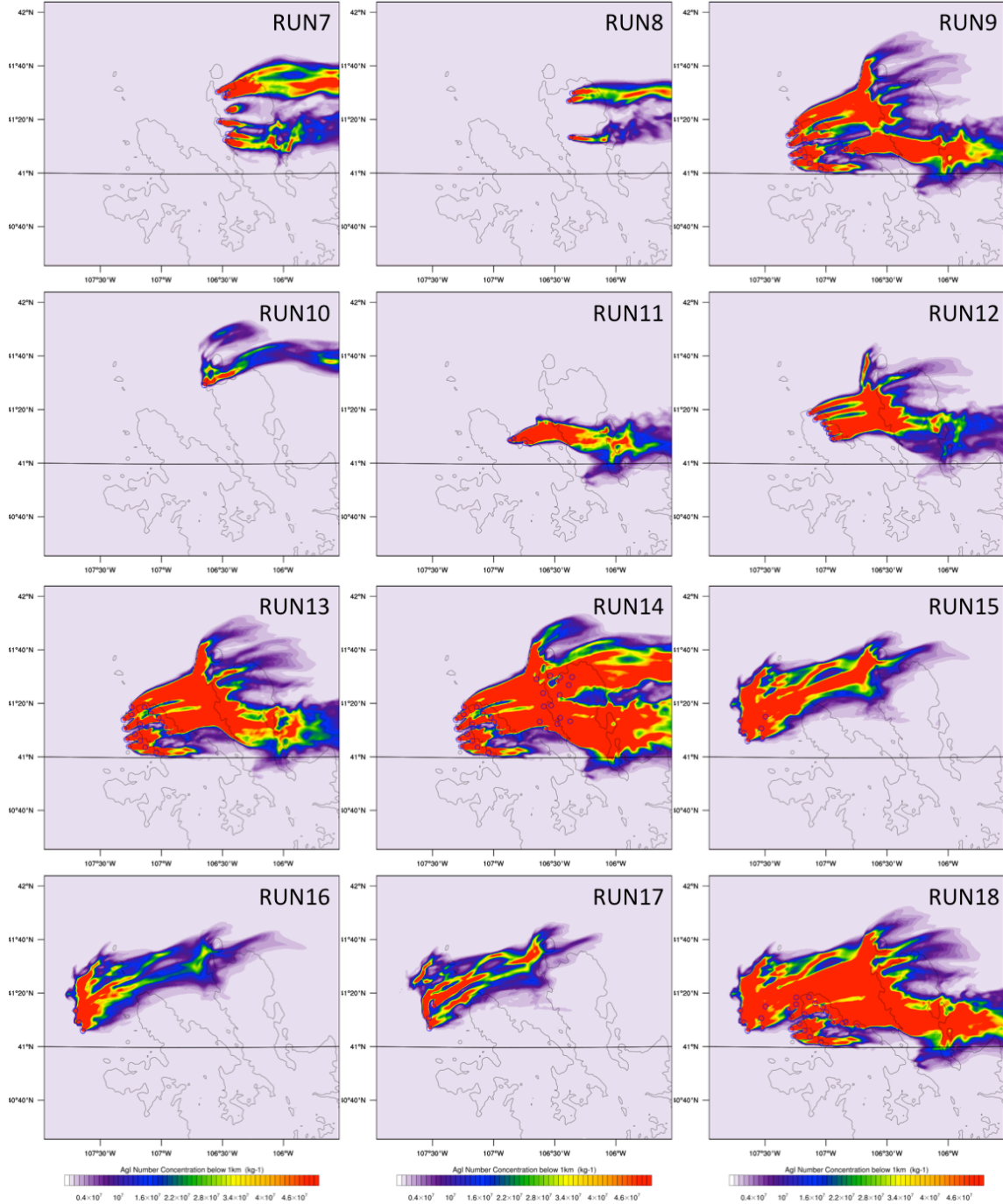


Figure 6.8. Average AgI concentration below 1 km AGL at the end of the seeding period for the same cases as in Figure 6.6.

The vertical cross sections (locations are shown in Figure 6.9) showing the simulated seeding impact on clouds for Run1 are illustrated in Figure 6.10. As a result of the stable and blocked flow conditions, the simulated impact of seeding was limited to a shallow layer over the mountain ranges where the SLW formed.

Cross-sections

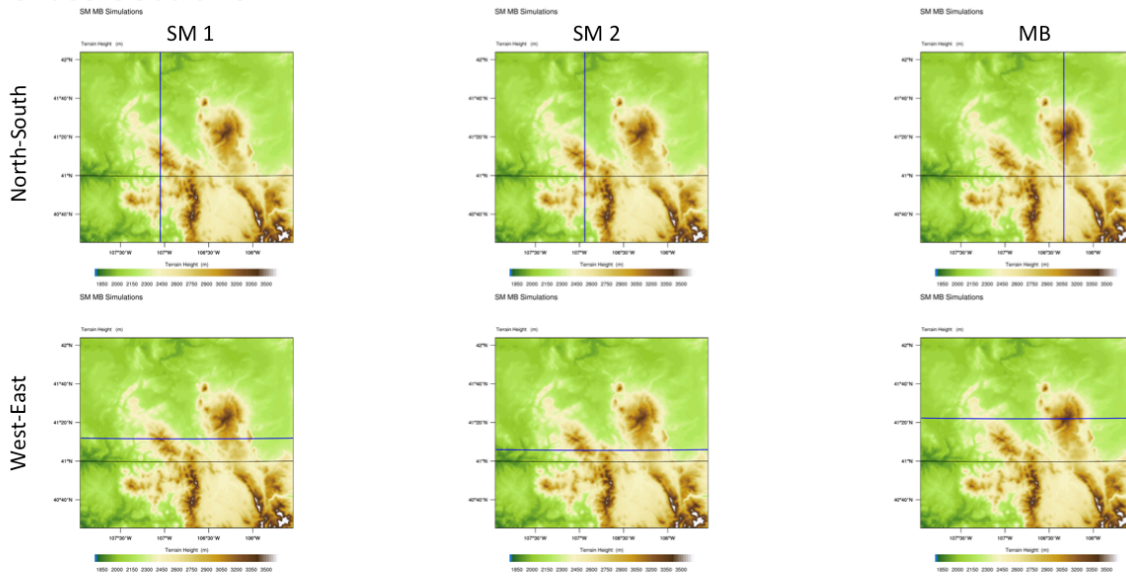


Figure 6.9. Locations of various vertical cross sections denoted as thick blue lines. Note: there are two cross section locations for Sierra Madre (SM1 and SM2), intersecting different points along those mountains.

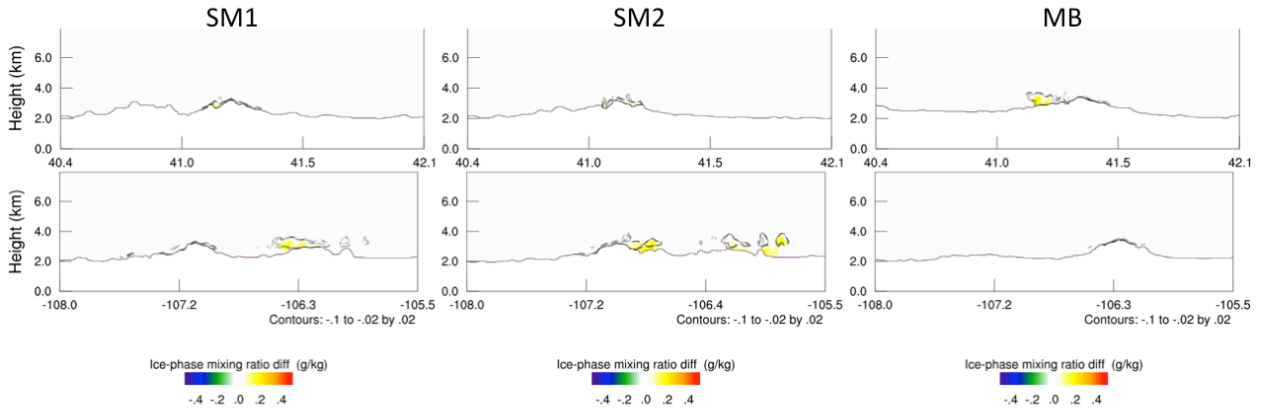


Figure 6.10. South-north (top row) and west-east (bottom row) cross sections of liquid and ice-phase mixing ratio differences between SEED and CTRL of Run1 at 0145 UTC in 23 January 2010 case. Black contours indicate liquid water mixing ratio difference from -0.1 to -0.02 g kg^{-1} in an interval of 0.02 g kg^{-1} . Color shaded is the mixed-phase mixing ratio difference from -0.5 to 0.5 g kg^{-1} .

The simulated seeding effect and simulated seeding impact areas over the entire domain, Sierra Madre Range, and Medicine Bow Range for each seeding experiment are listed in Table 6.4. These metrics in Table 6.4 quantify the results displayed in the maps from Figure 6.6. In this case, generators in the Medicine Bow Range did not contribute much to the simulated seeding-enhanced precipitation. Seeding from Sierra Madre generators generally provided the highest simulated seeding effects in both ranges, however, the absolute highest simulated seeding impact materialized in Run 14 over the Medicine Bow Range utilizing generators A+B+C from both Ranges. Run18, which only included Sierra Madre groups A–F, yielded a very high simulated impact in the Sierra Madre assessment area, as well as in the Medicine Bow assessment area. In each of the cases showing the strongest simulated seeding effects, greater than 70% of the assessment areas were impacted (Table 6.4, right columns). This estimate of the seeding impact area will be used in the streamflow benefits analysis presented in Section 12.

Table 6.4. Control precipitation (CTRL; acre-feet) followed by the simulated seeding effect (SE; acre-feet and % relative to CTRL precipitation) over the entire domain, Sierra Madre assessment area (> 8,000 ft, SM), and Medicine Bow assessment area (> 8,000 ft, MB) from all experiments for the 23 January 2010 case. In addition, the area affected by positive simulated seeding effects (PSE_A) is noted (km² and %) for each experiment and over the full domain, Sierra Madre assessment area, and Medicine Bow assessment area. The % impact area is relative to the total area of the domain, Sierra Madre assessment area, or Medicine Bow assessment area, which is listed in the CTRL row, respectively. Run1 is shaded in light gray to highlight it as the “baseline” experiment. The experiments that resulted in the largest Sierra Madre and Medicine Bow assessment area relative simulated seeding effects are shaded in light blue (are not always the same experiment).

Exp.	Effect	Domain	SM	MB	Effect	Domain	SM	MB
CTRL	Precip	13679	3354	3227	Area (km ²)	36288	2459	2468
Run1	SE (af)	999	557	380	PSE_A (km ²)	6315	1705	1978
	SE (%)	7	17	12	PSE_A (%)	17	69	80
Run2	SE (af)	919	556	325	PSE_A (km ²)	5547	1710	1801
	SE (%)	7	17	10	PSE_A (%)	15	70	73
Run3	SE (af)	242	2	198	PSE_A (km ²)	4172	158	1895
	SE (%)	2	0	6	PSE_A (%)	12	6	77
Run4	SE (af)	626	449	164	PSE_A (km ²)	4647	1690	1497
	SE (%)	5	13	5	PSE_A (%)	13	69	61
Run5	SE (af)	177	2	149	PSE_A (km ²)	3771	174	1767
	SE (%)	1	0	5	PSE_A (%)	10	7	72
Run6	SE (af)	688	417	246	PSE_A (km ²)	5024	1554	1744
	SE (%)	5	12	8	PSE_A (%)	14	63	71
Run7	SE (af)	125	1	104	PSE_A (km ²)	2824	138	1380
	SE (%)	1	0	3	PSE_A (%)	8	6	56
Run8	SE (af)	33	2	25	PSE_A (km ²)	1665	145	458
	SE (%)	0	0	1	PSE_A (%)	5	6	19
Run9	SE (af)	973	557	352	PSE_A (km ²)	6336	1715	1922
	SE (%)	7	17	11	PSE_A (%)	17	70	78
Run10	SE (af)	19	2	13	PSE_A (km ²)	1738	184	325
	SE (%)	0	0	0	PSE_A (%)	5	7	13
Run11	SE (af)	181	2	148	PSE_A (km ²)	2667	156	983
	SE (%)	1	0	5	PSE_A (%)	7	6	40
Run12	SE (af)	512	14	482	PSE_A (km ²)	3988	393	1949
	SE (%)	4	0	15	PSE_A (%)	11	16	79
Run13	SE (af)	1039	557	436	PSE_A (km ²)	6010	1713	1901
	SE (%)	8	17	14	PSE_A (%)	17	70	77
Run14	SE (af)	1089	557	481	PSE_A (km ²)	6354	1712	2012
	SE (%)	8	17	15	PSE_A (%)	18	70	82

Exp.	Effect	Domain	SM	MB	Effect	Domain	SM	MB
Run15	SE (af)	1183	605	173	PSE_A (km ²)	7714	1905	1344
	SE (%)	9	18	5	PSE_A (%)	21	77	54
Run16	SE (af)	1064	548	143	PSE_A (km ²)	7356	1920	1316
	SE (%)	8	16	4	PSE_A (%)	20	78	53
Run17	SE (af)	578	331	87	PSE_A (km ²)	6000	1716	1228
	SE (%)	4	10	3	PSE_A (%)	17	70	50
Run18	SE (af)	1776	900	435	PSE_A (km ²)	9016	2015	1942
	SE (%)	13	27	13	PSE_A (%)	25	82	79
Run19	SE (af)	1067	558	449	PSE_A (km ²)	6358	1707	1977
	SE (%)	8	17	14	PSE_A (%)	18	69	80

6.4.2. Case 2: 10 January 2014 results

For this case, the control run was integrated from 10 January 2014 1300 UTC to 10 January 2014 2300 UTC. Seeding simulations were integrated between 10 January 2014 1500 UTC to 10 January 2014 2100 UTC. The seeding experiments are listed in Table 6.5.

Table 6.5. Seeding simulations for the 10 January 2014 case. The SM “oriC” group consists of the one original Group C generator shown in Figure 5.5.

Run 1	SM A+B+oriC & MB A+B+C
Run 2	SM A+B+oriC
Run 3	MB A+B+C
Run 4	SM A
Run 5	MB A
Run 6	SM B
Run 7	MB B
Run 8	MB C
Run 9	SM A+B+oriC+D
Run 10	MB A (north generator only)
Run 11	SM D
Run 12	SM C
Run 13	SM E+F
Run 14	SM A+B+C+D+E+F
Run 15	SM A+B+C
Run 16	SM A+B+C+D

For the second case, the simulated natural precipitation covers a broader area and is slightly stronger in the Sierra Madre Range than in the Medicine Bow Range (Figure 6.11). The pattern of precipitation in the low terrain region upwind of the Sierra Madre Range and the cellular feature of the LWP indicated that the cloud was more convective over the Sierra Madre Range. Precipitation over the Medicine Bow Range is confined to higher terrain with the maximum on the upwind side of the highest peak. The LWP during and after the simulated seeding period

indicated that more SLW was available in the Sierra Madre Range than in the Medicine Bow Range in the early stage of the simulation period, but similar amounts of SLW were seen over the Medicine Bow Range later in the same simulation (Figure 6.12).

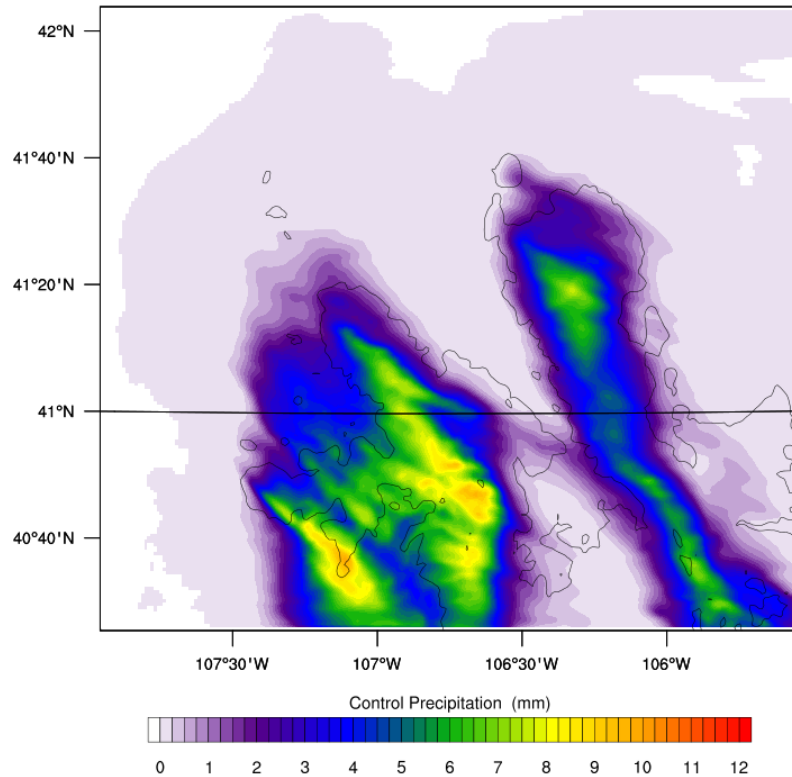


Figure 6.11. Same as Figure 6.4, but for the 10 January 2014 case.

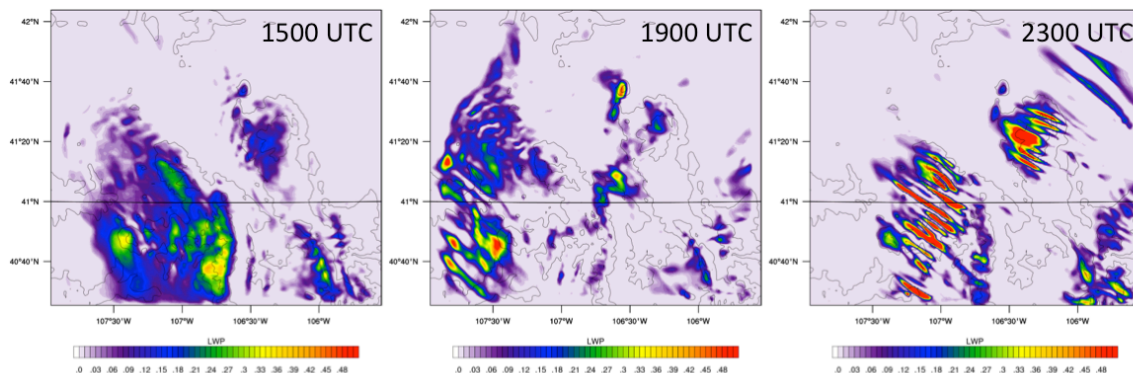


Figure 6.12. Same as Figure 6.5, but for the 10 January 2014 case.

The simulated seeding effects, and corresponding seeding generators used in all of the seeding experiments, except for Run16, are plotted in Figure 6.13. Due to the slightly unstable atmospheric conditions of this case, these simulations show impressions of negative seeding effects in the Sierra Madre Range. These negative “streaks” are the result of a convective cell being slightly dislocated between the control (CTRL) simulation and the seeding (SEED) simulation. These negative effects are often coupled with a streak of positive effects nearby, and therefore negate one another when calculating the area impacts. As a result, the simulated seeding effects over the Sierra Madre Range were rather weak. The simulated seeding impact in the Medicine Bow Range was limited to the upwind side, collocated with the SLW.

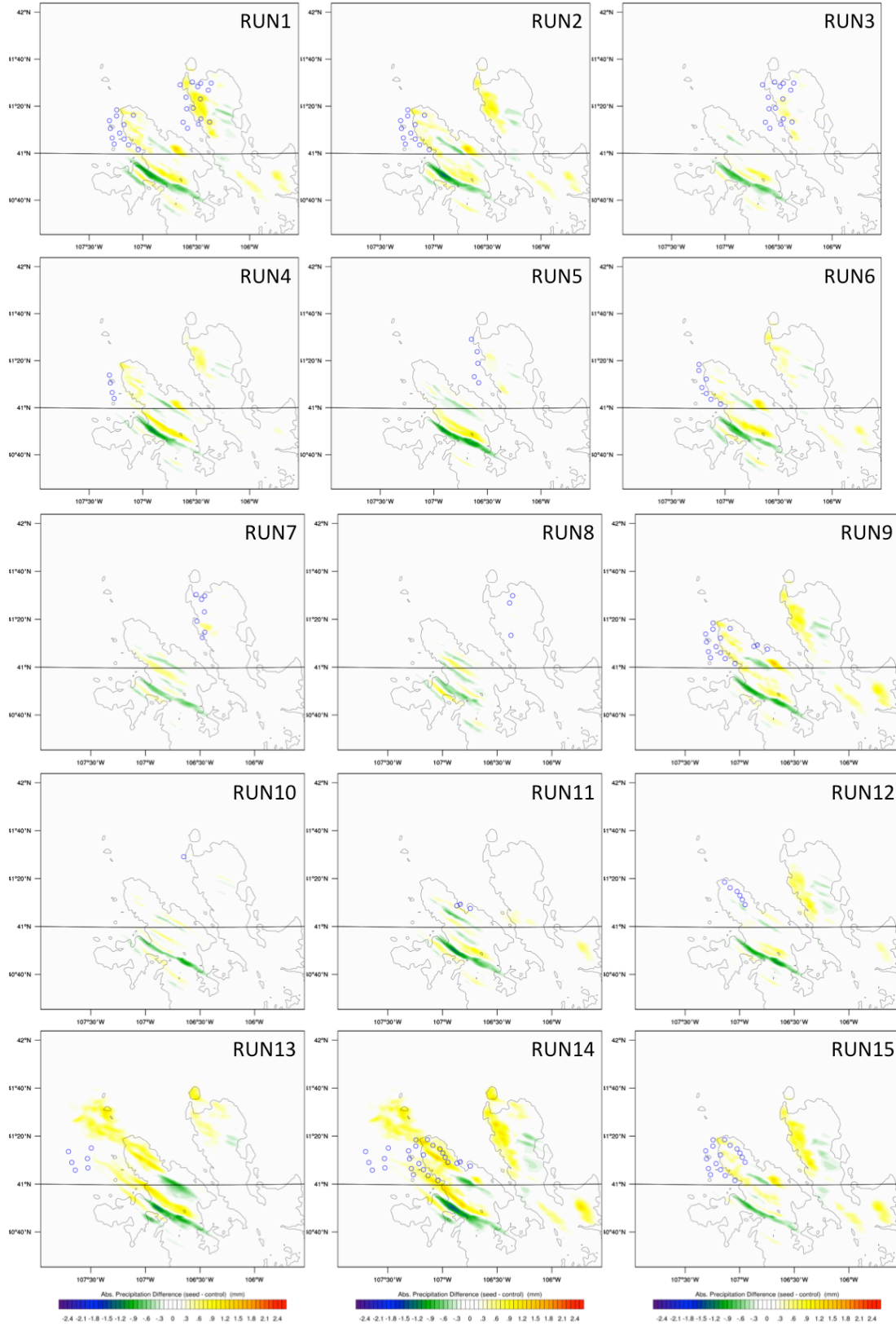
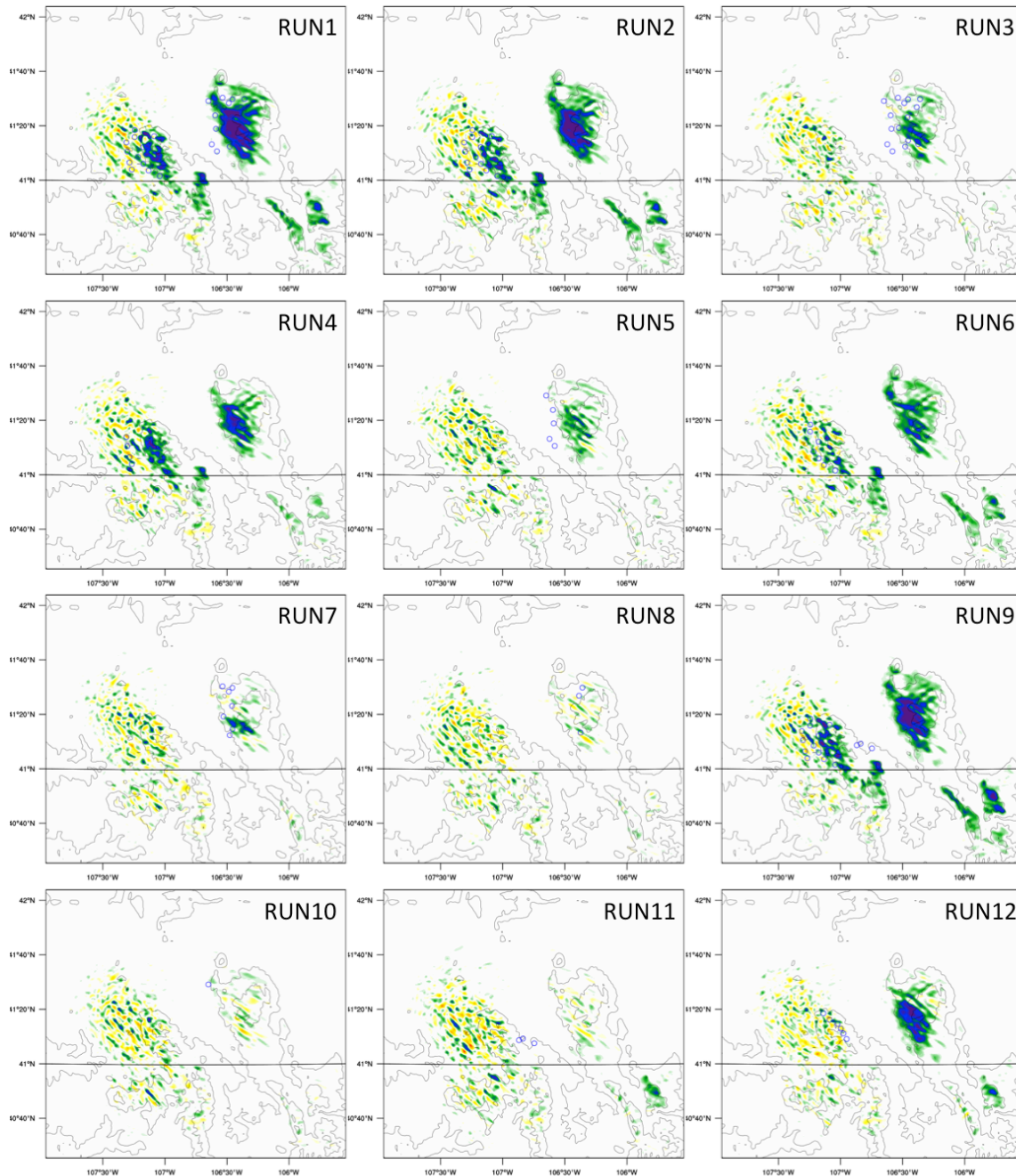


Figure 6.13. Same as Figure 6.6, but for the 10 January 2014 case without Run16.

The LWP depletion patterns are shown in Figure 6.14 for the same cases as in Figure 6.13. The unstable atmospheric conditions were reflected by the scattered positive and negative signals of the LWP difference field in the Sierra Madre Range. In case 2, Groups E and F, located in the far upwind region of the Sierra Madre Range (Run13 and Run14), depleted more LWP and generated higher simulated seeding effects in both Ranges. The AgI plume maps (Figure 6.15) show that the AgI particles from these two groups were transported around the north of the Sierra Madre Range and impacted the northwestern part of the Medicine Bow Range. The flow in the Medicine Bow Range was not blocked in this case, but only the upwind side had SLW to facilitate the simulated seeding effects shown in Figure 6.13 (Figure 6.14 and Figure 6.15).



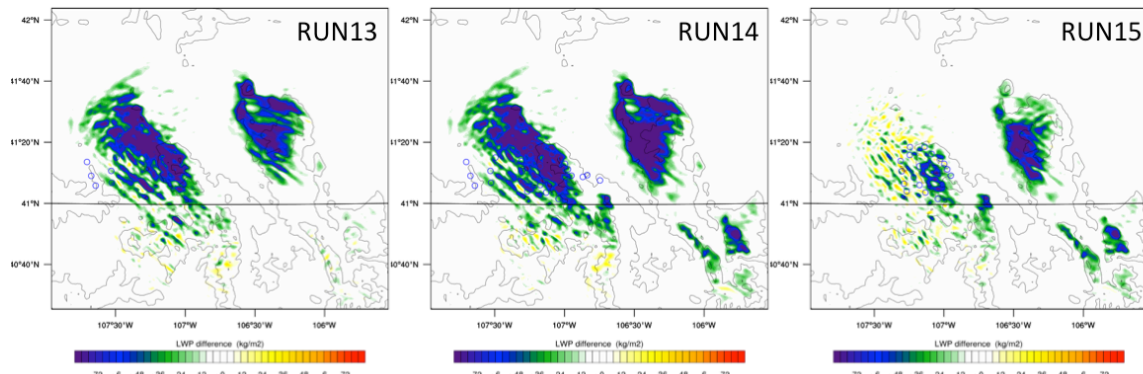


Figure 6.14. Accumulated LWP path difference (-0.8 to 0.8 mm) during the simulated seeding period between SEED and CTRL simulations for the same cases as in Figure 6.13.

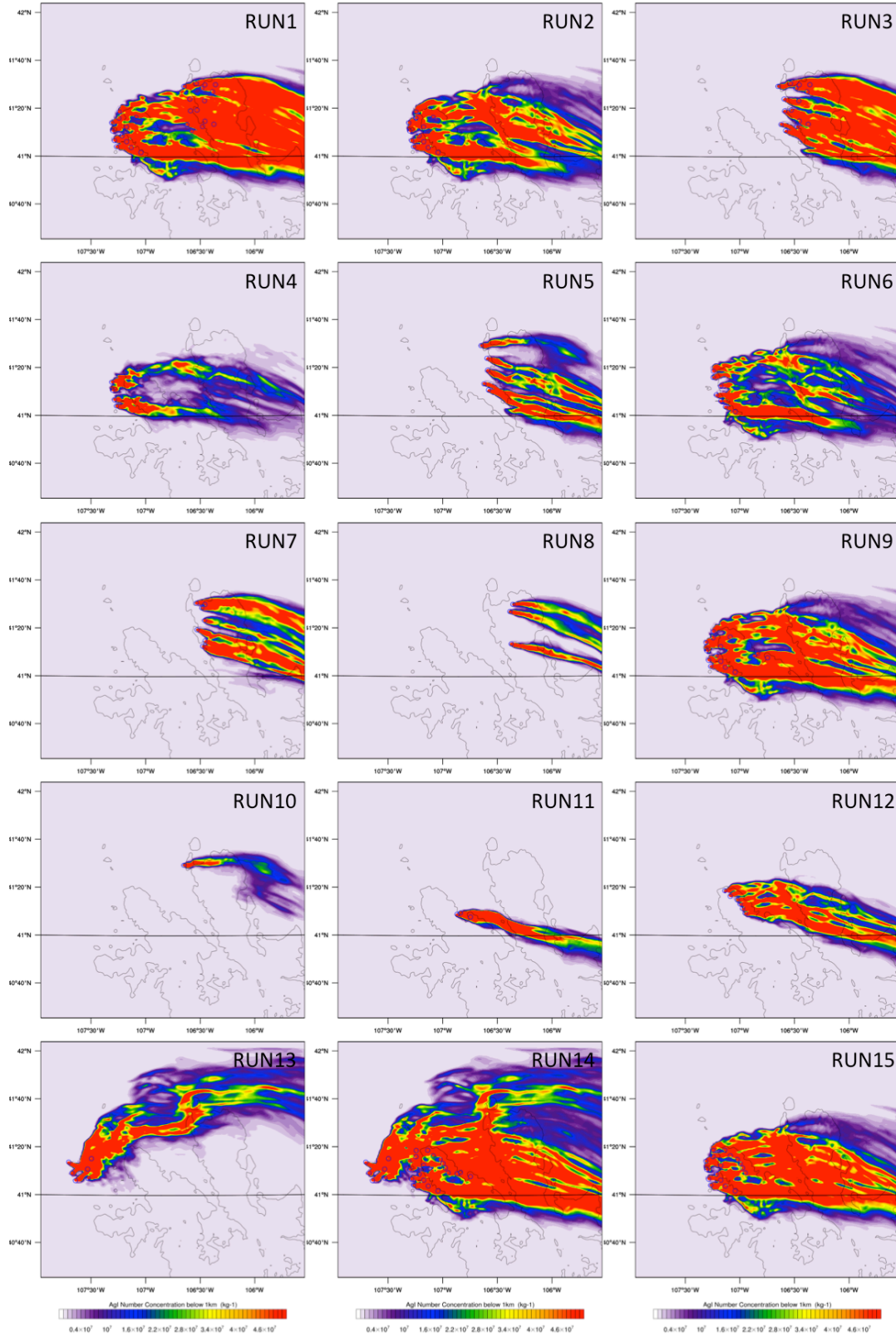


Figure 6.15. Average AgI concentration below 1 km AGL at the end of the simulated seeding period for the same cases as in Figure 6.13.

The vertical cross sections (locations are shown in Figure 6.9) showing the simulated seeding impact on clouds in the middle of the seeding period for Run1, and are illustrated in Figure 6.16. The simulated seeding impact showed convective features as the liquid-water depletion was cellular in nature. Over the Medicine Bow Range, the simulated seeding impact was limited to the upwind and low-level region where the SLW formed.

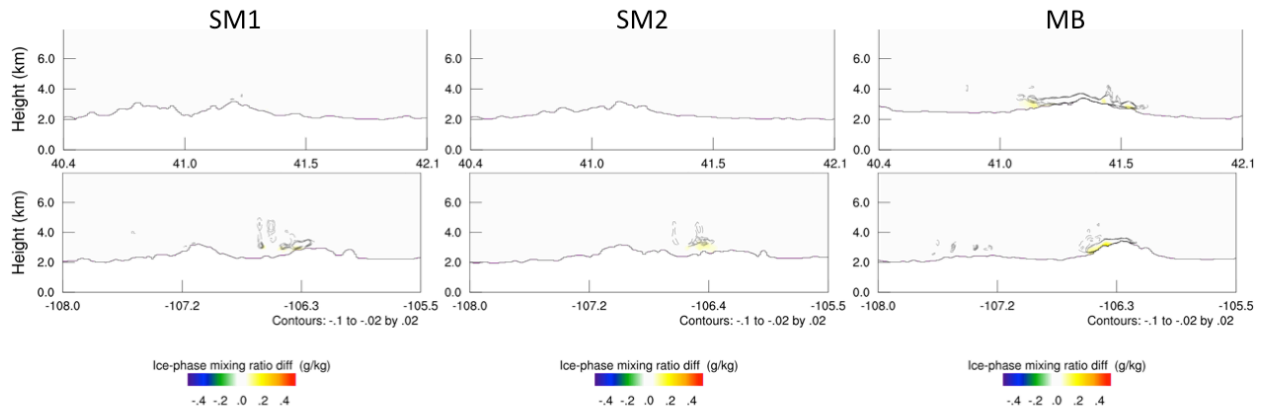


Figure 6.16. Same as Figure 6.10, but for the 10 January 2014 case at 1800 UTC. Top row is south-north cross section and bottom row is west-east cross section.

The control precipitation and simulated seeding effect over the entire domain, Sierra Madre assessment area, and Medicine Bow assessment area, from each of the seeding experiments are listed in Table 6.6. Case 2 has more natural (CTRL) precipitation than the first (23 January 2010) case. All experiments generated less simulated seeding effect compared with their counterparts in the 23 January 2010 case. Similarly, seeding in the Medicine Bow Range contributed little to the total effect, and seeding generated from the Sierra Madre Range resulted in the highest simulated seeding effect in both ranges (Run14). The relative impact area in this case is slightly less than the first case (23 January), roughly 60% for experiments with the highest simulated seeding effects (Table 6.6).

Table 6.6. Same as Table 6.4, but for the 10 January 2014 case.

Exp.	Effect	Domain	SM	MB	Effect	Domain	SM	MB
CTRL	Precip	37517	7212	5747	Area (km ²)	36288	2459	2468
Run1	SE (af)	577	234	234	PSE_A (km ²)	7051	1530	1430
	SE (%)	2	3	4	PSE_A (%)	19	62	58
Run2	SE (af)	482	273	150	PSE_A (km ²)	6521	1726	1125
	SE (%)	1	4	3	PSE_A (%)	18	70	46
Run3	SE (af)	144	41	144	PSE_A (km ²)	6521	1247	1570
	SE (%)	0	1	3	PSE_A (%)	18	51	64
Run4	SE (af)	247	175	72	PSE_A (km ²)	5879	1404	1049
	SE (%)	1	2	1	PSE_A (%)	16	57	43
Run5	SE (af)	125	48	87	PSE_A (km ²)	6376	1131	1476
	SE (%)	0	1	2	PSE_A (%)	18	46	60
Run6	SE (af)	365	184	107	PSE_A (km ²)	6418	1456	1229
	SE (%)	1	3	2	PSE_A (%)	18	59	50
Run7	SE (af)	50	36	69	PSE_A (km ²)	4876	1135	1256
	SE (%)	0	1	1	PSE_A (%)	13	46	51
Run8	SE (af)	9	1	14	PSE_A (km ²)	4696	1048	991
	SE (%)	0	0	0	PSE_A (%)	13	43	40
Run9	SE (af)	598	226	186	PSE_A (km ²)	7038	1521	1352
	SE (%)	2	3	3	PSE_A (%)	19	62	55
Run10	SE (af)	27	30	15	PSE_A (km ²)	5194	1183	1163
	SE (%)	0	0	0	PSE_A (%)	14	48	47
Run11	SE (af)	159	23	45	PSE_A (km ²)	6023	1194	986
	SE (%)	0	0	1	PSE_A (%)	17	49	40
Run12	SE (af)	263	56	166	PSE_A (km ²)	6940	1407	1284
	SE (%)	1	1	3	PSE_A (%)	19	57	52
Run13	SE (af)	982	287	194	PSE_A (km ²)	8546	1523	1482
	SE (%)	3	4	3	PSE_A (%)	24	62	60
Run14	SE (af)	1514	452	376	PSE_A (km ²)	10176	1623	1550
	SE (%)	4	6	7	PSE_A (%)	28	66	63
Run15	SE (af)	622	240	243	PSE_A (km ²)	7274	1605	1405
	SE (%)	2	3	4	PSE_A (%)	20	65	57
Run16	SE (af)	696	282	244	PSE_A (km ²)	7196	1686	1374
	SE (%)	2	4	4	PSE_A (%)	20	69	56

6.4.3. Case 3: 13 January 2014 results

For this case, the control run was integrated from 13 January 2014 0700 UTC to 13 January 2014 2100 UTC. Seeding simulations were integrated between 13 January 2014 0900 UTC to 13 January 2014 1900 UTC. The seeding experiments that were run are listed in Table 6.7. For this case, three extra ground-seeding simulations were conducted using the updated WRFV3.7.1 and

updated ASPEN (Run 14–16, Table 6.7). Because the WRF version, PBL, land-surface model, and microphysics were updated for these three simulations, the control simulation was re-run as well. Two ground-seeding simulations with a seeding time between 13 January 2014 0900 UTC to 1900 UTC were used to investigate the impact of the newly added AgI removal processes in the ASPEN. Airborne seeding was simulated between 1530 UTC and 1730 UTC at 3500 m MSL along the flight track shown in Figure 5.7.

Table 6.7. Seeding simulations of the 13 January 2014 case. The SM “oriC” group consists of the one original Group C generator shown in Figure 5.5. Runs listed in light green shading were run with WRF V3.7.1 using the updated ASPEN.

Run 1	SM A+B+oriC & MB A+B+C
Run 2	SM A+B+oriC
Run 3	MB A+B+C
Run 4	All (SM + MB)
Run 5	SM D
Run 6	SM B+C & MB A+B (north generator only)
Run 7	SM oriC
Run 8	MB A (north generator only)
Run 9	SM C
Run 10	SM E+F
Run 11	SM A+B+C+D+E+F
Run 12	SM A+B+C
Run 13	SM A+B+C+D
Run 14	SM A+B+C+D+E+F (Run 11) with the same AgI scavenging in the original ASPEN
Run 15	Same as Run 14, but with extra AgI removal processes as listed in Table 6.1
Run 16	Airborne seeding with extra AgI removal processes as listed in Table 6.1

In this third case, the simulated natural precipitation is much stronger and widespread in the Sierra Madre Range than in the Medicine Bow Range (Figure 6.17). Precipitation in both ranges is confined to areas of higher terrain. The precipitation maximum in the Medicine Bow Range is close to the highest peak. The LWP during and after the seeding period indicated that plenty of SLW was available in both Ranges throughout the seeding period (Figure 6.18).

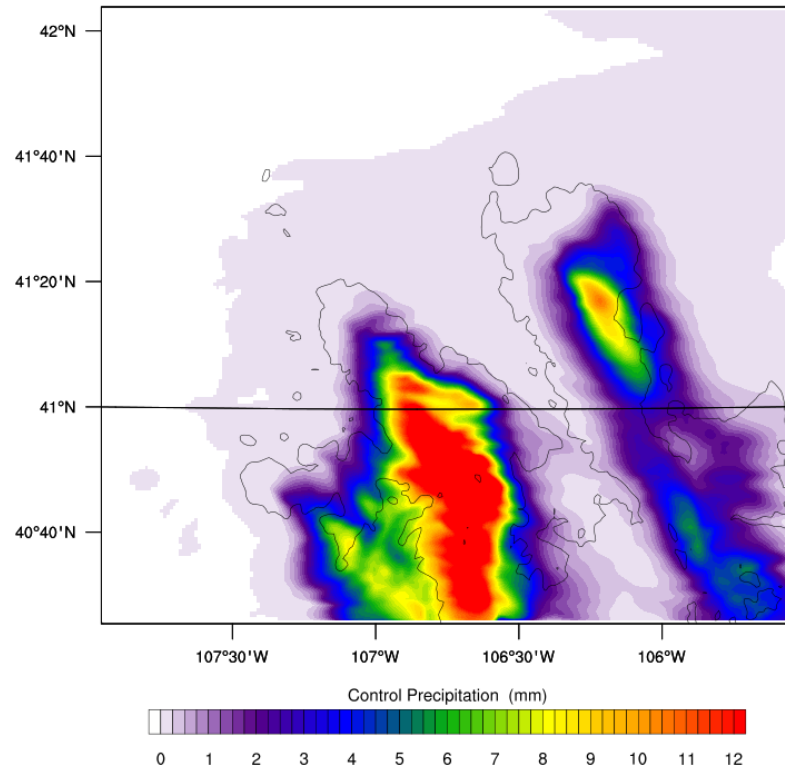


Figure 6.17. Same as Figure 6.4, but for the 13 January 2014 case.

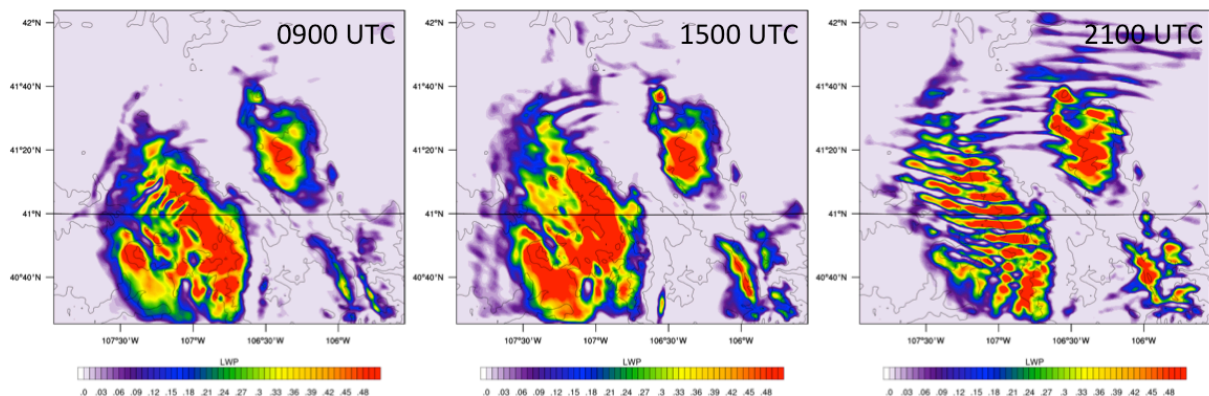


Figure 6.18. Same as Figure 6.5, but for the 13 January 2014 case.

The simulated seeding effects, and corresponding seeding generators used in of all seeding experiments, except for Run6, are plotted in Figure 6.19. The results show that the simulated seeding effects over the Medicine Bow Range are greater than the Sierra Madre, even when only Sierra Madre generator groups are turned on. The inclusion of generator groups E and F produce additional simulated seeding effects around the north ends of both ranges. There is a slight region of negative simulated seeding effect on the lee side of the Medicine Bow Range in almost every experiment, indicating that seeding shifted some precipitation to fallout more on the upwind side of the range.

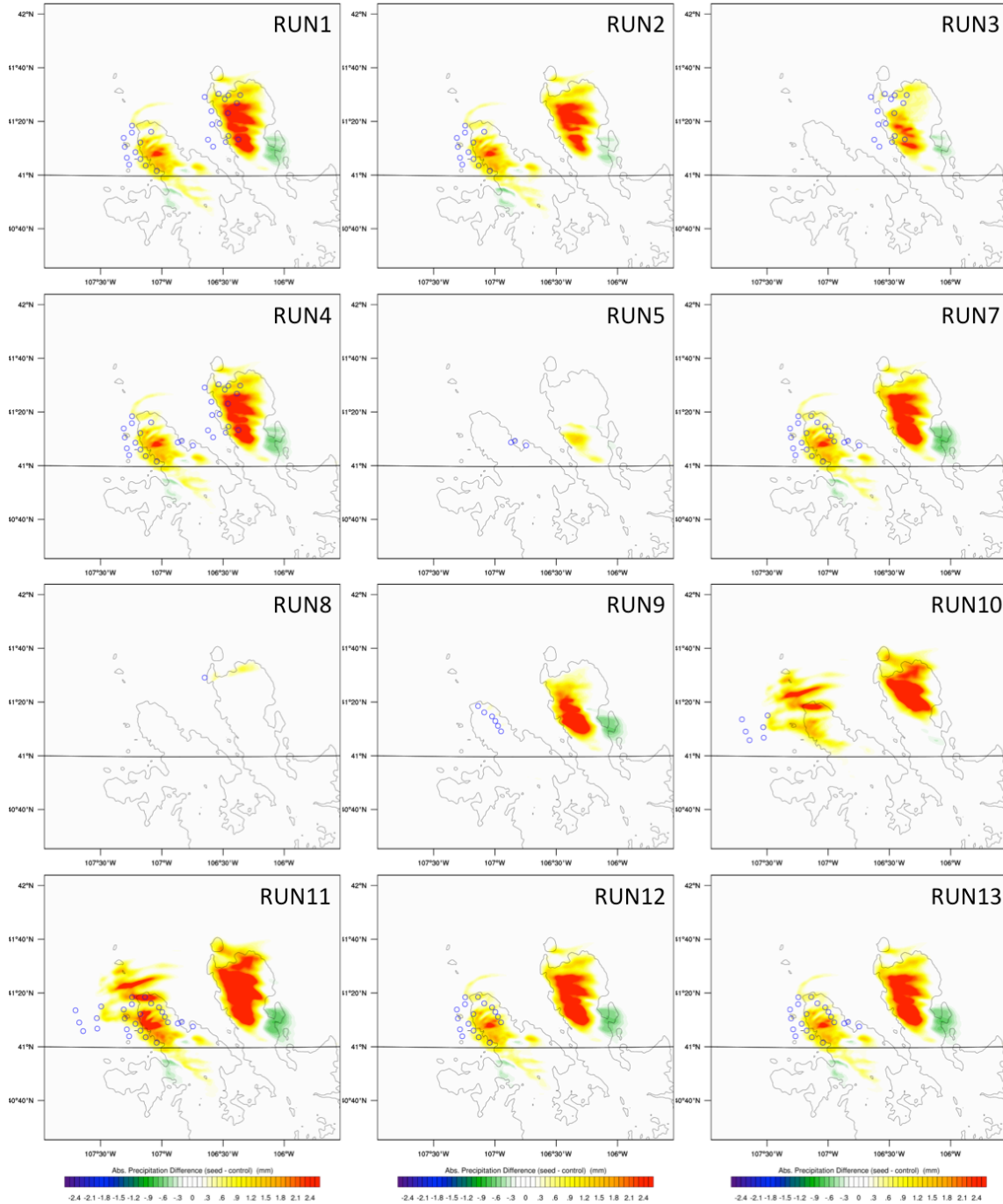


Figure 6.19. Same as Figure 6.6, but for the 13 January 2014 case without run6.

Case 3 LWP depletion patterns and the AgI plume concentration maps are shown in Figure 6.20 and Figure 6.21. The majority of the AgI plumes from the Medicine Bow generator groups were blocked, leaving a void of AgI over the areas of highest terrain in the Range. Nonetheless, sufficient AgI dispersed from the generators on the upwind side of the Medicine Bow Range to have a local simulated seeding impact. On the other hand, most of the AgI plumes from Sierra Madre generator groups dispersed adequately over the Sierra Madre Range (Figure 6.21). However, Groups E and F, in the far upwind region of the Sierra Madre Range, were completely

blocked as illustrated by the AgI plumes from these groups going around the north of the Range. Nonetheless, these plumes then impacted the northwestern corner of the Medicine Bow Range in this case (Figure 6.21). The high SLW and relatively stable atmospheric conditions in both ranges made the seeding very efficient in terms of depleting SLW (Figure 6.19 and Figure 6.20).

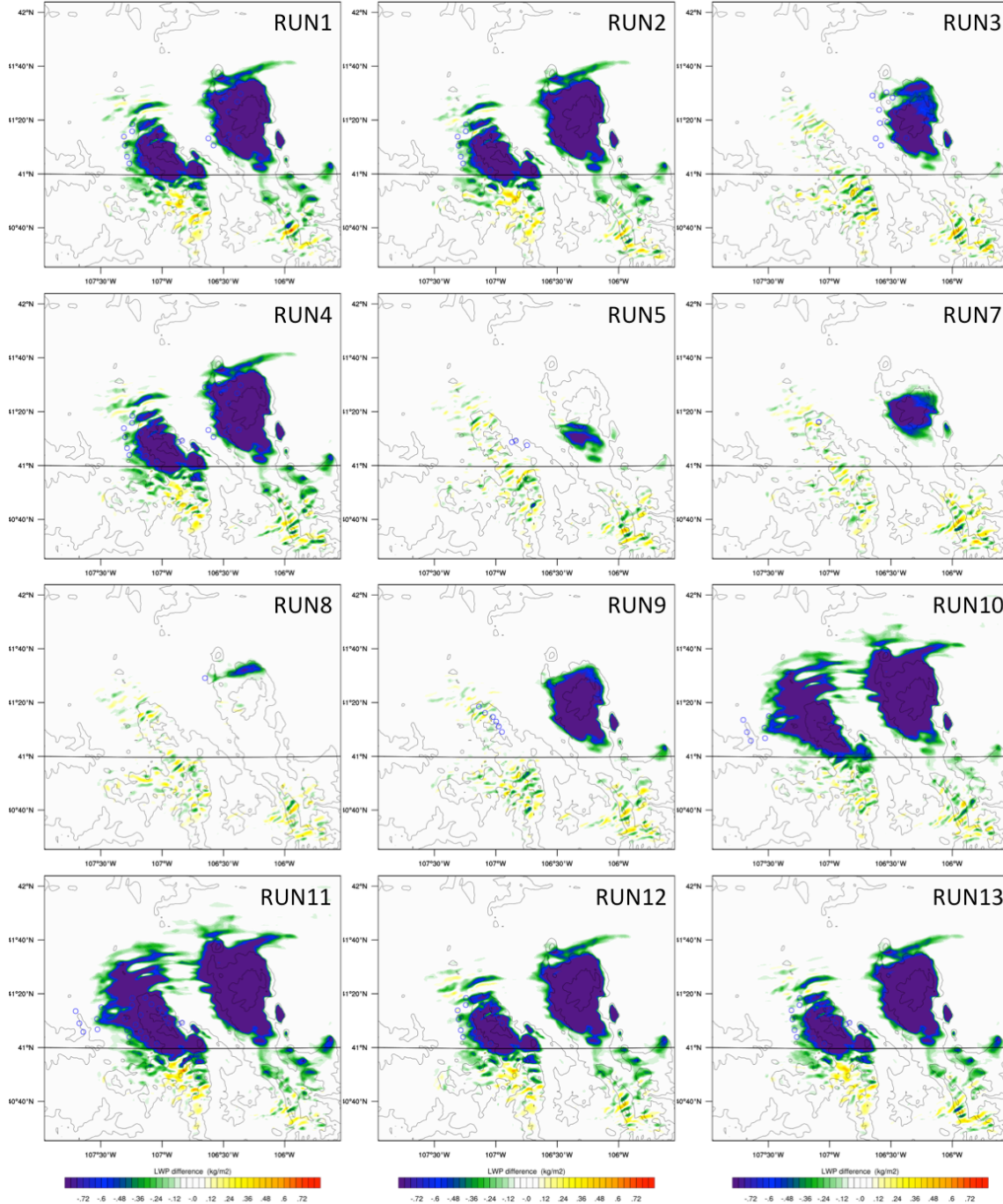


Figure 6.20. Accumulated LWP path difference (-0.8 to 0.8 mm) during the seeding period between SEED and CTRL simulations for the same cases as in Figure 6.19.

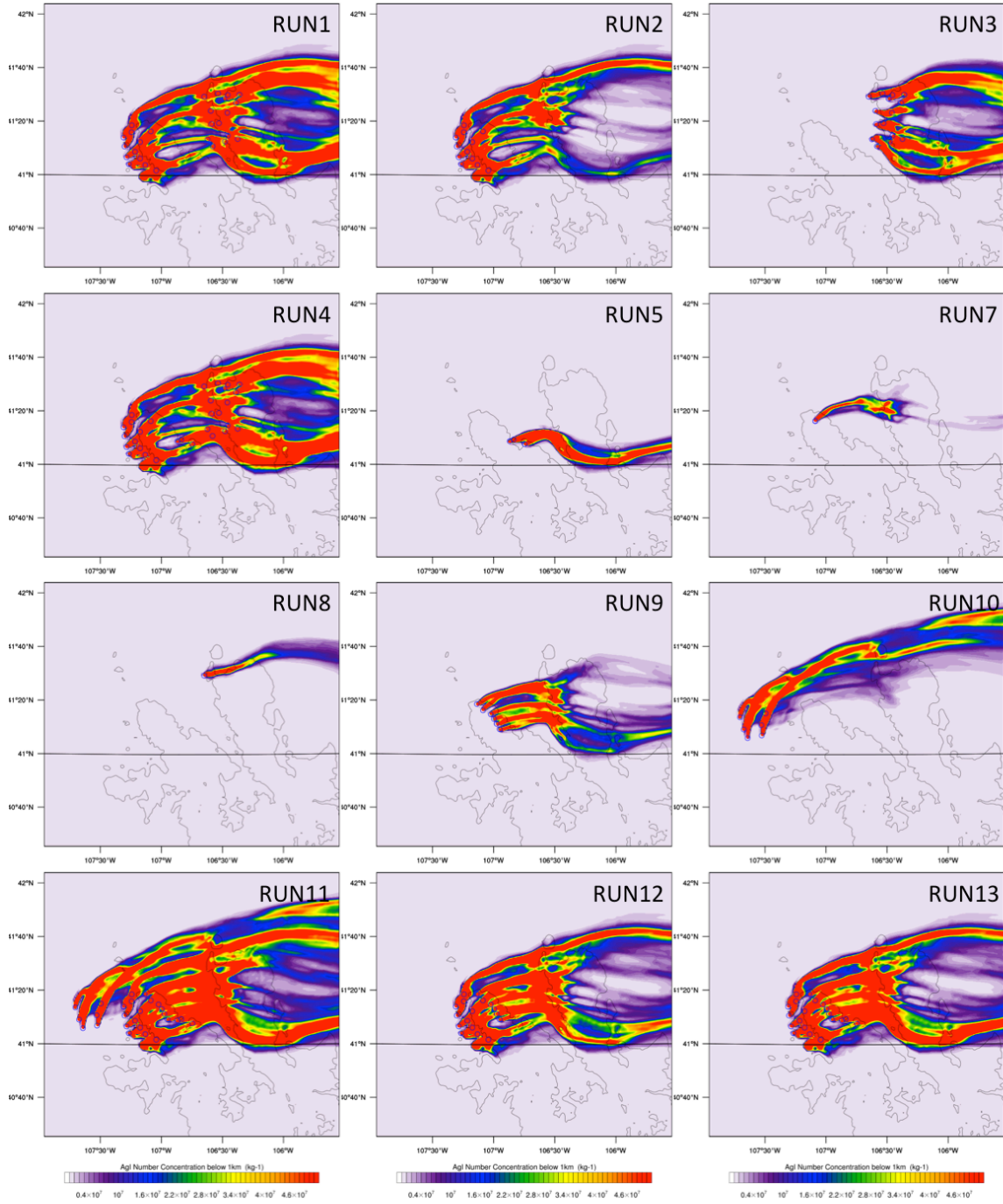


Figure 6.21. Average AgI concentration below 1 km AGL at the end of the seeding period for the same cases as in Figure 6.19.

The vertical cross sections (locations are shown in Figure 6.9) showing the simulated seeding impact on clouds are illustrated in Figure 6.22 for Run1. The seeding had relatively broad impacts in both ranges compared with the previous two cases.

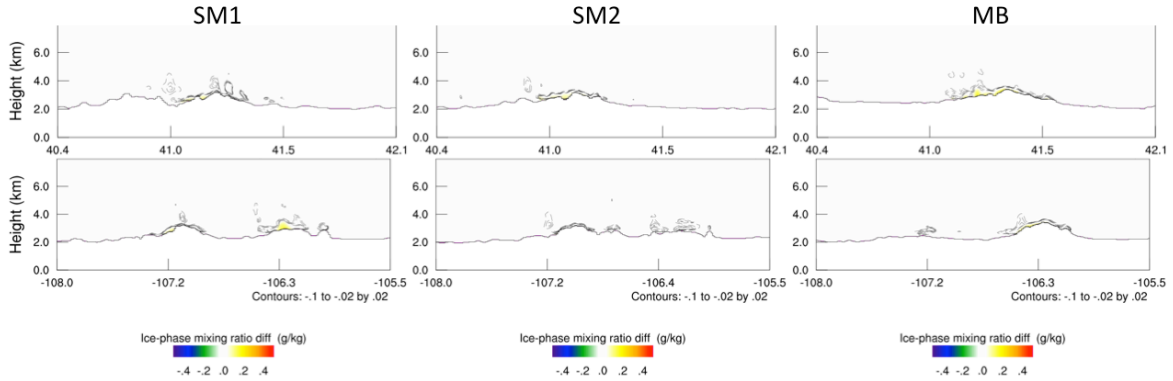


Figure 6.22. Same as Figure 6.10, but for run1 of the 13 January 2014 case at 1400 UTC.

Results using the modified model configuration (i.e. updated WRF version with updated ASPEN) changed slightly. The newly simulated control precipitation and LWP are shown in Figure 6.23 and Figure 6.24, respectively. The general patterns and magnitudes of the precipitation and LWP are similar between these new simulations and the previous ones using the original model configuration (i.e. WRFV3.4.1); however, the LWP distribution is smoother in the new run than the original one.

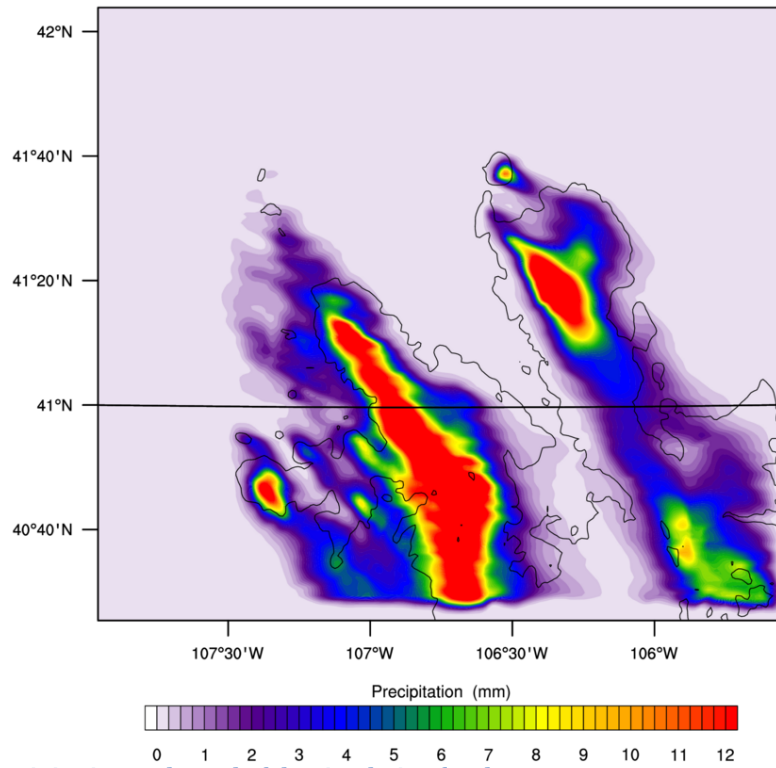


Figure 6.23. Control precipitation at the end of the simulation for the 13 January 2014 case.

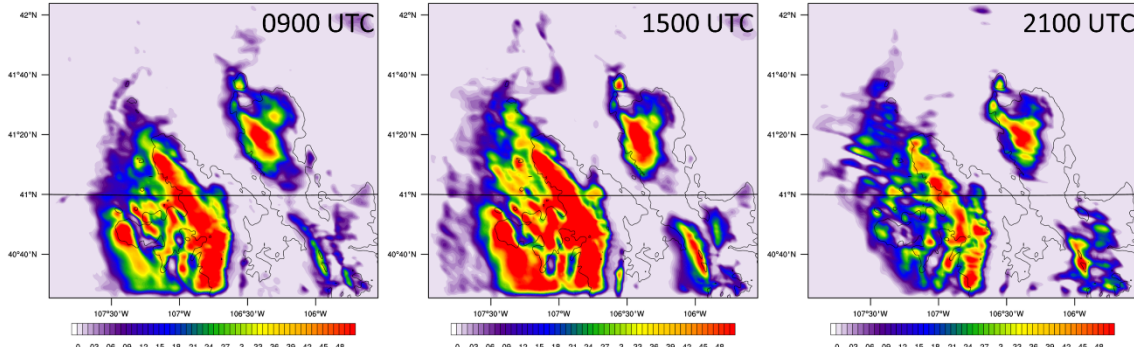


Figure 6.24. Liquid-water path below 1 km AGL at 0900, 1500 and 2100 UTC from the control simulation for the 13 January 2014 case.

The simulated seeding effects of the three extra seeding experiments (Runs 14–16) are plotted in Figure 6.25. Unlike the original simulations (i.e., Run 11 in Figure 6.19), all seeding simulations with the new WRF and ASPEN (Runs 14–16) produced a slightly negative impact in the upwind side of the Medicine Bow highest peak. A detailed analysis shows that the negative signal is associated with reduced precipitation that was simulated to fall as rain on the ground. The simulated seeding converted the rain into slower falling snow or graupel that fell in the downwind area. By comparing Run 14 (no AgI scavenging) with Run 15 (AgI scavenging), it is clear that the extra AgI removal processes in the updated ASPEN reduced the simulated seeding effect in both of the Ranges; however, the reduction was more evident in the Medicine Bow Range. Two hours of airborne seeding (Run 16) generated a broader area, but a smaller magnitude, of simulated seeding impacts in the Sierra Madre Range compared with most of the ground-seeding simulations for the same range. In addition, the simulated airborne-seeding effect in the Medicine Bow Range is weaker than it is for the ground-seeding cases.

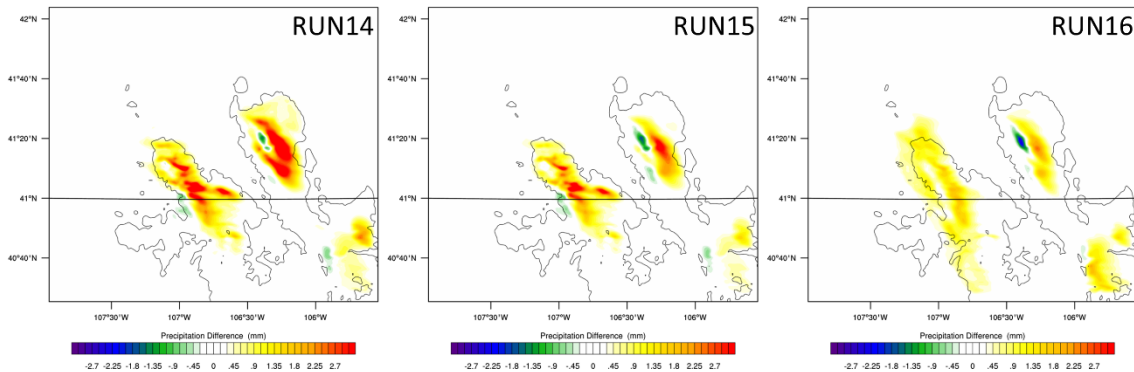


Figure 6.25. Seeding effect of precipitation of runs 14 to 16 for the 13 January 2014 case.

The LWP depletion patterns and the AgI maps are shown in Figure 6.26 and Figure 6.27, respectively, for these three simulations. The change of the PBL scheme and land-surface model reduced the stability in the upwind region of the Sierra Madre Range; therefore, the AgI plumes from generator groups E and F were advected over the Sierra Madre Range instead of going around it to the north, as the original simulations showed (Figure 6.21). The flow in the area upwind of the Medicine Bow is still blocked. However, due to the low-level wind direction, and the change in atmospheric stability upwind of the Sierra Madre in the new simulation, all AgI plumes were able to cross the Medicine Bow Range around the south. The extra AgI removal processes reduced both the LWP depletion and the AgI concentration especially in the Medicine

Bow Range, which corresponds to the simulated seeding effect (Figure 6.25). The AgI plumes covered a broader area and depleted liquid water in a greater area of the Sierra Madre Range in the airborne test than the ground-seeding tests. The AgI plume from simulated airborne seeding (i.e. Run 16) dispersed over both Ranges and is not subject to low-level atmospheric stability issues like plumes from ground-based generators (Figure 6.27).

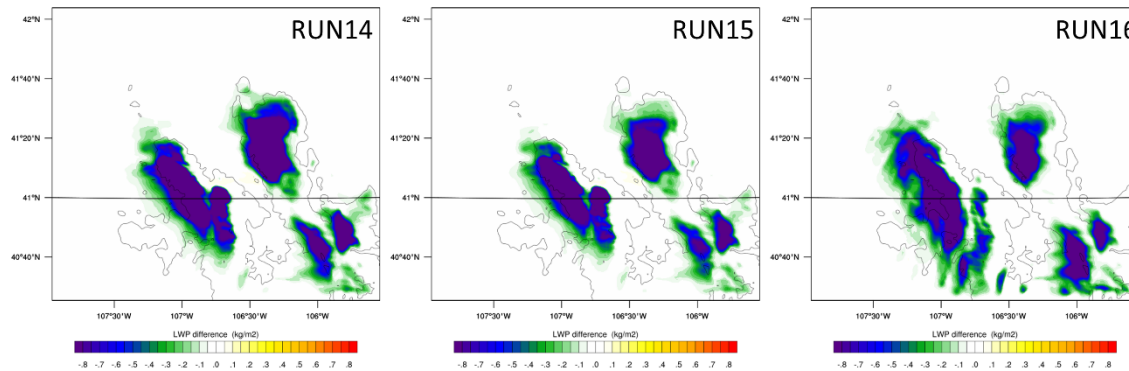


Figure 6.26. Accumulated LWP difference (-0.8 to 0.8 mm) during the seeding period between SEED and CTRL simulations of runs 14 to 16 for the 13 January 2014 case.

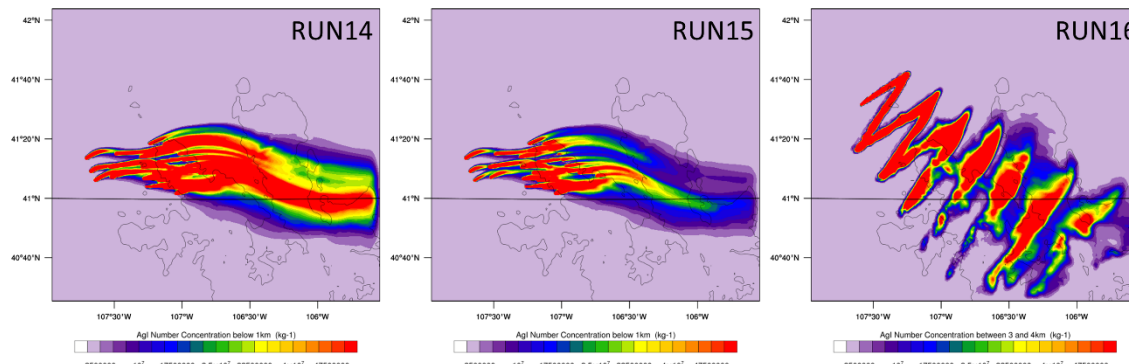


Figure 6.27. Average AgI concentration below 1 km AGL at the end of the seeding period of runs 14 and 15 and between 3 and 4 km MSL of run 16 for the 13 January 2014 case.

The vertical cross sections (locations are shown in Figure 6.9) showing the simulated airborne-seeding impact on clouds are illustrated in Figure 6.28 for the airborne seeding simulation (i.e. Run 16). The airborne seeding generated deeper impacts in both the liquid and ice phases of the cloud than the ground-seeding cases (Figure 6.22).

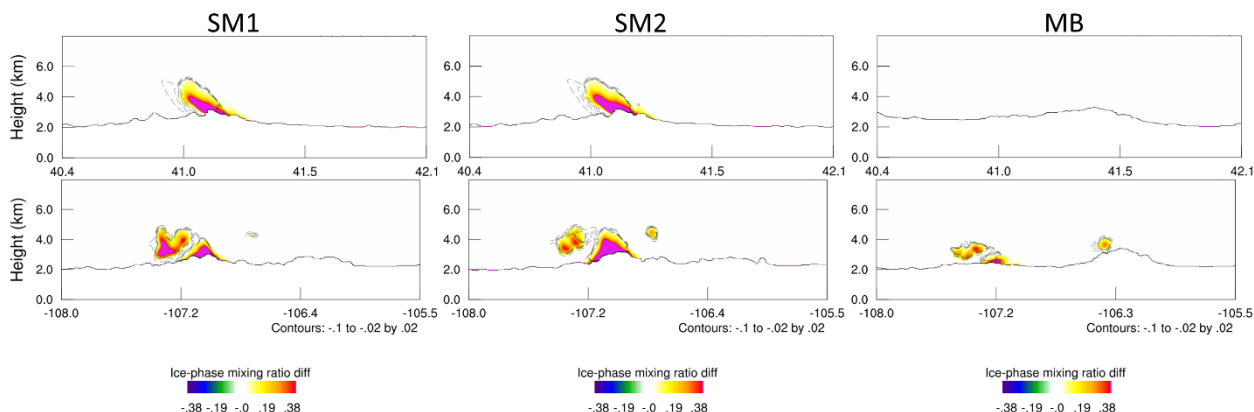


Figure 6.28. Vertical cross sections (south-north on the top and west-east at the bottom) of Run 16 at 1630 UTC for the 13 January 2014 case.

The control precipitation and simulated seeding effect over the entire domain, Sierra Madre assessment area, and Medicine Bow assessment area for each of the seeding experiments are listed in Table 6.8. This case has more natural (CTRL) precipitation than the first (23 January 2010) case and is similar to the second (10 January 2014) case. All experiments generated more simulated seeding effects compared with the previous two cases. Seeding simulated from Medicine Bow generators (Run3) resulted in more simulated seeding effects over the Medicine Bow Range compared with the previous two cases as well. Nonetheless, similar to the previous case, seeding simulated from Sierra Madre generators still resulted in the highest simulated seeding effects in both ranges (Run11). The relative seeding impact areas in cases with the highest simulated seeding effects are typically 70% or greater (Table 6.8). The new WRF model simulated more precipitation in the entire domain as well as each individual range, especially in the Medicine Bow Range. Run 14 produced more simulated seeding effect in the Sierra Madre Range, but less effect in the Medicine Bow Range and the entire domain than Run 11 (the original simulation using the same generator groups). The addition of AgI removal processes reduced the simulated seeding effect in all areas with substantial reduction in the downwind Medicine Bow Range (by more than 50%) compared with results without these processes. It also reduced the seeding-impacted area in the Medicine Bow Range. However, comparing the Run 15 simulated seeding effect in the Medicine Bow Range (754 AF) to that from Run 3 if run with the new model set up (805 AF, not shown), simulated seeding impacts in the Medicine Bow Range are similar from seeding only in the Sierra Madre Range to that of only seeding in the Medicine Bow Range. Two hours of simulated airborne seeding produced almost the same effects in both precipitation amount and impacted-area as the 10-hour ground-seeding using 26 generators from the Sierra Madre Range.

Table 6.8. Same as Table 6.4, but for the 13 January 2014 case. Results listed in light green shading were run with WRF V3.7.1 using the updated ASPEN.

Exp	Effect	Domain	SM	MB	Effect	Domain	SM	MB
CTRL	Precip	39842	9192	4568	Area (km ²)	36288	2459	2468
Run1	SE (af)	2645	760	1749	PSE_A (km ²)	7437	1779	1947
	SE (%)	7	8	38	PSE_A (%)	21	72	79
Run2	SE (af)	2411	769	1495	PSE_A (km ²)	7205	1749	1866
	SE (%)	6	8	33	PSE_A (%)	20	71	76
Run3	SE (af)	840	11	874	PSE_A (km ²)	4052	617	1946
	SE (%)	2	0	19	PSE_A (%)	11	25	79
Run4	SE (af)	2667	761	1780	PSE_A (km ²)	7399	1761	1970
	SE (%)	7	8	39	PSE_A (%)	20	72	80
Run5	SE (af)	173	6	192	PSE_A (km ²)	2699	619	745
	SE (%)	0	0	4	PSE_A (%)	7	25	30
Run7	SE (af)	353	19	353	PSE_A (km ²)	2985	714	1213
	SE (%)	1	0	8	PSE_A (%)	8	29	49
Run8	SE (af)	102	4	90	PSE_A (km ²)	2554	486	796
	SE (%)	0	0	2	PSE_A (%)	7	20	32
Run9	SE (af)	1295	30	1363	PSE_A (km ²)	3882	759	1694
	SE (%)	3	0	30	PSE_A (%)	11	31	69
Run10	SE (af)	3845	629	2063	PSE_A (km ²)	9083	1685	1507
	SE (%)	10	7	45	PSE_A (%)	25	69	61
Run11	SE (af)	5248	1162	2969	PSE_A (km ²)	10370	1816	1924
	SE (%)	13	13	65	PSE_A (%)	29	74	78
Run12	SE (af)	2790	766	1926	PSE_A (km ²)	7319	1771	1926
	SE (%)	7	8	42	PSE_A (%)	20	72	78
Run13	SE (af)	2795	762	1937	PSE_A (km ²)	7378	1769	1950
	SE (%)	7	8	42	PSE_A (%)	20	72	79
CTRL2	Precip	42528	10535	7464	Area (km ²)	36288	2459	2468
Run14	SE (af)	3895	1634	1601	PSE_A (km ²)	8222	2003	1836
	SE (%)	9	16	21	PSE_A (%)	23	81	74
Run15	SE (af)	2507	1335	754	PSE_A (km ²)	7269	1963	1584
	SE (%)	6	13	10	PSE_A (%)	20	80	64
Run16	SE (af)	2926	1090	495	PSE_A (km ²)	7583	1929	1360
	SE (%)	7	10	7	PSE_A (%)	21	78	55

6.4.4. Case 4: 21 February 2012 results

For this case, the control run was integrated from 21 February 2012 1300 UTC to 21 February 2012 2300 UTC. Seeding simulations were integrated between 21 February 2012 1500 UTC to 21 February 2012 2030 UTC, with ground seeding between 21 February 2012 1500 UTC to 2030 UTC.

Five extra seeding simulations were conducted for this case. Two ground-seeding simulations with seeding time from 21 February 2012 1500 UTC to 2030 UTC were used to investigate the impact of the AgI removal processes in the updated ASPEN. Three airborne-seeding simulations were run: two with the same seeding time window of 1900 UTC to 2130 UTC, but with one simulating seeding at 3,500 m MSL versus 4,500 m MSL for the other. The third airborne-seeding simulation used a longer seeding window of 1500 UTC to 2130 UTC at 3500 m MSL because the airborne-seeding conditions were considered good during this entire period. The seeding experiments are listed in Table 6.9.

Table 6.9. Seeding simulations of the 21 February 2012 case. The SM “oriC” group consists of the one original Group C generator shown in Figure 5.5. Runs listed in light green shading were run with WRF V3.7.1 using the updated ASPEN.

Run 1	SM A+B+oriC & MB A+B+C
Run 2	SM A+B
Run 3	MB A+B+C
Run 4	SM A+B+oriC+D
Run 5	SM C
Run 6	SM E+F
Run 7	SM A+B+C+D+E+F
Run 8	SM A+B+C
Run 9	SM A+B+C+D
Run 10	SM A+B+C+D+E+F with the same AgI scavenging in the original ASPEN
Run 11	Same as Run 10 but with extra AgI removal processes as listed in Table 6.1
Run 12	Airborne seeding with extra AgI removal processes as listed in Table 6.1 (AS)
Run 13	Same as Run 12 but at 4500 m MSL (ASH)
Run 14	Same as Run 12 but from 1500 to 2130 UTC (ASL)

For this case, the simulated natural precipitation is stronger and more widespread over the Sierra Madre Range than over the Medicine Bow Range (Figure 6.29). Sierra Madre precipitation is confined to the high terrain region. Precipitation in the Medicine Bow Range is on the lee side of the mountain with a weaker maximum than in the Sierra Madre Range. The LWP during and after the seeding period indicated that plenty of SLW was available in both Ranges throughout the seeding period, although there was clearly more SLW over the Medicine Bow Range (Figure 6.30).

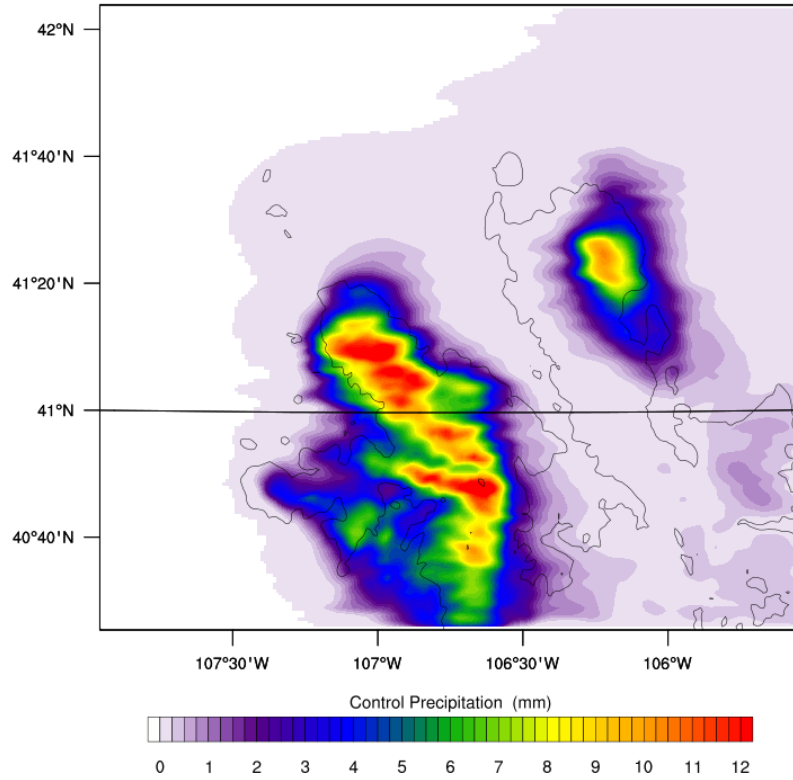


Figure 6.29. Same as Figure 6.4, but for the 21 February 2012 case.

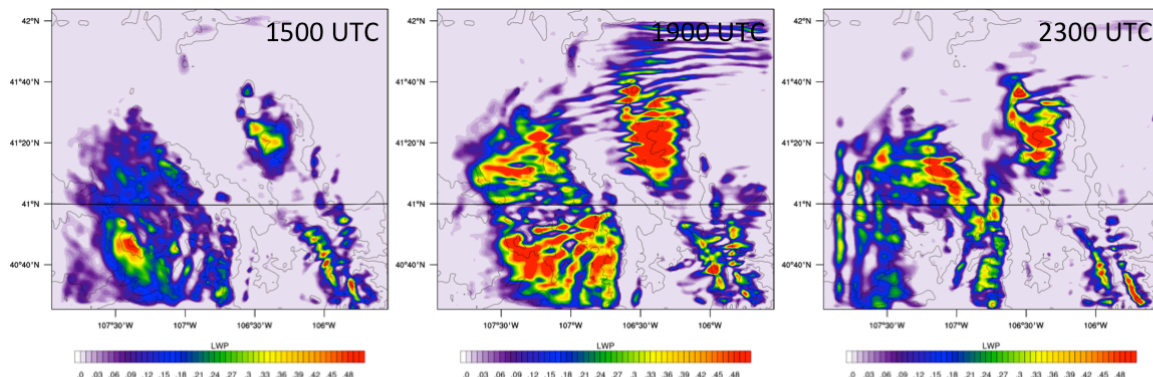


Figure 6.30. Same as Figure 6.5, but for the 21 February 2012 case.

The simulated seeding effects of all seeding experiments are plotted in Figure 6.31. The corresponding seeding generators are plotted on each panel. The simulations show that very little change in precipitation is simulated as the result of seeding over the Sierra Madre Range in any experiment. On the other hand, nearly every experiment has a similar spatial pattern of simulated seeding effects over the Medicine Bow Range, even in experiments for which no Medicine Bow generators were utilized. The simulated seeding effects in the Medicine Bow Range typically fall upwind of and at the peak, offset from where the natural precipitation maximum was located in the CTRL run (Figure 6.29 and Figure 6.31). In the experiments with the strongest simulated seeding effects over the Medicine Bow Range (i.e., Run7–Run9), there is a slight negative change in precipitation on the lee side of the range.

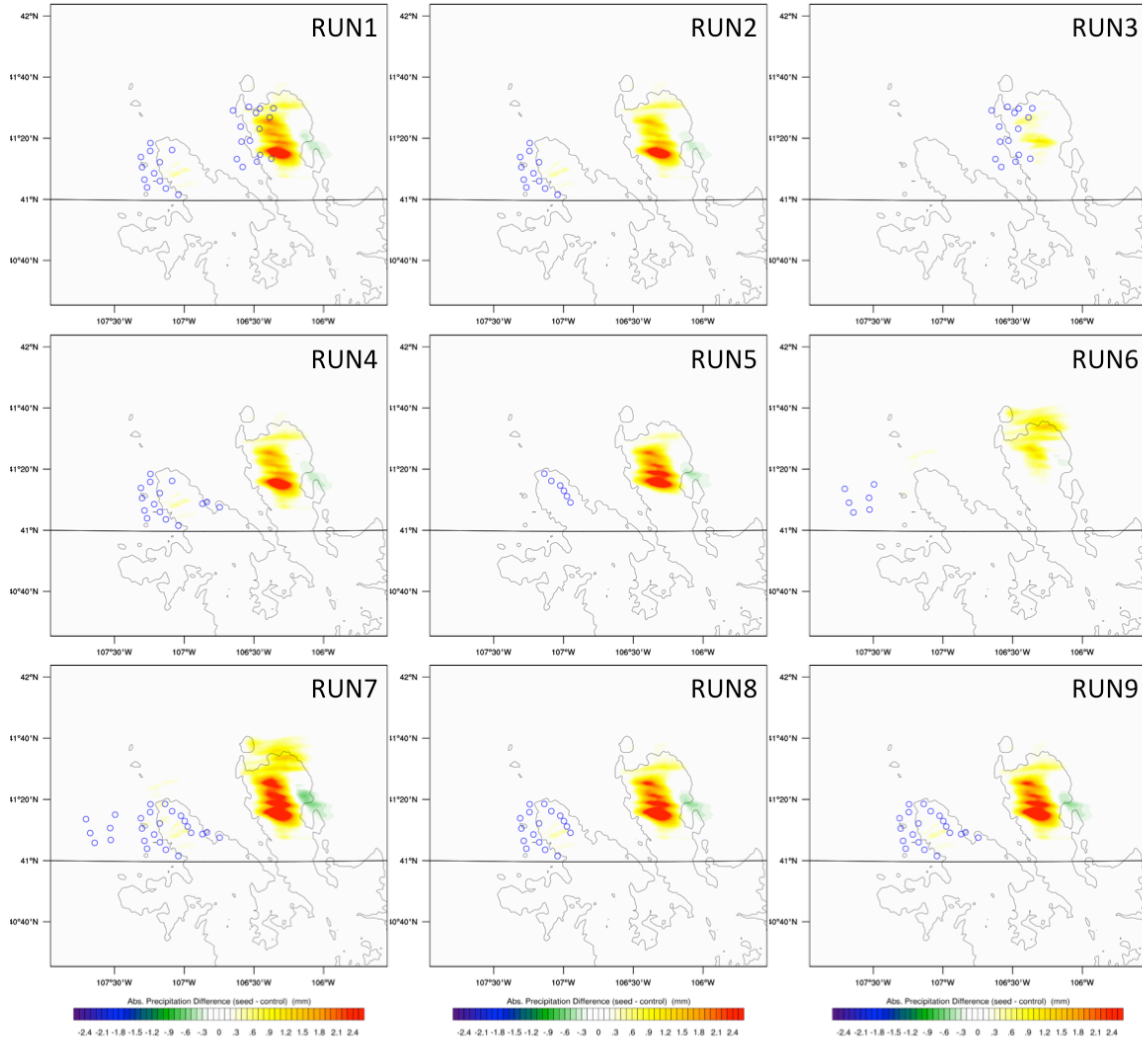


Figure 6.31. Same as Figure 6.6, but for the 21 February 2012 case with all runs.

The LWP depletion patterns corresponded to the simulated seeding effect maps for the same cases as in Figure 6.31 (Figure 6.32). Unlike some of the previous cases, such as the third (13 January 2014) case, the AgI plumes were not blocked by the terrain in these simulations (Figure 6.33). Even the AgI plume released from the low altitude generators in Sierra Madre Groups E and F was transported straight over the north end of the Sierra Madre Range by the prevailing southwesterly winds.

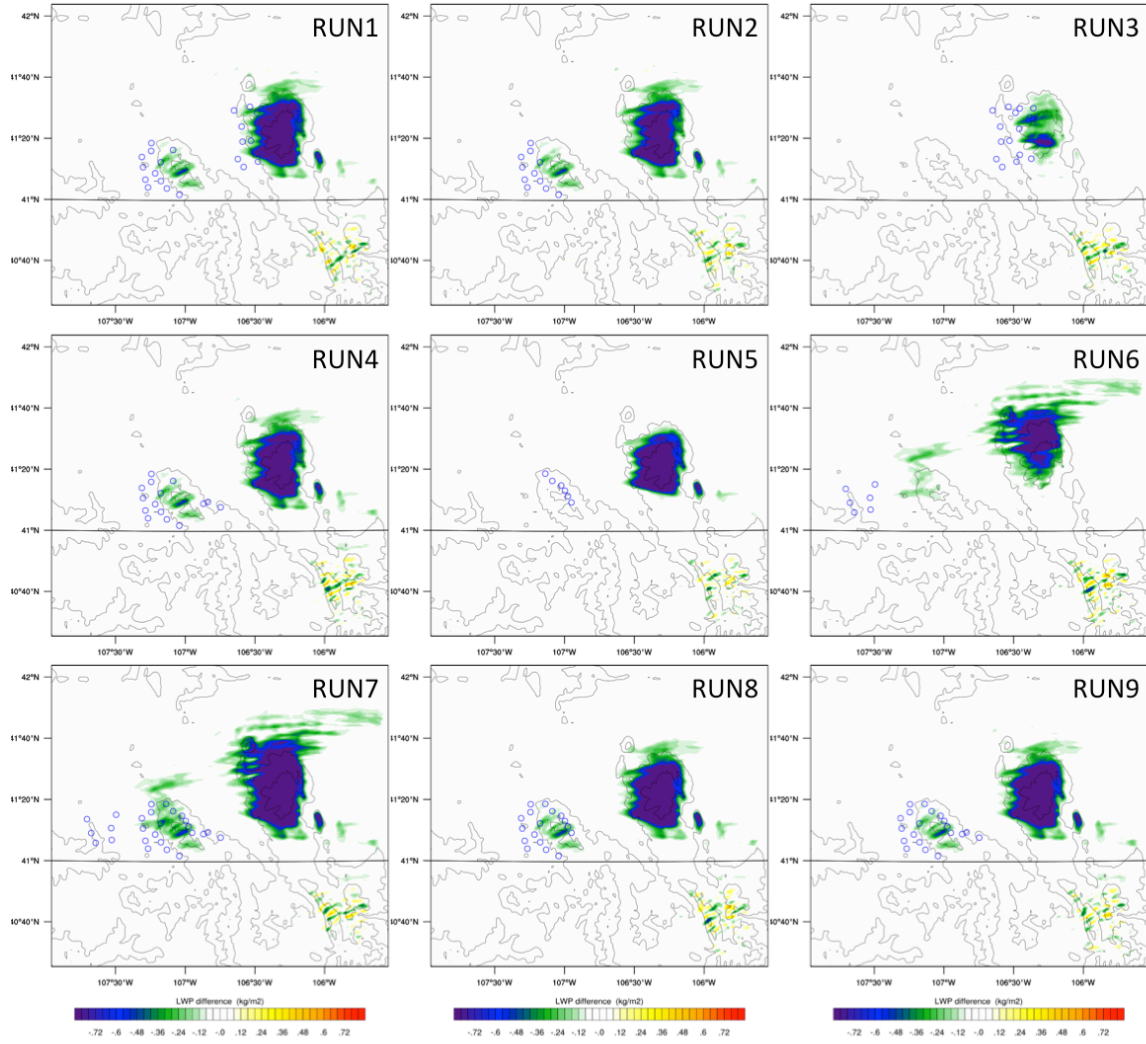


Figure 6.32. Accumulated LWP path difference (-0.8 to 0.8 mm) during the seeding period between SEED and CTRL simulations for the same cases as in Figure 6.31.

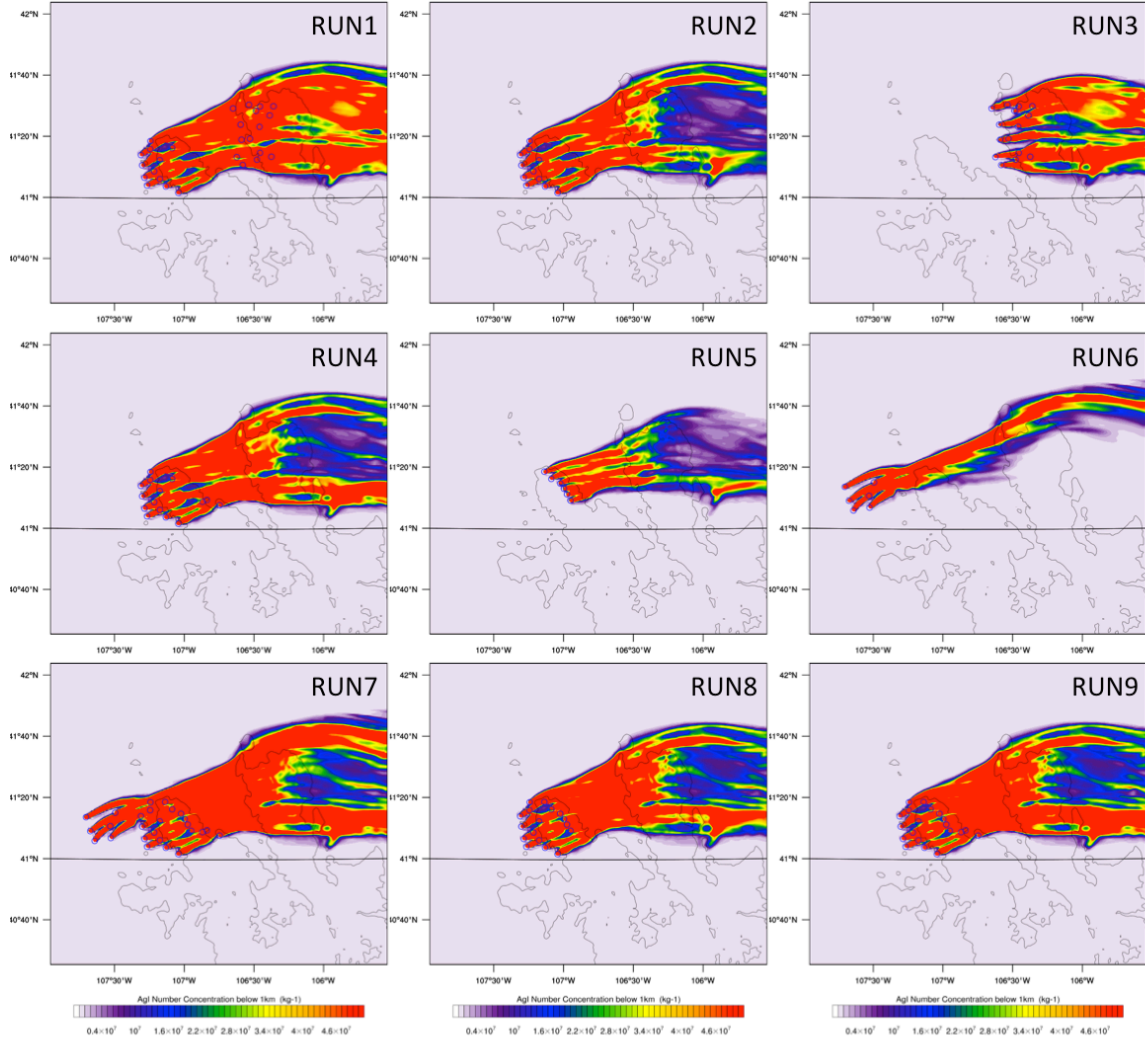


Figure 6.33. Average AgI concentration below 1 km AGL at the end of the seeding period for the same cases as in Figure 6.31.

The vertical cross sections (locations are shown in Figure 6.9) showing the simulated seeding impact on clouds are illustrated in Figure 6.34 for Run1. The impact of simulated seeding in the Sierra Madre Range is negligible, which agrees with the simulated seeding effect on precipitation. While there was SLW, the cloud-top temperatures over the Sierra Madre Range were colder than -20°C in this case, leading to natural precipitation efficiency. Moreover, the flow was strong and laminar, which confined the AgI plume close to the surface such that it was only able to impact a very shallow layer of the SLW in the Sierra Madre Range.

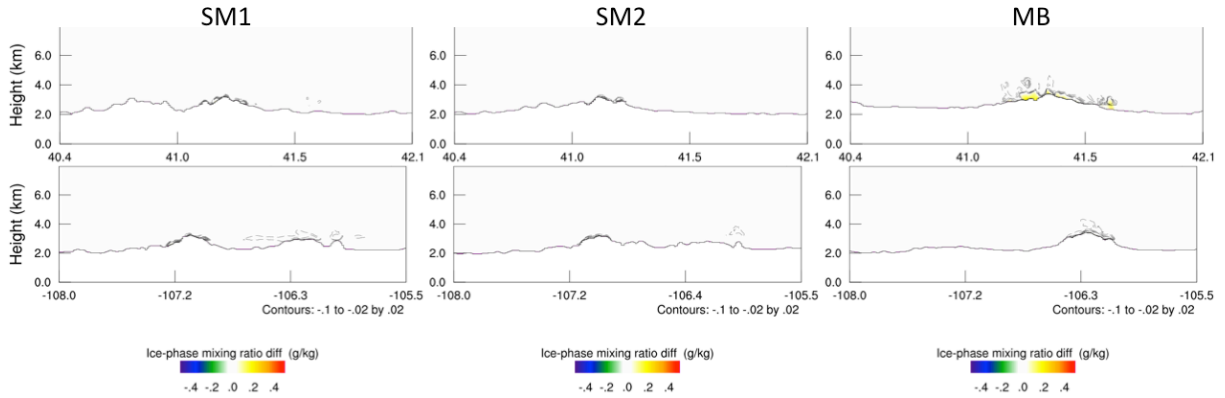


Figure 6.34. Same as Figure 6.10, but for the 21 February 2012 case at 1745 UTC.

The newly simulated control precipitation and LWP at the same times as Figure 6.29 are shown in Figure 6.35 and Figure 6.36, respectively. The general patterns and magnitudes of the precipitation and LWP are similar between the new simulation and the previous ones (WRFV3.4.1). Nonetheless, the precipitation maximum in the Medicine Bow Range was increased and shifted upwind relative to the original control run. The LWP distribution is smoother in the new run as well.

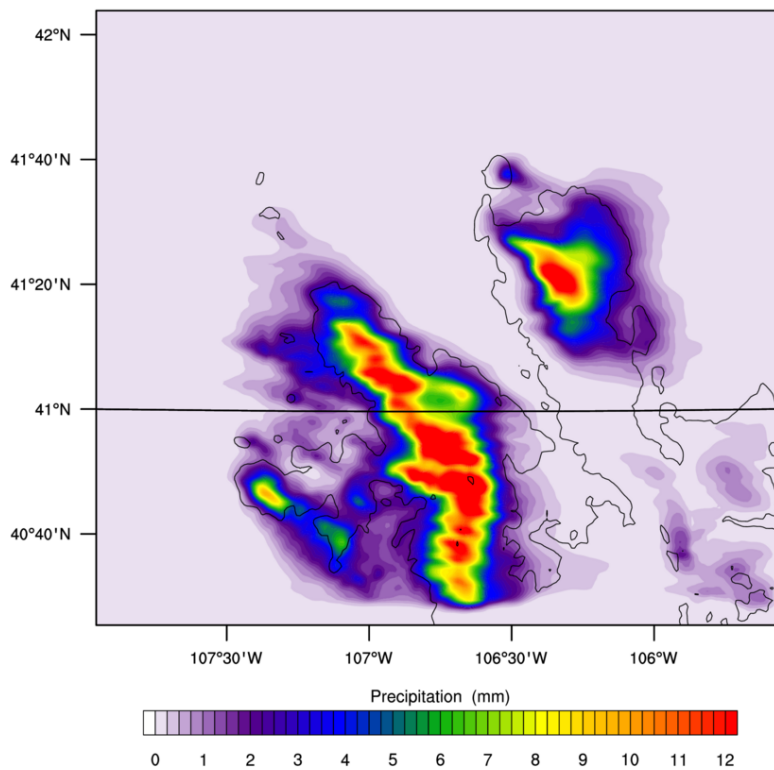


Figure 6.35. Control precipitation at the end of the simulation for the 21 February 2012 case.

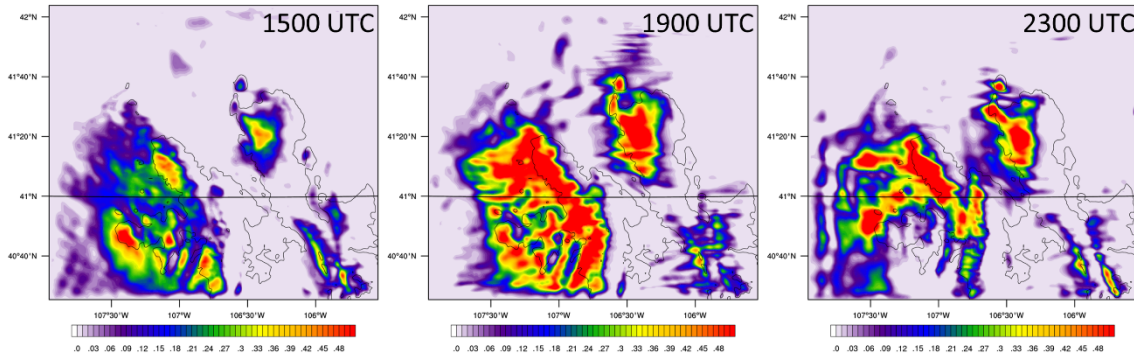


Figure 6.36. Liquid-water path below 1 km AGL at 1500, 1900 and 2300 UTC from the control simulation for the 21 February 2012 case.

The simulated seeding effects of the five extra seeding experiments are plotted in Figure 6.37. Again, similar to 13 January 2014 (Case 3), the new seeding runs with the new WRF and ASPEN converted rain into snow and graupel and thus produced a negative impact in the upwind side of the Medicine Bow Range, which was not present in the original seeding simulations. The extra AgI removal processes slightly reduced the simulated seeding effect in the Medicine Bow Range. Two and a half hours of airborne seeding generated a broader and larger magnitude of simulated seeding impact in the Sierra Madre Range than the ground-seeding case. The simulated airborne seeding effect in the Medicine Bow Range is weaker than the ground-seeding case. The airborne seeding at the higher altitude generated a stronger simulated seeding effect in the Sierra Madre Range, especially on the upwind side, but barely impacted the Medicine Bow Range. The longer airborne-seeding scenario (Run 14) produced the widest and strongest simulated seeding impacts in both Ranges.

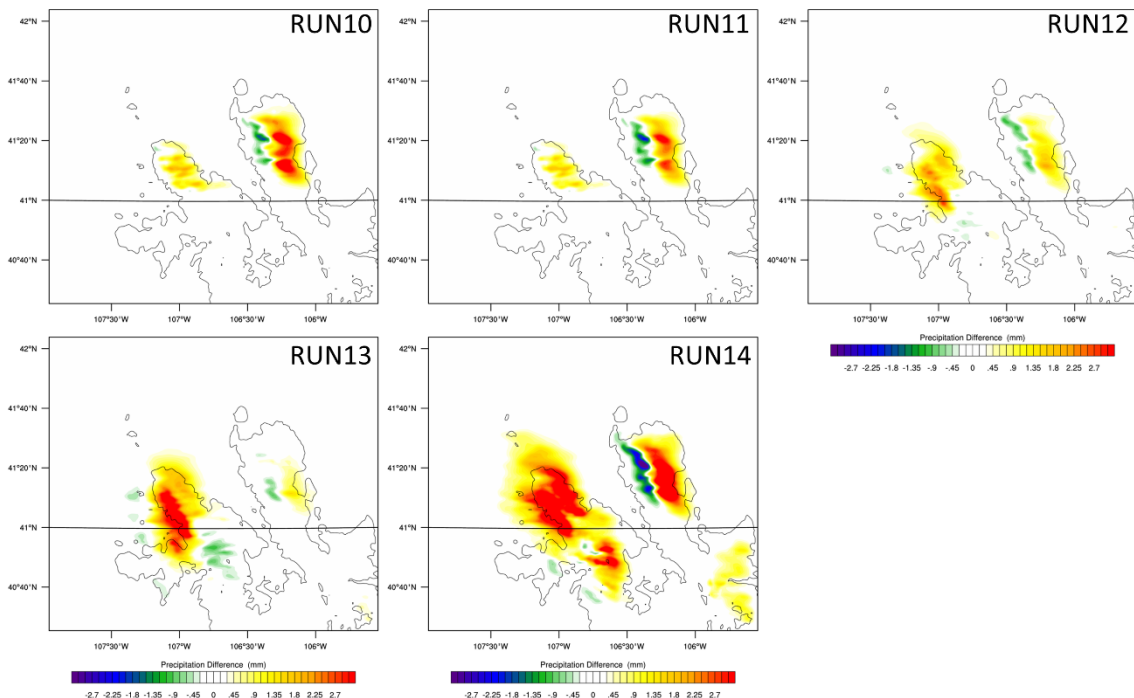


Figure 6.37. Simulated seeding effect on precipitation (mm) of Runs 10 to 14 for the 21 February 2012 case.

The LWP depletion patterns and the AgI maps are shown in Figure 6.38 and Figure 6.39, respectively, for these simulations. The atmospheric stability in both ranges was weaker in the new simulations, so that the AgI plumes from all generators passed over the ranges instead of going around them. The extra AgI removal processes reduced the AgI concentration in both ranges and slightly reduced the LWP depletion in the Medicine Bow Range. The AgI plumes covered a broader area and depleted the SLW in the same zigzag pattern. The same features are found in the high-altitude airborne-seeding run. The wind had a stronger northerly component in the ASH case than the AS case so that the Medicine Bow Range was less impacted by the high airborne seeding. In the AS simulation, the AgI plumes cover both areas for longer time than the other two airborne-seeding runs, which led to broader and stronger depletion of SLW and subsequently more simulated seeding-enhanced precipitation on the ground. For all airborne simulations, more liquid water in the Sierra Madre Range was depleted compared with the ground-seeding scenario.

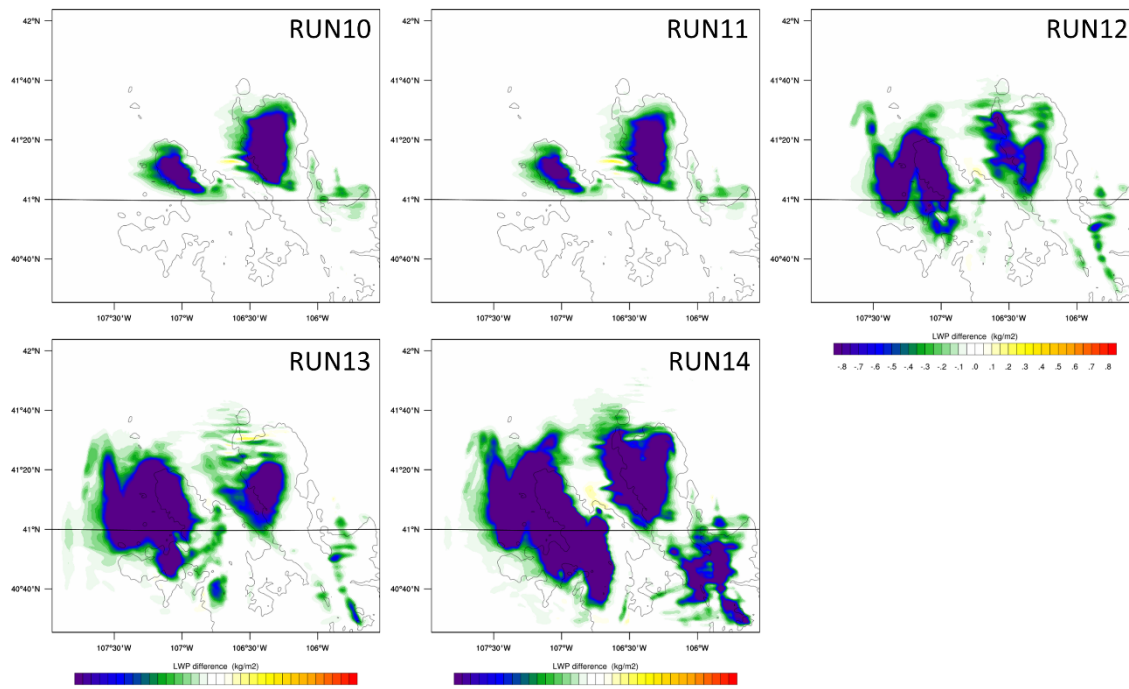


Figure 6.38. Accumulated LWP difference (-0.8 to 0.8 mm) during the seeding period between SEED and CTRL simulations of Runs 10 to 14 for the 21 February 2012 case.

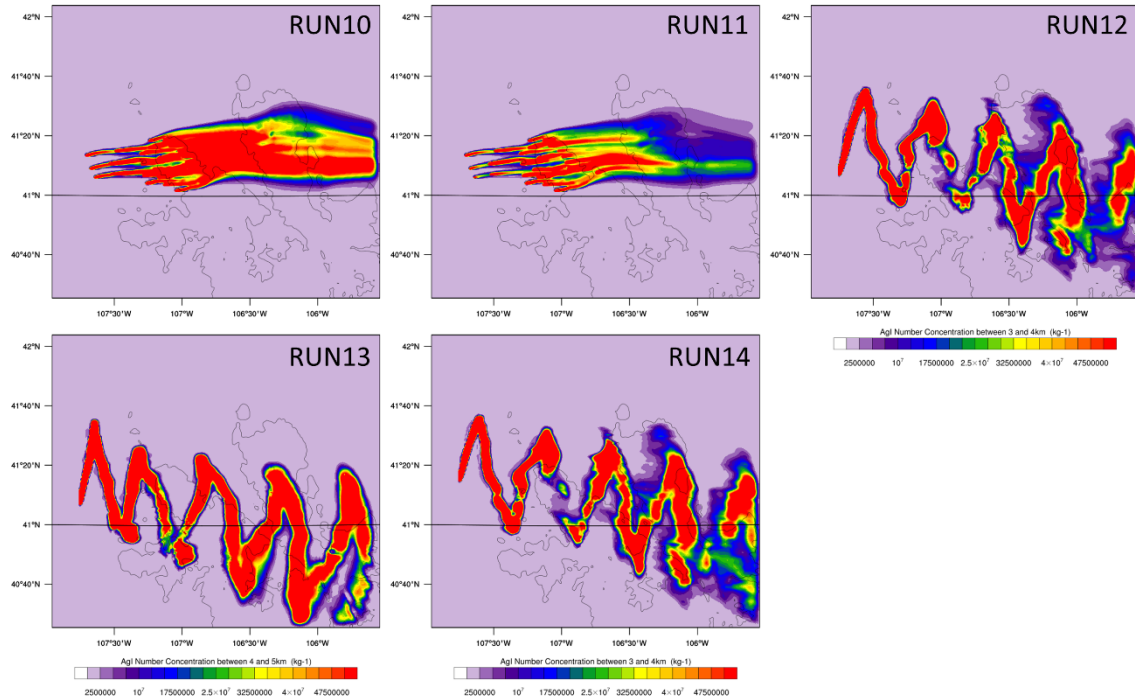


Figure 6.39. Average AgI concentration below 1 km AGL at the end of the seeding period of Runs 10 and 11, between 3 and 4 km MSL of Runs 12 and 14, and between 4 and 5 km MSL of Run 13 for the 21 February 2012 case.

The vertical cross sections showing the simulated seeding impact on clouds are illustrated in Figure 6.40 and Figure 6.41 for the AS and ASH runs. The high-altitude airborne-seeding simulation generated deeper and broader impacts in the Sierra Madre Range than the regular airborne-seeding altitude simulation.

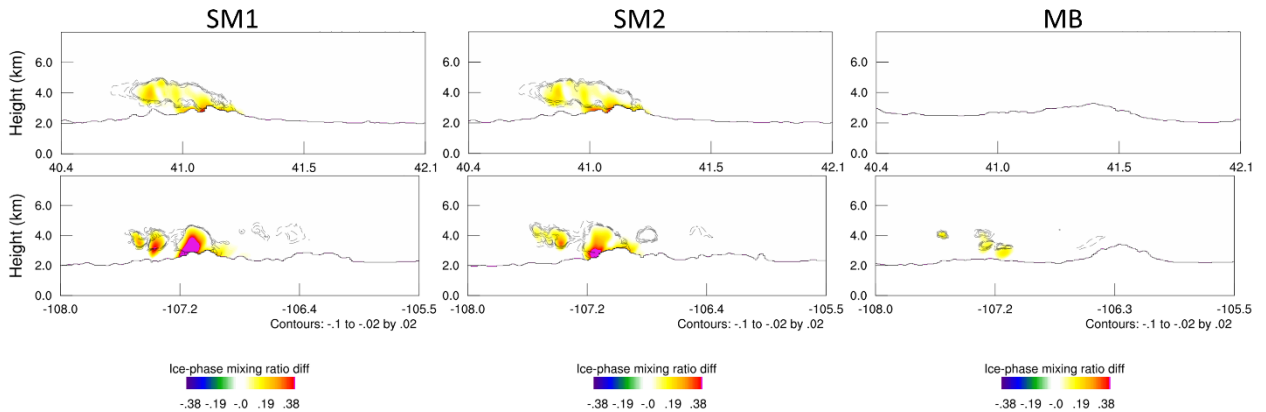


Figure 6.40. Vertical cross sections (south-north on the top and west-east at the bottom) of Run 12 at 2030 UTC for the 21 February 2012 case.

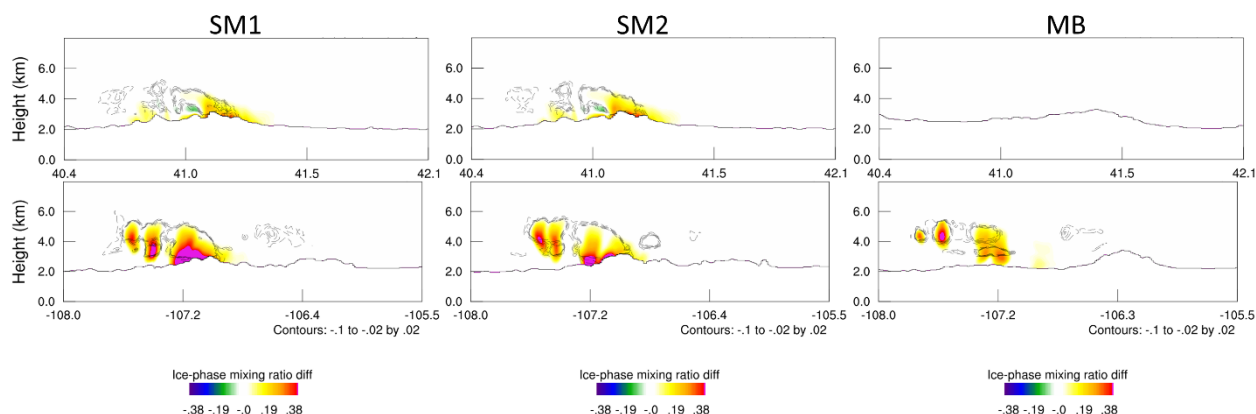


Figure 6.41. Vertical cross sections (south-north on the top and west-east at the bottom) of Run 13 at 2030 UTC for the 21 February 2012 case.

The control precipitation and simulated seeding effect over the entire domain, the Sierra Madre Range, and the Medicine Bow Range for each of the extra seeding experiments are listed in Table 6.10. The new WRF model simulated similar precipitation in the Sierra Madre Range and the entire domain, but more precipitation in the Medicine Bow Range. The Run10 simulation produced more simulated seeding effect in the Sierra Madre Range and the entire domain, but almost the same absolute simulated seeding effect in the Medicine Bow Range compared with Run7 (the same generator groups). The addition of AgI removal processes reduced the simulated seeding effect in all areas with substantial reduction in the downwind Medicine Bow Range (by about 50%) compared with results without these processes. It also reduced the seeding-impacted area in the Medicine Bow Range slightly. Two and a half hours of simulated airborne seeding produced almost the same effects in precipitation amount over the entire domain as the 5.5-hour ground-based seeding using 26 generators from the Sierra Madre Range. More simulated seeding effects in the Sierra Madre Range and less in the Medicine Bow Range were simulated by airborne seeding compared with ground-based seeding. High-altitude airborne seeding almost doubled the simulated seeding effect in the Sierra Madre Range relative to the regular altitude airborne-seeding run. A 6.5-hour window of airborne seeding almost doubled the simulated seeding effect in the Sierra Madre Range compared with the high altitude airborne-seeding run. All airborne-seeding simulations generated more simulated seeding effects and impacted broader areas than the ground-based seeding simulations.

The control precipitation and simulated seeding effect of the seeding experiments over the entire domain, the Sierra Madre Range, and the Medicine Bow Range are listed in Table 6.10. This case has more natural (CTRL) precipitation in the Sierra Madre Range than any of the other three cases. The simulated seeding effect in the Sierra Madre Range is very weak compared with the other cases as well. As shown in the previous cases, however, seeding simulated from Sierra Madre generators resulted in the greatest simulated seeding effects in both ranges (Run7). While the simulated seeding effect for the Sierra Madre Range was weak, and the associated impact area was also lower (~30%), the Medicine Bow Range relative simulated seeding impact area was similar to previous cases (~70% or greater).

Table 6.10. Same as Table 6.4, but for the 21 February 2012 case.

Exp	Effect	Domain	SM	MB	Effect	Domain	SM	MB
CTRL	Precip	29365	11278	3616	Area (km ²)	36288	2459	2468
Run1	SE (af)	951	72	864	PSE_A (km ²)	4090	776	1768
	SE (%)	3	1	24	PSE_A (%)	11	32	72
Run2	SE (af)	834	72	744	PSE_A (km ²)	4273	788	1748
	SE (%)	3	1	21	PSE_A (%)	12	32	71
Run3	SE (af)	224	0	225	PSE_A (km ²)	2116	57	1517
	SE (%)	1	0	6	PSE_A (%)	6	2	61
Run4	SE (af)	918	72	830	PSE_A (km ²)	4348	770	1822
	SE (%)	3	1	23	PSE_A (%)	12	31	74
Run5	SE (af)	809	2	842	PSE_A (km ²)	2143	155	1556
	SE (%)	3	0	23	PSE_A (%)	6	6	63
Run6	SE (af)	724	30	397	PSE_A (km ²)	5983	534	1281
	SE (%)	2	0	11	PSE_A (%)	16	22	52
Run7	SE (af)	1668	101	1294	PSE_A (km ²)	7073	860	1852
	SE (%)	6	1	36	PSE_A (%)	19	35	75
Run8	SE (af)	1109	72	1030	PSE_A (km ²)	4266	778	1793
	SE (%)	4	1	28	PSE_A (%)	12	32	73
Run9	SE (af)	1129	73	1048		4270	787	1849
	SE (%)	4	1	29		12	32	75
CTRL2	Precip	28511	10135	5336	Area (km ²)	36288	2459	2468
Run10	SE (af)	1789	480	1239	PSE_A (km ²)	3720	1125	1619
	SE (%)	6	5	23	PSE_A (%)	10	46	66
Run11	SE (af)	1212	394	758	PSE_A (km ²)	3248	1038	1463
	SE (%)	4	4	14	PSE_A (%)	9	42	59
Run12	SE (af)	1742	908	434	PSE_A (km ²)	6643	1505	1242
	SE (%)	6	9	8	PSE_A (%)	18	61	50
Run13	SE (af)	2714	1773	225	PSE_A (km ²)	7548	1572	1457
	SE (%)	10	18	4	PSE_A (%)	21	64	59
Run14	SE (af)	7497	3316	1295	PSE_A (km ²)	10315	2198	1338
	SE (%)	26	33	24	PSE_A (%)	28	89	54

6.5. Model Simulation Comparison with Observations

6.5.1. Comparison between model and observed soundings

During the WWMPP, project-specific soundings were launched from Saratoga, Wyoming in association with nearly every seeding case that was called. For each of the four test cases evaluated in this study, which are based upon WWMPP cases, the measurements from the soundings have been compared with the model results from near the sounding launch site (i.e.,

Saratoga) to assess how well the model simulations reproduced the thermodynamic environment of each case. The Saratoga sounding data are from 23 January 2010 23 UTC (Case 1), 10 January 2014 16 UTC (Case 2), 13 and 21 UTC 13 January 2014 (Case 3), 13 and 21 UTC 21 February 2012 (Case 4).

A scatterplot comparison of the sounding observations versus the model output for several thermodynamic variables is provided in Figure 6.42. From this view, it is clear that for most of the variables assessed, the model and observations compared very well with points nearly lying on the 1:1 line. The model output varied from Case 2 by simulating overly dry conditions, and there was approximately a 10-20-degree discrepancy between observed and modeled wind directions. Another discrepancy between observed and modeled data, was found in the modeled atmospheric stability as indicated by the Brunt-Väisälä frequency (Figure 6.42j). In four of the six soundings, the model was too stable (larger N) compared with the observations. Since N is the denominator in calculating Fr (Section 4.1.3), this error in model atmospheric stability also shows up as an error in Fr . Nonetheless, the Fr for all cases, in both the model and the observations, was greater than one, indicating that the atmosphere should not be blocking the flow of air over the barrier. Nonetheless, smaller-scale influences on atmospheric stability and wind speed can still impact the local Fr number such that localized blocking of the flow could still occur. Detailed comparisons of the skew- t plots illustrating the Saratoga sounding observations compared with the modeled soundings are shown in Figure 6.43–Figure 6.46. While the model does not always resolve rapid fluctuations in temperature or humidity, the soundings compare rather well in all cases.

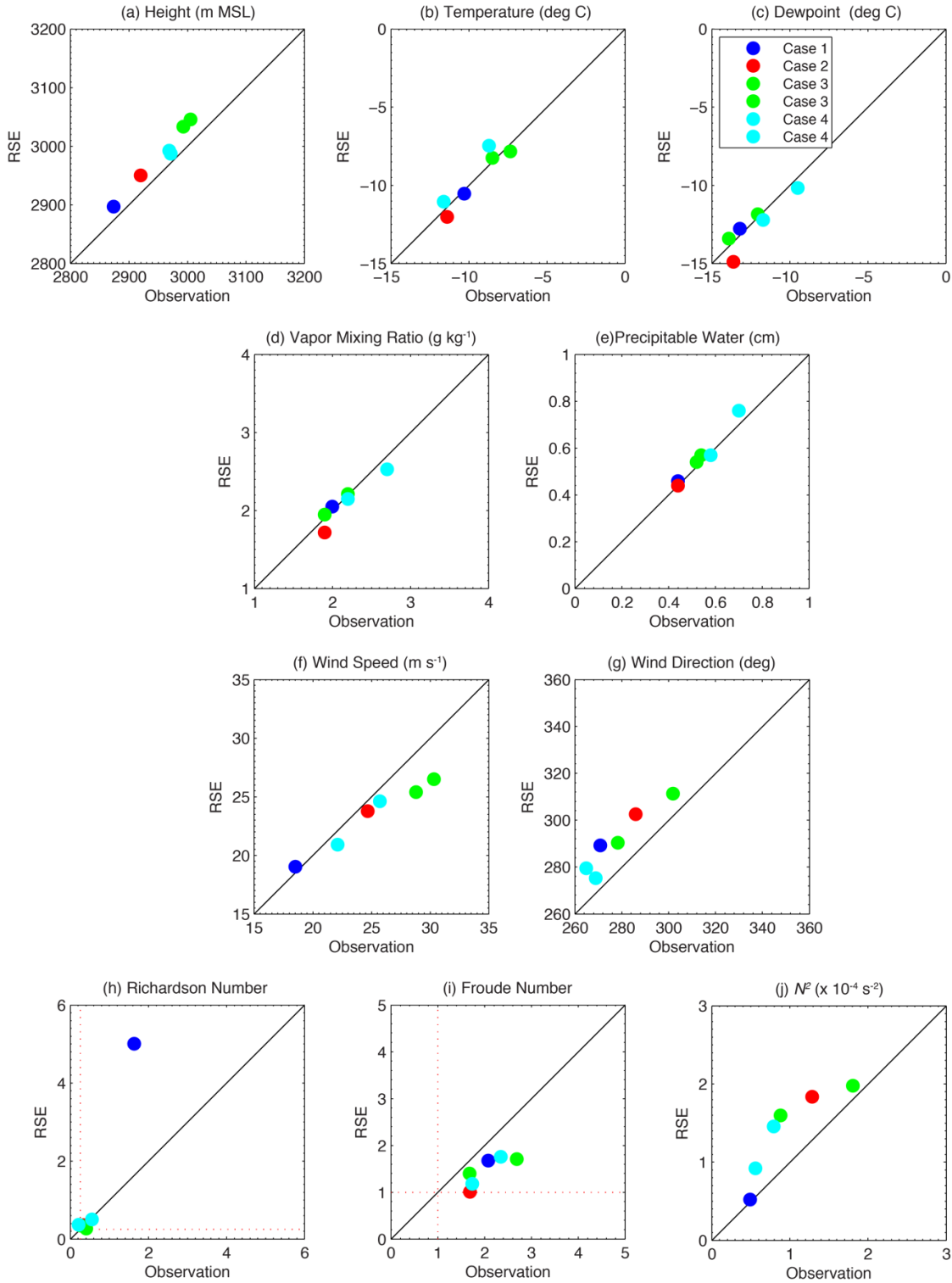


Figure 6.42. Scatter plots of observed and model-simulated (a) 700-hPa geopotential height (m MSL), (b) 700-hPa temperature ($^{\circ}\text{C}$), (c) 700-hPa dew point temperature ($^{\circ}\text{C}$), (d) 700-hPa vapor mixing ratio (g kg^{-1}), (e) precipitable water (cm), (f) 700-hPa wind speed (m s^{-1}), (g) 700-hPa wind direction (deg), (h) Richardson number, (i) Froude number, and (j) the squared of Brunt-Vaisala frequency (N^2 , s^{-2}). Filled dots are color-coded by RSE cases. The sounding data are from 23 January 2010 23 UTC (case 1), 10 January 2014 16 UTC (case 2), 13 and 21 UTC 13 January 2014 (case 3), 13 and 21 UTC 21 February 2012 (case 4).

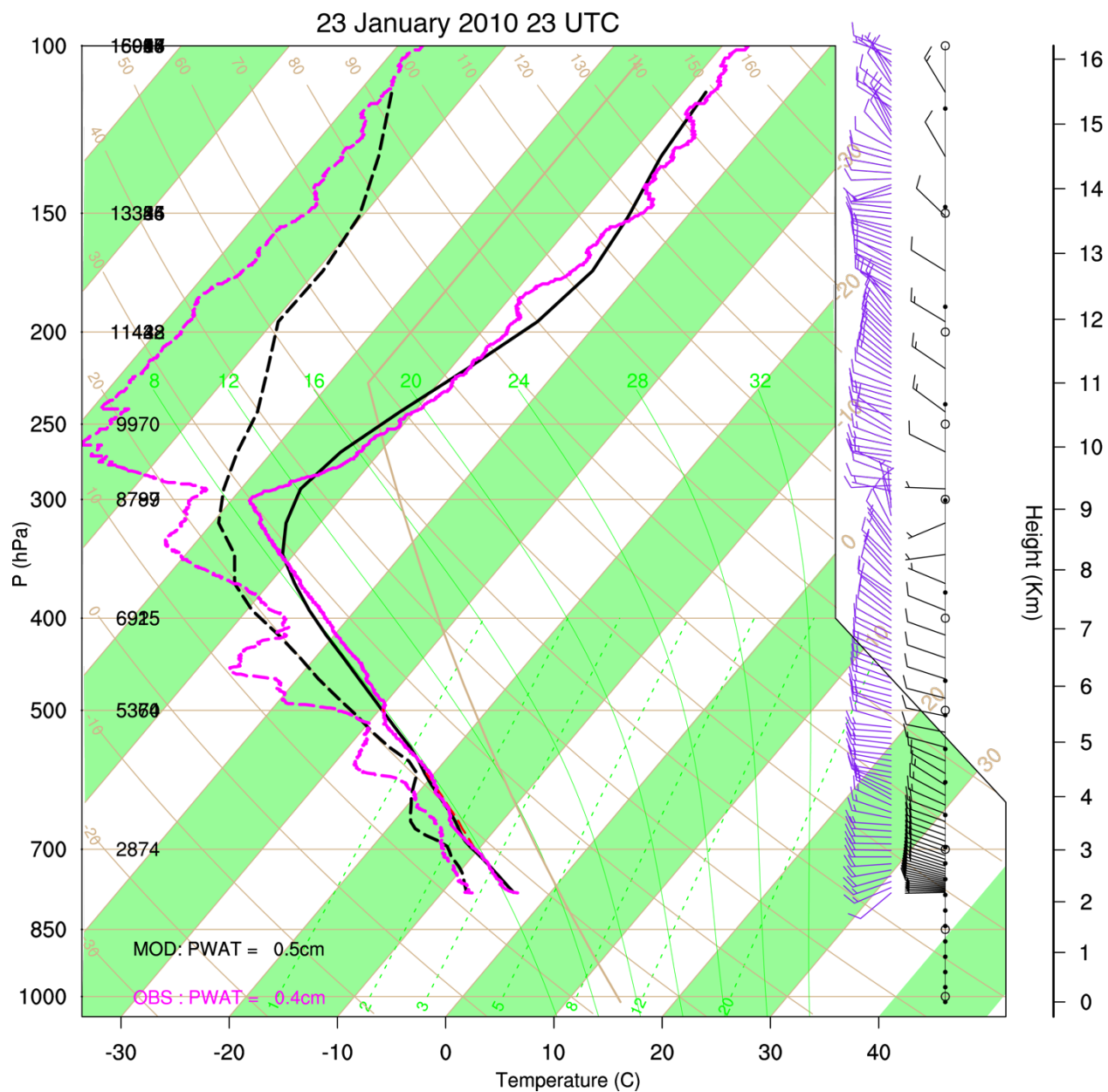


Figure 6.43. Skew-T comparison between the sounding launched from Saratoga and the RSE model-based sounding for 23 UTC on 23 January 2010 (Case 1).

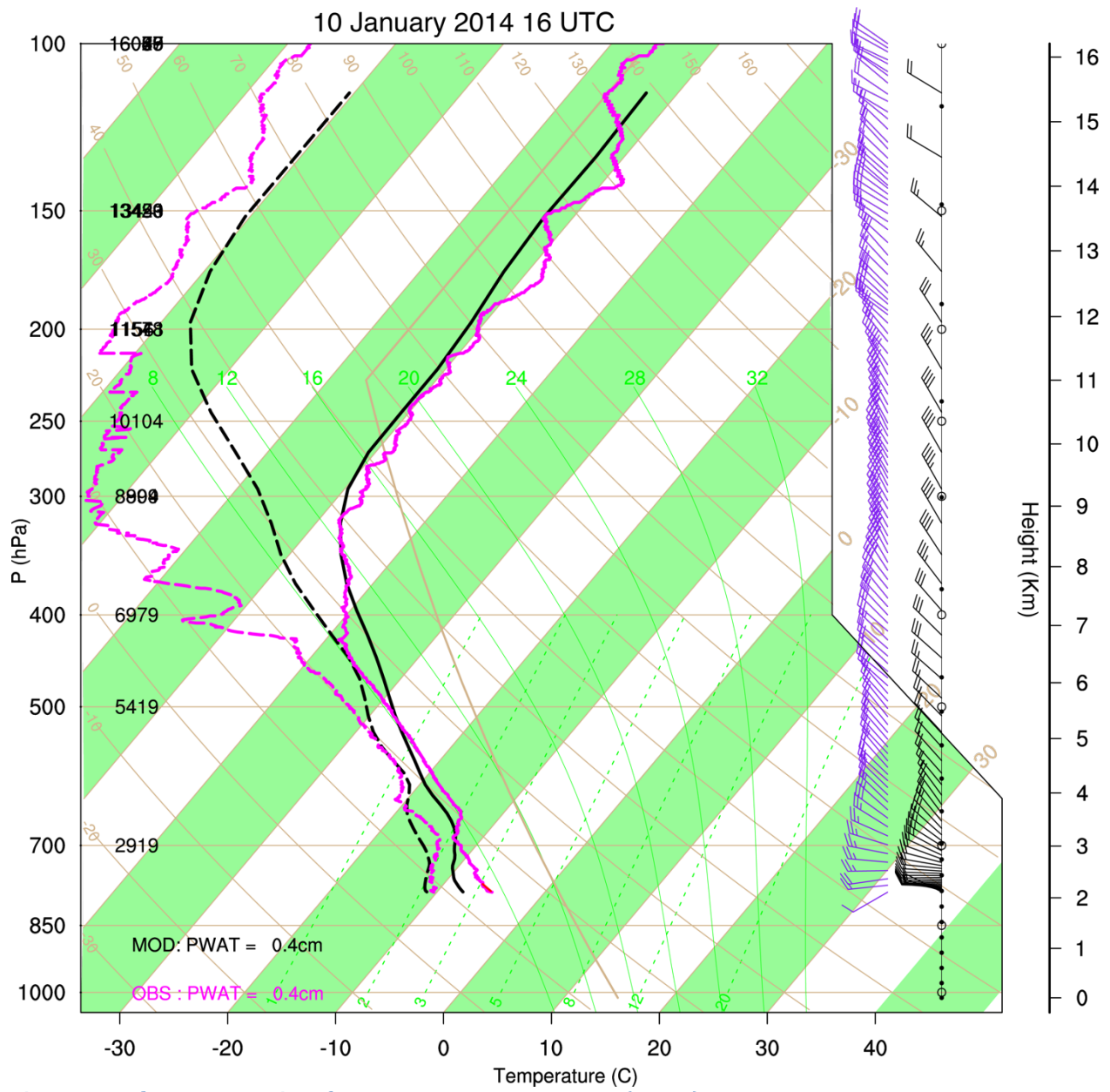


Figure 6.44. Skew-T comparison for 16 UTC on 10 January 2014 (Case 2).

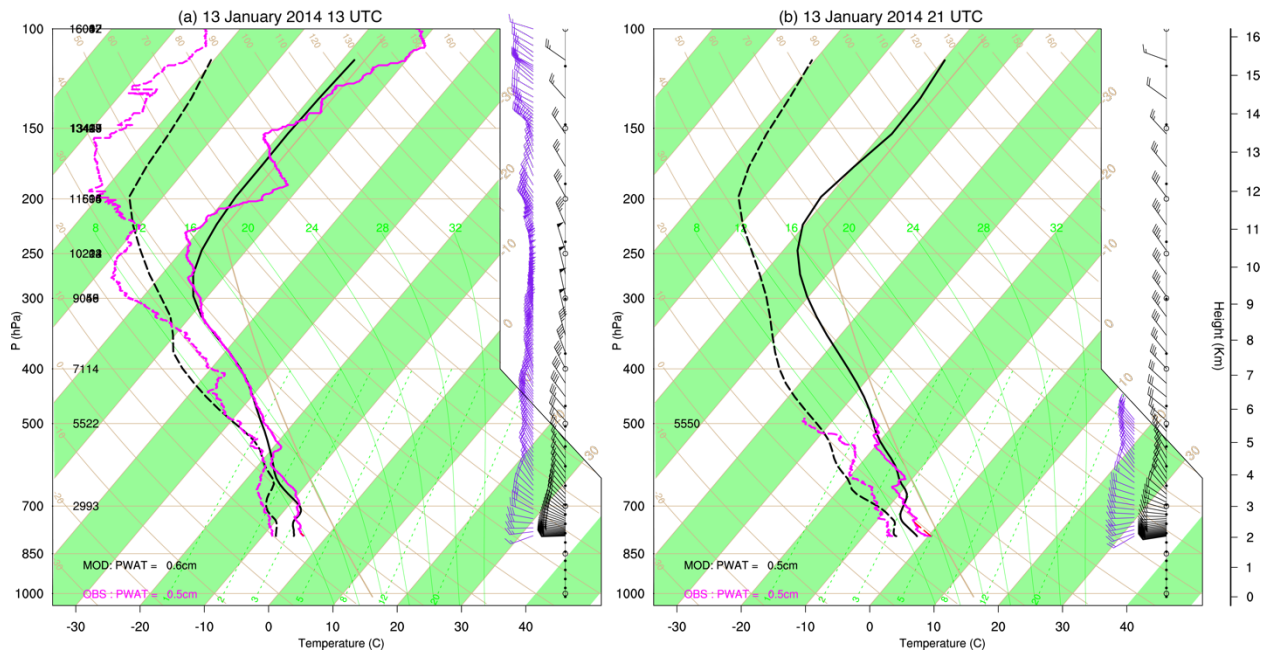


Figure 6.45. Skew-T comparison for (a) 13 UTC and (b) 21 UTC on 13 January 2014 (Case 3).

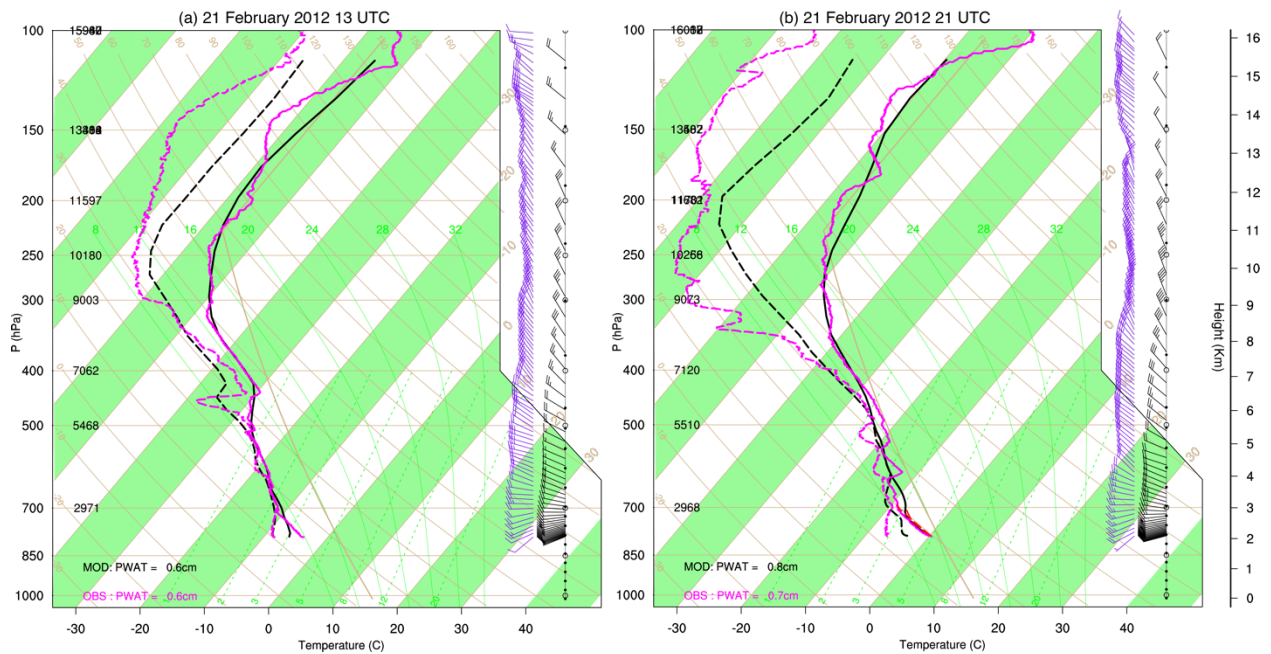


Figure 6.46. Skew-T comparison for (a) 13 UTC and (b) 21 UTC on 21 February 2012 (Case 4).

6.5.2. Comparison between model and observed precipitation

SNOTEL gauge data were analyzed compared with the control model simulations of the four test cases. The SNOTEL gauges in the region are illustrated on the map shown in Figure 4.3. In Case 1, precipitation amounts were generally low (< 5 mm) in both the SNOTEL observations

and modeled output (Figure 6.47). The spatial pattern of precipitation was almost equally distributed between both ranges in the modeled and observed results. In Case 2, the maximum precipitation accumulation was roughly 10 mm at most sites, with a few SNOTEL sites in the Medicine Bow showing higher accumulations not captured by the model. (Figure 6.48). In Case 3, maximum observed precipitation accumulations were as high as 15–20 mm, and there are some areas where the modeled SNOTEL values agree with the observations quite well (Figure 6.49). In this case, more precipitation fell in the Sierra Madre than the Medicine Bow, and the model captured that pattern properly. In Case 4, maximum precipitation amounts of 10–15 mm were observed in the Sierra Madre, with less in the Medicine Bow, and the model simulation reproduced those SNOTEL observations very well (Figure 6.50). Despite some weakness in reproducing SNOTEL observations in the Medicine Bow Range, the overall ability of the model to reproduce the spatial pattern of precipitation in both Ranges is adequate for the purposes of this study.

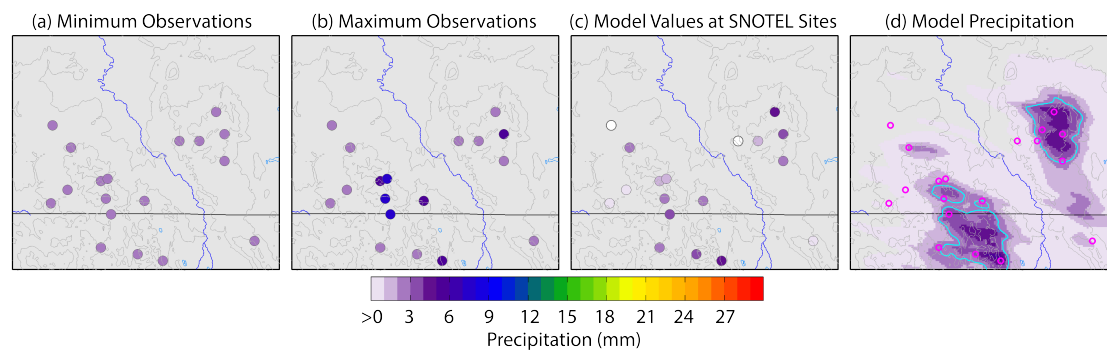


Figure 6.47. Maps of observed precipitation accumulation (mm) over the simulation period for the 23 January 2010 case (Case 1) from SNOTEL sites, with minimum accumulation in (a) and maximum accumulation in (b), compared with model-simulated precipitation accumulation at the SNOTEL sites (c) and the complete simulation of precipitation across the domain (d).

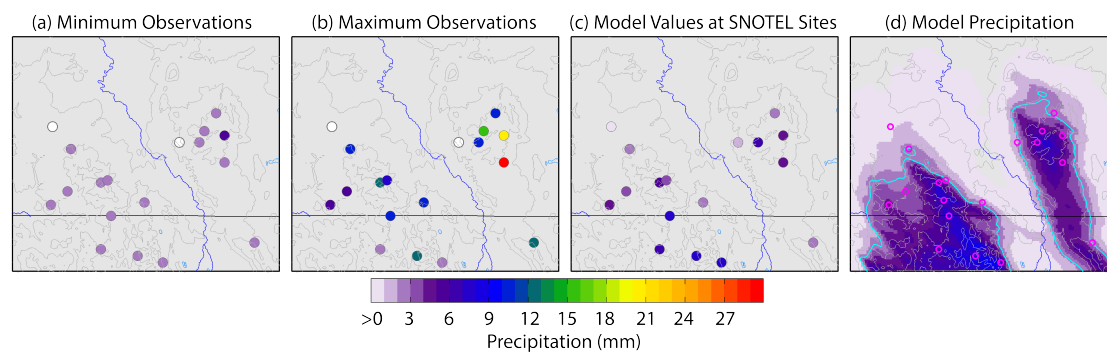


Figure 6.48. Same as Figure 6.47, but for 10 January 2014 (Case 2).

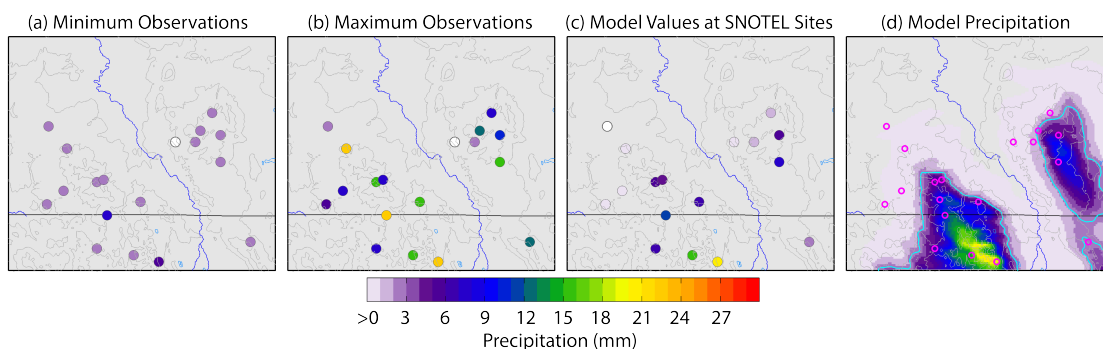


Figure 6.49. Same as Figure 6.47, but for 13 January 2014 (Case 3).

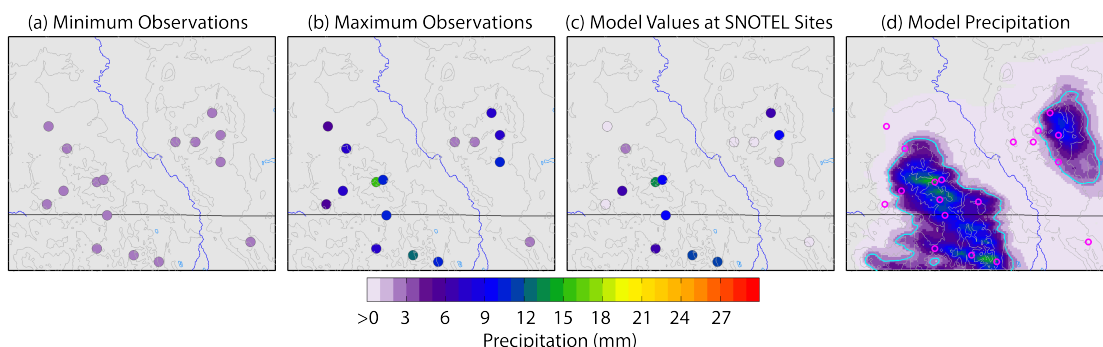


Figure 6.50. Same as Figure 6.47, but for 21 February 2012 (Case 4).

6.6. Summary of Case Study Simulation Results

Four “control” cases were selected from the WWMPP RSE research program to represent a range of suitable seeding conditions found in the Sierra Madre and Medicine Bow Ranges. To investigate the preliminary designs of a ground-based seeding program, these cases were assessed using NCAR’s WRF model configured with the original Thompson microphysics scheme and the original ASPEN. Different groups of generators were simulated to systematically determine the most effective configuration.

WRF simulations of the four “control” cases showed that: (1) the Sierra Madre Range often received more precipitation than the Medicine Bow Range, mainly due to the upwind position of the range; (2) convection can occur in the Sierra Madre Range while stratiform precipitation is simulated in the Medicine Bow Range; (3) SLW was present in both ranges throughout the simulations in all cases, which is a necessary condition for the seeding operation to commence.

WRF simulations of the ground-based seeding cases showed that: (1) seeding depleted SLW in a shallow layer close to the terrain and increased precipitation over the mountain; (2) flow over the Medicine Bow was usually blocked, or forced around the Range due to the steeper slope of the topography, although some of the lower elevation generator groups (i.e., E and F) placed upwind of the Sierra Madre Range were also occasionally blocked; (3) the simulated seeding effect was not as great if the natural cloud efficiently produced precipitation (i.e., Cases 2 and 4); (4) seeding simulations using only the Sierra Madre generators, including the upwind generator groups (i.e., E and F), resulted in the greatest combined simulated seeding effects in both Ranges for most of the cases tested.

One caveat to mention is that the original version of the ASPEN used in this study for the ground-based seeding simulations did not include precipitation scavenging of AgI particles, AgI self-coagulation, and AgI dry deposition processes. Without those AgI-removal processes in place, the particles being transported from the Sierra Madre Range to the Medicine Bow Range and the subsequent seeding impact in the Medicine Bow Range were overestimated. To address this deficiency, two of the ground-based seeding cases were re-run with only the Sierra Madre generators groups and the new ASPEN to evaluate how the additional AgI removal processes affected the cloud and precipitation, especially downwind in the Medicine Bow Range.

The results of ground-based seeding (Sierra Madre all generators) simulations, using only the Sierra Madre generators with the additional AgI removal processes (new ASPEN and microphysics scheme) reduced the AgI concentration and the simulated seeding effect in the Medicine Bow Range by 50% for both cases. However, seeding from Sierra Madre generators only produced similar or greater simulated seeding in the Medicine Bow Range compared with the Medicine Bow generators only seeding scenario (Run3 of the original simulations). In summary, the position of the Sierra Madre Range directly upwind of the Medicine Bow Range may provide an opportunity to strategically place generators in the Sierra Madre (only) that can effectively target both Ranges.

The 13 January 2014 and 21 February 2012 cases (Cases 3 and 4) were selected to investigate airborne-seeding impacts because these two cases exhibited conditions suitable for seeding by aircraft. When conditions are suitable, airborne seeding for a period of about two hours can produce similar simulated seeding effects similar to those from ground-based seeding. According to the model results, airborne-seeding simulations showed impacts over a deeper and broader portion of the atmosphere, and converted the SLW to precipitation more efficiently, than the ground-based seeding scenarios. Airborne seeding conducted upwind of both Ranges produced more of an impact on precipitation in the Sierra Madre than it did in the Medicine Bow Range when compared with the upwind ground-based seeding case. Based on these modeled results, an airborne program is recommended to be considered as an addition to the implementation of a ground-based program.

7. Task 6: Field Surveys: Proposed Ground-Based Generator Locations

Field surveys were conducted within the Ranges to identify potential ground-based generator locations to be used in development of the project design and the modeling exercise (Sections 5 and 6). This Section describes the selection of the potential sites, and the results of the field surveys. There were 19 ground-based generator locations previously surveyed and permitted for use during the WWMPP that were not revisited in the field for this study. During the field surveys conducted for this project, 27 new potential sites were visited and considered for inclusion in the preliminary project design.

7.1. Proposed Ground-Based Generator Locations: Siting Areas

The research and modeling conducted as part of the WWMPP identified numerous suitable ground-based generator sites that could be considered as part of the preliminary project design. The WWMPP research showed that, within each mountain range, there were multiple areas where the placement of additional generators would be best suited for increasing snowpack in the target areas. Figure 7.1 shows four areas within the Sierra Madre Range and five areas within the Medicine Bow Range considered for additional generator deployment. Topographic maps and on-line tools (e.g., Google Earth) were used to identify potential ground-based generator sites within these areas. Generator spacing, ease of installation and servicing, land ownership, access, elevation, and exposure were all considered.

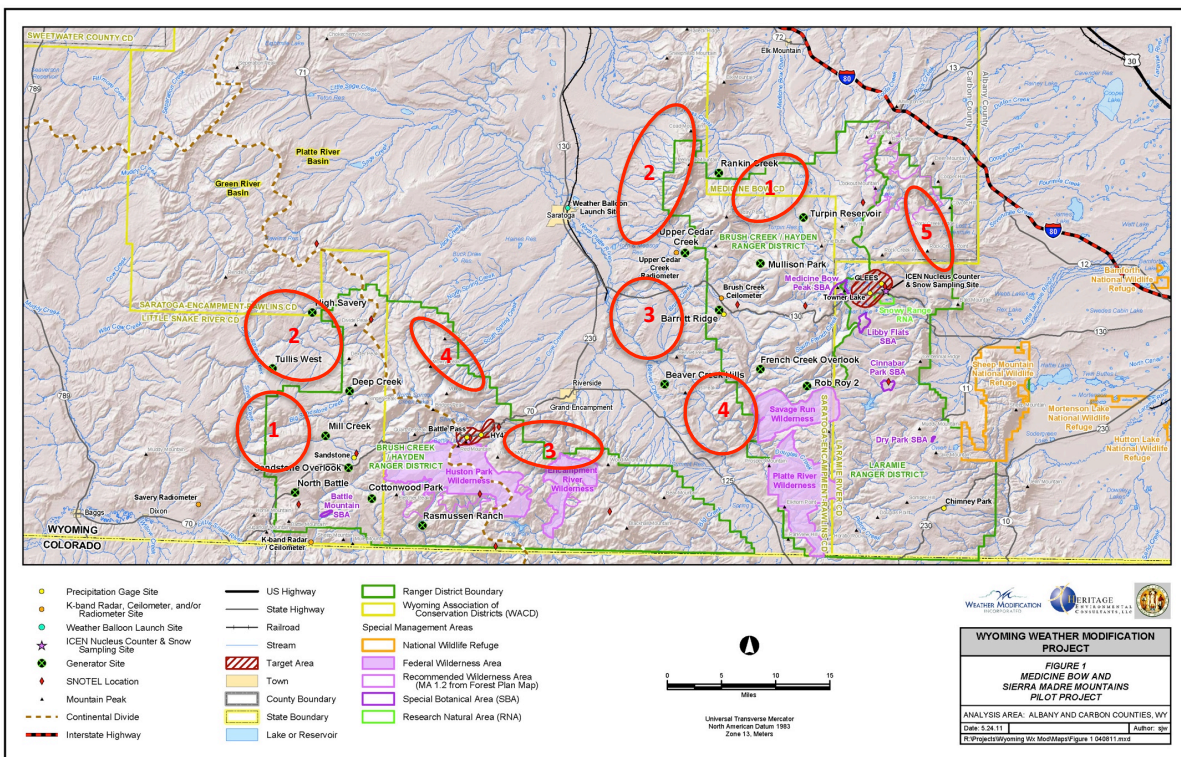


Figure 7.1. Siting areas for placement of additional proposed ground-based generators.

7.1.1. Proposed Ground-Based Generator Locations: Field Surveys

Staff from HEC and WMI conducted the field surveys in the Medicine Bow and Sierra Madre Ranges in September 2015. The goal was to assess the proposed generator locations for access issues (both for installation and maintenance during operations), exposure to winds that would loft the seeding plume into clouds and over the target, and permitting constraints.

During the field surveys, 27 potential generator sites located on federal and private lands within the Medicine Bow and Sierra Madre Ranges were evaluated:

- 1) 18 sites on USFS lands
- 2) 9 sites on private lands

The generator locations that were part of the 2015 field survey are shown in Figure 7.2. Proposed locations, land ownership, access descriptions and ratings, and brief descriptions of the sites are included in Table 7.1. Appendix A presents photographs of the sites. These sites all have a good potential for effective seeding.

Medicine Bow Range

Within the Medicine Bow Range, 14 potential generator sites located on federal and private lands were evaluated:

- 1) 9 sites on USFS lands
- 2) 5 sites on private lands

Sierra Madre Range

Within the Sierra Madre Range, 13 potential generator sites located on federal and private lands were evaluated:

- 1) 9 sites on USFS lands
- 2) 4 sites on private lands

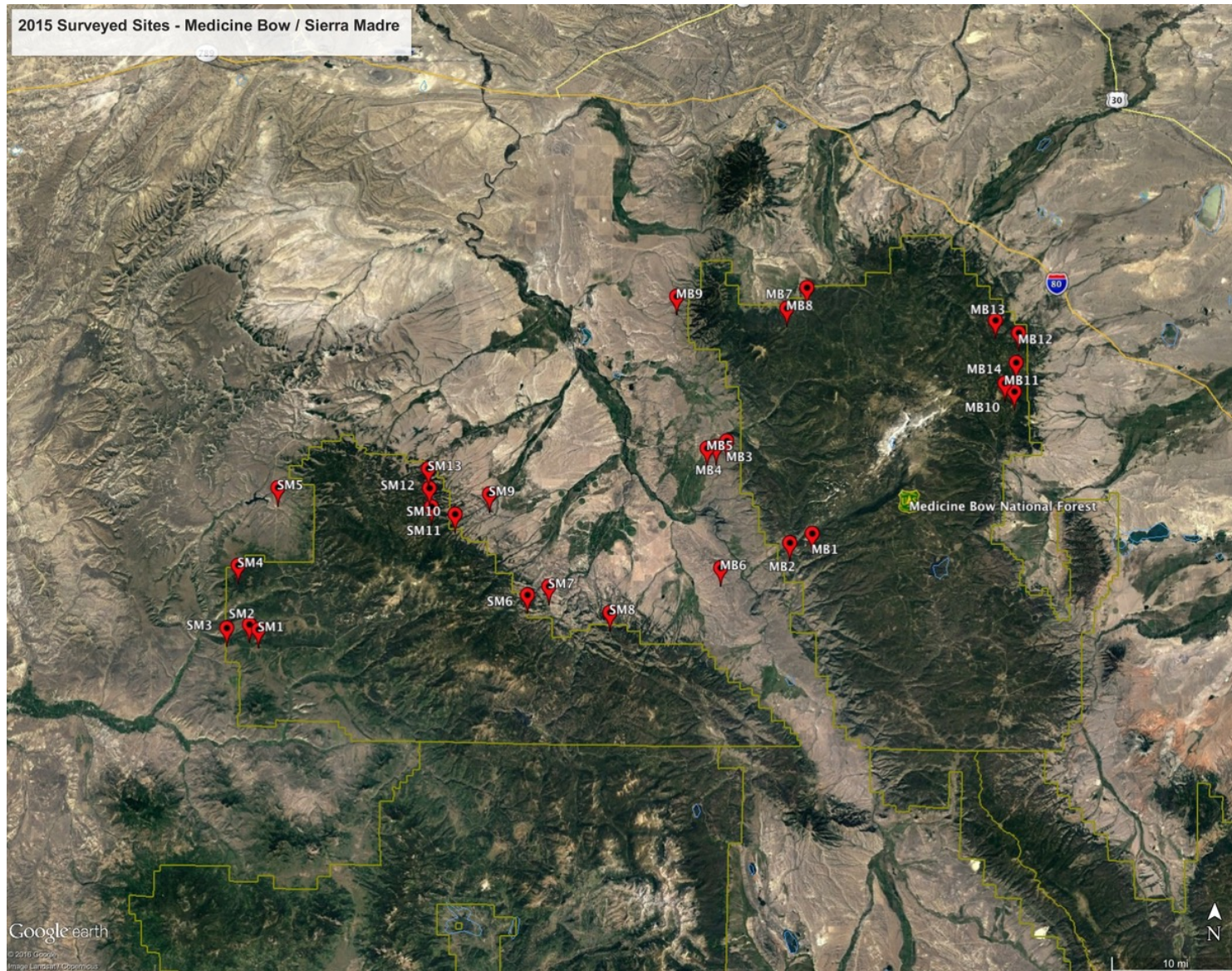


Figure 7.2. Proposed ground-based generator sites selected and visited in the field.

Table 7.1. Description of Proposed Ground-Based Generator Locations

<u>Survey Site ID</u>	<u>Site Name</u>	<u>Latitude</u>	<u>Longitude</u>	<u>T,R,S, ¼ ¼¹</u>	<u>Elevation (feet)</u>	<u>Ownership</u>	<u>Access Rating²</u>	<u>Notes</u>
Medicine Bow Range								
MB1	Sourdough Creek	41.222665	-106.441846	T15N R81W Sec 36 SENW	8,660	USFS	Class 1	Forest Road 500
MB2	Upper Bear Gulch	41.211881	-106.475211	T14N R81W Sec 03 SENE	8,223	USFS	Class 1	Forest Road 500 to BLM Road 3424 (Upper North Platte Road)
MB3	Francis Draw	41.327203	-106.571299	T16N R82W Sec 26 SENE	8,211	Private	Class 2	Brush Creek Ranch
MB4	Little Beaver Creek	41.321089	-106.587199	T16N R82W Sec 26 NWSW	7,960	Private	Class 1	Brush Creek Ranch
MB5	Brush Creek	41.318879	-106.600815	T16N R82W Sec 27 SESW	7,650	Private	Class 1	Brush Creek Ranch
MB6	Big Spring West	41.182793	-106.579272	T14N R82W Sec 14 SENW	7,870	Private	Class 3	Brush Creek Ranch
MB7	East Pass Creek	41.502008	-106.451227	T18N R81W Sec 25 SENW	8,540	USFS	Class 1	Forest Road 261 to 2-track up hill
MB8	Kennaday Peak	41.478211	-106.481662	T17N R81W Sec 03 SWNE	8,740	USFS	Class 1	Forest Road 261; clearcut.
MB9	Goetz Creek	41.491407	-106.648564	T18N R82W Sec 32 SWNW	7,550	Private	Class 1	Adjacent to Penock Mountain Wildlife Management Area

MB10	South Fork Mill Creek	41.384373	-106.137299	T16N R78W Sec 03 SENE	9,791	USFS	Class 1	Forest Road 329 near fire ring loop pullout; old clearcut
MB11	Middle Fork Mill Creek	41.393839	-106.152316	T16N R78W Sec 03 NWNW	9,925	USFS	Class 1	Forest Road 329 near fire ring loop pullout; old clearcut
MB12	Lost Lake	41.451147	-106.130654	T17N R78W Sec 14 NWNW	9,370	USFS	Class 1	Forest Road 329 near fire ring loop pullout; old clearcut
MB13	Cooper Creek	41.464983	-106.166561	T17N R78W Sec 09 NENW	9,900	USFS	Class 2	Forest Road 327; large bladed pullout
MB14	Rock Creek Point	41.417223	-106.13486	T17N R78W Sec 26 SWNW	9,700	USFS	Class 1	Forest Road 329; fire pit pullout; old clearcut
Sierra Madre Range								
SM1	Stemp Spring	41.107269	-107.276896	T13N R88W Sec 10 SWSE	8,100	USFS	Class 1	Forest Road 852
SM2	Sandstone Plateau	41.112835	-107.290831	T13N R88W Sec 09 SENE	7,956	USFS	Class 1	Forest Road 870 at 1C
SM3	West Sandstone Plateau	41.108371	-107.325516	T13N R88W Sec 08 SWSW	7,838	USFS	Class 1	Forest Road 852
SM4	Green Ridge	41.180101	-107.308628	T14N R88W Sec 17 SWSE	8,251	USFS	Class 2	Forest Road 877
SM5	Dirtyman Fork	41.269122	-107.250566	T15N R88W Sec 14 NESW	7,540	Private	Class 1	Sage Creek Road; Peter Hansen Ranch Trustees
SM6	Cooper Creek	41.150657	-106.870655	T14N R84W Sec 29 NESW	8,745	Private	Class 1	Forest Road 405 1D

SM7	Cushman Creek	41.160553	-106.838545	T14N R84W Sec 21 SESE	8,260	Private	Class 1	Carbon County Road 353
SM8	Purgatory Plateau	41.131664	-106.745975	T14N R83W Sec 32 SWSE	9,010	USFS	Class 2	Forest Road 409 1E; take Forest Road 409 1A to 1E; excellent access.
SM9	Heather Hill	41.264734	-106.929657	T15N R85W Sec 14 SWSW	8,010	Private	Class 1	Carbon County Road
SM10	Heather Creek	41.241571	-106.980915	T15N R85W Sec 29 SENW	8,680	USFS	Class 1	Forest Road 440 1A
SM11	Mowry Peak	41.249748	-107.016362	T15N R86W Sec 25 NWNW	9,485	USFS	Class 1	Forest Road 443 to unnamed camp road
SM12	Sharp Hill	41.270826	-107.019902	T15N R86W Sec 13 SENW	9,275	USFS	Class 1	Forest Road 443
SM13	Cherokee Creek	41.292766	-107.02195	T15N R86W Sec 12 NENW	8,860	USFS	Class 1	Forest Road 452

¹ Township, Range, Section, quarter

² Class 1 – access for installation/maintenance easy, propane truck accessible;

Class 2 – access for installation/maintenance relatively easy, may be short lengths of more difficult terrain or short distance with no existing access.

Class 3 – access for installation is more difficult; long distance and short sections rough roads; slow moving; winter access may be long distance
Class 4 – access for installation is more difficult; long distance and mostly rough roads; some tight turns; winter access may be long distance
Class 5 – extremely difficult; very rough and slow roads, more tight turns, steep slopes; winter access is a long snow mobile trip.

7.2. Proposed Viable Ground-based Generator Locations

As a result of the initial modeling simulations and the field survey, a total of 35 viable ground-based generator sites (Figure 7.3 and Figure 7.4) were identified for possible use in the preliminary project design. These proposed generator sites are organized into seven generator “groups” as described in Section 5: three groups in the Medicine Bow Range (Groups A, B, and C) and four groups in the Sierra Madre Range (Groups A, B, C, and D) (Table 7.2).

A total of 35 remotely controlled generator sites located on federal (USFS), state, and private lands are recommended with 15 in the Medicine Bow Range and 20 in the Sierra Madre Range:

- 1) 23 sites on USFS lands
- 2) 5 sites on state lands
- 3) 7 sites on private lands

7.2.1. Medicine Bow Range

The 15 remotely controlled generator sites located on federal, state, and private lands recommended within the Medicine Bow Range breakdown as follows:

- 1) 9 sites on USFS lands
- 2) 2 sites on state lands
- 3) 4 sites on private lands

Of these 15 sites, 8 were permitted and used in the WWMPP; 1 site was permitted but not used in the WWMPP. The remaining 6 sites are new and were surveyed in September 2015. All of the sites would allow access for installation, operations and maintenance purposes. (Table 7.2).

7.2.2. Sierra Madre Range

The 20 remotely controlled generator sites located on federal, state, and private lands recommended within the Sierra Madre Range breakdown as follows:

- 1) 14 sites on USFS lands
- 2) 3 sites on state lands
- 3) 3 sites on private lands

Of these 20 sites, 8 were permitted and used in the WWMPP; 1 site was permitted but not used in the WWMPP. Of the remaining 11 sites, 7 are new and were surveyed in September 2015. However, 4 of the new sites were added to the preliminary project design after the actual field surveys and therefore were evaluated using Google Earth and maps. All of the sites would allow access for installation, operations, and maintenance purposes (Table 7.2).

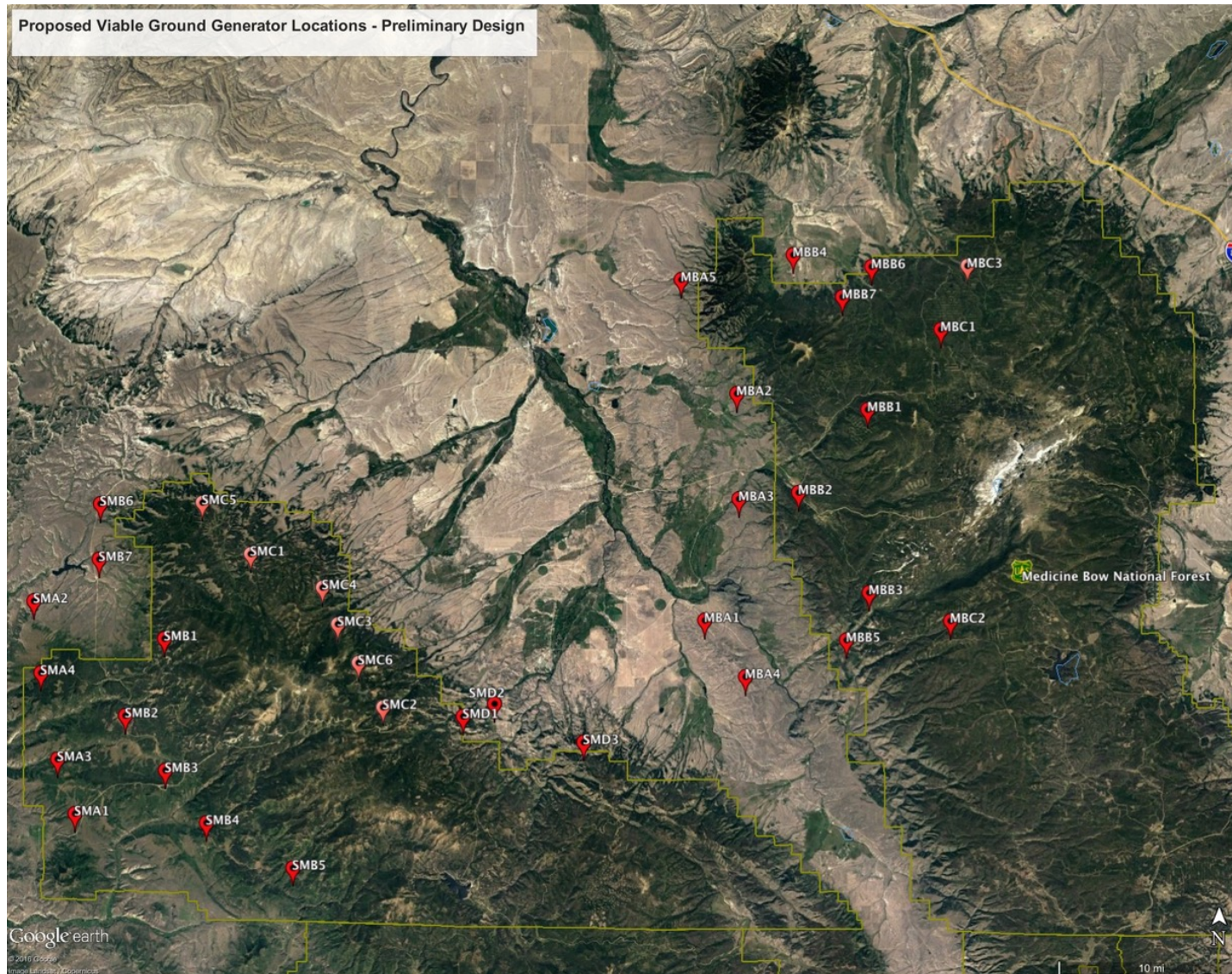


Figure 7.3. The final 35 proposed viable ground-based generator locations for the Preliminary Project Design. Consists of Sierra Madre Groups A-D and Medicine Bow Groups A-C, also illustrated in Figure 5.6.

Table 7.2. Description of Proposed Generator Locations – Preliminary Project Design

<u>Site ID</u>	<u>Site Name</u>	<u>Latitude</u>	<u>Longitude</u>	<u>T,R,S, ¼ ¼¹</u>	<u>Elevation (feet)</u>	<u>Ownership</u>	<u>Access Rating²</u>	<u>Notes</u>
Medicine Bow Range								
Group A								
MBA1	Beaver Creek Hills	41.226000	-106.621400	T15N R82W Sec 33 SENW	7,757	State	Class 2	Site used in WWMPP
MBA2	Upper Cedar Creek	41.403200	-106.593250	T17N R82W Sec 34 SENE	7,700	Private	Class 1	Site used in WWMPP
MBA3	Little Beaver Creek	41.321089	-106.587199	T16N R82W Sec 26 NWSW	7,960	Private	Class 1	New site for preliminary project design
MBA4	Big Spring West	41.182793	-106.579272	T14N R82W Sec 14 SENW	7,870	Private	Class 3	New site for preliminary project design
MBA5	Goetz Creek	41.491407	-106.648564	T18N R82W Sec 32 SWNW	7,550	Private	Class 1	New site for preliminary project design
Group B								
MBB1	Mullison Park	41.390800	-106.455300	T16N R81W Sec 1 NWNW	9,546	USFS	Class 2	Site used in WWMPP
MBB2	Barrett Ridge	41.326300	-106.526200	T16N R81W Sec 29 SENW	9,029	USFS	Class 2	Site used in WWMPP
MBB3	French Creek Overlook	41.248900	-106.452200	T15N R81W Sec 24 NWSW	8,857	USFS	Class 2	Site used in WWMPP
MBB4	Rankin Creek	41.511100	-106.532500	T18N R81W Sec 20 SWSW	7,980	State	Class 2	Site used in WWMPP
MBB5	Upper Bear Gulch	41.211881	-106.475211	T14N R81W Sec 03 SENE	8,223	USFS	Class 1	New site for preliminary project design

MBB6	East Pass Creek	41.502008	-106.451227	T18N R81W Sec 25 SENW	8,540	USFS	Class 1	New site for preliminary project design
MBB7	Kennaday Peak	41.478211	-106.481662	T17N R81W Sec 03 SWNE	8,740	USFS	Class 1	New site for preliminary project design
Group C								
MBC1	Turpin Reservoir	41.453052	-106.380240	T17N R80W Sec 10 SWSW	9,665	USFS	Class 2	Site used in WWMPP
MBC2	Rob Roy2	41.227554	-106.369120	T15N R80W Sec 34 SWNE	9,720	USFS	Class 1	Site used in WWMPP
MBC3	Willow Park	41.502800	-106.352200	T18N R80W Sec 26 NWSE	8,835	USFS	Class 2	Site permitted but not used in WWMPP
Sierra Madre Range								
Group A								
SMA1	North Battle	41.070410	-107.271470	T13N R88W Sec 27 SENE	7,594	State	Class 1	Site used in WWMPP
SMA2	Tullis West	41.235820	-107.317620	T15N R88W Sec 29 SWSE	7,890	State	Class 1	Site used in WWMPP
SMA3	Sandstone Plateau	41.112835	-107.290831	T13N R88W Sec 09 SENE	7,956	USFS	Class 1	New site for preliminary project design
SMA4	Green Ridge	41.180101	-107.308628	T14N R88W Sec 17 SESE	8,251	USFS	Class 2	New site for preliminary project design
Group B								
SMB1	Deep Creek	41.208300	-107.180300	T14N R87W Sec 4 SESE	8565	USFS	Class 2	Site used in WWMPP
SMB2	Mill Creek West	41.147700	-107.220700	T14N R87W Sec 31 NWNE	7990	USFS	Class 2	Site used in WWMPP
SMB3	Sandstone Overlook	41.105500	-107.178800	T13N R87W Sec 9 SESE	8369	USFS	Class 1	Site used in WWMPP

SMB4	Cottonwood Park	41.064900	-107.135600	T13N R87W Sec 25 NWSW	7977	USFS	Class 3	Site used in WWMPP
SMB5	Rasmussen Ranch	41.030700	-107.045600	T12N R86W Sec 10 NWNE	8160	USFS	Class 4	Site used in WWMPP
SMB6	High Savery	41.312490	-107.249220	T16N R88W Sec 36 NWSW	7843	State	Class 1	Site used in WWMPP
SMB7	Dirtyman Fork	41.269122	-107.250566	T15N R88W Sec 14 NESW	7,540	Private	Class 1	New site for preliminary project design
Group C								
SMC1	Jack Creek	41.275000	-107.091700	T15N R86W Sec 17 SWNE	8840	USFS	Class 2	Used prior to program start (2006-2007)
SMC2	Hidden Treasure Gulch	41.157694	-106.952606	T14N R85W Sec 28 NWNE	9505	USFS	Class 1	Google earth survey site
SMC3	Heather Creek	41.221617	-107.000006	T15N R85W Sec 31 NESW	9530	USFS	Class 3	Google earth survey site
SMC4	Chippewa Creek	41.249748	-107.016362	T15N R86W Sec 24 SWSW	9485	USFS	Class 3	New site for preliminary project design
SMC5	McLain Park	41.314406	-107.142670	T16N R87W Sec 35 NWSE	8669	USFS	Class 2	Google earth survey site
SMC6	Teddy Creek	41.191953	-106.978222	T14N R85W Sec 8 SESW	9792	USFS	Class 3	Google earth survey site
Group D								
SMD1	Cooper Creek	41.150657	-106.870655	T14N R84W Sec 29 NESW	8,745	Private	Class 1	New site for preliminary project design
SMD2	Cushman Creek	41.160553	-106.838545	T14N R84W Sec 21 SESE	8,260	Private	Class 1	New site for preliminary project design
SMD3	Purgatory Plateau	41.131664	-106.745975	T14N R83W Sec 32 SWSE	9,010	USFS	Class 2	New site for preliminary project design

¹ Township, Range, Section, quarter

² Class 1 – access for installation/maintenance easy, propane truck accessible;

Class 2 – access for installation/maintenance relatively easy, may be short lengths of more difficult terrain or short distance with no existing access.

Class 3 – access for installation is more difficult; long distance and short sections rough roads; slow moving; winter access may be long distance
Class 4 – access for installation is more difficult; long distance and mostly rough roads; some tight turns; winter access may be long distance
Class 5 – extremely difficult; very rough and slow roads, more tight turns, steep slopes; winter access is a long snow mobile trip.

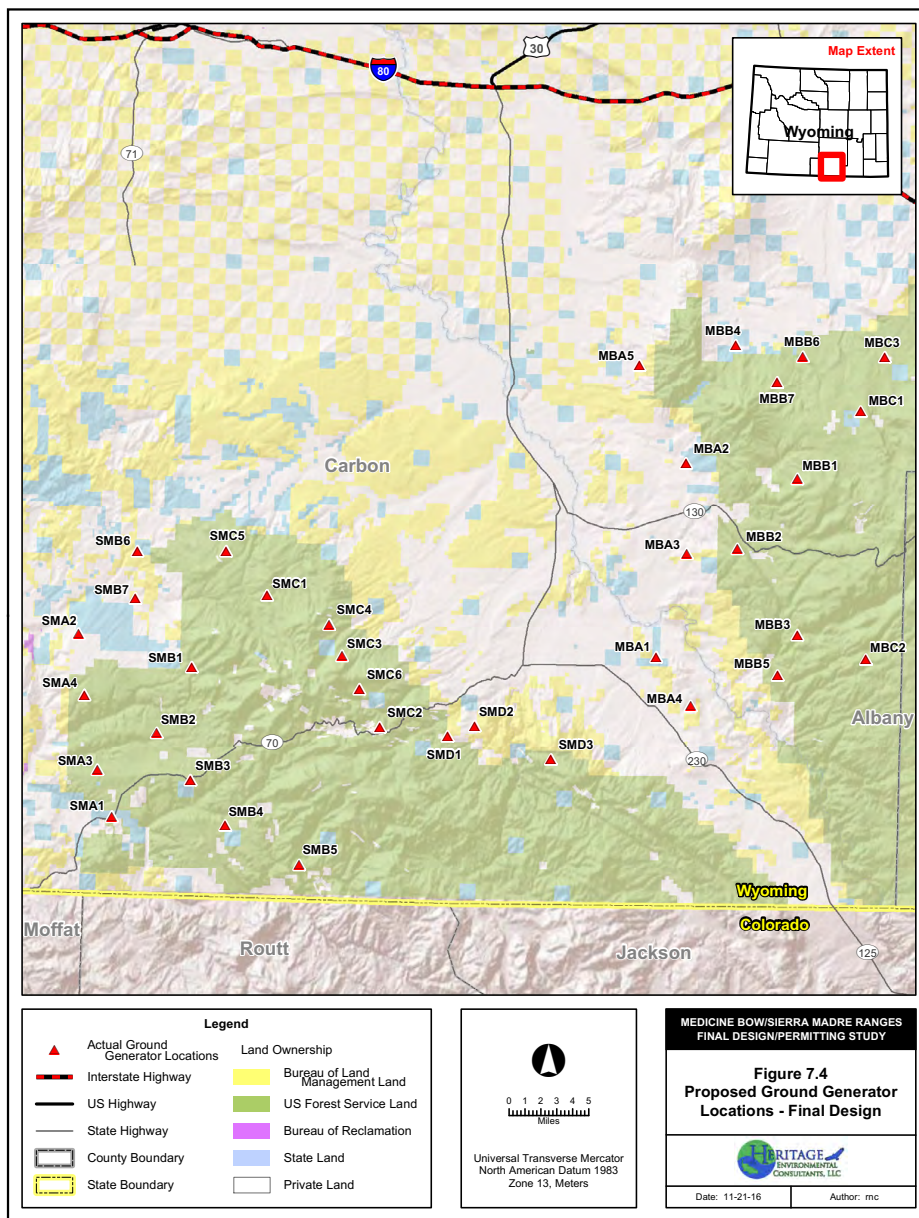


Figure 7.4. Land ownership map with proposed ground-based generator sites.

8. Task 7: Access/Easements & Environmental Permitting/Reporting

Effectively targeting clouds with seeding material is probably the most critical aspect affecting the outcome of cloud-seeding programs. For the Medicine Bow and Sierra Madre Ranges, understanding the climatology of winds during seedable conditions (Section 4), aided by numerical modeling of trajectories, is necessary to determine the general placement of cloud-seeding generators to reach the desired target area. Once the generator sites have been determined, logistical issues such as site access and land ownership become important. Accessibility of a potential generator site is necessary during both the summer (installation and pre-season preparatory work), and winter months (operations and maintenance). Two limiting factors for a site are sufficient access to deliver a large propane tank and the ability to fill propane tanks during the summer. If this is not feasible, smaller tanks may be used, but this requires more deliveries to the site, sometimes during the winter months when access to remote sites generally requires a tracked vehicle or a snow machine.

Land ownership dictates the types of permissions needed for permit acquisition, site access, and use. Generators located on public lands often require additional permitting and periodic reporting. Section 7 described the selection process of choosing an array of potential ground-based generator sites. Land ownership of the proposed ground-based generator locations for the preliminary project design is depicted in Figure 7.4. Although there are some tracts of private land to the west of the Medicine Bow and Sierra Madre Ranges that may be suitable for placing generators, the majority of the areas with the best siting opportunities are dominated by public lands, primarily federal lands administered by the USFS. State lands have been identified as possible generator locations, but are sparsely scattered throughout the area. The possibility of moving some of the generators in the Medicine Bow National Forest (MBNF) to small private inholdings in the MBNF may be feasible. Brief descriptions of the requirements for locating generators on private and public lands are described below.

8.1. Private Lands

The first step in siting a generator on private land is to contact the Landowner and ask for permission to do so. If the landowner is willing to allow the placement of a generator on their property, a lease agreement is established between the property owner and the operating entity, typically in the form of a Memorandum of Understanding (MOU). On some occasions, a fee is negotiated as part of the lease agreement and can vary depending upon the willingness of the property owner and the need to place a generator at that specific location. There is a substantial amount of private land near the Medicine Bow and Sierra Madre Ranges that may be suitable for siting ground-based generators; however, siting generators on private lands in the target area would require additional evaluation. In some cases, the generators may be too far away, or too low in elevation to effectively target the Ranges.

Additionally, some counties require a permit for the placement of a cloud-seeding generator on private lands. For this project, generators could potentially be located on private lands within Carbon County; however, the County does not require permits for ground-based generators.

8.2. Public Lands

The majority of the proposed generator locations are located on federally owned lands for two reasons: 1) because the area is dominated by federally owned lands in and near the target area and 2) because many of the proposed generator locations were used in the WWMPP and it is logical to use the same sites that were previously permitted for use in an operational weather modification program. The most effective generator locations will include lands under public ownership, whether it be a federal or state entity.

If a location is under federal ownership, such as the USFS or the Bureau of Land Management (BLM), a Special Use Permit (SUP) will be required for placement of the generator. As part of the permitting process, a National Environmental Policy Act (NEPA) review will be required. This process could result in a Categorical Exclusion (Cat Ex), an Environmental Assessment (EA), or an Environmental Impact Statement (EIS), as determined by the federal entity and the final project design. All proposed ground-based generators that are located on USFS administered lands (i.e., the MBNF) are administered by the Brush Creek Hayden Ranger District.

Placement of a generator on state or local government lands requires the approval of that entity and a lease agreement. For placement on Wyoming State lands, a Temporary Use Permit is required from the Office of State Lands and Investments. This process involves a site survey prior to submitting an application package. The application package includes comments from the current lessee, and payment to the State. For example, each generator permit in the Wind River Range costs \$100 annually. These permits are valid for 5 years. Renewals would be required for longer-term operations (e.g., an operational program longer than 5 years).

8.2.1. Medicine Bow National Forest Service Application

The WWDO submitted a Special Use Permit (SUP) application (SF299) to the MBNF on 22 February 2016. The application requested USFS approval to place up to 23 ground-based generators and six monitoring equipment sites on National Forest administered lands. The USFS replied by letter to the WWDO on 9 August 2016 explaining that the proposal failed to meet the minimum requirements of the initial screening criteria and would not be considered further (Appendix B).

The WWDO resubmitted the application with supplemental information (detailed project description, etc.) on 22 December 2016. This amended application requested a SUP for the period of 15 years, down from the original 30 years originally requested. The MBNF responded with a letter to the WWDO on 28 February 2017 initially accepting the SUP application and notifying the WWDO that USFS personnel would be in contact to discuss the application approval procedures (Appendix B).

8.3. Weather Modification Program Permitting

There have been no changes to the general permitting and reporting requirements for conducting cloud-seeding programs in the last 10 years. There are two entities that require some level of permitting and reporting: the State of Wyoming and the U.S. Department of Commerce through NOAA.

8.3.1. State of Wyoming Permit Requirements

Wyoming Statutes 9-1-905 to 9-1-907 contain legislative declarations concerning weather modification, the definition of weather modification, and weather modification permit requirements. These regulations are administered by the Wyoming State Engineer's Office (WSEO). The permit process through the WSEO requires an application outlining weather modification credentials, financial assurance, references, generator locations, target areas, and proposed procedures. The WSEO also requires monthly reports be submitted during the operational season.

8.3.2. Wyoming Game and Fish Department

The Governor of Wyoming issued the Sage Grouse Executive Order in 2008, establishing Core Population Areas for sage grouse across the state to avoid federal listing of the species as threatened or endangered. Many types of development within these Core Population Areas are prohibited or limited. Core Population Areas were established based on habitat, not land ownership; therefore, they affect federal, state, and private lands. There are Core Population Areas located west and north of the Medicine Bow Range, and east, north, and west of the Sierra Madre Range.

The Wyoming Game and Fish Department (WGFD) requested to review the locations of all 26 ground-based generators associated with the WWMPP, and it is anticipated that they would review the proposed generator locations for the Medicine Bow and Sierra Madre Ranges. If any are located in the Core Population Areas, an analysis on potential impacts to the species would have to be conducted and potential mitigation measures may be required.

8.3.3. National Oceanic and Atmospheric Administration Reporting

Public Law 92-205 requires all non-federally sponsored attempts to modify the weather be reported to the Secretary of Commerce. The process involves the submittal of Initial, Interim, and Final reports covering weather modification activities for individual target areas. An Initial report is required each year cloud seeding is planned, and at least 10 days prior to the start of the activity.

A Final report must be submitted within 45 days after the completion of the weather modification activity. The information required in the Interim and Final reports include:

- 1) number of weather modification days each month;
- 2) number of modification days for purposes of increasing rain or snow, reduction of hail, fog or other;
- 3) hours of apparatus operation (airborne or ground); and
- 4) type and amount of cloud seeding agent used.

Public Law 92-205 is a reporting requirement, and establishes no regulatory authority, whereas the State of Wyoming permit requirements provide for non-compliance penalties.

9. Task 8: Establishment of Operational Criteria

Criteria for operational winter orographic cloud-seeding programs have been developed by the American Society of Civil Engineers (ASCE 2004 and 2016), and by the Weather Modification Association (WMA 2014). This study examines the potential for effective glaciogenic seeding through the introduction of IN from ground-based and airborne means. The utilization of LP to induce homogeneous nucleation, is not considered an effective means of seeding agent dispersion for this project because the flow downwind of the seeding site may often—though temporarily—warm the LP plume above 0 °C, resulting in evaporation of the cloud. For this reason, AgI was determined to be the most suitable for the Medicine Bow and Sierra Madre Mountains.

9.1. Information Sources

Among the most critical data for establishing seeding thresholds are upper air temperatures and winds, and the existence of SLW relative to the project target area. The more accurate this information, the better the seeding decisions will be. Toward this objective, two instruments can play vital roles. In addition to these, or in the instance these instruments are not available, high-resolution tailored forecast models can also provide valuable guidance for making seeding decisions.

9.1.1. Soundings

On-demand project soundings would provide real-time vertical atmospheric temperature and wind profiles, as well as the Froude number (e.g., Pokharel et al. 2014a), a stability index that allows prediction of whether environmental winds will flow up and over the mountains or around them. Using project rawinsondes will provide solid guidance for both wind flow and seeding temperatures. The nearest soundings available are routinely conducted by the National Weather Service (NWS) near Riverton, Wyoming (160 miles to the northwest of the project area), Denver, Colorado (140 miles to the southeast), and Grand Junction, Colorado (180 miles to the southwest). All of these locations are too far removed to accurately reflect current atmospheric conditions in the project area; therefore, localized soundings would be necessary to verify seeding temperature criteria.

9.1.2. Radiometer

Microwave radiometers sited with an unobstructed view of the Medicine Bow and Sierra Madre Ranges would provide real-time cloud LWC over the range, critical for successful seeding. In the absence of real-time liquid cloud water data, its presence must be inferred by the presence of cloud mass over the range and/or prognostic numerical model output. One such option is the aircraft icing product from the NOAA Aviation Weather Center (AWC) available at <https://www.aviationweather.gov/icing/fip>.

The Medicine Bow and Sierra Madre Ranges are considered a “dual barrier” because the Ranges are closely located, and therefore frequently impacted by the same passing storm systems. This means the Sierra Madre Range is often being upwind of the Medicine Bow Range during

seedable conditions. The optimal use for radiometers, as detectors of liquid cloud water, is to site the equipment with a view of the clouds on the predominantly upwind side of the range. The western flanks of both ranges are the predominantly upwind sides; therefore, a single radiometer cannot adequately cover both ranges. If a single radiometer were sited between the two ranges, the view of the Sierra Madre Range would be of the downwind slope, and therefore not useful. This issue might be solved by deploying two radiometers, each with an upwind view of passing storm systems.

9.1.3. Other Sources

Additional real-time information available via the internet, useful for evaluating potential seeding conditions includes the following:

- NOAA and NWS data:
 - surface observations,
 - prognostic numerical models, included gridded data,
 - satellite imagery: visible, infrared, and multi-spectral;
- NRCS SNOTEL sites (can provide temperature data near the 700-hPa level), typically with a 1–2 hour latency;
- select real-time webcams near the ranges (during daylight, for cloud cover);
- University of Utah Mesowest mesonet data displays of surface winds and temperatures.

9.2. Ground-Based Seeding with Ice Nuclei

When IN are generated, either by the combustion of seeding solution or pyrotechnic, the nuclei remain in the atmosphere until they (a) nucleate ice which grows into precipitation, or (b) they are scavenged by precipitation. With time, other processes may remove them more slowly. Once created, the IN plume can travel considerable distances downwind before becoming so dilute that it is no longer detectable. If ground-based ice nucleus generators (INGs) are deployed, an array of remote-controlled INGAs would be used to seed clouds upwind of the targeted portions of the range, when flow regimes (winds) and temperature profiles are suitable. The proposed ground-based generator locations are shown in Figure 7.3. Manually operated generators would not be feasible for the most part because the proposed sites are all well removed from populated areas, and many are at higher elevations generally not readily accessible during winter storms. Therefore, all proposed ground-based generators deployed should be remotely controlled.

In any given seeding event, activating the generators would be determined by the prevailing wind speed and direction. The number of generators used will depend upon the extent of the seedable conditions over the target area. The AgI-based seeding agent would be released at a rate of approximately 25 g h^{-1} from each active generator.

Seeding would be guided by an on-site meteorologist, aided by weather observations, real-time microwave radiometer observations of cloud liquid water, and prognostic numerical models.

The recommended seeding criteria for ground-based IN seeding are:

1. The temperature at the 700-hPa pressure level ($\sim 10,000 \text{ ft MSL}$) should be less than or equal to -6°C .

2. The wind direction is such that the proper transport of the ice nuclei will occur, from the selected ground-based generators to the target.
3. Liquid cloud water is observed, predicted, or otherwise believe to exist over the range.
4. No seeding suspension criteria are met (Section 9.5).

The rationale for these criteria has been adopted from those employed by the WWMPP (Breed et al. 2014), but modified to expand the seeding window slightly, acknowledging that some positive impacts (increases in snowfall) can be attained at -6°C (warmer than the WWMPP temperature criterion of -8°C). These activation temperatures are for the IN from a seeding solution tested by DeMott (1997), known to function in the condensation-freezing mechanism, also used in the WWMPP. This curve is shown in Figure 9.1, along with the analogous curve for the glaciogenic cloud-seeding pyrotechnic manufactured by Ice Crystal Engineering (ICE). The pyrotechnic-generated IN are also known to function by the condensation-freezing mechanism (DeMott 1999).

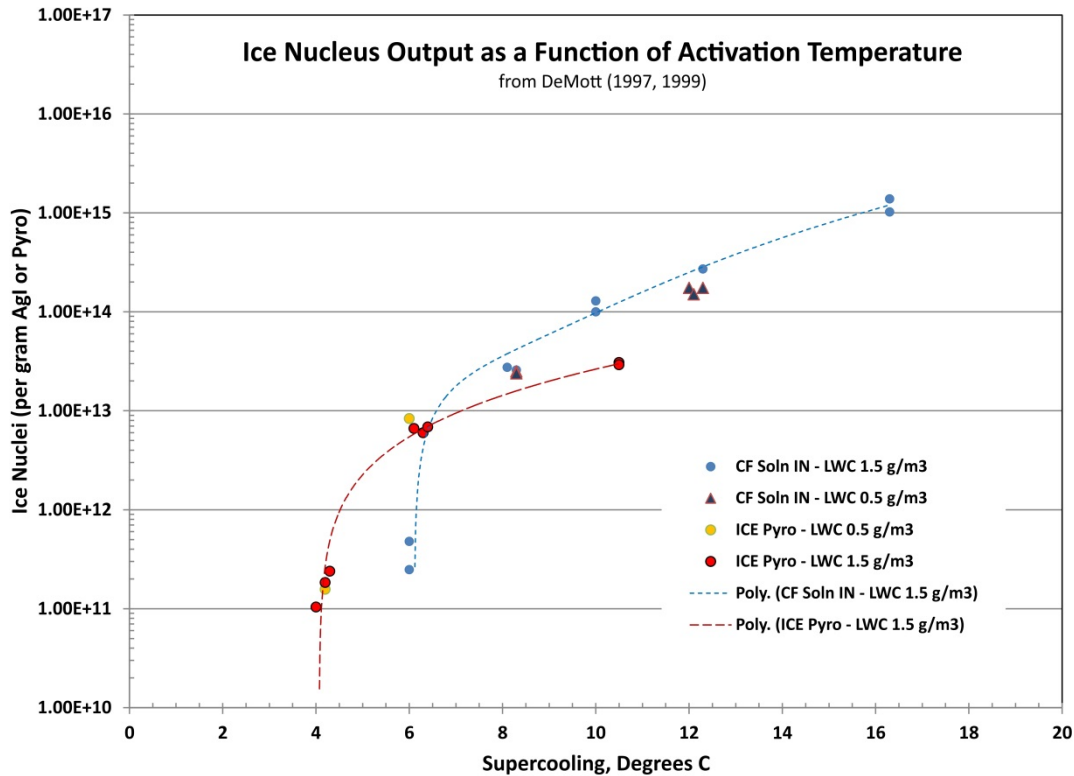


Figure 9.1. Yield as a function of supercooling for a condensation-freezing nucleus produced by the seeding solution used in the WWMPP (blues), and another condensation-freezing nucleus produced by pyrotechnics manufactured by Ice Crystal Engineering (red, yellow). (Data from DeMott 1997, 1999.)

Seeding with remote-controlled ground-based generators can begin when seeding criteria are met over either range. Whenever suitable conditions exist, seeding can continue for as long as conditions remain favorable, at least as long as the requisite consumables are available at the generators in use. Because consumables are replenished between storm systems as needed throughout the season, this should not pose any limitations on the duration of any seeding events.

9.3. Airborne Seeding with Ice Nuclei

Any aircraft deployed for wintertime glaciogenic seeding must be well maintained and certified for flight in icing conditions. Such a certification does not mean that flight operations can be conducted indefinitely in icing conditions, but rather that the aircraft has been proven to function safely in transient icing.

The recommended seeding criteria for airborne AgI seeding are:

1. The temperature at the flight altitude should be less than or equal to -6°C . This criterion is more flexible than that for ground-based seeding, as the aircraft can fly higher to target colder clouds, if necessary.⁶
2. The aircraft flight path allows the winds to transport the resulting ice crystals and precipitation to the target area.
3. The aircraft crew has observed SLW.
4. No seeding suspension criteria are met.

With regard to (3) above, radiometer or other observations of liquid cloud water can be used to suggest when airborne-seeding operations might be effectively undertaken, but *in situ* observations by the aircraft will confirm the existence of SLW. It should also be noted that in many cases, radiometers in cloud-seeding programs are operated at fixed, or at least very limited azimuths (directions), and so the presence or absence of liquid water is not necessarily indicative of conditions over the entire range, but rather a “spot” measurement. It is possible, even probable, that liquid water may often be encountered by the aircraft when the radiometer sees none because an aircraft will fly through portions of the orographic clouds not sampled by a radiometer. Thus, the presence of liquid water indicated by a radiometer should not be the sole means of confirming its existence. Prognostic numerical model output may also be useful.

Thus, the norm for airborne seeding is for the aircraft to:

- fly to the desired seeding area, determined by the altitude, distance, and direction appropriate for the day,
- find the SLW to be targeted,
- climb slightly above the liquid-water layer, and
- seed the SLW zone.

Airborne seeding can continue as long as:

- the supercooled cloud persists, or
- the accumulation of ice on the aircraft does not make departure from the supercooled cloud necessary, or
- all seeding materials on board are expended, or
- fuel is diminished, forcing a return to base.

⁶ There is an upper limit to the seeding altitude. The cloud must be deep enough and the precipitation process initiated early enough that resulting precipitation falls on the target. If the seeding altitude is too high and/or the wind is too strong, the resulting snow may not develop fast enough to precipitation on the barrier.

9.4. Seeding Season

Throughout the WWMPP, cloud seeding was conducted from 2008–2014, and each season started 15 November and concluded (after an early-project change) after 30 April. However, during those WWMPP seasons, only seven EUs met the research seeding criteria on 1 April or later. In these six seasons, operations were suspended once, in March 2011, so these numbers reflect only five winters. Recall that operational cloud seeding criteria for operations are less stringent than those for research, as the 700-hPa temperature need be only as cold as -6°C instead of -8°C . Another benefit to operational seeding is that it can be conducted whenever conditions are suitable over either Range, whereas the seeding criteria for the research study had to be met over both Ranges simultaneously.

Furthermore, only ground-based seeding was conducted during the WWMPP. Airborne seeding, an option explored by this study, enables seeding to be conducted at higher altitudes. This is important because late-season, higher-altitude opportunities (as temperatures warm) will sometimes be possible when ground-based seeding is not.

Based on this information, ground-based seeding opportunities would be most effective between 15 November and 15 April for each season. The window of opportunity for airborne seeding can be expanded on both ends, beginning 1 November and ending 1 May each season.

9.5. Suspension Criteria

For safety, all seeding programs should have suspension criteria established prior to the commencement of field operations (ASCE 2016). Such criteria should identify thresholds and conditions that will stop or suspend seeding, and also outline how any stoppage of operations will be communicated to project personnel. Further, all cessations are expected to be documented for the public record.

Operational suspension criteria have been established for the Wind River Range Weather Modification Program, conducted in the 2014–2015, and 2015–2016 winter seasons. These criteria were based on those implemented for the WWMPP, but modified to reflect differences between research and operations. The following criteria are recommended for an operational program being implemented in the Medicine Bow or Sierra Madre Ranges. These criteria are expected to govern all decisions on the operations of the generators.

Snowfall histories are used to determine the Historic Range of Natural Variability (HRNV) for a given SNOTEL facility. These historic SWE values are then combined and a median is established for a period of time, usually 10–20 years of recorded history. This median is then used to set the HRNV by the day or month of any recorded year. The criteria used for the Sierra Madre/Medicine Bow program design was developed using 30 years of historical data to determine an HRNV at the upper range of 140%.

Cloud seeding in the target area, or portions of the target area will be suspended if any of the criteria listed below exist:

1. Range-wide SWE indicated by designated NRCS SNOTEL sites (Figure 9.2) exceeds a percentage of the long-term median defined by a linear upper limit of 85% of the 30-year

(1981–2010) median 1 April SWE for the site on 15 November (normal program start), and increasing to 140% of the median 1 April SWE as of 1 April . If seeding is to continue after 1 April, the upper limit will remain fixed at 140% of the 1 April median value, until season end⁷.

2. Reservoir storage for flood control, based upon hydrologic estimates of total snowpack using all available data, is deemed insufficient.
3. There exists potential for significant rain-on-snow events at elevations above 8,500 ft MSL. Occasionally such events, have the potential to produce short-term winter season flooding. The area of risk would not be targeted until after the risk had passed.
4. The NWS office having responsibility for the forecast in the target area has issued notice of a severe winter weather event. The target area predicted to be affected would not be targeted until the risk had passed.
5. There exists an extreme avalanche risk in a specific target area. The area of risk would not be targeted until the risk had passed.
6. If regions within the target areas are affected by wildfire, the Forest Service shall be consulted prior to the next cloud-seeding season to determine if there is need for suspension(s) that account(s) for the newly burned areas.
7. Care will be taken to avoid targeting major highways to avoid impact on transportation corridors. The two highways that cross the Medicine Bow and Sierra Madre Ranges are Wyoming Highways 130 and 70, both of which are closed during the winters. Otherwise, Interstate 80, which passes north of both ranges, will not be significantly affected because the interstate is located upwind of any potential seeding activities. Thus, the seeding agent would generally move away from the roadway, and toward the mountains themselves.
8. Seeding can be suspended at any time upon direction from the program sponsor.

In addition, in the event of a localized situation that affects only a portion of the target area, operational seeding activities will be restricted to non-affected portions of the target area. An example of such a situation would be a wildfire burn scar that elevates erosion risks during spring runoff (Criterion 6). Conditions defined in Criterion 5 would also trigger this type of localized suspension. In such cases, seeding activities that may impact the affected area would not be conducted.

In the event conditions change and suspension criteria no longer exist, seeding operations may be resumed, and documented appropriately.

⁷The operational excess snowpack seeding suspension criterion now uses medians rather than means, and the 1981-2010 period of record. The upper limit of 140% is used because this corresponds approximately to one standard deviation above the long-term medians, meaning that snowpack at this level would still be well within the limits of natural variability. It is here noted that the *lowest* SWE suspension threshold currently employed in the western United States is 140%, including programs in Idaho, Utah, Nevada, and California.



Figure 9.2. The locations of NRCS SNOTEL sites in the Sierra Madre and Medicine Bow Ranges are shown. All but Little Snake River were also used in the WWMPP for snowpack evaluation.

10. Task 9: Environmental and Legal Considerations

As mentioned above in Section 9, well-designed research and operational cloud-seeding programs incorporate seeding suspension criteria to stop or suspend seeding activities that could generate unsafe conditions due to increases in precipitation produced from cloud seeding and atypical natural precipitation events. These criteria tend to focus on specific concerns such as suspension of seeding when there is the potential for flash flooding.

There are, however, other environmental concerns such as downwind (extra-area) effects, or potential impacts on water and soil quality, that are raised relevant to the practice of cloud seeding. This Section describes a few of the more common environmental concerns associated with cloud seeding.

10.1. Downwind (Extra-area) Effects

Perhaps the most frequently asked question regarding the establishment of a cloud-seeding program in an area that has not been involved in previous cloud-seeding programs, is whether areas downwind of the intended target area will experience less precipitation during seeded periods. The analysis of precipitation in areas downwind of cloud-seeding programs suggest that the amount of downwind precipitation is not significantly changed.

As described in the WWMPP Draft Executive Summary (WWDC 2014), potential extra-area effects due to cloud seeding were evaluated for the Sierra Madre and Medicine Bow Mountains. Potential extra-area effects from seeding were evaluated using the WRF model coupled with the cloud seeding parameterization (Xue et al. 2013a, b). Given the observational constraints of the WWMPP, no measurements were available to validate the model results beyond the intended seeding target areas at the time of this study. Nonetheless, model validation studies to date show promise for the model's ability to capture the trends and distribution in precipitation, LWP, and thermodynamic structure. However, the validity of the model has been shown to vary by case and has not been explicitly validated for this study.

During the WWMPP, WRF simulations were set up and conducted to investigate the simulated extra-area seeding effect from seeding the Wind River Range during the month of February 2013. A control simulation (CTRL) was run continuously for the entire month without any seeding prescribed. The outputs of CTRL were evaluated to identify potential seeding opportunities for the Wind River Range according to appropriate environmental conditions such as temperatures between -6 and -18 °C, SLW content greater than 0.05 g kg^{-1} , and ice saturation ratio greater than 1.04. No other dispersion factors were considered, such as wind speed and direction. Six cases were identified for the Wind River Range during this month-long period. An additional month-long simulation was also conducted with seeding prescribed.

Figure 10.1 shows the natural precipitation from the CTRL run as well as changes in precipitation due to the simulated seeding. The natural (CTRL) precipitation accumulated mostly in high-altitude areas. Results from the simulated seeding run showed enhancements in the Wind River Range, but also generated some positive and negative effects outside of that target area. The extra-area effects were small in area and magnitude and randomly distributed, except for

two small areas just west of the Wind River Range, which experienced a large negative seeding impact. Simulated seeding enhanced precipitation in the target region by 3%, and by an order of magnitude less in the extra-area region. It is also interesting to note that the very distant Sierra Madre and Medicine Bow Ranges were also impacted by seeding during this seeding simulation. This is likely due to the predominant northwesterly flow transporting AgI southeastward during this simulation.

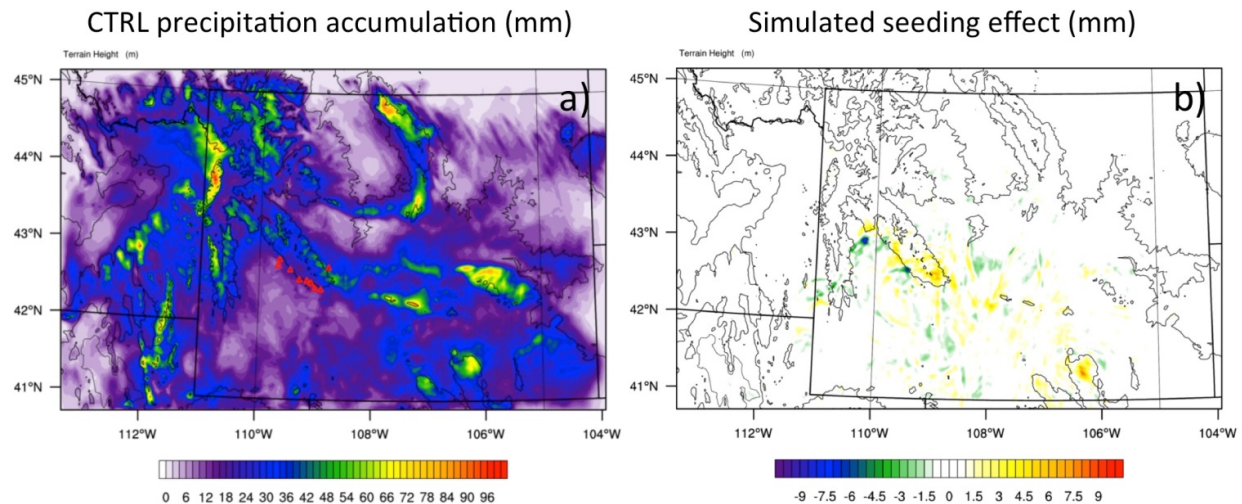


Figure 10.1. The accumulated precipitation (mm) from CTRL (left), and the simulated seeding effect (difference in precipitation from the seeding simulation minus CTRL; mm) for the WR seeding cases (right).

In addition to assessing the changes in precipitation, the model output was analyzed for changes in total precipitable water, which is a sum of all model-simulated atmospheric water vapor and hydrometeors (cloud droplets, rain, snow, ice, graupel) in the cloud. This was performed to compare the impact of cloud seeding on the total mass of available water in the atmosphere. The maximum model simulated change in total precipitable water was a reduction of 0.25% on 22 February. The simulated change in total precipitable water varied by seeding case, with some cases having much lower simulated percent changes. For instance, one seeding case had a simulated reduction in total precipitable water of only 0.07%.

The key preliminary result from this WWMPP study is that the net effect of all simulated seeding on precipitation in areas outside of the intended targets (i.e., extra-area effects) was quite small (less than 0.5%). This is consistent with the conclusions from previous studies (Long 2001, DeFelice et al. 2014).

Long (2001) reviewed information from a variety of both winter and summer programs. One winter research program that is perhaps most relevant to wintertime programs was conducted by Colorado State University scientists in the Climax, Colorado area. This mountainous area is located in the central Colorado Rockies. Quoting from Long (2001), “In order to detect downwind precipitation effects drifting from the Climax target area, various time lags of precipitation data from hourly stations in downwind locales were considered. Significant ratios of seeded to not-seeded precipitation were found downwind east and northeast of the Climax

area. This suggests *increases* in precipitation on the order of 15–25% downwind of the intended target area.” Long makes a summary statement in his paper as follows: “Downwind precipitation effects have been observed in geographic areas and time frames that are about the same magnitude as primary effects intended for the target area. There is little evidence of a decrease in precipitation outside the target area.”

Solak et al. (2003) analyzed potential downwind effects from an operational winter program. This paper examined the precipitation that fell in areas located in eastern and southeastern Utah and western Colorado located downwind of a long-term winter cloud-seeding program that has been conducted since 1974 in the central and southern Wasatch Mountains of Utah. The abstract from this paper states “Estimations of effects on precipitation downwind of a long-standing operational snowpack augmentation project in Utah are made, using an adaptation of the historical target/control regression technique which has been used to estimate the seasonal effects over more than twenty seasons within the project’s target area. Target area analyses of December–March high-elevation precipitation data for this project indicate an overall seasonal increase of about 14%. Estimations of downwind effects are calculated for distance bands downwind as far as 150 miles. The downwind analyses indicate increases of similar magnitude to those for the target, expressed as percentages or ratio values, extending to about 100 miles downwind. Beyond 100 miles, the ratio values decay, reaching about 1.0 (e.g., no effect) at about 125 miles. Expressed as average-depth precipitation amounts, the target area precipitation difference is about 1.4 inches of additional water, while the values within downwind distance bands range from 0.4 to 0.25 inches, reaching zero at about 125 miles.”

A workshop, jointly sponsored by the WMA) and the ASCE, was held at the annual meeting of the WMA in April 2012. The topic of this workshop was the potential for extra-area effects from cloud-seeding programs. After this meeting, a paper was published on this topic (DeFelice et al. 2014). It states, “The results described in this paper make a strong case for enhanced precipitation, or a direct seeding effect, in extra-area regions from the conduct of seeding programs. They did not reveal regional impacts to the water balance, nor to the natural precipitation on a regional scale. This suggests that cloud seeding would not dry up the atmosphere or lead to summer drought, contrary to a popular belief. Cloud seeding typically benefits both ‘Peter and Paul.’” Further, “The spatial extent of the positive ‘extra-area’ seeding effect may extend to a couple hundred kilometers. Both microphysical (static) and dynamical (dynamic) effects of seeding appear to be contributors to these ‘extra-area’ effects.”

In summary, extra-area effects do not appear to show decreases in precipitation downstream of cloud-seeding activities, and oftentimes show slight increases in downstream precipitation. Therefore, negative effects downstream of the Medicine Bow and Sierra Madre Ranges would not be expected as a result of cloud seeding in this area.

10.2. Environmental Impacts of Seeding Agents

Silver (Ag) in the form of AgI has been used as an ice nucleant in weather modification projects over the past 60 years. The ice nucleating properties of AgI were first reported by Vonnegut (1947). Vonnegut hypothesized that AgI acts as an effective ice nucleant because its crystal lattice structure resembles water ice and described a practical way to generate large numbers of AgI

particles by combusting a solution of dissolved AgI in acetone. Using this method, one gram of AgI can produce $>10^{16}$ IN at temperatures of about -20°C . Because of the extremely large number of IN produced by the method, very little AgI is required to significantly increase the local ice nucleus population. In ideal conditions, a large fraction of the AgI particles released during cloud-seeding operations create ice and are incorporated into the snowfall. Particles of AgI that do not act as IN may also be deposited on the ground by scavenging and dry deposition processes. Because the AgI particles are less than one micrometer, they will, , be transported in the atmosphere over large distances disappearing into the global atmospheric Ag background, if not captured in cloud particles. Only a very small percentage of the AgI particle mass is expected to dissolve during snowmelt because it is a very insoluble salt. The impact of cloud seeding on natural levels of Ag in the environment (primarily aquatic ecosystems) has become an environmental concern because Ag in the form of its free ion (Ag^+) has been found to be toxic to fish and a subset of other aquatic organisms (Bianchini et al. 2002; Di Toro et al. 2001). It is important to note that *the toxic Ag^+ ion is not a product of AgI* and is not released into the environment by cloud seeding (Golden et al. 2011).

Several 1970s-era studies examined the environmental and health impacts of cloud seeding in the United States, including Harris (1981), Howell (1977), and Klein (1978). A more comprehensive list of worldwide laboratory and field studies is contained in the WMA's 2009 "Position Statement on the Environmental Impact of Using Silver Iodide as a Cloud Seeding Agent" (WMA 2009). The conclusion of the policy statement is: "The published scientific literature clearly shows ***no environmentally harmful effects*** arising from cloud seeding with silver iodide aerosols have been observed, nor would be expected to occur. Based on this work, the WMA finds that AgI is environmentally safe as it is currently being used in the conduct of cloud-seeding programs."

Cardno Entrix (2011) references four multi-year studies that were conducted on cloud seeding from 1977 to 2006, including the geochemistry and toxicity of AgI. These studies are also unanimous in their conclusion that AgI used in cloud seeding is practically insoluble, does not tend to dissociate to its component ions of Ag and I, and is not bioavailable in the aquatic environment but instead remains in soils and sediments.

Williams and Denholm (2009) provide an in-depth literature review of the toxicity of AgI on the environment, as well as the most recent monitoring results of the large-scale SPERP study, an 11-year cloud-seeding research program designed to assess the technical, economic, and environmental feasibility of augmenting snowfall in the Snowy Mountain Region of New South Wales, Australia. The literature review summarizes findings from both field and laboratory toxicity studies, including studies on fish and amphibians. The authors concluded that there is no compelling evidence that the use of AgI for the SPERP would result in an adverse ecotoxicological impact on the study area environment.

Monitoring by the Desert Research Institute (DRI) of past cloud-seeding projects in and near the Walker Basin in Nevada has not detected an increase in Ag above levels naturally present in soil and streams (i.e., baseline numbers are not elevated). DRI uses ultra-sensitive laboratory methods that can detect parts per trillion concentrations (USBR 2010).

Edwards and Simeral (2006) note the toxicity of Ag^+ in the aquatic environment is a function of its speciation, complexation, and interaction with competing cations. Thus, its toxicity is not necessarily related to the total aqueous metal concentration, but rather site-specific aquatic chemistry.

It is important to note that while laboratory studies have demonstrated the potential toxicity of Ag^+ to aquatic organisms, no actual reports of Ag toxicity in the environment were discovered, even for heavily polluted water bodies. Because of the lack of case studies, aquatic toxicity is still largely theoretical (Edwards and Simeral 2006).

Findings from the WWMPP state, “Trace chemistry analyses of water and soil samples were conducted for all three ranges following each operational season. These analyses demonstrated a negligible environmental impact of the seeding operations within the three mountain ranges, with silver concentrations in the water ranging in the parts per trillion and background concentrations in the soil being in the parts per billion range. These concentrations are far less than would be expected from other potential (background) sources of silver and measured concentrations in water sources were about three orders of magnitude less than values considered hazardous to environmental system or human health” (WWDC 2014).

All of these studies are consistent in concluding the contribution of AgI to the environment from cloud seeding is negligible (i.e., in quantities too small to be measured) compared with background levels and are well below threshold limits for human safety, aquatic organisms, and water quality standards.

Overall, the conclusions reached in the published scientific literature center around these points, and are applicable to the ecosystems contained within the area associated with the Medicine Bow and Sierra Madre Ranges:

- Background levels of Ag far exceed Ag contributed from cloud-seeding projects. Ag is found naturally and through industrial emissions. Ag is a trace element in many organisms. Numerous studies report no detected AgI in samples of cloud-seeded areas vs. control areas.
- In studies in which Ag (all compounds and all sources) was detected, it was in the range of 0.1 to 0.01 micrograms per liter. The U.S. Public Health Service established a concentration limit of 50 micrograms per liter in public water supply. In a 1978 study, cloud seeding AgI was estimated to contribute 0.1% of overall silver emissions (Eisler 1996).
- The quantities of AgI used in cloud seeding are minute because very little material is needed to form the desired ice crystals. Furthermore, cloud-seeding material is dispersed over very large areas. In sampling water bodies in mountain areas of California subject to long-term cloud seeding, no detectable silver above the natural background was found in seeded target area water bodies, precipitation and lake sediment samples, nor any evidence of Ag accumulation after more than 50 years of continuous seeding operations (Stone et al 1995; Stone 2006).
- Silver toxicity depends on the concentration of active, free Ag^+ ions. AgI is considered water insoluble and not able to bioaccumulate to toxic levels. This insoluble property is what makes AgI maintain its structure and serve as an effective cloud-seeding agent.

Some silver compounds are toxic, especially to aquatic organisms in laboratory studies. However, in an environmental setting AgI is immobilized and is not bioavailable. Studies were conducted as part of an environmental monitoring effort to determine whether cloud seeding was impacting Sierra Nevada alpine lakes. No evidence was found that Ag from seeding operations was detectable above the background level. There was also no evidence of an impact on lake water chemistry, which is consistent with the insoluble nature and long times required to mobilize any AgI released over these watersheds. Comparisons of Ag with other naturally occurring trace metals measured in lake and sediment samples collected from the Mokelumne watershed in the Sierra Nevada indicate that the Ag was of natural origin (Stone 2006).

- Soil, sediment, and water-silver toxicity is very low even at high total Ag concentrations. Most Ag is bound into a compound such as AgI and is not available for absorption. Organic matter in the water column (colloids) and sediments bind Ag⁺ ions, and Ag is strongly bonded to particulate matter. These factors result in low bioavailability, and therefore low toxicity. Because of this, very low amounts of Ag are absorbed from food; most is passed through the body of aquatic and terrestrial organisms.
- Although Ag⁺ ions from soluble silver salts have been shown to be toxic to aquatic species, this is not the case with insoluble silver salts such as AgI, which is not bioavailable and thus of little environmental concern.

10.3. General Statements on Potential Environmental Impacts of Cloud Seeding

Numerous studies have been conducted in the western United States related to the potential environmental impacts of winter cloud seeding. Most of these studies were funded under the U.S. Bureau of Reclamation's (USBR) "Project Skywater". Four programs of note concerned with wintertime programs were:

- Potential Ecological Impacts of Snowpack Augmentation in the Uinta Mountains, Utah. A 1981 report from Brigham Young University authored by Kimball Harper (Harper 1981) summarizing the results of a four-year study.
- Ecological Impacts of Snowpack Augmentation in the San Juan Mountains, Colorado. A 1976 report edited by Harold Steinhoff (Colorado State University) and Jack Ives (University of Colorado) summarizing the results of a five-year study (Steinhoff and Ives 1976).
- The Medicine Bow Ecology Project. A 1975 report on studies conducted in the Medicine Bow Mountains of southern Wyoming (Knight et al. 1975).
- The Sierra Ecology Study. A five-volume report summarizing work on possible impacts on the American River Drainage in California (Smith et al. 1980, Berg et al. 1980).

In general, the findings from these studies were that significant environmental effects due to the possible conduct of cloud-seeding programs in these areas were not expected to occur. A couple of examples that support this conclusion are as follows:

A statement made in the final report on the San Juan Mountains program (Steinhoff and Ives 1976): “The results of the San Juan Ecology Project suggest that there should be no immediate, large-scale impacts on the terrestrial ecosystems of these mountains following an addition of up to 30 percent of the normal snowpack, but with no addition to maximum snowpacks. Further, much of the work reported here suggests that compensating mechanisms within the study’s ecosystems are such that any impacts would be buffered, at least for short periods of time, and of lesser magnitude than the changes in snow conditions required to produce them.”

The USBR published an “Environmental Assessment and Finding of No Significant Impact (Harris 1981) for the Sierra Cooperative Pilot Project (SCPP). Quoting from the introduction of this report:

“This document and the project environmental assessment serve as the basis for determination that no further action is necessary to comply with the National Environmental Policy Act of 1969 (Public Law 91-190) for the following reasons:

- 1) The Sierra Cooperative Pilot Project Environmental Assessment examines a research program designed to seed, on a randomized basis, some of the cloud types, which occur within winter storms in the Sierra Nevada of California and Nevada. The increase in annual precipitation expected from seeding all eligible storms during an average or less-than-average year would be 10 to 15 percent. The annual precipitation increase expected from randomized seeding of selected cloud types would be 5 to 7.5 percent. The report analyzes the potential effect of these increases upon weather elements, hydrologic and physiographic phenomena, plant and animal communities, the human environment, and land and water resource use in the project area. It also discusses possible impacts of the seeding agents, dry ice and silver iodide. The report concludes the research program will not result in significant or adverse effects upon the environment.
- 2) Consultation with Federal and State agencies has resulted in the determination that this project will not affect endangered or threatened species of plants or wildlife or their habitats in a significant or adverse manner.
- 3) Archeological and historic sites and sites of extraordinary aesthetic value will not be significantly or adversely affected by the project.
- 4) Project activities and resultant increases in precipitation will not affect the human environment, lifestyle, or existing land and water resource use in a significant or adverse manner. The project design includes suspension criteria to prevent operations during periods that would lead to public safety hazards.”

A more recent environmental assessment was completed by the USBR for the Walker River Basin located in the east central Sierra Nevada Mountains of California and west central Nevada (USBR 2010). A Finding of No Significant Impact (FONSI) was issued for this project by the USBR (USBR 2010). The following is the summary statement from the FONSI: “Based on the analysis of the environmental impacts as described in the Environmental Assessment for the Walker River Basin Cloud Seeding Project, Reclamation has determined that the proposed federal action will not significantly affect the quality of the human environment, thus an environmental impact statement is not required. This Finding of No Significant Impact (FONSI)

is supported by the Environmental Assessment for the Walker River Basin Cloud Seeding Project.”

10.4. Legal Implications

There are legal implications associated with the conduct of cloud-seeding programs. Water ownership is a primary example. Most state regulations claim ownership of surface waters while they are within the state, and they can be distributed according to the existing water rights in the area. The State of Wyoming considers water developed by cloud seeding as part of the natural water supply and subject to all applicable laws.

Another legal consideration is whether cloud-seeding program sponsors have legal responsibilities for any perceived damages caused by the seeding activities. For example, if seeding is conducted and a flood occurs in or near the program’s target area, would the sponsors be liable? This is sometimes referred to as the possible “consequential effects” of cloud seeding. To prevent such situations, it is important to have adequate safeguards built into the design of seeding programs to suspend seeding operations in questionable circumstances (Section 9).

Weather modification operators also have the option to carry a special type of insurance commonly known as “consequential effects of cloud-seeding liability insurance.” This insurance protects the operator and sponsor from legal defense costs, and also provides reasonable assurance of protection to the public in the event that damages are caused as a result of cloud seeding.

Cloud-seeding programs are subject to permitting and reporting requirements. Both state and federal requirements would be associated with the proposed Medicine Bow and Sierra Madre operational program. These requirements are summarized in Section 8.

11. Task 10: Evaluation Methodology

The critical necessity for weather modification research and operational programs is the evaluation and validation of results. Objectivity, repeatability, and predictability are primary requirements in weather-modification studies. Independent confirmation of a seeding effect with strong physical and statistical evidence is crucial. With more emphasis on statistical studies and randomization in the past decade, there has been some improvement in the evaluation and validation of cloud-seeding activities. The recent advances in numerical models that simulate seeding are noteworthy, and can be complementary in contributing to both the statistical, and the physical evidence of seeding. The goal of this task is to develop and summarize statistical and physical methodologies for evaluating the efficacy of the proposed cloud-seeding program.

11.1. Statistical Evaluation

Statistical evaluation may detect a change in a response variable (i.e., seeding effect), as specified by the seeding conceptual model (Section 3.1.1). The objective is to show that the behavior of seeded clouds is clearly outside the scope of natural variability. In a statistical experiment, the response variable is the variable being investigated for the seeding effect. While the variable could be any expected change along the steps of the conceptual model, such as AgI detection in the target area, increased concentrations of ice particles, or enhanced radar reflectivity, a measurement of the result (seasonally accumulated precipitation, 1 April SWE, or a measure of streamflow) is usually of more interest. For example, in the WWMPP study, the response variable for the Medicine Bow and Sierra Madre targets was the 4-hour accumulation of liquid-equivalent precipitation in each target area as measured by high-resolution precipitation gauges. These changes, or seeding effects, have proven to be relatively small when compared with natural variability. Therefore, it is most common to compare target (seeded) measurements to control (unseeded) measurements – so-called target/control evaluation. This is the method to detect and quantify, with some measure of confidence, seeding effects from an operational program. As such, it has been recognized or recommended as a preferred method in ASCE standards, and various weather-modification permitting regulations.

11.1.1. Target/Control Method

The most widely used approach to evaluating operational cloud-seeding programs is the comparison of events in the target area to events in one or more control areas (which are unaffected by the seeding). The 2006 Wyoming Range Feasibility Study (NAWC 2006) described this method in great detail, and the review and results are still applicable to the Medicine Bow and Sierra Madre Ranges target area evaluation. The appeal of this method for operational programs is its use of measurements from the SNOTEL or streamflow gauge networks, which have been established over a long time. It is critical to identify appropriate control areas that are highly correlated to the target area(s), and have been unaffected by precipitation augmentation activities for an extended period. One technique is to calculate the precipitation as a percentage of normal (over some historical period). The target and control area can be compared in terms of a percentage of normal, and a ratio of increase in precipitation can be calculated. However, the use of ratios carries a risk of error. If the target and control have similar precipitation patterns, the expected value of the target-control ratio is expected to be greater than one. However, the value depends on the distributions of rainfall events in the target and control area.

The validity of these ratios depends on two assumptions: 1) no other differences are confounded with the operational/historical seed/no seed difference; and 2) variability of precipitation between one set of years and the next set behaves like the variability of two independent random samples of years. The first assumption, in which no other differences have confounded with the operational/historical comparison, is referred to as “lack of bias.” Biases arising from unrecognized temporal or spatial trends that may have been present during the seeding period need to be reconciled. For example, Silverman (2007) presents an analysis technique that accounts for biases due to natural differences in streamflow between the target and control and, by taking advantage of the high correlation between the target and control. The second assumption underlying the validity of the statistical methods addresses the variability of precipitation from year to year. As knowledge is gained about the effects of land-use changes, climatic shifts, and large-scale dynamic cycles (i.e., El Nino) on precipitation in the West, that knowledge may be useful in further adjusting long-term records for these known variations. The practical issue is whether the statistical methods used in operational/historical evaluations of cloud seeding are valid when based on fluctuating yearly precipitation data. Making the assumption of normality for annual precipitation data is highly suspect. However, many statistical methods are quite robust and can account for departures from the assumptions under which the evaluations were derived. Different statistical approaches, such as historical regression and ratio statistics, can be used to compare target to control variables.

11.1.2. Evaluation by Historical Regression

Relationships between target and control are commonly described statistically via regression calculations on historical data. The historical regression method of comparing target and control is considered more sophisticated than a ratio comparison. In addition to obtaining an estimate of the effects of seeding upon precipitation, the historical regression method provides an estimate of the probability that the departure from the predicted value, for any seeded storm, is entirely due to chance. Many examples of this technique have been described (e.g., Silverman 2007, 2010; Griffith et al. 2009; 2011, NAWC 2006).

The historical regression method consists of the following steps:

1. Select a variable affected by seeding (e.g., SWE, streamflow).
2. Acquire records of the variable to be tested for a non-seeded historical duration of more than 20 years (requires precipitation gauges with a long historical record).
3. Records are partitioned in the target and control area. The meteorology in the target and control area should be similar, and the control area should be unaffected by the seeding. The correlation between precipitation in the target and control area should be greater than 0.9, and target and control areas should not be downwind of other seeding projects. As more seeding programs are implemented in the Western U.S. mountains, this latter criterion will become more challenging to meet.
4. Use target and control data from the unseeded period to develop an equation (regression) that predicts the amount of target area precipitation.
5. The regression equation is applied to the seeded period to estimate what target precipitation might have been without the seeding.

The target and control area often is the same fixed geographical area, and comparisons are made between measurements collected during the seeding and those from a period without the seeding. Alternatively, the control area might be a geographically fixed area adjacent to (and meteorologically similar to) the target area. The historical regression method can also involve multiple control areas. Controls can also be introduced based on observed meteorological variables other than precipitation. In this case, the objective is to find a multiple correlation coefficient higher than that for any single control area. However, the addition of new control variables usually reaches a point of diminishing return due to intercorrelation amongst controls.

There is no guarantee that long-term climatological trends, or biases arising from temporal or spatial trends that may have been present during the seeding period, will not change a target-control relationship. To address this possibility, it is recommended that the historical regression analysis method for the selection of control areas be followed, and to be watchful for any changes in weather patterns that could distort the target-control relationship.

11.1.3. Evaluation by Ratio Statistics

Using ratio statistics is an alternative method for detecting and quantifying seeding effects, using target and controls. Ratio statistics relate totals, or means, of precipitation at different times and in different areas (with seeding or without seeding), on a seeding target or a control area, or on two alternate targets. The totals accumulate all seeded or unseeded experimental units at all stations of a particular area. Because daily, or even weekly, precipitation tends to have highly skewed distributions, ratio methods may not be satisfactorily robust and prone to the effect of outliers. Replacing them by statistics that censor outliers increases robustness but does so at the risk of ignoring possible large effects of seeding. Biases occur when operational data are compared with historical records in an *a posteriori* evaluation of non-randomized seeding programs. Gabriel and Petrondas (1983) have shown that reliable conclusions cannot be drawn from comparisons of operational data with historical records, and have demonstrated the problems encountered in trying to do so. The calculated p-values are likely to be lower than the true level of significance and the calculated confidence limits are likely to be more precise than they really are. Because of these problems, standard statistical methods are prone to indicate effects when there might not be any.

Although ratio statistics are explained in Gabriel (1999), a clear example is given in Silverman (2007) in the analysis of the Kings River operational seeding program (Henderson 2003). In this analysis, bias adjustments were made in accordance with Gabriel and Petrondas (1983) and robust results of seeding effects were presented. In general, the use of ratio statistics presents an analysis technique that addresses some of the caveats highlighted in other analysis methods. Using the regression ratio, which takes advantage of correlations over an entire measurement period (unseeded and seeded), and adjusting for biases decreases the variance and facilitates the detection of smaller effects due to seeding.

11.2. Numerical Model Evaluation

Computer models are now capable of predicting the transport of seeding plumes, their microphysical response in clouds, and the fallout of seeding-enhanced precipitation. Running the WRF model with a cloud-seeding parameterization (i.e., ASPEN, Xue et al. 2013a, b) to show

spatial variability and quantified simulated seeding effects, can aid in the design of cloud-seeding programs. Similarly, the seeding parameterization in WRF can be applied to seeded and natural storms to statistically analyze seeding effects – a virtual seeding experiment – as was done for the WWMPP (WWDC 2014). Although the model has yet to be thoroughly validated, this approach has the potential to transform how cloud-seeding programs are evaluated. Running seeded versus unseeded model simulations to determine a plausible seeding effect is less expensive than conducting a long-term, randomized, statistically significant seeding experiment. Moreover, the model provides a true “control” experiment, whereas in a randomized experiment, actual seeding operations would have to be intermittently suspended when seedable storms were present. For this approach to have merit, the ability of the model simulation to reproduce the actual observed storm characteristics in the control and seeded simulations needs to be thoroughly validated against observations. For the purposes of this study, model simulations of all the WWMPP RSE cases has been completed to assess whether or not the model is able to reproduce the observed results of that statistical experiment. Those results can be found in Section 21.

Additionally, various plume-modeling approaches have been successfully applied to winter orographic cloud-seeding conditions, based on spot observations for model verification. Plume models depend on input from observations or more often a three-dimensional weather model to “drive” the plume model with winds, temperature, pressure, underlying topography, and land-use. The advantage of using plume models is the ability to include many simulations with these relatively simple models (e.g., SCIPUFF – Sykes and Gabruk 1997, the Hybrid Single-Particle Lagrangian Integrated Trajectory (HYSPLIT), Stochastic Time-Inverted Lagrangian Transport (STILT), and Flexible Particle (FLEXPART) models). DRI’s Lagrangian particle dispersion model (LAP) has been used to predict plume transport from AgI generators (NAWC 2006). Some of these simulations have been subject to independent verification through studies of the Ag content of snow. Another method used to validate plume dispersion is to map IN or tracer concentrations using aircraft (e.g., Boe et al 2014). Careful comparison of observations against validate model output is necessary for building confidence that numerical models faithfully portray seeding plumes.

11.3. Physical Evaluation

Physical evidence constitutes the measurement of key steps within the chain of events associated with the seeding conceptual model and establishes the physical plausibility that seeding effects suggested by the results of statistical evaluations could have been caused by the seeding. The physical evidence enables the establishment of a cause-and-effect relationship between seeding and the changes in the response variables as documented in the statistical evaluation. However, such relationships do not directly address whether seeding changes the total precipitation reaching the ground.

Physical evidence is usually accomplished: 1) by means of case studies on the behavior of seeded and unseeded clouds, and 2) through the identification and measurement of response variables associated with the seeding conceptual model. Response variables are parameters that represent key steps in the chain of physical events as described by the seeding conceptual model. Such parameters must be capable of being measured to the degree necessary to discern the anticipated changes due to seeding. A recent example of such an approach is the ASCII program,

which utilized a suite of instruments to examine relevant parameters (Geerts et al. 2010; Pokharel et al. 2014a, b).

A number of instruments and analysis techniques for evaluating an operational program are listed below:

- Installation of additional precipitation measurement sites.
 - When historical data are not available in a critical area, the installation of additional precipitation measurement equipment is valuable, especially when conducting a historical regression analysis.
 - Accurately measuring snowfall at unmanned high-elevation sites is difficult. Main issues are clogging at the top of the snow gauge and blow-by of snowflakes past the snow gauge. The best location for a snow gauge is in small clearings in forested areas to help reduce the impact of wind influence. Uncertainty in snow measurements could be greater in magnitude than a seeding effect; therefore, siting multiple gauges at any given site (redundancy) is helpful to ascertain the uncertainty in the measurement itself.
 - SNOTEL sites may provide the only type of standard precipitation measurements at high-elevation areas targeted by many winter cloud-seeding programs in the Western U.S. They are not ideal for estimating seeding effect, given the low temporal (hourly) and measurement (0.1 inch) resolution of these gauges.
- Installation of additional streamflow gauges. This is especially helpful at sites with historical records, but no longer have gauges. These sites could be the basis for statistical evaluation of streamflow changes. In addition, these gauges would augment streamflow information useful to the planning authorities.
- Additional atmospheric soundings (weather balloons) and radiometer data. Not only are observations of current atmospheric conditions useful for making operational seeding decisions, but also for program evaluation and model validation.
- Addition of a meteorological tower site(s). While the location(s) for the site(s) would need to be evaluated, meteorological observations in these data-sparse regions would be useful for model validation.
- Deploy a millimeter-wave radar (e.g., the Wyoming Cloud Radar) during periods of opportunity. These measurements provide information about cloud structure at scales not available from operational NEXRAD radars, which can aid in physical evaluation of cloud seeding. The value of such data was established during ASCII.
- Deploy an X-band radar at a site that allows remote operation to obtain measurements of clouds over the mountainous regions where operational NEXRAD radars cannot see. This radar would not need to be continuously manned, but would require power and internet access.
- Collect snow samples for trace chemistry analysis to verify targeting. This technique is used for assessing the effectiveness of the targeting of seeding effect by determining whether Ag is present in areas that use AgI as the seeding agent.
 - Snow samples collected prior to cloud seeding or from non-seeded storms are analyzed to establish the natural background Ag content for comparison with snow samples taken from seeded storms.
 - Warburton et al (1996) demonstrates how trace chemical assessment techniques strengthen traditional target and control precipitation analyses.

- The addition of a control aerosol along with an active seeding aerosol (Warburton et al 1995) can give estimates of seeding effectiveness.
- The combination of silver-in-snow samples along with model predictions of the transport of seeding plumes over sampling sites verifies targeting, and supports any indications of positive seeding effect indicated by statistical evaluations.
- Make IN measurements, like those performed in the Medicine Bow Range during WWMPP. Without an easily accessible site in the target area, it may be best to measure downwind to investigate plume transport.
- Validate cloud-seeding plume dispersion by using aircraft to map concurrently released tracer concentrations in clouds. Previously, this type of work was done using SF₆ tracer in Utah storm events (Holroyd et al. 1995, Heimbach et al. 1997).
- Evaluate particle dispersion over the target area using trace gas releases at generator sites and gas samplers at the target area.
- Instrumentation to provide temperature, wind, cloud water content, and cloud droplet sizes could be added to the seeding aircraft. This would gather quantitative information about cloud properties and would better inform the seeding decision making, as well facilitate evaluation of the conditions prior to and during seeding when compared with the seeding conceptual model.
- The objective would be to keep the instrumentation at a minimum, so that it could be utilized during operations without the need of an instrument operator and with minimal maintenance.
- If higher-elevation remote generators have continuous connectivity, the addition of icing-rate meters would provide real-time physical verification of the existence of seeding conditions.
- Consider new technologies for collecting data relevant to the seeding conceptual model, such as other remote sensing-instruments or unmanned airborne vehicles as a platform for stability analysis (in valleys) or winds affecting plume transport and diffusion from lower elevation generators.

11.4. Evaluation Methodology Summary

Statistical analyses using the target/control method are commonly used to evaluate operational programs because of their long history in developing the technique and the publically available data (i.e., SNOTEL, streamflow gauges) that are used. The target/control method is capable of providing fairly robust results and is also cost effective. However, finding appropriate controls can be challenging. Numerical modeling using the recently developed seeding parameterization (i.e., ASPEN) is emerging as another cost-effective tool for evaluating seeding effects. Ongoing validation efforts and continued development of the model are providing evidence of its reliability. A number of physical measurements would also aid in the evaluation of the operational seeding program, such as adding streamflow gauges and local meteorological stations. Moreover, the addition of supplementary instrumentation (i.e. soundings, radiometers, and radar) not only aids in program evaluation, but also in program decision making to identify suitable cases for seeding. The deployment of specialized instruments would also be useful in helping further model validation and determining seeding effectiveness.

12. Task 11: Potential Benefits/Hydrologic Assessment

The potential benefits of streamflow from cloud seeding were calculated two ways. One method estimated the change in streamflow relative to a change in precipitation using regressions of historical precipitation and streamflow records, either from gauge measurements and/or long-term model simulation. This method was similar to that used in other weather-modification feasibility studies (i.e., Wyoming Range, Bighorn Mountains). In this design study, the 8-year, high-resolution model simulation (Liu et al. 2016, WRF-CONUS) was used to establish this relationship. However, there are several assumptions required for this approach (i.e., magnitude of seeding effect, relationship of winter snowfall to streamflow runoff, etc.), which contributes to a substantial range of uncertainty in the results.

Secondly, a new method utilizes the WRF-Hydro hydrological model, coupled with results of cloud-seeding simulations from the WWMPP. While there are still inherent uncertainties associated with this method, many of the assumptions needed for the previous regression method are explicitly simulated.

12.1. WRF-CONUS Model Estimates of Seeding Effects on Streamflow

12.1.1. WRF-CONUS Simulation of Runoff

A first-order estimate of the potential change in streamflow (runoff) in the study area from snowfall augmentation from cloud seeding was made using precipitation and runoff simulated by the high-resolution WRF-CONUS simulation (Section 4.1.2). Model output of runoff includes both surface and sub-surface runoff from the Noah-MP Land Surface Model (LSM). The WRF-CONUS simulation was not run with a hydrological model, which would give detailed hydrological routing of runoff to water bodies such as streams, rivers, and lakes. Therefore, the current dataset does not allow for an estimate of runoff amount that distributes to specific rivers/streams. However, the model dataset allows us to examine the spatial distribution of runoff and give insight to the relationship between the distribution of precipitation and runoff.

Figure 12.1 shows precipitation, runoff, and evapotranspiration for the annual, November–April (winter), and May–October (summer) periods using the 2000–2008 WRF-CONUS simulation. Overall, more of this domain is bounded within the North Platte River Basin, and as a result, most of the precipitation, runoff, and evapotranspiration occurs in this basin compared with the Green River Basin. The high-elevation snowfall is very important, driving the majority of the annual precipitation from which the majority of runoff also results. Consistent with the SNOTEL analysis shown in Section 4.2.1, most of the precipitation occurs in the winter months as well. The spatial distribution of runoff is symmetric with respect to the mountain in both ranges. Most runoff from high elevations occurs during the early summer months because the snowmelt occurs largely in May and June. The slight runoff at low elevations in the November–April period comes from snowmelt (and rain) in early April at these heights. Evapotranspiration is very small during winter, primarily due to cold temperatures and snow-covered surfaces, while it is high during the warm (summer) season and greater at higher elevations due to increased availability of water (i.e., precipitation). Across the whole domain, the runoff ratio (ratio of runoff to precipitation) is ~0.2, but it generally increases with elevation, such that above 8,000 ft it is ~0.6 or greater (Figure 12.2). Both the runoff ratio and runoff maps (Figure 12.1–Figure

12.2) show that more runoff goes to the North Platte River Basin than the Green River Basin (Table 12.2).

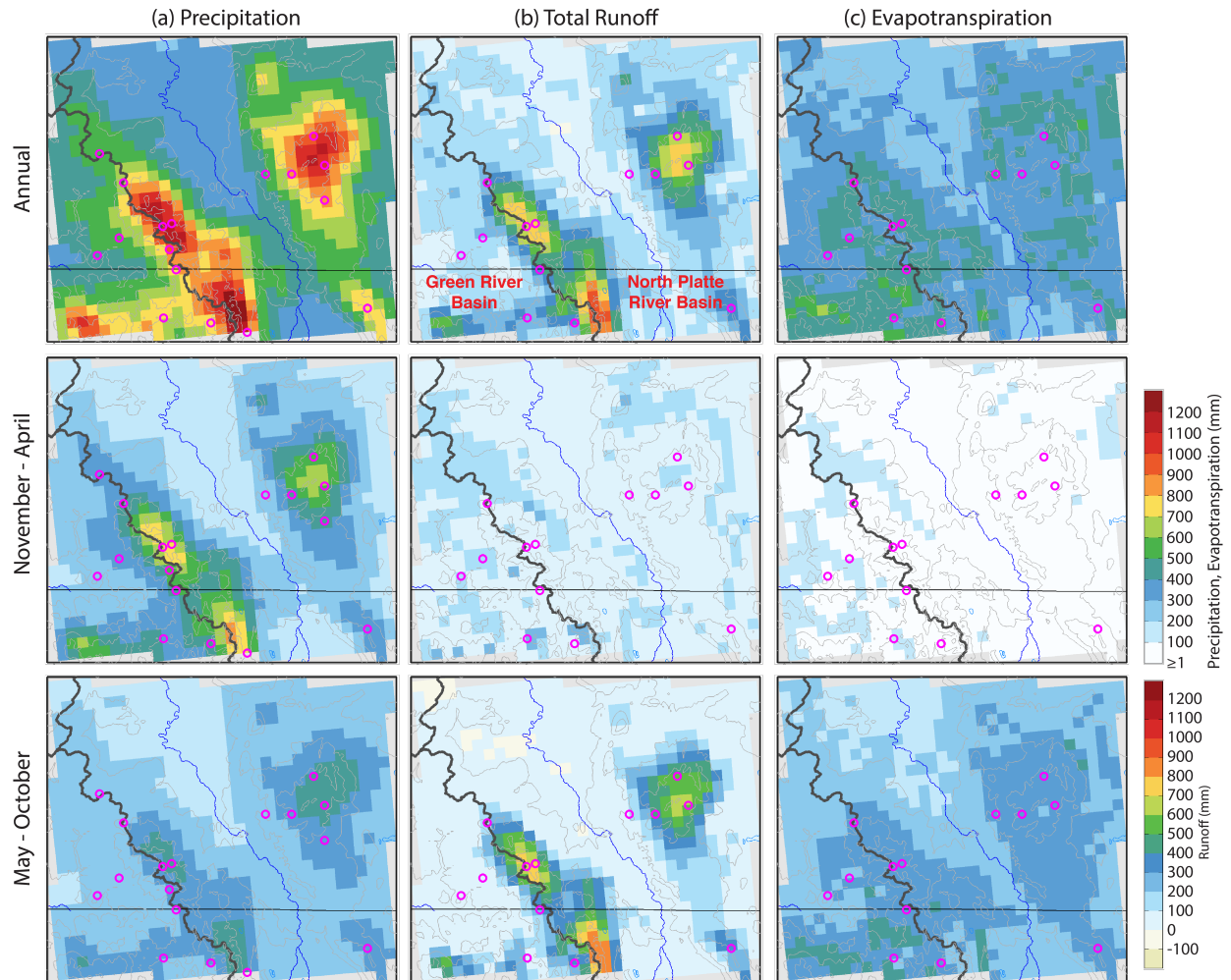


Figure 12.1. WRF-CONUS simulation of (a) precipitation, (b) total runoff (surface and sub-surface runoff), and (c) evapotranspiration averaged over 2000–2008. Top panels show annual precipitation, runoff, and evapotranspiration. Middle and bottom panels are for November – April, and May – October, respectively. The thick black solid line indicates the hydrological basins: west of the divide is the Green River basin and east of the divide is the North Platte River basin. The thin straight black line is the Colorado-Wyoming state border.

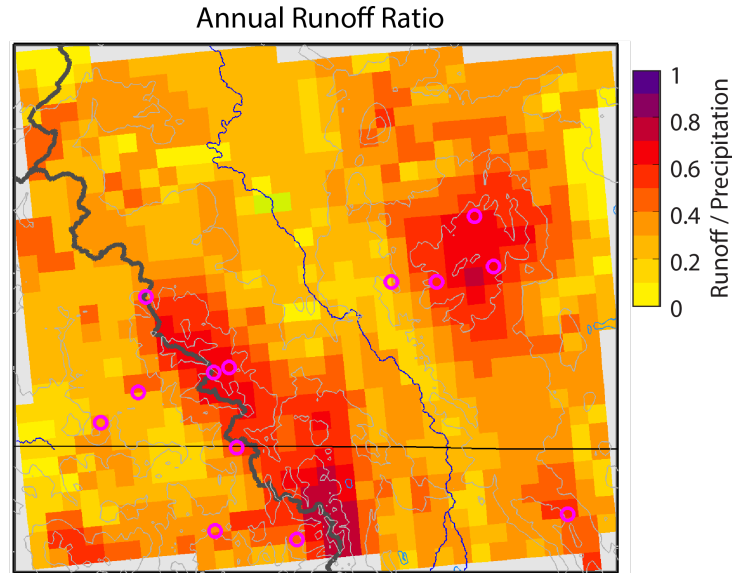


Figure 12.2. Ratio of annual total runoff to annual precipitation from the 8-year averaged WRF-CONUS model data. The thick black line is the divide between the North Platte River Basin to the east and the Green River Basin to the west.

The WRF-CONUS model-based annual precipitation calculated over the study area shown in Figure 12.2 is 543 mm with 36% as runoff (198 mm) and 59% of the annual precipitation is snowfall (Table 12.1). This means that 59% of 198 mm runoff (i.e., 116 mm) is from snowmelt and the other 82 mm from rainfall (Table 12.1).

The breakdown of these values for each of the two basins is similar to that determined for the entire study area (Table 12.1). In the North Platte River Basin, the annual precipitation is 536 mm with 37% going to runoff (199 mm). Snowfall is 59% of the annual precipitation, which means that 59% of the 199 mm runoff is snowmelt and the remainder from rain. The average annual precipitation in the Green River basin is slightly greater (593 mm) than in the North Platte River Basin. However, the runoff ratio in the Green River basin is 36%—similar to the runoff ratio in the North Platte River basin. Of the 593 mm of annual precipitation in the Green River Basin, 63% is snow, which leads to 134 mm of runoff from snowmelt and the other 78 mm from rainfall.

Table 12.1: 8-year average annual precipitation, runoff, runoff ratio, snowfall and rainfall averaged over the study area (Figure 12.1), North Platte River basin, and Green River basin. Values in parentheses for the snowfall and rainfall indicate the ratio of snowfall and rainfall to total precipitation. Note that the basin-averaged values are only for the area that appears in Figure 12.1, not including the entire basin.

	Annual Precipitation (mm)	Annual Runoff (mm)	Runoff / Precipitation	Annual Snowfall (mm)	Annual Rainfall (mm)
Study Area	543	198	36 %	323 (59%)	220 (41%)
N. Platte River Basin	536	199	37 %	315 (59%)	221 (41%)
Green River Basin	593	212	36 %	373 (63%)	220 (37%)

Figure 12.3 and Figure 12.4 are scatter plots showing the relationship between April–July WRF-CONUS simulated runoff over the North Platte River Basin and Green River Basin above 8,000 ft (MSL) to May 1 SWE. Traditionally, April 1 SWE is used; however, we have used the May 1 SWE as a parameter for this study because the peak SWE usually occurs in May and demonstrates a better relationship to the April–July runoff. The two variables show a good relationship, as expected, given values at individual model grid points are being correlated, resulting in a linear correlation coefficient of 0.97 for the North Platte and 0.94 for the Green River Basin. The least-squared fit through the data points has a coefficient of determination of 0.94 and 0.89, respectively.

Figure 12.3 and Figure 12.4 show scatter plots of April–July total runoff from the WRF-CONUS simulation above 8,000 ft MSL versus May 1 SWE over each basin. Data points are from model grid values in each basin. Table 12.2 provides three metrics on the snowpack and runoff: the basin-average May SWE above 8,000 ft in each basin, basin-total annual runoff, and April–July runoff. The model indicates that most of the runoff from > 8,000 ft elevation occurs in the April–July period, during which time it is just over 1,000,000 AF for the North Platte River Basin and close to 400,000 AF for the Green River Basin, on average over the eight-year simulation. Note that the domain of study is mostly within the North Platte River Basin, which is part of why the total runoff is higher for this basin.

The percentage increase in streamflow resulting from a given percentage increase in SWE varies, depending upon whether conditions are dry or wet. Using the best-fit line for the runoff and May 1 SWE from the WRF-CONUS simulation (Figure 12.3 and Figure 12.4), the ratio of snowpack increase to streamflow increase is estimated to be 0.59 for the North Platte River Basin and 0.63 for the Green River Basin (Table 12.2). The results of Super and McPartland (1993) indicated that the ratio of snowpack increase to streamflow increase observed at several locations in Colorado, Utah, and Wyoming varied between 0.6 and 2.1 with a median of 1.05. Detailed hydrological models tend to show ratios much lower than 1.0 (e.g., Acharya et al. 2011). Based on all these factors, a ratio of 0.60 will be used to calculate seeding effects on streamflow.

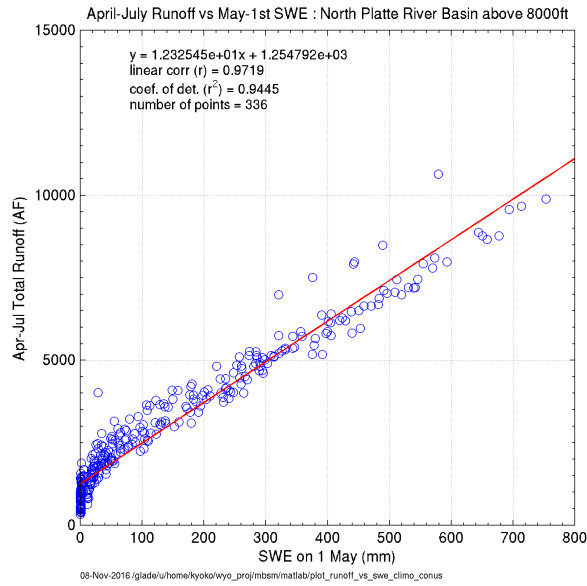


Figure 12.3. Scatter plot of total runoff (acre feet) from the WRF-CONUS model simulation in the North Platte River Basin above 8,000 ft MSL during April through July compared with SWE (mm) on May 1st. Red line shows the least-squared fit. r^2 is the coefficient of determination and r is the linear correlation coefficient.

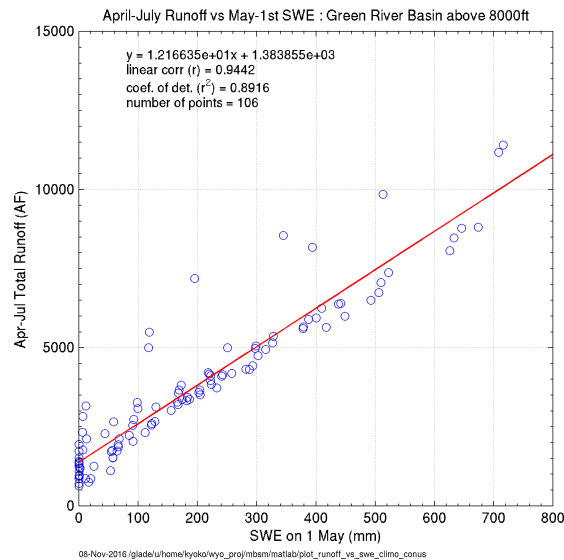


Figure 12.4. Scatter plot of total runoff (acre feet) from the WRF-CONUS model simulation in the Green River Basin above 8,000 ft MSL during April through July compared with SWE (mm) on May 1st. Red line shows the least-squared fit. r^2 is the coefficient of determination and r is the linear correlation coefficient.

Table 12.2. 8-yr (2000–2008) average annual and April–July total runoff per river basin in acre feet for areas > 8,000 ft in elevation calculated from the WRF-CONUS model simulations.

	North Platte River Basin	Green River Basin
Basin average May 1 SWE	144.7 mm	195.7 mm
Avg annual total runoff (AF)	1,289,165	471,582
Avg Apr-Jul total runoff (AF)	1,020,999	399,078
Ratio of % change in runoff to % change in snowpack	0.59	0.63

12.1.2. Assumptions for Estimating Seeding Effects on Streamflow

Seasonal Percentage of Seedable Snowpack

Results from seeding project evaluations have been interpreted incorrectly sometimes because of the many methods available for estimating seeding effects. Some report seasonal seeding impacts, which are appropriate if the measurement is a seasonal or integrated value such as with streamflow gauge data and 1 May SWE measurements. Experimental seeding projects usually measure precipitation in some form on a case-by-case basis, such as with the BRE, SPERP, and the WWMPP. When using results from these types of seeding evaluations to estimate seeding impacts on seasonal snowpack, it is necessary to also assess how often the experimental seeding events occurred in a season or how much precipitation fell during those “seedable” conditions. A climatological evaluation of a project design should include a parameter that translates seeding events or seedable conditions into a seasonal estimate.

Section 4.5 provides the seasonal estimate of the frequency of seedable conditions for the Medicine Bow and Sierra Madre Ranges. For ground-based seeding in the western regions of the Medicine Bow and Sierra Madre, seedable conditions occurred during storm periods accounting for 38–39% of the total winter (November–April) precipitation on average for the 8-year climatology (Table 4.9). In the more restrictive seeding criteria of the WWMPP, designed for a ground-seeding program, about 30% of the total precipitation occurred during seedable conditions (Ritzman et al. 2015). This difference may be in part due to the warmer maximum temperature criteria threshold used in this study (-6°C), which would allow for more seeding opportunities in this study compared with the colder maximum temperature threshold used in the WWMPP (-8°C).

Airborne-seeding conditions over the western regions occurred during periods affecting 56–58% of the total precipitation on average for the 8-year climatology (Section 4.5). For the calculations used in estimating the streamflow changes due to cloud seeding, the lower value of each of the estimates from the climatological analysis is used (e.g., 38% for ground-based seeding and 56% for airborne seeding).

Areal Coverage

If the technique for estimating seasonal snowpack changes resulting from seeding is based upon measuring the impact at a single point (as was the case for the WWMPP analysis), then a factor for areal coverage of the seeding impacts is required. This is because the response variable (i.e.,

the measure of the seeding effect) in the WWMPP was determined at one measurement point or small area. The areal coverage is then necessary to extrapolate that result to the larger target area. However, if the response variable, and hence the seeding effect, is derived from an areal measurement (i.e., over a target area), such as in the SPERP measurements or from three-dimensional model simulations, then there is no need to perform this extrapolation. The technique used in this study for estimating streamflow changes is based upon the preliminary WWMPP analysis, because it is an estimate of seeding impacts on a *seasonal* basis, which is necessary for streamflow estimation. The model evaluation performed as part of Section 6 only simulated a few cases, given the resources available to this study, and therefore cannot be utilized directly to estimate streamflow benefits. Since these estimates are based upon the preliminary WWMPP analysis, an areal coverage parameter is needed.

The areal coverage of seeding effects varies depending on the storm and seeding conditions. The preliminary WWMPP evaluation technique used a range of 50–80% (WWDC 2014). An examination of the case studies in Section 6.4 shows that this remains a reasonable coverage estimate for the current tested project designs.

12.1.3. Regression-based Estimates of Streamflow Changes due to Seeding

The technique used in the draft WWMPP report (WWDC 2014) for calculating streamflow changes is essentially repeated here using the preliminary WWMPP seeding results (5–15% per season relative to seedable storms), but using other parameters specific to the current operational project design. Although there is clearly a range of possible values, the percentage of precipitation accumulation that occurred when ground-based or airborne-seeding criteria existed is assumed to be a fixed 38% or 56%, respectively, of seasonal precipitation—the average value from the climatology results (Table 4.9). Similarly, the conversion of streamflow increase to precipitation increase (percentage) is assumed to be a fixed ratio of 0.60. The total April–July runoff into the North Platte and Green River Basins from the Medicine Bow and Sierra Madre Ranges above 8,000 ft MSL was estimated at approximately 1,400,000 AF (Table 12.2, combined) and the areal coverage of seeding in the assessment area (50–80%). The combined influence of these variables on potential increases in streamflow are demonstrated in Figure 12.5. Note that there is a difference in the maximum seeding temperature threshold used in this study (–6 °C) compared with that used in the WWMPP (–8°C). Since the efficiency of AgI activation has been shown to be less at warmer temperatures, the seeding effects (i.e., 5–15% per season relative to seedable storms) preliminarily reported by the WWMPP (WWDC 2014) may be greater than what could be realized for cases identified using this warmer temperature threshold. Nonetheless, the warmer temperature threshold allows for many additional cases to be considered seedable (Section 4.4), and if each of those cases also contribute to the seasonal seeding effect, the reduced magnitude of seeding effects due to reduced AgI activation efficiency could potentially be offset because more cases would be seeded and thereby could accrue similar seasonal results. Nonetheless, this caveat in the analysis should be kept in mind when interpreting the results.

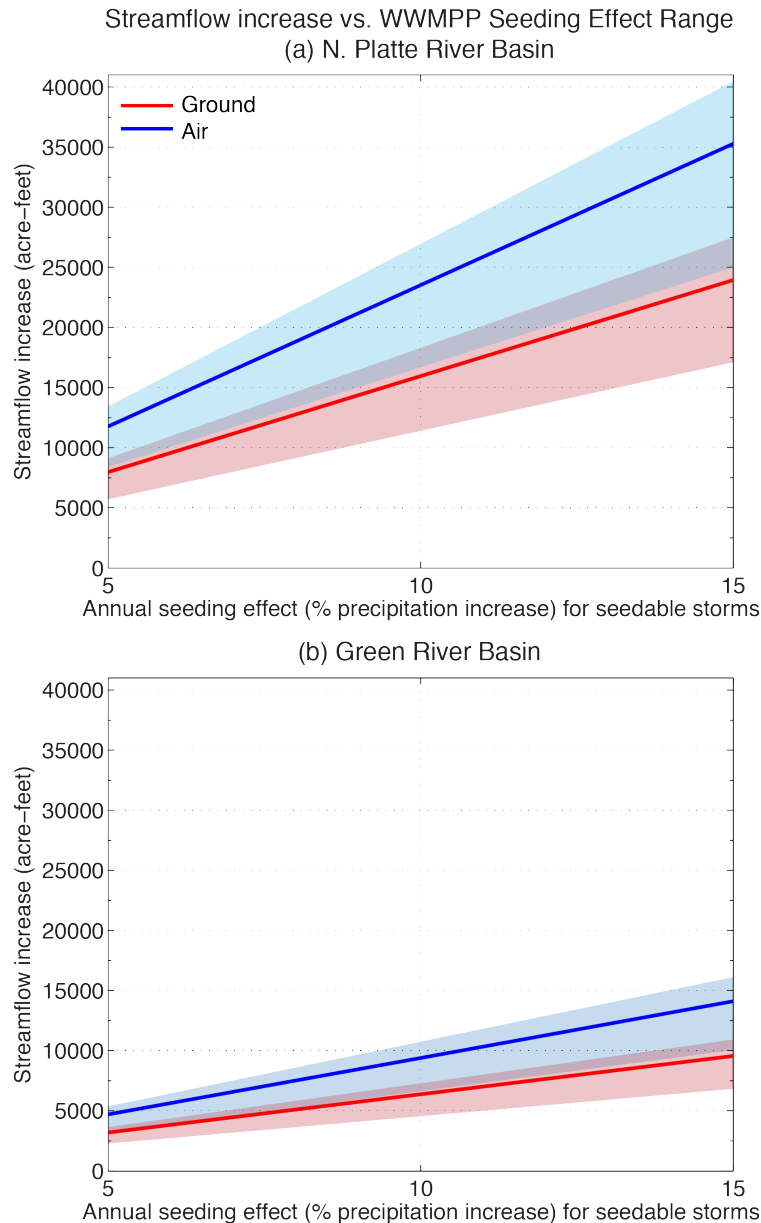


Figure 12.5. Estimates of streamflow increases into the (a) North Platte River Basin and (b) Green River Basin using the 5, 10, 15% levels of seasonal seeding effects for seedable storms from the draft WWMPP report. The streamflow calculations include adjustments to relate the seeding effects to total assessment area precipitation, which requires an estimate of assessment area seeding coverage. The range of streamflow estimates for the various levels of area coverage (50–80%) are denoted by the different color-shaded areas. Different colors represent the estimates based on a ground-based (red) or airborne-based (blue) seeding program. The 70% area coverage (solid lines within the color-shaded areas) are used for streamflow estimates assumed in the benefit/cost calculations. Note: there is overlap between the shaded regions, which is indicated by the light purple shaded areas.

Table 12.3. Streamflow increase estimates using various seeding impact parameters for a ground-based seeding program (5, 10, 15% seeding effect and 50-80% seeding impact area). Estimated April–July streamflow increases (AF) are provided using the 70% impact area (shaded row) estimated increases.

Method	Seeding Effect Scenario		
Seeding effect (increase)	5%	10%	15%
Seasonal seeding impact (38% seeding precip/total precip)	1.14%	2.28%	3.42%
50% assessment area coverage	0.57%	1.14%	1.71%
70% assessment area coverage	0.80%	1.60%	2.39%
80% assessment area coverage	0.91%	1.82%	2.74%
Apr-Jul Streamflow Increase (AF) North Platte @ 1,000,000 AF total	7,980	15,960	23,940
Apr-Jul Streamflow Increase (AF) Green River @400,000 AF total	3192	6384	9576
Apr-Jul Streamflow Increase (AF) North Platte and Green River Basins combined @1,400,000 AF total	11,172	22,344	33,516

Table 12.4. Same as Table 12.3, except for an airborne-seeding program.

Method	Seeding Effect Scenario		
Seeding effect (increase)	5%	10%	15%
Seasonal seeding impact (56% seeding precip/total precip)	1.68%	3.36%	5.04%
50% assessment area coverage	0.84%	1.68%	2.52%
70% assessment area coverage	1.18%	2.35%	3.53%
80% assessment area coverage	1.34%	2.69%	4.03%
Apr-Jul Streamflow Increase (AF) North Platte @ 1,000,000 AF total	11,760	23,520	35,280
Apr-Jul Streamflow Increase (AF) Green River @400,000 AF total	4,704	9,408	14,112
Apr-Jul Streamflow Increase (AF) North Platte and Green River Basins combined @1,400,000 AF total	16,464	32,928	49,392

12.2. WRF-Hydro Simulation of Seeding Impacts on Streamflow

To assess the impact of cloud seeding on surface hydrology, and water resources in particular, atmospheric forcing data from two WRF simulations (water years 2010 and 2012) were fed through the WRF-Hydro modeling framework to simulate snow states and streamflow. The modeling domain chosen (Figure 12.6) is centered over the Medicine Bow and Sierra Madre Ranges where ground-based glaciogenic seeding activities were being targeted. Eight USGS stream-gauge points were chosen for analysis. Their delineated upstream headwaters are shown in the domain overview. The size of the region is around 24,000 km² ranging from northern Colorado to central Wyoming. However, the cloud seeding took place over the Medicine Bow and Sierra Madre Ranges.

WxMod Overview

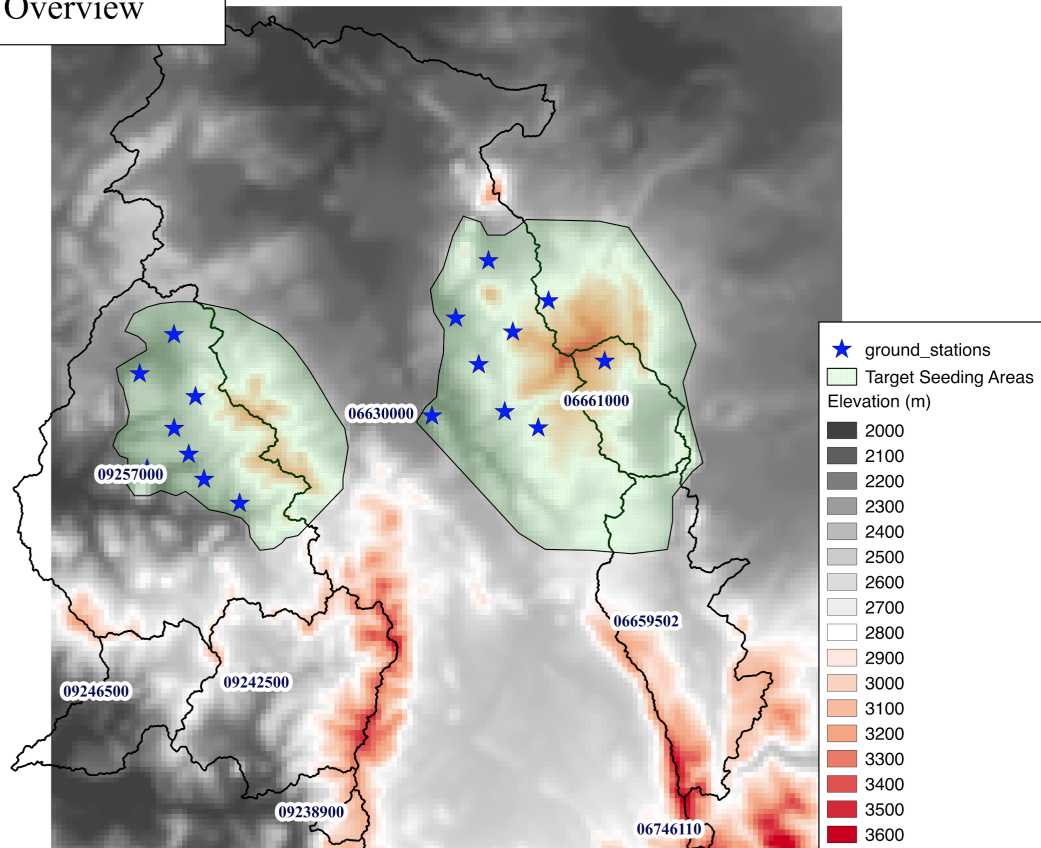


Figure 12.6. Overview of the WRF-Hydro modeling domain, along with seeding ground-based stations and targeted regions for increased precipitation.

12.2.1. Description of WRF-Hydro and Methods for this Study

The community WRF-Hydro modeling system was used as the hydrologic modeling framework for quantifying the spatially distributed patterns of snowpack, snowmelt, runoff, and streamflow impacts from cloud seeding. The WRF-Hydro system is a multi-scale, multi-physics modeling framework, which allows for flexible representation of spatial elements and hydrologic processes. Figure 12.7 shows the workflow for the WRF-Hydro modeling system. The column land-surface physics in this study, including vertical representation of snowpack, snowmelt, infiltration, vertical soil water transport, and evapotranspiration were modeled using the community Noah-MP LSM deployed on a 1-km spatial resolution grid. Once the column land-surface states and fluxes have been calculated, they are disaggregated to a higher-resolution terrain routing grid. For this study, that grid is a 250-m resolution grid. Surface runoff, ponded water, and soil moisture are disaggregated to the routing grid to route water at the surface and subsurface using a steepest descent method. The details of the diffusive wave overland flow formulation and the Boussinesq subsurface flow formulation are described in Gochis et al. (2015).

In addition to the 250-m routing grid, a pre-defined channel network is used to route water along streamflow reaches within the domain. This channel network is based on the National Hydrography Dataset Plus Version 2.1 (NHDPlus V2) streamflow network. Routing along the channel network is performed using Muskingum Cunge, which depends on the channel length

and pre-defined parameters for various stream order values. Once water routed on the high-resolution routing grid reaches a high-resolution grid cell defined within the channel network, the water is placed into the channel reach for channel routing. Figure 12.8 shows the NHDPlus V2 channel network across the modeling domain, which contains approximately 10,000 individual reaches. This high-resolution spatial discretization of land surface and channel hydrologic processes provides a first-in-time physical description of the hydrologic impacts of cloud seeding activities.

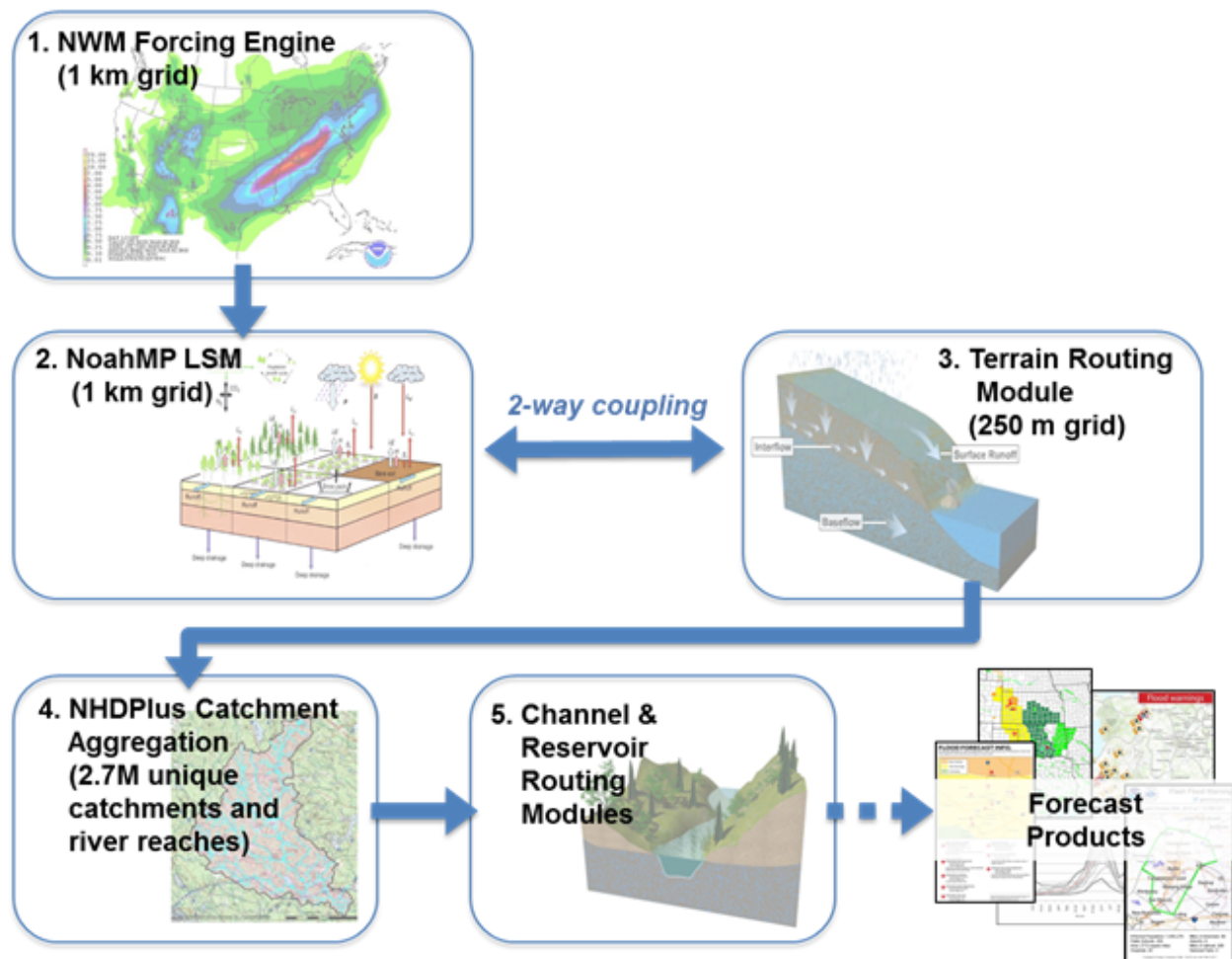


Figure 12.7. WRF-Hydro sequence of operations used in this study and in the NOAA National Water Model (NWM).

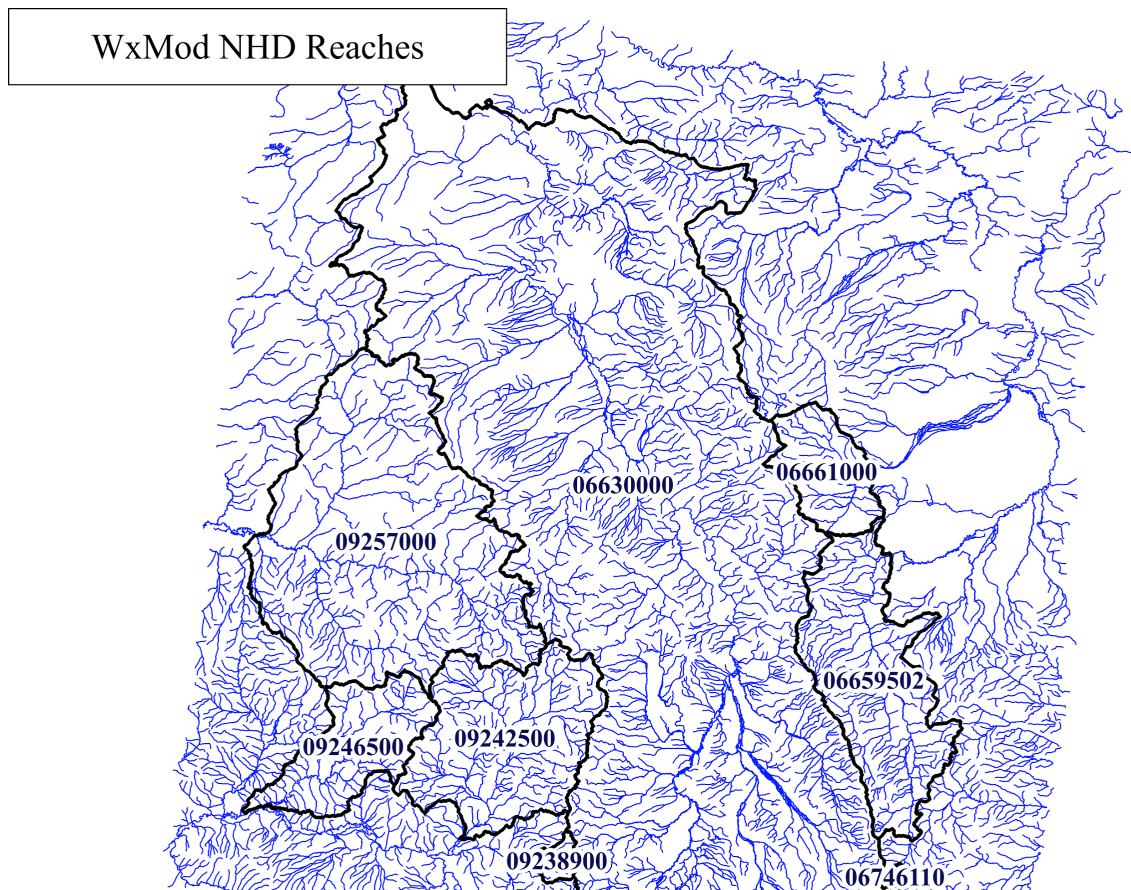


Figure 12.8. Overview of NHDPlus V2 reaches across modeling domain.

Three simulations were run during the 2010 and 2012 water years, covering multiple cloud-seeding periods between November and May of each year. The Noah-MP LSM component was run at an hourly time step, with high-resolution lateral routing taking place every 6 seconds (steepest descent). For the 2010 water year, the simulations began on 15 November 2009, while the simulations began on 16 November 2011 for the 2012 water year. The model was initiated with a multi-year spin up to ensure equilibrium of land-surface hydrologic states. While simulated cloud-seeding activities occurred during the winter/early spring period, typically through early April, the WRF-Hydro hydrologic simulations continued to the end of the water year (1 October) to capture the streamflow response from the seeding throughout the remainder of the water year, thereby providing a complete assessment of full water budget and water resources impacts.

The first simulation was run using forcing from the National Land Data Assimilation System (NLDAS) as a reference in order to establish a baseline simulation to compare against and ensure the WRF-forced simulations were within reasonable bounds. Hourly NLDAS forcing fields (precipitation, surface temperature, surface pressure, incoming shortwave radiation, specific humidity, incoming longwave radiation, U-wind, and V-wind components) were subsetting from hourly downscaled NLDAS fields that covered the continental United States. These larger NLDAS fields were processed for retrospective simulations of the NOAA National Water Model (NWM-<http://water.noaa.gov/about/nwm>), which is a similar configuration of the community

WRF-Hydro system. Because of the relatively coarse resolution of the NLDAS forcing data (12 km), fields of temperature, humidity, pressure, and incoming shortwave radiation are topographically downscaled to the 1-km WRF-Hydro/Noah-MP LSM grid. Processing forcing data for the two WRF model simulations that account for the seeding process was a multi-step process. Throughout the course of each snow season, a continuous unseeded WRF simulation (“control forecast”) produced hourly output on a 2-km Lambert conformal grid centered over the region. Forcing data needed for WRF-Hydro from the control forecast were interpolated to the 1-km WRF-Hydro/Noah-MP LSM modeling domain using bilinear interpolation. For a select set of precipitation events throughout the winter season, two additional WRF simulations were run for the period encapsulating the precipitation event. Of these two WRF simulations, one had no cloud seeding and thus served as a “control” case, while the other WRF simulation contained a physics-based representation of cloud seeding (Xue et al. 2013) during periods when the WWMPP randomized seeding events occurred. The precipitation fields from these two simulations were also interpolated to the modeling domain. After interpolation took place, a difference between the two event-based precipitation fields was calculated and added to the original interpolated continuous hourly WRF control forecast forcing. Once the continuous WRF forecast simulations ended in April, the NLDAS forcing data, with no additional adjustment for seeding activities, was used in place to carry the hydrologic simulations to the end of the water year.

12.2.2. WRF-Hydro Results

A first step in assessing the impact of the cloud seeding on local hydrology and water resources was to perform a summation of the precipitation differences across the two snow seasons. Figure 12.9 shows the spatial difference in SWE between the non-seeded and seeded run for 1 May 2010, along with the accumulated precipitation differences. As expected, the concentrations of highest precipitation gains are co-located within the key cloud-seeding target areas and associated changes in WRF-simulated precipitation. Net increases here are in excess of 5 mm, with a few isolated locations exceeding 7 mm of total liquid-water equivalent of precipitation. However, downwind, out of area impacts can also be seen, leading to small increases (1–3 mm) across southern portions of the modeling domain. There are also a few scattered areas of small decreases in accumulated precipitation. However, these regions are small compared with the area covered by either neutral precipitation gains, or precipitation gains. Figure 12.10 shows accumulated precipitation differences for the 2012 water year. The behavior is similar to 2010, except the peaks are slightly lower over the Medicine Bow and Sierra Madre Ranges. The southern portion of the modeling domain contains slightly less positive accumulated precipitation differences. However, the scattered nature of small net decreases is similar in nature to the 2010 analysis.

Because the cloud seeding occurred when conditions supported frozen precipitation, the vast majority, if not all, of the precipitation increases fell as snow. The spatial pattern of SWE increases/decreases matches the contour pattern of precipitation increases fairly well (both in spatial distribution and magnitude; Figure 12.9). This supports the notion that not only a majority of the precipitation from cloud seeding was frozen, but also a majority of it is being held in the snowpack prior to melt out in the spring. Figure 12.10 shows the same SWE and precipitation difference, but for 1 April 2012. This date was chosen as opposed to 1 May as the melt season began earlier in 2012 than in 2010, translating to an earlier peak SWE date. As with the 2010

water year, the spatial SWE difference field matches the precipitation difference field in pattern and magnitude.

May 1st, 2010 SWE/Precipitation Difference

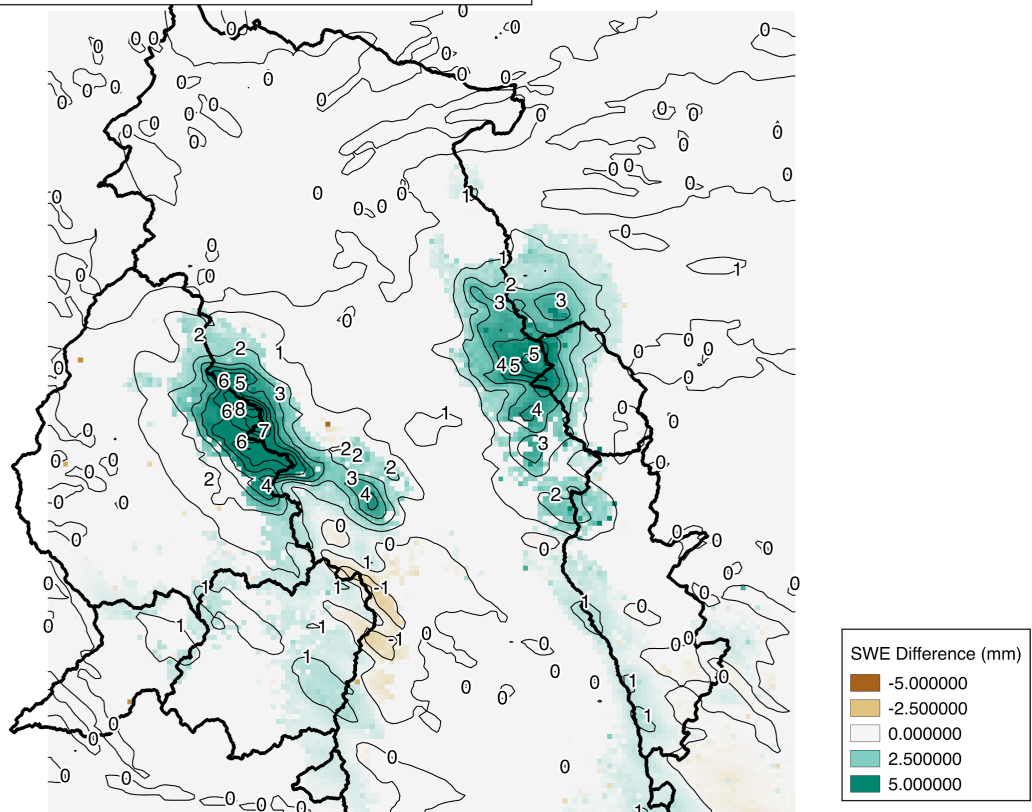


Figure 12.9. Difference between seeded and unseeded SWE for 1 May 2010 (colored), along with accumulated precipitation difference (mm) (contour).

April 1st, 2012 SWE/Precipitation Difference

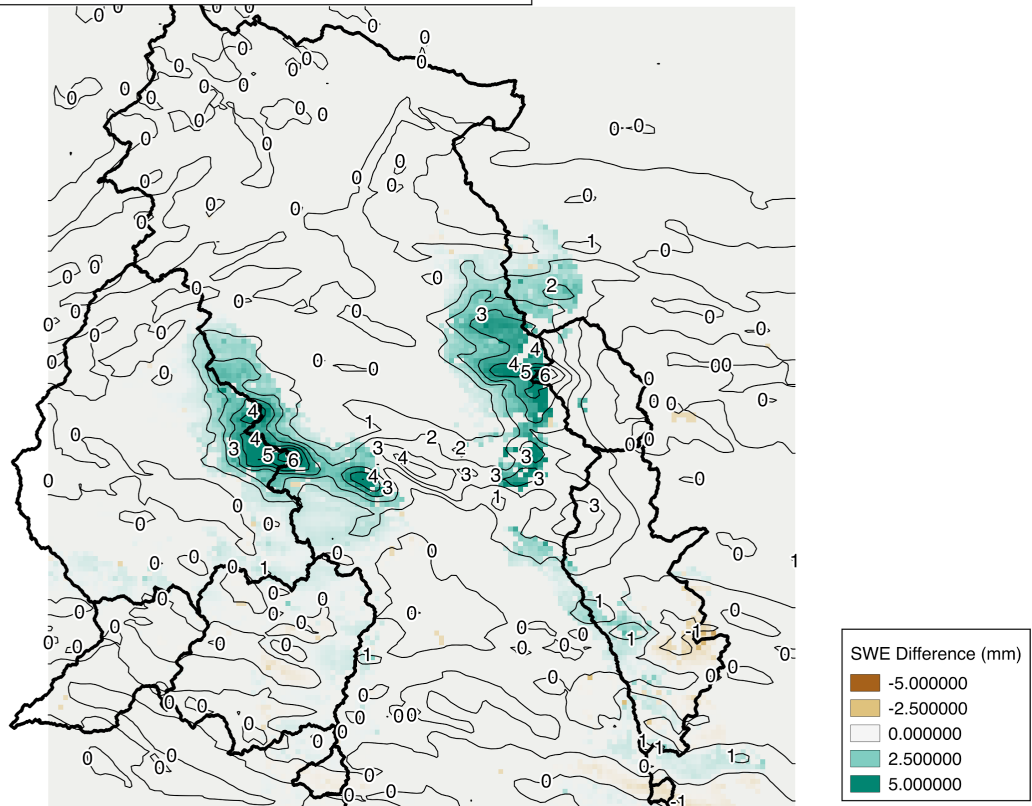


Figure 12.10. Difference between seeded and unseeded SWE for 1 April 2012 (colored), along with accumulated precipitation difference (mm) (contour).

While water is routed along nearly 10,000 channel reaches within the domain, the impacts of seeding activities, both positive and negative, are focused over a more limited area of the domain. Referring back to Figure 12.6, output at eight channel reach locations corresponding to USGS gauges were chosen for analysis. Streamflow was analyzed from the beginning of the simulation period to the end of the water year (1 October). Differences in streamflow were converted to a volume by integrating the hourly instantaneous streamflow discharge values (cubic meters per second) over time. Table 12.5 and Table 12.6 show results of these differences in terms of AF and percent difference from the non-seeded to seeded simulations for the eight basins. The two largest basins (ID #6630000 and #9257000) experienced gains of 0.25%–0.50%, respectively. Their combined gain in AF ranged from a little over 4,000 AF during the 2010 water year to a little over 6,000 AF during the 2012 water year. When all eight basins are combined, the total gain for the 2010 water year is approximately 7,750 AF (Table 12.5). For the 2012 water year, the combined gains were less, at just under 5,000 AF (Table 12.6). While there were a couple basins that experienced a net loss of streamflow, their combined losses for both water years only totaled around 40 AF, which is very small when compared with total gains. Figure 12.11 and Figure 12.12 show the distribution of total gains/losses across the domain by each basin for the 2010 water year and 2012 water year, respectively. Figure 12.13 and Figure 12.14 show the same gains/losses in terms of percent change. The majority of the gains are found

in the more northern basins where the majority of the cloud seeding took place. The southern basins have either very little change, or a very small net loss in streamflow.

Table 12.5. Summary streamflow results for the 2010 water year by basin.

<u>Basin ID#</u>	<u>Percent Change</u>	<u>Acre-Feet Change</u>
6630000	0.240	3928.97
6610000	0.538	495.97
9257000	0.402	2152.78
9246500	0.222	188.11
6659502	0.159	397.19
9242500	0.161	593.64
9238900	0.046	17.19
6746110	-0.209	-21.98
8-Basin Total	0.257	7751.87

Table 12.6. Summary streamflow results for the 2012 water year by basin.

<u>Basin ID#</u>	<u>Percent Change</u>	<u>Acre-Feet Change</u>
6630000	0.413	3377.67
6610000	1.267	306.08
9257000	0.232	716.03
9246500	-0.010	-3.80
6659502	0.252	290.35
9242500	0.056	122.46
9238900	-0.050	-7.81
6746110	-0.081	-3.89
8-Basin Total	0.311	4797.09

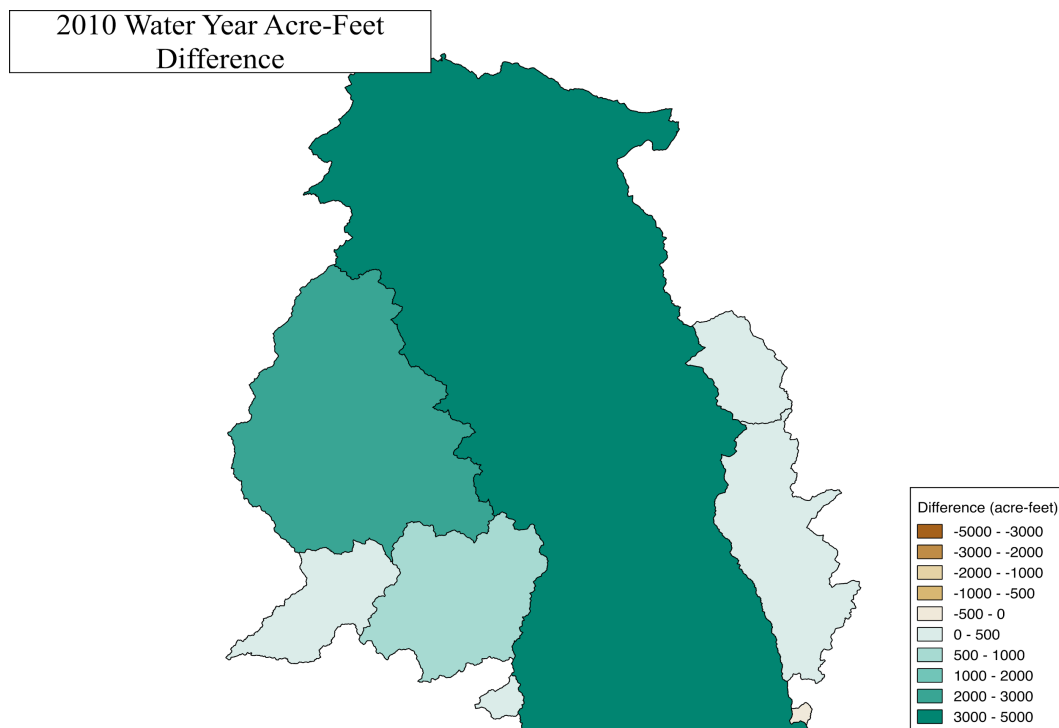


Figure 12.11. Total accumulated streamflow differences for the 2010 water year from the non-seeded to seeded simulation by basin.

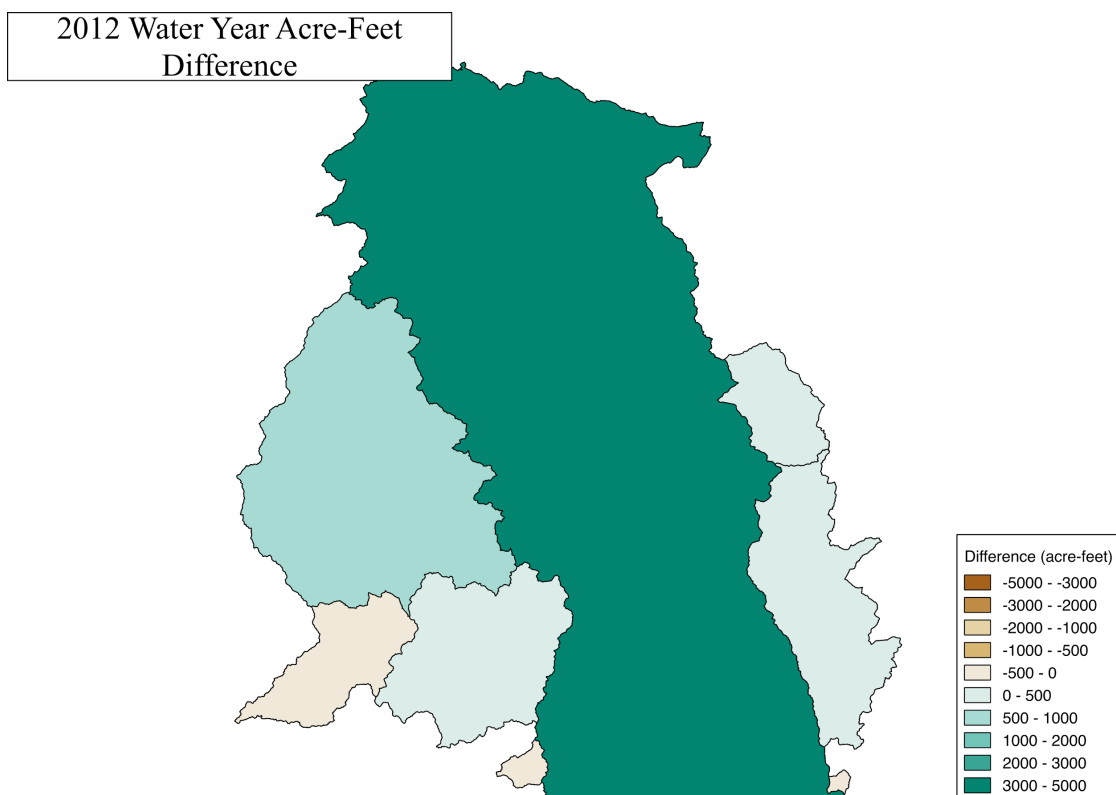


Figure 12.12. Total accumulated streamflow differences for the 2012 water year from the non-seeded to seeded simulation by basin.

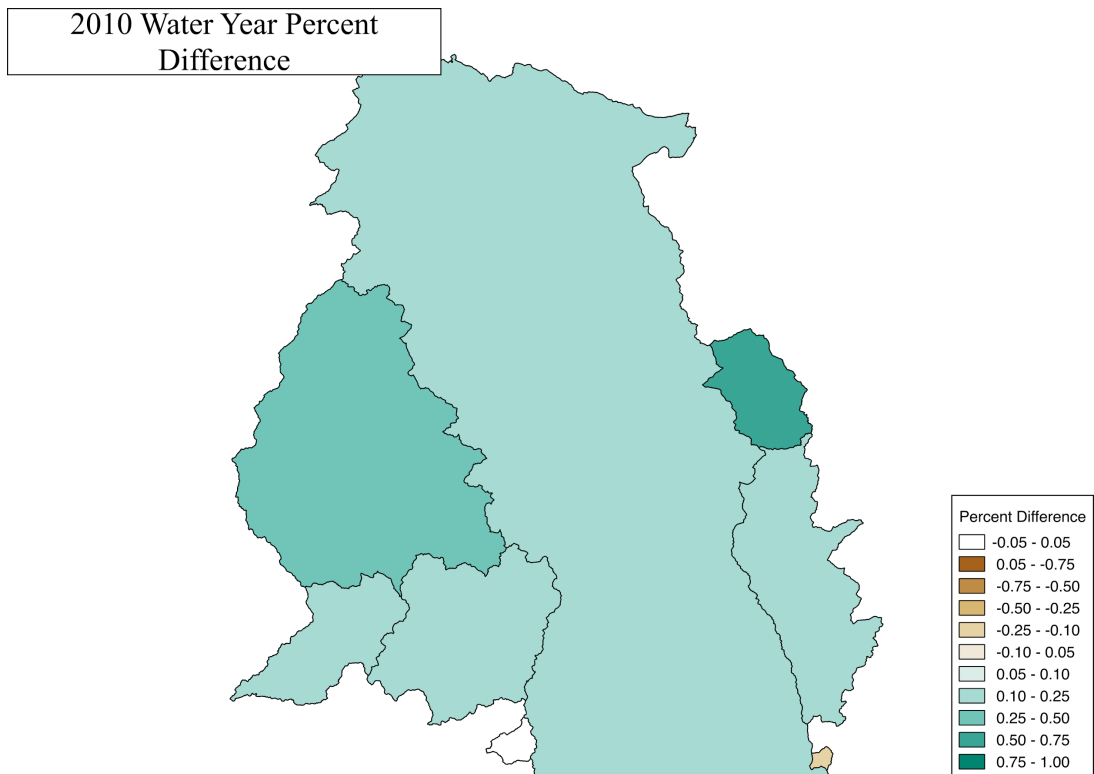


Figure 12.13. Total percent streamflow differences for the 2010 water year from the non-seeded to seeded simulation by basin.

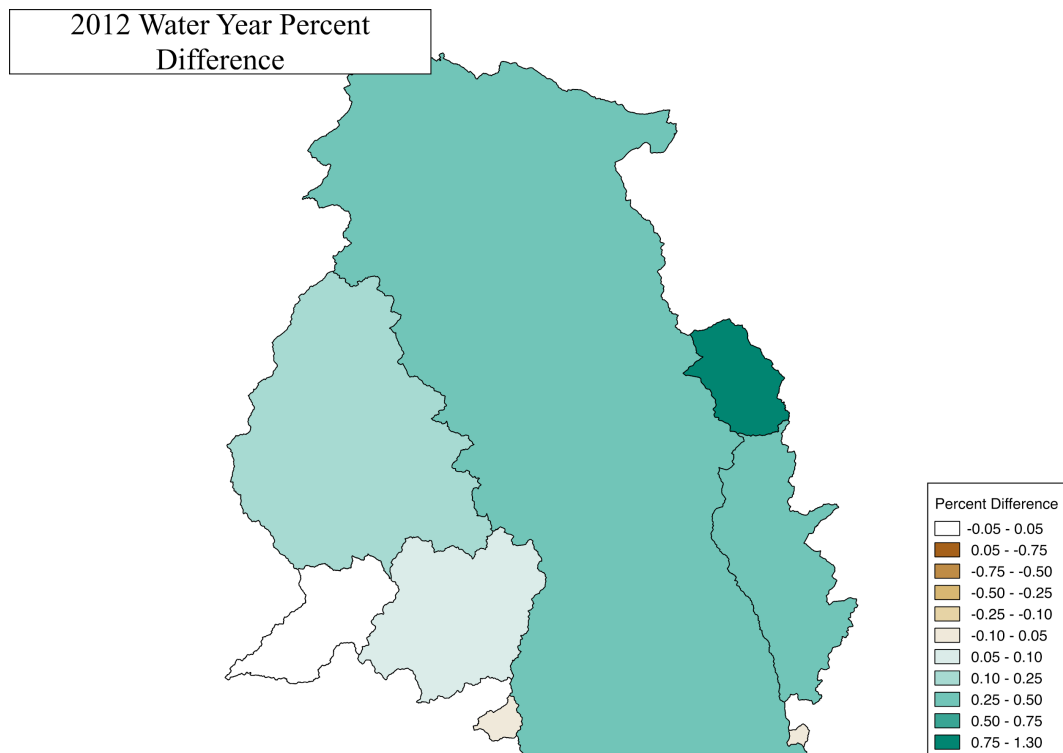


Figure 12.14. Total percent streamflow differences for the 2012 water year from the non-seeded to seeded simulation by basin.

To examine the temporal and spatial patterns of the streamflow gains/losses in-depth, additional analysis was performed to understand the local hydrologic response due to the cloud seeding. Figure 12.15 shows a time-series plot of the difference in streamflow between the non-seeded and seeded results for basin #6630000, which is the largest basin in the modeling domain. There are a few instances early in the melt season where streamflow decreases slightly. This may be attributed to a delay in snowmelt due to a deeper snowpack taking slightly longer to ripen prior to melt out. However, the remainder of the melt season shows a net increase of streamflow in the cloud-seeding experiments that peaks during June. Figure 12.16 shows a spatial distribution of accumulated streamflow gains/losses by each of the 10,000 NHDPlus V2 channel reaches represented in WRF-Hydro for 15 June 2010. While there are a few reaches where small net losses occurred, there is a large percentage of channel reaches where streamflow increased. Not surprisingly, the gains are near or downstream of where the snowpack increased as a result of the seeding activities represented in the WRF model simulations. It is interesting to note how the results propagate downstream to the basin outlets, in some cases, far from where the cloud seeding took place. Figure 12.17 shows the same results for 15 May 2012. As with the 2010 water year, the streamflow response propagates well beyond the cloud-seeding region. It is also noted that there was a positive streamflow response that extends to the east from the modeling domain into eastern Wyoming.

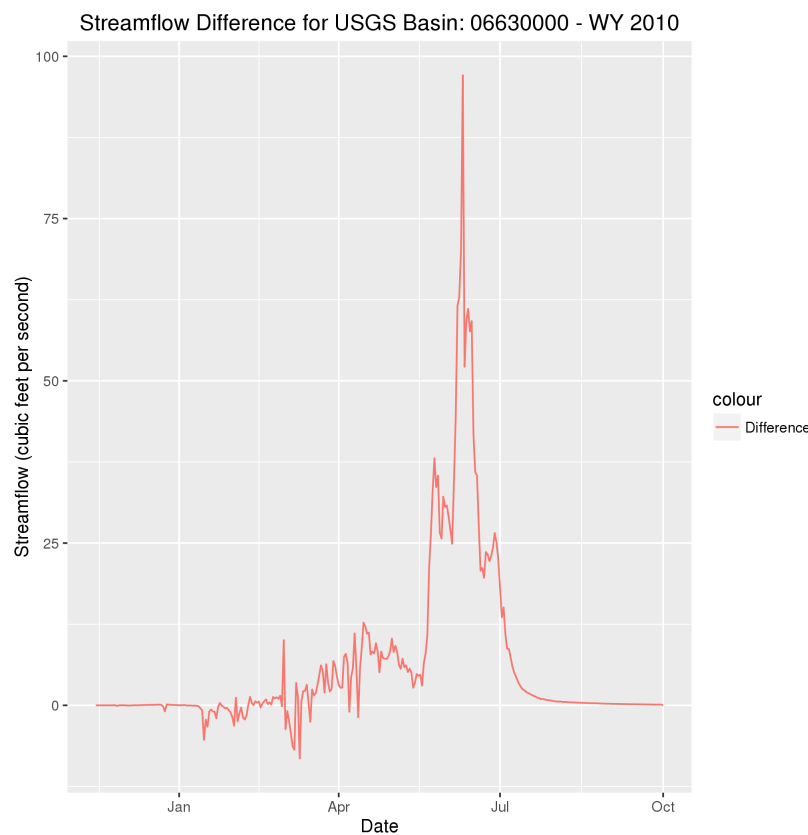


Figure 12.15. Difference in streamflow (ft³/s or cfs) between the non-seeded and seeded simulation during the 2010 water year at site #6630000.

WRF Hydro Model

2010-06-15 Analysis

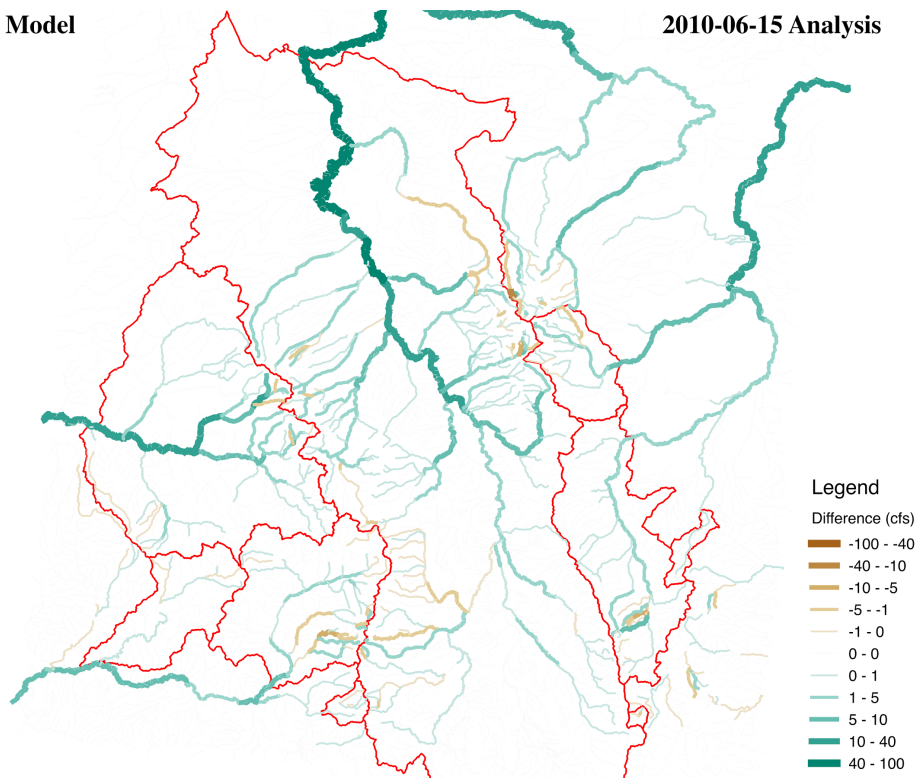


Figure 12.16. Streamflow differences (ft^3/s , or cfs) for 15 June 2010 for each channel reach in the modeling domain.

WRF Hydro Model

2012-05-15 Analysis

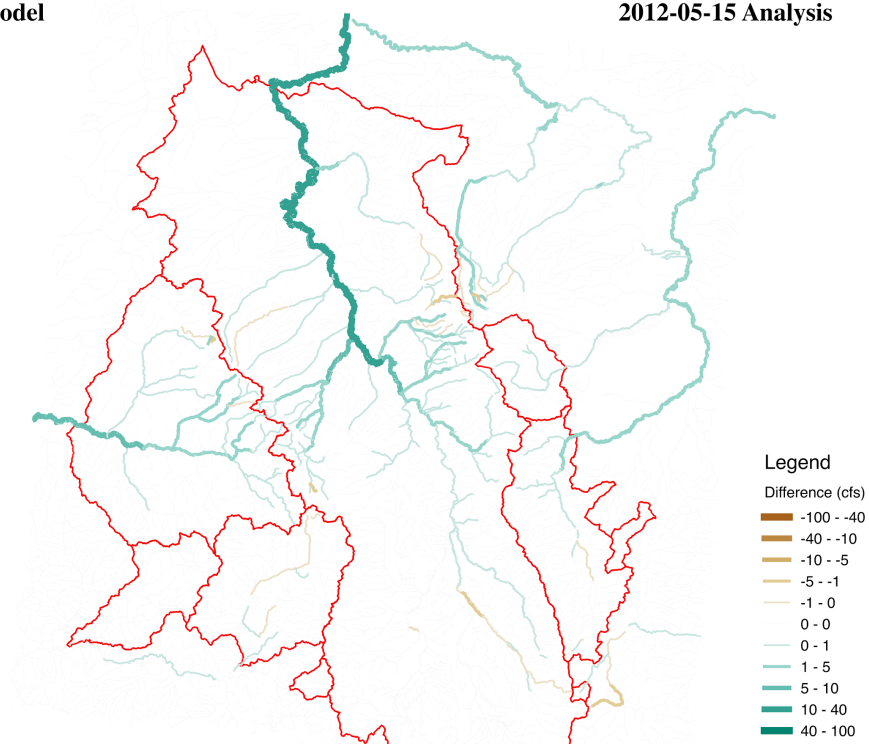


Figure 12.17. Streamflow differences for 15 May 2012 for each channel reach in the modeling domain.

As with any hydrologic study, accurately modeling streamflow to compared with observations is critical for assessing model strengths and weaknesses. Figure 12.18 and Figure 12.19 show accumulated streamflow during the 2010 and 2012 water years, respectively, compared with observations. Overall, all simulations, including the NLDAS-only forced model run, tend to overestimate streamflow for the largest basin in the modeling domain. For all of the model runs performed in this study, very minimal calibration was performed. Model parameters used for this study were selected during a large-scale calibration effort undertaken with the upgrade of the National Water Model (NWM) from version 1.0 to 1.1. Key United States Geological Survey (USGS) unregulated basins were selected across the continental United States for calibration against observed streamflow. The Dynamically Dimensioned Search (DDS) algorithm was used to adjust parameters. Once parameter convergence was met, the parameters were divided into ecological regions that shared similar physiographic and biological characteristics with the basins calibrated. This process leads to a calibrated parameter dataset for the U.S. that was subsetted for the domain used in this study. Even though regions of the U.S. were calibrated in this version of the model, not all basins studied in this project were locally calibrated. Without local calibration, and using regionalized model parameters can result in significant uncertainty in the final model parameter value specification. This uncertainty needs to be recognized in the interpretation of the results. More detailed work, beyond the initial scope of this project, is needed to improve upon model parameter specifications in these experiments and, in turn, reduce uncertainty in the results reported here.

The default model run using NLDAS meteorological forcing proves that additional calibration is warranted (Figure 12.18 and Figure 12.19). Nevertheless, the signal between the seeding and no-seeding WRF model simulations obtained from this study are robust. It is also worth noting that this basin is fairly large with man-made water management infrastructure (e.g., reservoirs and irrigation diversions) that will significantly alter natural flow conditions. While WRF-Hydro has a reservoir function to account for lake storage and reservoir management, it is very difficult to account for in distributed hydrologic simulations. Therefore, these results should be interpreted as “natural” flow responses to seeding perturbations.

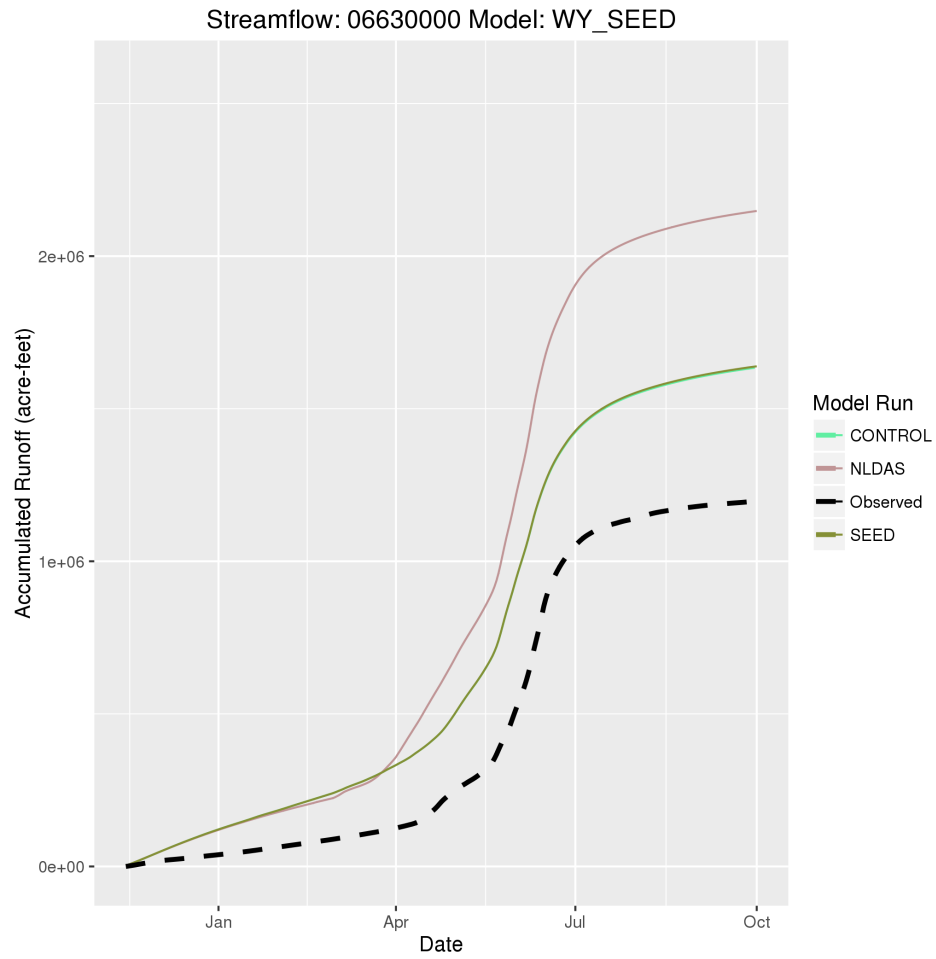


Figure 12.18. Accumulated streamflow for all three simulations and against observations for the 2010 water year at site #6630000.

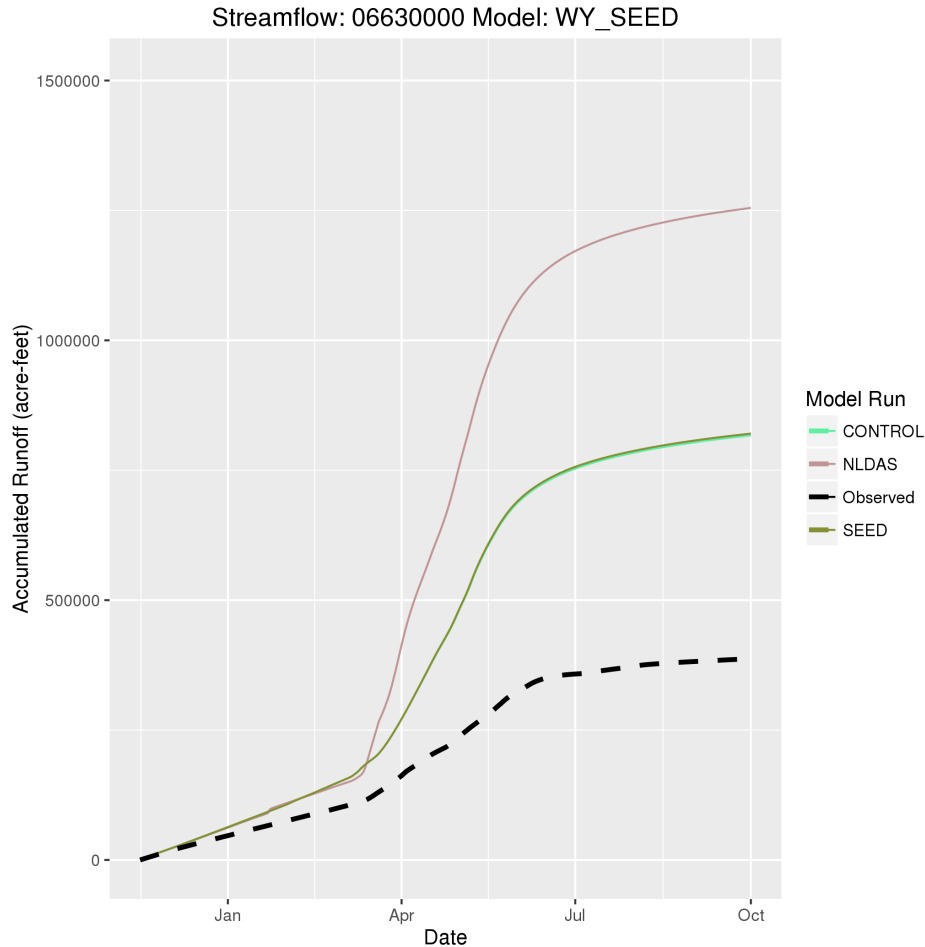


Figure 12.19. Accumulated streamflow for all three simulations and against observations for the 2012 water year at site #6630000.

To assess model performance over basins where these factors are minimized, additional analysis was performed over three USGS GAGES-II “reference” basins, which contain no significant diversions in the headwaters regions. Figure 12.20 is an overview of the basins within the domain. It should be noted a fourth basin (#9245000) is excluded from the analysis because observations were lacking for the gauge site associated with that basin. Figure 12.21–Figure 12.23 show accumulated streamflow for both water years compared with observations. Basin #6622700 shows reasonable agreement with the NLDAS-based simulations and observations, although the model overestimated streamflow for the 2010 water year while underestimating slightly for the 2012 water year. Basin #6632400 was in good agreement with observations for all three simulations for the 2010 water year. The WRF-Hydro simulations driven by WRF simulations underestimated discharge significantly for the 2012 water year at #6632400. However, the NLDAS-driven WRF-Hydro simulation was in very good agreement with observations. Collectively, these variations in WRF-Hydro simulated responses point out potential issues and uncertainties with the baseline WRF precipitation forcings. The performance for #6623800 was similar to #6632400.

USGS GAGES-II Basins

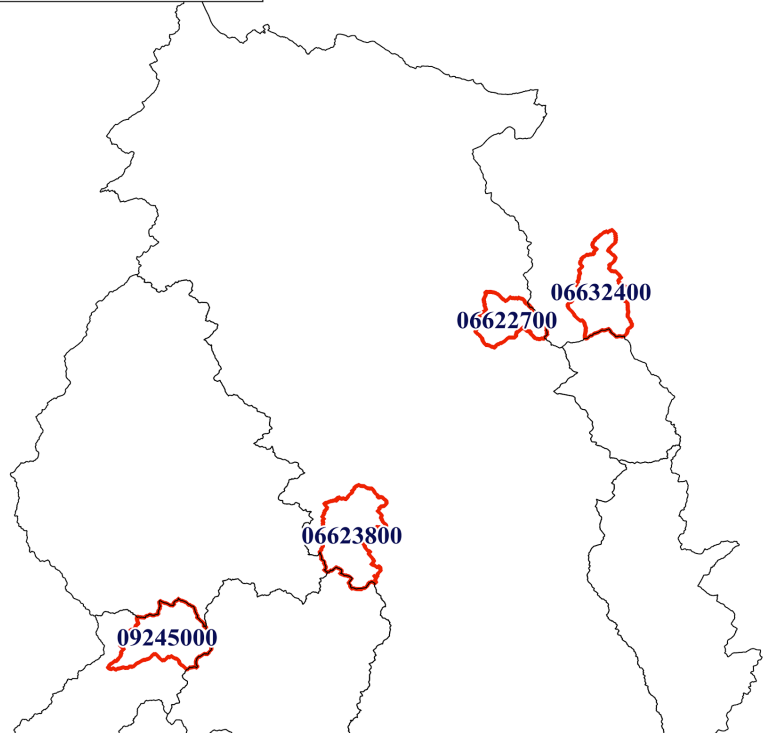


Figure 12.20. Overview of USGS GAGES-II basins located near the cloud seeding regions.

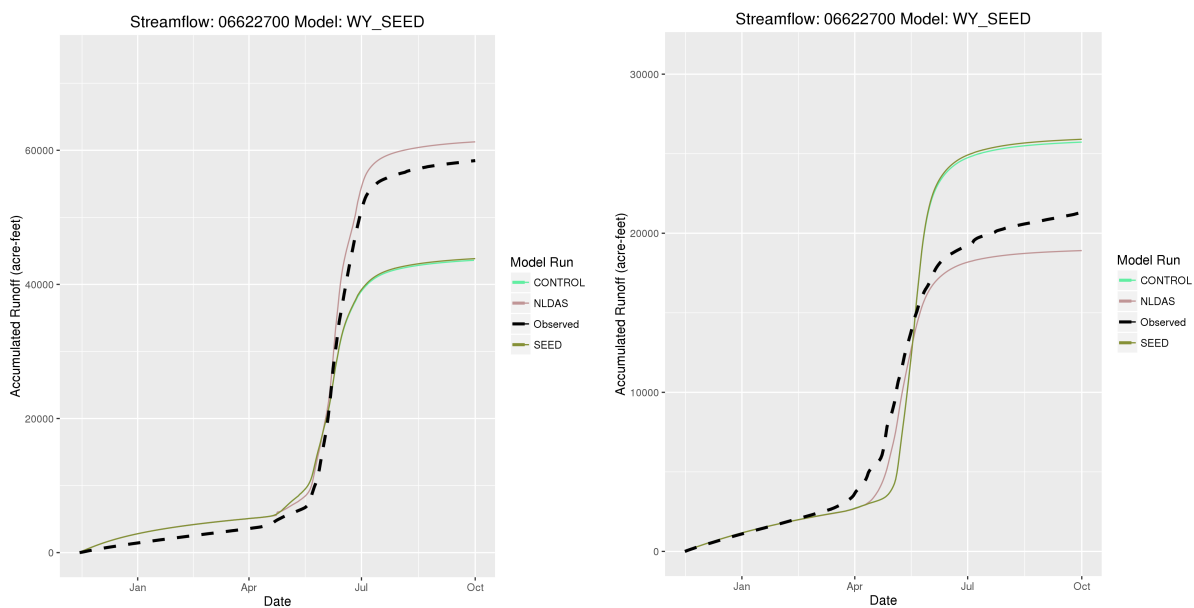


Figure 12.21. Simulated streamflow for the 2010 and 2012 water years for USGS site #6622700.

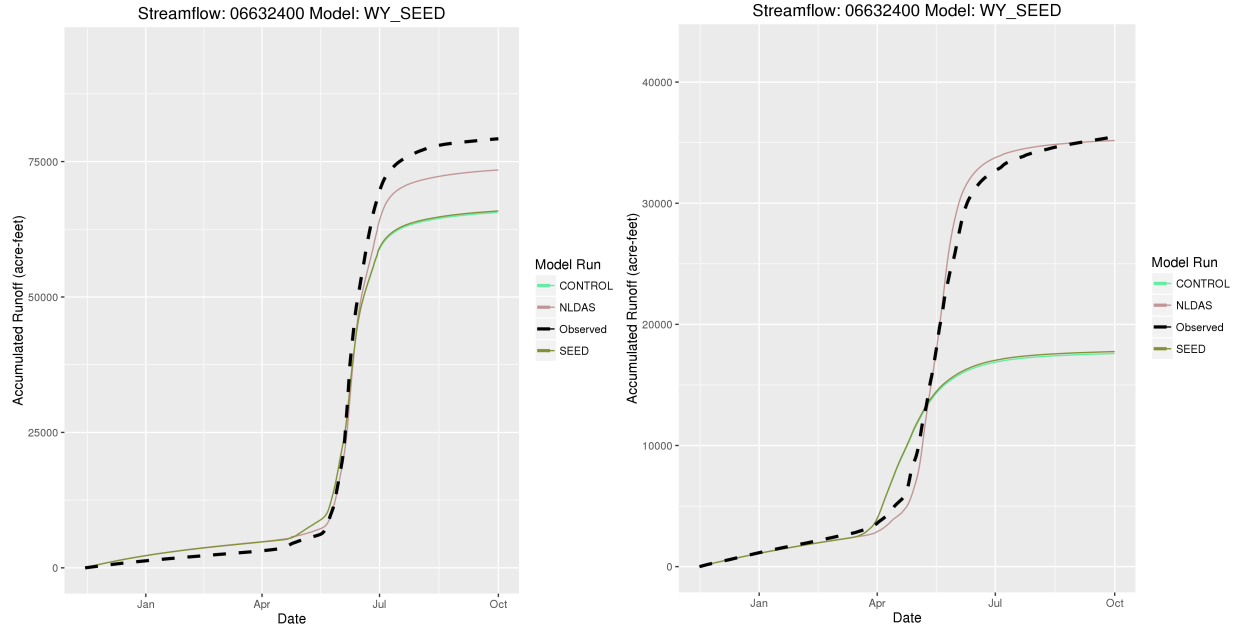


Figure 12.22. Simulated streamflow for the 2010 and 2012 water years for USGS site #6632400.

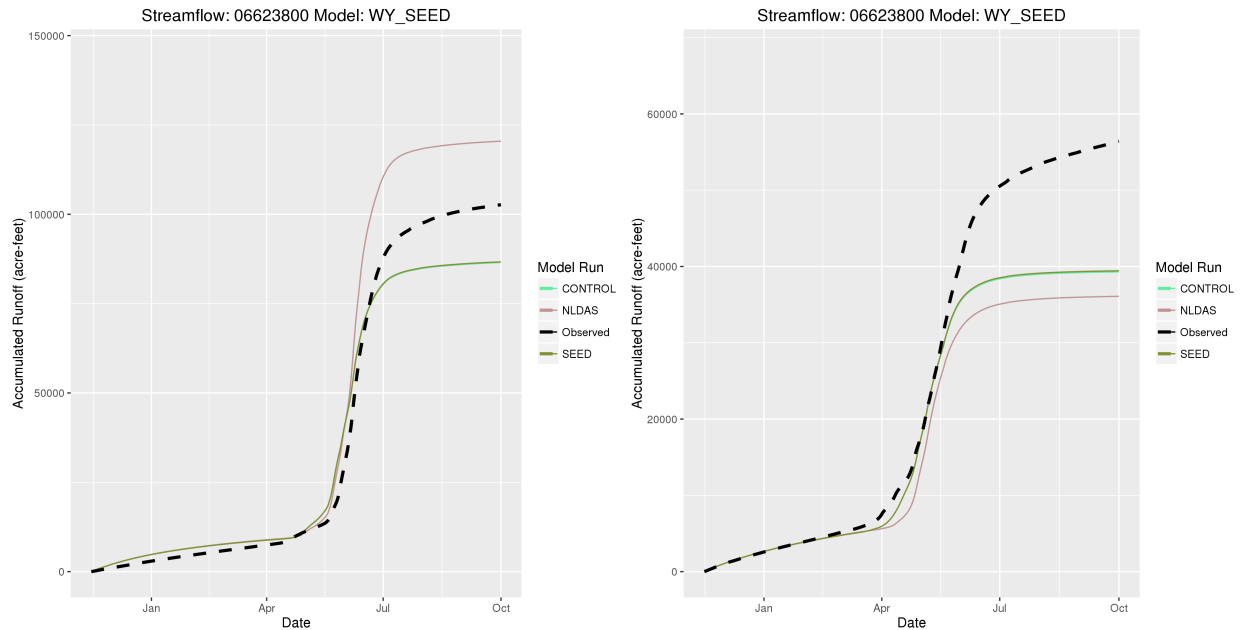


Figure 12.23. Simulated streamflow for the 2010 and 2012 water years for USGS site #6623800.

12.2.3. WRF-Hydro Analysis Summary

The analysis presented in this report demonstrates the potential hydrologic response from cloud-seeding experiments over the course of a snow season. Experiments conducted over the course of two snow seasons were performed in a seeding module within the WRF model. Differences between the seeded and unseeded simulations were driven through the physics-based, spatially distributed, community WRF-Hydro modeling framework to assess detailed impacts on snow

and streamflow response across the region. Analysis showed there was a net positive increase of both SWE and streamflow. While the percent of accumulated runoff increases across various USGS basins ranged only from 0.5–1.3%, the total net increase in streamflow in terms of volume ranged from 5,000–7,000 AF, which may be significant for certain water resources applications. Interestingly, modeled hydrologic impacts from cloud seeding propagated far from the target seeding regions to several km away at the outlet of some of the larger basins.

It is also important to note that the seeding simulations driving the seeding WRF-Hydro run were based upon limited seeding scenarios due to the nature of the WWMPP experiment. In the WWMPP, only one of the two mountain ranges was seeded at any given time, yet conditions meeting the criteria for seeding were required to be met in both ranges at the same time. Therefore, if both ranges had been seeded simultaneously and the impacts were similar for both ranges, there exists the potential for twice as much overall increase in snowpack across the basins of interest. Moreover, seeding was limited to 4-hour periods (with a 4-hour period of no seeding in between), and the temperature criterion for calling a seeding case was colder than typical operational programs. Therefore, it is possible that there were additional periods that could have been seeded, but were not during the WWMPP. As a result, if seeding was simulated during water years 2010 and 2012 for all periods when seeding conditions were met, the simulated seeding effects could have been more than currently simulated. In fact, the seeding effects could have potentially doubled (if not more than doubled) if an operational program was implemented targeting both mountain ranges at the same time, yielding similar seeding effects in both ranges, and without any limits imposed on the seeding periods.

Overall results show that cloud seeding can provide a means for increasing streamflow on a small, but potentially important, scale in regions where snowmelt-driven runoff is a primary source for water resources. However, the changes in streamflow found in this study illustrate that changes in streamflow are not a direct 1 to 1 increase or decrease in streamflow relative to precipitation changes. This is because substantial portions of the precipitation augmented by seeding operations will be sequestered by other watershed processes, such as increases in evapotranspiration and snowpack sublimation. This latter fact is hypothesized to be relevant for hydroclimatic regions where evaporative demand is significantly greater than precipitation. In such regions, marginal increases in streamflow should be expected in relation to changes in precipitation. In other regions where evaporative demand is not as great, proportionately larger increases in streamflow may result. Ongoing research is exploring these regional differences.

12.3. Synthesis of Results from Multiple Methods

The regression method presented in Section 12.1 calculated a range of total streamflow increase between ~11,170 and 49,390 AF, depending on the assumed method of seeding (ground versus airborne) and the assumed magnitude of the seeding effect (5, 10, 15%, all assuming a 70% impact area; Table 12.3–Table 12.4), while the WRF-Hydro method found 5,000–7,750 AF (Table 12.5–Table 12.6). The WRF-Hydro simulation method reduces some of the uncertainties in the traditional regression analysis, because it does not need to assume anything about the spatial distribution or magnitude of the seeding effect. Rather, those attributes from the simulated seeding cases are directly ingested as forcing into the WRF-Hydro simulation. However, at the present time, this simulation represented only two years of simulated seeding cases from the WWMPP, whereas the regression analysis represented a multi-year average scenario from the

climatology analysis. Therefore, averaging the results from the two years of WRF-Hydro simulations yields 6,375 AF of average additional streamflow.

Moreover, the regression analysis results were based upon less stringent conditions for seeding than imposed during the WWMPP (i.e., the climatology analysis used a warmer temperature criterion, no time limit on seeding periods, etc.). The 4-hour time-limit criterion and, in particular, the fact that only one target was seeded at a time, in the WWMPP will likely yield reduced seeding effects on streamflow from the WRF-Hydro method than what is estimated using the climatology analysis regression method. The reduction will depend on how long seeding criteria were actually met beyond the 4-hour limit imposed by the WWMPP, but it will likely be reduced by at least half given only one target was seeded at a time in the WWMPP. If the average WRF-Hydro results were doubled, to account for the limited seeding time periods simulated based upon the WWMPP criteria, the results indicate approximately 12,500 AF of additional streamflow could be produced from cloud seeding. This estimate is consistent with the regression analysis results for a ground-based scenario with just over a 5% annual seeding effect (in seedable storms) with an assumed 70% impact area. As a result, 12,500 AF of additional streamflow will be highlighted going forward for the cost-benefit analysis.

13. Task 12: Cost Estimates

The costs for a winter orographic cloud-seeding program designed to increase snowpack in the Medicine Bow or Sierra Madre Ranges of Wyoming would depend upon the following factors:

- the portions of the ranges targeted;
- the number of ground-based INGs deployed (Sections 5, 6, and 15);
- annual program duration (when seeding starts and stops each season);
- service contract duration (the number of operational seasons);
- the amount of the ground-based and airborne-seeding equipment to be deployed;
- whether or not the project is conducted via contract with a commercial operator, in-house (by the sponsor(s), or a blend of the two); and
- the possibility of sharing operational resources with other cloud-seeding programs.

The details and scope of each of these are discussed in the following sections.

13.1. Project Scope

The most direct approach to estimating project cost is to consider both ranges in their entirety for the predominant flow regimes (wind conditions) identified in Section 4. In such a case, the project scope will match that defined in Sections 5 and 6. However conceptually, it is possible to reduce the scope of the project to support operations in one range and not the other, and still develop an effective and less expensive cloud-seeding program. For these cost projections, estimates for each range are prepared independently, and the total cost for targeting both ranges is also provided.

As discussed in Section 7, a total of 35 potential ground-based generator sites were identified for the preliminary project design. Each of these sites has differing aspect (orientation with respect to terrain), exposure to wind flow, and elevation. While all are “good” sites, not all are necessary to build an effective cloud-seeding program. Determining which ones should be used for operations and which should not is based upon:

- generator proximity to each other (overlap of ice nucleus plumes);
- climatology (frequency of winds that would allow effective use);
- results of the cloud seeding simulations; and
- whether ground-based seeding would occasionally be complemented by airborne seeding.

Following an assessment of the original 35 generators based on these criteria, 23 sites were selected as the best suited for ground-based operations (Figure 13.1).

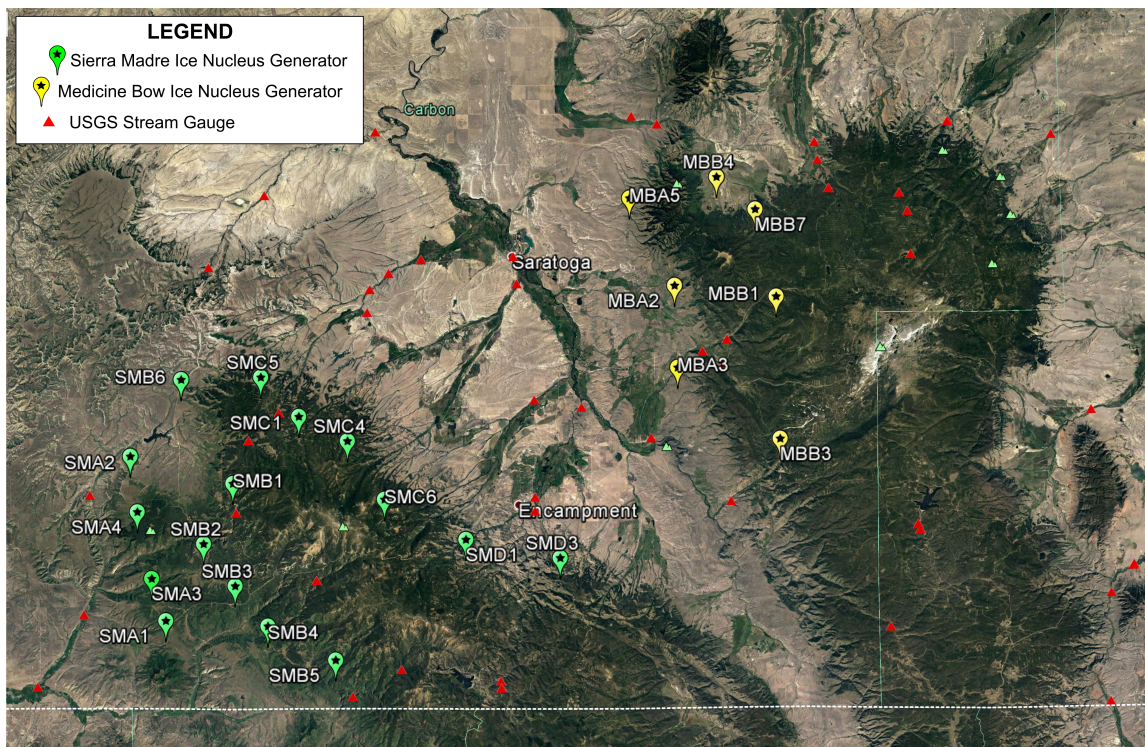


Figure 13.1. The subsets of all potential ice nucleus generator sites recommended for ground-based seeding operations in the Sierra Madre Range (left, green, 16 sites), and Medicine Bow Range (right, yellow, 7 sites). The locations of the U.S. Geological Survey (USGS) stream gaging sites are also shown (red triangles).

The sites chosen will allow seeding to occur over the greatest range of more predictable wind directions and speeds. It is noted that while IN plumes produced by lower-elevation generators may be capped in some stable situations, this is less likely in stronger wind regimes. Thus, sites farther upwind of the mountains will often afford effective targeting when winds are stronger. In these stronger wind regimes, there is insufficient time for snow crystal growth to precipitation from seeding by generators sited in or closer to the higher elevations.

13.2. Length of Program Season

The duration of a winter seeding season is largely determined by the climatology (Section 4). Typically, the beginning of the season is determined by when cloud temperatures become cold enough to allow glaciogenic seeding to produce snow, as defined by a temperature criterion of -6°C ($+21^{\circ}\text{F}$) (Section 9).

Likewise, the end of the season is determined by the typical date when the orographic clouds are no longer routinely cold enough to support ice crystal growth. Ground-based seeding opportunities during the WWMPP decreased markedly after the end of March, such that operational seasons typically came to an end by early, or mid-April. From this, the operational, ground-based seeding season is defined as five months (15 November – 15 April) for this study.

13.3. Deployment of Ground-Based Ice Nucleus Generators

The deployment cost for the ground-based IN generators will depend upon the following considerations.

- A. *Whether the generators are leased or purchased, and whether the generators will be manually operated, remotely controlled, or a mix of the two.* Given the locations of the generators proposed herein, manual operation is not considered a viable option, so these cost estimates assume all INGs will be remote-controlled units. The INGs are also assumed to be leased, rather than purchased, as this has been the precedent in recent Wyoming operations.
- B. *The amount of seeding agent and other consumables (nitrogen, propane) used by each ING, which will vary depending upon the number and duration of the seeding opportunities.* For the cost estimates in Table 13.1, the frequency of operations is based on those for the same two ranges during the WWMPP, but with modifications. The cost estimates were modified because the WWMPP criteria allowed seeding only when weather conditions over both ranges were suitable. Seeding operations were not conducted when weather conditions were suitable over only one range or the other, which occurred with some frequency. Additional adjustments have to be made because the seeding temperature threshold will be 2 °C (3.6 °F) warmer, which widens the window of opportunity for seeding, therefore impacting potential program costs. Finally, this project design places additional INGs in locations that will allow seeding to occur under some wind regimes that heretofore were not considered seedable. For example, the WWMPP seeding was limited to wind directions from the southwest through the west-northwest, whereas this design also includes some northerly and even northeasterly flow regimes to be seeded. When all the factors are considered, it is estimated that each ING could be operated for approximately 125 hours during a typical winter season.
- C. *The scope of the service and maintenance requirements for the INGs.* Once deployed, a single two-person technician team can keep a large number of INGs operating through an entire season. The number of technicians needed is determined not only by the number of generators deployed, but their proximity to each other, therefore, in some circumstances it is possible for a team to service generators on multiple ranges. Using the WWMPP as an operational blueprint, it is reasonable to assume that one team will service all the generators proposed in this study. Costs are estimated accordingly and provided in Table 13.1.

Table 13.1. Estimated operational costs of a five-month, ground-based seeding program in the Medicine Bow and Sierra Madre Ranges. Cost are based upon direct and personnel costs as of the fourth quarter of calendar year 2016.

Cost Category		<i>Combined Medicine Bow and Sierra Madre Ranges</i>
		<i>Remote-Controlled Generators (23)</i>
Deployment¹	Personnel	\$30,148 ⁶
	Direct Costs⁴	\$4,615
Operations²	Personnel	\$239,160 ⁷
	Direct Costs⁵	\$150,025
Expendables and Other Reimbursable Costs³		\$232,737
Estimated Totals		\$656,685
¹ Initial deployment costs amortized over five seasons ² Assumes an average of 57 hours per generator ³ Seeding agents, propane, etc., as applicable ⁴ Direct costs include lodging and per diem of field personnel, vehicle mileage, and shop lease. ⁵ Direct costs include generator lease costs, lodging and per diem of field personnel, shop lease, and vehicle mileage. ⁶ Three technicians working three days per generator (staging, deployment, and power up), off-season maintenance, and 0.5 month administrative support. ⁷ Maintenance, service, operations, and meteorological support (forecasting, seeding decision-making), program administration.		

The effects of seeding in each range is provided in Section 12, specifically in Figure 12.9 and Figure 12.10.

13.4. Airborne Seeding

Recent investigations found that winter orographic seeding via aircraft can be effective often when ground-based seeding is not (Xue et al. 2016, Geresdi et al. 2016). Thus, seeding by aircraft can increase the frequency of seeding opportunities above those identified for ground-based seeding alone. The primary reason is that the seeding range by aircraft is flexible, whereas seeding from fixed, ground-based generators is not.

Airborne seeding does not rely entirely on wind direction or speed to effectively target clouds suitable for seeding, whereas ground-based generators rely entirely on wind speed and direction to ensure that seeding material reaches the targeted clouds. In addition, if temperatures suitable for seeding are higher in the atmosphere, and therefore, potentially out of the reach of a ground-based generator AgI plume, the aircraft can be flown at those altitudes, provided there is still enough time for any ice crystals formed to fall the greater distance to the surface within the target. Utilizing aircraft seeding alone removes concerns regarding the deployment of, or access

to, ground-based seeding equipment, and any of the obstacles associated with the operation and maintenance of the equipment in harsh winter conditions.

However, aircraft operations have their own costs and limitations. Not only must the aircraft be leased (not owned) and configured for seeding, but the flight crew must be experienced for the work. Moreover, aircraft have limited on station (flight) times and cannot fly in low-level clouds too close to the mountains. To determine whether the inclusion of airborne seeding is an economically viable option in the Medicine Bow and Sierra Madre ranges, the results of the storm climatology (Section 4) were used to identify the frequency of situations when the lower atmosphere is not conducive to transporting ground-based seeding material over the mountain. There may also be situations when SLW is present at altitudes suitable for seeding, but at a higher altitude than may be reliably targeted with ground-based generators.

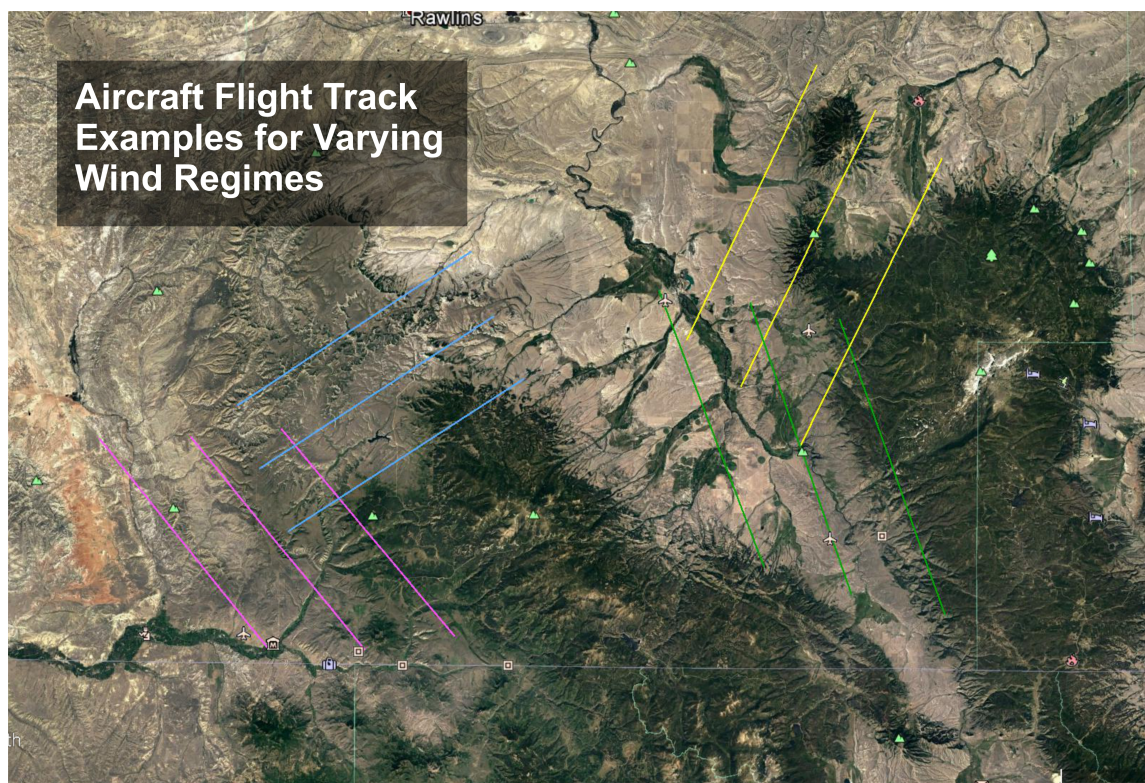


Figure 13.2. Potential aircraft flight tracks for airborne-seeding operations are shown. Location relative to the target range is determined by wind direction, distance from the range by wind speed.

For the operational cost estimates presented in Table 13.2, a single, piston-engine aircraft certified for flight in known icing conditions was considered. This cost estimate assumes that the aircraft would be operated during each season by a crew of two for 100 flight hours. The amount of seeding agent (pyrotechnics) required for the 100 flight hours was estimated and included in the overall cost calculation, as were fuel and hangar costs.

Table 13.2. Estimated operational costs of a possible five-month airborne-seeding program in the Medicine Bow and/or Sierra Madre Ranges.

Cost Category		Single Range	Both Ranges
		Seeding Aircraft ²	Seeding Aircraft ³
Deployment¹	Personnel	\$ 4,641	\$ 4,641
	Direct Costs	\$ 3,844	\$ 3,844
Operations	Personnel	\$ 180,400	\$ 180,400
	Direct Costs	\$ 101,200	\$ 105,825
Expendables and Other Reimbursable Costs⁴		\$ 51,486	\$ 67,070
Estimated Totals		\$ 341,571	\$ 361,780
¹ Twin-engine piston aircraft, certified for flight in known icing conditions ² Assumes an average of 60 flares of each type, each month, 20 flight hours per month ³ Assumes an average of 80 flares of each type, each month, 20 flight hours per month ⁴ Seeding agents, aircraft fuel, etc., as applicable Personnel costs include salaries of the flight crew (2 pilots) and meteorologist. Direct costs include lodging, per diem, aircraft lease (includes maintenance and insurance), fuel, seeding agent, and hangar and office space.			

For an operational program using only remotely controlled ground-based INGs, the estimated annual costs for a typical season are approximately \$657,000 (Table 13.1). For an airborne program using a single twin-engine seeding aircraft, operational costs would be approximately \$360,000 (Table 13.2). Both cost estimates were based on the current cost of labor, fuel, seeding material, and other expendables as of the fourth quarter of calendar year 2016. If the airborne program was expanded to six months to exploit the aircraft's ability to effectively target colder (higher) clouds earlier and later in the season, such a program would cost approximately \$67,000 more (~\$408,000).

13.5. Possible Cost Savings

Costs presented here reflect all aspects of an operational program and do not consider any of the various avenues through which a cost savings might be realized. There are several means by which a program could potentially cut costs, and those options are explored in the Sections that follow.

13.5.1. Sharing Operational Resources

If there are other cloud-seeding programs operating in the vicinity, collaboration and cooperation with those projects could result in significant savings. For example, if the general weather patterns and storm events have similar timing, and the same meteorological support established for one program might service both. The weather data used to predict, initiate, and terminate seeding events is readily available through the Internet, so utilizing meteorological support teams to forecast for more than one project and/or target area is reasonable.

Similarly, once INGs are deployed, a single team of field technicians can support up to two dozen or more INGs, providing they are not located too far apart geographically. Thus, depending upon the number of generators operated by nearby projects, it may make sense to share technicians between programs for ING service and maintenance calls. However, if a major weather event removes multiple generators from service in the targets areas, restoration service to all generators will take longer.

13.5.2. The Number of Operational Seasons

A cost savings can also be realized by lengthening project contracts. Multi-season project contracts can be conducted more affordably than single-season contracts, primarily for two reasons. First, a company contracted to conduct or assist in cloud-seeding operations will be assured that the program will be conducted for more than one season. and could manage the company's resources accordingly. Resources include both physical resources, such as the INGs, vehicles, and shops, as well as the seasonal project personnel. Secondly, expenses are minimized when consumables not used during one season can be carried over to the next. Typically, this includes seeding agent, propane, nitrogen, and helium (the last, if rawinsondes are part of the project). Another advantage to the multi-season project contract is as project personnel expertise (e.g., local weather forecasting, knowledge of terrain, project logistics, etc.) increases from season to season, the efficiency and effectiveness of the program can be expected to increase. In the end, the longer a project contract, the greater the potential savings.

13.5.3. Project Implementation Mode

There are two methods of program implementation. One is to hire an experienced firm to provide the equipment, personnel, and consumables to conduct the cloud-seeding project. The other is for the project sponsors to purchase and/or construct the requisite equipment and consumables, and train their own personnel to conduct operations. A third option would be a blend of the two; to outsource some project assignments, while conducting other project activities "in house". A comparison of the pros and cons of the first two approaches is provided in Table 13.3.

The cost estimates presented in Table 13.3, columns 1 & 2, are based upon turn-key operations. Columns 3 and 4 are included because significant cost savings can result if the sponsor's infrastructure and staffing allow for the sponsor to perform some of the activities themselves. However, the calculation of such circumstance-specific savings is beyond the scope of this operational design study.

Table 13.3. Contracted versus self-run projects, or project components.

Element	Leasing / Hiring		Purchasing / Self-Service	
	1 Pros	2 Cons	3 Pros	4 Cons
A Ice Nucleus Generators	Consultant in charge of equipment procurement, and/or construction. Consultant provides all technical services (i.e., siting, installation, maintenance, replacement, repair and dismantle services). No additional project sponsor staff is required (staff resource savings).	Lease fees may exceed actual generator purchase costs in long-term. Indirect expenses for technician services (i.e. salary, time, travel, company overhead fees, etc.) are incurred by the funding sponsor.	Purchase expenses will be recouped if equipment is utilized long-term (5 – 7 years, A2). Project sponsor is able to provide all technical services (A1). Indirect expenses (A2) for project sponsor staff are already accounted for.	A long-term cloud-seeding project is required to attain “owner/operator” cost savings. Additional expenses will occur if outside expertise is required to perform any technical services (A1).
B Aircraft	Consultant responsible for aircraft and associated equipment procurement expenses. Consultant provides all required aircraft services and manpower. Lease fees include actual flight hours, and “stand-by” time. No purchase or installation of seeding equipment fees. No additional “in-house” project sponsor staff is required (staff resource savings).	The deployment costs include the salaries and living expenses for aircraft mechanics, technicians, meteorologists, and pilots), are paid by the funding sponsor	Project sponsor staff is able to provide all required aircraft services. Salaries for specialized professional services (B2), and indirect expenses (B2), are already accounted for. Aircraft can be used for ancillary purposes (i.e., transport) when not employed for cloud seeding.	Project sponsor responsible for aircraft & associated equipment procurement expenses. All aircraft expenses (e.g., “stand-by” fees) are absorbed by the project sponsor, however, if the sponsor regularly stores, operates & maintains aircraft, this may not greatly impact known expenditures.
C IN generator Technicians	No training required. Technician fees are incurred only while “on project” at a pre-determined rate. No additional “in-house” project sponsor staff is required (staff resource savings).	Indirect expenses for technician services (A2) are incurred by the funding sponsor.	Project sponsor staff is able to provide all technical services (A1). Indirect expenses for project sponsor staff are already accounted for (A2).	Additional expenses will occur if outside expertise is required to perform any technical services (A1). Project sponsor staff workloads may increase.

Element	Leasing / Hiring		Purchasing / Self-Service	
	1 Pros	2 Cons	3 Pros	4 Cons
D <i>Forecasting and Seeding Operations</i>	Consultant meteorologist is able to perform required services, and possesses local weather expertise. Meteorologist expenses are incurred only while “on project” at a pre-determined rate. No additional “in-house” project sponsor staff is required (staff resource savings). Indirect expenses for meteorological services can be reduced if forecasting support is provided "off site" via the Internet. “On-site” expenses (lodging, per diem) are not incurred.	Indirect expenses for meteorological services are incurred by the funding sponsor (A2). A lack of local weather expertise may result in additional operational expenses.	Project sponsor meteorologist is able to perform required services and possesses local weather expertise. Indirect expenses for meteorological staff are already accounted for (A2).	Additional expenses will occur if outside expertise is required to perform any meteorological services. A lack of local weather expertise may result in additional operational expenses. Project sponsor staff workloads may increase.
E <i>Radiometer</i>	Consultant absorbs all equipment purchase expenses. Consultant provides all technical services (A1). No additional “in-house” project sponsor staff is required (staff resource savings).	Lease fees may exceed actual radiometer purchase cost in long-term. Indirect expenses for technician services (A2) are incurred by the funding sponsor.	Purchase expenses will be recouped if equipment is utilized long-term (~5 years). Project sponsor is able to provide all technical services (A1). Indirect expenses (A2) for project sponsor staff are already accounted for.	Project sponsor responsible for purchase of equipment. A long-term cloud-seeding project is required to attain “owner/operator” cost savings. Additional expenses will occur if outside expertise is required to perform any technical services (A1).
F <i>Rawinsondes</i>	Consultant absorbs all equipment purchase expenses. Consultant provides all technical services (A1). No additional project sponsor staff is required (staff resource savings).	Lease fees may exceed actual sounding equipment purchase costs (i.e., calibration box and receiver) in long-term. Indirect expenses for technician services (A2) are incurred by the funding sponsor.	Purchase expenses will be recouped if equipment is utilized long-term (~5 years). Project sponsor is able to provide all technical services (A1). Indirect expenses (A2) for project sponsor staff are already accounted for	Project sponsor responsible for purchase of equipment. A long-term cloud-seeding project is required to attain “owner/operator” cost savings. Additional expenses will occur if outside expertise is required to perform any technical services (A1).

14. Task 13: Preliminary Cost/Benefit Analyses

The ASCE Guidelines for Cloud Seeding to Augment Precipitation (2006) provides a discussion of feasibility studies that are recommended prior to the initiation of an operational cloud-seeding program. The Guidelines suggest two questions to be answered:

- 1) Is the program technically feasible?
- 2) Is the program economically feasible?

Both questions need to be answered in the affirmative for the program to be considered truly feasible. Effectively evaluating the economic feasibility of a program is performed by considering the potential benefit compared with the estimated cost of providing this benefit (i.e., the common benefit/cost ratio). For example, if the estimated additional streamflow produced through cloud seeding costs \$5/AF and the value of this water to the primary users (there can be secondary and tertiary beneficiaries) is \$20/AF, then a 4/1 ratio is the result; stated more pragmatically; there is a potential for \$4 in return for each dollar spent. The ASCE Guidelines recommend that a target benefit-to-cost ratio should be at least $\sim 5/1$. The following will examine some preliminary benefit/cost estimates.

Section 12 of this report gives estimates of the potential average increases in April–July runoff from the Medicine Bow and Sierra Madre Ranges assessment areas into the North Platte and Green River Basins separately, and also combined. Considering that program costs would be the same for (and shared by) each basin, basin-combined estimates of streamflow increases will be used going forward. The projected range of streamflow increases for ground-based seeding if the annual seeding effect in seedable storms ranges from 5% to 15% (using a 70% impact area) is $\sim 11,170$ to $33,510$ AF. For airborne seeding, using the same assumptions, the estimates in potential streamflow increase range from $\sim 16,460$ to $49,390$ AF.

14.1. The Value of Water near the Medicine Bow and Sierra Madre Ranges

To estimate the benefit/cost ratio, the value of water in the region must be established first. The value of water from those portions of the Upper North Platte and Green River that originate in the Medicine Bow and Sierra Madre Ranges varies considerably, largely depending upon water use.

As of August 2016, contracts for water from the Pathfinder Reservoir on the North Platte established a “readiness-to-serve” charge of \$5/AF, whether the water is withdrawn or not, with the water taken in the withdrawal itself priced at \$25/AF; thus, the total cost would be \$30/AF. From that reservoir, water taken under the Platte River Recovery Implementation Program (NE Nebraska) sells for \$51/AF for environmental purposes. This price applies to the first 38,400 AF in any 8-year period; if exceeded, price rises to \$65/AF.

In the Green River Basin, water contracts with the State of Wyoming for water from Fontenelle Reservoir set the readiness-to-serve charge from \$5-10/AF, with water for industrial purposes sold within the \$42–\$65/AF range.

14.2. Value of Augmented April-July Streamflow

Assuming a value of water between \$30–\$65/AF, various benefit/cost ratios can be established for the ground-versus-airborne program scenarios. Table 14.1 and Table 14.2 enumerate the various program costs required to meet different benefit/cost ratios assuming water costs of \$30/AF.

Based on the cost estimates for a ground-seeding program provided in Table 13.1, ground-based seeding would be cost effective with a 1/1 benefit-to-cost ratio if greater than 22,240 AF additional streamflow were produced. The cost estimate for an airborne-seeding program provided in Table 13.2 suggests that an airborne program would be cost effective at a 1/1 ratio for all estimated levels of additional streamflow.

As shown in Table 14.1, to achieve the 5/1 ratio recommended by the ACSE Guidelines, a ground-based seeding program would need to cost less than \$201,060 and achieve a streamflow increase of 33,510 AF. If the seeding program only produced an additional 12,500 AF, as estimated by the WRF-Hydro simulations in Section 12, then the ground-based program would have to cost less than \$75,000 to meet the 5/1 ratio for a water cost of \$30/AF. Given the operational cost estimates provided in Table 13.1, none of the ground-based programs meet the 5/1 ratio, and cannot be considered economically feasible.

Likewise, assuming a water cost of \$30/AF, and comparing program costs to meet the 5/1 ratio in Table 14.2 with the estimated airborne program costs provided in Table 13.2, an airborne-seeding program would not be economically feasible either. However, if water costs more than \$30/AF, then an airborne-seeding program could be economically feasible at the 5/1 ratio, as illustrated in Figure 14.1 below.

Table 14.1. Cost of a Ground-based Program to Generate Different Benefit/Cost Ratios, assuming a water cost of \$30 and impact area of 70%. The estimated annual increase in streamflow from seeding based upon the WRF-Hydro simulation is included in the far right column (shaded in gray) for comparison.

Benefit/Cost Ratio	Cost of Program 11,170^{G5} AF Increase	Cost of Program 22,340^{G10} AF Increase	Cost of Program 33,510^{G15} AF Increase	Cost of Program 12,500^{WH} AF Increase
1/1	\$335,100	\$670,200	\$1,005,300	\$375,000
2/1	\$167,550	\$335,100	\$502,650	\$187,500
3/1	\$111,700	\$223,400	\$335,100	\$125,000
4/1	\$83,775	\$167,550	\$251,325	\$93,750
5/1	\$67,020	\$134,040	\$201,060	\$75,000
^{G5} , ^{G10} , and ^{G15} Projected yield for ground-based seeding if annual seeding effect in seedable storms is 5, 10, and 15%, respectively.				
^{WH} Projected yield for ground-based seeding predicted by the WRF-Hydro model.				

Table 14.2. Cost of an Airborne Program to Generate Different Benefit/Cost Ratios (assuming \$30 water cost and 70% impact area).

Benefit/Cost Ratio	Cost of Program 16,460^{A5} AF Increase	Cost of Program 32,930^{A10} AF Increase	Cost of Program 49,390^{A15} AF Increase
1/1	\$493,800	\$987,900	\$1,481,700
2/1	\$246,900	\$493,950	\$740,850
3/1	\$164,600	\$329,300	\$493,900
4/1	\$123,450	\$246,975	\$370,425
5/1	\$98,760	\$197,580	\$296,340
^{A5} , ^{A10} , and ^{A15} Projected yield for airborne seeding if annual seeding effect in seedable storms is 5, 10, and 15%, respectively.			

14.3. Cost per Acre Foot Estimates

Calculations of program costs for different seeding options and benefit/cost ratios are given in Table 14.1 and Table 14.2. Table 14.3 provides the estimated costs per AF of ground-based and aircraft seeding to be compared with the cost of water per AF. These estimated program costs per AF are also illustrated in Figure 14.1. Based on the estimated operational program costs provided in Section 13 and assuming the cost of water between \$30–\$65/AF, at a 1/1 benefit/cost ratio, an airborne program costs less per AF than the cost of water, while the ground-based program costs similar to that of water. At a per-AF-estimated cost of \$53, the WRF-Hydro simulation results would suggest a ground-based seeding program would only be cost effective at a 1/1 benefit/cost ratio for the higher range of water costs. In Figure 14.1, a 5/1 ratio is met when the dashed line falls inside or below the gray shaded area. Assuming a \$30–\$65/AF range in water costs (illustrated by the gray shaded area), an airborne program would meet the 5/1 benefit/cost ratio if seeding produced a 10% or greater annual seeding effect relative to seedable storms; however, the ground-based seeding program would still not meet the 5/1 benefit/cost ratio in any of the estimated levels of seeding effect.

Table 14.3. Annual Costs Breakdown of Seeding Options for the Proposed Winter Cloud-seeding program and Estimated Cost/AF of augmented streamflow (using 70% impact area assumption for ground and airborne).

Item	Remote Generators (23)	Seeding Aircraft (one)
Est. Total	\$656,685	\$361,780
Est. Cost/A.F. for 5% Seeding Effect	\$59	\$22
Est. Cost/A.F. for 10% Seeding Effect	\$29	\$11
Est. Cost/A.F. for 15% Seeding Effect	\$20	\$7
Est. Cost/A.F. for Simulated Seeding Effect with WRF-Hydro	\$53	N/A

Water and program costs vs. streamflow increases from seeding

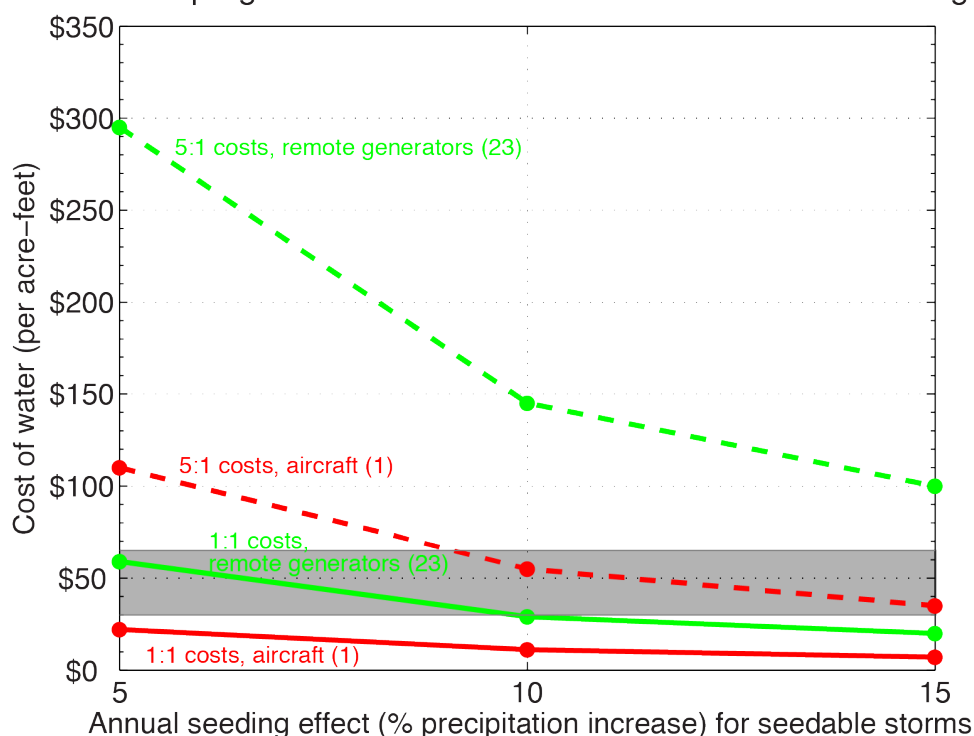


Figure 14.1. Cost of water for usage categories and for two estimates of annual seeding program costs (using 70% impact area) for the three levels of estimated streamflow increases resulting from WWMPP annual seeding effects for seedable storms (5, 10, 15%; Section 12). Gray shading indicates estimated water costs (\$30-\$65/AF). The solid green and red lines indicate the cost for the 23 remote ground-based generator seeding option versus the single aircraft airborne-seeding option, respectively, expressed as program costs per acre-feet of streamflow increase (essentially a 1:1 ratio). The dashed green and red lines show the corresponding 5:1 ratios of water costs to program costs.

14.4. Cost/Benefit Summary Remarks

The cost/benefit calculations presented herein were based upon the most sophisticated datasets, models, and/or methods, and resources available at the time of the study. That said, neither method is without uncertainty; there are a number of assumptions made in calculating the cost/benefit estimates to be considered when interpreting the results. Perhaps the most significant assumption is that the seeding program options summarized in Table 14.3 produce the estimated increases in streamflow contained in Section 12, and Table 14.1–Table 14.2. The streamflow estimates in Section 12 were calculated using two methods: 1) the range of preliminary WWMPP seasonal seeding effects for seedable storms⁸ (5-15%), and 2) a WRF-Hydro simulation of two seasons of WWMPP randomized seeding events. The first method is based on the WWMPP preliminary results, which in turn, are based on the program design of the WWMPP (i.e., up to 8 generators per mountain barrier deployed in a given period). It is quite possible that the seeding effects would have scaled up (or down) with more (or fewer) generators used. Therefore, this study assumes that the range of seeding effects from the draft WWMPP report encompasses the

⁸ The results from the WWMPP were used due to limited resources that prevented new simulations from being run on a *seasonal* basis explicitly for the Medicine Bow and Sierra Madre Ranges operational seeding program designs that were evaluated in this study.

reasonable range of seasonal seeding effects that may be realized by the various program design options summarized in Table 14.3. Additionally, this method assumes that there would be a 0.60 relationship between increases in seasonal winter precipitation and April–July runoff.

For the second method, the seeding cases simulated as part of the WWMPP were limited to 4-hour periods (with mandatory no seeding for 4 hours in between each), only seeding one barrier at a time, and the seeding temperature criterion was more stringent than is typically used for operational programs. Moreover, the WRF-Hydro approach only included two years of cases, and is not representative of a longer-term average year.

Additional cost/benefit calculation assumptions include the following.

- Consistently being able to obtain the estimated seeding effects provided in Section 12.
- The value of the augmented streamflow would be \$30/AF.
No additional components to the program, such as collecting rawinsonde and radiometer data, the provision of near real-time sophisticated modeling support for identification of “seedable” situations or targeting the AgI nuclei and forecasting potential seeding effects on precipitation, or any evaluation exercises. Any additions of this type or encountering unexpected costs during the performance of the seeding program would lower the calculated benefit/cost ratio information because the cost estimates in Table 14.3 do not provide for any such variations to the programs.

Another point to consider is that the calculated values in Table 14.1 and Table 14.2 are for average conditions. This study doesn’t take into account the possibility of whether benefit/cost ratios would rise in above normal years and fall in below normal years, or consider whether seeding effect increases would remain the same, or vary, in years with above and below normal precipitation. Also, the estimated benefits are primary benefits to identifiable water users in the immediate area. There may be secondary and even tertiary benefits from augmenting precipitation in the Medicine Bow and Sierra Madre Ranges. Examples include benefits gained from augmented streamflow that flows out of the North Platte or Green River Basins in Wyoming; value to agriculture, industrial and municipal uses; and enhanced hydroelectric generation (a non-consumptive use). Positive effects may occur in the forests of the intended target areas as well as the enhancement of recreational activities like fishing and boating.

15. Task 14: Finalization of Project Design

To initiate the permitting requirements (Section 16) for an operational cloud-seeding program designed to target the Medicine Bow and Sierra Madre Mountains, a SUP application would be required by the USFS. A meeting was held on 11 February 2016 at NCAR in Boulder, CO to discuss the project results to date and arrive at a preliminary project design to be submitted as part of the SUP application. Attendees at this meeting were Prof. Terry Deshler (Univ. Wyoming), Mr. Barry Lawrence and Ms. Jeni Cederle (WWDO), Mr. Patrick Golden (HEC), Mr. Bruce Boe (WMI), and Drs. Roy Rasmussen, Sarah Tessendorf, and Lulin Xue (NCAR).

The approach for the permit application portion of this study was to provide a maximum number of potential ground-based generators that could be used in the Medicine Bow and Sierra Madre Mountains operational cloud-seeding program, and assessed through the federal NEPA process. At this meeting a total of 35 ground-based generator sites were identified for possible use, with the placement of up to 23 generators on USFS lands.

The recommended operational design, based on the test simulations discussed in Section 6, were narrowed down from the preliminary total of 35 generator sites to a final total of 23 sites composed of sites from Sierra Madre Groups A, B, C, and D, as well as Medicine Bow Groups A and B (Figure 13.1). The Medicine Bow Group C generator sites were eliminated because the simulations showed that they produced negligible impacts in the Medicine Bow assessment area. Theoretically, the negligible seeding impact of the Medicine Bow Group C generators may be due to proximity of the site locations to the crest of the barrier, thereby reducing the time available for the AgI plume to impact the assessment area. Within the remaining generator groups, some sites were eliminated for their proximity to other sites as discussed in Section 13.1.

The final project design of 23 ground-based generators includes 16 in the Sierra Madre and 7 in the Medicine Bow (Figure 15.1). The model indicated that seeding from sites in the Sierra Madre can produce positive simulated effects on the Medicine Bow, and therefore, one approach to developing a cost effective operational program would be placing generators only in the Sierra Madre to target both mountain ranges. Of the 16 proposed sites in the Sierra Madre, 6 were sited specifically to target the Medicine Bow. However, to target the Medicine Bow under northwesterly winds, which occurs roughly one-third of the time that seedable conditions occur in the Medicine Bow (Figure 4.31), some sites are still necessary in the Medicine Bow on the western and northwestern slopes.

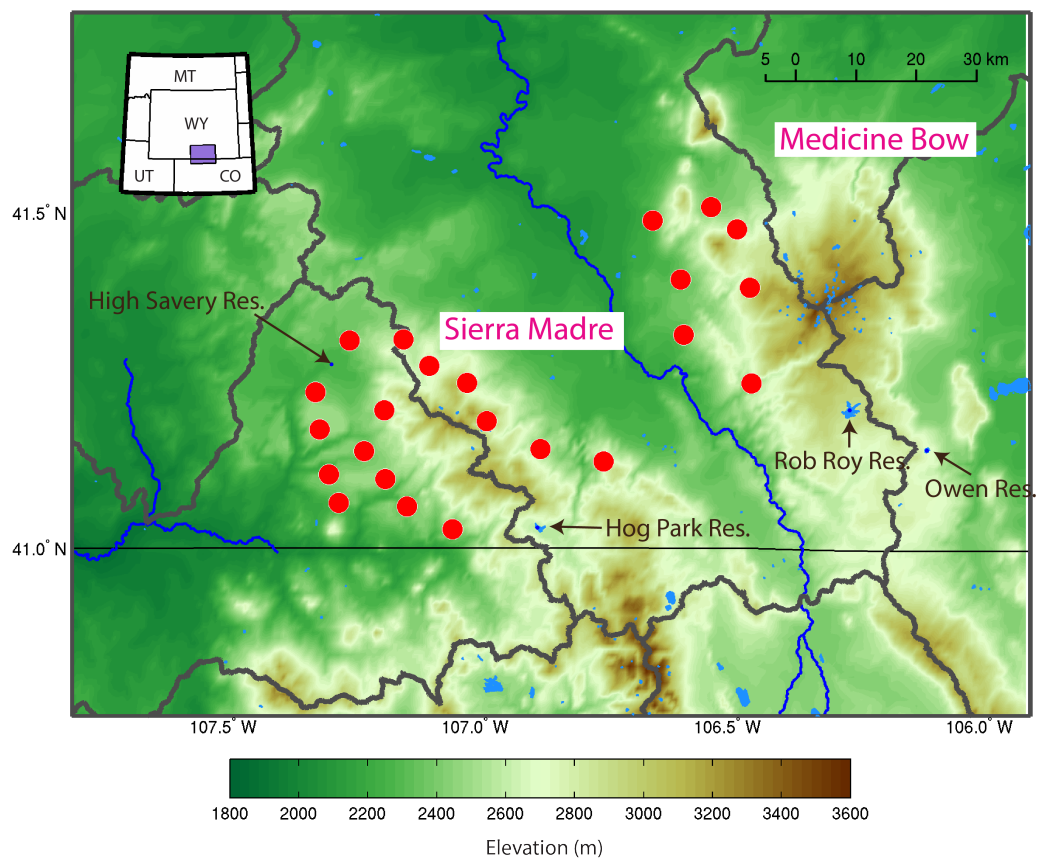


Figure 15.1. Map of the Final Recommended Project Design for 23 ground-based generator sites in the Medicine Bow and Sierra Madre Ranges.

16. Task 15: Environmental Analysis and Permitting

This task includes preparation of applicable permits for federal, state, and private lands for the final operational program and associated environmental analyses (e.g., development of NEPA documentation). As described in Section 8.2.1, the WWDO submitted a SUP application to the MBNF on 22 February 2016. The application requested USFS approval to place up to 23 ground-based generators and 6 monitoring equipment sites on National Forest administered lands. The MBNF replied with a letter to the WWDO on 9 August 2016 explaining that the proposed project failed to meet the minimum requirements of the initial screening criteria (Appendix B). The WWDO resubmitted the application with supplemental information (detailed project description, etc.) on 22 December 2016. This amended application requested a SUP for the period of 15 years, down from the original 30 years originally requested. The MBNF responded with a letter to the WWDO on 28 February 2017 initially accepting the SUP application and notifying the WWDO that USFS personnel would be in contact to discuss the application approval procedures (Appendix B). The WWDO is currently waiting to be contacted on this matter.

17. Task 16: Discretionary Task

In this task, discretionary project funds were authorized by the WWDO project manager to accommodate variations in the scope of work as the project developed, or as new issues were discovered during the project. The contract for services for this study is interconnected with the Bighorn Mountains Siting and Design Study (NCAR 2017). Approval for the use of discretionary funds was provided to deploy a high-resolution snow gauge in the northern end of the Bighorn Mountains, and is reported on in the final report for the Bighorn Mountains. At the time of this report, no discretionary funds were used for the Medicine Bow and Sierra Madre project.

18. Task 17: Reports and Executive Summaries

This task requires preparing digital and paper copies of a final report and executive summary provided to the WWDC at the completion of this study. This report serves as the deliverable required for this task. An executive summary that summarizes the purpose, primary results, and recommendations from this study has been compiled in a short document.

19. Task 18: Report Presentations

This task requires the findings of this study be presented at two separate meetings/public hearings held within the vicinity of the study area.

The WWDO held one public hearing in Saratoga, WY on 11 July 2017, in the Platte Valley Community Center. The hearing was called to order by Jeni Cederle, and presentations were given by Drs. Sarah Tessendorf and Roy Rasmussen of NCAR, along with Bruce Boe (WMI) and Patrick Golden (HEC). The meeting attendee list is provided in Table 19.1. Public comments were recorded and responded to. Documents pertaining to this public hearing are provided in Appendix C.

A presentation of the study results may also be requested by the WWDC and held in Cheyenne, WY to occur at a later date.

Table 19.1. Attendee list (other than presenters) from the public hearing held in Saratoga, WY on 11 July 2017.

Name	Agency		Name	Agency
Jeni Cederle	WWDO		Barry Lawrence	WWDO
Harry LaBonde	WWDO		Joe Parsons	Saratoga Encampment Rawlins Conservation Dist.
Emma Dierks	Bigfoot 99		Daniel Manville	Jackson Co., Walden, CO
Craig Blumenshine	Wyoming PBS			

20. Task 19: Climatological Monitoring of the Study Area

Datasets that may be used to monitor the climatology of the study area for the November 2015–April 2016 season are summarized below. These datasets are publicly available on the internet, and URLs to access those data have been provided. No additional datasets were collected during the course of this study.

The following list provides URLs for the available observational data sets used in this study.

- SNOTEL precipitation and snowpack measurements.
 - Real-time and historical precipitation and snowpack measurements are available at <http://www.wcc.nrcs.usda.gov/snow/>.
 - Provides temporal resolution of hourly and daily observations.
- USGS streamflow records.
 - Real-time stream gauge measurements are available at http://waterdata.usgs.gov/wy/nwis/current/?type=flow&group_key=huc_cd
 - Historical data can be retrieved from a how-to page via <http://waterdata.usgs.gov/nwis>

21. Task 20: Model Evaluation of the WWMPP RSE using an Ensemble Approach

This task requires a model-based evaluation of the WWMPP RSE using the WRF cloud-seeding parameterization. The goal of this work is to reproduce the statistical results of the RSE, thereby providing evidence of the cloud-seeding parameterization's ability to estimate realistic effects of cloud seeding.

21.1. Description of Ensemble Modeling Approach

The traditional statistical approach to cloud-seeding evaluation involves a randomized seeding program in which a target is randomly selected to either be seeded or not seeded, and a covariate measurement to account for natural storm variability. This approach was applied to the quality-controlled snow-gauge data from the WWMPP and resulted in a 3.3% increase in seeding that was not statistically significant (WWDC 2014). While a statistical approach can provide robust results in cases in which the seeding effect is relatively large, the number of cases needed becomes quite high when the seeding effect is small. This was the case for the statistical analysis of the WWMPP program. Due to the high cost of running a cloud-seeding program, it was simply not possible or realistic to collect additional Experimental Units (EUs) to achieve statistical significance.

As part of the WWMPP, a cloud-seeding module was developed by Xue et al. (2013a,b) and implemented into the Weather Research and Forecast (WRF) model through the Thompson et al. (2008) microphysical scheme. This allowed us to conduct simulations for each EU with and without seeding. To this end, a pair of deterministic model simulations was conducted for each EU, one that simulated seeding and one without seeding to serve as the control. The seeding effect was then estimated as the net increase in precipitation realized by differencing the two runs. It was determined, however, due to the initial condition and model uncertainty, that one deterministic pair of simulations for each of the EUs is only one possible outcome of model-estimated seeding, and thus there is a need to fully estimate the likely seeding effect through additional simulations.

To address this issue, an ensemble modeling approach was applied to the EUs of the RSE. This involves performing many simulations of each EU using different initializations and model physics configurations and then calculating the ensemble mean and spread of the ensemble members. The ensemble approach has become standard practice in weather forecasting since the 1990s based on Lorenz's (1963) ground-breaking results showing that small perturbations in the initial condition of the atmosphere can lead to a significant change in the forecast, and thus a single deterministic forecast is not likely representative of the actual forecast. This requires the use of probabilistic methods, such as running many ensemble members forced with appropriate perturbations to estimate the most likely outcome.

The ensemble approach provides a range of plausible solutions allowing one to better estimate the likely outcome through the ensemble mean, and also estimate the likely range of possible outcomes through the ensemble spread. In order for the spread to accurately estimate confidence

and realistic variability (Slingo and Palmer 2011), the ensemble needs to appropriately sample the likely uncertainty in: 1) the initial conditions driving the model, and 2) the uncertainty in the model formulation.

In the following, we use these guidelines in creating an appropriate ensemble to estimate the impact of cloud seeding for the RSE. In addition, three requirements are needed to conduct a robust ensemble analysis of seeding effect:

1. the model physics needs to accurately estimate precipitation over orographic barriers;
2. the seeding effect needs to be well characterized; and
3. sufficient numbers of ensemble members need to be created to reliably estimate the likely seeding effect.

Regarding the first requirement, Ikeda et al. (2010) and Rasmussen et al. (2011) have shown that the WRF model configured with the Thompson microphysics (Thompson et al. 2008) is able to estimate orographic precipitation in Colorado and Wyoming within 5-10%.

Regarding the second requirement, Xue et al. (2013a,b) developed a cloud-seeding module to estimate the impacts of orographic cloud seeding using AgI for both ground and airborne seeding. While the scheme has been verified for AgI dispersion (Boe et al. 2014; Xue et al. 2014), the seeding effect, while reasonable, has some uncertainty, requiring the creation of ensemble members to sample this uncertainty.

Regarding the third requirement, the high-speed NCAR supercomputer (Yellowstone) makes possible the creation of tens of ensemble members for each EU in a reasonable amount of time. As will be shown here, three different initializations were used. For each of these, there were 8 model configurations for the unseeded (making a total of 24 control runs) and 24 model configurations for the seeded (a total of 72 seeded runs from each of the 118 EUs. This results in the creation of 8,496 seeded simulations and 2,832 unseeded simulations. To estimate the impact of seeding, each of these ensemble members consisted of a seeded and corresponding control (no seeding) simulation pair.

21.2. Ensemble formulation

Based on the above discussion, the WRF model was used to conduct model simulations for each EU by running a 24-hr simulation for the outer 2.7-km-grid spacing domain and a 12-hr simulation centered on the time of the EU for the inner 900-m domain (Figure 21.1). The inner domain is initialized 12 hours into the outer domain simulation. Table 21.1 provides further information on the model configuration used.

Since each EU is only 4 hours long, the probability of a single high-resolution simulation capturing the snow-gauge accumulation of precipitation for that specific time period is quite low (Rossa et al. 2008). However, by capturing the likely variability in initial conditions and model physics using the ensemble approach, the model simulation of snow-gauge accumulation is significantly improved. Part of this improvement is because biases in the time-dependent forcing of precipitation (i.e. moisture flux, synoptic or mesoscale forcing) are reduced by the averaging process to produce an ensemble mean and the non-time-dependent forcing, such as orographic uplift, is reinforced (Rasmussen et al. 2011).

The following modeling approach and analysis method (summarized in Table 21.2) was used to address these requirements:

1. Uncertainty in model forcing
 - a. ECMWF ReAnalysis-Interim (ERA-Interim), Climate Forecasting System Re-analysis (CFSR) and North American Regional Re-analysis (NARR) re-analysis products are used as initial and boundary conditions for the all the conditions in Table 21.2. These re-analyses represent three of the most commonly used and accurate estimates of the 4D historical atmospheric conditions currently available.
2. Uncertainty in boundary-condition treatment
 - a. Boundary conditions with and without hydrometeors (traditional WRF boundary condition treatment does not include hydrometeors at the boundary between model domains; this capability was added to the model for this experiment, first column under Control Simulations section in Table 21.2).
3. Uncertainty in model physics for natural cloud and precipitation processes
 - a. Different PBL schemes for atmospheric environments, cloud and precipitation (second column under Control Simulations in Table 21.2). We chose to use two PBL schemes (MYNN and YSU in Table 21.2) to represent model uncertainties associated with boundary-layer effects on natural clouds. These two schemes represent the two dominant approaches to simulate the PBL.
 - b. Different Cloud Condensation Nuclei (CCN) backgrounds for cloud and precipitation (third column under Control Simulations in Table 21.2). The climatology of CCN concentration was based on 7-years of GOCART climatology following Thompson and Eidhammer (2014) and (CCN in Table 21.2) is used as the standard background while 1/5 of the climatology is used as the clean background and 5 times the climatology is used as the polluted background.
 - c. Different Ice Nuclei (IN) parameterizations for cloud and precipitation (column 4 under Control Simulations in Table 21.2). The Cooper 1986 (IN1) and Meyer et al. (1992) (IN2) ice nucleation parameterizations are used to represent different ice initiation processes.
4. Uncertainty in seeding processes
 - a. Different PBL for AgI dispersion. The MYNN and YSU schemes were both used for this purpose.
 - b. The default AgI activation (second column under Seeding Simulations in Table 21.2) followed DeMott (1995) and Meyers et al. (1995) parameterization. To capture the likely uncertainty due to activation rate, the default rate was increased by a factor of 5 for one of the ensemble members, and decreased by a factor of 5 for another ensemble member.
 - c. AgI removal (second column in third major column in Table 21.2) included AgI self-coagulation, scavenging of AgI by hydrometeors, and AgI dry deposition (Xue et al. 2013a). This removal rate was increased and decreased by a factor of five to capture the likely uncertainty due AgI removal processes.
5. Uncertainty in spatial and temporal distribution of precipitation
 - a. Precipitation in 3x3 grids surrounding the gauge sites was analyzed to address spatial uncertainty of the precipitation

- b. Precipitation 4-hr accumulations using different lags from the start time of seeding (30 and 60 minutes) were analyzed to address temporal uncertainty of the precipitation formation due to seeding

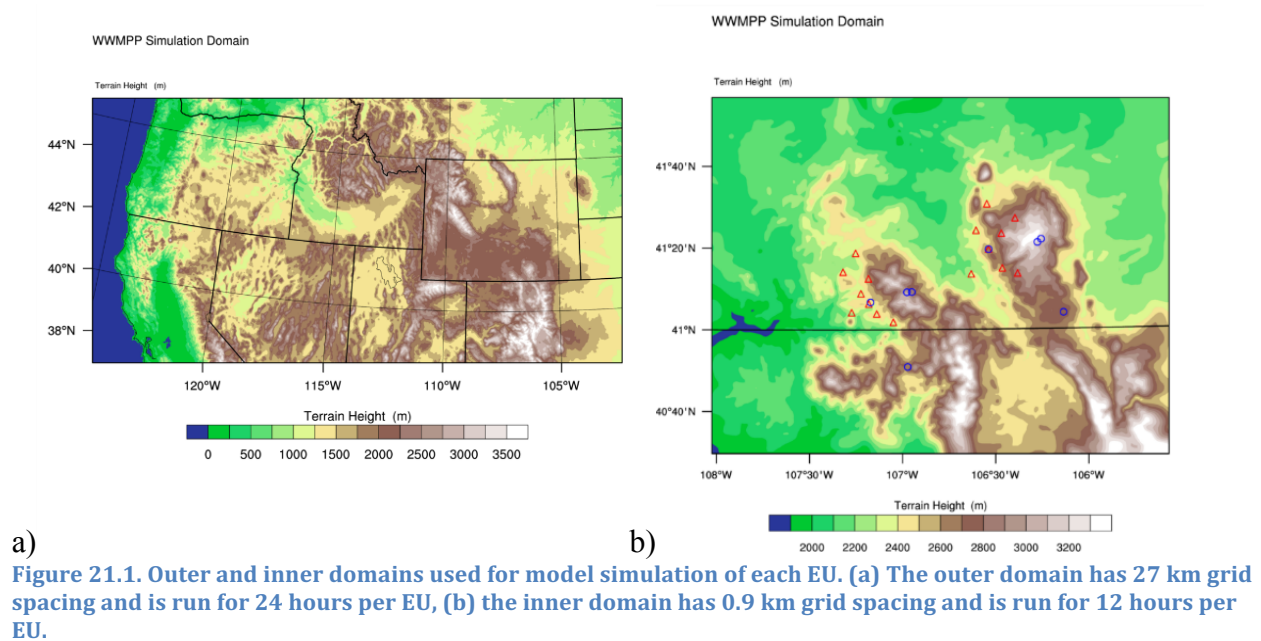


Table 21.1. Aspects of the model configuration utilized in all simulations.

Domain	2700 m domain	900 m domain
Horizontal grids	720 x 360	231 x 180
Vertical levels	81 terrain following Eta levels	
Time step	12 s	5 s
PBL scheme	Mellor–Yamada–Nakanishi–Niino (MYNN) 2.5 order	MYNN/YSU
Microphysics scheme	Thompson and Eidhammer (2014) scheme	Thompson-Eidhammer (2014) with the seeding parameterization

Table 21.2. Summary of ensemble model configurations.

Note: AS2 (AN2) = 0.2 * AS1 (AN1) and AS3 (AN3) = 5 * AS1 (AN1).

IN1 is Cooper (1986) ice nucleation parameterization and IN2 is Meyers et al. (1992).

HYD BC = hydrometeors in the boundary. NO HYD BC = no hydrometeor.

Control simulations					Seed simulations		
ID	Boundary condition	PBL scheme	CCN	IN	ID	AgI nucleation	AgI scavenging
C1	HYD BC	MYNN	CCN	IN1	S1	AN1	AS1
C2		YSU	CCN	IN1			
C3		MYNN	0.2 CCN	IN1			
C4		MYNN	20 CCN	IN1	S2	AN2	AS2
C5		MYNN	CCN	IN2			
C6		MYNN	0.2 CCN	IN2			
C7		MYNN	20 CCN	IN2	S3	AN3	AS3
C8	NO HYD BC	MYNN	CCN	IN1			

21.3. Verification of the Ensemble Modeling Approach

The WRF model results are compared to the RSE gauge data to establish confidence that the model is able to provide a reasonable estimate of precipitation over the Sierra Madre and Medicine Bow Ranges.

The distributions of paired errors for all 118 EUs between snow-gauge observations and the model at the gauge site serving as the target and the control (thus the location of the gauge site will vary depending on which mountain range is the target or control) indicate errors nearly equally distributed about zero for every model configuration (Figure 21.2–Figure 21.3). The results are given as box and whisker plots, and mean differences. The same paired error analysis was conducted for the each of the model configurations for the covariate gauge sites and further support these conclusions (not shown). This indicates that there was no single model configuration in the ensemble biasing the statistical results in a given direction. Moreover, these results show that the ERA-Interim model initialization had the least spread of error compared to the NARR and CFSR, which had a wider magnitude of errors.

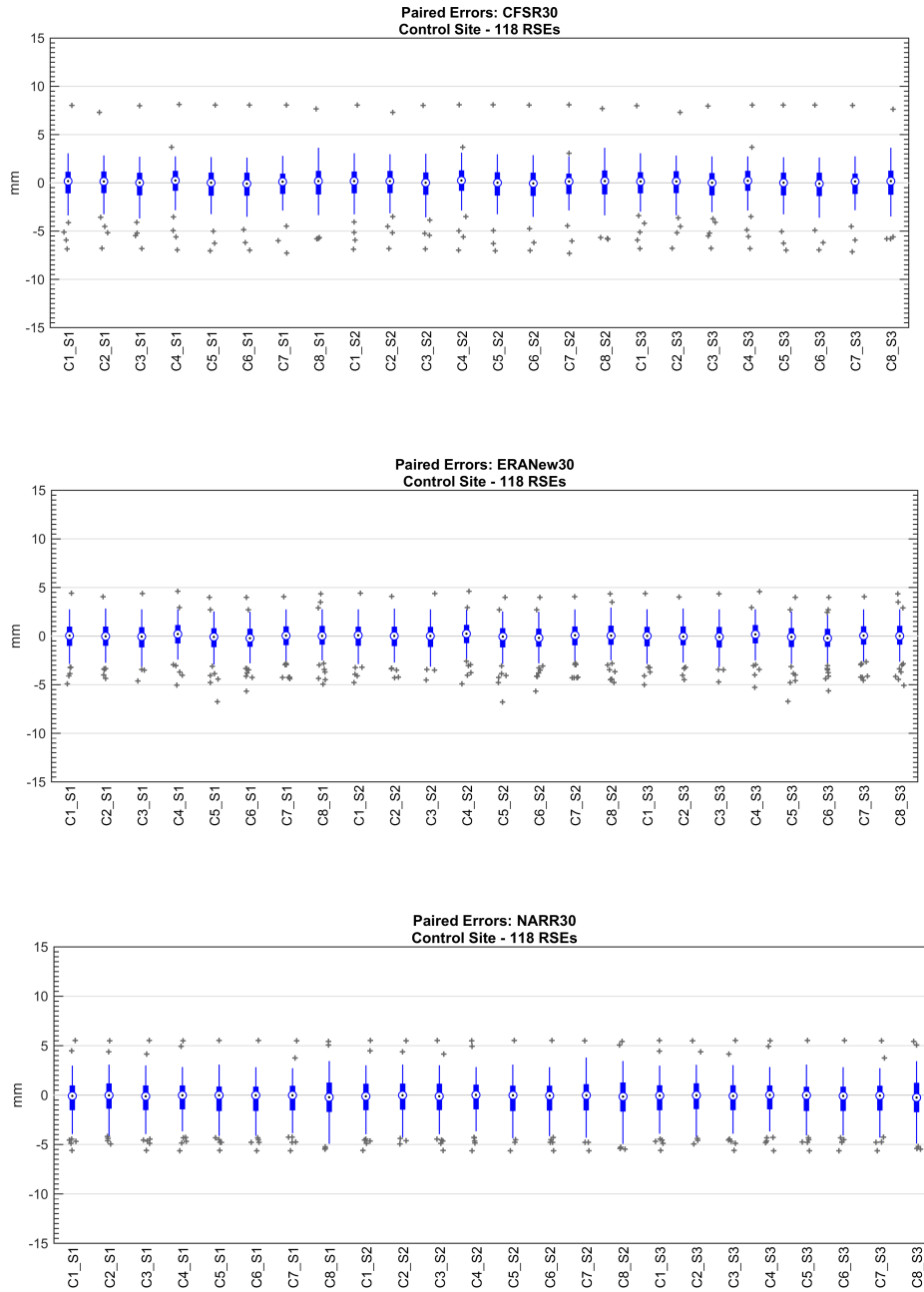


Figure 21.2. Paired errors for the gauge location declared as the control of all 1118 RSE cases. Error is the model 4-hr precipitation minus the 4-hr gauge-measured precipitation. a) All 24 ensemble members per RSE case initialized with CFSR, b) All 24 ensemble members per RSE case initialized with ERA-Interim, and c) All 24 ensemble members per RSE case initialized with the NARR reanalysis.

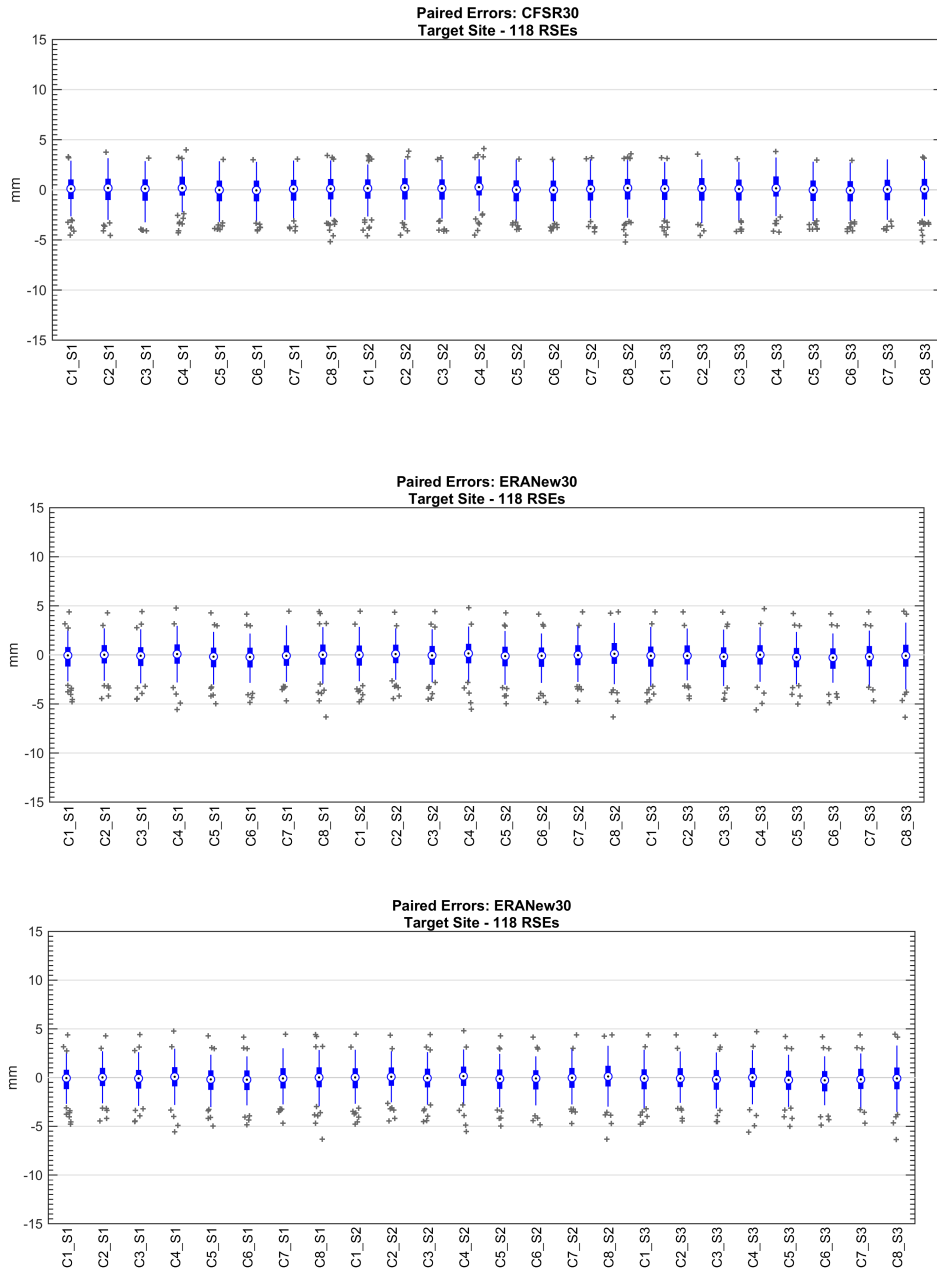


Figure 21.3. Paired errors for the gauge location declared as the target for all 118 RSE cases. Error is the model 4-hr precipitation minus the 4-hr gauge-measured precipitation. a) All 24 ensemble members per RSE case initialized with CFSR, b) All 24 ensemble members per RSE case initialized with ERA-Interim, and c) All 24 ensemble members per RSE case initialized with the NARR reanalysis.

Figure 21.4 provides a paired analysis of the 4-hr precipitation accumulation differences of the ensemble mean for each EU and each re-analysis compared to the snow-gauge observations at each gauge site. The data pairs are for the specific EU ensemble simulation (24 members for each re-analysis) with the corresponding EU gauge accumulation. The results show that the model ensemble mean provides an excellent estimate of the observed precipitation based on the mean difference between the observations and model ensemble mean being close to zero for all

the snow-gauge sites, and the distribution of the differences nearly symmetric about zero. These results suggest that the current model ensemble is providing a reasonable estimate of the actual precipitation observed during the 6-year experiment.

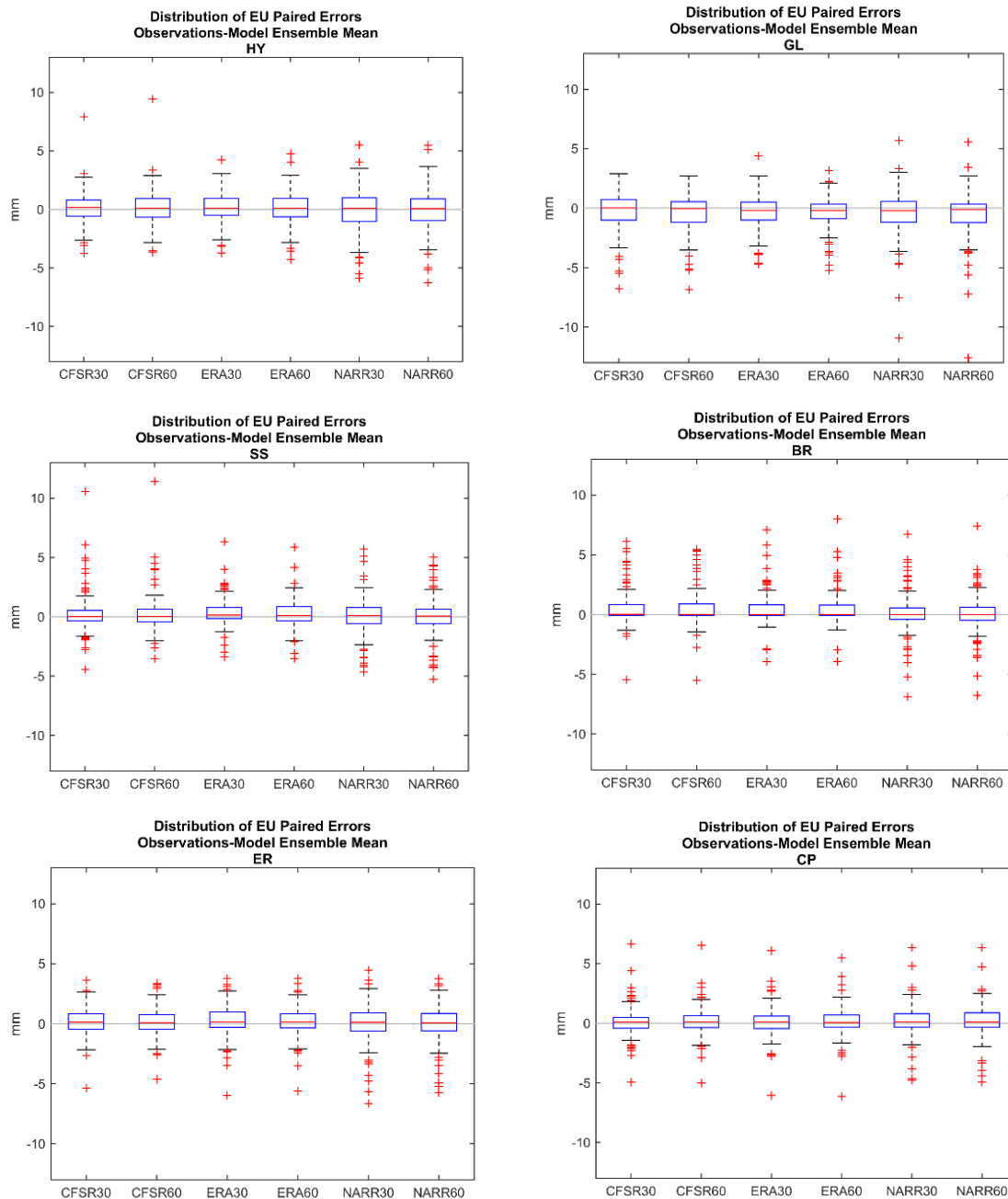


Figure 21.4. Distribution of EU paired errors by subtracting the ensemble mean of the 24 ensemble members run using each re-analysis from the 4-hr observed precipitation accumulation at each gauge. Each box and whisker plot represents the paired differences of the 118 EU cases. Each plot provides the results for a particular EU snow-gauge location (see Figure 1 for details). HY is Highway 47 (target in the Sierra Madre range), GL is Glees (target in the Medicine Bow range), SS is Sandstone (upwind co-variate site in the Sierra Madre range), BR is Barrett Ridge (upwind co-variate in the Medicine Bow range), ER is Elk River (southern co-variate for the Sierra Madre range), and CP is Chimney Park (southern co-variate for the Medicine Bow range). The box represents 25

to 75% of the differences, while the whiskers 5 to 95% of the data. Outliers are shown as plus signs. The mean difference is represented by the horizontal red line. Results are shown in each plot for the three different analyses (CFSR, ERA and NARR) and for seeding onset lag times of 30 and 60 minutes (CFSR30, CFSR60, etc.). The statistical design specified that the lag to estimate seeding effect at a gauge site would be 30 minutes from the start of seeding.

Figure 21.5 shows the model-estimated seeding effect (seeding simulation 4-hr precipitation accumulation minus control simulation precipitation) at the targeted gauge site for each seeded EU. Note that there is a wide variety of seeding effects, with the smaller amounts more frequent. The frequency plot of the model-estimated seeding (Figure 21.6) shows that the seeding effect resembles an exponential distribution. This result is consistent with the distribution of radiometer-measured and model-simulated integrated liquid water also resembling an exponential distribution (not shown), suggesting that the seeding effect is proportional to the amount of supercooled liquid water present.

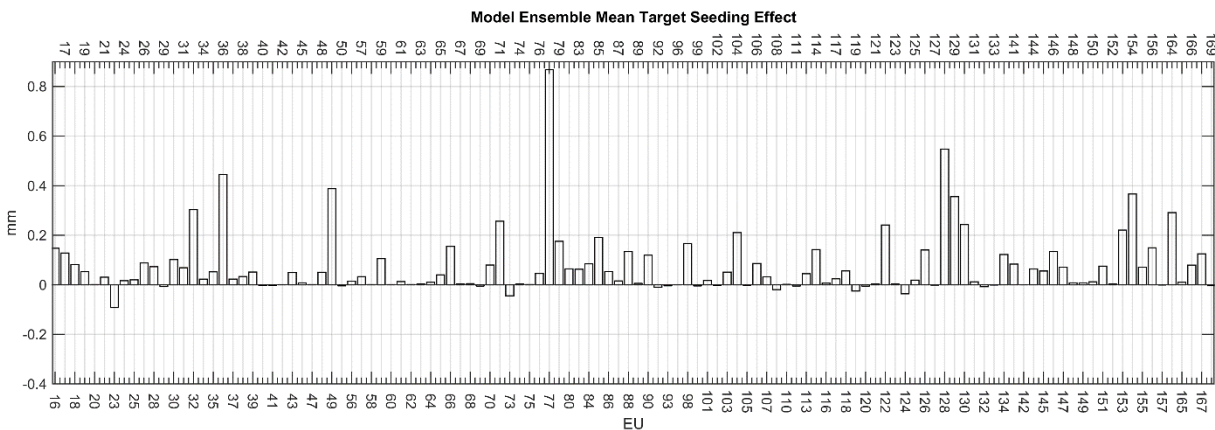


Figure 21.5. ERA-Interim model-estimated seeding effect (seeding simulation 4-hr precipitation accumulation minus control simulation precipitation) for the targeted gauge site (mm), either GL or HY, in each EU from the model ensemble mean.

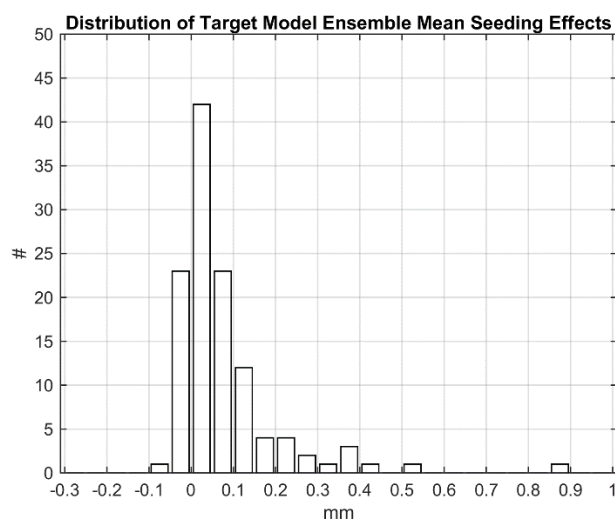


Figure 21.6. Frequency of ERA-Interim model-estimated seeding effect for the target gauge sites, either GL or HY, combined from the model ensemble mean.

21.4. Evaluation of the WWMPP using the Ensemble Modeling Approach

The model ensemble mean seeding effect for the Sierra Madre and Medicine Bow target gauge sites, individually and combined, is given in Figure 21.7. The results show a mean model-estimated seeding effect of ~5% for the two ranges. The 25th percentile is 3% and the 75th percentile is 7%.

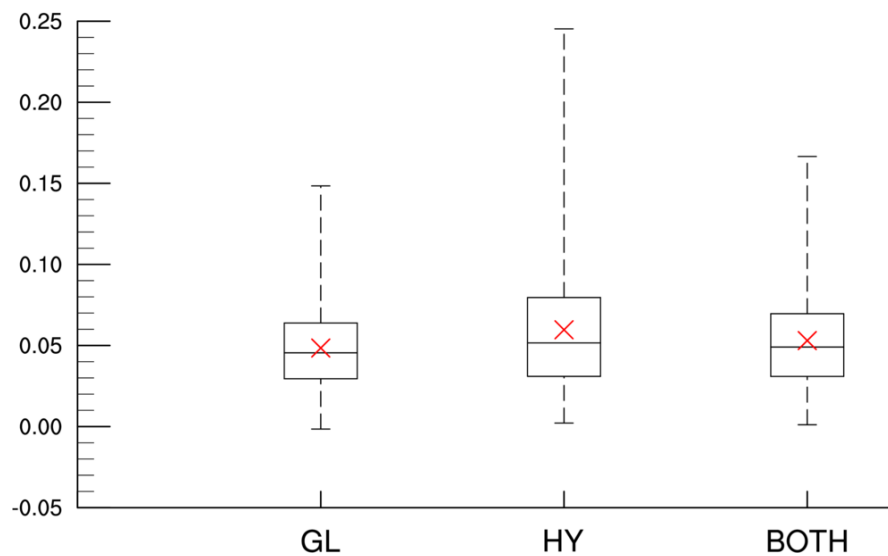


Figure 21.7. Distributions of the fractional increase in precipitation at the Medicine Bow range target (GL), the Sierra Madre target (HY) and both (average of the two) based on the difference between seed and no-seed model ensemble simulations (8,946 EU cases simulated). The horizontal bar is the median and the red X the mean value. The top and bottom of the boxes represent the quartile ranges.

21.5. Summary of RSE Ensemble Modeling Study

Instead of collecting additional cases at large expense, an ensemble modeling approach to estimate the impact of ground-based seeding was conducted and presented. The modeling approach has the advantage that both the conditions with and without seeding can be simulated, allowing the difference of the model simulations to estimate the seeding effect. An ensemble approach allows one to better account for initial conditions, model biases and random errors in the model simulations. A prerequisite to using a model, however, is that the simulations reasonably represent reality. The WWMPP RSE snow-gauge data were used to perform this function. The inter-comparison between the model ensemble simulations and the snow-gauge data per EU showed reasonable agreement in terms of the model mean and median errors being close to zero, with the distribution of errors in the paired comparison symmetric about zero error in most cases.

The above comparison was made with twenty-four model ensemble members for each of three re-analysis forcing datasets, with a total of 8,946 simulations to simulate each of the 118 EUs. This approach minimized potential biases due to time-variation of forcings of precipitation for each EU, and emphasized the orographically forced component of precipitation.

The results of the model ensemble in which the paired seeding effect was estimated for each ensemble member produced mean precipitation enhancement of 5%, with an inner quartile range of 3 to 7%. These results provide a robust estimate of the impact of ground based cloud seeding in the Sierra Madre and Medicine Bow Ranges in Wyoming that accounts for key uncertainties in both initial conditions and model physics.

21.6. Next Steps for Modeling the Effects of Cloud Seeding

This study estimated the likely additional precipitation produced by ground-based seeding of AgI over the Sierra Madre and Medicine Bow mountain ranges in Wyoming using a seeding parameterization applied to the WRF model. The next step is to use observations to verify that the model estimate of seeding effect is reasonable. This would require specific field studies for both ground and airborne seeding.

21.7. Application of the Ensemble Approach to other Mountain Ranges

It is tempting to apply the ensemble approach to other mountain ranges to estimate potential seeding effects. However, verifying that the model is estimating snowfall and supercooled liquid water correctly through observational comparisons is still necessary. It is also important to verify that the model-generated wind and thermodynamic structure of storms is also observed in appropriate data from the mountain range of interest. If this is performed and the model-generated seeding effect is also verified, then the ensemble approach provides a powerful tool to estimate the likely seeding effect due to AgI seeding in orographic clouds for both ground and airborne seeding. While this approach requires a significant investment of time and money, the statistical approach to evaluating cloud-seeding programs using snow-gauge observations from either ground or airborne seeding can often require over 1,000 cases to detect the signal from the noise, depending on the strength of the *a priori* unknown seeding signal.

In addition, if the number of cases is less than that needed number to achieve statistical significance, it is tempting to re-stratify the data to obtain some useful trends. The current results suggest that such re-stratification has a high probability of committing the error of multiplicity, and is thus highly discouraged.

22. Summary and Recommendations

This Final Design and Permitting Study establishes an operational weather modification program targeting the Medicine Bow and Sierra Madre Ranges in southern Wyoming. This study was led by NCAR with collaboration from WMI and HEC. Twenty tasks were identified by the WWDC for the study, including: scoping and project meetings; reviewing previous studies and data; climatological analysis of the project area; development of a preliminary project design; model evaluation of the preliminary project design; field surveys of potential ground-based generator locations; assessing the access/easements and permitting/reporting for potential generator sites; operational criteria development; a review of environmental and legal considerations; provide cloud seeding evaluation methods; potential benefits analysis; cost estimates; developing a cost/benefit analysis of the potential program; finalizing the project design; environmental analysis and permitting; discretionary tasks; preparation of the report itself; giving presentations on the final results; climatological monitoring of the study area; and a model evaluation of the WWMPP RSE.

22.1. Summary

Two public scoping meetings were held at the start of the project in locations near the Medicine Bow and Sierra Madre Ranges. The first meeting was held in Saratoga, Wyoming on 21 September 2015, and the second in Savery, Wyoming on 24 September 2015. The meetings provided the public with an overview of the scientific concept of cloud seeding, a summary of the previous weather modification studies in Wyoming, and a description of the plans for the current study.

A review of previous data found that numerous research investigations have improved the understanding of how to use AgI seeding to enhance snowfall in winter orographic clouds. These include the recently concluded Wyoming Range Phase II Feasibility Study and the WWMPP. The results of these studies were reviewed in the preparation of this report to ensure it remains consistent with the most recent recommendations for cloud-seeding program design. Noteworthy results from the draft WWMPP report asserted that while the RSE was statistically inconclusive, an “accumulation of evidence” analysis approach suggested precipitation increases of 5–15% in seedable storms over a winter season. It also demonstrated the capability of numerical models to realistically simulate snowfall distributions, as well as simulate seeding effects via a seeding parameterization. The results of the WWMPP were utilized in this study.

The review of previous data suggested that liquid propane seeding would be an inefficient option for the Medicine Bow and Sierra Madre Mountains because it must be released in the supercooled cloud to be effective. Manual, ground-based AgI generators were also determined to be challenging to deploy and operate in the target area, given the limited options for accessible and effective generator placement. For manual generators to be activated and deactivated during the winter months, locations should be sited at lower elevations around the Medicine Bow and Sierra Madre Ranges, potentially creating a situation in which the AgI plume could frequently be blocked and unable to disperse over the mountains.

A climatological analysis of the Medicine Bow and Sierra Madre Ranges was performed as part of the WWMPP by Ritzman et al. (2015). However, the criteria for seeding during that study

was based upon criteria for the WWMPP *research* program. For the purposes of developing an operational cloud-seeding program, a climatology analysis was conducted based on seeding criteria applicable to an *operational* cloud-seeding program. The climatology analysis indicated that the predominant 700-hPa wind direction impacting the targeted areas is westerly. Similarly, the western regions of both mountain ranges were shown to have the most frequent occurrence of seedable conditions for both ground-based and airborne techniques. Results from the Sierra Madre southern region climatology analysis showed that there were enough opportunities for ground-based seeding to warrant the placement of a few generators in that area. The climatology analysis also suggested that the eastern regions of both ranges were not suitable for ground-based seeding given the low frequency of suitable conditions materializing on the eastern slopes, as well as the limiting wind directions and atmospheric stability that would diminish seeding opportunities. Airborne seeding was shown to be feasible in all geographical regions of both ranges, and opportunities were frequent enough to warrant an airborne program if deemed cost effective. The annual fraction of November–April precipitation that fell under seedable conditions was 38% for ground-based seeding and approximately 56% for airborne seeding. These percentages are based upon the climatological analysis results for the western regions and were utilized in the streamflow benefits estimation.

Preliminary Project Design, Model Evaluation, and Field Surveys

To test a wide variety of program design options based upon results of the climatological analysis, several groups of potential ground-based generator sites were established. Initially, seven groups of generators were tested; however, following the initial iteration of cloud-seeding model simulations, additional generators were placed with an existing Group, and two new Groups of generator sites were created to investigate potential seeding impacts from generators located upwind of the ranges. The preliminary project design focused on ground-based seeding and/or airborne seeding with an operational season of mid-November through mid-April (e.g., 15 November – 15 April), utilizing silver iodide, or more specifically, a silver iodide-salt compound as the seeding agent.

Four “control” cases were selected from the WWMPP RSE research program to represent a range of suitable seeding conditions found in the Sierra Madre and Medicine Bow Ranges. To investigate the potential designs of a ground-based seeding program, the original ASPEN was incorporated into the original Thompson microphysics scheme (Thompson et al. 2004, 2008) within WRF.

WRF simulations of these four “control” cases showed that: (1) the Sierra Madre received more precipitation than Medicine Bow, mainly due to the upwind location of the range; (2) convection can occur in the Sierra Madre while more stratiform precipitation is simulated in the Medicine Bow; (3) SLW was present in both ranges throughout the simulations in all cases, which is a necessary condition for seeding operations to commence.

WRF simulations of the ground-based seeding cases showed that: (1) seeding depleted SLW in a shallow layer close to the terrain and increased precipitation over the mountain; (2) flow over the Medicine Bow was usually blocked, or forced around the range due to the steeper slope of the topography, although flow from some of the lower elevation generator groups (i.e., Groups E and F) placed upwind of the Sierra Madre were also occasionally blocked; (3) the simulated seeding

effect was not as great if the natural cloud efficiently produced precipitation (Cases 2 and 4); (4) seeding simulated from all Sierra Madre generators, including those in the upwind generator Groups E and F, produced the greatest combined simulated precipitation increases in *both* ranges for most of the cases tested.

Cases 3 and 4 (13 January 2014 and 21 February 2012) were selected to investigate airborne-seeding impacts on the Sierra Madre and Medicine Bow regions because these two cases exhibited conditions suitable for seeding by aircraft.

One caveat to mention is that the original version of the ASPEN used in this study for the ground-based seeding simulations did not include precipitation scavenging of AgI particles, AgI self-coagulation, or AgI dry deposition processes. Therefore, the particles transported from the Sierra Madre to the Medicine Bow and the subsequent simulated seeding impacts in the Medicine Bow were overestimated. To address this overestimation, two of the ground-based seeding cases were re-run using only the Sierra Madre generator groups and the new ASPEN to better understand how the additional AgI-removal processes affected the cloud and precipitation, especially downwind in the Medicine Bow Range.

The results of the ground-based seeding simulations (only Sierra Madre generators) with the additional AgI-removal processes (new ASPEN and microphysics scheme) reduced the AgI concentration and the simulated seeding effect in the Medicine Bow region by 50% for both of the re-run cases. However, similar or greater simulated seeding effects still resulted in the Medicine Bow from AgI released from sites in the Sierra Madre compared with the seeding scenario using only the Medicine Bow generators to target the Medicine Bow. (Run 3 of the original simulations). In light of these limited results, it can be reasonably deduced that ground-based generators strategically placed in the Sierra Madre Range (only), could effectively target both the Sierra Madre and Medicine Bow Ranges.

When conditions are suitable, airborne seeding for a period of about 2 hours can produce similar simulated seeding effects as those from ground-based seeding. According to modeling results, airborne-seeding simulations showed impacts over a deeper and broader portion of the atmosphere, and converted the SLW to precipitation more efficiently than the ground-based seeding scenarios. Airborne seeding conducted upwind of both Ranges produced more of an impact on precipitation in the Sierra Madre than it did in the Medicine Bow Range when compared with the upwind ground-based seeding case.

During the field surveys conducted for this project, 27 potential ground-based generator sites were visited, and considered for inclusion in the operational project design. Of these 27 sites, 18 were located on federal lands, and 9 on private lands within the Medicine Bow and Sierra Madre Ranges. For each location, land ownership, access descriptions and ratings, and brief descriptions of the sites were provided (Table 7.1). As a result of the modeling exercise and field surveys, a total of 35 viable generator sites located on federal, state, and private lands were identified with 23 located on USFS land.

To initiate the permitting requirements for an operational cloud-seeding program designed to target the Medicine Bow and Sierra Madre Ranges, a SUP application was submitted to the

USFS on 22 February 2016. The approach for the permit application portion of this study (Section 16) was to provide a maximum number of potential ground-based generators that could be used in the Medicine Bow and Sierra Madre Mountains operational cloud-seeding program, and would be assessed through the federal NEPA process. The application requested USFS approval to place up to 23 ground-based generators on National Forest administered lands. The MBNF replied with a letter to the WWDO on 9 August 2016 explaining that the proposed project failed to meet the minimum requirements of the initial screening criteria (Appendix B). The WWDO resubmitted the application on 22 December 2016. The MBNF responded with a letter to the WWDO on 28 February 2017 initially accepting the SUP application and notifying the WWDO that USFS personnel would be in contact to discuss the application approval procedures. The WWDO is currently waiting to be contacted on this matter.

The total number of viable generator sites was reduced from 35 to 23 ground-based generators⁹ based off iterative cloud-seeding model simulations. The final project design of 23 ground-based generators includes 16 in the Sierra Madre and 7 in the Medicine Bow. The model simulations indicated that seeding from sites in the Sierra Madre can produce positive simulated effects on the Medicine Bow, and therefore, one approach to developing a cost-effective operational program would be to place generators only in the Sierra Madre to target both mountain ranges. Of the 16 proposed sites in the Sierra Madre, 6 were sited specifically to target the Medicine Bow.

Operational Criteria and Other Program Considerations

Operational seeding criteria were developed for possible ground-based seeding operations as well as for potential seeding with an aircraft. Among the most critical data for establishing operational seeding criteria are upper air temperatures, wind direction and speed, and the existence of SLW relative to the project target area. Weather observations to determine when the operational criteria are met are available in real time via a variety of products available on the internet. In order to obtain project specific weather information the deployment of project soundings and a radiometer is recommended, but not required. A well-designed research or operational cloud-seeding program will incorporate seeding suspension criteria to stop or suspend seeding activities that could generate unsafe conditions due to increases in precipitation. Suspension criteria recommended for an operational program being implemented in the Medicine Bow and Sierra Madre Mountains can be found in Section 9.5.

Other program considerations account for environmental concerns such as downwind (extra-area) effects, or potential impacts to water and soil quality resulting from the practice of cloud seeding. Numerous studies have been conducted in the western United States related to the potential environmental impacts of winter cloud seeding. These studies found that significant environmental effects related to the conduct of cloud-seeding programs in these areas were not expected to occur.

⁹ Note that not all of these are on USFS land, and therefore this set of 23 slightly differs from the 23 included in the USFS permit application.

Potential Benefits, Cost Estimates, and Benefit/Cost Analysis Summary

Estimates of streamflow changes due to seeding impacts were calculated two ways. One method estimated the change in streamflow relative to a change in precipitation using regressions of historical precipitation and streamflow records, either from gauge measurements and/or a long-term model simulation. This method was similar to that used in other recent Wyoming weather-modification feasibility studies (i.e., Wyoming Range, Bighorn Mountains). In this design study, the WRF-CONUS simulation was used to establish this relationship. However, there are several assumptions required for this approach, which contribute to a substantial range of uncertainty in the final results.

Secondly, streamflow changes from seeding were estimated using a new method that utilizes the WRF-Hydro hydrological model, coupled with results of cloud-seeding simulations from the WWMPP. While there are still inherent uncertainties associated with this method, many of the assumptions associated with the previous regression method were removed.

The results of the two methods compared well. The regression method found a range of total streamflow increase between ~11,170 and ~49,390 AF, depending on the assumed method of seeding (ground versus airborne) and the assumed magnitude of the seeding effect (5, 10, 15%, all assuming a 70% impact area), while the WRF-Hydro method found 5,000–7,750 AF. The WRF-Hydro simulation method helped reduce some of the uncertainties in the traditional regression analysis, because it did not need to assume anything about the spatial distribution or magnitude of the seeding effect. Rather, those attributes from the simulated seeding cases were directly ingested as forcing into the WRF-Hydro simulation. However, at the time, this simulation represented only two years of simulated seeding cases from the WWMPP, whereas the regression analysis represented an 8-year-average scenario from the climatology analysis. Moreover, the regression analysis results were based upon less stringent conditions for seeding than imposed during the WWMPP (i.e., temperature criterion, 4-hour seeding periods, etc.). If the WRF-Hydro results were averaged together and then doubled, to account for the limited seeding periods simulated based upon the WWMPP criteria, the results indicate approximately 12,500 AF of additional streamflow could be produced from cloud seeding. This estimate is consistent with the regression analysis result (~11,170 AF) for a ground-based scenario with just over a 5% annual seeding effect (in seedable storms) using an assumed 70% impact area.

Cost estimates were prepared for two different seeding program options:

- 3.) a program with 23 remote-controlled ground-based generators (estimated annual cost: \$656,685), and
- 4.) a single stand-alone aircraft seeding program (estimated annual cost: \$361,780).

A preliminary benefit/cost analysis was performed using the estimated range of enhanced average April – July runoff values. ASCE Guidelines were used to determine whether the program would be considered feasible. The Guidelines suggest that two questions be answered: is the proposed program technically feasible and is the proposed program economically feasible? An affirmative answer to both questions is required for the program to be considered feasible. *The evidence presented in this study is that the program is technically feasible.*

For a proposed program to be economically feasible, the ASCE Guidelines recommend that a proposed program have an estimated benefit/cost ratio of 5/1. To determine the benefit/cost ratio several assumptions need to be considered (e.g., area and magnitude of seeding impact, value of the water, etc.), and were included in the ratio calculations for this study. Of the possible seeding options and levels of seeding effects, airborne seeding met the 5/1 ratio assuming 10% or greater seeding effect, and also the actual value of water. Ground seeding does not meet the 5/1 ratio, primarily due to the higher program cost compared with airborne seeding. If the ground-seeding program costs could be reduced (by reducing the number of total generators) while still achieving the desired seeding effect, ground seeding might be more cost effective.

Model Evaluation of the WWMPP RSE

Instead of collecting additional randomized cases at great expense, an ensemble modeling approach to estimate the impact of ground-based seeding was conducted. This approach is advantageous because conditions with and without seeding can be simulated, allowing the difference of the model simulations to estimate the seeding effect. An ensemble approach also better accounts for initial condition uncertainty, model biases, and random errors in the model simulations.

A prerequisite to using a model, however, is that the simulations reasonably represent reality. The WWMPP RSE snow-gauge data and sounding data were used to perform this function. The inter-comparison between the model ensemble simulations and the snow-gauge data per Experimental Unit (EU) showed reasonable agreement in terms of the model mean with median errors being close to zero. In addition, the distribution of errors in a paired comparison between model and gauges was symmetric about zero error in most cases. The inter-comparison to sounding data showed that the model simulation reasonably simulated the mesoscale structure of the storms.

This snow-gauge comparison was made with twenty-four model ensemble members for each of three re-analysis forcing datasets with no seeding simulated, with a total of 8,946 simulations to simulate each of the 118 EUs. This approach minimized potential biases due to poor representation of time-variations in forcings of precipitation for each EU, and emphasized the orographically forced component of precipitation.

The results of the model ensemble approach with and without seeding estimated a mean enhancement of precipitation of 5%, with an inner quartile range of 3 to 7%. These results provide a robust estimate of the impact of ground-based cloud seeding in the Sierra Madre and Medicine Bow Ranges in Wyoming that accounts for key uncertainties in both initial conditions and model physics.

22.2. Conclusions and Recommendations

Based on the results of this study, an operational cloud-seeding program targeting the Medicine Bow and Sierra Madre Ranges is technically feasible. This is supported by the climatological analysis and cloud-seeding model evaluation presented herein, as well as the results previously ascertained in the same project area during the WWMPP.

Based on the results of this study it can be concluded that an operational cloud-seeding program targeting the Medicine Bow and Sierra Madre Ranges would be economically feasible depending on which type of operational program is implemented (ground or air). The cost effectiveness of a cloud-seeding program is dependent on several factors, including the cost of water and the level of seeding effect expected to be achieved. Based on the results of this analysis, airborne seeding is a cost-effective program design option given lower overall program costs, fewer seeding restrictions due to wind direction or atmospheric stability, and no required permitting fees. However, airborne seeding is limited by aircraft on-station time, which is not reflected in the climatology analysis. For example, a single aircraft may not be able to seed for the entirety of a seedable period if that period is longer than the aircraft can be on station (due to fuel consumption, crew duty limits, etc.). The climatology analysis did not exclude long seedable periods given the aircraft on-station time is currently unknown (dependent on the actual aircraft type selected for the seeding program, the extent of icing conditions encountered in a given flight, etc.). However, accounting for this could lead to reduced precipitation that falls when conditions are seedable by a single aircraft. None of the ground-based seeding scenarios met the 5/1 ratio, and therefore cannot be considered economically feasible. However conceptually, a ground-based seeding program could become more cost effective if the number of generators in the design were reduced to lower overall program costs, while maintaining seeding effects similar to those presented in this study.

22.2.1. Recommendations

Based on the results of this study, several recommendations specific to the design and conduct of an operational cloud-seeding program in the Medicine Bow and Sierra Madre Ranges are presented here.

- Seeding should be conducted using AgI as the seeding agent.
- The seeding season for ground based and/or airborne operations should be 15 November–15 April.
- Aircraft seeding is considered technically and economically feasible, whereas ground-based seeding is considered technically feasible only, therefore it is recommended that aircraft seeding be conducted.
- To address whether or not ground-based seeding could be considered economically feasible, an investigation focused on optimizing the operational design in relation to cost and seeding effectiveness should be considered.
- To validate the effects from seeding with either proposed program design, modeled simulations of additional test cases (ideally an entire season of seeding cases), should be considered.
- Basic seeding criteria should be based on readily available (and quickly accessible) meteorological data.
- To accurately assess seeding criteria specifically in the study area, a program would benefit from deploying project-specific instrumentation (i.e., radiometer and soundings), but these would add costs to operate the program that were not accounted for in the benefit/cost analysis for this study.
- To attempt to reduce overall program cost, a study to investigate sharing operational resources (i.e., aircraft, staff, weather data, etc.) between seeding programs targeting multiple mountain ranges in the region should be considered.

- To determine the most cost-effective approach to sharing operational resources, an evaluation of all the Wyoming (proposed and operational) weather modification projects, for multiple project designs (ground-based and airborne) should be considered.
- The implementation of a statewide, real-time modeling system would provide guidance in determining storm seedability, especially if multiple cloud-seeding programs are implemented within the state. A forecast modeling system will generate a cost savings by identifying storms with high seeding potential, therefore maximizing cloud-seeding impacts. The model can also serve as a basis for seasonal program evaluation.

Appendix A: Photos from Field Surveys

Photos from the field surveys of potential generator sites

Medicine Bow Range

Site MB1 – Sourdough Creek. Clockwise, from upper left: north, west, south, and east.



Site MB2 – Upper Bear Gulch. Clockwise, from upper left: north, west, south, and east.



Site MB3 – Francis Draw. Clockwise, from upper left: north, west, south, and east.



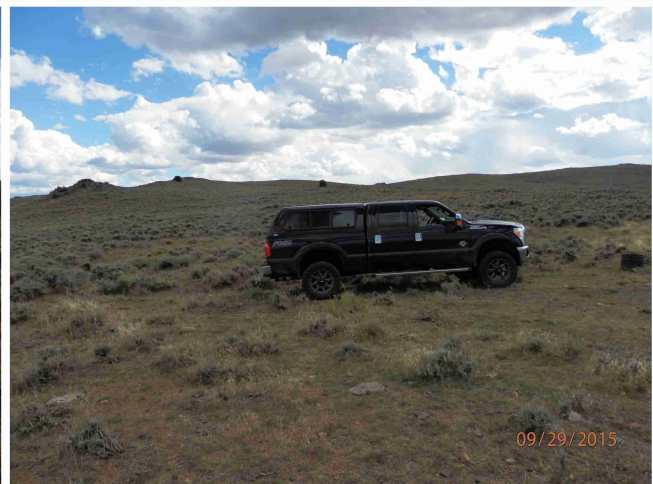
Site MB4 – Little Beaver Creek. Clockwise, from upper left: north, west, south, and east.



Site MB5 – Brush Creek. Clockwise, from upper left: north, west, south, and east.



Site MB6 – Big Spring West. Clockwise, from upper left: north, west, south, and east.



Site MB7 – East Pass Creek. Clockwise, from upper left: north, west, south, and east.



Site MB8 – Kennaday Peak. Clockwise, from upper left: north, west, south, and east.



Site MB9 – Goetz Creek. Clockwise, from upper left: north, west, south, and east.



Site MB10 – South Fork Mill Creek. Clockwise, from upper left: north, west, south, and east.



Site MB11 – Middle Fork Mill Creek. Clockwise, from upper left: north, west, south, and east.



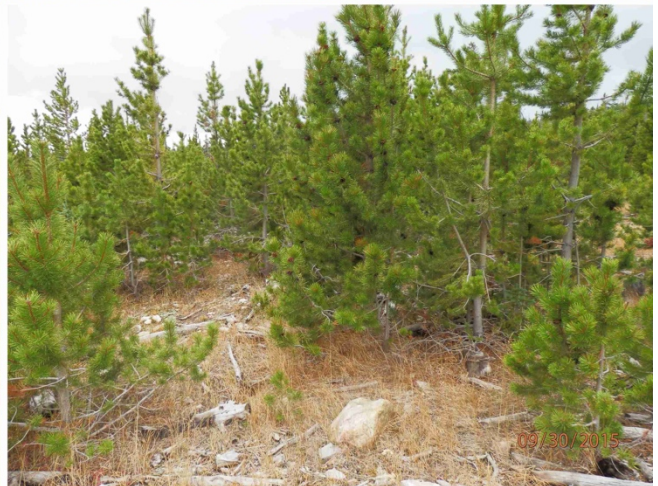
Site MB12 – Lost Lake. Clockwise, from upper left: north, west, south, and east.



Site MB13. Copper Creek. Clockwise, from upper left: north, west, south, and east.



Site MB14 – Rock Creek Point. Clockwise, from upper left: north, west, south, and east.

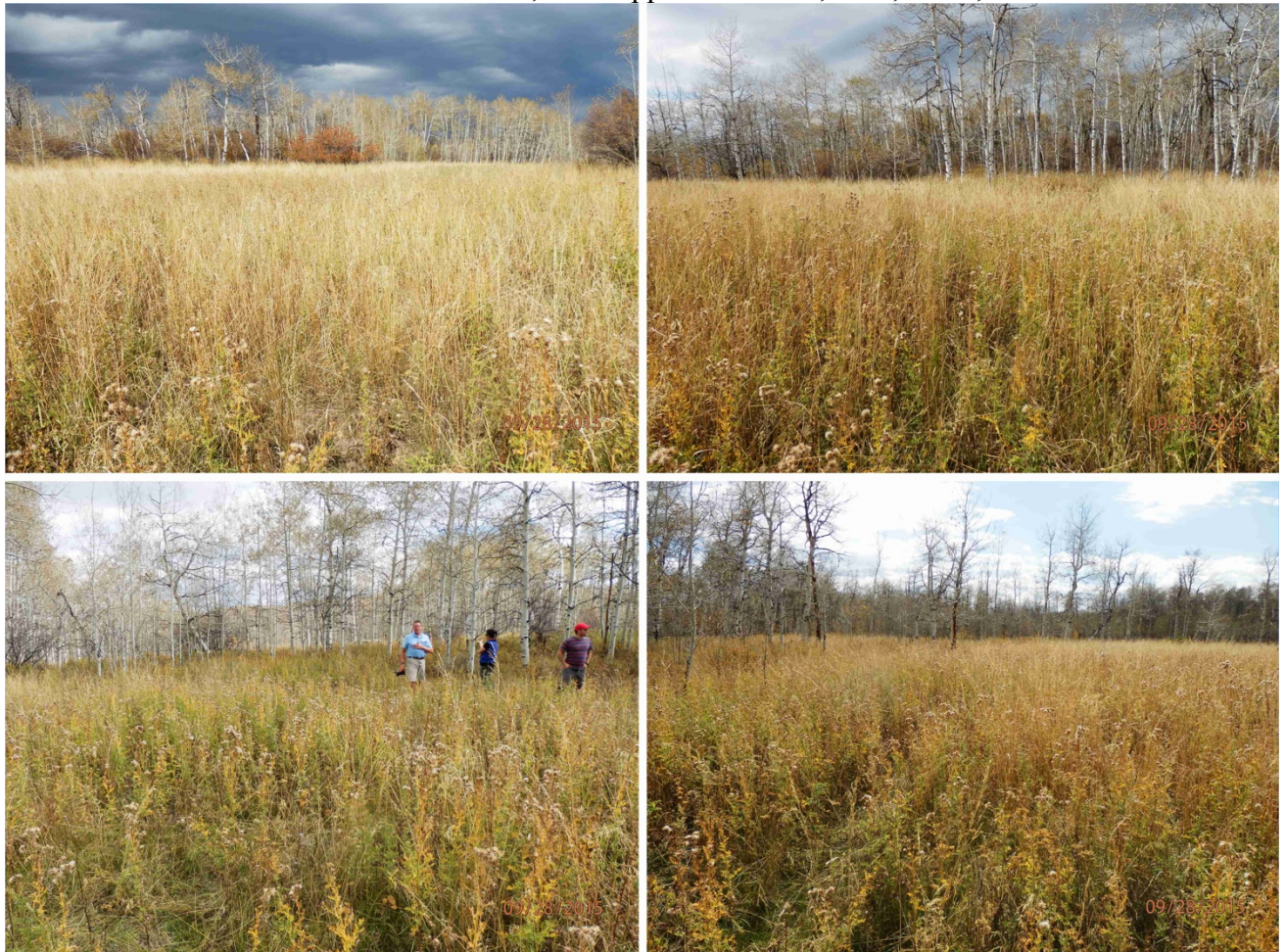


Sierra Madre Range

Site SM1 – Stemp Spring. Clockwise, from upper left: north, west, south, and east.



Site SM2 – Sandstone Plateau. Clockwise, from upper left: north, west, south, and east.



Site SM3 – West Sandstone Plateau. Clockwise, from upper left: north, west, south, and east.



Site SM4 – Green Ridge. No photos were taken because site is 250 feet from F3 and looks the same.



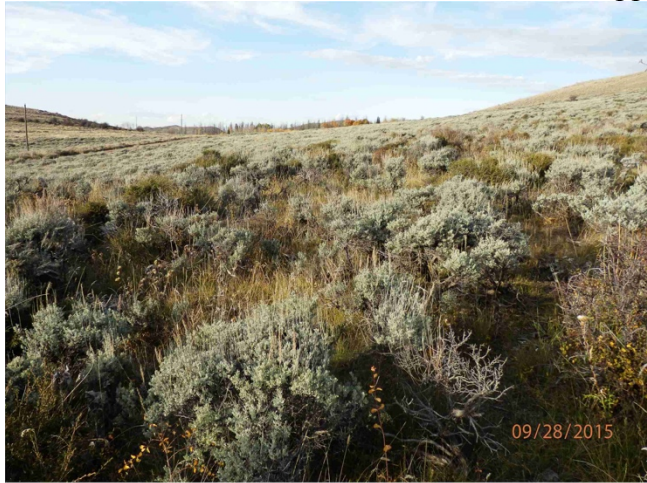
Site SM5 – Dirtyman Fork. Clockwise, from upper left: north, west, south, and east.



Site SM6 – Cooper Creek. Clockwise, from upper left: north, west, south, and east.



Site SM7 – Cushman Creek. Clockwise, from upper left: north, west, south, and east.



Site SM8 – Purgatory Plateau. Clockwise, from upper left: north, west, south, and east.



Site SM9 – Heather Hill. Clockwise, from upper left: north, west, south, and east.



Site SM10 – Heather Creek. Clockwise, from upper left: north, west, south, and east.



Site SM11 – Mowry Peak. Clockwise, from upper left: north, west, south, and east.



Site SM12 – Sharp Hill. Clockwise, from upper left: north, west, south, and east.



Site SM13 – Cherokee Creek. Clockwise, from upper left: north, west, south, and east.



Appendix B: Letters from the USFS



Forest
Service

Medicine Bow-Routt National Forests
and Thunder Basin National Grassland

2468 Jackson Street
Laramie, WY 82070
307-745-2300
FAX: 307-745-2398

File Code: 2720; 2320; 2520

Date: August 9, 2016

Harry C. LaBonde, Jr., PE
Director
Wyoming Water Development Commission
6920 Yellowtail Road
Cheyenne, WY 82002

RECEIVED

AUG 10 2016

WY WATER DEVELOPMENT
COMMISSION

Dear Mr. LaBonde:

I received your proposal, dated February 22nd, 2016, to operate a weather modification program on the Medicine Bow National Forest (MBNF). In August of 2006, the U.S. Forest Service (USFS) issued a permit to Weather Modification, Inc. to conduct a cloud-seeding research study, on behalf of the Wyoming Water Development Commission (WWDC), in the MBNF. The permit was issued as a research permit. Although the WWDC collaborated with Weather Modification, Inc. for a weather modification research study on the MBNF, you are a new proponent and the proposal is for a new type of use.

Proposals for new uses of National Forest System (NFS) lands are initially screened for the minimum requirements in *36 Code of Federal Regulations (CFR) 251.54(e)(1)(i)-(ix)* and *Forest Service Handbook (FSH) 2709.11 sec. 12.21*. Proposed uses that do not meet all of the minimum requirements shall not receive further consideration (*36 CFR 251.54(e)(2)*).

Screening criteria #1, of the initial screening of proposals, states "*The proposed use is consistent with the laws, regulations, orders, and policies establishing or governing national Forest System lands...*" I reviewed your proposal for consistency with Forest Service policy regarding weather modification on NFS lands. Forest Service Manual (FSM) 2724.24 provides guidance on issuing special use authorizations for weather modification devices. FSM 2323.45 provides direction on the management of weather modification that affect congressionally designated wilderness areas:

FSM 2323.45 Do not permit long-term weather modification programs that produce, during any part of successive years, a repeated or prolonged change in the weather directly affecting wilderness areas.

The stated purpose of the proposed use is, "to increase the volume of water available for irrigation, power generation, and downstream flows of several major rivers." The term requested is 30 years. In the project background you state, "The project would target specific watersheds near and within designated wildernesses for an anticipated 5 to 15% increase in snowpack in seeded storms (an estimated 30% of all winter storms are seedable in any given year)." The target watersheds are in the MBNF and include the Huston Park, Encampment River, Savage Run, and Platte River Wilderness Areas.



Caring for the Land and Serving People

Printed on Recycled Paper



The proposed use is to operate a long-term weather modification program that would produce a repeated change in the weather directly affecting wilderness areas in the MBNF. This use of NFS lands would not be consistent with *FSM 2323.45*, therefore I find that your proposal does not meet criteria 1 of the initial screening criteria requirements and shall not receive further consideration as proposed.

Findings that a proposal fails to meet the initial screening criteria are not subject to administrative appeal (*FSH 2709.11 sec. 12.22(1)(d)*). Please find your original proposal enclosed with this letter.

When the Forest Service commented on the Weather Modification Feasibility Study proposal in 2004 we informed the WWDC that the Forest Service does not allow long-term weather modification programs that produce, during any part of successive years, a repeated or prolonged change in the weather directly affecting wilderness areas (see attached letter dated 12/21/2004).

The Forest Service supports properly designed and scientifically and technically sound snow augmentation or other weather modification activities carried out by cooperators, provided those activities and anticipated results are consistent with all applicable laws and regulations governing the administration and management of NFS lands (*FSM 2522.12b*). The Medicine Bow-Routt National Forests and Thunder Basin National Grassland is prepared to work with the WWDC and the State of Wyoming to develop future proposals for weather modification programs that would not be in conflict with our management direction for congressionally designated wilderness areas and provide guidance on applicable laws, regulations, and policies related to weather modification activities on NFS lands.

If you have further questions contact Nathan Haynes, Realty Specialist, at (307)745-2430 or nhaynes@fs.fed.us.

Sincerely,



DENNIS L. JAEGER
Forest Supervisor

cc: Jim Bedwell, Deb Ryon, Ralph Swain, Sandy Henning



United States
Department of
Agriculture

Forest
Service

Medicine Bow-Routt National Forests
and Thunder Basin National Grassland

2468 Jackson Street
Laramie, WY 82070
307-745-2300
Fax: 307-745-2398

File Code: 2720; 2520; 2320
Date: February 24, 2017

Harry C. LaBonde, Jr., PE
Director
Wyoming Water Development Commission
6920 Yellowtail Road
Cheyenne, WY 82002

RECEIVED

FEB 28 2017

WY WATER DEVELOPMENT OFFICE

Dear Mr. LaBonde:

I received your proposal, dated December 22nd, 2017, to operate a weather modification program on the Medicine Bow National Forest (MBNF). In August of 2006, the MBNF issued a research permit to Weather Modification, Inc. to conduct a cloud-seeding research study, on behalf of the Wyoming Water Development Commission (WWDC). Although the WWDC collaborated with Weather Modification, Inc. for this research study on the MBNF, you are a new proponent and the proposal is for a new type of use.

Proposals for new uses of National Forest System (NFS) lands are initially screened for the minimum requirements in *36 Code of Federal Regulations (CFR) 251.54(e)(1)(i)-(ix)* and *Forest Service Handbook (FSH) 2709.11 sec. 12.21*. A proposal that passes the initial screening proceeds to second-level screening outlined in *36 CFR 251.54(e)(5)(i)-(v)* and *FSH 2709.11 sec. 12.32*.

My determination is that your proposal meets all of the initial and second-level screening criteria. I accept your proposal as a formal application for a Special Use Authorization to operate a weather modification program on the MBNF. Formal applications for Special Use Authorizations are considered a proposed action for purposes of the National Environmental Policy Act (NEPA). Proposed actions must be evaluated pursuant to NEPA, its implementing regulations, and agency NEPA procedures.

You will be contacted by my staff in the coming weeks to discuss our procedures for processing the application and estimated time requirements. If you have any question contact Nathan Haynes, Realty Specialist, at (307)745-2430 or nhaynes@fs.fed.us.

Sincerely,

DENNIS L. JAEGER
Forest Supervisor



Caring for the Land and Serving People

Printed on Recycled Paper



Appendix C: Public Hearing Documents

These documents include notices of publication regarding the hearing, the agenda for the hearing, sign in sheet listing attendees of the hearing, a public hearing summary, and a response to public comment.

Wyoming Water Development Commission
6920 Yellowtail Rd
Cheyenne, WY 82002

From:
Rawlins Daily Times
Adams Publishing Group, INC.
P.O. Box 370
Rawlins, WY 82301-370
FEDERAL TAX ID. #83-0141320

LEGAL ADVERTISING AFFIDAVIT

DESCRIPTION OF ADVERTISEMENT: MedBow Sierra Madre

PUBLISHED: June 20, 27 & July 4, 2017

LEGAL PUBLICATION NO: 7661

THE STATE OF WYOMING)
SS,
COUNTY OF CARBON)

I, Emily Kirk,
Do solemnly swear that I am the
Marketing Director

of the Rawlins Daily Times, a newspaper of general
circulation published daily (except Sunday and
Monday), in the CITY OF RAWLINS, CARBON
COUNTY, WYOMING; that the notice of which the
attached is a true copy, was published in said
newspaper for


Three (3)
Publications, the first publication having been made
on the

20th day of June, A.D. 2017

and the last publication having been made on the

4th day of July A.D. 2017

that said notice was published in the regular and entire
issue of said paper during the period and times of
publication aforesaid and that the notice was
published in the newspaper proper and not in a
supplement. So help me God.


Subscribed and sworn to before me, this
4th day of July A.D. 2017

Printer's Fees: \$121.50

Notary Public 
Julia Sabo - Notary Public
County of Carbon State of Wyoming
My Commission Expires: 12/22/2019

12/22/19

Public Notice
Presentation of Study Results and Public Hearing on
the Wyoming Weather Modification Medicine
Bow/Sierra Madre Final Design and Permitting
Study
When: July 11, 2017 at 6:30 pm
Where: Platte Valley Community Center
210 W. Elm St.
Saratoga, WY 82331
The Wyoming Water Development Commission
will hold public hearings to receive comments on
the above listed project. The Commission will also
be seeking information as to whether the proposed
project functions and services can be served by any
person, association or corporation engaged in pri-
vate enterprise.
Representatives of the Water Development Com-
mission and the project sponsor will be present to
explain the proposed project and to record com-
ments.
For further information contact:
Wyoming Water Development Office, 6920 Yel-
lowtail Road,
Cheyenne, Wyoming 82002 (307/777-7626)
Published: June 20, 27 & July 4, 2017
No. 7661

*** Proof of Publication ***

Casper Star-Tribune
P.O. Box 80, Casper, WY 82602-0080, ph 307-266-0500

AFFIDAVIT OF PUBLICATION

STATE OF WYOMING)
COUNTY OF NATRONA)

I, the undersigned, being a person in the employ of the Casper Star-Tribune, a newspaper published in CASPER, NATRONA COUNTY, WYOMING, and, knowing the facts herein set forth do so solemnly swear that a copy of the notice as per clipping attached was printed and published

Daily

Weekly

In the regular and entire issue of said newspaper, and not in any supplement thereof, for 3 Consecutive Days Weeks

commencing with issue dated June 20, 2017
ending with issue dated July 5, 2017

Wyoming Water Development
6920 Yellowtail Rd.
Cheyenne, WY 82002

NOTICE

Presentation of Study Results and Public Hearing on the Wyoming Weather Modification Medicine Bow Sierra Madre Final Design and Permitting Study

When: July 11, 2017 at 6:30 pm
Where: Platte Valley Community Center
210 W. Elm St.
Saratoga, WY 82331

The Wyoming Water Development Commission will hold public hearings to receive comments on the above listed project. The Commission will also be seeking information as to whether the proposed project functions and services can be served by any person, association or corporation engaged in private enterprise.

Representatives of the Water Development Commission and the project sponsor will be present to explain the proposed project and to record comments.

For further information contact:

Wyoming Water Development Office,
6920 Yellowtail Road,
Cheyenne, Wyoming 82002
(307)777-7626

Published: June 20, 27 & July 5, 2017
Legal No: 24989

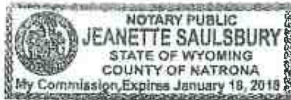
ORDER NUMBER 24989

Shaun Kithers
Signed

Subscribed in my presence and sworn to before me this

6th day of July 2017

Jeannette Saulsbury



PUBLISHED ON: 06/20/2017, 06/27/2017, 07/05/2017

TOTAL AD COST: 198.52

FILED ON: 7/5/2017

**Medicine Bow and Sierra Madre Range
Weather Modification Design and Permitting Study
Draft Final Results Public Hearing**

Tuesday July 11th, 2017 6:30-8:30 p.m.
Platte Valley Community Center
Saratoga, Wyoming

WELCOME – Jeni Cederle, Project Manager, Wyoming Water Development Office (WWDO), Cheyenne, WY

- A. Welcome
- B. Pass around sign-in sheet
- C. Open public hearing

OVERVIEW OF CURRENT STUDY – Sarah Tessendorf, National Center for Atmospheric Research (NCAR) and Bruce Boe, Weather Modification International (WMI)

- A. Introduction of project team
- B. Summary of tasks
- C. Review of WWMPP
- D. Climatology study
- E. Overview of design options

MODEL EVALUATION OF PROGRAM DESIGNS – Roy Rasmussen, NCAR

- A. RSE model evaluation
- B. Model evaluation of design options
- C. Design iterations based on model results
- D. Recommended design

PROGRAM CONSIDERATIONS – Bruce Boe, WMI, and Patrick Golden, Heritage Environmental Consultants

- A. Operational criteria
- B. Field surveys of potential generator sites
- C. Permitting
- D. Environmental and legal implications

COST BENEFIT ANALYSIS – Roy Rasmussen, NCAR, and Bruce Boe, WMI

- A. Potential benefits analysis
- B. Cost estimates
- C. Benefit/cost analysis

SUMMARY AND RECOMMENDATIONS – Sarah Tessendorf, NCAR

DISCUSSION / WRAP UP

**WYOMING WATER DEVELOPMENT COMMISSION (WWDC) PUBLIC HEARING
WEATHER MODIFICATION MEDICINE BOW/SIERRA MADRE FINAL DESIGN & PERMITTING STUDY - PUBLIC HEARING**

Date: July 11, 2017 – 6:30pm

Hearing Location: Platte Valley Community Center, Saratoga, WY

Name	Representing / Location	Email
Joni Cederte	WWDC / Cheyenne	cedertej@wyo.gov
Bruce Boe	WMI / Fargo	bboe@weather-mod.com
Pitt Golden	Heritage / Denver	pgolden@heritage-ec.com
Sarah Tessen Dorf	NCAR	SarahT@ucar.edu
Roy Rasmussen	NCAR	rasmus@ucar.edu
Emma Diants	Bigfoot 99	emma@bigfoot99.com
Harry LaBouche	WWDC	harry.labouche@wyo.gov
DANIEL MANVILLE	JACKSON COUNTY / WACAPEN, CO	MANVILLE.DAN@GMAIL.COM
Barry Lawrence	WWDC / CHEYENNE	Barry.Lawrence@wyo.gov
Craig Blumenshine	Wyoming PBS	craig@wyomingpbs.org
Joe Parsons	SEACD	joe.lserid@grail.com



Wyoming Water Development Office

6920 YELLOWTAIL ROAD

CHEYENNE, WY 82002

TELEPHONE: (307) 777-7626





WYOMING WATER DEVELOPMENT OFFICE

6920 Yellowtail Road
Cheyenne, WY 82002

Phone: (307) 777-7626
wwdc.state.wy.us

Matthew H. Mead
Governor

Commissioners

Nick Bettas	Kellen K. Lancaster
Karen Budd-Falen	Sheridan Little
David Evans	Jeanette Sekan
Gerald E. Geis	Larry Suchor
Clinton W. Glick	Rodney Wagner

Harry C. LaBonde, Jr., P.E.
Director

To: Katie Talbot

From: Jeni Cederle, Project Manager

CC: Hearing Record

Date: July 26, 2017

Re: Weather Modification, Medicine Bow and Sierra Madre Final Design and Permitting Study - July 11, 2017 Public Hearing

A public hearing was held on July 11, 2017 at the Platte Valley Community Center, 210 W. Elm Street, Saratoga, Wyoming to present the draft study results and accept public comment concerning the Wyoming Water Development Commission's Weather Modification, Medicine Bow & Sierra Madre Final Design and Permitting Study. The hearing was declared open at 6:30 p.m. and closed at approximately 8:21 p.m. The hearing notice was published three times in the state-wide Casper Star-Tribune newspaper and local Rawlins Daily Times. Eleven people attended the hearing, and a recording of the hearing is available at the Water Development Office.

The public hearing was held pursuant to Wyoming Statute 41-2-114(b)(iii). During the course of the presentation, the consultant provided clarification and answered technical questions posed by the audience regarding the study results. One substantive verbal comment was received at the hearing. Joe Parsons, District Manager of the Saratoga – Encampment – Rawlins Conservation District (SERCD) provided comment for the record. The SERCD comment is summarized below:

- The SERCD commented on the results of the previous Wyoming Weather Modification Pilot Program (WWMPP) having produced a “null” value.
- The SERCD pointed out that the modeling results of the 7/11/17 public hearing were based off the previous WWMPP study results, and are now showing a positive result.
- The SERCD questions whether or not the positive modeling result is realistic.

Written/email comments were accepted and included as part of the public record if received by July 21, 2017. One email comment was received prior to the close of the comment period and will be included as part of the public record.

Comments to be included for the public record were received from:

Ms. Arla Strasser
Board Chair
Saratoga-Encampment-Rawlins Conservation District (SERCD)
P.O. Box 633
Saratoga, WY 82331

Enc.
Hearing Agenda
Comments Received

Response to Public Comment



WYOMING WATER DEVELOPMENT OFFICE

6920 Yellowtail Road
Cheyenne, WY 82002

Phone: (307) 777-7626
wwdc.state.wy.us

Matthew H. Mead
Governor

Commissioners

Nick Bettas	Kellen K. Lancaster
Karen Budd-Falen	Sheridan Little
David Evans	Jeanette Sekan
Gerald E. Geis	Larry Suchor
Clinton W. Glick	Rodney Wagner
Harry C. LaBonde, Jr., P.E. Director	

October 2, 2017

Saratoga-Encampment-Rawlins Conservation District
P.O. Box 633
Saratoga, WY 82331

SUBJECT: Comment Response Concerning the Medicine Bow/Sierra Madre Weather
Modification Final Design and Permitting Study Results

Introduction:

The 2015 Wyoming Legislature appropriated funds to be spent developing a final operational project design and initiate the permitting process for weather modification activities in the Medicine Bow/Sierra Madre Mountains (MBSM). The results of the study were presented to the public at a public hearing on July 11, 2017 at 6:30 p.m., at the Platte Valley Community Center in Saratoga, WY.

Overview of Comments Received:

During the course of the presentation of results, the consultant provided clarification and answered technical questions posed by the audience. The Saratoga-Encampment-Rawlins Conservation District (SERCD) also submitted a written comment that was received via email prior to the close of the comment period (July 11, 2017 – July 21, 2017). One substantive verbal comment was provided by Mr. Joe Parsons, District Manager of the SERCD for the record at the hearing. The content of the verbal comment mirrors concerns addressed in the written submission. This document has been developed to serve as a response to the verbal & written comments received from the SERCD.

Comment and Response:

Comment:

Request that the Wyoming Water Development Office (WWDO) continue to provide outreach and discussion with the SERCD regarding any action or decisions pertaining to the Proposed Project.

Response:

The WWDO appreciates SERCD's interest in the proposed MBSM weather modification project. We have worked diligently to maintain open lines of communication, and outreach in regards to all weather modification activities, and will continue to do so.

Comment(s):

"While previous studies in the area showed no increase in water from weather modification activities, additional spring water runoff could compound the recently altered patterns of spring water runoff from the beetle-killed forest and increased areas of recent forest fires if the Proposed Project results in adding more snow water equivalent to the system."

"Models can be developed to show desired outcomes. We believe the previous multi-year weather modification study project conducted is more accurate than the model in determining snow increase."

Response: (from NCAR)

The previous multi-year research project (the Wyoming Weather Modification Pilot Program (WWMPP)) statistical analysis did not show beyond a reasonable doubt there was a seeding effect due to the lack of statistical significance in the result. Having a lack of statistical significance means that the result cannot indicate if there is, or is not, a seeding effect. There are many reasons why statistical experiments fail to show conclusive results, from experimental design limitations to not obtaining a representative (or large enough) sample of cases to overcome the degree of natural variability in the system. The latter is often a highly contributing factor to inconclusive statistical results.

In our work at NCAR, we have been developing numerical models to forecast and simulate the weather for many decades. Our goal is to develop systems that can predict a variety of weather phenomena with the highest degree of accuracy that is possible with the available computing resources and scientific understanding of the processes that are the basis for the numerical formulations of the model itself. We strive to compare our models with high quality observations in order to evaluate how well they perform, using the actual observed conditions as the basis for performance (not any particular desired outcome).

During the WWMPP, a new parameterization was developed to explicitly simulate the impacts of silver iodide (AgI) in our weather model. One goal for developing this parameterization was to utilize models to evaluate cloud seeding, since statistical programs have long been fraught with inconclusive results given the lack of a truly controlled experiment and large natural

variability in the weather. With the model, the precipitation from a control simulation without seeding can be subtracted from the precipitation simulated with seeding. This provides a model-based estimate of the impact (both in magnitude and spatial distribution) of seeding. However, models are far from perfect and must be validated with observations. Our evaluation of these simulations with precipitation measurements from the WWMPP indicated that the model performed well in some cases, but less so in others. Thus, there is uncertainty in the model that needed to be accounted for.

A way to account for the uncertainty in models is to run an ensemble of model simulations to get a spread of results. This is the work that was conducted by NCAR after the WWMPP, as part of the recent MBSM Final Design and Permitting Study, and results were presented at the public hearing on July 11, 2017. The results of the ensemble modeling simulations show that the ensemble method is able to capture the trends in the precipitation observations and replicate the results of the original research-based random statistical experiment.

Our recent results using the ensemble mean, that were presented at the public hearing on July 11, 2017, suggest that the seeding effect in the Medicine Bow/Sierra Madre Mountains from the WWMPP was on the order of 5% relative to precipitation that fell during seedable storms in a given winter season.

Comment:

"To date, we are simply told 'excess water falls under Wyoming water law.' With an already over adjudicated water problem in the upper Platte Valley, we request an expanded explanation for what will occur if excess water from the Proposed Project comes to fruition."

Response:

Parties offering financial sponsorship, or benefiting from Wyoming weather modification activities will not be allowed to claim a right to any increase in water attributable to cloud seeding, and any increase in the water supply shall be considered part of the natural water supply and shall not be specifically claimed by any Party. Any excess water that is reasonably expected to be a result of cloud seeding activities is to be considered part of the natural water supply subject to all applicable laws. No water rights will be assigned to additional water supplies.

Comment:

SERCD questions "how large expenditures to conduct weather modification activities can be justified when the previous pilot project [WWMPP] showed no net increase in snowpack."

Response:

Initially, the State of Wyoming appropriated funds to research the science and technology behind cloud seeding in order to determine its effectiveness. The results of a 10 year research program provided multiple layers of evidence suggesting that cloud seeding used to augment winter snowpack is a viable and cost effective technology to implement. Based on those results, the Wyoming Legislature has directed the WWDO to transition from research based

cloud seeding programs, to operational programs. Expenditures for operational cloud seeding programs are magnitudes less expensive compared to research based cloud seeding programs (i.e., 2015 Wind River Range (WRR) Funding Recommendation, 2016 WRR Funding Recommendation). A cost savings can also be realized when operational programs are “grouped” together to take advantage of sharing project resources (i.e., weather forecasting, aircraft, maintenance support). Lastly, implementing a collaborative funding approach in developing cloud seeding programs can create a cost savings. All cost saving options will be considered by the WWDO should the Proposed Project move towards implementation.

Comment:

“We believe caution should be exercised in obtaining outside funding partners for the Proposed Project. These outside interests may not be forthright in full disclosure of what they expect in return for helping fund the Proposed Project.”

Response:

The WWDO appreciates the SERCD’s concern regarding the installation of a collaborative funding approach to weather modification in the state of Wyoming. A collaborative funding approach aims to unite all in-basin water users, as well as those benefiting from increased water supplies downstream, under an umbrella agreement to sponsor cloud seeding activities. As mentioned previously, any excess in water that is reasonably expected to be a result of cloud seeding activities is to be considered part of the natural water supply subject to all applicable laws. Furthermore, it is the duty of the WWDO and the State of Wyoming Attorney General’s Office to fully vet any type of collaborative funding agreement(s).

Comment:

“Should the Proposed Project move forward, we recommend aerial cloud seeding be the method of application versus the use of ground generators.”

Response:

The WWDO appreciates the SERCD’s support of the implementation of an airborne cloud seeding program for the MBSM. Results of the Final Design and Permitting Study suggest that aircraft seeding is technically feasible and the most cost effective method to be utilized for the region. The WWDC/SWC and the Office will make every effort to carry out our fiduciary responsibilities to the citizens of Wyoming in the development and funding structure utilized to implement a cloud seeding program in the MBSM.

References

- Acharya, A., T. Piechota, H. Steven, and G. Tootle, 2011: Modeled streamflow response under cloud seeding in the North Platte River watershed. *J. Hydrology*, **409**, 305–314.
- ASCE, 2004: Standard Practice for the Design and Operation of Precipitation Enhancement Projects. ASCE/EWRI 42-04, Reston, Virginia, 58p.
- ASCE, 2006: Guidelines for Cloud Seeding to Augment Precipitation. ASCE Manuals and Reports on Engineering Practice No. 81. ASCE, Reston, VA. 181 p.
- ASCE, 2016: Guidelines for Cloud Seeding to Augment Precipitation. ASCE Manuals and Reports on Engineering Practice No. 81 (Third Edition). ASCE, Reston, VA. 220 p.
- Auer, A.H., Jr., D.L. Veal, and J.D. Marwitz, 1969: Observations of ice crystal and ice nucleus concentrations in stable cap clouds. *J. Atmos. Sci.*, **26**, 1342–1343.
- Auer, A.H., 1972: Inferences about ice nucleation from ice crystal observations. *J. Atmos. Sci.*, **29**, 311–317.
- Barker, D.M., W. Huang, Y.-R. Guo, A.J. Bourgeois and Q.N. Xiao, 2004: A three-dimensional variational data assimilation system for MM5: Implementation and initial results. *Mon. Wea. Rev.*, **132**, 897–914.
- Barlage, M., and Coauthors, 2010: Noah land surface model modifications to improve snowpack prediction in the Colorado Rocky Mountains. *J. Geophys. Res.*, **115**, D22101, doi:10.1029/2009JD013470.
- Berg, N. H., and J.L. Smith, 1980: "An Overview of Societal and Environmental Responses to Weather Modification." *The Sierra Ecology Project*, **5**, Office of Atmospheric Resources Management, Bureau of Reclamation, U.S. Department of the Interior (USDI), Denver, CO.
- Bergeron, T., 1949: The problem of artificial control of rainfall on the globe. I. General effects of ice-nuclei in clouds. *Tellus*, **1**, 32–43.
- Bianchini, A., M. Grosell, S.M. Gregory, and C.M. Wood, 2002: Acute silver toxicity in aquatic animals is a function of sodium uptake rate, *Environmental Science & Technology*, **36**, 1763–1766.
- Boe, B.A., J.A. Heimbach, Jr., T.W. Krauss, L. Xue, X. Chu, and J.T. McPartland, 2014: The dispersion of silver iodide particles from ground-based generators over complex terrain, Part 1: Observations with Acoustic Ice Nucleus Counters. *J. Appl. Meteor. Climatol.*, **53**, 1325–1341.
- Breed, D., R. Rasmussen, C. Weeks, B. Boe, and T. Deshler, 2014: Evaluating winter orographic cloud seeding: Design of the Wyoming Weather Modification Pilot Project (WWMPP), *J. Appl. Meteor. Climatol.*, **53**, 282–299.
- Brier, G.W., 1974: Chapter 5. Design and Evaluation of Weather Modification Experiments, in *Weather and Climate Modification*, Wilmut Hess, Ed., John Wiley and Sons, New York, 842 pp.
- Cardno ENTRIX, 2011: Geochemistry and Impacts of Silver Iodide Use in Cloud Seeding. May 2011. 35 pages.
- Chen, S. and J. Dudhia, 2000: Annual Report: WRF Physics. *NCAR/MMM Internal Report* available at <http://www.mmm.ucar.edu/wrf/users/docs>.
- Coons, R.D., R.C. Gentry, and R. Gunn, 1948: First partial report on the artificial production of precipitation: Stratiform clouds, Ohio. *Bull. Amer. Met. Soc.*, **29**, 266–269.
- Cooper, W.A., and G. Vali, 1981: The origin of ice in mountain cap clouds. *J. Atmos. Sci.*, **38**, 1244–1259.

- Cooper, W.A., 1986: Ice initiation in natural clouds. *Precipitation Enhancement – A Scientific Challenge, Meteor. Monogr.*, No. 43, Amer. Meteor. Soc., 29-32.
- DeFelice, T.P., J. Golden, D. Griffith, W. Woodley, D. Rosenfeld, D. Breed, M. Solak and B. Boe, 2014: Extra area effects of cloud seeding - An updated assessment. *Atmos. Res.*, **135–136**, p. 193–203.
- DeMott, P.J., 1995: Quantitative descriptions of ice formation mechanisms of silver iodide-type aerosols. *Atmos. Res.*, **38**, 63-99.
- DeMott, P.J., 1997: Report to North Dakota Atmospheric Resource Board and Weather Modification Incorporated on tests of the ice nucleating ability of aerosols produced by the Lohse airborne generator. Report from Dept. Atmos. Sci., Colorado State Univ., Fort Collins, CO, 15 pp.
- DeMott, P.J., 1999: Report to Ice Crystal Engineering on Tests of Ice Nucleating Ability of Aerosols Produced by New Formulation Pyrotechnics - July 1999. Cloud Simulation and Aerosol Laboratory, Department of Atmospheric Science, Colorado State University, Fort Collins, CO, USA 80523, 19 p.
- Dennis, A.R., 1980: *Weather Modification by Cloud Seeding*. Academic Press, New York, 267 pp.
- Deshler, T. and G. Vali, 1985: The accretion of ice particles by rime during dry growth. *J. Atmos. Sci.*, **42**, 193–202.
- Di Toro, D.M., H.E. Allen, H.L. Bergman, J.S. Meyer, P.R. Paquin, and R.C. Santore, 2001: Biotic Ligand Model of the acute toxicity of metals. 1. Technical basis. *Environmental Toxicology and Chemistry*, 20:2383-2396.
- Edwards, R., and D. Simeral, 2006: Baseline Silver Concentrations in Freshwater and Snow in the Wyoming Weather Modification Project Target Area. Division of Hydrologic Sciences and Division of Atmospheric Sciences, Desert Research Institute. 42 pages.
- Eisler, R., 1996: Silver Hazards to Fish, Wildlife, and Invertebrates: A Synoptic Review, Contaminant Hazard Reviews, 32, Patuxent Wildlife Research Center, U.S. National Biological Service, Laurel, MD.
- Findeisen, W., 1938: Colloidal meteorological processes in the formation of atmospheric precipitation. *Meteor. Z.*, **55**, 121-133.
- Gabriel, K.R., 1999: Ratio statistics for randomized experiments in precipitation stimulation. *J. Appl. Meteor.*, **38**, 290–301.
- Gabriel, K.R. and D. Petrondas, 1983: On using historical comparisons in evaluating cloud seeding operations. *J. Climate Appl. Meteor.*, **22**, 626–631.
- Geerts, B., Q. Miao, Y. Yang, R. Rasmussen, and D. Breed, 2010: An airborne profiling radar study of the impact of glaciogenic cloud seeding on snowfall from winter orographic clouds. *J. Atmos. Sci.*, **67**, 3286–3302.
- Geresdi, I., R. M. Rasmussen, W. Grabowski, and B. Bernstein, 2005: Sensitivity of freezing drizzle formation in stably stratified clouds to ice processes. *Meteor. Atmos. Phys.*, **88**, 91–105.
- Geresdi, I., L. Xue, R. Rasmussen, 2016: Evaluation of Orographic Cloud Seeding Using Bin Microphysics Scheme. Part I: Two-dimensional approach. *J. Appl. Meteor. Climatol.*, in review.
- Givati, A., and D. Rosenfeld, 2005: Separation between cloud-seeding and air-pollution effects. *J. Appl. Meteor.*, **44**, 1298–1314.

- Gochis, D.J., W. Yu, and D.N. Yates, 2013: *The WRF-Hydro model technical description and user's guide, version 1.0*. NCAR Technical Document. 120 pages. Available online at: http://www.ral.ucar.edu/projects/wrf_hydro/
- Golden, J.H., 1995: The NOAA Atmospheric Modification Program – A 1995 update. *J. Wea. Modif.*, **27**, 110–112.
- Golden, P., A. Heyvaert, R. Edwards, and J. Thomas, 2011: Idaho Power Company Payette Basin Silver Sampling Final Report. Field Sampling June – August 2010. 152 pages.
- Grant, L.O., and P.W. Mielke Jr., 1967: A randomized cloud seeding experiment at Climax, Colorado, 1960-1965. *Proceedings of the Fifth Berkeley Symposium on Mathematical Statistics and Probability*, Vol 5., University of California Press, 115- 131.
- Grant, L.O., 1986: Hypotheses for the Climax wintertime orographic cloud seeding experiments. *Meteorological Monographs* Vol. 21, No. 43., Precipitation Enhancement: A Scientific Challenge. American Meteorological Society, 105-108.
- Griffith, D.A., M.E. Solak, D.P. Yorty, A.W. Huggins, and D. Koracin, 2006: A Level II Weather Modification Feasibility Study for the Salt River and Wyoming Ranges, Wyoming. North American Weather Consultants (NAWC) Report to the Wyoming Water Development Commission, 261 pp. [also referenced as NAWC, 2006]
- Griffith, D.A., M.E. Solak and D.P. Yorty, 2009: 30+ winter seasons of operational cloud seeding in Utah. *J. Wea. Modif.*, **41**, 23–37.
- Griffith, D.A., D.P. Yorty and M.E. Solak, 2011: A winter operational cloud seeding program: Upper Gunnison River Basin, Colorado. *J. Wea. Modif.*, **43**, 29–43.
- Hallett, J., and S.C. Mossop, 1974: Production of secondary ice particles during the riming process. *Nature*, **249**, 26–28.
- Harper, K.T., 1981: Potential Ecological Impacts of Snowpack Augmentation in the Uinta Mountains, Utah. Brigham Young University Report to the Utah Division of Water Resources, 291 pp.
- Harris, E. R., 1981: “Sierra Cooperative Pilot Project - Environmental Assessment and Finding of No Significant Impact”. U.S. Bureau of Reclamation Report, 196 pp.
- Heimbach, J.A., W.D. Hall, A.B. Super, and 1997: Modeling and observations of valley-released silver iodide during a stable winter storm over the Wasatch Plateau of Utah. *J. Wea. Mod.*, **29**, 33-41.
- Heimbach, J.A., A.B. Super, B.A. Boe, G. Langer, and J.T. McPartland, 2008: Comparison of two acoustic ice nucleus counters. *J. Wea. Modif.*, **40**, 54–63.
- Henderson, T.J., 2003: The Kings River weather resources management program. *J. Wea. Modif.*, **35**, 45–51.
- Hicks and Vali, 1973: Ice nucleation in clouds by liquefied propane spray. *J. Appl. Meteor.*, **12**, 1025–1034.
- Holroyd, E.W., J.A. Heimbach, Jr., and A.B. Super, 1995: Observations and model simulations of AgI seeding within a winter storm over Utah’s Wasatch Plateau. *J. Wea. Mod.*, **27**, 36-56.
- Hong, S.-Y., Y. Noh, and J. Dudhia, 2006: A new vertical diffusion package with an explicit treatment of entrainment processes. *Mon. Wea. Rev.*, **134**, 2318–2341, doi:10.1175/MWR3199.1.
- Hoose, C., and O. Mcöhler, 2012: Heterogeneous ice nucleation on atmospheric aerosols: A review of results from laboratory experiments. *Atmos. Chem. Phys. Discuss.*, **12**, 12 531–12 621.

- Howell, W., 1977: Environmental Impacts of Precipitation management: results from Project Skywater. *Bureau of Reclamation: Division of Atmospheric Water Resources*: 488-501.
- Huggins, A. W., 1995: Mobile microwave radiometer measurements: Spatial characteristics of supercooled cloud water and cloud seeding implications. *J. Appl. Meteor.*, **34**, 432–446.
- Huggins, A.W. 2009: Summary of studies that document the effectiveness of cloud seeding for snowfall augmentation. *J. Wea. Modif.*, **41**, 119–126.
- Iacono, M. J., J. S. Delamere, E. J. Mlawer, M. W. Shephard, S. A. Clough, and W. D. Collins, 2008: Radiative forcing by long-lived greenhouse gases: Calculations with the AER radiative transfer models, *J. Geophys. Res.*, **113**, D13103, doi:10.1029/2008JD009944.
- Ikeda, K., and Coauthors, 2010: Simulation of seasonal snowfall over Colorado. *Atmos. Res.*, **97**, 462–477.
- Johnson, J. B., and D. Marks, 2004: The detection and correction of snow water equivalent pressure sensor errors. *Hydrological Processes*, **18**, 3513–3525.
- Klein, D.A., 1978: *Environmental Impacts of Artificial Ice Nucleating Agents*. Dowden, Hutchinson & Ross, Inc., Stroudsburg, Pennsylvania.
- Klemp, J.B., W.C. Skamarock, and O. Fuhrer. 2003: Numerical consistency of metric terms in terrain-following coordinates. *Mon. Wea. Rev.*, **131**, 1229–1239.
- Knight, D. H., and Coauthors, 1975: "The Medicine Bow Ecology Project." *Final Report to Bureau of Reclamation*, University of Wyoming, Laramie, WY.
- Kraus, E.B., and P. Squires, 1947: Experiments on the simulation of clouds to produce rain. *Nature*, **159**, 489–491.
- Langmuir, I., 1948: The growth of particles in smokes and clouds and the production of snow from supercooled clouds. *Proc. Am. Philos. Soc.*, **92**, 167.
- Liu, C., and co-authors, 2016: Continental-scale convection-permitting modeling of the current and future climate of North America. *Climate Dynamics*. doi:10.1007/s00382-016-3327-9
- Long, A. B., 2001: Review of downwind extra-area effects of precipitation enhancement. *J. Wea. Modif.*, **33**, 24–45.
- Lorenz, E., 1963: Deterministic Nonperiodic Flow, *J. Atmos. Sci.*, **20**, 130 – 141.
- Ludlam, F.H., 1955: Artificial snowfall from mountain clouds. *Tellus*, **7**, 277-289.
- Manton, M.J., and L. Warren, 2011: A confirmatory snowfall enhancement project in the Snowy Mountains of Australia. Part II: Primary and associated analyses. *J. Appl. Meteor. Climatol.*, **50**, 1448–1458.
- Manton, M.J., L. Warren, S. L. Kenyon, A.D. Peace, S.P. Bilish, and K. Kemsley, 2011: A confirmatory snowfall enhancement project in the Snowy Mountains of Australia. Part I: Project design and response variables. *J. Appl. Meteor. Climatol.*, **50**, 1432–1447.
- Manton, M.J., J. Denholm, K. Kemsley, S. L. Kenyon, A. Peace, J. Speirs, and L. Warren (2015): Analysis of a snowfall enhancement project in the Snowy Mountains of Australia. *Submitted to the J. Appl. Meteor. Climatol.*
- Meyers, M.P., P.J. DeMott, and W.R. Cotton, 1992: New primary ice nucleation parameterizations in an explicit cloud model. *J. Appl. Meteor.*, **31**, 708-721.
- Meyers, M. P., P. J. DeMott, and W. R. Cotton, 1995: A Comparison of Seeded and Non-seeded Orographic Cloud Simulations with an Explicit Cloud Model. *J. Appl. Meteor.*, **34**, 834 – 846.
- Mielke, P.W. Jr., L.O. Grant, C.F. Chapell, 1971: An independent replication of the Climax wintertime orographic cloud seeding experiment. *J. Appl. Meteor.*, **10**, 1198-1212.

- Mielke, P.W. Jr., G.W. Brier, L.O. Grant, G.J. Mulvey, and P.N. Rosenweig, 1981: A statistical reanalysis of the replicated Climax I and II wintertime orographic cloud seeding experiments. *J. Appl. Meteor.*, **20**, 643–659.
- Mikalakes, J., J. Dudhia, D. Gill, T. Henderson, J. Klemp, W. Skamarock, and W. Wang, 2004: The Weather Research and Forecast Model: Software Architecture and Performance. *Proceeding of the Eleventh ECMWF Workshop on the Use of High Performance Computing in Meteorology. 25 - 29 October 2004, Reading, U.K.*
- NAWC, 2006: [see Griffith et al. 2006]
- NCAR, 2017: Weather Modification–Bighorn Mountains Siting and Design Study. Report prepared for Wyoming Water Development Commission, State of Wyoming, 288 pages.
- National Research Council (NRC), 2003: *Critical Issues in Weather Modification Research*. National Academy Press, 123 pp.
- Niu, G.-Y., and co-authors, 2011: The community Noah land surface model with multiparameterization options (Noah-MP): 1. Model description and evaluation with local-scale measurements. *J. Geophys. Res.*, **116**, D12109, doi: 10.1029/2010JD015139.
- Pokharel, B., B. Geerts, and X. Jing, 2014a: The impact of ground-based glaciogenic seeding on orographic clouds and precipitation: a multi-sensor case study. *J. Appl. Meteor. Climatol.*, **53**, 890–909.
- Pokharel, B., B. Geerts, X. Jing, K. Friedrich, J. Aikens, D. Breed, R. Rasmussen, and A. Huggins, 2014b: The impact of ground-based glaciogenic seeding on clouds and precipitation over mountains.: A multi-sensor case study of shallow precipitating cumuli. *Atmos. Res.*, **147–148**, 162–182.
- Politovich, M.K., and G. Vali, 1983: Observations of liquid water in cloud of Elk Mountain. *J. Atmos. Sci.*, **40**, 1300–1312.
- Rangno, A.L., and P.V. Hobbs, 1987: A reevaluation of the Climax cloud seeding experiments using NOAA published data. *J. Clim. Appl. Meteor.*, **26**, 757–762.
- Rangno, A.L., and P.V. Hobbs, 1993: Further analyses of the Climax cloud seeding experiments. *J. Appl. Meteor.*, **32**, 1837–1847.
- Rasmussen, R., and Coauthors, 2011: High-resolution coupled climate runoff simulations of seasonal snowfall over Colorado: A process study of current and warmer climate. *J. Climate*, **24**, 3015–3048.
- Rasmussen, R., and Coauthors, 2012: How well are we measuring snow? The NOAA/FAA/NCAR Winter Precipitation Test Bed: *Bull. Amer. Meteorol. Soc.*, **93**, 811–829.
- Rasmussen, R., and Coauthors, 2014: Climate change impacts on the water balance of the Colorado Headwaters: High-resolution regional climate model simulations. *J. Hydro. Meteor.*, **15**, 1091–1116.
- Rauber, R. M., and L. O. Grant, 1986: The characteristics of cloud water over the mountains of northern Colorado during wintertime storms. Part II: Spatial distribution and microphysical characteristics. *J. Climate Appl. Meteor.*, **25**, 489–504.
- Reisner, J. R.M. Rasmussen, and R.T. Bruintjes, 1998: Explicit forecasting of supercooled liquid water in winter storms using the MM5 mesoscale model. *Quart. J. Roy. Meteor. Soc.*, **124**, 1071–1107.
- Reynolds, D.W., 1996: The effects of mountain lee waves on the transport of liquid propane-generated ice crystals. *J. Appl. Meteor.*, **35**, 1435–1456.

- Reynolds, D.W., 2015: Literature Review and Scientific Synthesis on the Efficacy of Winter Orographic Cloud Seeding. Draft Report to the U.S. Bureau of Reclamation, CIRES, Boulder, CO, 148 pp.
- Ritzman, Jaclyn, 2013: What Fraction of Winter Precipitation over the Sierra Madres and Medicine Bows was Treated during the Wyoming Weather Modification Pilot Project?, MS Thesis, Univ. of Wyoming, 96 pp.
- Ritzman, J., T. Deshler, K. Ikeda, and R. Rasmussen, 2015: Estimating the fraction of winter orographic precipitation that is produced under conditions meeting the seeding criteria from the Wyoming weather modification pilot project. *J. Appl. Meteor. Climatol.*, **54**, 1202–1215.
- Rogers, D.C., and G. Vali, 1987: Ice crystal production by mountain surfaces. *J. Clim. Appl. Meteor.*, **26** 1152–1168.
- Rossa, A. M., P. Nurmi, and E. E. Ebert, 2008: Overview of methods for the verification of quantitative precipitation forecasts. *Precipitation: Advances in Measurement, Estimation and Prediction*, S. C. Michaelides, Ed., Springer, 418–450.
- Schaefer, V.J., 1946: The production of ice crystals in a cloud of supercooled water droplets. *Science*, **104**, 457–459.
- Serreze, M. C., M. P. Clark, R. L. Armstrong, D. A. McGinnis, and R. S. Pulwarty, 1999: Characteristics of the western United States snowpack from snowpack telemetry (SNOTEL) data. *Water Resour. Res.*, **35**, 2145–2160.
- Serreze, M. C., M. P. Clark, and A. Frei, 2001: Characteristics of large snowfall events in the montane western United States as examined using snowpack telemetry (SNOTEL) data. *Water Resour. Res.*, **37**, 675–688.
- Silverman, B.A., 2007: On the use of ratio statistics for the evaluation of operational cloud seeding programs. *J. Wea. Modif.*, **39**, 50–60.
- Silverman, B.A., 2010: An evaluation of eleven operational cloud seeding programs in the watersheds of the Sierra Nevada Mountains. *Atmos. Res.*, **145**, 526–539.
- Skamarock, W. C., J. B. Klemp, J. Dudhia, D. O. Gill, D. M. Barker, W. Wang, and J. G. Powers, 2005: A description of the Advanced Research WRF version 2. NCAR Tech. Note NCAR/TN-4681STR, 88 pp. [Available online at www.mmm.ucar.edu/wrf/users/docs/arw_v2.pdf.]
- Skamarock, W. C., J.B. Klemp, J. Dudhia, D.O. Gill, D.M Barker, 2008: A description of the Advanced Research WRF version 3. NCAR Tech. Note NCAR/TN-475+STR
- Slingo, J. and T. Palmer, 2011: Uncertainty in weather and climate prediction, *Philosophical Transactions A*, **369**, 4751 – 4767.
- Solak, M.E., D.P. Yorty and D.A. Griffith, 2003: Estimations of downwind cloud seeding effects in Utah. *J. Wea. Mod.*, **35**, 52–58.
- Smith, J. L., Erman, D. C., Hart, D. D., Kelly, D. W., Klein, D. A., Koch, D. L., Linn, J. D., Moyle, P. M., Ryan, J. H., and Woodard, R. P., 1980. "An Evaluation of Possible Effects of Weather Modification On Lake and Stream Biota in the American River Basin, California." *The Sierra Ecology Project*, **2**, (5), Office of Atmospheric Water Resources Management, Bureau of Reclamation, USDI, Denver, CO.
- Steinhoff and Ives, 1976: Ecological Impacts of Snowpack Augmentation in the San Juan Mountains of Colorado, Final Report of the San Juan Ecology Project to the Bureau of Reclamation from Colorado State University, Contract No. 14-06-D-7052, 489 pp.

- Stone, R.H., K. Smith-Miller, and P. Neeley, 1995: *Mokelumne Watershed Lake Water and Sediment Silver Survey*. Final Report to the Pacific Gas and Electric Company, Technical and Ecological Services, San Ramon, CA.
- Stone, R.H., 2006: *2006 Mokelumne Watershed Lake Water and Sediment Survey*. Final Report to the Pacific Gas and Electric Company, Technical and Ecological Services, San Ramon, CA.
- Super, A.B., 1974: Silver iodide plume characteristics over the Bridger Mountain Range, Montana. *J. Appl. Meteor.*, **13**, 62–70.
- Super, A.B., 1986: Further exploratory analysis of the Bridger Range winter orographic seeding experiment. *J. Clim. Appl. Meteor.*, **25**, 1926–1923.
- Super, A.B., 1999: Summary of the NOAA/Utah Atmospheric Modification Program: 1990–1998. *J. Wea. Modif.*, **31**, 51–75.
- Super, A.B., and J.A. Heimbach, Jr., 1983: Evaluation of the Bridger Range winter cloud seeding experiment using control gauges. *J. Appl. Meteor.*, **22**, 1989–2011.
- Super, A.B., and J.A. Heimbach, Jr., 1988: Microphysical effects of wintertime cloud seeding with silver iodide over the Rocky Mountains, Part II: Observations over the Bridger Range, Montana. *J. Appl. Meteor.*, **27**, 1152–1165.
- Super, A.B., and J.T. McPartland, 1993: Preliminary estimates of increased runoff from additional high elevation snowfall in the Upper Colorado River Basin. *J. Wea. Modif.*, **25**, 74–81.
- Super, A.B., and J. A. Heimbach, Jr., 2005: Feasibility of snowpack enhancement from Colorado winter mountain storms: Emphasis on supercooled liquid water and seeding with silver iodide and propane. Final Report to Technical Services Center, Bureau of Reclamation, Denver, CO, 13 November 2005, 73 pp.
- Sykes, R. I., and R. S. Gabruk, 1997: A second-order closure model for the effect of averaging time on turbulent plume dispersion. *J. Appl. Meteor.*, **36**, 1038–1045.
- Tessendorf, S.A., B. Boe, B. Geerts, M.J. Manton, S. Parkinson, and R. Rasmussen, 2015: The future of winter orographic cloud seeding: a view from scientists and stakeholders. *Bull. Amer. Meteor. Soc.*, **96**, 2195–2198.
- Thompson, G., R. M. Rasmussen, and K. Manning, 2004: Explicit forecasts of winter precipitation using an improved bulk microphysics scheme. Part I: Description and sensitivity analysis. *Mon. Wea. Rev.*, **132**, 519–542.
- Thompson, G., P. R. Field, R. M. Rasmussen, and W. D. Hall, 2008: Explicit forecasts of winter precipitation using an improved bulk microphysics scheme. Part II: implementation of a new snow parameterization. *Mon. Wea. Rev.*, **136**, 5095–5115.
- Thompson, G. and T. Eidhammer, 2014: A study of aerosol impacts on clouds and precipitation development in a large winter cyclone. *J. Atmos. Sci.*, **71**, 3636–3658.
- Trihydro Corporation, 2006: *Platte River Basin Plan Final Report*, Wyoming Water Development Commission. Report, May 2006. 421 pp.
- USBR, 2010: Environmental Assessment for the Walker River Basin Cloud Seeding Project. Lahonton Basin Area Office, Carson City, Nevada. Mid-Pacific Region. 80 pp.
- USBR, 2010: Finding of No Significant Impact, Walker River Basin Cloud Seeding Project. FONSI No: LO-10-05, 7 p.
- Vonnegut, B., 1947: The nucleation of ice formation by silver iodide. *J. Appl. Phys.*, **18**, 593–595.

- Warburton, J.A., R.H. Stone, and B.L. Marler, 1995: How the transport and dispersion of AgI aerosols may affect detectability of seeding effects by statistical methods. *J. Appl. Meteor.*, **34**, 1929–1941.
- Warburton, J.A., S.K. Chai, and L.G. Young, 1996: A new method of assessing snowfall enhancement with silver iodide seeding using physical and chemical techniques. *J. Appl. Meteor.*, **35**, 1569–1573.
- Williams, B.D., and J.A. Denholm, 2009: Assessment of the Environmental Toxicity of Silver Iodide-With Reference to a Cloud Seeding Trial in the Snowy Mountains of Australia. *J. Wea. Modif.*, **41**, 75–96.
- WMA, 2009: Weather Modification Association (WMA) Position Statement on the Environmental Impact of Using Silver Iodide as a Cloud Seeding Agent. WMA, Salt Lake City, 5 pp.
- WMA, 2014: Code of Ethics. Weather Modification Association document adopted April 2014 by WMA membership, Reno, Nevada.
- WWC Engineering, AECOM, and ERO Resources Corp., 2010: *Green River Basin Plan*. Report to the Wyoming Water Development Commission, Basin Planning Program. 189 pp.
- WWDC, 2014: The Wyoming Weather Modification Pilot Program – Level II Study, Draft Executive Summary, NCAR, 15 pp. (available at <http://wwdc.state.wy.us/>)
- Xue, L., A. Teller, R. M. Rasmussen, I. Geresdi, and Z. Pan, 2010: Effects of aerosol solubility and regeneration on warm-phase orographic clouds and precipitation simulated by a detailed bin microphysical scheme. *J. Atmos. Sci.*, **67**, 3336–3354.
- Xue, L., A. Teller, R. M. Rasmussen, I. Geresdi, Z. Pan, and X. Liu, 2012: Effects of aerosol solubility and regeneration on mixed-phase orographic clouds and precipitation. *J. Atmos. Sci.*, **69**, 1994–2010.
- Xue, L., and Coauthors, 2013a: AgI cloud seeding effects as seen in WRF simulations. Part I: Model description and idealized 2D sensitivity tests. *J. Appl. Meteor. Climatol.*, **52**, 1433–1457.
- Xue, L., S. Tessendorf, E. Nelson, R. Rasmussen, D. Breed, S. Parkinson, P. Holbrook, and D. Blestrud, 2013b: AgI cloud seeding effects as seen in WRF simulations. Part II: 3D real case simulations and sensitivity tests. *J. Appl. Meteor. Climatol.*, **52**, 1458–1476.
- Xue, L., X. Chu, R. Rasmussen, D. Breed, B. Boe, and B. Geerts, 2014: The dispersion of silver iodide particles from ground-based generators over complex terrain, Part 2: WRF Large-Eddy simulations vs. Observations. *J. Appl. Meteor. Climatol.*, **53**, 1342–1361.
- Xue, L., R. Edwards, A. Huggins, R. Rasmussen, S. A. Tessendorf, P. Holbrook, D. Blestrud, M. Kunkel, B. Glenn and S. Parkinson, 2016: WRF Large-Eddy simulations of chemical tracer deposition and seeding effect over complex terrain from ground- and aircraft-based AgI generators. *J. Appl. Meteor. Climatol.*, to be resubmitted.
- Yang, D., B.E. Goodison, J.R. Metcalfe, V.S. Golubev, R. Bates, T. Pangburn, and C.L. Hanson, 1998: Accuracy of NWS 8" standard nonrecording precipitation gauge: results and application of WMO intercomparison. *J. Atmos. Oceanic Technol.*, **15**, 54–68.

List of Acronyms

AF – Acre-feet or acre-foot
AgI – Silver iodide
AGL – Above Ground Level
AINC – Acoustic Ice Nucleus Counter, aka the NCAR ice nucleus counter
AS – Airborne Seeding (level 3–4 km MSL)
ASCE – American Society of Civil Engineers
ASCI – AgI Seeding Cloud Impact Investigation, a National Science Foundation-funded study of cloud seeding in Wyoming that utilized the seeding facilities from the WWMPP
ASH – Airborne Seeding (level 4–5 km MSL)
ASPEN – AgI Seeding Parameterization
AWC – Aviation Weather Center
AWRR – Atmospheric Water Resources Research
BLM – U.S. Bureau of Land Management
BOPU – Board of Public Utilities
BRE – Bridger Range Experiment (southwestern Montana)
Cat Ex – Categorical Exclusion
CCN – Cloud Condensation Nuclei
CFSR – Climate Forecast System Reanalysis
CONUS – Continental United States
DRI – Desert Research Institute
EA – Environmental Assessment
ECMWF – European Centre for Medium-Range Weather Forecasts
EIS – Environmental Impact Study
EMO – Elk Mountain Observatory
ERA – ECMWF Re-Analysis
EU – Experimental Unit
FLEXPART – Flexible Particle
FONSI – Finding of No Significant Impact
Fr – Froude Number, an index of how flow interacts with a mountain barrier
GFS – Global Forecast System
GS – Ground Seeding (level 0–1 km AGL)
HEC – Heritage Environmental Consulting
HRNV – Historical Range of Natural Variability
HYSPLIT – HYbrid Single-Particle Lagrangian Integrated Trajectory
(http://www.arl.noaa.gov/documents/Summaries/Dispersion_HYSPLIT.pdf)
ICE – Ice Crystal Engineering
IN – Ice Nuclei
INGs – Ice Nucleus Generators
IPC – Idaho Power Company
LES – Large Eddy Simulation
LP – Liquid Propane
LSM – Land Surface Model
LWC – Liquid water content
LWP – liquid water path (a vertical integration of LWC)
MBNF – Medicine Bow National Forest

MOU – Memorandum of Understanding
 MSL – Mean Sea Level
 MYJ – Mellor Yamada Janjic PBL scheme
 MYNN – Mellor Yamada Nakanishi Niino PBL scheme
 NARR – North American Regional Reanalysis
 NAWC – North American Weather Consultants
 NCAR – National Center for Atmospheric Research
 NCEP – National Centers for Environmental Prediction
 NEPA – National Environmental Policy Act
 NLDAS – National Land Data Assimilation System
 NOAA – National Oceanic and Atmospheric Administration
 NRC – National Research Council
 NRCS – Natural Resource Conservation Service
 NRRI – Natural Resources Research Institute
 NWS – National Weather Service
 PBL – Planetary Boundary Layer
 RAL – Research Applications Laboratory, a part of NCAR
 RCM – Regional Climate Model
 RSE – Randomized Statistical Experiment, analysis part of the WWMPP
 RT-FDDA – WRF real-time four-dimensional data assimilation modeling system
 SCPP – Sierra Cooperative Pilot Project
 SEO – State Engineer’s Office
 SLW – supercooled liquid water
 SNOTEL – Snow Telemetry, a snow gauge network operated by the NRCS
 SPERP – Snowy Precipitation Enhancement Research Program (Snowy Mountains of Australia)
 STILT – Stochastic Time-Inverted Lagrangian Transport
 SUP – Special Use Permit
 SWE – Snow water equivalent
 TAT – Technical Advisory Team, created as part of the WWMPP
 USBR – United States Bureau of Reclamation
 USFS – United States Forest Service
 USGS – United States Geological Survey
 WGFD – Wyoming Game and Fish Department
 WMA – Weather Modification Association
 WMI – Weather Modification, Inc.
 WRF – Weather Research and Forecast model
 WRF-Hydro – WRF Hydrological model
 WSEO – Wyoming State Engineer’s Office
 WWDC – Wyoming Water Development Commission, the State body directing the WWDO
 WWDO – Wyoming Water Development Office
 WWMPP – Wyoming Weather Modification Pilot Program
 YSU – Yonsei University PBL scheme